frontiers | Research Topics

Frontiers in Wolbachia biology

2023

Edited by
Takema Fukatsu, Mark Taylor, Didier Bouchon, Yuval Gottlieb, Steve Perlman, George Tsiamis, Karyn Nicole Johnson and Elizabeth McGraw

Published in
Frontiers in Microbiology

ISSN 1664-8714
ISBN 978-2-8325-5723-5
DOI 10.3389/978-2-8325-5723-5

About Frontiers

Frontiers is more than just an open access publisher of scholarly articles: it is a pioneering approach to the world of academia, radically improving the way scholarly research is managed. The grand vision of Frontiers is a world where all people have an equal opportunity to seek, share and generate knowledge. Frontiers provides immediate and permanent online open access to all its publications, but this alone is not enough to realize our grand goals.

Frontiers journal series

The Frontiers journal series is a multi-tier and interdisciplinary set of open-access, online journals, promising a paradigm shift from the current review, selection and dissemination processes in academic publishing. All Frontiers journals are driven by researchers for researchers; therefore, they constitute a service to the scholarly community. At the same time, the *Frontiers journal series* operates on a revolutionary invention, the tiered publishing system, initially addressing specific communities of scholars, and gradually climbing up to broader public understanding, thus serving the interests of the lay society, too.

Dedication to quality

Each Frontiers article is a landmark of the highest quality, thanks to genuinely collaborative interactions between authors and review editors, who include some of the world's best academicians. Research must be certified by peers before entering a stream of knowledge that may eventually reach the public - and shape society; therefore, Frontiers only applies the most rigorous and unbiased reviews. Frontiers revolutionizes research publishing by freely delivering the most outstanding research, evaluated with no bias from both the academic and social point of view. By applying the most advanced information technologies, Frontiers is catapulting scholarly publishing into a new generation.

What are Frontiers Research Topics?

Frontiers Research Topics are very popular trademarks of the *Frontiers journals series*: they are collections of at least ten articles, all centered on a particular subject. With their unique mix of varied contributions from Original Research to Review Articles, Frontiers Research Topics unify the most influential researchers, the latest key findings and historical advances in a hot research area.

Find out more on how to host your own Frontiers Research Topic or contribute to one as an author by contacting the Frontiers editorial office: frontiersin.org/about/contact

Frontiers in Wolbachia biology 2023

Topic editors

Takema Fukatsu — National Institute of Advanced Industrial Science and Technology (AIST), Japan

Mark Taylor — Liverpool School of Tropical Medicine, United Kingdom

Didier Bouchon — University of Poitiers, France

Yuval Gottlieb — Hebrew University of Jerusalem, Israel

Steve Perlman — University of Victoria, Canada

George Tsiamis — University of Patras, Greece

Karyn Nicole Johnson — The University of Queensland, Australia

Elizabeth McGraw — The Pennsylvania State University (PSU), United States

Citation

Fukatsu, T., Taylor, M., Bouchon, D., Gottlieb, Y., Perlman, S., Tsiamis, G., Johnson, K. N., McGraw, E., eds. (2024). *Frontiers in Wolbachia biology 2023*. Lausanne: Frontiers Media SA. doi: 10.3389/978-2-8325-5723-5

Table of contents

05 Editorial: Frontiers in *Wolbachia* biology 2023
Takema Fukatsu, Yuval Gottlieb, George Tsiamis, Elizabeth McGraw, Steve Perlman, Didier Bouchon, Karyn Johnson and Mark J. Taylor

08 Toward novel treatment against filariasis: Insight into genome-wide co-evolutionary analysis of filarial nematodes and *Wolbachia*
Arporn Wangwiwatsin, Siriyakorn Kulwong, Jutarop Phetcharaburanin, Nisana Namwat, Poramate Klanrit, Watcharin Loilome, Wanchai Maleewong and Adam J. Reid

23 Modeling emergence of *Wolbachia* toxin-antidote protein functions with an evolutionary algorithm
John Beckmann, Joe Gillespie and Daniel Tauritz

34 Patterns of asexual reproduction of the soybean aphid, *Aphis glycines* (Matsumura), with and without the secondary symbionts *Wolbachia* and *Arsenophonus*, on susceptible and resistant soybean genotypes
Rosanna Giordano, Everett P. Weber, Ryan Mitacek, Alejandra Flores, Alonso Ledesma, Arun K. De, Theresa K. Herman, Felipe N. Soto-Adames, Minh Q. Nguyen, Curtis B. Hill and Glen L. Hartman

51 Using *Wolbachia* to control rice planthopper populations: progress and challenges
Yan Guo, Jiayi Shao, Yanxian Wu and Yifeng Li

63 Symbiotic *Wolbachia* in mosquitoes and its role in reducing the transmission of mosquito-borne diseases: updates and prospects
Awoke Minwuyelet, Giulio Petronio Petronio, Delenasaw Yewhalaw, Andrea Sciarretta, Irene Magnifico, Daria Nicolosi, Roberto Di Marco and Getnet Atenafu

75 Combinations of the azaquinazoline anti-*Wolbachia* agent, AWZ1066S, with benzimidazole anthelmintics synergise to mediate sub-seven-day sterilising and curative efficacies in experimental models of filariasis
Shrilakshmi Hegde, Amy E. Marriott, Nicolas Pionnier, Andrew Steven, Christina Bulman, Emma Gunderson, Ian Vogel, Marianne Koschel, Alexandra Ehrens, Sara Lustigman, Denis Voronin, Nancy Tricoche, Achim Hoerauf, Marc P. Hübner, Judy Sakanari, Ghaith Aljayyoussi, Fabian Gusovsky, Jessica Dagley, David W. Hong, Paul O'Neill, Steven A. Ward, Mark J. Taylor and Joseph D. Turner

92 Bacterial community and genome analysis of cytoplasmic incompatibility-inducing *Wolbachia* in American serpentine leafminer, *Liriomyza trifolii*
Ajeng K. Pramono, Ardhiani K. Hidayanti, Yohsuke Tagami and Hiroki Ando

103 Improved metagenome assemblies through selective enrichment of bacterial genomic DNA from eukaryotic host genomic DNA using ATAC-seq
Lindsey J. Cantin, Julie C. Dunning Hotopp and Jeremy M. Foster

120 Cross-validation of chemical and genetic disruption approaches to inform host cellular effects on *Wolbachia* abundance in *Drosophila*
Zinat Sharmin, Hani Samarah, Rafael Aldaya Bourricaudy, Laura Ochoa and Laura Renee Serbus

133 Development, feeding, and sex shape the relative quantity of the nutritional obligatory symbiont *Wolbachia* in bed bugs
Marius Poulain, Elodie Rosinski, Hélène Henri, Séverine Balmand, Marie-Laure Delignette-Muller, Abdelaziz Heddi, Romain Lasseur, Fabrice Vavre, Anna Zaidman-Rémy and Natacha Kremer

144 Dual RNA-seq in filarial nematodes and *Wolbachia* endosymbionts using RNase H based ribosomal RNA depletion
Lindsey J. Cantin, Vanessa Gregory, Laura N. Blum and Jeremy M. Foster

158 *Wolbachia* endosymbionts in *Drosophila* regulate the resistance to Zika virus infection in a sex dependent manner
Ghada Tafesh-Edwards, Margarita Kyza Karavioti, Klea Markollari, Dean Bunnell, Stanislava Chtarbanova and Ioannis Eleftherianos

169 *In vitro* extracellular replication of *Wolbachia* endobacteria
Lara Vanessa Behrmann, Kirstin Meier, Jennifer Vollmer, Chukwuebuka Chibuzo Chiedu, Andrea Schiefer, Achim Hoerauf and Kenneth Pfarr

183 Three feminizing *Wolbachia* strains in a single host species: comparative genomics paves the way for identifying sex reversal factors
Pierre Grève, Bouziane Moumen and Didier Bouchon

frontiers | Frontiers in Microbiology

TYPE Editorial
PUBLISHED 11 November 2024
DOI 10.3389/fmicb.2024.1513314

OPEN ACCESS

EDITED AND REVIEWED BY
Daisuke Kageyama,
National Agriculture and Food Research Organization (NARO), Japan

*CORRESPONDENCE
Takema Fukatsu
✉ t-fukatsu@aist.go.jp

RECEIVED 18 October 2024
ACCEPTED 21 October 2024
PUBLISHED 11 November 2024

CITATION
Fukatsu T, Gottlieb Y, Tsiamis G, McGraw E, Perlman S, Bouchon D, Johnson K and Taylor MJ (2024) Editorial: Frontiers in *Wolbachia* biology 2023.
Front. Microbiol. 15:1513314.
doi: 10.3389/fmicb.2024.1513314

Editorial: Frontiers in *Wolbachia* biology 2023

Takema Fukatsu[1,2,3]*, Yuval Gottlieb[4], George Tsiamis[5], Elizabeth McGraw[6], Steve Perlman[7], Didier Bouchon[8], Karyn Johnson[9] and Mark J. Taylor[10]

[1]Bioproduction Research Institute, National Institute of Advanced Industrial Science and Technology, Tsukuba, Japan, [2]Graduate School of Life and Environmental Sciences, University of Tsukuba, Tsukuba, Japan, [3]Department of Biological Sciences, Graduate School of Science, The University of Tokyo, Tokyo, Japan, [4]Koert School of Veterinary Medicine, Robert H. Smith Faculty of Agriculture, Food and Environment, The Hebrew University of Jerusalem, Rehovot, Israel, [5]Department of Sustainable Agriculture, University of Patras, Agrinio, Greece, [6]Department of Biology, The Pennsylvania State University, University Park, PA, United States, [7]Department of Biology, University of Victoria, Victoria, BC, Canada, [8]Ecologie et Biologie des Interactions, Université de Poitiers, Poitiers, France, [9]Australia School of Biological Sciences, The University of Queensland, Brisbane, QLD, Australia, [10]Department of Tropical Disease Biology, Liverpool School of Tropical Medicine, Liverpool, United Kingdom

KEYWORDS

***Wolbachia*, symbiont, genome, insect, nematode**

Editorial on the Research Topic
Frontiers in *Wolbachia* biology 2023

Wolbachia is likely the most successful endosymbiotic bacteria associated with insects and other arthropods, as well as nematodes (Werren et al., 2008). Over the past several decades, its widespread presence across the vast range of arthropod in the terrestrial ecosystem, as well as its various biological attributes, have led to an explosive development in *Wolbachia* research. These include the induction of striking reproductive phenotypes, namely cytoplasmic incompatibility (CI), male-killing (MK), feminization (Fem) and parthenogenesis induction (PI) (Kaur et al., 2021); obligatory and conditional beneficial fitness consequences such as nutrient provisioning and resistance to parasites, pathogens and viruses (Hamilton and Perlman, 2013; Pimental et al., 2021); essentiality for host growth, development and survival (Zug and Hammerstein, 2015; Taylor et al., 2005); and others. The biology of *Wolbachia* is not only a captivating area of basic research that covers host-microbe interactions ranging from cell-biology and physiology to ecology and evolution (Serbus et al., 2008; Sanaei et al., 2021), but it is also an important applied research field that contributes to *Wolbachia*-mediated control of vector-borne infectious diseases and pests (Iturbe-Ormaetxe et al., 2011; Ross et al., 2019), and *Wolbachia*-targeted prevention and remedy of filariasis (Taylor et al., 2005; Johnson et al., 2021).

Since the 1st *Wolbachia* Conference held at Crete, Greece, in 2000, *Wolbachia* Conferences have biennially provided a very active and important forum for world's researchers working on *Wolbachia* and other microbial symbionts of arthropods, nematodes etc. The 11th *Wolbachia* Conference was initially planned to be held on 5th-10th July 2020, but because of the COVID pandemic, it was finally postponed to 11th-16th June 2023 and held so successfully. In collaboration with the 11th *Wolbachia* Conference, the Research Topic "*Frontiers in Wolbachia Biology 2023*" was launched to provide a forum to overview achievements recently emerging in this research field. In total, 12 original research articles and two review articles are compiled in the Research Topic, which cover a variety of topics regarding the *Wolbachia* biology.

The reproductive manipulations induced by *Wolbachia* infection are among the focal Research Topics of the *Wolbachia* biology. While several (putative) effector proteins responsible for CI, MK and PI phenotypes have been uncovered for several insect systems including fruit flies, mosquitoes, moths and wasps (Beckmann et al., 2017; LePage et al., 2017; Perlmutter et al., 2019; Katsuma et al., 2022; Arai et al., 2023; Fricke and Lindsay, 2024), considering the diversity of the effector molecules (Cifs, Oscar, Wmk, Pifs, etc.), more extensive survey is needed for understanding the diversity and commonality of the *Wolbachia*-induced reproductive phenotypes. Pramono et al. reported a CI-inducing *Wolbachia* genome from a leaf-mining pest fly *Liriomyza trifolii*. Grève et al. reported the genomes of three feminizing *Wolbachia* strains from the pill bug *Armadillidium vulgare*. Beckmann et al. attempted a modeling approach using an evolutionary algorithm as to how CI-inducing and rescuing proteins evolve. These studies provide basic information toward our better understanding of the biology of *Wolbachia* and its intricate reproductive phenotypes.

Wolbachia-mediated control measures against mosquito-borne diseases comprise the recent focal topic in this research field, which are mainly based on *Wolbachia*-mediated suppression of pathogen infections and CI-driven spread of *Wolbachia* infection into host populations (Iturbe-Ormaetxe et al., 2011; Ross et al., 2019). Tafesh-Edwards et al. investigated innate immune responses of the fruit fly *Drosophila melanogaster* after Zika virus infection. They found that some immune-related genes such as *drosocin* and *puckered* are upregulated in a female specific manner, whereas the activity of RNA interference and Toll signaling remain unaffected. Minwuyelet et al. reviewed previous studies on utilization of *Wolbachia* for reducing the transmission of mosquito-borne diseases. Guo et al. also overviewed the *Wolbachia*-mediated technologies for suppressing the transmission of mosquito-borne pathogens, and argued application of the technologies to control of rice pest planthoppers.

Wolbachia is difficult to culture *ex vivo*. Thus far, several *Wolbachia* culture systems have been developed, where the fastidious endosymbiotic bacteria can be maintained only when co-cultured with insect cell lines (Masson and Lemaitre, 2020). On the other hand, it was reported that *Wolbachia* purified from insect cells could be maintained in cell-free culture media for at least 1 week without loss of viability or infectivity (Rasgon et al., 2006). Here Behrmann et al. monitored the proliferation of a *Wolbachia* isolate from the mosquito *Aedes albopictus* in a host cell-free *in vitro* culture system by quantitative PCR. By supplementing a mosquito cell membrane fraction and fetal bovine serum, extracellular *Wolbachia* replication for up to 12 days was detected. Notably, even after the *ex vivo* maintenance for 12 days, the *Wolbachia* cells could establish infection to a fresh mosquito cell line, suggesting the possibility that *Wolbachia* might be amenable to some experimental or genetic manipulations using such cell-free culture systems.

Population dynamics of *Wolbachia* within host cells and tissues is important for understanding phenotypic consequences of the symbiont infection such as fitness effects, intensity of reproductive manipulation, level of reproductive performance, and others (López-Madrigal and Duarte, 2019). Sharmin et al. attempted to elucidate the molecular and cellular mechanisms involved in regulation of intra-host *Wolbachia* titer by adopting chemical and genetic approaches using *Drosophila* fruit flies. In total, 37 chemical inhibitors targeting 14 host cellular/molecular processes, which were reported to affect intracellular bacterial abundance in previous studies, were administrated to *D. melanogaster* and *D. simulans*, and examined for their effects on *Wolbachia* titers. Finally, 5 compounds were identified to significantly increase the intra-host *Wolbachia* titers, which were associated with host Imd signaling, Calcium signaling, Ras/mTOR signaling, and Wnt signaling functions, suggesting that these host mechanisms may negatively regulate the *Wolbachia* titers. By making use of ample molecular genetic tools available for *D. melanogaster*, genetic disruption assays confirmed that disruption of Wnt and mTOR pathways upregulates the *Wolbachia* titers, uncovering that interactions of Wnt and mTOR pathways with autophagy may underlie the negative regulation over *Wolbachia* population. Poulain et al. reported detailed population dynamics of the *Wolbachia* strain *w*Cle associated with the common bedbug *Cimex lecturalius*. In the bedbug, the *Wolbachia* cells densely and endocellularly populate the well-developed symbiotic organs, called the bacteriomes, where the specific *Wolbachia* strain synthesizes B vitamins that are deficient in host's blood meal (Hosokawa et al., 2010; Nikoh et al., 2014). In this context, the population dynamics data of *w*Cle in the bedbug will provide insight into how the exceptional *Wolbachia* strain that turned into an obligatory nutritional mutualist contributes to survival and proliferation in the life cycle of the blood-sucking insect pest that is recently re-emerging worldwide (Doggett and Lee, 2023). Giordano et al. investigated reproductive performance of the soybean aphid *Aphis glycines* infected with or without the facultative symbionts *Arsenophonus* and/or *Wolbachia* under different aphid and soybean genotypes. These studies highlight how *Wolbachia* population is controlled and integrated into the endosymbiotic system in cellular, physiological and ecological contexts.

Since *Wolbachia* is indispensable for survival and reproduction of filarial nematodes, *Wolbachia*-targeting drugs are regarded as promising for medical prevention and remedy of filariasis (Johnson et al., 2021). Hegde et al. reported that an azaquinazoline anti-*Wolbachia* agent, AWZ1066S, facilitates the sterilizing and curing effects of benzimidazole in an experimental model of filariasis. Wangwiwatsin et al. reported *in silico* screening of co-evolving protein sequences between host filarial nematodes and their *Wolbachia* endosymbionts, which identified candidate "hub" genes that may connect multiple host-symbiont interactions and thus may provide potential drug targets via disruption of host-*Wolbachia* interactions.

For genomic and transcriptomic studies, the preparation of *Wolbachia*-derived DNA/RNA usually suffers heavy contamination of host-derived DNA/RNA due to the endosymbiotic nature of *Wolbachia*. Cantin, Dunning Hotopp et al. reported an improved procedure for metagenomic assembly of *Wolbachia* genome through selective enrichment of bacterial DNA from nematode host DNA using ATAC-seq technique. Cantin, Gregory et al. also reported an improved procedure for dual RNA-seq in filarial nematodes and *Wolbachia* endosymbionts using RNase H based ribosomal RNA depletion. These technical improvements may be

useful for *Wolbachia* studies of not only nematodes but also insects and other arthropods.

In conclusion, the Research Topic provides a valuable overview of the recent research progress in the field of *Wolbachia* biology. We hope that this Research Topic shows future directions of this research field, which will be manifested in the forthcoming 12th *Wolbachia* Conference to be held at Okinawa, Japan, from 13th to 19th April 2025 (https://web.tuat.ac.jp/~insect/wolbachia2025/).

Author contributions

TF: Writing – original draft, Writing – review & editing. YG: Writing – review & editing. GT: Writing – review & editing. EM: Writing – review & editing. SP: Writing – review & editing. DB: Writing – review & editing. KJ: Writing – review & editing. MT: Writing – review & editing.

Funding

The author(s) declare financial support was received for the research, authorship, and/or publication of this article. TF was funded by the Japan Science and Technology Agency (JST) ERATO grant no. JPMJER1902.

Conflict of interest

The authors declare that the research was conducted in the absence of any commercial or financial relationships that could be construed as a potential conflict of interest.

The author(s) declared that they were an editorial board member of Frontiers, at the time of submission. This had no impact on the peer review process and the final decision.

Publisher's note

References

Arai, H., Anbutsu, H., Nishikawa, Y., Kogawa, M., Ishii, K., Hosokawa, M., et al. (2023). Combined actions of bacteriophage-encoded genes in *Wolbachia*-induced male lethality. *iScience* 26, 106842. doi: 10.1016/j.isci.2023.106842

Beckmann, J. F., Ronau, J. A., and Hochstrasser, M. (2017). A *Wolbachia* deubiquitylating enzyme induces cytoplasmic incompatibility. *Nat. Microbiol.* 2:17007. doi: 10.1038/nmicrobiol.2017.7

Doggett, S. L., and Lee, C. Y. (2023). Historical and contemporary control options against bed bugs, *Cimex* spp. *Annu. Rev. Entomol.* 68, 169–190. doi: 10.1146/annurev-ento-120220-015010

Fricke, L. C., and Lindsay, A. R. I. (2024). Identification of parthenogenesis-inducing effector proteins in *Wolbachia*. *Genome Biol. Evol.* 16:evae036. doi: 10.1093/gbe/evae036

Hamilton, P. T., and Perlman, S. J. (2013). Host defense via symbiosis in *Drosophila*. *PLoS Pathog.* 9:e1003808. doi: 10.1371/journal.ppat.1003808

Hosokawa, T., Koga, R., Kikuchi, Y., Meng, X.-Y., and Fukatsu, T. (2010). *Wolbachia* as a bacteriocyte-associated nutritional mutualist. *PNAS* 107, 769–774. doi: 10.1073/pnas.0911476107

Iturbe-Ormaetxe, I., Walker, T., and O' Neill, S. L. (2011). *Wolbachia* and the biological control of mosquito-borne disease. *EMBO Rep.* 12, 508–518. doi: 10.1038/embor.2011.84

Johnson, K. L., Hong, W. D., Turner, J. D., O'Neill, P. M., Ward, S. A., and Taylor, M. J. (2021). Anti-*Wolbachia* drugs for filariasis. *Trends Parasitol.* 37, 1068–1081. doi: 10.1016/j.pt.2021.06.004

Katsuma, S., Hirota, K., Matsuda-Imai, N., Fukui, T., Muro, T., Nishino, K., et al. (2022). A *Wolbachia* factor for male killing in lepidopteran insects. *Nat. Commun.* 13:6764. doi: 10.1038/s41467-022-34488-y

Kaur, R., Shropshire, J. D., Cross, K. L., Leigh, B., Mansueto, A. J., Stewart, V., et al. (2021). Living in the endosymbiotic world of *Wolbachia*: a centennial review. *Cell Host Microb.* 29, 879–893. doi: 10.1016/j.chom.2021.03.006

LePage, D. P., Metcalf, J. A., Bordenstein, S. R., On, J., Perlmutter, J. I., Shropshire, J. D., et al. (2017). Prophage WO genes recapitulate and enhance *Wolbachia*-induced cytoplasmic incompatibility. *Nature* 543, 243–247. doi: 10.1038/nature21391

López-Madrigal, S., and Duarte, E. H. (2019). Titer regulation in arthropod-*Wolbachia* symbioses. *FEMS Microbiol. Let.* 366:fnz232. doi: 10.1093/femsle/fnz232

Masson, F., and Lemaitre, B. (2020). Growing ungrowable bacteria: overview and perspectives on insect symbiont culturability. *Microbiol. Mol. Biol. Rev.* 84, e00089–e00020. doi: 10.1128/MMBR.00089-20

Nikoh, N., Hosokawa, T., Moriyama, M., Oshima, K., Hattori, M., and Fukatsu, T. (2014). Evolutionary origin of insect–*Wolbachia* nutritional mutualism. *PNAS* 111, 10257–10262. doi: 10.1073/pnas.1409284111

Perlmutter, J. I., Bordenstein, S. R., Unckless, R. L., LePage, D. P., Metcalf, J. A., Hill, T., et al. (2019). The phage gene wmk is a candidate for male killing by a bacterial endosymbiont. *PLoS Pathog.* 15:e1007936. doi: 10.1371/journal.ppat.1007936

Pimental, A. C., Cesar, C. S., Martins, M., and Cogni, R. (2021). The antiviral effects of the symbiont bacteria *Wolbachia* in insects. *Front. Immunol.* 11:626329. doi: 10.3389/fimmu.2020.626329

Rasgon, J. L., Gamston, C. E., and Ren, X. (2006). Survival of *Wolbachia pipientis* in cell-free medium. *Appl. Environ. Microbiol.* 72, 6934–6937. doi: 10.1128/AEM.01673-06

Ross, P. A., Turelli, M., and Hoffmann, A. A. (2019). Evolutionary ecology of *Wolbachia* releases for disease control. *Annu. Rev. Genet.* 53, 93–116. doi: 10.1146/annurev-genet-112618-043609

Sanaei, E., Charlat, S., and Engelstädter, J. (2021). *Wolbachia* host shifts: routes, mechanisms, constraints and evolutionary consequences. *Biol. Rev.* 96, 433–453. doi: 10.1111/brv.12663

Serbus, L. R., Casper-Lindley, C., Landmann, F., and Sullivan, W. (2008). The genetics and cell biology of *Wolbachia*-host interactions. *Annu. Rev. Genet.* 42, 683–707. doi: 10.1146/annurev.genet.41.110306.130354

Taylor, M. J., Bandi, C., and Hoerauf, A. (2005). *Wolbachia* bacterial endosymbionts of filarial nematodes. *Adv. Parasitol.* 60, 245–284. doi: 10.1016/S0065-308X(05)60004-8

Werren, J. H., Baldo, L., and Clark, M. E. (2008). *Wolbachia*: master manipulators of invertebrate biology. *Nat. Rev. Microbiol.* 6, 741–751. doi: 10.1038/nrmicro1969

Zug, R., and Hammerstein, P. (2015). Bad guys turned nice? A critical assessment of *Wolbachia* mutualisms in arthropod hosts. *Biol. Rev.* 90, 89–111. doi: 10.1111/brv.12098

frontiers | Frontiers in Microbiology

TYPE Original Research
PUBLISHED 22 March 2023
DOI 10.3389/fmicb.2023.1052352

OPEN ACCESS

EDITED BY
Amparo Latorre,
University of Valencia,
Spain

REVIEWED BY
Christina Toft,
Instituto de Biología Integrativa de Sistemas (UV+CSIC), Spain
Mónica Asunción Hurtado Ruiz,
University of Jaume I, Spain
Alexandra Grote,
Broad Institute,
United States

*CORRESPONDENCE
Arporn Wangwiwatsin
✉ arpowa@kku.ac.th

SPECIALTY SECTION
This article was submitted to Microbial Symbioses, a section of the journal Frontiers in Microbiology

RECEIVED 26 September 2022
ACCEPTED 16 February 2023
PUBLISHED 22 March 2023

CITATION
Wangwiwatsin A, Kulwong S, Phetcharaburanin J, Namwat N, Klanrit P, Loilome W, Maleewong W and Reid AJ (2023) Toward novel treatment against filariasis: Insight into genome-wide co-evolutionary analysis of filarial nematodes and *Wolbachia*. *Front. Microbiol.* 14:1052352. doi: 10.3389/fmicb.2023.1052352

Toward novel treatment against filariasis: Insight into genome-wide co-evolutionary analysis of filarial nematodes and *Wolbachia*

Arporn Wangwiwatsin[1,2,3]*, Siriyakorn Kulwong[1,2,3], Jutarop Phetcharaburanin[1,2,3], Nisana Namwat[1,2,3], Poramate Klanrit[1,2,3], Watcharin Loilome[1,2,3], Wanchai Maleewong[4] and Adam J. Reid[5,6]

[1]Department of Biochemistry, Faculty of Medicine, Khon Kaen University, Khon Kaen, Thailand, [2]Cholangiocarcinoma Research Institute, Khon Kaen University, Khon Kaen, Thailand, [3]Khon Kaen University Phenome Centre, Khon Kaen University, Khon Kaen, Thailand, [4]Department of Parasitology, Faculty of Medicine, Khon Kaen University, Khon Kaen, Thailand, [5]Parasite Genomics Group, Wellcome Sanger Institute, Hinxton, United Kingdom, [6]The Gurdon Institute, University of Cambridge, Cambridge, United Kingdom

Infectious diseases caused by filarial nematodes are major health problems for humans and animals globally. Current treatment using anti-helminthic drugs requires a long treatment period and is only effective against the microfilarial stage. Most species of filarial nematodes harbor a specific strain of *Wolbachia* bacteria, which are essential for the survival, development, and reproduction of the nematodes. This parasite-bacteria obligate symbiosis offers a new angle for the cure of filariasis. In this study, we utilized publicly available genome data and putative protein sequences from seven filarial nematode species and their symbiotic *Wolbachia* to screen for protein–protein interactions that could be a novel target against multiple filarial nematode species. Genome-wide *in silico* screening was performed to predict molecular interactions based on co-evolutionary signals. We identified over 8,000 pairs of gene families that show evidence of co-evolution based on high correlation score and low false discovery rate (FDR) between gene families and obtained a candidate list that may be keys in filarial nematode–*Wolbachia* interactions. Functional analysis was conducted on these top-scoring pairs, revealing biological processes related to various signaling processes, adult lifespan, developmental control, lipid and nucleotide metabolism, and RNA modification. Furthermore, network analysis of the top-scoring genes with multiple co-evolving pairs suggests candidate genes in both *Wolbachia* and the nematode that may play crucial roles at the center of multi-gene networks. A number of the top-scoring genes matched well to known drug targets, suggesting a promising drug-repurposing strategy that could be applicable against multiple filarial nematode species.

KEYWORDS

filarial nematode, *Wolbachia*, co-evolution, mirrortree, protein–protein interactions, genomics

1. Introduction

Filarial nematodes comprise multiple species and they are a major health problem globally. These parasites cause diseases such as lymphatic filariasis (elephantiasis), onchocerciasis (river blindness), and dirofilariasis (heartworm disease), resulting in disfigurement, social stigma, and, in some cases, permanent disability. These diseases affect up to 50 million people worldwide, and over 1.5 billion people are at risk of infection. Some species also cause diseases in animals, making filariasis a problem for both human and veterinary medicine (Vos et al., 2016; Lustigman et al., 2017). The life cycle of the filarial nematode involves biting insect vectors and mammalian hosts. In the mammalian host, the larval stages reside in regional lymphatic vessels or nodules and develop into mating adults, which release microfilaria into the circulation system (Cross, 2011).

The majority of filarial nematodes co-exist with an obligatory endosymbiotic bacterium called *Wolbachia*, a gram-negative alphaproteobacterium in the order Rickettsia. *Wolbachia* is present in all life stages of the nematode, with a marked increase once the nematode passes from insect vector to mammalian host, and another sharp increase as the nematodes develop into adults (Fenn and Blaxter, 2004; McGarry et al., 2004). The presence of *Wolbachia* is essential for worm survival, development, embryogenesis, and reproduction (Scott et al., 2012; Taylor et al., 2013). At the molecular level, *Wolbachia*–filarial nematode interactions are associated with haem metabolism, nucleotide metabolism, fatty acid synthesis, as well as folic acid synthesis (Slatko et al., 2010; Taylor et al., 2013). When the phylogenetic trees of the nematode and the *Wolbachia* are compared, they closely reflect one another, suggesting co-evolution between the nematode and the Wolbachia – a phenomenon often found in organisms with a long-term, tightly associated relationship (Bandi et al., 1999; Casiraghi et al., 2001; Ferri et al., 2011). The elimination of filarial nematode infection might be achieved through disruption of this essential symbiotic relationship, either by targeting the bacterium or targeting the molecular interactions between the worm and the bacterium. The latter approach is potentially more specific for filariasis treatment and may reduce the risk of antibiotic resistance.

Current treatment with anthelminthic drugs such as ivermectin is sub-optimal against the adult stage (Basáñez et al., 2008; Diawara et al., 2009; Tamarozzi et al., 2011). Signs of drug resistance have been observed (Schwab et al., 2006; Laman et al., 2022); hence, alternative treatments are urgently needed. New treatment trials have focused on killing the *Wolbachia* endosymbiont as well as the nematode by using a combination of antibiotics and anthelminthic drugs (Taylor et al., 2014; Turner et al., 2017). Treating experimentally infected animal models with antibiotics affected the reproduction capacity of the nematodes, as indicated by the reduced number of microfilaria, and eventually the killing of the adult stage (Bandi et al., 1999; Volkmann et al., 2003; Aljayyoussi et al., 2017; Specht et al., 2018). However, mass-drug administration of antibiotics disrupts the microbiota of the treated individual as well as risks the eventual development of antibiotic-resistant bacteria. Screenings for other anti-*Wolbachia* drugs, as well as attempting to target nematode–*Wolbachia* interactions, are underway (Landmann et al., 2012; Scott et al., 2012; Poopandi et al., 2021). However, these attempts often focus on a single filarial nematode species. Recently, with the publicly available genomes for many filarial nematode species and their *Wolbachia*, we aim to reveal targets that could be relevant against multiple species.

Proteins that interact with one another tend to co-evolve to maintain their functions, and this allows researchers to use co-evolutionary signals to predict protein–protein interactions within a species, known as the *mirrortree* approach (Pazos and Valencia, 2001; Goh and Cohen, 2002). In this well-established approach, one can predict protein–protein interactions by comparing amino acid sequences in related species and screen for gene trees that are very similar to each other (Shoemaker and Panchenko, 2007; Pazos and Valencia, 2008; Ochoa et al., 2015). This approach has been tested with data from multiple species, both prokaryotic and eukaryotic genomes (Goh and Cohen, 2002; Mier et al., 2017). Over time, the methods have been further developed to improve their accuracy and utility (Ochoa and Pazos, 2014). In particular, some genes may appear to be co-evolving because of the phylogenetic signal between species. Therefore, the Tree-of-Life (tol) mirrortree approach subtracts the species trees from the gene tree prior to gene co-evolutionary analysis (Pazos et al., 2005). Furthermore, a *p*-value calculation that is designed for analyzing multiple phylogenetic trees can be applied to the analysis of each gene pair (Ochoa et al., 2015). The approach has revealed a signal of co-evolution between interacting gene products in the mitochondrial and nuclear genomes (Ochoa and Pazos, 2014), which suggest that the approach could be applicable to interactions that occur between different species (two sets of genomes).

Here, we used publicly available genome data of seven species of filarial nematodes and their *Wolbachia*, namely, *Brugia malayi*, *Brugia pahangi*, *Dirofilaria immitis*, *Wuchereria bancrofti*, *Litomosoides sigmodontis*, *Onchocerca volvulus*, and *Onchocerca ochengi*, and applied co-evolutionary screening at the protein sequence level (mirrortree approach) to predict molecular interactions between the filarial nematode and the *Wolbachia*. By integrating the orthologous genes in the nematode and *Wolbachia* across seven species, the outcome provided here is expected to be applicable against the range of filariasis-causing agents. The results are consistent with the known biology of the symbiotic relationship as well as provide pointers to specific molecules and pathways that can be shortlisted for further anti-filarial screening.

2. Materials and methods

2.1. Source of genomic data

Publicly available genomic data of filarial nematode and its symbiotic *Wolbachia* are obtained from multiple databases, as shown in Table 1. All annotated genes of each species were collected as FASTA format of amino acid sequences.

2.2. Annotation of *Brugia pahangi Wolbachia* genome

For *Wolbachia* of *B. pahangi*, the reference genome was available as a by-product of *B. pahangi* genome sequencing (International Helminth Genomes Consortium, 2019) but no annotation was provided. We, therefore, annotated this genome using prokka (version 1.13; Seemann, 2014) with default parameters and using its default core BLAST+ database, UniProtKB (SwissProt), for protein-coding genes.

TABLE 1 Genome data used for analysis.

Organism	Nematode sequence source and version	Wolbachia sequence source and version
Brugia malayi	WormBase ParaSite: r13 (PRJNA10729)	Ensembl Bacteria: r44 (GCA_000008385)
Brugia pahangi	WormBase ParaSite: r13 (PRJEB497)	WormBase ParaSite: r13 (PRJEB497)
Onchocerca ochengi	WormBase ParaSite: r13 (PRJEB1204)	Ensembl Bacteria: r44 (GCA_000306885.1)
Onchocerca volvulus	WormBase ParaSite: r13 (PRJEB513)	RefSeq (GCF_000530755.1)
Wuchereria bancrofti	WormBase ParaSite: r13 (PRJNA275548)	RefSeq (GCF_002204235.2)
Dirofilaria immitis	WormBase ParaSite: r13 (PRJEB1797)	nematodes.org (wDi.2.2)
Litomosoides sigmodontis	WormBase ParaSite: r13 (PRJEB3075)	nematodes.org (wLs.2.0)

2.3. Overview of the co-evolutionary screening workflow

The workflow is presented in Figure 1. In brief, orthologous groups for the protein sequences of seven filarial nematode species and seven *Wolbachia* species were identified. Orthologous groups with one gene from each species (of either nematodes or bacteria) were kept for downstream analysis. Within each group, protein sequences were aligned using MUSCLE, and a distance matrix between species was created with codeml using the Dayhoff matrix. The species tree distance matrices of the nematodes or *Wolbachia* were created and subtracted from the gene distance matrices by taking away from each gene tree value the distance between corresponding species in the species tree distance matrix based on the tol-mirrortree method (Pazos et al., 2005). Then, the subtracted gene trees were used for correlation analysis. After the species-tree subtraction, the distance matrices from each 1-to-1 orthologous group of the nematode were then compared with the distance matrices of the *Wolbachia* in an all-against-all manner. The correlation coefficients between the nematode and *Wolbachia* matrices were used as an indicator of phylogenetic tree similarity, and hence the co-evolution signal between each pair of nematode–*Wolbachia* gene groups (Pazos and Valencia, 2001). Statistical significance of the correlation was assessed using the *p*-value calculation based on the method of pMT *p*-value Ochoa et al. (2015), followed by multiple-testing correction using the Benjamini–Hochberg method (Benjamini and Hochberg, 1995). Nematode–*Wolbachia* gene pairs with the top scores for both correlation coefficient and pMT *p*-value were taken for further functional analysis.

2.4. Identification of 1-to-1 ortholog

OrthoMCL (version 1.4; Li et al., 2003) was used to identify orthologous groups with one gene from each species (1-to-1 ortholog). For the nematode dataset, all protein sequences from all seven species were combined and used as a reference database for BLASTp (version 2.2.26; Altschul et al., 1990). BLASTp for each protein sequence was performed with -e 0.01. The BLASTp result and a table containing a list of gene IDs for each species were used as input for OrthoMCL run with mode 3. The output from OrthoMCL was filtered to keep only the orthologous groups with one gene from each nematode species. The same pipeline was applied to the *Wolbachia* dataset to obtain the *Wolbachia* 1-to-1 orthologous groups.

2.5. Gene sequence alignment and analysis of evolutionary distances

Within each 1-to-1 orthologous group, the protein sequences of its member were aligned using MUSCLE alignment (version 6.4.2; Edgar, 2004). The distance matrix between each protein sequence within a group was calculated with the Dayhoff matrix using *codeml* (version 4.9; Yang, 2007) with default parameters and runmode = −2. Each distance matrix was converted into a distance vector while maintaining the species order across all groups, and these vectors were then used for correlation analysis.

2.6. Removal of speciation background from gene evolutionary distances

Based on the method of Pazos et al. (2005), subtracting species trees can help remove the correlation that is a result of co-evolution at the species level. In this study, the species tree of the nematodes and the *Wolbachia* was generated by concatenating all of their aligned 1-to-1 orthologs, using a script concatenate_fasta_alignments.py available from Aunin et al. and their associated GitHub[1] (Aunin et al., 2020). GBlocks (version 0.91b; Castresana, 2000) was us ed to remove alignment positions with poor quality (containing missing sequences from at least one species). Distance matrix and distance vectors were created in the same way as the gene orthologous groups. The species tree distance vector of the nematode was subtracted from each nematode gene distance vector, and the same process was performed for the *Wolbachia* species tree. The resulting gene distance vectors, with species tree subtracted, were then used for the calculation of Pearson's correlation coefficient.

2.7. Correlation between nematode and *Wolbachia* genes

Each distance vector of the nematodes, with or without species tree subtraction, was correlated with all distance vectors of the *Wolbachia* in an all-against-all manner. Following the method developed by Pazos and Valencia (2001), the similarity of the distance vectors, i.e., the similarity of the phylogenetic trees, was measured by Pearson's correlation coefficient. The *p*-value for each correlation was calculated using the

1 https://github.com/adamjamesreid/hepatocystis-genome

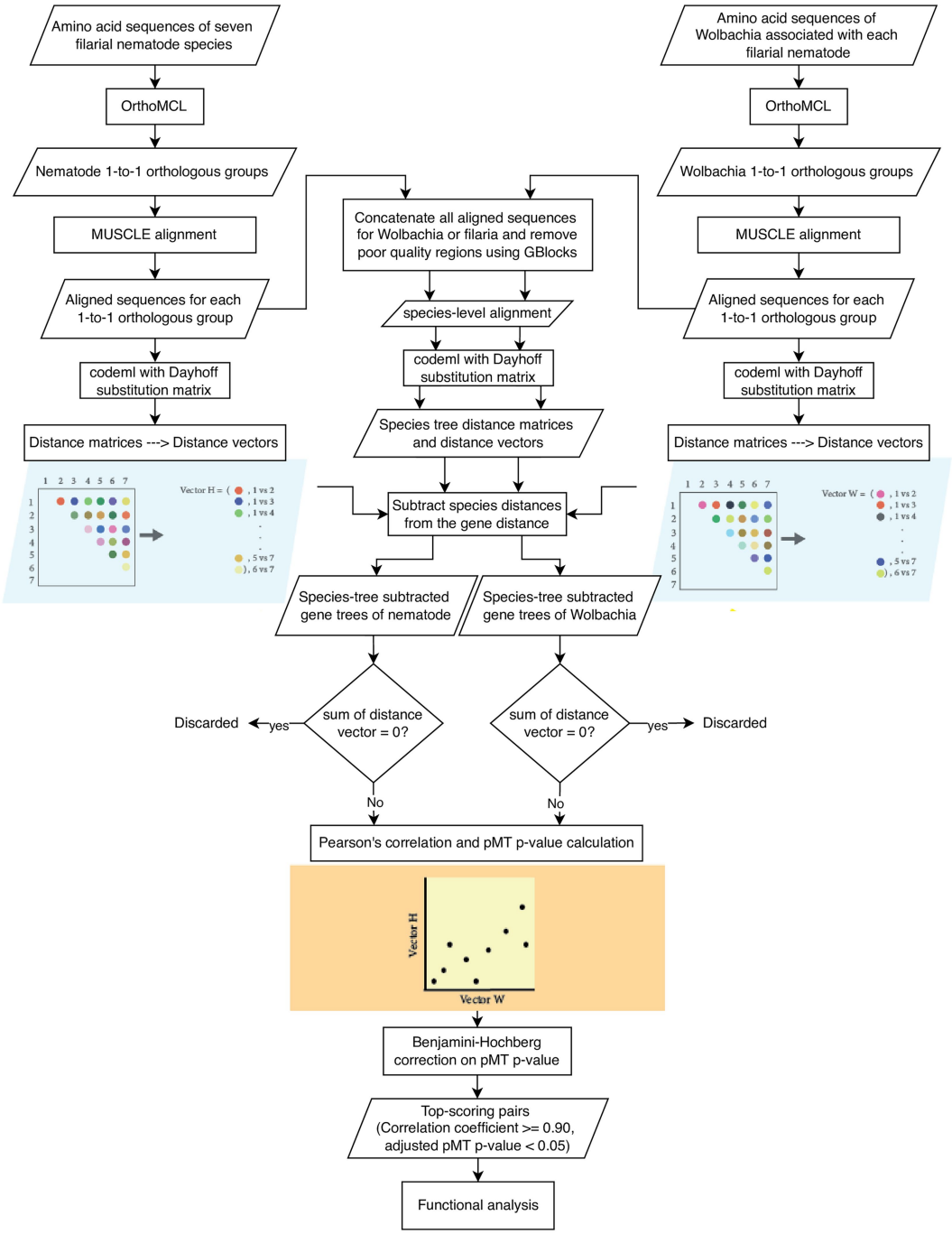

FIGURE 1
Analysis workflow. Rectangles indicate processes. Parallelograms indicate data. Diamonds indicate decisions and filtering. The conversion of a distance matrix to its distance vector, and the correlation analysis of distance vectors are shown here for only one matrix from nematode and *Wolbachia* each.

pMT method of Ochoa et al. (2015), which has been designed specifically for the mirrortree approach. It accounts for the fact that each value between the distance vectors is not entirely independent of one another because they are limited by the species present in each tree. Therefore, when creating the background distribution for *p*-value calculation, the pMT method limits its randomization to only shuffle the data points of the same species between trees. By doing so, the resulting background distribution will be trees that each contain all species, and each species is present only once in a given tree – a more realistic situation for phylogenetic data. Each branch shuffling is counted as one iteration. For our analysis, with ~5,000 ortholog groups and 7 branches in each group, the pMT was run with 100,000 iterations. The pMT *p*-values were corrected for multiple testing using the Benjamini–Hochberg method.

2.8. Functional analysis of top-scoring results

To investigate the genes with the strong co-evolutionary signal between the nematodes and the *Wolbachia*, top-scoring genes

(Pearson's correlation coefficient ≥ 0.90, Benjamini–Hochberg adjusted pMT *p*-value < 0.05) between nematodes and *Wolbachia* with species tree subtraction were used for downstream analyses.

Genes from *B. malayi* (Bm) and *Wolbachia* associated with *B. malayi* (wBm) were used for downstream functional analyses due to its more complete genome among all filarial nematodes in this study. GO term annotations for *B. malayi* genes were obtained from WormBase ParaSite release 13 (Howe et al., 2017; Bolt et al., 2018) using the "BioMart" feature. GO term annotation of *Wolbachia* associated with *B. malayi* was obtained using InterProScan (version 5.55-88.0; Jones et al., 2014). The InterProScan was run using default parameters with -goterms -pa. GO term enrichment was performed using topGO (Alexa and Rahnenfuhrer, 2021) with a weight algorithm and Fisher's exact test using all annotated genes of *B. malayi* or *Wolbachia* associated with *B. malayi* as the background dataset. GO term enrichment was performed separately for genes of *B. malayi* or *Wolbachia* associated with *B. malayi*.

Cytoscape (version 3.8.2; Shannon et al., 2003) was used for visualizing the network of co-evolving groups and for identifying groups that appeared to be centers of potential interactions. Only the connections linking nematode and *Wolbachia* genes were included in the network analysis and not the nematode-nematode or *Wolbachia*-*Wolbachia* connections. Nematode and *Wolbachia* nodes with a high number of connections (correlated with multiple gene groups from their symbiotic partner) were annotated as the top 5% and top 1% most highly connected nodes, which refer to being above 95% quartile and 99% quartile, respectively. These top 5% nodes and their first neighbors (nodes that were directly connected to them) were isolated from the full network and further investigated.

2.9. KEGG pathway mapping

The top-scoring genes of *B. malayi* and *Wolbachia* associated with *B. malayi* were mapped to KEGG ID using KEGG BlastKOALA (version 2.2; Kanehisa and Goto, 2000; Kanehisa et al., 2016) with amino acid sequences as query and searched against either *B. malayi* (taxonomy ID 6279) or *Wolbachia* of *B. malayi* (taxonomy ID 292805) reference. The resulting KEGG IDs were visualized on reference KEGG pathways using KEGG Mapper (version 5.0; Kanehisa et al., 2022). Green color denotes *Wolbachia* genes; yellow and red colors denote nematode genes. The denser colors represent the top 5% and top 1% most highly connected nodes of *Wolbachia* and nematode, respectively.

2.10. Druggability screening

The top 1% most highly connected nodes of the *Wolbachia* and nematode were screened for known drug targets using DrugBank online[2] (version 5.1.9; Wishart et al., 2006) using the "target search" feature. The amino acid sequences of the *B. malayi* and *Wolbachia* associated with *B. malayi* were used as input. BLAST parameters were used as a default in the DrugBank online (cost to open a gap = −1, cost to extend a gap = −1, penalty for mismatch = −3, reward for match = 1, and expectation value (*E*-value) for reporting = 10^{-5}, with low compositional complexity masking/filtering). Resulting target hits were further filtered for those with "approved" or "vet-approved" status.

2 https://go.drugbank.com/

3. Results

The seven nematode genomes used in this study had an average of 12,102 protein-coding genes (range 10,246–14,674), and the *Wolbachia* genomes had 845 protein-coding genes (range 647–1,119). We identified 4,506 orthologous groups of genes for the filarial nematodes and 539 groups for the *Wolbachia* (1-to-1 orthologs only).

3.1. A number of genes appeared to co-evolve between nematode and *Wolbachia*

To evaluate gene-level co-evolution between the nematode and *Wolbachia*, each of the 1-to-1 ortholog groups of the nematode was paired and correlated with those of the *Wolbachia*. The resulting Pearson's correlation coefficient scores, without species tree subtraction, had a mean of 0.503 (range −0.632 to 1; Figure 2A), with a higher correlation coefficient indicating a stronger co-evolutionary signal. After applying a mirrortree-specific *p*-value (pMT) followed by the Benjamini–Hochberg method for multiple testing correction (adjusted pMT *p*-value <0.05) and Pearson's correlation coefficient score cutoff value ($r \geq 0.90$), 39,537 out of 2,428,734 pairs (1.6%) of nematode–*Wolbachia* genes were identified as top-scoring pairs (Figures 2B,C).

To reduce the influence of co-evolution at the species level on gene-level co-evolution, species trees for the nematode and the *Wolbachia* were created and their distance matrices were subtracted from each gene distance matrix of the nematodes or *Wolbachia*, respectively. Pearson's correlation coefficient of the subtracted gene distance matrices ranged from −0.990 to 0.998, with a mean of −0.004 (Figure 2A). After applying pMT followed by the Benjamini–Hochberg method for multiple testing correction (adjusted *p*-value <0.05), 254,276 passed this adjusted *p*-value cutoff, but with a correlation coefficient score as low as 0.57 (Figures 2D,E). Based on the distribution of the correlation coefficient (Figure 2A), we further applied a correlation coefficient cutoff value of 0.90, resulting in a total of 8,285 pairs of nematode–*Wolbachia* genes being identified as top-scoring pairs (adjusted pMT *p*-value of <0.05, Pearson's correlation coefficient > 0.90).

3.2. Top-scoring pairs revealed the co-evolution of gene expression regulation and multiple biosynthesis processes

The total top-scoring pairs from the tol-mirrortree + pMT method (8,285 pairs) were used for functional analyses to investigate the biological implications of these putatively co-evolving genes. Genes of *B. malayi* (Bm) or *Wolbachia* associated with *B. malayi* (wBm) were used as group representatives due to the high quality of the *B. malayi* genome compared to other filarial nematode species.

For *B. malayi*, 1,959 genes were present in the 8,285 top-scoring pairs (some genes were in multiple pairs; i.e., co-evolving with multiple *Wolbachia* genes). GO term enrichment of these genes revealed enrichment in biological processes related to phosphorylation, histone modification, developmental regulation, gene expression

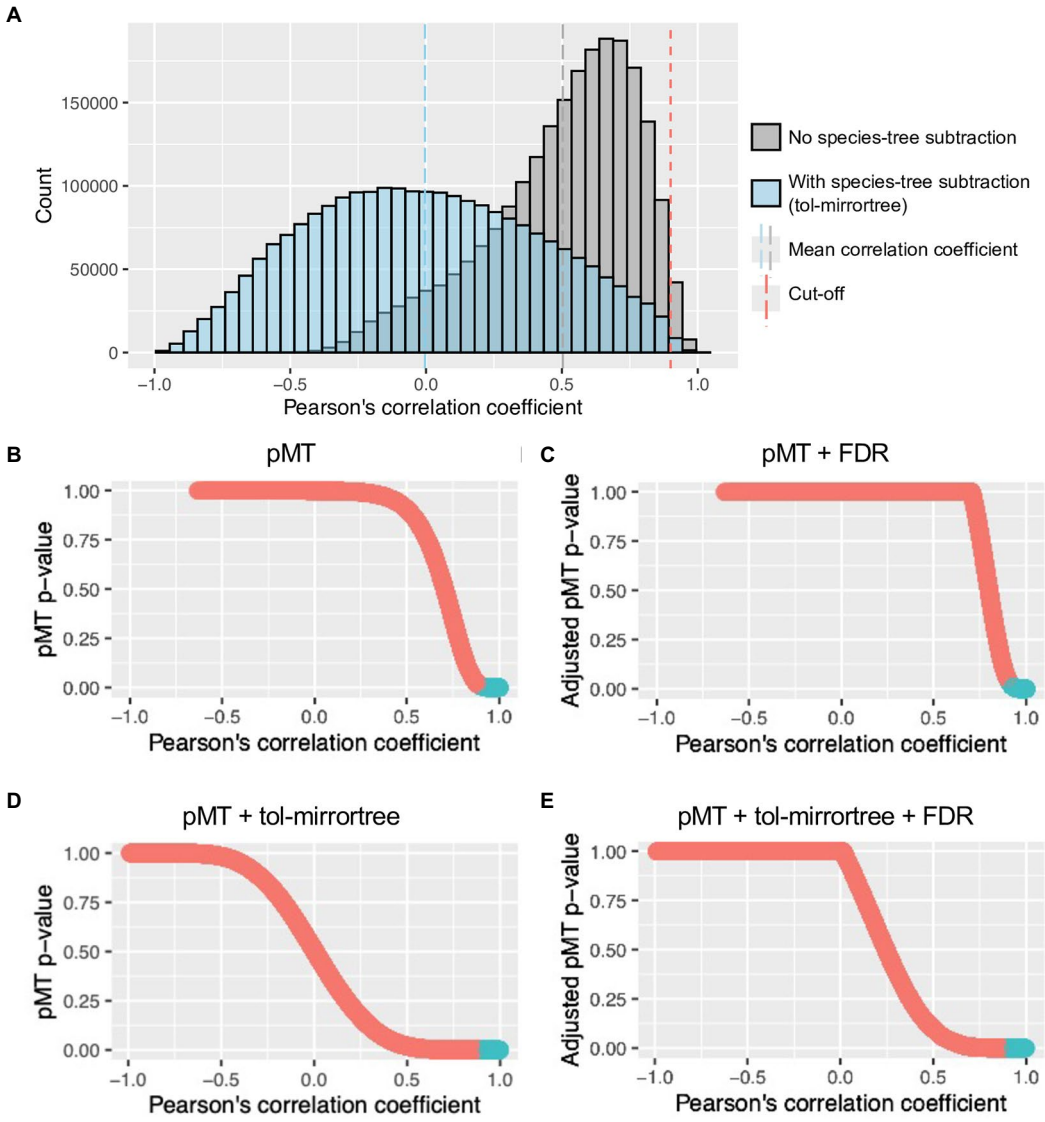

FIGURE 2
Distribution of Pearson's correlation coefficient and pMT value of ps. **(A)** Distribution of Pearson's correlation coefficient of *Wolbachia*–nematode gene tree comparisons with (blue) or without (gray) species tree subtraction (tol-mirrortree). Blue and gray dash lines are means of correlation coefficients with and without species tree subtraction, respectively. Red dash line indicates a cutoff value used for selecting top-scoring genes (Pearson's correlation coefficient≥0.9). **(B–E)** Relationship between Pearson's correlation coefficient and (Benjamini–Hochberg adjusted) pMT *p*-value after different combination of corrections. Blue sections are *Wolbachia*–nematode correlation that pass both cutoff values (Pearson's correlation coefficient≥0.9 and adjusted pMT-*p*-value<0.05).

regulation, and mRNA processing (Figure 3; Supplementary Figure S1; Supplementary Table S1). For molecular functions, enriched GO terms were related to transferase activity, signaling *via* MAPK, calmodulin, GTP, serine/threonine phosphatase, translation, and ribosomal processes (Supplementary Table S1). The cellular component GO terms suggested events related to alternative splicing (*spliceosomal complex* and *U4/U6 x U5 tri-snRNP complex*), translation (*large ribosomal subunit*), and vesicle transport (*clathrin-coated vesicle*, *transport vesicle*, and *phagocytic vesicle*; Supplementary Table S1).

For *Wolbachia*, 386 genes were present in the top-scoring pairs. Only a small number of GO terms were identified as enriched in the *Wolbachia* genes in the top-scoring pairs. Nevertheless, the number of top-scoring genes that were found under these GO terms covered almost or all genes annotated with such GO terms (gene ratio ~ 1), suggesting a strong signal for functional enrichment (Figure 3; Supplementary Figure S1; Supplementary Table S2). These enriched GO terms were related to amino acid synthesis (*lysine biosynthetic process via diaminopimelate*; Supplementary Figure S2), *fatty acid biosynthesis* (Supplementary Figure S3), oxidation reduction (particularly with enzymes in fatty acid synthesis, TCA cycle, and co-factor biosynthesis), and peptidase activity (Supplementary Table S2).

3.3. Some co-evolving genes were an apparent hub of potential interactions

A number of gene orthologous groups were connected to multiple gene groups of the symbiotic partner. Focusing on the nematode, and

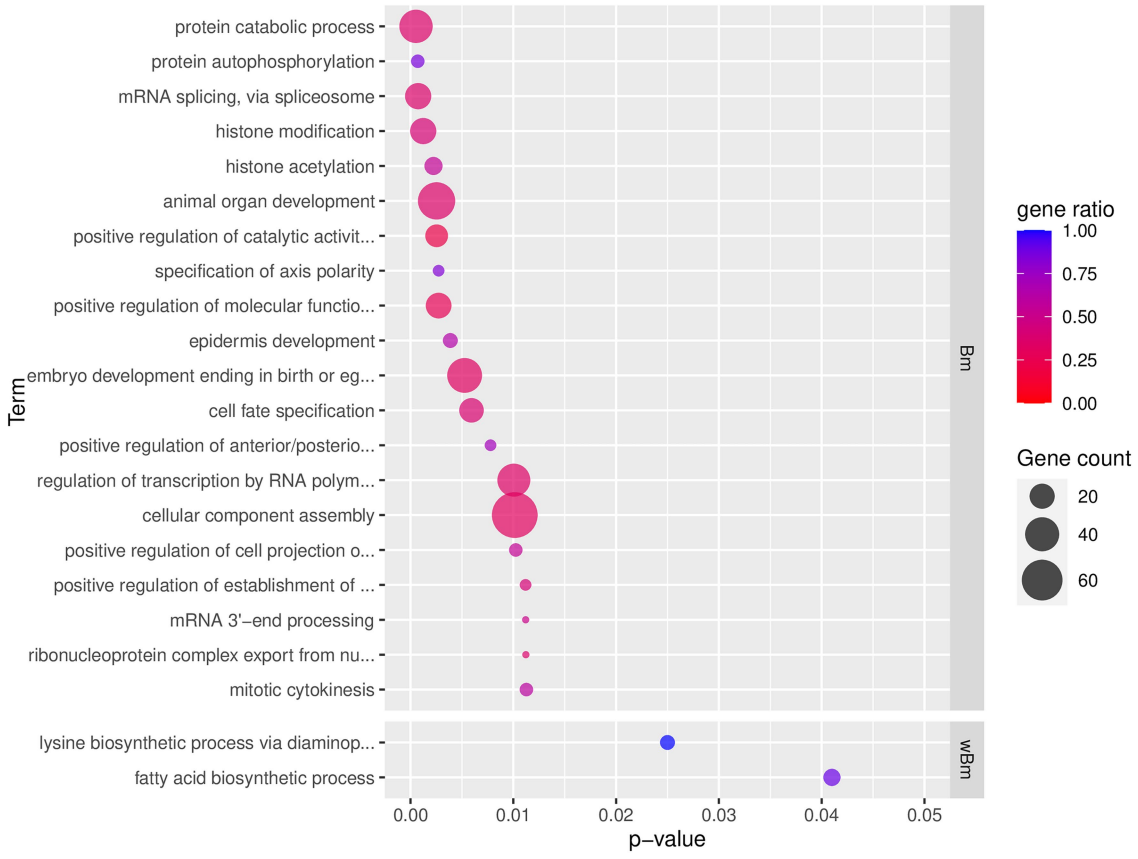

FIGURE 3
Top 20 enriched GO term of *B. malayi* and *Wolbachia* of *B. malayi* genes in top-scoring pairs. Only the top 20 enriched GO terms, ranked by *p*-value, of the biological processes type (BP) are shown. *p*-value refers to the *p*-value reported by topGO analysis. Gene count indicates the number of genes with that GO term in the input top-scoring gene list. Gene ratio is the number of genes with that GO term in the input list divided by a total number of genes in the genome annotated with that GO term. Full list of enriched GO terms of the BP type is presented in Supplementary Figure S1. The complete GO enrichment results with GO ID, full GO term description, and the top-scoring genes in each GO term are shown in Supplementary Table S1 (for *B. malayi*) and Supplementary Table S2 (for *Wolbachia* of *B. malayi*). *Wolbachia*'s lysine biosynthesis and fatty acid synthesis networks and their co-evolving genes in the nematode are further explored in Supplementary Figures S2, S3, respectively. Interactive networks can be found in Cytoscape session file (Supplementary File S1).

using *B. malayi* as a group representative, the top 1% most highly connected nodes (20 nodes) were orthologous groups related to kinase and signaling activities including *stress-activated protein kinase JNK* (involved in various pathways related to stress responses and cell differentiation), *EGL-15* (contained tyrosine-protein kinase receptor domain), *Bm6186* (belonged to ribose-phosphate diphosphokinase family which is involved in catalyzing PRPP – an essential precursor for purine and pyrimidine biosynthesis), and *SOS-1* (involved in activation of RAS/MAPK pathway and regulation of growth, cell differentiation, and survival). Other groups among the top 1% can be related to the regulation of gene expression, translation, RNA pre-processing, and alternative splicing. These included *vab-3* (containing the homeobox domain), *NPAX-2* (predicted to affect transcription factor activity *via* DNA binding), *TBP-1* (TATA-box binding protein), *LIN-40* (predicted to have histone deacetylase binding activity), *MBD-2* (Methyl-CpG Binding Domain Protein), the 40S and 60S ribosomal proteins, *Integrator complex subunit 11* (involved in transcription of small RNA involved in spliceosome), *CWF19* (part of spliceosome), and *fcp-1* (involved in dephosphorylation of RNA polymerase II C-terminal domain) (Table 2; Supplementary Table S3; Supplementary Files S1, S2).

Among *Wolbachia* orthologs, the top 1% most highly connected nodes (four nodes) included the *aspartate-semialdehyde dehydrogenase* (*ASD*) gene that encodes an essential enzyme in the biosynthesis of amino acids in bacteria (Harb and Abu, 1998) and an enzyme in the electron transport chain (*NADH:ubiquinone oxidoreductase chain D*; *nuoD*), the ATPase *dnaA* that activates the initiation of DNA replication, and *dihydrolipoamide dehydrogenase E3 component* (*DLD*) that forms a subunit of several enzyme complexes that are largely involved in energy production *via* breaking down of biomolecules (Table 2; Supplementary Table S3; Supplementary Files S1, S2).

To investigate genes that may have co-evolved with multiple symbiotic partner's genes, and hence could be hubs of the interactions, the top 5% most highly connected nodes of both nematode and *Wolbachia* and their first neighbors (orthologous groups of their symbiotic partner) were selected for producing a network (Figure 4A). Intriguingly, all of the top 1% most highly connected nodes were part of a single connected component, here referred to as Network 1 (Figure 4A). This Network 1 contained a total of 613 genes, with 66 genes being the top 5% most highly connected nodes (accounting for 65% of all the top 5% nodes;

TABLE 2 Top 1% most highly connected nodes in the nematode and *Wolbachia*.

Gene ID		Gene information
Wolbachia of B. malayi	AAW70634	Gene: Wbm0042 (Aspartate-semialdehyde dehydrogenase)
	AAW70716	Gene: Wbm0125 (NADH:ubiquinone oxidoreductase chain D)
	AAW70865	Gene: Wbm0276 (ATPase involved in DNA replication initiation, DnaA)
	AAW71149	Gene: Wbm0561 (Dihydrolipoamide dehydrogenase E3 component)
B. malayi	WBGene00222081	Gene: Bma-jnk-1 (Stress-activated protein kinase JNK)
	WBGene00222891	Gene: Bm2630 (Cleft lip and palate associated transmembrane protein 1, putative)
	WBGene00223114	Gene: Bma-rps-2.1 (40S ribosomal protein S2)
	WBGene00223516	Gene: Bma-ints-11 (Integrator complex subunit 11)
	WBGene00223630	Gene: Bma-vab-3 (Variable ABnormal morphology, PAX6 ortholog)
	WBGene00223673	Gene: Bma-cwf-19 L1 (CwfJ C-terminus 1 containing protein)
	WBGene00224135	Gene: Bma-fcp-1 (RNA polymerase II subunit A C-terminal domain phosphatase)
	WBGene00224457	Gene: Bma-npax-2 (Paired domain-containing protein)
	WBGene00224470	Gene: Bm4209 (FAD_binding_2 domain-containing protein)
	WBGene00224578	Gene: Bma-unc-108 (Ras-related protein Rab-2A)
	WBGene00224796	Gene: Bma-egl-15 (fibroblast growth factor receptor EGL-15)
	WBGene00226117	Gene: Bma-tbp-1 (TATA-box-binding protein-1)
	WBGene00226303	Gene: Bma-lin-40 (metastasis associated 1 family member 2 ortholog)
	WBGene00226342	Gene: Bma-sos-1 (Son Of Sevenless Homolog 1)
	WBGene00226447	Gene: Bm6186 (ribose-phosphate diphosphokinase family member)
	WBGene00229500	Gene: Bma-rpl-7A.3 (60S ribosomal protein L7a)
	WBGene00230969	Gene: Bm10708/Bma-ztf-18.2 (Zinc Finger domain-containing)
	WBGene00231010	Gene: Bma-mbd-2 (methyl-CpG binding domain protein 2)
	WBGene00233173	Gene: Bm12912 (DET1 Partner Of COP1 E3 Ubiquitin Ligase)
	WBGene00234073	Gene: Bma-xpb-1 (General transcription and DNA repair factor IIH helicase subunit XPB)

Supplementary Table S3). GO term enrichment of the genes in Network 1 revealed multiple processes and functions well-known for the *Wolbachia*–filarial nematode relationship, for example, *determination of adult lifespan*, *regulation of oviposition*, *dauer larval development*, *flavin adenine dinucleotide binding*, *NAD binding*, *mRNA splicing*, post-translational processes such as protein folding and localization, and various terms related to developmental control (Figure 4B). However, the enrichment results also point to functions not previously associated with *Wolbachia*–nematode interactions including *vesicle-mediated transport*, *histone acetylation*, *positive regulation of transcription by RNA polymerase II*, and *protein autophosphorylation*. For the *protein autophosphorylation* GO term, seven nematode genes across its genome were annotated with such GO term, with five of these found in Network 1, and the GO term appeared as the most significant enriched GO term (Figure 4B; Supplementary Figure S4; Supplementary Tables S4, S5).

Upon investigation of the *protein autophosphorylation* GO terms, all of the five nematode genes were related to serine–threonine kinase and mitogen-activated protein kinase. These are *dual specificity tyrosine-phosphorylation-regulated kinase 1* (*DYRK1*), *tousled-like kinase* (*TLK*), *DYRK2/3/4*, *calcium/calmodulin-dependent protein kinase I* (*CAMK1*), and *serine/threonine-protein kinase ULK2* (*ULK2; ATG1*; Supplementary Table S4). Human orthologs of these serine/threonine kinases are known to be involved in the regulation of cell differentiation and proliferation, survival, development, autophagy, calcium signaling processes, DNA replication, transcription, DNA repair, and chromosome segregation (Safran et al., 2021). Even though four, out of five, of these nematode kinases were neither among the top 1% nor top 5% nodes, they showed a signal of co-evolution with all of the four *Wolbachia* top 1% nodes which were largely related to energy metabolism, amino acid biosynthesis, and DNA replication (Figure 5; Supplementary File S1).

In contrast, one of the kinases, *DYRK1,* was among the top 5% most highly connected nodes of the nematode genes (Figure 5; Supplementary File S1; Supplementary Table S3). This nematode DYRK1 appeared to co-evolve with some of the top 1% most connected genes in *Wolbachia* including *DLD* and *nuoD* genes. It was also connected to two top 5% most connected Wolbachia genes *undecaprenyl pyrophosphate synthase* (*UPPS*; involved in the production of precursor for bacterial cell wall biosynthesis) and *phosphoenolpyruvate synthase regulatory protein* (*ppsR*; another serine/threonine kinase, now in *Wolbachia*, that regulate the conversion of pyruvate to phosphoenolpyruvate (PEP) which can be used for gluconeogenesis or energy production).

In addition, other *Wolbachia* genes that appeared to co-evolve with the nematode *DYRK1* included an ATPase component *VirB4* of bacterial type 4 secretion system (T4SS), as well as a membrane fusion protein *hasE* which belongs to the type 1 secretion system (T1SS). These two secretion system components, *VirB4* (T4SS) and *HasE* (T1SS), also co-evolved with the nematode *p38* gene, also known as *mitogen-activated*

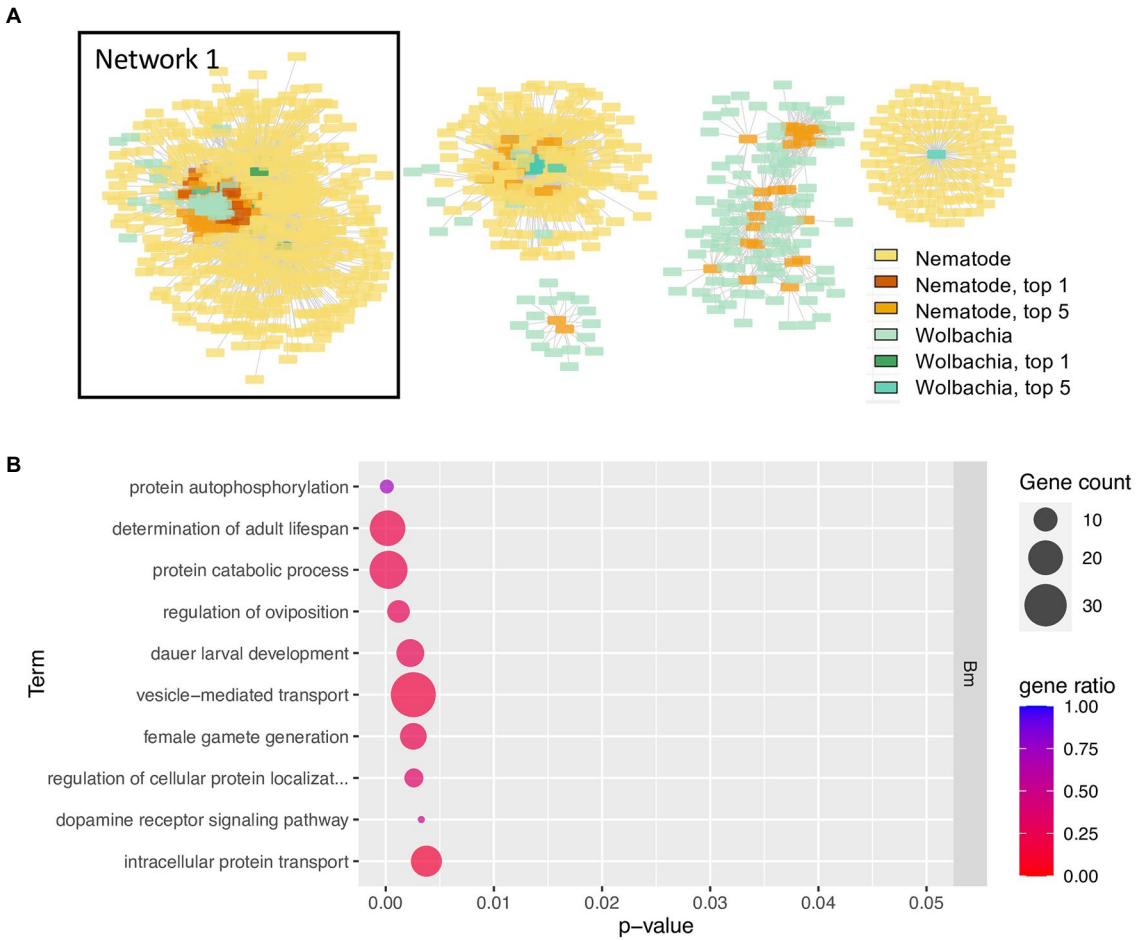

FIGURE 4
Network of top 5% most highly connected genes and enriched biological processes of Network 1 **(A)** The network contains the top 5% most highly connected genes of the *Wolbachia* and of the nematodes and their co-evolving genes in the symbiotic partner. Colors in yellow-red tone indicate genes in nematodes; blue–green tone indicates genes in *Wolbachia*, with deeper colors indicating the top 5% or top 1% most connected genes. List of all genes in Network 1 is provided in Supplementary Table S3. Interactive networks can be found in Cytoscape session file (Supplementary File S1). (B) Enriched GO terms of *B. malayi* genes in Network 1, a network that contains all top 1% most connected nodes. Only the top 10 enriched GO terms, ranked by *p*-value, of the biological processes type (BP) are shown. *p*-value refers to the *p*-value reported by topGO analysis. Gene count indicates the number of genes with that GO term in the input top-scoring gene list. Gene ratio is the number of genes with that GO term in the input list divided by a total number of genes in the genome annotated with that GO term. Full list of enriched GO terms, BP type, in Network 1, is presented in Supplementary Figure S4. The complete GO enrichment results for Network 1 with GO ID, full GO term description, and the top-scoring genes in each GO term are in Supplementary Table S4 (for *B. malayi*) and Supplementary Table S5 (for *Wolbachia* of *B. malayi*). Nematode's genes in Network 1 with GO annotation *determination of adult lifespan* and their co-evolving genes in the *Wolbachia* are further explored in Supplementary Figure S5.

protein kinase 14 (*MAPK14*), which is involved in a huge variety of biological processes including cell differentiation, transcription regulation, development, and responses to stresses. *VirB4* (a T4SS component), *HasE* (a T1SS component), and *p38* were all in the network of genes connected to the second enriched GO term *determination of adult lifespan* (Figure 4B; Supplementary Table S4; Supplementary File S1). Among genes in this network, another secretion system component *HasD*/*AprD* gene was present which positions as an ATP-binding cassette in T1SS (Supplementary Figure S5; Supplementary File S1).

3.4. Candidate drug targets from the highly connected genes

In addition to revealing the potentially novel biology of *Wolbachia*–filarial nematode interaction, the highly connected nodes may also be useful as potential drug targets since disrupting their function may corrupt some of the key interactions between the nematode and its obligate symbiont, as well as affect the biological processes of the nematode or *Wolbachia* directly. To investigate the potential of nematode–*Wolbachia* co-evolving genes as novel drug targets, we searched for sequence similarity to known drug targets by screening the top 1% most highly connected nodes of *B. malayi* and *Wolbachia* of *B. malayi* using DrugBank Online[3] (Wishart et al., 2006). Among the 24 genes comprising the top 1% of nodes used for the target search, eight sequences were similar to known drug targets with BLAST E-value of <0.00001, which was a default setting of DrugBank Online and a cutoff value used by other drug-target studies (e.g., Rajamanickam et al., 2020; Table 3; Supplementary Table S6).

3 https://go.drugbank.com/

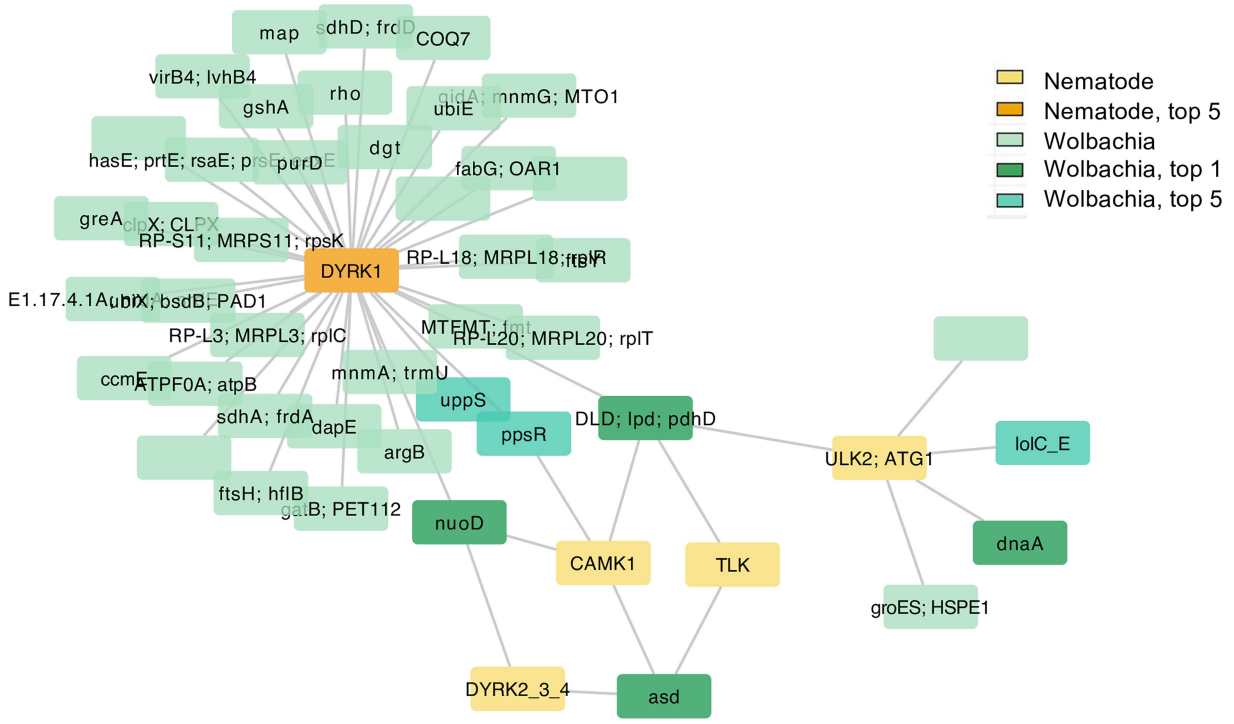

FIGURE 5
Genes in Network 1 that co-evolved with nematode genes annotated with GO term *protein autophosphorylation*. The nematode genes annotated with GO term *protein autophosphorylation* (five nodes in yellow and orange) and their first neighbors (*Wolbachia* genes) were selected from all genes that passed the cutoff value and viewed as a separated network here. Colors in yellow-red tone indicate genes in nematodes; blue–green tone indicates genes in *Wolbachia*, with deeper colors indicating the top 5% or top 1% most connected genes. Interactive networks can be found in Cytoscape session file (Supplementary File S1).

TABLE 3 Target hits on DrugBank Online of the top 1% genes.

Top 1% nodes with matched targets on DrugBank	DrugBank top target	Top target *E*-value	Top target bit score	The number of drugs for all identified targets
AAW70716	NADH dehydrogenase [ubiquinone] iron–sulfur protein 2, mitochondrial (Humans)	0	561.222	2
AAW71149	Dihydrolipoyl dehydrogenase, mitochondrial (Humans)	5.28E−134	394.815	11
WBGene00222081	Mitogen-activated protein kinase 10 (Humans)	0	590.497	18
WBGene00223114	40S ribosomal protein S2 (Humans)	3.82E−134	379.407	1
WBGene00224470	Fumarate reductase flavoprotein subunit (*Shewanella frigidimarina*)	4.27E−73	242.276	2
WBGene00224578	Rho-related GTP-binding protein RhoB (Humans)	2.93E−21	85.8853	7
WBGene00224796	Fibroblast growth factor receptor 1 (Humans)	1.36E−122	401.364	96
WBGene00226447	Phosphoribosylpyrophosphate synthetase (*Plasmodium falciparum*)	1.82E−48	167.933	1

Full list of matched drug targets and related drugs is in Supplementary Table S6. Visualization of this data is in Figure 6 and Supplementary File S3.

Overall, the target sequence hits that pass the E-value and bit score cutoff value cover a range of common drug targets including enzymes, receptors, and binding proteins. Top hits to DrugBank targets include *NADH dehydrogenase*, *dihydrolipoyl dehydrogenase* (*DLD*), *mitogen-activated protein kinase 10*, *40S ribosomal protein S2*, *fumarate reductase flavoprotein subunit*, *Rho-related GTP-binding protein RhoB*, *fibroblast growth factor receptor 1*, and *phosphoribosylpyrophosphate (PRPP) synthetase* (Table 3; Figure 6; Supplementary Table S6; Supplementary File S3). The drugs identified included albendazole, a known broad-spectrum anthelmintic drug used against *Taenia solium* and *Echinococcus granulosus*, which was coupled with antibiotics for killing filarial nematodes (Turner et al., 2017; Laman et al., 2022). Moreover, two of the nematode kinases were similar to multiple kinases in the DrugBank Online database. Kinases are widely targeted enzymes in many diseases including cancer, immune-related diseases, and infections. As a result, multiple drugs that are small molecule

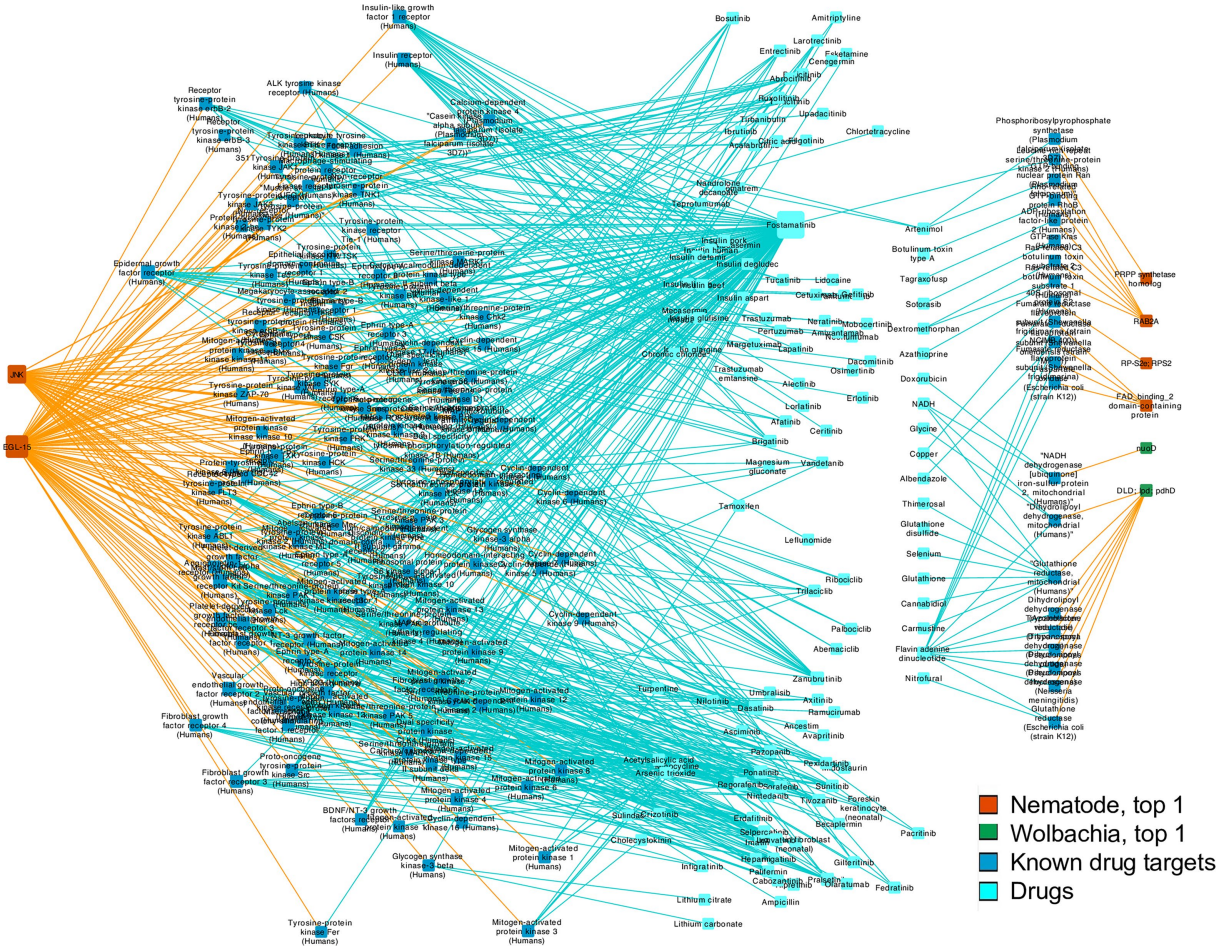

FIGURE 6
Drug-gene network Connections between genes from the top 1% most highly connected nodes of nematodes and *Wolbachia* genes, and their matched drug targets from DrugBank Online search, and related drugs acting on the drug targets based on DrugBank Online report. Gene nodes without a matched drug target are not shown. Node sizes indicate the degree of connections, i.e., how many edges are connected to a given node. Orange edges link genes in our study and known drug targets. Blue edges link known drug targets to their relevant drugs.

kinase inhibitors were identified in our search, such as imatinib, nilotinib, dasatinib, and fostamatinib (Table 3; Figure 6; Supplementary Table S6; Supplementary File S3).

4. Discussion

In this study, we performed a genome-wide co-evolutionary analysis between gene families of the filarial nematode and their obligate *Wolbachia* symbiont using publicly available genome data to seek protein–protein interactions that could be keys for their symbiotic relationship. The results showed that co-evolving genes were consistent with the known metabolic processes between the nematode–*Wolbachia* interactions and suggested gene-level details as well as potentially novel interactions. The co-evolving genes were involved in a range of metabolic and signaling processes including amino acid, lipid, carbohydrate, and nucleotide metabolism, regulation of transcription through transcription factor binding and epigenetic modification, pre-mRNA splicing, post-translational modification, signal transduction, and bacterial transport system. Some genes may be co-evolving with multiple other genes, suggesting potentially prominent roles in the interactions. Moreover, highly connected, co-evolving genes share sequence similarity and protein domains highly similar to known targets of approved drugs. It is worth noting that some of these drugs may also affect human drug target homologs and, therefore, their potential side effects should be taken into account. This information may help prioritize candidate targets that can be further tested for drug re-purposing and can lead to better treatment for at-risk populations of filariasis worldwide.

Due to their essential regulatory roles in various biological processes, protein kinases have been proposed as drug targets against parasitic infections, from protozoa to helminths (Beckmann and Grevelding, 2010; O'Connell et al., 2015; Kesely et al., 2016; Wu et al., 2021). In our data, two kinases were among the top 1% of most highly connected genes and showed high similarity to known drug targets. In addition, multiple serine/threonine kinases were part of the network that contained all of the top 1% most connected genes. Three of the kinase inhibitors identified on DrugBank online, i.e., imatinib, nilotinib, and dasatinib, have been tested against microfilaria, L3, and adult *B. malayi* and resulted in reduced survival rates in all stages (O'Connell et al., 2015). In addition, *MAPK*, *FGFR*, *SOS*, and *JNK*, all in the top 1% nodes of the nematode and each of them connected to overlapping sets of *Wolbachia* genes, are part of MAPK signaling

pathways, which are generally known to control cell proliferation (Avruch et al., 2001) and have roles in pro-inflammatory pathogenesis in patients with filariasis (Babu et al., 2011).

Wolbachia and filarial nematodes rely on metabolic substrate provisioning from one another (Taylor et al., 2013). For example, filarial nematode spp. is known to possess the pathway for producing PRPP, but the steps from PRPP to the production of purine precursor (IMP) turn out to be incomplete (International Helminth Genomes Consortium, 2019). *Wolbachia* is thought to supply nucleotides to its nematode host and to take pyruvate and amino acids from the nematode to use it as an energy source and for the production of other biomolecules (Foster et al., 2005; Taylor et al., 2013; Voronin et al., 2019). Consistent with this knowledge, our data revealed, among the top 1% most connected nodes, a putative *Wolbachia DLD* gene, which encodes a component participating in breaking down amino acids (BCKD enzyme), and conversion between pyruvate and acetyl-CoA (pyruvate dehydrogenase), both can lead to the release of energy. Our dataset suggested that *Wolbachia* DLD may be co-evolving with nematode genes involved in RNA, protein, and nucleotide synthesis, all of which require energy input. In addition, *Wolbachia DLD* appeared to co-evolve with nematode's putative *PRPP synthetase*, an essential enzyme for the production of PRPP, a key precursor for purine and pyrimidine biosynthesis. The potential connections between intermediate enzymes in amino acid and pyruvate metabolism in *Wolbachia* and biosynthesis in filaria suggested that their metabolic interactions may be more complex than previously thought.

Another gene among the top 1% in *Wolbachia* was annotated as *NADH dehydrogenase Fe-S* which forms part of Complex I in the electron transport chain. From our data, it may co-evolve with a nematode gene *fumarate reductase flavoprotein subunit*, which catalyzes the conversion of succinate to fumarate and forms part of Complex II in the electron transport chain. Previous data suggested that *Wolbachia* may aid its host in generating ATP *via* a mitochondrial-like function in somatic tissue based on high expression of ATPase and components of the electron transport chain (Darby et al., 2012). Our data further provide specific players that may be involved, suggesting a possibility that Complex I and Complex II may be interacting across species. Furthermore, Complex I and Complex II systems in filaria were previously proposed as potential targets, particularly the fumarate reductase protein, which was a known target for albendazole/benzimidazole (Barrowman et al., 1984; Gupta and Srivastava, 2005; Ahmad and Srivastava, 2007).

The involvement of fatty acid synthesis in the filarial nematode–*Wolbachia* relationship is not well understood. However, *Wolbachia* can affect lipid profiles in arthropod host and can modulate viral infection (Caragata et al., 2013; Molloy et al., 2016). Nematode and bacteria are capable of glyoxylation shunting which shortcuts the TCA cycle and utilizes fatty acid as a source of acetyl-CoA for gluconeogenesis and energy metabolism (International Helminth Genomes Consortium, 2019; Curran et al., 2020). Fatty acid would be required for growth and reproduction, and it is also an essential precursor for the production of steroid hormones including reproductive hormones. Our data showed that multiple *Wolbachia* genes in the fatty acid biosynthesis pathway may co-evolve with highly connected genes in the filarial nematode. The roles of fatty acid synthesis in filarial nematode–*Wolbachia* interaction may warrant further investigation.

Finally, much of the literature on filarial nematodes and *Wolbachia* focuses on the involvement of T4SS, which facilitate the transport of molecules from bacteria to the inside of host cells. In particular, T4SS is a major exchanger of effector proteins and small metabolites such as nucleotides and their precursors, and it is involved in the control of gene expression and germline development in filarial nematodes (Rancès et al., 2008; Slatko et al., 2010; Darby et al., 2012; Li and Carlow, 2012; Carpinone et al., 2018; Lindsey, 2020; Chevignon et al., 2021). Our data identified an ATPase component of the T4SS and also two components of the T1SS, another key bacterial secretion system that translocates proteins across the outer membrane into the extracellular space. T1SS is rarely investigated in the *Wolbachia*–filarial nematode interactions. However, the system is widespread in gram-negative bacteria and is involved in the secretion of peptidase, lipase, and toxin, as well as drug efflux (Thomas et al., 2014; Morgan et al., 2017; Kanonenberg et al., 2018). One of the genes identified in our analysis, the *HasD*/*AprD* gene, is important in *Pseudomonas fragi*, another Pseudomonadota gram-negative bacteria in the same phylum as *Wolbachia*, for its secretion of protease (Wang et al., 2021). A recent study showed that *Wolbachia* is important for microfilaria exsheathment, a process that requires proteolysis (Quek et al., 2022). Although less well-studied, T1SS is present in *Wolbachia* of both insects and filarial nematodes (Lindsey, 2020). The apparent co-evolution of T1SS components with various kinase enzymes, and with genes regulating development, stress response, and survival, suggests that the less studied T1SS could be an interesting novel avenue for *Wolbachia*–nematode communication and the signaling pathways that the communication may trigger.

Our approach has revealed gene sets that are relevant to the known biology between the filarial nematode and its *Wolbachia*. It has also allowed us to suggest interesting novel targets for further study. However, its power is limited to those proteins with one-to-one orthologs in each species which show a clear signal of co-evolution given our particular methodology. This is probably not the case for the majority of proteins that interact between the host and symbiont. Moreover, genes that had paralogs or were absent in at least one species or were missing due to their stage of the reference genome were excluded from the analyses. This may explain why our result, although pointing to relevant biological pathways and processes, was able to identify only a small number of genes in some pathways.

In addition to providing candidate drug targets and a list of conceivably repurposable drugs, this study paved a number of avenues, whereby the interactions between *Wolbachia* and filarial nematodes could be further investigated. Future validation of the interactions can utilize spatial information of the predicted interacting pairs and tracking of metabolic intermediates. The list of potential drugs and their targets may guide future investigations aimed at enhancing drug specificity toward filarial or *Wolbachia* proteins. Importantly, our analysis was based on genes shared across multiple filarial nematode species; hence, the implication provided is expected to be applicable to a wide range of filariasis diseases. Improvements in the availability of genome sequences for further filarial nematode species and their *Wolbachia* have the potential to improve the power of our approach, and it could be easily applied to other host-symbiont or host-pathogen systems.

Data availability statement

Publicly available datasets were analyzed in this study. This data can be found here: Table 1. The codes used for data analysis were deposited at: https://github.com/akoiwang/filaria-wolbachia-coevolution.

Author contributions

AW: conceptualization, data curation, funding acquisition, formal analysis, investigation, methodology, visualization, project administration, writing–original draft preparation, and writing–review and editing. SK: data curation, formal analysis, investigation, and visualization. JP: formal analysis, investigation, methodology, visualization, and writing–review and editing. NN: formal analysis, investigation, resources, and writing–review and editing. PK: formal analysis, investigation, and writing–review and editing. WL: formal analysis, investigation, resources, and writing–review and editing. WM: funding acquisition, resources, and supervision. AR: conceptualization, resources, software, validation, and supervision. All authors contributed to the article and approved the submitted version.

Funding

This study was supported by the Thailand Research Fund (TRF) and the Office of the Higher Education Commission (OHEC) (MRG6280068).

Acknowledgments

We thank Prapon Wilairat and Thanat Chookajorn for their comments on the scope of work during its initial stage. We thank David Ochou for additional insight into the use of the mirrortree approach and helpful discussion. We thank James Cotton for providing the assembly of *Wolbachia* of *B. pahangi* used in this analysis. We thank members of the Parasite Genomics team at the Wellcome Sanger Institute for their comments, discussions, and insights; in particular, we thank Matt Berriman, James Cotton, Eleanor Stanley, Martin Hunt, Hayley Bennett, and Anna Protasio. Computationally demanding data analyses were performed on high-performance computing facilities at Wellcome Sanger Institute and Khon Kaen University's Office of Digital Technology.

Conflict of interest

The authors declare that the research was conducted in the absence of any commercial or financial relationships that could be construed as a potential conflict of interest.

Publisher's note

All claims expressed in this article are solely those of the authors and do not necessarily represent those of their affiliated organizations, or those of the publisher, the editors and the reviewers. Any product that may be evaluated in this article, or claim that may be made by its manufacturer, is not guaranteed or endorsed by the publisher.

Supplementary material

The Supplementary material for this article can be found online at: https://www.frontiersin.org/articles/10.3389/fmicb.2023.1052352/full#supplementary-material

References

Ahmad, R., and Srivastava, A. K. (2007). Biochemical composition and metabolic pathways of filarial worms Setaria cervi: search for new antifilarial agents. *J. Helminthol.* 81, 261–280. doi: 10.1017/S0022149X07799133

Alexa, A., and Rahnenfuhrer, J. (2021). topGO: Enrichment analysis for gene ontology. R package version 2.46.0.

Aljayyoussi, G., Tyrer, H. E., Ford, L., Sjoberg, H., Pionnier, N., Waterhouse, D., et al. (2017). Short-course, high-dose rifampicin achieves *Wolbachia* depletion predictive of curative outcomes in preclinical models of lymphatic Filariasis and onchocerciasis. *Sci. Rep.* 7:210. doi: 10.1038/s41598-017-00322-5

Altschul, S. F., Gish, W., Miller, W., Myers, E. W., and Lipman, D. J. (1990). Basic local alignment search tool. *J. Mol. Biol.* 215, 403–410. doi: 10.1016/S0022-2836(05)80360-2

Aunin, E., Böhme, U., Sanderson, T., Simons, N. D., Goldberg, T. L., Ting, N., et al. (2020). Genomic and transcriptomic evidence for descent from *plasmodium* and loss of blood schizogony in Hepatocystis parasites from naturally infected red colobus monkeys. *PLoS Pathog.* 16:e1008717. doi: 10.1371/journal.ppat.1008717

Avruch, J., Khokhlatchev, A., Kyriakis, J. M., Luo, Z., Tzivion, G., Vavvas, D., et al. (2001). Ras activation of the Raf kinase: tyrosine kinase recruitment of the MAP kinase cascade. *Recent Prog. Horm. Res.* 56, 127–156. doi: 10.1210/rp.56.1.127

Babu, S., Anuradha, R., Kumar, N. P., George, P. J., Kumaraswami, V., and Nutman, T. B. (2011). Filarial lymphatic pathology reflects augmented toll-like receptor-mediated, mitogen-activated protein kinase-mediated proinflammatory cytokine production. *Infect. Immun.* 79, 4600–4608. doi: 10.1128/IAI.05419-11

Bandi, C., McCall, J. W., Genchi, C., Corona, S., Venco, L., and Sacchi, L. (1999). Effects of tetracycline on the filarial worms *Brugia pahangi* and *Dirofilaria immitis* and their bacterial endosymbionts *Wolbachia*. *Int. J. Parasitol.* 29, 357–364. doi: 10.1016/S0020-7519(98)00200-8

Barrowman, M. M., Marriner, S. E., and Bogan, J. A. (1984). The fumarate reductase system as a site of anthelmintic attack in Ascaris suum. *Biosci. Rep.* 4, 879–883. doi: 10.1007/BF01138170

Basáñez, M.-G., Pion, S. D. S., Boakes, E., Filipe, J. A. N., Churcher, T. S., and Boussinesq, M. (2008). Effect of single-dose ivermectin on Onchocerca volvulus: a systematic review and meta-analysis. *Lancet Infect. Dis.* 8, 310–322. doi: 10.1016/S1473-3099(08)70099-9

Beckmann, S., and Grevelding, C. G. (2010). Imatinib has a fatal impact on morphology, pairing stability and survival of adult Schistosoma mansoni in vitro. *Int. J. Parasitol.* 40, 521–526. doi: 10.1016/j.ijpara.2010.01.007

Benjamini, Y., and Hochberg, Y. (1995). Controlling the false discovery rate: a practical and powerful approach to multiple testing. *J. R. Stat. Soc.* 57, 289–300. doi: 10.1111/j.2517-6161.1995.tb02031.x

Bolt, B. J., Rodgers, F. H., Shafie, M., Kersey, P. J., Berriman, M., and Howe, K. L. (2018). "Using WormBase ParaSite: an integrated platform for exploring helminth genomic data" in *Eukaryotic genomic databases*. ed. M. Kollmar (New York, NY: Springer New York), 471–491.

Caragata, E. P., Rancès, E., Hedges, L. M., Gofton, A. W., Johnson, K. N., O'Neill, S. L., et al. (2013). Dietary cholesterol modulates pathogen blocking by *Wolbachia*. *PLoS Pathog.* 9:e1003459. doi: 10.1371/journal.ppat.1003459

Carpinone, E. M., Li, Z., Mills, M. K., Foltz, C., Brannon, E. R., Carlow, C. K. S., et al. (2018). Identification of putative effectors of the type IV secretion system from the *Wolbachia* endosymbiont of *Brugia malayi*. *PLoS One* 13:e0204736. doi: 10.1371/journal.pone.0204736

Casiraghi, M., Anderson, T. J., Bandi, C., Bazzocchi, C., and Genchi, C. (2001). A phylogenetic analysis of filarial nematodes: comparison with the phylogeny of *Wolbachia* endosymbionts. *Parasitology* 122, 93–103. doi: 10.1017/S0031182000007149

Castresana, J. (2000). Selection of conserved blocks from multiple alignments for their use in phylogenetic analysis. *Mol. Biol. Evol.* 17, 540–552. doi: 10.1093/oxfordjournals.molbev.a026334

Chevignon, G., Foray, V., Pérez-Jiménez, M. M., Libro, S., Chung, M., Foster, J. M., et al. (2021). Dual RNAseq analyses at soma and germline levels reveal evolutionary innovations in the elephantiasis-agent *Brugia malayi*, and adaptation of its *Wolbachia* endosymbionts. *PLoS Negl. Trop. Dis.* 15:e0008935. doi: 10.1371/journal.pntd.0008935

Cross, J. H. (2011). "Filarial Nematodes" in *Medical Microbiology*. ed. S. Baron (Galveston (TX): University of Texas Medical Branch at Galveston)

Curran, D. M., Grote, A., Nursimulu, N., Geber, A., Voronin, D., Jones, D. R., et al. (2020). Modeling the metabolic interplay between a parasitic worm and its bacterial endosymbiont allows the identification of novel drug targets. *eLife* 9:e51850. doi: 10.7554/eLife.51850

Darby, A. C., Armstrong, S. D., Bah, G. S., Kaur, G., Hughes, M. A., Kay, S. M., et al. (2012). Analysis of gene expression from the *Wolbachia* genome of a filarial nematode supports both metabolic and defensive roles within the symbiosis. *Genome Res.* 22, 2467–2477. doi: 10.1101/gr.138420.112

Diawara, L., Traoré, M. O., Badji, A., Bissan, Y., Doumbia, K., Goita, S. F., et al. (2009). Feasibility of onchocerciasis elimination with ivermectin treatment in endemic foci in Africa: first evidence from studies in Mali and Senegal. *PLoS Negl. Trop. Dis.* 3:e497. doi: 10.1371/journal.pntd.0000497

Edgar, R. C. (2004). MUSCLE: multiple sequence alignment with high accuracy and high throughput. *Nucleic Acids Res.* 32, 1792–1797. doi: 10.1093/nar/gkh340

Fenn, K., and Blaxter, M. (2004). Quantification of *Wolbachia* bacteria in *Brugia malayi* through the nematode lifecycle. *Mol. Biochem. Parasitol.* 137, 361–364. doi: 10.1016/j.molbiopara.2004.06.012

Ferri, E., Bain, O., Barbuto, M., Martin, C., Lo, N., Uni, S., et al. (2011). New insights into the evolution of *Wolbachia* infections in filarial nematodes inferred from a large range of screened species. *PLoS One* 6:e20843. doi: 10.1371/journal.pone.0020843

Foster, J., Ganatra, M., Kamal, I., Ware, J., Makarova, K., Ivanova, N., et al. (2005). The *Wolbachia* genome of *Brugia malayi*: endosymbiont evolution within a human pathogenic nematode. *PLoS Biol.* 3:e121. doi: 10.1371/journal.pbio.0030121

Goh, C.-S., and Cohen, F. E. (2002). Co-evolutionary analysis reveals insights into protein–protein interactions. *J. Mol. Biol.* 324, 177–192. doi: 10.1016/S0022-2836(02)01038-0

Gupta, S., and Srivastava, A. K. (2005). Biochemical targets in filarial worms for selective antifilarial drug design. *Acta Parasitol.* 50, 1–18.

Harb, O. S., and Abu, K. Y. (1998). Identification of the aspartate-beta-semialdehyde dehydrogenase gene of legionella pneumophila and characterization of a null mutant. *Infect. Immun.* 66, 1898–1903. doi: 10.1128/IAI.66.5.1898-1903.1998

Howe, K. L., Bolt, B. J., Shafie, M., Kersey, P., and Berriman, M. (2017). WormBase ParaSite − a comprehensive resource for helminth genomics. *Mol. Biochem. Parasitol.* 215, 2–10. doi: 10.1016/j.molbiopara.2016.11.005

International Helminth Genomes Consortium (2019). Comparative genomics of the major parasitic worms. *Nat. Genet.* 51, 163–174. doi: 10.1038/s41588-018-0262-1

Jones, P., Binns, D., Chang, H.-Y., Fraser, M., Li, W., McAnulla, C., et al. (2014). InterProScan 5: genome-scale protein function classification. *Bioinformatics* 30, 1236–1240. doi: 10.1093/bioinformatics/btu031

Kanehisa, M., and Goto, S. (2000). KEGG: Kyoto encyclopedia of genes and genomes. *Nucleic Acids Res.* 28, 27–30. doi: 10.1093/nar/28.1.27

Kanehisa, M., Sato, Y., and Kawashima, M. (2022). KEGG mapping tools for uncovering hidden features in biological data. *Protein Sci.* 31, 47–53. doi: 10.1002/pro.4172

Kanehisa, M., Sato, Y., and Morishima, K. (2016). BlastKOALA and GhostKOALA: KEGG tools for functional characterization of genome and metagenome sequences. *J. Mol. Biol.* 428, 726–731. doi: 10.1016/j.jmb.2015.11.006

Kanonenberg, K., Spitz, O., Erenburg, I. N., Beer, T., and Schmitt, L. (2018). Type I secretion system-it takes three and a substrate. *FEMS Microbiol. Lett.* 365, 1–10. doi: 10.1093/femsle/fny094

Kesely, K. R., Pantaleo, A., Turrini, F. M., Olupot-Olupot, P., and Low, P. S. (2016). Inhibition of an erythrocyte tyrosine kinase with imatinib prevents *plasmodium falciparum* egress and terminates parasitemia. *PLoS One* 11:e0164895. doi: 10.1371/journal.pone.0164895

Laman, M., Tavul, L., Karl, S., Kotty, B., Kerry, Z., Kumai, S., et al. (2022). Mass drug administration of ivermectin, diethylcarbamazine, plus albendazole compared with diethylcarbamazine plus albendazole for reduction of lymphatic filariasis endemicity in Papua New Guinea: a cluster-randomised trial. *Lancet Infect. Dis.* 22, 1200–1209. doi: 10.1016/S1473-3099(22)00026-3

Landmann, F., Foster, J. M., Slatko, B. E., and Sullivan, W. (2012). Efficient in vitro RNA interference and immunofluorescence-based phenotype analysis in a human parasitic nematode, *Brugia malayi*. *Parasit. Vectors* 5:16. doi: 10.1186/1756-3305-5-16

Li, Z., and Carlow, C. K. S. (2012). Characterization of transcription factors that regulate the type IV secretion system and riboflavin biosynthesis in *Wolbachia* of *Brugia malayi*. *PLoS One* 7:e51597. doi: 10.1371/journal.pone.0051597

Li, L., Stoeckert, C. J. Jr., and Roos, D. S. (2003). OrthoMCL: identification of ortholog groups for eukaryotic genomes. *Genome Res.* 13, 2178–2189. doi: 10.1101/gr.1224503

Lindsey, A. R. I. (2020). Sensing, signaling, and secretion: a review and analysis of Systems for Regulating Host Interaction in Wolbachia. *Genes* 11:813. doi: 10.3390/genes11070813

Lustigman, S., Grote, A., and Ghedin, E. (2017). The role of "omics" in the quest to eliminate human filariasis. *PLoS Negl. Trop. Dis.* 11:e0005464. doi: 10.1371/journal.pntd.0005464

McGarry, H. F., Egerton, G. L., and Taylor, M. J. (2004). Population dynamics of *Wolbachia* bacterial endosymbionts in *Brugia malayi*. *Mol. Biochem. Parasitol.* 135, 57–67. doi: 10.1016/j.molbiopara.2004.01.006

Mier, P., Alanis-Lobato, G., and Andrade-Navarro, M. A. (2017). Protein-protein interactions can be predicted using coiled coil co-evolution patterns. *J. Theor. Biol.* 412, 198–203. doi: 10.1016/j.jtbi.2016.11.001

Molloy, J. C., Sommer, U., Viant, M. R., and Sinkins, S. P. (2016). *Wolbachia* modulates lipid metabolism in Aedes albopictus mosquito cells. *Appl. Environ. Microbiol.* 82, 3109–3120. doi: 10.1128/AEM.00275-16

Morgan, J. L. W., Acheson, J. F., and Zimmer, J. (2017). Structure of a type-1 secretion system ABC transporter. *Structure* 25, 522–529. doi: 10.1016/j.str.2017.01.010

O'Connell, E. M., Bennuru, S., Steel, C., Dolan, M. A., and Nutman, T. B. (2015). Targeting filarial Abl-like kinases: orally available, food and drug administration-approved tyrosine kinase inhibitors are microfilaricidal and macrofilaricidal. *J. Infect. Dis.* 212, 684–693. doi: 10.1093/infdis/jiv065

Ochoa, D., Juan, D., Valencia, A., and Pazos, F. (2015). Detection of significant protein co-evolution. *Bioinformatics* 31, 2166–2173. doi: 10.1093/bioinformatics/btv102

Ochoa, D., and Pazos, F. (2014). Practical aspects of protein co-evolution. *Front. Cell Dev. Biol.* 2:14. doi: 10.3389/fcell.2014.00014

Pazos, F., Ranea, J. A. G., Juan, D., and Sternberg, M. J. E. (2005). Assessing protein co-evolution in the context of the tree of life assists in the prediction of the interactome. *J. Mol. Biol.* 352, 1002–1015. doi: 10.1016/j.jmb.2005.07.005

Pazos, F., and Valencia, A. (2001). Similarity of phylogenetic trees as indicator of protein-protein interaction. *Protein Eng.* 14, 609–614. doi: 10.1093/protein/14.9.609

Pazos, F., and Valencia, A. (2008). Protein co-evolution, co-adaptation and interactions. *EMBO J.* 27, 2648–2655. doi: 10.1038/emboj.2008.189

Poopandi, S., Sundaraj, R., Rajmichael, R., Thangaraj, S., Dhamodharan, P., Biswal, J., et al. (2021). Computational screening of potential inhibitors targeting MurF of *Brugia malayi Wolbachia* through multi-scale molecular docking, molecular dynamics and MM-GBSA analysis. *Mol. Biochem. Parasitol.* 246:111427. doi: 10.1016/j.molbiopara.2021.111427

Quek, S., Cook, D. A. N., Wu, Y., Marriott, A. E., Steven, A., Johnston, K. L., et al. (2022). *Wolbachia* depletion blocks transmission of lymphatic filariasis by preventing chitinase-dependent parasite exsheathment. *Proc. Natl. Acad. Sci. U. S. A.* 119:e2120003119. doi: 10.1073/pnas.2120003119

Rajamanickam, K., Yang, J., Chidambaram, S. B., and Sakharkar, M. K. (2020). Enhancing drug efficacy against mastitis pathogens-an in vitro pilot study in Staphylococcus aureus and Staphylococcus epidermidis. *Animals (Basel)* 10:2117. doi: 10.3390/ani10112117

Rancès, E., Voronin, D., Tran-Van, V., and Mavingui, P. (2008). Genetic and functional characterization of the type IV secretion system in *Wolbachia*. *J. Bacteriol.* 190, 5020–5030. doi: 10.1128/JB.00377-08

Safran, M., Rosen, N., Twik, M., BarShir, R., Stein, T. I., Dahary, D., et al. (2021). "The GeneCards suite" in *Practical guide to life science databases*. eds. A. Imad and K. Takeya (Singapore: Springer Nature Singapore), 27–56.

Schwab, A. E., Churcher, T. S., Schwab, A. J., Basáñez, M.-G., and Prichard, R. K. (2006). Population genetics of concurrent selection with albendazole and ivermectin or diethylcarbamazine on the possible spread of albendazole resistance in *Wuchereria bancrofti*. *Parasitology* 133, 589–601. doi: 10.1017/S003118200600076X

Scott, A. L., Ghedin, E., Nutman, T. B., McREYNOLDS, L. A., Poole, C. B., Slatko, B. E., et al. (2012). Filarial and *Wolbachia* genomics: filarial and *Wolbachia* genomics. *Parasite Immunol.* 34, 121–129. doi: 10.1111/j.1365-3024.2011.01344.x

Seemann, T. (2014). Prokka: rapid prokaryotic genome annotation. *Bioinformatics* 30, 2068–2069. doi: 10.1093/bioinformatics/btu153

Shannon, P., Markiel, A., Ozier, O., Baliga, N. S., Wang, J. T., Ramage, D., et al. (2003). Cytoscape: a software environment for integrated models of biomolecular interaction networks. *Genome Res.* 13, 2498–2504. doi: 10.1101/gr.1239303

Shoemaker, B. A., and Panchenko, A. R. (2007). Deciphering protein–protein interactions. Part II. Computational methods to predict protein and domain interaction partners. *PLoS Comput. Biol.* 3:e43. doi: 10.1371/journal.pcbi.0030043

Slatko, B. E., Taylor, M. J., and Foster, J. M. (2010). The *Wolbachia* endosymbiont as an anti-filarial nematode target. *Symbiosis* 51, 55–65. doi: 10.1007/s13199-010-0067-1

Specht, S., Pfarr, K. M., Arriens, S., Hübner, M. P., Klarmann-Schulz, U., Koschel, M., et al. (2018). Combinations of registered drugs reduce treatment times required to deplete *Wolbachia* in the Litomosoides sigmodontis mouse model. *PLoS Negl. Trop. Dis.* 12:e0006116. doi: 10.1371/journal.pntd.0006116

Tamarozzi, F., Halliday, A., Gentil, K., Hoerauf, A., Pearlman, E., and Taylor, M. J. (2011). Onchocerciasis: the role of *Wolbachia* bacterial endosymbionts in parasite biology, disease pathogenesis, and treatment. *Clin. Microbiol. Rev.* 24, 459–468. doi: 10.1128/CMR.00057-10

Taylor, M. J., Hoerauf, A., Townson, S., Slatko, B. E., and Ward, S. A. (2014). Anti-*Wolbachia* drug discovery and development: safe macrofilaricides for onchocerciasis and lymphatic filariasis. *Parasitology* 141, 119–127. doi: 10.1017/S0031182013001108

Taylor, M. J., Voronin, D., Johnston, K. L., and Ford, L. (2013). *Wolbachia* filarial interactions: *Wolbachia* filarial cellular and molecular interactions. *Cell. Microbiol.* 15, 520–526. doi: 10.1111/cmi.12084

Thomas, S., Holland, I. B., and Schmitt, L. (2014). The type 1 secretion pathway – the hemolysin system and beyond. *Biochim. Biophys. Acta* 1843, 1629–1641. doi: 10.1016/j.bbamcr.2013.09.017

Turner, J., Sharma, R., Al Jayoussi, G., Tyrer, H. E., Gamble, J., Hayward, L., et al. (2017). Albendazole and antibiotics synergize to deliver short-course anti-*Wolbachia* curative treatments in preclinical models of filariasis. *Proc. Natl. Acad. Sci. U. S. A.* 114, E9712–E9721. doi: 10.1073/pnas.1710845114

Volkmann, L., Fischer, K., Taylor, M., and Hoerauf, A. (2003). Antibiotic therapy in murine filariasis (Litomosoides sigmodontis): comparative effects of doxycycline and rifampicin on *Wolbachia* and filarial viability. *Tropical Med. Int. Health* 8, 392–401. doi: 10.1046/j.1365-3156.2003.01040.x

Voronin, D., Schnall, E., Grote, A., Jawahar, S., Ali, W., Unnasch, T. R., et al. (2019). Pyruvate produced by Brugia spp. via glycolysis is essential for maintaining the mutualistic association between the parasite and its endosymbiont, *Wolbachia*. *PLoS Pathog.* 15:e1008085. doi: 10.1371/journal.ppat.1008085

Vos, T., Allen, C., Arora, M., Barber, R. M., Bhutta, Z. A., Brown, A., et al. (2016). Global, regional, and national incidence, prevalence, and years lived with disability for 310 diseases and injuries, 1990–2015: a systematic analysis for the global burden of disease study 2015. *Lancet* 388, 1545–1602. doi: 10.1016/S0140-6736(16)31678-6

Wang, G., Li, Q., Tang, W., Ma, F., Wang, H., Xu, X., et al. (2021). AprD is important for extracellular proteolytic activity, physicochemical properties and spoilage potential in meat-borne *Pseudomonas fragi*. *Food Control* 124:107868. doi: 10.1016/j.foodcont.2021.107868

Wishart, D. S., Knox, C., Guo, A. C., Shrivastava, S., Hassanali, M., Stothard, P., et al. (2006). DrugBank: a comprehensive resource for in silico drug discovery and exploration. *Nucleic Acids Res.* 34, D668–D672. doi: 10.1093/nar/gkj067

Wu, K., Zhai, X., Huang, S., Jiang, L., Yu, Z., and Huang, J. (2021). Protein kinases: potential drug targets against *Schistosoma japonicum*. *Front. Cell. Infect. Microbiol.* 11:691757. doi: 10.3389/fcimb.2021.691757

Yang, Z. (2007). PAML 4: phylogenetic analysis by maximum likelihood. *Mol. Biol. Evol.* 24, 1586–1591. doi: 10.1093/molbev/msm088

frontiers | Frontiers in Microbiology

TYPE Original Research
PUBLISHED 09 June 2023
DOI 10.3389/fmicb.2023.1116766

OPEN ACCESS

EDITED BY
Daisuke Kageyama,
National Agriculture and Food Research Organization (NARO), Japan

REVIEWED BY
Jackson Champer,
Peking University, China
Mónica Asunción Hurtado Ruiz,
Jaume I University, Spain

*CORRESPONDENCE
John Beckmann
✉ beckmann@auburn.edu

RECEIVED 05 December 2022
ACCEPTED 23 May 2023
PUBLISHED 09 June 2023

CITATION
Beckmann J, Gillespie J and Tauritz D (2023) Modeling emergence of *Wolbachia* toxin-antidote protein functions with an evolutionary algorithm.
Front. Microbiol. 14:1116766.
doi: 10.3389/fmicb.2023.1116766

Modeling emergence of *Wolbachia* toxin-antidote protein functions with an evolutionary algorithm

John Beckmann[1]*, Joe Gillespie[2] and Daniel Tauritz[3]

[1]Department of Entomology and Plant Pathology, Auburn University, Auburn, AL, United States, [2]Department of Microbiology and Immunology, School of Medicine, University of Maryland, Baltimore, Baltimore, MD, United States, [3]Department of Computer Science and Software Engineering, Auburn University, Auburn, AL, United States

Evolutionary algorithms (EAs) simulate Darwinian evolution and adeptly mimic natural evolution. Most EA applications in biology encode high levels of abstraction in top-down population ecology models. In contrast, our research merges protein alignment algorithms from bioinformatics into codon based EAs that simulate molecular protein string evolution from the bottom up. We apply our EA to reconcile a problem in the field of *Wolbachia* induced cytoplasmic incompatibility (CI). *Wolbachia* is a microbial endosymbiont that lives inside insect cells. CI is conditional insect sterility that operates as a toxin antidote (TA) system. Although, CI exhibits complex phenotypes not fully explained under a single discrete model. We instantiate in-silico genes that control CI, CI factors (*cifs*), as strings within the EA chromosome. We monitor the evolution of their enzymatic activity, binding, and cellular localization by applying selective pressure on their primary amino acid strings. Our model helps rationalize why two distinct mechanisms of CI induction might coexist in nature. We find that nuclear localization signals (NLS) and Type IV secretion system signals (T4SS) are of low complexity and evolve fast, whereas binding interactions have intermediate complexity, and enzymatic activity is the most complex. Our model predicts that as ancestral TA systems evolve into eukaryotic CI systems, the placement of NLS or T4SS signals can stochastically vary, imparting effects that might impact CI induction mechanics. Our model highlights how preconditions and sequence length can bias evolution of *cifs* toward one mechanism or another.

KEYWORDS

***Wolbachia*, cytoplasmic incompatibility, toxin antidote, evolutionary algorithm, reproductive parasitism, evolution, simulation, artificial intelligence**

Introduction

TA systems typically involve two linked genes encoding a toxin and antidote (Yamaguchi et al., 2011). They skew Mendelian inheritance in their favor by addicting organisms to the presence of an antidote and killing offspring that do not inherit the TA module, via the toxin. Thus, they ensure inheritance in the next generation by post segregational killing. Ancestrally, TA systems might have arisen as selfish systems linked to the replication of prokaryotic plasmids (Rankin et al., 2012). How TA systems evolve is a chicken-egg paradox: a lone toxin is detrimental to host fitness and an antidote without a linked cognate toxin could be beneficial,

neutral, or detrimental, dependent on context. Prior models predict that TA systems assemble with selection on plasmids in contexts of genomic conflict or in situations where antidotes have beneficial functions in addition to toxin rescue (Rankin et al., 2012).

Wolbachia are bacteria that live inside insects (Hertig and Wolbach, 1924; Hertig, 1936; Werren et al., 2008). *Wolbachia* have the capability to conditionally sterilize mosquitos in a phenotype called CI (Laven, 1953, 1967a,b; Yen and Barr, 1971, 1973). CI is a unique biological instantiation of a TA system. The CI phenotype is useful to applied entomology (Laven, 1967b; Xi et al., 2005; Zheng et al., 2019). CI is currently applied as a biocontrol mechanism preventing the transmission of mosquito borne diseases across the world and on multiple continents in various applications. Mosquitos infected with *Wolbachia* exhibit reduced ability to transmit flaviviruses like Dengue and Zika (Teixeira et al., 2008; Ye et al., 2015). Ongoing attempts use the selective pressure of *cifs* to spread beneficial (probiotic) *Wolbachia* infections into wild mosquito populations to limit disease (Ross et al., 2022). At the molecular level, the beneficial spread of *Wolbachia* is linked to the function of *cif* TA genes.

Much of the evolutionary dynamics of CI has been well described at the population level. CI is common because it increases equilibrium frequencies and infection persistence, thereby increasing the chances of *Wolbachia* being transferred to new species hosts (Turelli et al., 2022). Yet in the insect, selection does not act to preserve or increase CI rates (Turelli, 1994). Importantly, evolutionary dynamics and selective pressures operating at the lowest molecular level and at the moment CI emerged in evolutionary history have never been described.

The genes that control this conditional sterility are two linked genes dubbed *cifs* that form complex TA systems (Beckmann and Fallon, 2013; Beckmann et al., 2017, 2019b). Uniquely, this TA system is viral, bacterial, and eukaryotic because it is encoded within/near WO-phages whose genomes reside in intracellular bacterial endosymbionts, which reside in insect hosts. The TA systems express extended phenotypes impacting the eukaryotic insect host. *Cifs* are uniquely positioned in that their evolutionary origin necessitates a functional jump from bacteria to eukaryotes. The *cif* TA system encodes a sperm delivered embryo killer toxin and a cognate rescuing antidote. If the insect host loses *Wolbachia*, remaining toxin sterilizes males, and these populations do not reproduce. Therefore, female insects keep *Wolbachia* because the antidotes are useful in the presence of toxins encountered in male sperm. Importantly, purifying selection does preserve the *cif* antidotes (Merçot and Poinsot, 1998; Meany et al., 2019; Driscoll et al., 2020); and on lower levels in the context of genomic conflict, selection can act to assemble the biochemical domains of toxin antidote systems (Rankin et al., 2012). Perhaps this is how the first CI system assembled. Though once assembled, selection on the insect level does not act to preserve the bacterial toxins which tend to pseudogenes and/or are replaced by subsequent invading *cif* systems (Martinez et al., 2020; Beckmann et al., 2021).

While molecular details on CI function are emerging, one problem is that rules governing induction of sterility via the *Wolbachia* TA system are debated. In general, the system behaves as a classical TA module, meaning one gene named *cifB* is inducer and its cognate partner *cifA* acts as antidote (Beckmann et al., 2019b). However, there remains unresolved nuance in the mechanism. Currently all data support the hypothesis that the first operon gene, *cifA*, is antidote (Beckmann et al., 2017; Shropshire et al., 2018). However, induction of CI and the exact source of the toxicity appears more, or less, complex in various models. The two main models each have empirical evidence to support them. These models are the TA model (Poinsot et al., 2003; Beckmann et al., 2019a,b) and the 2 × 1 model (Shropshire et al., 2019; Shropshire and Bordenstein, 2019). The TA model is more parsimonious and significant evidence supports it in fruit flies, mosquitos, yeast models, and structural studies (Beckmann et al., 2017, 2019c; Bonneau et al., 2019; Adams et al., 2021; Xiao et al., 2021; Horard et al., 2022; Sun et al., 2022). In contrast, the 2 × 1 model posits that a single gene acts as rescue factor, but induction of sterility requires both *cifA* and *cifB* genes (LePage et al., 2017; Shropshire and Bordenstein, 2019).

Our hypothesis is that both models coexist in nature as alternate variations of the broader TA theme. These variations might arise as CI evolves from a simple prokaryotic TA module into a eukaryotic CI system (see Figures 1A,B). To explain, induction of sperm sterility in a eukaryote via a prokaryotic TA module necessitates the evolution of additional functions beyond toxin and antidote. In support of this hypothesis, prior models predicted that beneficial functions in addition to antidote functionality are prerequisites for TA module emergence (Rankin et al., 2012). In our case, *Wolbachia* must first secrete the toxin out one of its Sec-independent secretion systems; for the remainder of this study, we implicate the Rickettsiales *vir* homolog (*rvh*) type IV secretion system (T4SS) for CI protein secretion. T4SS substrates require a signal sequence, usually found at the C-terminus. Once secreted, the toxin must localize into the nucleus via a nuclear localization signal (NLS). Thus in simple terms, for a CI system to evolve requires additions of secretion signals and nuclear localization signals. In TA systems, the two proteins bind each other. There is a likely possibility that binding of *cifA* to *cifB* occurs prior to secretion and thus one protein might drag the other through a given secretion system. Under this hypothesis, it is possible that T4SS and NLS sequences could evolve in either antidote or toxin genes in different insect hosts. If the *cifA* antidote acquires an NLS and T4SS signal but *cifB* has neither, this leads to additional complexity in the system necessitating cooperative induction of sterility by *cifA* and *cifB* (hence a 2 × 1). While most empirical work evidences a strict TA in four known orthologs (cid^{wPip}, cid^{wHa}, cin^{wNo}, and cin^{Ott}), there is indication of 2×1 in two systems (cid^{wMel} and cin^{wPip}). Our research did not focus on determining if one model was correct at the complete expense of the other, but rather seeks to understand evolutionary pressures and selective mechanisms that might bias evolution of one model over another. Understanding the precise molecular mechanisms underlying the *cif* TA system and its evolution contributes information to "fine-tune" *Wolbachia* based biocontrol. Once we have perfect knowledge for how the *cif* TA sterility is induced, we can design the most efficient and parsimonious transgene insertions to reconstruct sterility in transgenic mosquitos as a biotechnological tool (i.e., with 2 genes or 1).

It was our goal to gain insights on the molecular evolution of CI by modeling CI's emergence with an evolutionary algorithm. Using EAs to model natural evolution has been a productive application (Lenski et al., 2003; Messer, 2013; Haller and Messer, 2016; Haller and Messer, 2019). Modeling gene drives in mosquitos with EAs, machine learning, and computer simulation has provided insights that predicted efficacy of actual biocontrol tools (Champer et al., 2018, 2022; Li and Champer, 2023). Biological evolution can be modeled by EAs at different ecological levels. Various abstractions and assumptions are made by any given model. EAs are typically top-down ecological

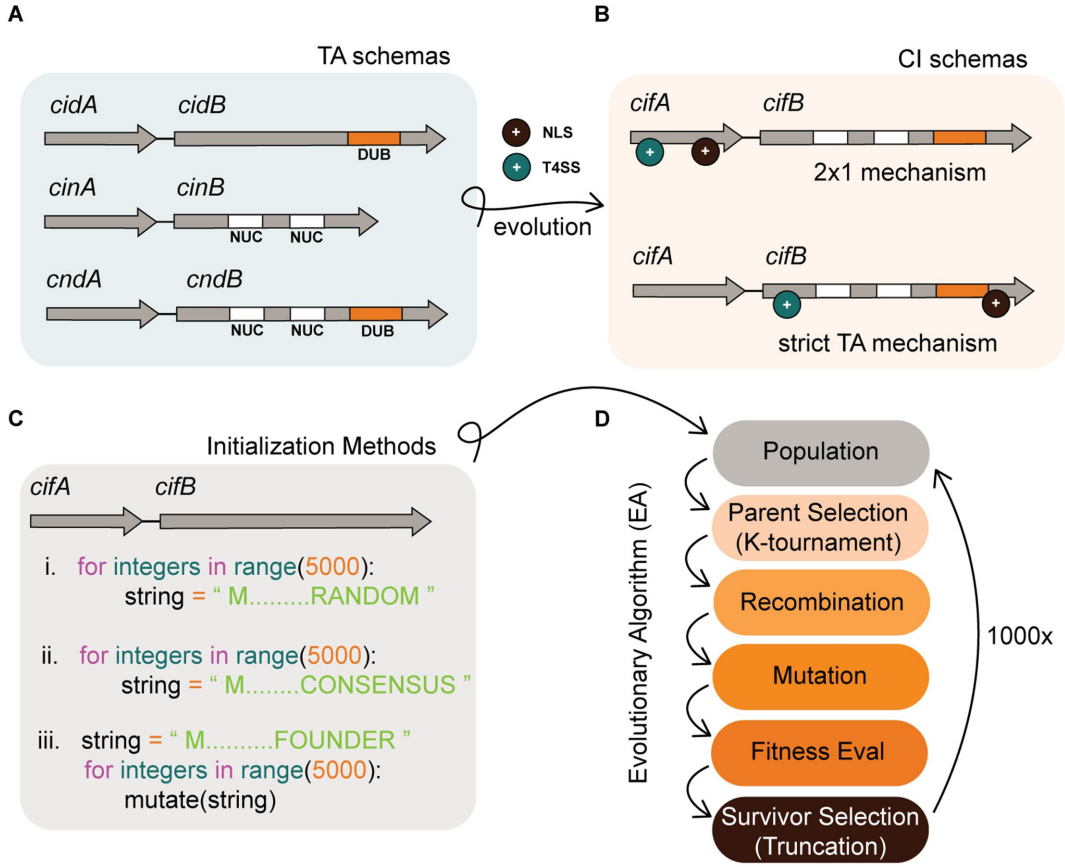

FIGURE 1
Background infographic. **(A)** Schemas of Wolbachia TA modules in a more ancestral prokaryotic form. To evolve into CI systems, ancestral TA modules must add more complex features including an NLS (+ black circle) and a T4SS (+ cyan circle). **(B)** CI system schemas might evolve into two descriptive models which include the 2 × 1 and strict TA model. The location where NLS or T4SS features evolve could impact the mechanistic induction of CI. A CI schema where both NLS and T4SS features co-occur in cifA alone is predicted to require both cifA and cifB for induction. In contrast, if these features co-occur in cifB, then cifB would be sufficient for induction of CI and behave as a strict TA module. **(C)** *In silico* simulation of this evolution requires an initial instantiation of a population of TA strings. Our experiments tested three distinct methods of instantiation that include (i) instantiating random strings, (ii) instantiating semi-random strings comporting to conserved cif consensus sequence, and (iii) instantiating a single individual and deriving an entire population by mutagenesis of that founder. **(D)** After instantiation of the population, it evolves under the selective pressure of a fitness function and follows discrete generations. Our algorithm selects parents by *K*-tournament and distributes these individuals into a mating pool. Offspring are generated by recombination of parents wherein two strings swap discrete sub-strings to create a new child. After recombination, child strings are mutated. Fitness of the TA is then evaluated, and survivors are selected based upon truncation survivor selection. In truncation, the population is sorted and the lowest fitness individuals that fall below a threshold are culled such that population numbers remain at the carrying capacity. The algorithm terminates after 1,000x generations.

models modeling populations of organisms. Top down EAs model gene flow of beneficial or deleterious traits. Within populations, each organism can be assigned a fitness value. Organisms and their genes can then mate, recombine, mutate, and die. These EA implementations tend toward Wright-Fisher models and often obey set rules. These models are useful for questions on evolutionary theory and adeptly model gene drives and selective sweeps, etc. However, the actual coded implementations are often abstract and difficult to translate into the evolution of amino acid sequence.

Popular bottom-up EA frameworks that modeled evolution upwards toward complexity are also abstract because they implemented computer assembly functions like "push" and "pop" as analogies of protein and metabolic pathways (Lenski et al., 2003; Adami and LaBar, 2015). These studies have demonstrated that in bottom-up simulations, simple functions can give rise to more complex functions (like add and multiply) through evolution; however, these are abstract analogies, not actual DNA code. There is a gap in implementations of bottom-up biological models. Bottom-up implementations could implement DNA code as the starting point and model how code changes. A bottom-up implementation should instantiate the lowest levels of selection on actual genes (Dawkins, 1976) and test the lowest level of function which is protein translations of that code. The *in silico* genes could be mutated and recombined as actual DNA molecules and fitness can determined by bioinformatic algorithms comparing string sequence similarity to proteins of known function. Our coded framework presented herein is novel in this respect.

Evolutionary algorithms are perfect for studying protein string evolution because the search space of protein strings is vast (considering 20 possible amino acids and strings in lengths of thousands $=20^{1000}$ unique strings). Research implementing codon based EAs is in early stages (Loose et al., 2006; Wnętrzak et al., 2018;

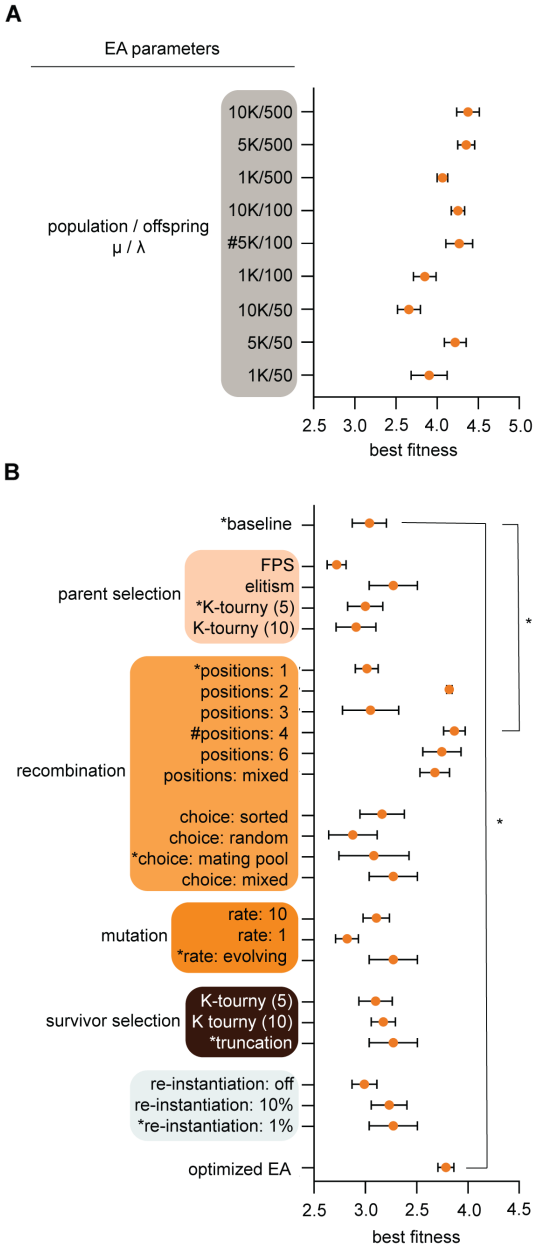

FIGURE 2
Evolutionary algorithms (EA) parameters were optimized for evolution and computational speed. **(A)** Population parameters were pre-tested to configure population (μ) and offspring (λ) sizes for subsequent larger experiments. Parameters (*Y*-axis) and best individual fitness (*X*-axis) were logged after 100 generations of simulated evolution. We chose 5K/100 [see hashtag (#)] for population/offspring (μ/λ) because it yielded high fitness, diverse outcomes, and fast computation time. **(B)** EA parameters were tuned by recording best fitness after populations [μ/λ: 1000/100] were evolved for 100 generations. A baseline configuration (asterisks, *) was held constant while individual parameters were varied. Choosing the highest yielding fitness configuration for each parameter is shown at bottom as the "optimized EA," though this was not necessarily *the best* because parameters exhibited interdependence. The optimized EA and baseline with 4-point crossover recombination evolved significantly better than baseline $p < 0.0001$ by One-way ANOVA with Tukey *post hoc* analysis. We used the baseline configuration with 4-point crossover recombination for subsequent experiments. Results show means and standard deviation from five trial runs after 100 generations. To briefly explain algorithmic terminology, *FPS* is fitness proportional parent selection

(Continued)

Figure 2 (Continued)
which assigns mating probability as proportional to fitness; *Elitism* ranks parents on fitness and sends the most fit individuals into the mating pool, *recombination* swaps DNA from two mated individuals at 1, 2, 3, 4, 6, or mixed points respectively; *mating choice sorted* sorts the mating pool and individuals mate with a partner closest to their fitness score, *mating choice random* allows individuals within the mating pool to randomly pick any other mate in the population; *mating choice mating pool* allows random choice of mates from within the mating pool only; *mating choice mixed* rolls a dice and chooses any method stochastically, *mutation rate* number indicates the number of dice rolls each individual child undergoes for chances to iteratively mutate the chromosome (the dice is an equal probability of 4 options to do nothing, bit flip, insert, or delete), *truncation* and *K-tournament* are selection methods described in EA-Class methods below, *re-instantiation* is a method to maintain diversity and it instantiates new TA modules from scratch and allows them to immigrate into the population at a set rate each generation.

Yoshida et al., 2018; Boone et al., 2021). For example, a few studies tested machine learning guided mutations and used EAs to design novel antimicrobial peptides (AMPs) (Loose et al., 2006; Yoshida et al., 2018; Boone et al., 2021). These researchers guided evolution from known AMP strings rather than evolving novel de-novo protein strings. These studies provide some support for the concept of using sequence similarity as a proxy for fitness. Here we use sequence similarity to *cif* consensus sequences as fitness proxy to process simulations orders of magnitude faster than possible with bioassay. To gain a better understanding of *cif* evolution, we encoded *cif* TA genes directly as chromosomes within a population based EA and observed the evolution of their strings (see Figures 1C,D).

Materials and methods

EA design

An overlapping generations (μ + λ) EA was coded in Python 3[1] where population size (μ) was 5,000 individuals and offspring (λ) was 100. Other variations were tested (see Figure 2A). Within the EA, code classes included an EA class (running the EA simulation functions, main methods, and data logging capacities), a TA class (housing the chromosome instantiations), and a main driver. The driver receives input from an editable JSON configuration file. All configuration files and outputs were saved and stored for reproducibility. The random seed is configurable for reproducibility.

EA class

EA algorithms are stochastic in nature. Evolutionary trajectories can proceed down different routes or converge. Thus, our main EA experiments consisted of 30 runs each (Figures 3, 4). Main methods within the EA class included class resets (to reset logs and class variables after each run); methods for population instantiation. In-Silico simulation of this evolution requires an initial instantiation

1 https://www.python.org/

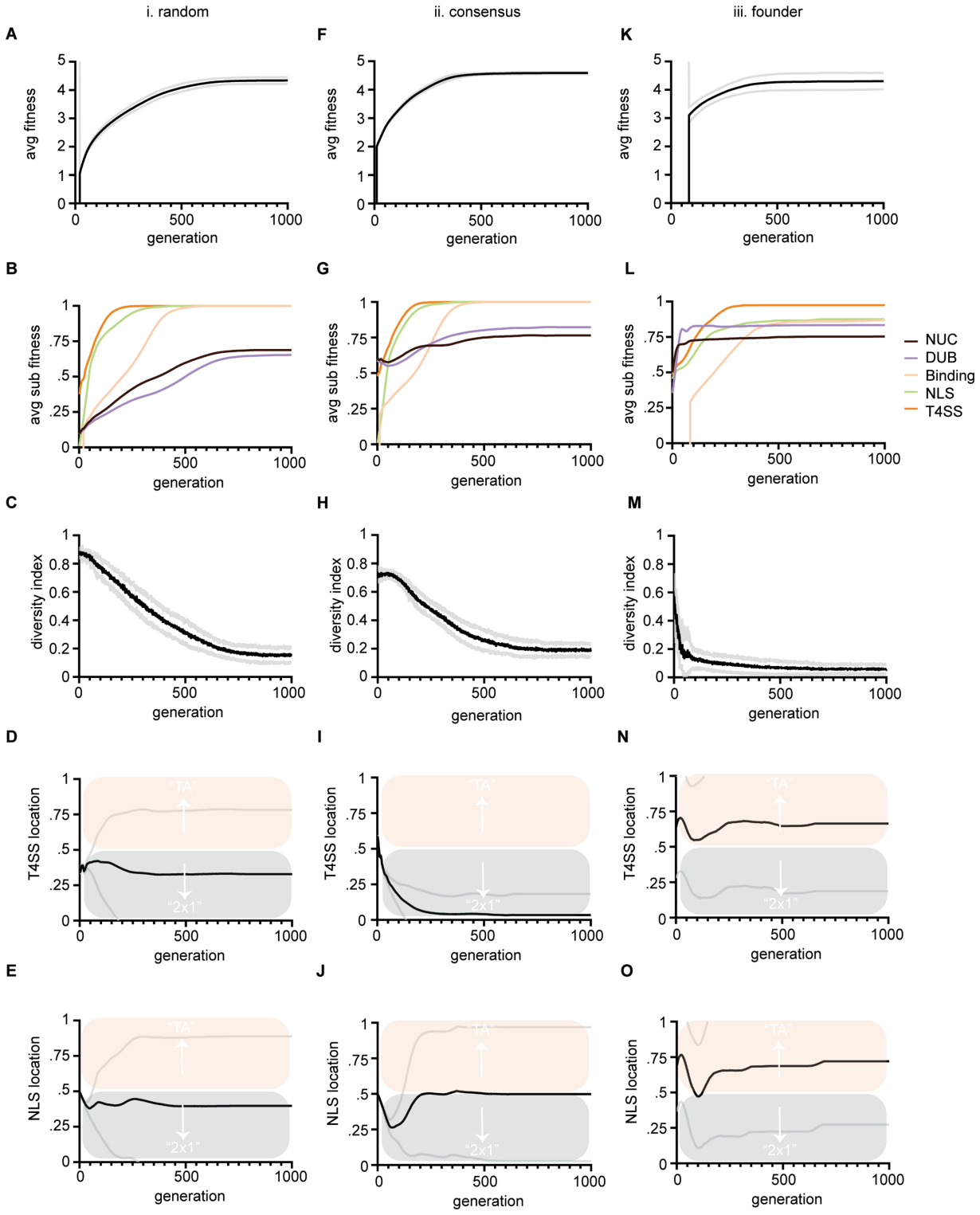

FIGURE 3
Output data from three large evolution experiments. Columns (i-iii) show results from three different instantiation methods described in Figure 1. Rows show average fitness of all TAs within a population versus generations **(A,F,K)**. Average sub-feature fitness of all TAs within a population versus generations **(B,G,L)**; Diversity index versus generations, where lower numbers indicate more similarity in string sequence and therefore loss of diversity **(C,H,M)**; Average T4SS site location of the population (black line) versus generations **(D,I,N)**; Average NLS site location (black line) of the population versus generations **(E,J,O)**. Scoring for T4SS and NLS sites is as follows: a score of 0 indicates that the site evolved in the antidote gene (*cifA*) and a 1 indicates that the site evolved in the toxin gene (*cifB*); therefore a score of 0.5 means that half the population had the site in *cifA* and the other half had the site in *cifB*. Mean values are plotted with black or colored lines. Standard deviation is marked in gray lines. Bias above 0.5 indicates preferential evolution of TA and below 0.5, 2×1. Panels **(D,I,N)** are all significantly different from each other at termination, (p <0.05) by one-way ANOVA with Tukey *post hoc* analysis. Panels **(E,O)** were significantly different by the same.

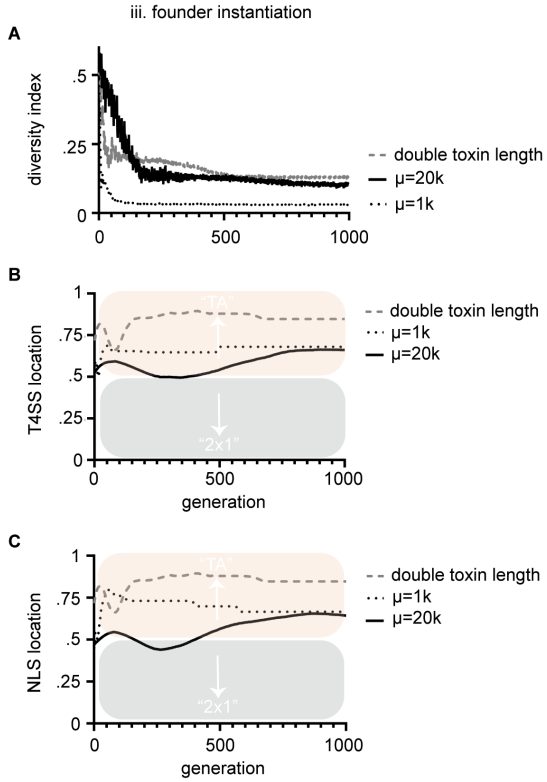

FIGURE 4
Parameters that control bias in the location of NLS and T4SS signals were tested. **(A)** We were able to control starting diversity by changing population size (μ). Small populations of 1,000 had significantly less diversity than populations of 20,000 by Mann–Whitney *U* test. In turn, these changes significantly altered the bias of the signal during the course of evolution, but not the final result [see dotted line vs. solid line in **(B,C)**; T4SS location and NLS location respectively]. The most significant terminal impact on bias of signal location was when we increased the average length of the toxins (see dashed line in **B,C**). Panels **(B,C)** are T4SS and NLS sites is as above. Mean values are plotted with black or colored lines. In **(B)** terminal conditions of doubling toxin length to μ=20k were significantly different for T4SS signal locations (p <0.05) by unpaired t-test with Welch's correction. These experiments all were performed under the third [(iii) founder] method of instantiation.

of a population of TA strings. Our experiments tested three distinct methods of instantiation that include (i) instantiating random strings, (ii) instantiating semi-random strings comporting to conserved *cif* consensus sequence, and (iii) instantiating a single individual and deriving an entire population by mutagenesis of that founder; sorting functions that sorted TA populations based on fitness; parent selection methods (which finally used K-tournament of $K = 5$ after preliminary testing; see Figure 2B). *K*-tournament selection runs multiple fitness tournaments among a few individuals chosen randomly from the population. Winners of a tournament with the best fitness are sent to the mating pool array to be selected for recombination. In experiments recombination used 4-point crossover recombination, but we tested other modes (Figure 2B). Mutation methods utilized an algorithm that randomly locates DNA base pairs and flips to a random choice of A, T, G, or C. Mutation also encoded insertion and deletion functions with randomly sized indels. The mutation method evaluates fitness by calling the fitness evaluation method from the TA class (see below). After fitness evaluation, survivors were selected via truncation survivor selection. Other survivor selection regimes were tested (Figure 2B). Truncation sorts the population and culls the lowest fitness individuals in a number equivalent to the number of offspring added per generation. Thus, carrying capacity remains constant at $\mu = 5{,}000$. Data logging functions were encoded, for example, calculateAverageFitness(), which tallies an average TA fitness. A termination condition method was coded but not used in final experiments. Logs were recorded in output files and saved. We tracked 15 quantifiable observations: (1) highestTAFitness_HTF, (2) avgBindingFitness_ABF, (3) avgDUBFitness_ADF, (4) avgNucFitness_ANF, (5) avgTAfitness_ATF, (6) avgToxinLength_ATL, (7) avgToxinAALength_ATAL, (8) avgAntidoteLength_AAL, (9) avgAntidoteAALength_AAAL, (10) avgTAMutationRate_ATMR, (11) avgNLSSITELocation_NLSL, (12) avgTypeIVSITELocation_TYPL, (13) avgNLSFitness_ANLSF, (14) avgT4SSFitness_AT4F, (15) diversityIndex_DI.

TA class

TA class individuals were instantiated with chromosomes encoding the string toxin and string antidote in DNA code. TAs additionally hold class variables including a nuclease score (measuring how well the toxin schema matches a known *cin* toxin consensus sequence) and a deubiquitylating (DUB) score (measuring how well the toxin schema matches a known *cid* toxin consensus sequence) (Gillespie et al., 2018). They also hold a NLS score which is determined by presence or absence of a "KRAR" string (Rossi et al., 1993) and a T4SS score determined by presence or absence of a "R-X(7)-R-X-R-X-R" string (Vergunst et al., 2005). All functional domains including nuclease domain, deubiquitylating domain, NLS, and T4SS signals are detected through a pairwise alignment algorithm and can be given partial scores if parts of the sequence are present. Pairwise alignment is built into the EA by importation of the Biopython[2] module's pairwise2 method. "Biopython is a set of freely available tools for biological computation written in Python by an international team of developers." The pairwise2 method is called with a −1 gap penalty, a −0.1 gap extension penalty, and a false condition so that end gaps are not penalized. A binding score (measuring how well the pair bind each other) is determined by our own algorithm. This algorithm is based on a sliding window that slides two strings together in comparison to find and tally a score of the best matching residue configurations. Precisely 11 charged residues are known to underlie *cifA* and *cifB* binding (Xiao et al., 2021). Therefore, if a sliding window detects an alignment of K with D, a score would be increased by 1 and the process continues. Repelling charges are penalized by −1. A total matched binding sequence should not exceed 11 binding residues in accordance with crystal structure data (Xiao et al., 2021). Class methods within the TA class include standard "getters" and "setters" [i.e., setSchemata() which instantiates the toxin strings], a translation method that translates the DNA code into proteins, a coded number parser to facilitate binding evaluations with integers rather than strings (to speed up computation), sub component fitness evaluation methods, and a "to string" reporting method.

2 https://biopython.org/

Main class

The main driver simply imports and stores the JSON configuration files. It instantiates the EA class. Finally, it initiates the simulation.

Calculating fitness

The fitness function for an individual TA pair is defined as the sum of its binding score, nuclease score, deubiquitylating score, NLS score, and T4SS signal score. Each sub-component fitness can maximally be 1 and therefore the max fitness of a perfect TA is 5. To elaborate precisely on how sequence similarity is used as a proxy for fitness, we describe the situation for DUB fitness. The DUB domain is a catalytic sequence of amino acids that conforms to a schema. The DUB schema in *cifs* is precisely, "HWVTLVI---------YY-DSL--------I---L-----D---------QQ-DG---CG----EN," where dashes (−) are interchangeable spaces (*do not cares*) and letters are requirements of specific amino acids in specific positions. A perfect alignment score of 1 for a *cif* DUB would match this schema. Anything not conforming to the schema is penalized by the alignment algorithm for gaps and mismatches. The schema for the nuclease domain is as follows, "DL-LL-R----------PIIIELK----------DLVL----------PIGLELK." These two consensus schemas were originally derived directly from compilation of diverse CI and CI-like toxins (Gillespie et al., 2018). Schemas for NLS and T4SS signals are also pulled from literature and listed on the preceding TA Class description. Thus, by using sequence similarity to conserved schemas and the binding algorithm (described above) we can sum elements for a perfect TA fitness score of 5. Parsimony pressure is applied if a TA genome exceeds a threshold of 4,500 DNA base pairs (this is an estimate of average *cif* TA size) and pressure increases corresponding to the length of the additional extraneous code. Parsimony pressure thus acts to minimize the coding length of TA pairs and accurately reflects selective pressures inducing reduction of *Wolbachia* genomes. *In toto*, a final fitness score involves the sum of the five functional component scores with a penalty function subtracting a coefficient parsimony penalty based on sequence length. All code is publicly available for inspection and reuse on github.

Experimental setup

The EA evolves populations of TAs and evaluates their fitness. Simulations were initialized via three distinct methods described in Figure 1C. How the simulation is initiated impacts the levels of inherent diversity in the starter population. Methods i–iii decrease in starting diversity from most to least, respectively. After 1,000 generations the simulation is terminated, and data collected. Data collected is given above and was graphed in Graphpad's Prism software. Experiments were conducted with 30 runs each.

Statistical analysis

For experiments generating multiple comparisons like optimizing the EA (Figures 2, 3) we employed one-way ANOVA with Tukey *post hoc* analysis using Graphpad Prism software. We compared values present at the final generation at termination of the simulation. *p*-values were considered significant if less than the standard 0.05. In Figure 4, terminal data were compared using unpaired two-tailed *t*-test with Welch's correction.

Results and discussion

Validating and tuning the EA's fitness function

One prerequisite of implementing an EA is an ability to evaluate fitness of individuals. A protein's function and thus its fitness is encoded in primary structure (amino acid strings). Protein function can be predicted by comparing strings to others with known function. Therefore, we use sequence similarity to *cif* domains as a proxy of fitness and thereby apply selective pressure. In our EA an individual in-silico *cif* is constituted of the two DNA genes and their translated protein strings. Many individual TA pairs are instantiated within populations. The EA mutates and recombines them exactly as DNA can mutate and recombine. Fitness of individual TA pairs is modelled as a sum of (1) how well a toxin can kill a cell (based on sequence similarity to known killer toxin domains from *cins* and *cids*) and (2) how well the antidote binds its partner toxin (modeled as matching charged residues within cognate TA pairs). Additionally, we add (3) NLS and (4) T4SS signal domains as additional summed components of fitness. We then quantified where NLS and T4SS signals evolved during simulations (in *cifA* or *cifB*) and tracked biased emergence of 2×1 versus TA.

After initial design (Figure 1), coding, and parameter optimization (Figure 2), we determined that the EA evolved efficiently and observed that population sizes of 5,000 individuals with offspring sizes of 100 individuals were optimal because they yielded high fitness, diverse outcomes, and fast computation time (Figure 2A). These assumptions have flaws (for example nature is not an algorithm that optimizes parameters to speed up evolution; discussed below), but these settings served as a starting point. Next, we tested different algorithmic methodologies for parent selection, recombination, mutation, survivor selection, and a "re-instantiation" method immigrating 10, 1%, or 0% de-novo individuals (described in methods). Results show means and standard deviation from five trial runs after 100 generations. Our goal was to determine optimal algorithms for maximizing *cif* fitness within simulation time periods. After observing EA behavior, we determined to use a "baseline" configuration of K-tournament selection where $K = 5$ for parent selection. Selected parents are transitioned to the mating pool where mating only occurs between individuals within that selective sub-population. Mating of TA parents is implemented with 4-point crossover recombination with a self-adaptive mutation rate to generate offspring TAs. The self-adaptive mutation rate is encoded within an individual's chromosome and can change if higher or lower mutation rates contribute to better fitness. Offspring TAs are loaded back into the main population ($\mu + \lambda$) and compete for survival via truncation, which culls the lowest fitness individuals. Subsequent experiments used these conditions unless otherwise specified.

Tracking evolution of cif domains shows that NLS and T4SS signals are quick to evolve

We performed three large experiments based upon three methods of instantiating populations. Our intention was to determine if starting preconditions biased preferential evolution of NLS or T4SS signals in *cifA* versus *cifB*. Any bias might indicate conditions under which 2 × 1 or strict TA mechanisms would arise from the evolutionary process. In these first tests, the EA successfully evolved and evaluated the fitness of TA modules. In all experiments fitness of individuals gradually increased toward 5 (Figures 3A,F,K). The rising fitness values over the course of the simulation indicates that our code is selecting for progressive *cif* assembly. All three simulations show a start at low average TA fitness which improves as more successful TAs evolve and overtake the population.

We tracked each sub-component of fitness including nuclease, DUB, NLS, and T4SS signal evolution (Figures 3B,G,L). As each component assembles in the evolving *cifs*, their corresponding fitness values move upwards to 1. The speed at which each domain reaches 1 indicates how difficult it is to evolve. These data also indicate our code works correctly as fitness of each sub-component increases with each generation towards a max score of 1. Importantly these data also indicate the inherent complexity of each sub-component and clearly show that NLS and T4SS signals are relatively quick to evolve in simulations (Figure 3; green and orange lines respectively). Binding is of intermediate complexity and arises slower (Figure 3; yellow lines). Nuclease and DUB catalytic domains are slow to evolve and do not completely reach perfect consensus sequences within the timeline of the evolutionary experiment (Figure 3; black and purple lines respectively). These data are in concordance with the given complexity of the domains. For example, the NLS is only 4 residues ("KRAR") whereas max binding fitness requires 11 matching residues in both toxin and antidote, and consensus sequences of catalytic domains must match 23 conserved residues within their schemas.

The five components' relative evolvability (or inherent speed of their evolution) indicates that CI systems might frequently lose, replace, adapt, and move NLS and T4SS signals, whereas binding and catalytic domains are more likely to remain conserved in-place due to difficulty of evolving them in the first place. If they are destroyed, they cannot quickly be replaced, whereas NLS and T4SS signals might be "fungible." We note that a full spectrum of T4SS signals has yet to be identified and this simulation only implements one example (Atmakuri et al., 2003; Nagai et al., 2005; Schulein et al., 2005; Vergunst et al., 2005; Huang et al., 2011).

To facilitate data interpretation, we point out that Figures 3A–C, F–H,K–M are simply controls that demonstrate that the simulations are programmed correctly. The results leading to conclusions about 2 × 1 vs. TA systems are contained in Figures 3D,E,I,J,N,O. These data plot the proportion of T4SS signals found in cifA/cifB (Figures 3D,I,N) and the proportion of NLS signals found in cifA/cifB (Figures 3E,J,O) for the populations under the three different simulations. In the plots, a score of 0 (below the midline and into the blue) indicates that the site evolved in the antidote gene (*cifA*) and implies 2 × 1 function has evolved whereas a score of 1 (above the midline and into the salmon) indicates that the site evolved in the toxin gene (*cifB*) implying a TA function has evolved; a score of 0.5 means that half the population had these sites in *cifA* and the other half had the site in *cifB*.

In many simulations, the algorithm terminates with both (2 × 1 and TA) models co-existing. These data indicate that both strict TA and 2 × 1 systems could co-exist and might even inter-convert between mechanisms on evolutionary time scales with drift, mutation, and recombination. These in-silico observations are congruent with empirical literature demonstrating both systems are apparently extant (Beckmann et al., 2017; LePage et al., 2017; Shropshire et al., 2018; Shropshire and Bordenstein, 2019; Adams et al., 2021; Sun et al., 2022). Cautiously, we note that these observations are premised on assumptions that there must be some conditions selecting for the evolution of CI; these ecological conditions are not yet completely defined (Turelli, 1994; Martinez et al., 2020; Beckmann et al., 2021) yet must exist under some context that gives rise to CI and *cifs;* perhaps amongst discrete spatial limitations and genomic competitions (Rankin et al., 2012). Importantly, our model simply justifies how multiple CI mechanisms might evolve to coexist on the amino acid level.

Parameters of simulations bias evolution of TA versus 2×1

When we measured where NLS and T4SS signals evolved (in *cifA* or *cifB*) under three different starting conditions [method (i) random, (ii) consensus, and (iii) founder; see Figures 1C,D] we detected biases in the evolutionary trajectory of one model over another (Figures 3D,I, N,E,J,O). After random instantiation (method i.) both NLS and T4SS signals' scores were slightly less than 0.5 indicating a slight preference for evolution of those sequences in *cifA* genes (Figures 3D,E). After semi-random instantiation (method ii.) there was strong bias to evolve the T4SS within *cifA* genes indicating a bias toward 2 × 1 (Figure 3I). Only in the third method did both NLS and T4SS signals preferentially evolve in the *cifB* gene, thereby indicating bias toward TA mechanisms (Figures 3N,O). Each method showed statistically different termination conditions for T4SS locations with all p-values <0.05. Method i significantly differed from method iii with respect to termination condition of NLS signal. Importantly, these results indicate that our model can detect significant evolutionary bias toward one mechanism over another and that preconditions at the start of evolution can bias the evolutionary trajectory toward either 2 × 1 or TA mechanisms.

We next sought to understand the conditions that drove biased evolution of one mechanism over another. Interestingly, some Culex mosquito populations maintain Wolbachia populations that contain multiple diversifying *cid* systems (Altinli et al., 2018; Bonneau et al., 2019). To monitor *cif* genetic diversity within the populations we tracked a diversity index, which was determined by randomly sampling 10 toxins from the population each generation and calculating the average similarity of those 10 toxins' amino acid strings. In populations where individual TAs fix and overtake the population, diversity decreases to zero (Figures 3C,H,M). After 1,000 generations, most populations are overtaken by one or a few TAs of high fitness. In method (iii), which resulted in biased evolution of strict TA systems, the diversity index was lowest (see Figure 3M). We tested whether diversity directly drove bias by altering the relative levels of genetic diversity within the population. We controlled this by simply changing population size (μ). Smaller populations carried less diversity (Figure 4A). The relative diversity did alter the course and

path of evolution, but not the outcome, which always converged on TA mechanisms (Figures 4B,C). Thus, population diversity did not drive the bias toward either TA or 2×1. We next tested whether length of the toxin protein impacted the outcome. When we doubled the size of the average size of the toxins, we significantly raised the bias of the model toward the TA model (Figure 4). We discuss the theoretical impacts of these observations below. Importantly, these observations demonstrate that we have successfully encoded an EA that evolves and tracks *cif* amino acid evolution.

To elaborate on the question of which instantiation method is more biologically realistic, we suggest the following thoughts. One assumption is that a prokaryotic TA model preceded the evolution of CI. There is evidence for this in the fact that *cif* operons have been observed within plasmids of *Rickettsia* (a sister lineage of *Wolbachia*), lending plausibility to the hypothesis that CI emerged from an ancestral prokaryotic TA plasmid selection system (Gillespie et al., 2018). If this hypothesis is correct, method (i) random instantiation, is not biologically relevant as it begins selection on all four components simultaneously from completely random sequences. In contrast, method (ii) assumes a prokaryotic TA system already exists and reasonably comports with some known toxin consensus sequences then selects for the addition of NLS and T4SS signals in the jump from prokaryotic TA to eukaryotic CI. This method is biologically relevant only for the first emergence of CI's evolution in deep evolutionary history. In that situation and according to the data observed here, this model shows preference for the evolution of 2×1 systems, but not to the complete exclusion of TA systems. The third instantiation method which started a population based on an individual founding sequence, method (iii), exhibited strong bias of NLS and T4SS assembly in *cifB* genes, indicating strong preference for a strict TA functionality. Notably, this model had the least diversity within its population and likely reflects more accurately the actual evolution in *Wolbachia* systems where an insect is colonized by a founder strain and diversity is only encountered in sporadic co-infections that only occur rarely in evolutionary history, but are likely the source for CI gene evolution if phages exchange genes during coinfection. Therefore, our analysis can explain the observed bias in favor of strict TA functionality by about 60% of studied *cif* orthologs; notably in our simulation method (iii) the bias was also about 60%. To be cautious, however, we note that only ~6 ortholog TA pairs have been studied in detail and it remains to be seen whether the observed frequency of TA or 2×1 functionalities is some relic of sample bias. After emergence of TAs, our model's data predicts they flux periodically from 2×1 to strict TA. Future studies can utilize this framework to determine more conditions that give rise to 2×1 versus TA systems.

Increasing length of toxin biases evolution toward TA mechanisms

Instantiation method (iii), where a population is generated by a founder, more accurately reflect the day-to-day evolution of *Wolbachia* organisms in their hosts. In each insect, the *Wolbachia* encountered will be entirely derived from the ancestor of that infection and therefore recombination with sequences of radically different *cifs* is unlikely, though not impossible due to mobility of WO phage viruses and infrequent co-infections. Method (iii) most accurately reflects these conditions and in this model, there was strong bias toward the evolution of strict TA functionality (Figure 3). This suggests that over time, most (~3/4) CI systems should end up in a state of strict TA functionality with some variation induced by ongoing flux of NLS and T4SS signals. One of the key factors seemingly controlling this evolution is simply the length of the corresponding antidote and toxin (Figure 4). Because the NLS and T4SS signals are of low complexity and evolve quickly, they should stochastically arise more often in what is the longer gene of the pair. Of all syntenic *cif* operons, the length of the toxin is always longer than the length of the antidote. This also indicates a simple bias toward strict TA if NLS and T4SS signals simply drift into the larger ORF. Biology is complex, yet factors having the biggest role in these mechanistic biases might be as simple as gene length. However, sequence length does not explain everything about the model. In data from method (ii), where the strongest bias toward 2×1 was observed, the toxins and antidotes on average are the same size. Therefore, size does not account for all the forces driving bias in either direction.

Conclusion, future directions, and limitations

The hypotheses and take-homes from our model are thus: (1) CI might evolve from less complex prokaryotic TA systems (Figure 1). (2) TA systems can convert to CI systems by the addition of at minimum NLS and T4SS signals (Figure 1) though these domains may not be completely sufficient. (3) Where NLS and T4SS signals evolve (in *cifA* or *cifB*) is predicted to be the determinant of 2×1 or strict TA mechanics (Figure 1). (4) In cases where CI and *cifs* diverge from a single founder, method (iii), the evolution is biased toward strict TA systems, but not at full exclusion of 2×1 systems (Figures 3N,O). (5) In our model, sequence length can predispose bias of signal evolution in a location; simply meaning that if B genes are longer than A genes, it is more likely that NLS and T4SS signals will arise inside them first. Finally, (6) Codon-based EAs can be applied in a bottom-up approach to address questions related to the evolution of protein strings.

In future experiments we plan to utilize this framework to test additional sequences of NLS and T4SS signals. Importantly, the signals we used are not the only ones that exist in nature. There can be cryptic and/or bi-partite combinatorial sequence motifs that contribute to secretion and localization (Schulein et al., 2005). To add to the nuance, our algorithm does not account for redundant sequences. For example, it does not quantify if additional NLS or T4SS signals evolve elsewhere, beyond the first. It would be interesting to re-program the system to measure and tally if multiple NLS and T4SS signals are evolving and where they are. One prediction our model makes is that because NLS and T4SS signals are of low complexity, there may be multiple redundant signals within the same gene. In future experiments we will look for this.

Our model makes many assumptions. One assumption we made, to begin analysis somewhere, is that the parameters causing the fastest evolution of *cifs* in simulations were apt to simulate the natural evolutionary dynamics of these TA modules. However, evolution within the natural organism might not be so ideal. Therefore, favoring the most efficient methodologies and parameters to evolve high fitness quickly might be incongruent with nature. Although we grounded the evolution of the EA in real biology using actual *cif*

sequences and known binding features. The benefit of our coded framework is that it can be modified to test and address future criticisms and hypotheses. For example, while we have only implemented the 2 × 1 and strict TA mechanisms, if ever a possibility of a third mechanism is observed or postulated, we can add that possibility to the code base.

Finally, our model encodes and models evolution of the most primal or basal level of CI (the amino acids). It is not an ecological model assessing TA allele fixation in populations. It would be inappropriate to directly compare our model with prior ecological models (Turelli, 1994; Rankin et al., 2012); although our model could be imported into those models as a foundation. The natural evolution of selfish TA elements involves multiple levels of evolutionary dynamics. For example, *cif* systems exist within WO-phages that exist within *Wolbachia* bacteria that live within insect hosts that live within populations. *Cifs* impact evolution and population dynamics on all these levels. Future models might incorporate our codon-based EA as a subcomponent of a larger multi-competitive EA framework. Such a program might provide vast insights into the complex evolutionary dynamics inherent to *Wolbachia* biology and make predictions about actual CI gene function.

Data availability statement

The original contributions presented in the study are included in the article/supplementary material, further inquiries can be directed to the corresponding author.

Author contributions

JB conceived of, conducted the experiments, and wrote the first draft manuscript. DT conceived of experiments and edited the manuscript. JG edited the manuscript. All authors contributed to the article and approved the submitted version.

Funding

Funding was provided by Auburn University's Department of Entomology and Plant Pathology startup funds (JB) and US Department of Agriculture Hatch Grant USDA AFRI (ALA015-4-19178) and USDA HATCH (ALA015-1-18014). JG acknowledges support from the NIH/NIAID (R21 AI146773, R21 AI156762, and R21 AI166832).

Acknowledgments

We thank Jason Barbieri, David Edwards, and Dennis Brown for constructive comments on the project design and manuscript.

Conflict of interest

The authors declare that the research was conducted in the absence of any commercial or financial relationships that could be construed as a potential conflict of interest.

Publisher's note

References

Adami, C., and LaBar, T. (2015). From entropy to information: biased typewriters and the origin of life. *ArXiv*. Available at: https://arxiv.org/abs/1506.06988

Adams, K. L., Abernathy, D. G., Willett, B. C., Selland, E. K., Itoe, M. A., and Catteruccia, F. (2021). *Wolbachia* cifB induces cytoplasmic incompatibility in the malaria mosquito vector. *Nat. Microbiol.* 6, 1575–1582. doi: 10.1038/s41564-021-00998-6

Altinli, M., Gunay, F., Alten, B., Weill, M., and Sicard, M. (2018). *Wolbachia* diversity and cytoplasmic incompatibility patterns in *Culex pipiens* populations in Turkey. *Parasit. Vectors* 11:198. doi: 10.1186/s13071-018-2777-9

Atmakuri, K., Ding, Z., and Christie, P. J. (2003). VirE2, a type IV secretion substrate, interacts with the VirD4 transfer protein at cell poles of *Agrobacterium tumefaciens*. *Mol. Microbiol.* 49, 1699–1713. doi: 10.1046/j.1365-2958.2003.03669.x

Beckmann, J. F., Bonneau, M., Chen, H., Hochstrasser, M., Poinsot, D., Merçot, H., et al. (2019b). The toxin-antidote model of cytoplasmic incompatibility: genetics and evolutionary implications. *Trends Genet.* 35, 175–185. doi: 10.1016/j.tig.2018.12.004

Beckmann, J. F., Bonneau, M., Chen, H., Hochstrasser, M., Poinsot, D., Merçot, H., et al. (2019a). Caution does not preclude predictive and testable models of cytoplasmic incompatibility: a reply to Shropshire et al. *Trends Genet.* 35, 399–400. doi: 10.1016/j.tig.2019.03.002

Beckmann, J. F., and Fallon, A. M. (2013). Detection of the *Wolbachia* protein WPIP0282 in mosquito spermathecae: implications for cytoplasmic incompatibility. *Insect Biochem. Mol. Biol.* 43, 867–878. doi: 10.1016/j.ibmb.2013.07.002

Beckmann, J. F., Ronau, J. A., and Hochstrasser, M. (2017). A *Wolbachia* deubiquitylating enzyme induces cytoplasmic incompatibility. *Nat. Microbiol.* 2:17007. doi: 10.1038/nmicrobiol.2017.7

Beckmann, J. F., Sharma, G. D., Mendez, L., Chen, H., and Hochstrasser, M. (2019c). The Wolbachia cytoplasmic incompatibility enzyme CidB targets nuclear import and protamine-histone exchange factors. *eLife* 8:e50026. doi: 10.7554/eLife.50026

Beckmann, J. F., Van Vaerenberghe, K., Akwa, D. E., and Cooper, B. S. (2021). A single mutation weakens symbiont-induced reproductive manipulation through reductions in deubiquitylation efficiency. *Proc. Natl. Acad. Sci.* 118:e2113271118. doi: 10.1073/pnas.2113271118

Bonneau, M., Caputo, B., Ligier, A., Caparros, R., Unal, S., Perriat-Sanguinet, M., et al. (2019). Variation in Wolbachia cidB gene, but not cidA, is associated with cytoplasmic incompatibility mod phenotype diversity in *Culex pipiens*. *Mol. Ecol.* 28, 4725–4736. doi: 10.1111/mec.15252

Boone, K., Wisdom, C., Camarda, K., Spencer, P., and Tamerler, C. (2021). Combining genetic algorithm with machine learning strategies for designing potent antimicrobial peptides. *BMC Bioinform.* 22:239. doi: 10.1186/s12859-021-04156-x

Champer, J., Liu, J., Oh, S. Y., Reeves, R., Luthra, A., Oakes, N., et al. (2018). Reducing resistance allele formation in CRISPR gene drive. *Proc. Natl. Acad. Sci.* 115, 5522–5527. doi: 10.1073/pnas.1720354115

Champer, S. E., Oakes, N., Sharma, R., García-Díaz, P., Champer, J., and Messer, P. W. (2022). Modeling CRISPR gene drives for suppression of invasive rodents using a supervised machine learning framework. *PLoS Comput. Biol.* 17:e1009660. doi: 10.1371/journal.pcbi.1009660

Dawkins, R. (1976). *The selfish gene*. New York: Oxford University Press.

Driscoll, T. P., Verhoeve, V. I., Brockway, C., Shrewsberry, D. L., Plumer, M., Sevdalis, S. E., et al. (2020). Evolution of Wolbachia mutualism and reproductive

parasitism: insight from two novel strains that co-infect cat fleas. *PeerJ* 8:e10646. doi: 10.7717/peerj.10646

Gillespie, J. J., Driscoll, T. P., Verhoeve, V. I., Rahman, M. S., Macaluso, K. R., and Azad, A. F. (2018). A tangled web: origins of reproductive parasitism. *Genome Biol. Evol.* 10, 2292–2309. doi: 10.1093/gbe/evy159

Haller, B. C., and Messer, P. W. (2016). SLiM 2: flexible, interactive forward genetic simulations. *Mol. Biol. Evol.* 34, 230–240. doi: 10.1093/molbev/msw211

Haller, B. C., and Messer, P. W. (2019). SLiM 3: forward genetic simulations beyond the Wright–fisher model. *Mol. Biol. Evol.* 36, 632–637. doi: 10.1093/molbev/msy228

Hertig, M. (1936). The Rickettsia, *Wolbachia pipientis* (gen. Et sp.n.) and associated inclusions of the mosquito, *Culex pipiens*. *Parasitology* 28, 453–486. doi: 10.1017/S0031182000022666

Hertig, M., and Wolbach, S. B. (1924). Studies on Rickettsia-like micro-organisms in insects. *J Med Res* 44, 329–374.7.

Horard, B., Terretaz, K., Gosselin-Grenet, A. S., Sobry, H., Sicard, M., Landmann, F., et al. (2022). Paternal transmission of the *Wolbachia* CidB toxin underlies cytoplasmic incompatibility. *Curr. Biol.* 32, 1319–1331.e5. doi: 10.1016/j.cub.2022.01.052

Huang, L., Boyd, D., Amyot, W. M., Hempstead, A. D., Luo, Z. Q., O'Connor, T. J., et al. (2011). The E block motif is associated with *Legionella pneumophila* translocated substrates. *Cell. Microbiol.* 13, 227–245. doi: 10.1111/j.1462-5822.2010.01531.x

Laven, H. (1953). Reciprocally differentiable crossing of mosquitoes (Culicidae) and its significance for plasmatic heredity. *Z. Indukt. Abstamm. Vererbungsl.* 85, 118–136.

Laven, H. (1967a). *Chapter 7: speciation and evolution in Culex pipiens*, vol. *251* (Elselvier: Academic Press), 251–275.

Laven, H. (1967b). Eradication of *Culex Pipiens* Fatigans through cytoplasmic incompatibility. *Nature* 216, 383–384. doi: 10.1038/216383a0

Lenski, R. E., Ofria, C., Pennock, R. T., and Adami, C. (2003). The evolutionary origin of complex features. *Nature* 423, 139–144. doi: 10.1038/nature01568

LePage, D. P., Metcalf, J. A., Bordenstein, S. R., On, J., Perlmutter, J. I., Shropshire, J. D., et al. (2017). Prophage WO genes recapitulate and enhance Wolbachia-induced cytoplasmic incompatibility. *Nature* 543, 243–247. doi: 10.1038/nature21391

Li, J., and Champer, J. (2023). Harnessing Wolbachia cytoplasmic incompatibility alleles for confined gene drive: a modeling study. *PLoS Genet.* 19:e1010591. doi: 10.1371/journal.pgen.1010591

Loose, C., Jensen, K., Rigoutsos, I., and Stephanopoulos, G. (2006). A linguistic model for the rational design of antimicrobial peptides. *Nature* 443, 867–869. doi: 10.1038/nature05233

Martinez, J., Klasson, L., Welch, J. J., and Jiggins, F. M. (2020). Life and death of selfish genes: comparative genomics reveals the dynamic evolution of cytoplasmic incompatibility. *Mol. Biol. Evol.* 38, 2–15. doi: 10.1093/molbev/msaa209

Meany, M. K., Conner, W. R., Richter, S. V., Bailey, J. A., Turelli, M., and Cooper, B. S. (2019). Loss of cytoplasmic incompatibility and minimal fecundity effects explain relatively low Wolbachia frequencies in *Drosophila mauritiana*. *Evolution* 73, 1278–1295. doi: 10.1111/evo.13745

Merçot, H., and Poinsot, D. (1998). And discovered on Mount Kilimanjaro. *Nature* 391:853. doi: 10.1038/36021

Messer, P. W. (2013). SLiM: simulating evolution with selection and linkage. *Genetics* 194, 1037–1039. doi: 10.1534/genetics.113.152181

Nagai, H., Cambronne, E. D., Kagan, J. C., Amor, J. C., Kahn, R. A., and Roy, C. R. (2005). A C-terminal translocation signal required for dot/Icm-dependent delivery of the Legionella RalF protein to host cells. *Proc. Natl. Acad. Sci.* 102, 826–831. doi: 10.1073/pnas.0406239101

Poinsot, D., Charlat, S., and Mercot, H. (2003). On the mechanism of Wolbachia-induced cytoplasmic incompatibility: confronting the models with the facts. *BioEssays* 25, 259–265. doi: 10.1002/bies.10234

Rankin, D. J., Turner, L. A., Heinemann, J. A., and Brown, S. P. (2012). The coevolution of toxin and antitoxin genes drives the dynamics of bacterial addiction complexes and intragenomic conflict. *Proc. Biol. Sci.* 279, 3706–3715. doi: 10.1098/rspb.2012.0942

Ross, P. A., Robinson, K. L., Yang, Q., Callahan, A. G., Schmidt, T. L., Axford, J. K., et al. (2022). A decade of stability for wMel Wolbachia in natural *Aedes aegypti* populations. *PLoS Pathog.* 18:e1010256. doi: 10.1371/journal.ppat.1010256

Rossi, L., Hohn, B., and Tinland, B. (1993). The VirD2 protein of *Agrobacterium tumefaciens* carries nuclear localization signals important for transfer of T-DNA to plant. *Mol Gen Genet* 239, 345–353. doi: 10.1007/bf00276932

Schulein, R., Guye, P., Rhomberg, T. A., Schmid, M. C., Schröder, G., Vergunst, A. C., et al. (2005). A bipartite signal mediates the transfer of type IV secretion substrates of *Bartonella henselae* into human cells. *Proc. Natl. Acad. Sci. U. S. A.* 102, 856–861. doi: 10.1073/pnas.0406796102

Shropshire, J. D., and Bordenstein, S. R. (2019). Two-by-one model of cytoplasmic incompatibility: synthetic recapitulation by transgenic expression of cifA and cifB in *Drosophila*. *PLoS Genet.* 15:e1008221. doi: 10.1371/journal.pgen.1008221

Shropshire, J. D., Leigh, B., Bordenstein, S. R., Duplouy, A., Riegler, M., Brownlie, J. C., et al. (2019). Models and nomenclature for cytoplasmic incompatibility: caution over premature conclusions - a response to Beckmann et al. *Trends Genet.* 35, 397–399. doi: 10.1016/j.tig.2019.03.004

Shropshire, J. D., On, J., Layton, E. M., Zhou, H., and Bordenstein, S. R. (2018). One prophage WO gene rescues cytoplasmic incompatibility in *Drosophila melanogaster*. *Proc. Natl. Acad. Sci.* 115, 4987–4991. doi: 10.1073/pnas.1800650115

Sun, G., Zhang, M., Chen, H., and Hochstrasser, M. (2022). The CinB nuclease from wNo *Wolbachia* is sufficient for induction of cytoplasmic incompatibility in *Drosophila*. *MBio* 13, e03177–e03121. doi: 10.1128/mbio.03177-21

Teixeira, L., Ferreira, Á., and Ashburner, M. (2008). The bacterial symbiont Wolbachia induces resistance to RNA viral infections in *Drosophila melanogaster*. *PLoS Biol.* 6:e1000002. doi: 10.1371/journal.pbio.1000002

Turelli, M. (1994). Evolution of incompatibility-inducing microbes and their hosts. *Evolution* 48, 1500–1513. doi: 10.1111/j.1558-5646.1994.tb02192.x

Turelli, M., Katznelson, A., and Ginsberg, P. S. (2022). Why *Wolbachia*—induced cytoplasmic incompatibility is so common. *Proc. Natl. Acad. Sci.* 119:e2211637119. doi: 10.1073/pnas.2211637119

Vergunst, A. C., van Lier, M. C. M., den Dulk-Ras, A., Grosse Stüve, T. A., Ouwehand, A., and Hooykaas, P. J. J. (2005). Positive charge is an important feature of the C-terminal transport signal of the VirB/D4-translocated proteins of Agrobacterium. *Proc. Natl. Acad. Sci.* 102, 832–837. doi: 10.1073/pnas.0406241102

Werren, J. H., Baldo, L., and Clark, M. E. (2008). Wolbachia: master manipulators of invertebrate biology. *Nat. Rev. Microbiol.* 6, 741–751. doi: 10.1038/nrmicro1969

Wnętrzak, M., Błażej, P., Mackiewicz, D., and Mackiewicz, P. (2018). The optimality of the standard genetic code assessed by an eight-objective evolutionary algorithm. *BMC Evol. Biol.* 18:192. doi: 10.1186/s12862-018-1304-0

Xi, Z., Khoo, C. C., and Dobson, S. L. (2005). Wolbachia establishment and invasion in an *Aedes aegypti* laboratory population. *Science* 310, 326–328. doi: 10.1126/science.1117607

Xiao, Y., Chen, H., Wang, H., Zhang, M., Chen, X., Berk, J. M., et al. (2021). Structural and mechanistic insights into the complexes formed by *Wolbachia* cytoplasmic incompatibility factors. *Proc. Natl. Acad. Sci.* 118:e2107699118. doi: 10.1073/pnas.2107699118

Yamaguchi, Y., Park, J. H., and Inouye, M. (2011). Toxin-antitoxin systems in bacteria and archaea. *Annu. Rev. Genet.* 45, 61–79. doi: 10.1146/annurev-genet-110410-132412

Ye, Y. H., Carrasco, A. M., Frentiu, F. D., Chenoweth, S. F., Beebe, N. W., van den Hurk, A. F., et al. (2015). Wolbachia reduces the transmission potential of dengue-infected *Aedes aegypti*. *PLoS Negl. Trop. Dis.* 9:e0003894. doi: 10.1371/journal.pntd.0003894

Yen, J. H., and Barr, A. R. (1971). New hypothesis of the cause of cytoplasmic incompatibility in *Culex pipiens* L. *Nature* 232, 657–658. doi: 10.1038/232657a0

Yen, J. H., and Barr, A. R. (1973). The etiological agent of cytoplasmic incompatibility in *Culex pipiens*. *J. Invertebr. Pathol.* 22, 242–250. doi: 10.1016/0022-2011(73)90141-9

Yoshida, M., Hinkley, T., Tsuda, S., Abul-Haija, Y. M., McBurney, R. T., Kulikov, V., et al. (2018). Using evolutionary algorithms and machine learning to explore sequence space for the discovery of antimicrobial peptides. *Chem* 4, 533–543. doi: 10.1016/j.chempr.2018.01.005

Zheng, X., Zhang, D., Li, Y., Yang, C., Wu, Y., Liang, X., et al. (2019). Incompatible and sterile insect techniques combined eliminate mosquitoes. *Nature* 572, 56–61. doi: 10.1038/s41586-019-1407-9

frontiers | Frontiers in Microbiology

TYPE Original Research
PUBLISHED 31 August 2023
DOI 10.3389/fmicb.2023.1209595

OPEN ACCESS

EDITED BY
Chih-Horng Kuo,
Academia Sinica, Taiwan

REVIEWED BY
Giuseppe Massimino Cocuzza,
University of Catania, Italy
Aaron Lorenz,
University of Minnesota Twin Cities, United States

*CORRESPONDENCE
Rosanna Giordano
✉ rgiordan@fiu.edu
Everett P. Weber
✉ everett.p.weber@dartmouth.edu

†These authors have contributed equally to this work and share first authorship

RECEIVED 21 April 2023
ACCEPTED 25 July 2023
PUBLISHED 31 August 2023

CITATION
Giordano R, Weber EP, Mitacek R, Flores A, Ledesma A, De AK, Herman TK, Soto-Adames FN, Nguyen MQ, Hill CB and Hartman GL (2023) Patterns of asexual reproduction of the soybean aphid, *Aphis glycines* (Matsumura), with and without the secondary symbionts *Wolbachia* and *Arsenophonus,* on susceptible and resistant soybean genotypes.
Front. Microbiol. 14:1209595.
doi: 10.3389/fmicb.2023.1209595

Patterns of asexual reproduction of the soybean aphid, *Aphis glycines* (Matsumura), with and without the secondary symbionts *Wolbachia* and *Arsenophonus,* on susceptible and resistant soybean genotypes

Rosanna Giordano[1,2*†], Everett P. Weber[3*†], Ryan Mitacek[4], Alejandra Flores[5], Alonso Ledesma[6], Arun K. De[7], Theresa K. Herman[8], Felipe N. Soto-Adames[9], Minh Q. Nguyen[10], Curtis B. Hill[11] and Glen L. Hartman[4]

[1]Institute of Environment, Florida International University, Miami, FL, United States, [2]Puerto Rico Science Technology and Research Trust, San Juan, Puerto Rico, [3]Office of Institutional Research, Dartmouth College, Hanover, NH, United States, [4]Department of Crop Sciences, University of Illinois Urbana-Champaign, Urbana, IL, United States, [5]Department of Physiology and Biophysics, School of Medicine, Case Western Reserve University, Cleveland, OH, United States, [6]College of Agricultural, Consumer and Environmental Sciences, University of Illinois Urbana-Champaign, Urbana, IL, United States, [7]Animal Sciences Division, ICAR-Central Island Agricultural Research Institute, Port Blair, India, [8]USDA-Agricultural Research Service, Urbana, IL, United States, [9]Division of Plant Industry, Florida Department of Agriculture and Consumer Services, Gainesville, FL, United States, [10]Neochromosome, Inc., Long Island City, NY, United States, [11]Agricen Sciences, Pilot Point, TX, United States

Plant breeding is used to develop crops with host resistance to aphids, however, virulent biotypes often develop that overcome host resistance genes. We tested whether the symbionts, *Arsenophonus* (*A*) and *Wolbachia* (*W*), affect virulence and fecundity in soybean aphid biotypes Bt1 and Bt3 cultured on whole plants and detached leaves of three resistant, *Rag1*, *Rag2* and *Rag1 + 2,* and one susceptible, *W82*, soybean genotypes. Whole plants and individual aphid experiments of *A. glycines* with and without *Arsenophonus* and *Wolbachia* did not show differences in overall fecundity. Differences were observed in peak fecundity, first day of deposition, and day of maximum nymph deposition of individual aphids on detached leaves. Bt3 had higher fecundity than Bt1 on detached leaves of all plant genotypes regardless of bacterial profile. Symbionts did not affect peak fecundity of Bt1 but increased it in Bt3 (*A*+*W*+) and all Bt3 strains began to deposit nymphs earlier than the Bt1 (*A*+*W*–). *Arsenophonus* in Bt1 delayed the first day of nymph deposition in comparison to aposymbiotic Bt1 except when reared on *Rag1 + 2*. For the Bt1 and Bt3 strains, symbionts did not result in a significant difference in the day they deposited the maximum number of nymphs nor was there a difference in survival or variability in number of nymphs deposited. Variability of number of aphids deposited was higher in aphids feeding on resistant plant genotypes. The impact of *Arsenophonus* on soybean aphid patterns of fecundity was dependent on the aphid biotype and plant genotype. *Wolbachia* alone had no detectable impact but may have contributed to the increased fecundity of Bt3 (*A*+*W*+). An individual based model, using data from the detached leaves experiment and with intraspecific competition removed, found patterns similar to those observed in the greenhouse and growth chamber experiments including

a significant interaction between soybean genotype and aphid strain. Combining individual data with the individual based model of population growth isolated the impact of fecundity and host resistance from intraspecific competition and host health. Changes to patterns of fecundity, influenced by the composition and concentration of symbionts, may contribute to competitive interactions among aphid genotypes and influence selection on virulent aphid populations.

KEYWORDS

soybean aphid, reproduction, resistant soybean varieties, symbionts, *Wolbachia*, *Arsenophonus*, *Hamiltonella*

Introduction

Aphids feed on plant phloem, a source of food composed mostly of diluted sugars, amino acids, and a range of proteins and RNA molecules, some produced in response to environmental stresses (van Bel and Gaupels, 2004; Lough and Lucas, 2006; Turgeon and Wolf, 2009). As with other insects that feed on nutrient-poor food, aphids are associated with intracellular symbiotic organisms that contribute to their acquisition of nutrients. Most species within the Aphidoideae, except for members of the Cerataphidini tribe, who are colonized by symbiotic yeast (Fukatsu and Ishikawa, 1992), are associated with the obligate symbiotic bacteria *Buchnera aphidicola* (Buchner, 1965; Munson et al., 1991a,b; Vogel and Moran, 2013), a relationship estimated to have begun *circa* 150 Ma (Moran et al., 1993; Von Dohlen and Moran, 2000). This long association has rendered them inextricably tied; aphids deprived of *B. aphidicola* cannot reproduce and attempts at *in vitro* culturing of the bacterium have failed. The obligate *B. aphidicola* is not the only symbiont associated with aphids. Insects in general, and aphids in particular, are associated with a panoply of facultative or secondary symbionts, some of which have been shown to render fitness benefits to the host (Montllor et al., 2002; Tsuchida et al., 2002; Oliver et al., 2003, 2007; Tsuchida et al., 2004; Scarborough et al., 2005; Russell and Moran, 2006; Łukasik et al., 2012, 2013; Henry et al., 2013). The presence of symbiotic bacteria in insects may affect their interaction with plants including facilitating the colonization of resistant plants (Hebert et al., 2007; Francis et al., 2010; Frago et al., 2012; Biere and Tack, 2013). Moreover, the intimate association between aphids and plants has facilitated the transfer of bacteria across these two kingdoms, allowing the opportunity for bacteria to commonly infect aphids and establish new niches (Caspi-Fluger and Zchori-Fein, 2010; Li et al., 2017).

The soybean aphid, *Aphis glycines* Matsumara 1917 (Hemiptera, Aphididae) is native to Eastern Asia (Wang et al., 1994; Van Der Berg et al., 1997; Blackman and Eastop, 2000) and a recent invader in North America where, after its detection in 2000, it quickly spread throughout the midwestern U.S. and southern provinces of Canada (Hunt et al., 2003; Venette and Ragsdale, 2004; Giordano et al., 2020). The spread of the soybean aphid was facilitated by the diffused availability of the primary and overwintering host plant, invasive plant species *Rhamnus cathartica* L. (Buckthorn) (Ragsdale et al., 2004), and by widespread cultivation of soybean, *Glycine max,* the secondary and summer host, in the agricultural landscape of North America, where there is also a general lack of geographical impediments to aerial dispersal (Wallin and Loonan, 1971; Irwin et al., 1988; Loxdale et al., 1993; Irwin et al., 2007). As observed with other invasive species (Elton, 2000), the soybean aphid has reached higher population densities and confers greater damage to the soybean crop in its invasive range compared to its native range (Liu et al., 2004; Ragsdale et al., 2004; Wu et al., 2004; Tilmon et al., 2011). If left untreated, damage due to the soybean aphid can cause significant yield losses to the soybean crop (Song et al., 2006; Kim C.S. et al., 2008; Johnson et al., 2009; Song and Swinton, 2009; Ragsdale et al., 2011). Soybean pest control is largely managed with neonicotinoid pesticide sprays or seed treatments (Johnson et al., 2009; Ragsdale et al., 2011; Myers and Hill, 2014; Bahlai et al., 2015). However, the widespread use of neonicotinoids is likely to be curtailed as they are implicated in the decline of pollinators and other insects with a ripple effect on their invertebrate and vertebrate predators (Di Prisco et al., 2013; Hallmann et al., 2014; Sánchez-Bayo, 2014). Sustainable alternatives include biological control measures (McCarville and O'Neal, 2012; Hallett et al., 2013; Heimpel et al., 2013) and host plant resistance (Li et al., 2004; Hill et al., 2004a,b, 2006a,b, 2012; Mardorf et al., 2010; McCarville and O'Neal, 2012, 2013; Wiarda et al., 2012; Hesler et al., 2013; Fox et al., 2014; McCarville et al., 2014). However, before the widespread field use of soybean aphid resistant genotypes could be completed, four soybean aphid biotypes able to overcome the resistance were identified (Kim K.-S. et al., 2008; Hill et al., 2010, 2012; Alt and Ryan-Mahmutagic, 2013; Pawlowski et al., 2014).

Resistant plant genotypes are a valuable, effective, and ecologically sustainable tool not only to control damage by aphids but also to limit the spread of diseases that affect soybean (i.e., Neupane et al., 2019; Barros et al., 2023). However, 72 virulent aphid biotypes have developed among 17 aphid species affecting at least 10 crop plants, with the greatest number of biotypes seen in *Diuraphis noxia*, the Russian wheat aphid, on wheat (Smith and Chuang, 2014). The mechanisms of aphid virulence are not well understood. Evidence, however, suggests that anatomical structures and chemical responses associated with the intake and digestion of plant phloem, and interactions with symbionts may also play a role (Bansal et al., 2013; Smith and Chuang, 2014; Bansal and Michel, 2015).

The specific way virulent soybean aphid biotypes overcome resistance genes in soybean is not known (Natukunda and MacIntosh, 2020). Previous reports with other aphids suggest that the ability of aphids to overcome plant resistance may be the result of mutation, gene regulation, gene amplification (Bass and Field, 2011; Bass et al., 2013; Feyereisen et al., 2015) and/or contributions of bacterial symbionts (Zytynska and Weisser, 2016). The soybean aphid harbors *Buchnera*, as with the great majority of aphids, as well as *Arsenophonus*,

Wolbachia and *Hamiltonella*. *Arsenophonus* (Wille and Hartman, 2009; Bansal et al., 2013; Wenger and Michel, 2013; Wulff et al., 2013), is a bacterium that infects a variety of arthropod hosts (Duron et al., 2008; Nováková et al., 2009; Jousselin et al., 2013). Host effects attributed to the action of *Arsenophonus* range from male-killing in parasitic wasps (Huger et al., 1985; Werren et al., 1986; Gherna et al., 1991; Darby et al., 2010; Duron et al., 2010) to protection from parasitism in psyllids (Hansen et al., 2007). *Arsenophonus* infections in Asian and US populations of the soybean aphid have been reported (Bansal et al., 2013; Wulff et al., 2013). Despite the widespread occurrence of *Arsenophonus*, studies have shown it did not confer protection to soybean aphids from attack by three parasitoid species or by the aphid fungal pathogen *Pandora neoaphidis* (Remaudiere & Hennebert) (Wulff et al., 2013). *Arsenophonus* infection also did not influence soybean aphid virulence on *Rag* soybean aphid resistant genotypes, although infected aphids developed higher populations than the corresponding uninfected isolines (Wulff and White, 2015).

The soybean aphid is infected with the widely occurring Rickettsial arthropod symbiont *Wolbachia,* as well as *Hamiltonella,* and several extracellular bacteria (Bai et al., 2010; Liu et al., 2012; Bansal et al., 2013). *Wolbachia* have thus far been reported solely from invertebrates where they can elicit a range of effects from cytoplasmic incompatibility to male-killing (Stevens et al., 2001; Fenn and Blaxter, 2007; Werren et al., 2008; Kaur et al., 2021). *Hamiltonella defensa* has been documented in aphids, psyllids and whiteflies (Clark et al., 1992; Sandström et al., 2001; Russell et al., 2013). In aphids it has been shown to provide protection against parasitoid wasps (van der Wilk et al., 1999; Oliver et al., 2003, 2005, 2007; Ferrari et al., 2004; Moran et al., 2005; Bensadia et al., 2006; Degnan and Moran, 2007).

The association of Rickettsia with plants is exceedingly rare and a single report exists of a plant-pathogenic Rickettsia, causing papaya bunchy top disease (Davis et al., 1998). Evidence thus far indicates that the plant environment is not favorable for *Wolbachia* reproduction (Perlman et al., 2006; Weinert et al., 2009). We could not identify any report of *H. defensa* infecting plants. Conversely, *Arsenophonus* includes two well-characterized species, *Phlomobacter fragariae* and *Arsenophonus phytopathogenics,* that have been reported to be restricted to the phloem of plants and dependent on inter-plant transmission by their planthopper host: *Cixius wagneri* (China) (Hemiptera: Cixiidae) and *Pentastiridius leporinus* (L.) (Hemiptera: Cixiidae) respectively (Bressan et al., 2009; Bressan, 2014).

Given the influence that both intra-and extra-cellular bacterial symbionts have been shown to exert on their hosts, whether invertebrate or vertebrate, understanding the impact of bacterial infection on the traits of a major agricultural pest such as the soybean aphid may lead to important insights regarding their role as pests. The rapid development of soybean aphid virulence on resistant genotypes is of special concern, as resistant soybean genotypes hold the promise of providing pest control while minimizing detrimental impacts to the environment caused by pesticides (Natukunda and MacIntosh, 2020). We therefore tested whether *Arsenophonus* and *Wolbachia* have an effect on the expression of virulence and fecundity in the soybean aphid using two well-established laboratory strains of *A. glycines* and their corresponding *Arsenophonus* and *Wolbachia* free equivalents reared on whole plants and detached leaves of resistant and susceptible soybean genotypes.

Materials and methods

We conducted three no-choice fecundity experiments. Two experiments introduced a fixed number of aphids to a caged whole plant (greenhouse and growth chamber experiments). A third experiment consisted of individual aphids reared on single detached plant leaves in petri dishes to determine the fecundity of individual aphids (detached leaves experiment). Analysis of the detached leaves experiment included an individual based model simulating the whole plant experiments using the detached leaves data.

Soybean genotypes and aphid strains

All experiments used four soybean plant genotypes obtained from Brian Diers at the University of Illinois. Three were soybean aphid-resistant lines: (1) LD11-4576a (*Rag1*), (2) LD11-5431a (*Rag2*), (3) LD10-30014 (*Rag1*, *Rag2*), and (4) Williams 82 (*W82*) a line that has no known resistance to soybean aphid feeding.

Five soybean aphid strains were used with varying symbiont profiles (Supplementary Table S1): (1) Bt1 (*A*+*W*−), avirulent on *Rag1*, *Rag2* and *Rag1* + *2* soybean plants (Li et al., 2004; Hill et al., 2004a,b, 2006a,b), was collected in Urbana, IL shortly after the soybean aphid was first detected in North America and kept in culture in our laboratory since 2000. The genome of this strain was recently sequenced (Giordano et al., 2020; Mathers, 2020; Wenger et al., 2020). All strains used harbor the obligate symbiont *Buchnera*. We determined that the Bt1 laboratory strain was infected with *Arsenophonus* and *Hamiltonella* but not infected with *Wolbachia* which it likely lost while in culture because all world-wide field populations tested have been found to be infected with *Wolbachia* (Giordano et al., in preparation). (2) Bt1 (*A*−*W*−), is an isofemale line derived from Bt1 via the microinjection of ampicillin (Sigma, St. Louis, MO). (3) Bt3 (*A*+*W*+), is avirulent on *Rag1* and virulent on *Rag2* soybean plants (Hill et al., 2010) and has been in culture since 2007 when it was collected from its overwintering host *Rhamnus frangula* in Springfield Fen, Indiana. This Bt3 laboratory strain is infected with *Hamiltonella*, *Arsenophonus* and *Wolbachia*. (4) Bt3 (*A*−*W*+) strain was derived from Bt3 via microinjection with ampicillin (Sigma, St. Louis, MO) while (5) Bt3 (*A*−*W*−) was derived by the microinjection of Bt3 with doxycycline hyclate (Sigma, St. Louis, MO). It was not possible to clear the strain of *Wolbachia* without also clearing *Arsenophonus*. We therefore could not generate a Bt3 (*A*+*W*−) strain. Results from the screening and curing of aphid strains can be found in Supplementary Figures S1–S3. Primers used for the screening can be found in Supplementary Tables S2, S3. Methods used to microinject aphids with antibiotics to eliminate specific bacteria can be found in Supplementary material.

Soybean aphid strains used in all experiments were cultured on detached leaves of soybean variety *W82* placed in petri dishes (100 × 20 mm) at 25°C under a 16 h photoperiod. Fifteen to 20 apterous adult females were placed on each leaf and allowed to lay nymphs. Twenty-two to three-day-old nymphs were transferred to fresh soybean leaves and reared to adulthood. Offspring that were 2–3 day old produced by this second generation of nymphs were utilized for the experiments.

Plant cultivation, insect cages and greenhouse and growth chamber experiments

All plants were grown in 13 cm diameter plastic pots using soil-less medium (LC1 Sunshine Mix, Sungro Horticultural Distribution Inc., Agawam, MA) and 15 mL of slow-release fertilizer pellets (Osmocote 19-6-12) spread evenly over the growth medium to an approximate density of 2–3 pellets per cm^2 following planting. Three seeds of each soybean genotype were planted per pot and thinned to one plant per pot after emergence, then grown to the VC stage for use in growth chamber or greenhouse experiments or V1–V3 stage for use in detached leaf experiments.

Plants for the growth chamber experiment were reared in a Conviron PGR15 (Manitoba, Canada) illuminated with 500 µmol m^2s^{-1} PAR fluorescent and incandescent lamps programmed for a 16-h photoperiod at a constant 22°C. Plants remained in the same growth chamber under the same conditions after the application of aphids and containment cages.

Growth chamber experiment cages consisted of a clear flexible plastic tube 10.5 × 45 cm with an opaque plastic top and two opposing, rectangular side silk (Rose Brand, Sun Valley, CA; vanilla, non-flame retardant, SILK0031) panels of 6 × 25.5 cm placed 3 cm from the top for ventilation. Cages for the greenhouse experiment were 17.78 × 17.78 × 40.64 cm and consisted of a wood frame and bottom with a plexiglass top and paneled on all four sides with silk. For both experiments, single VC-age plants were placed inside each cage and inoculated with 20 soybean aphid nymphs. Aphid populations on whole plants were enumerated 14 days after inoculation. We used a nonparametric scale to rate the health of the plants based on that of Hill et al. (2006a): (1) Good—little to no evidence of damage; (2) Fair—some chlorosis; (3) Poor—chlorosis with some leaf damage; (4) Very Poor—chlorosis, leaf distortion and stunting.

Detached leaf experiment

In the detached leaves experiment, fecundity of individual aphids was followed through their entire life cycle. For this experiment single unifoliate leaves with petioles were obtained from plants in the V1 or V2 stage of each variety and placed in individual petri dishes (100 × 20 mm) with a small cotton pad imbued with water wrapped around the petiole. A single aphid was placed on the top (adaxial) surface of each leaf with a fine sable paintbrush. Petri dishes were wrapped around the edge and sealed with parafilm (Bemis, Neenah, WI). Dishes were arranged on stainless steel trays so that leaves were fully illuminated and their order on the trays was rotated daily. To ensure that no contamination occurred between aphid strains in separate dishes, each strain was placed in a separate incubator. Trays were rotated daily in each chamber. Petri dishes were monitored daily, leaves were changed every 4 days, and deposited nymphs were counted and removed daily for 18 days. Petri dishes in which aphids trapped themselves in the cotton and died were eliminated from the study. The experiment was conducted at 25°C in Percival reach-in plant growth chambers, Model E-22 L, with a light intensity of 500 micromoles/m^2/s, from sixteen 17 W cool white, fluorescent lamps and two 25 W incandescent lamps with a cycle of 16 h light and 8 h dark.

Experimental design

The greenhouse and growth chamber experiments used three replicates of each of the 20 treatments (four soybean genotypes and five aphid strains) for a total of 60 plants per experiment. For the greenhouse experiment, caged pots were placed in pairs, in trays without holes and arranged using a randomized block design to account for the pairing. For the detached leaf experiment, all 20 treatments (four soybean genotypes and five aphid strains) were included. The experiment began with 12 replicates for each treatment, except for Bt3 (*A−W−*) reared on the susceptible *W82* soybean leaves that had 13 replicates. Two trials, run at different times, were conducted for the plant growth chamber experiment and a single trial was conducted in the greenhouse.

PCR test for *Arsenophonus* and *Wolbachia* bacteria

The infection profile of test *A. glycines* laboratory strains, Bt1 (*A+W−*), and Bt3 (*A+W+*), was determined in the following manner: DNA was extracted from freshly killed aphids using the DNA Micro Kit (Qiagen, Valencia, CA) following the manufacturer's protocol but with the following two changes: a 10 min incubation at 70°C after addition of the lysis buffer (AL) and the use of Wizard SV Mini columns (Promega) as these give a higher DNA yield. Specimens were macerated with a polypropylene pestle (Bel-Art Products) while viewing the specimen under a dissecting scope. Individual aphid specimens were tested with *Wolbachia* and *Arsenophonus* specific primers both as a screening tool during the process of generating the cured Bt1 and Bt3 lines as well as to confirm the infection profile of a subset of the initial and final aphids in the whole plant experiments and all the aphids that survived to the end of the detached leaves experiment. The bacterial screening primers and their respective protocols used were as follows: (1) *Wolbachia* screen: *dnaA* 2F (5′-acaattggttatatcagctg-3′) and *dnaA* 2R (5′-tacatagctatttgygttgg-3′) (Casiraghi et al., 2003) (95°C 3 min; followed by 35 cycles of 95°C 30s, 52°C 30s, 72°C 1 min); *Arsenophonus* screen: Gly1-2F (5′-cgcgtmaagccaatctaagattg-3′) designed for this work and 480R ("-cacggtactggttcactatcggtc-3′) (Sandström et al., 2001) (95°C 3 min, followed by 35 cycles of 95°C 30s, 56°C 30s, 72°C 1 min). Screening was also conducted for additional symbiotic bacteria. The list of these primers, protocols and results can be found in the supporting information (Supplementary Tables S2, S3). PCR's were conducted using 2 µL of the extracted genomic DNA, Illustra PuReTaq Ready-To-Go PCR beads (GE Healthcare), 1 µL each of 10 µM primers listed above and 21 µL of water. PCR products were run on agarose gels and visualized using GelGreen (Biotium) nucleic acid stain to verify whether amplification of the correct gene fragment had taken place. PCR products destined for sequencing were cleaned using the QIAquick PCR purification Kit (Qiagen), and concentration of DNA was measured using a Nanodrop ND-1000 spectrophotometer (Thermo Scientific). PCR products were sequenced using 20 µL reactions containing 3 µL of Big Dye v3.1 (Applied Biosystems), 1.6 µL of 2 µM primer and variable amounts of DNA and water depending on the PCR product concentration. Amount of DNA to be used in a sequencing reaction was calculated based on 5 ng of

DNA per 100 bp of PCR product to be sequenced. Sequencing reactions were cleaned using PERFORMA® Ultra 96-Well Plate (Edge Bio, Gaithersburg, Maryland) and run on the Applied Biosystem 3730xl DNA Analyzer (Life Technologies) at the University of Illinois Keck Center. Sequences were analyzed using the Sequencher® v5.0 (Gene Codes Inc., Ann Arbor, Michigan) and manually aligned using PAUP version 4.0.

Individual based population model

We developed a simple population model in SAS IML (Supplementary material 1a, b) which modeled the greenhouse and growth chamber whole plant experiments using the individual leaf experiment data. As with the whole plant experiment, each model run began with 20 individuals and ran for 14 days. Data for each individual in the model were randomly selected from the individual fecundity curves of the specific aphid biotype grown on the respective soybean variety used in the individual leaf experiment. Each day of the model, the number of individuals produced (sum of all individuals produced for the day) was determined and that number of individuals randomly selected and added as new individuals in the model starting at that day of the model run. Missing values in the matrix represent points when the aphid is no longer alive or was not yet added to the model. Zero values were used to indicate that an individual is present but not producing offspring. The number of individuals was calculated as the number of non-missing values for a given day. The model was run 3,000 times with all five aphid biotypes and four soybean varieties.

This simple model incorporates the cumulative impact of all aspects of the fecundity curves to produce an idealized fecundity rate based upon optimal conditions and does not include intraspecific competition. The model therefore isolates the impact of the different soybean varieties on aphid population growth.

Analysis methods

Whole plant—growth chamber and greenhouse experiments

Prior to analysis, aphid population counts were transformed by adding one and taking the log base 10 to correct for non-constant variance among the treatments. Variance homogeneity tests indicated that the variance between the two trials were not significant, therefore data from both trials were combined in the final analysis.

In the greenhouse experiment, cages were set up in pairs as part of a randomized complete block design. Cage pair was therefore used as a random factor in the greenhouse model. Tukey–Kramer adjustments were used for post-hoc analyses.

Several methods were tried to transform the count data from the fecundity experiment conducted in the growth chamber and greenhouse. The data were overdispersed when analyzed using a Poisson model, therefore, we used a generalized linear model (Proc Genmod, SAS ver. 9.4) with a negative binomial distribution and a log link function as suggested by Agresti (2002).

Detached leaves experiment

We characterized overall fecundity (the number of aphid nymphs deposited by individual aphids over the duration of the experiment), as well as the pattern of fecundity (day first nymph deposited, maximum number of nymphs deposited in a day, and day maximum number of nymphs were deposited), and survival rate. We also tested whether there was a pattern of variability in fecundity among the different aphid strains on the different soybean genotypes.

For the four measures that were analyzed, (1) total number of nymphs, (2) maximum number of nymphs, (3) day of first nymph, and (4) the day of maximum nymphs deposited, transformations were unsuccessful at normalizing the data or reducing hetero-skedasticity. For the same measures listed above, if the interaction term of soybean variety by aphid strain was not found to be significant, the analysis was rerun without the interaction term.

Detached leaves: aphid fecundity—total nymphs deposited per aphid

A generalized linear model (Proc Genmod, SAS ver. 9.4) with a negative binomial distribution and a log link function as suggested by Agresti (2002) was used. Tukey–Kramer post-hoc analyses were used to compare least square means.

Detached leaves: characterization of fecundity—maximum nymphs deposited

A weighted least squares approach, modeling the mean response, was used for the analysis (Proc Catmod, SAS ver. 9.4). Contrasts compare the maximum number of aphids deposited on the susceptible *W82* soybean genotype to each of the three other genotypes. Contrasts also compared lab aphid strains Bt1 ($A+W-$) to Bt3 ($A+W+$), as well as each of these strains to their derived antibiotic treated strains: Bt1 ($A+W-$) to and Bt1 ($A-W-$) and Bt3 ($A+W+$) to Bt3 ($A-W-$) and Bt3 ($A-W+$), and the two latter antibiotic treated strains to each other. A Bonferroni adjustment was used to determine alpha for multiple comparisons.

Detached leaves: characterization of fecundity—day first nymph deposited

A weighted least squares approach was not an acceptable analysis for comparing the first day that aphids were deposited due to a problem with linear dependence. Cochran–Mantel–Haenszel row mean score (Proc Freq, SAS ver. 9.4) was therefore used to assess the effect of soybean genotype and aphid strain on first day of nymph deposition. If an aphid did not deposit nymphs, it was removed from the analysis.

Detached leaves: characterization of fecundity—day maximum number of nymphs deposited

We analyzed the day that the maximum number of nymphs were deposited using a generalized linear model (Proc Genmod, SAS ver.

9.4) with a negative binomial distribution with an identify link function. The Poisson distribution resulted in an overdispersed model and a log link resulted in failure of the relative Hession convergence criteria. Tukey–Kramer post-hoc analyses were used to compare least square means.

Detached leaves: survival analysis

Two models were used to assess the effect of soybean genotype on the survival of different strains of aphids. A logistic regression event/trials model via Proc Logistic (SAS ver. 9.4) was used to model the effect of survival to day 14. In addition, Proc Phreg (SAS ver 9.4) was used to model survival functions over the duration of the study. In both cases non-significant interactions and variables were removed until only significant factors were left in the model.

Detached leaves: variability of fecundity

We used a model II ANOVA to determine whether soybean genotype had an impact on the variability of the total number of nymphs produced (Proc Nested, SAS ver. 9.4). Only aphids that survived to the end of the experiment were included in the analysis. The analysis does not allow for unequal sample size, thus a random sample of seven samples from each aphid strain/genotype combination was used in the analysis. The analysis was repeated 10 times, with a different selection of samples, to ensure that results were consistent. The *p*-values presented are averages of the *p*-values from the 10 runs. Because post-hoc tests are limited in model II ANOVAs, a set of tests were run comparing Bt1 (*A*+*W*−) to Bt3 (*A*+*W*+), Bt1 (*A*+*W*−) to Bt1 (*A*−*W*−), and Bt3 (*A*+*W*+) to each of its antibiotic-treated sub-strains Bt3 (*A*−*W*+) and Bt3 (*A*−*W*−). Comparisons were also made between the susceptible *W82* genotype and each of the resistant genotypes (*Rag1*, *Rag2*, *Rag1*+*2*) using only data from Bt1 (*A*+*W*−) and Bt3 (*A*+*W*+). As with the overall analyses, 10 runs each, using seven random samples were used for the post-hoc tests and the *p*-value was averaged over all runs. The alpha used in these analyses was Bonferroni adjusted to account for multiple tests.

Individual based population model

We ran the same ANOVA model used for the whole plant experiments for successive sets of three models representing the three replicates used in the greenhouse and growth chamber experiments (each run was randomly selected so successive model selection is still random). We calculated the average *p* value for each main effect and interaction for the 1,000 model experiments.

Results

Reproduction on whole plants

There was a significant interaction between aphid strain and soybean genotype for the greenhouse (df = 12, $X^2 = 22.53$, $p = 0.0320$) and environmental chamber experiments (df = 12, $X^2 = 39.49$, $p < 0.0001$), demonstrating aphid biotype specificity toward plant host genotypes. In both experiments, all strains of Bt3 had significantly higher aphid counts than the two strains of Bt1 (Figure 1) when grown on *Rag2*.

The two Bt1 strains, (*A*+*W*−) and (*A*−*W*−), behaved similarly, with reduced fecundity on all resistant genotypes, the three Bt3 strains, (*A*+*W*+), (*A*−*W*−), (*A*−*W*+), also behaved similarly to each other with higher fecundity on *W82* and *Rag2* and lower fecundity on *Rag1* and *Rag1* + *2* (Figure 1). There was no significant difference in the performance of all three Bt3 strains on *Rag1* (letter f), *Rag 2* (letter a), or *Rag 1* + *2* (letter d); likewise, there was no significant difference for Bt1 strains on *Rag1*, *Rag1* + *2* (letter g), or *Rag 2* (letters e, f) (Figure 1). In the greenhouse experiment, Bt3 (*A*−*W*+) had significantly lower aphid counts on *W82* plants (Figure 1A), and all three plants were severely damaged by aphid feeding as compared to the other plants at the end of the experiment. The three plants in this latter treatment were, respectively, classified as very poor, poor, and fair (using the non-parametric plant health scale referred to in the methods) at the end of the experiment. No other treatment in the greenhouse had all three plants classified as poor or fair. The susceptible *W82* genotype in the environmental chamber did not have such decrease in aphid numbers (Figure 1B). **T**here was not a significant difference attributable to the presence or absence of *Wolbachia* or *Arsenophonus* in the aphids.

Detached leaves: fecundity of individual aphids

Average number and cumulative number of nymphs deposited per day per genotype leaf over the duration of the experiment (Figure 2) were characterized by the overall fecundity (the number of nymphs deposited by individual aphids for the duration of the experiment); pattern of fecundity (maximum number of nymphs deposited in a day, day first nymph deposited, and day maximum number of nymphs were deposited); and survival rate.

Detached leaves: overall fecundity

The interaction between aphid clonal strain and soybean genotype was not significant (df = 12, $X^2 = 10.32$, $p = 0.5883$); however, both main effects were significant (soybean genotype $X^2 = 48.33$, df = 3, $p < 0.0001$; aphid strain $X^2 = 15.21$, df = 4, $p = 0.0043$). In Tukey–Kramer *post hoc* tests fecundity on all four soybean genotypes were significantly different from each other (Figure 3A). The susceptible *W82* plants had the highest number of aphid nymphs deposited (63 ± 0.94 nymphs deposited), while the *Rag1* plants had the lowest number of nymphs deposited over the same time-period (37 ± 2.32 nymphs deposited). The two Bt1 strains had significantly lower fecundity than the three Bt3 strains. The pattern of overall fecundity, with the susceptible genotype (*W82*) having the highest and *Rag1* the lowest number, was consistent across all aphid strains (Figure 3A); however, Bt1 (*A*+*W*−) and Bt1 (*A*−*W*−) deposited significantly fewer nymphs on all genotypes compared to the three Bt3 strains on the same genotypes (Figure 3B). The cumulative number of nymphs deposited between

10.3389/fmicb.2023.1209595

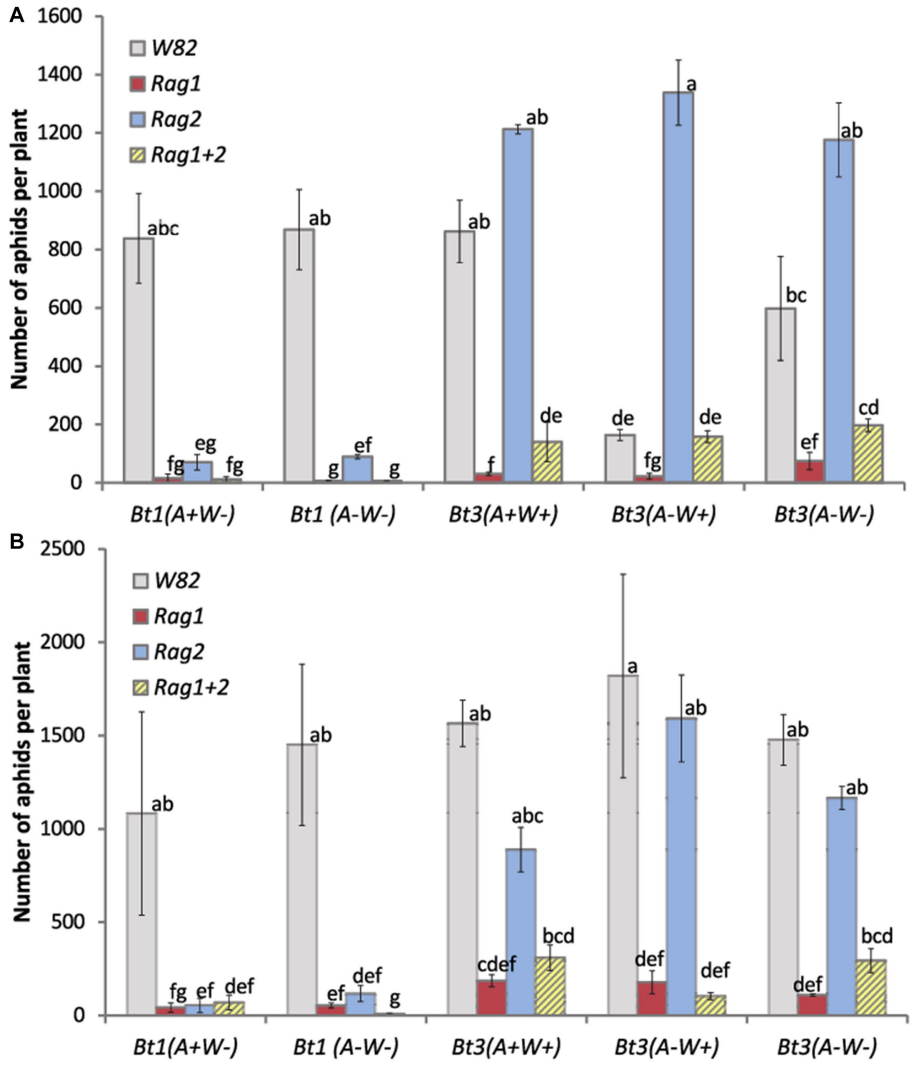

FIGURE 1
Both aphid strain and soybean genotype affected aphid population size in whole plant experiments. Average number of aphids per plant for 5 clonal strains of aphids [Bt1(*A*+*W*−), Bt1(*AW*−), Bt3(*A*+*W*+), Bt3(*A*−*W*+), Bt3(*A*−*W*−)], grown on caged whole plants in a greenhouse **(A)** and an environmental chamber **(B)** on 4 genotypes of soybean (*W82*, *Rag1*, *Rag2*, *Rag1 + 2*). Counts were made at the end of the experiment. Data were analyzed with a general model using a negative binomial distribution and a log link function. There was a significant interaction between aphid strain and soybean genotype for the greenhouse (df = 12, $X^2 = 22.53$, $p = 0.0320$) and environmental chamber experiments (df = 12, $X^2 = 39.49$, $p < 0.0001$). Means with the same letter are not significantly different using Tukey–Kramer *post hoc* comparisons ($p < 0.05$). The study included three replicates of each aphid strain/soybean variety combination for both experiments.

Bt1 and Bt3 strains on *Rag2* can be observed in Figure 2B. The presence or absence of *Wolbachia* and *Arsenophonus* did not significantly affect fecundity within the two Bt1 and three Bt3 aphid strains (Figure 3B).

Detached leaves: pattern of fecundity—maximum aphids deposited

For the maximum number of nymphs deposited, the interaction term of soybean genotype by aphid strain was not significant (df = 12, $X^2 = 19.26$, $p = 0.08214$) and was therefore removed, prior to running the main effects model. Both soybean genotype (df = 3, $X^2 = 92.83$, $p < 0.001$) and aphid strain (df = 4, $X^2 = 46.79$, $p < 0.0001$) were significant. A total of eight contrasts were tested in this experiment resulting in a Bonferroni adjusted alpha level of 0.0063. Aphids grown on the susceptible genotype (*W82*) had a higher maximum number of nymphs deposited than those cultured on any resistant genotype (*Rag1*, *Rag2*, *Rag1 + 2*) (Figure 4A). There was not a significant difference between Bt1 (*A*+*W*−) and Bt1 (*A*−*W*−), but Bt1 (*A*+*W*−) had significantly lower maximum number of nymphs deposited than Bt3 (*A*+*W*+) (Figure 4B). Bt3 (*A*+*W*+) had significantly higher maximum number of nymphs deposited than either Bt3 (*A*−*W*+) or Bt3 (*A*−*W*−), but Bt3 (*A*−*W*+) and Bt3 (*A*−*W*−) were not significantly different from each other. *Arsenophonus* significantly impacted Bt3 but not Bt1.

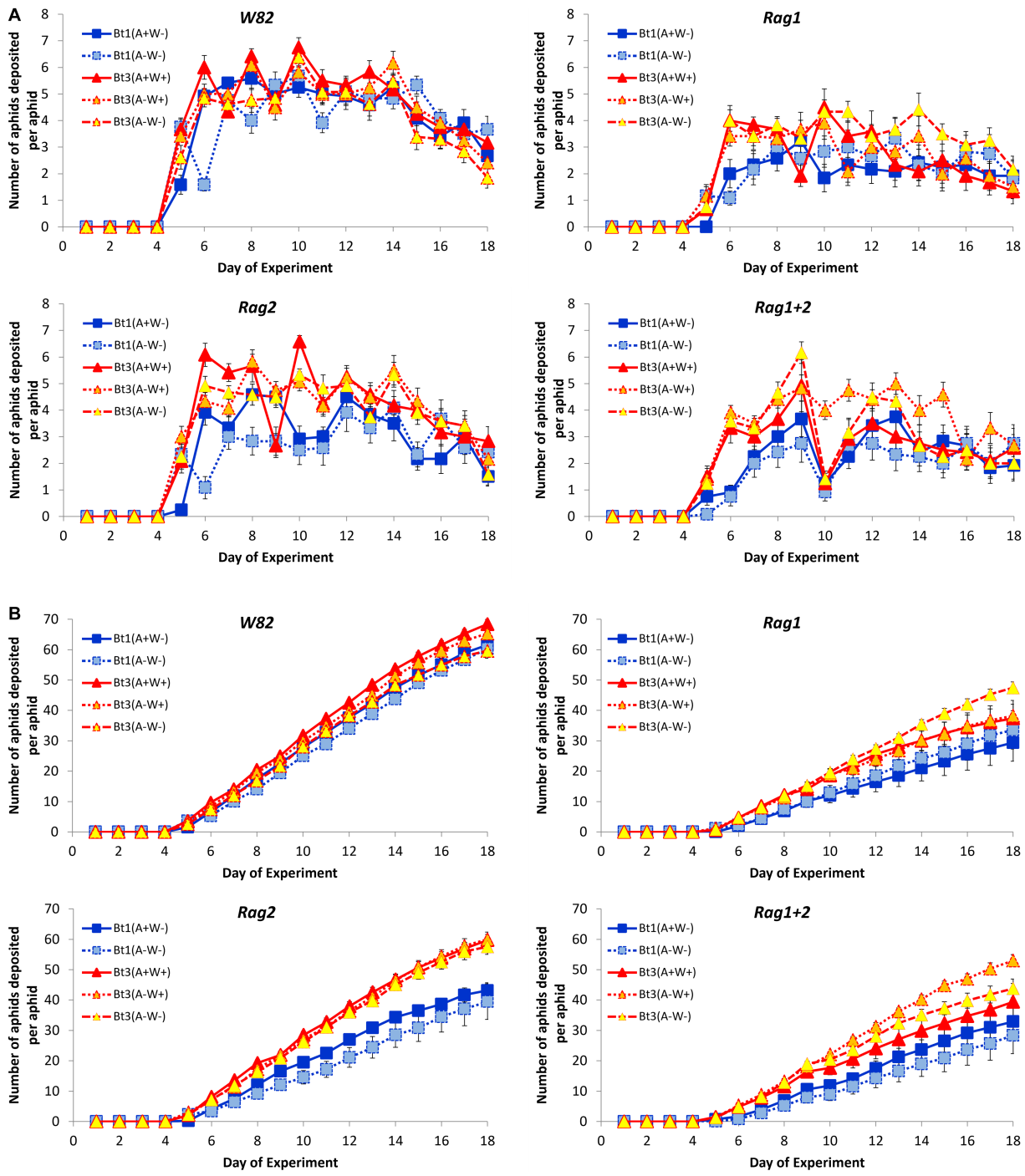

FIGURE 2
Pattern of cumulative and daily aphid nymph deposition by individual aphids on detached leaves. Average number **(A)** and cumulative number **(B)** of aphids deposited per day by strain for individual aphids grown on detached leaves of four soybean genotypes (*W82*, *Rag1*, *Rag2*, and *Rag1 + 2*). Error bars are standard errors of the average number of aphid nymph deposited. Characterizations of the fecundity curves are described in the text.

Detached leaves: characterization of fecundity—day first nymph deposited

There was a significant difference in the day that the first nymph was deposited (Cochran–Mantel–Haenszel row mean scores differ df = 4, $X^2 = 25.23$, $p < 0.0001$). When on the *W82* plant genotype all aphid strains deposited nymphs earlier than on resistant genotypes (Table 1). The Bt1(*A*+*W*−) strain deposited nymphs later than the other strains on all plant genotypes except for *Rag1 + 2* genotype where Bt1(*A*−*W*−) was the most delayed. *Arsenophonus* impacted the day of first nymph deposition in Bt1 but not Bt3.

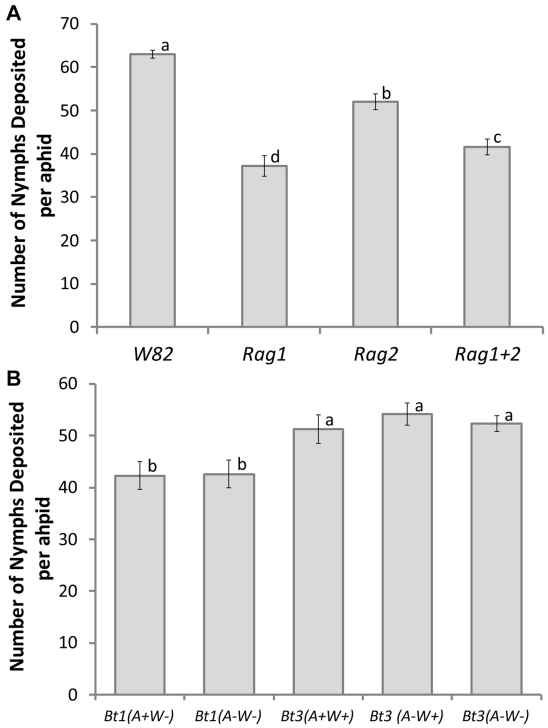

FIGURE 3
Aphid strain and soybean genotype affected number of aphid nymphs deposited on detached leaves. Average number of nymphs deposited per aphid over a 14-day period for 5 clonal strains of aphids [Bt1(*A* + *W*–), Bt1(*A*–*W*–), Bt3(*A* + *W*+), Bt3(*A*–*W*–), Bt3(*A*–*W*–)] cultured on detached leaves of 4 soybean genotypes (*W82*, *Rag1*, *Rag2*, *Rag1* + *2*). Data presented by soybean genotype **(A)** and aphid strain **(B)**. Data were analyzed with a general model using a negative binomial distribution and a log link function. Soybean variety was a significant factor in the number of nymphs deposited per aphid (X^2 = 48.33, df = 3, p < 0.0001) as was aphid strain (X^2 = 15.21, df = 4, p = 0.0043). Means with the same letter are not significantly different using Tukey–Kramer *post hoc* comparisons (p < 0.05). The study included 12 replicates of each aphid strain/soybean genotype combination except for Bt3 (*A*–*W*–) on *W82* soybean which had 13 replicates.

Detached leaves: characterization of fecundity—day maximum number of nymphs were deposited

Bt3(*A*+*W*+) was the first strain to deposit the maximum number of nymphs in a day, while Bt1(*A*–*W*–) was the last, but there was not a significant difference within the Bt1 or Bt3 strains (Figure 5) (Aphid strain effect df = 4, X^2 = 14.13, p = 0.0069). Neither soybean genotype nor the interaction was significant (strain x genotype interaction df = 12, X^2 = 17.93, p = 0.1179; genotype df = 3, X^2 = 1.53, p = 0.6752). *Arsenophonus* and *Wolbachia* did not impact the day maximum number of nymphs were deposited.

Detached leaves: survival analysis

Aphid strain had no effect on survival, but soybean genotype was a significant factor (proc logistic X^2 = 15.3293, p = 0.0016; Proc Phreg Wald X^2 = 14.70, df = 3, p = 0.0021). Aphid strains had significantly lower survival rates on *Rag1* and *Rag1* + *2* compared to the susceptible genotype (*W82*). Survival rates and functions of aphids for all strains on *Rag2* were not significantly different from aphids on the *W82* genotype (Figure 6). *Arsenophonus* and *Wolbachia* did not impact survival of aphids.

Detached leaves: variability of fecundity

There was a significant difference in the variability of total fecundity per aphid on the different genotypes (df = 3, p < 0.0001) but not among aphid strains (df = 4, p < 0.05). The analysis only included aphids that survived the entire experiment (18 days, 7 aphids per aphid strain, soybean genotype combination, see methods for more information on sample size), providing a conservative measure of variability. Aphids cultured on the susceptible genotype (*W82*) had less variability in the total number of nymphs deposited when compared to the resistant *Rag* soybean genotypes (Figure 7). No comparisons were made among the resistant genotypes. *Arsenophonus* and *Wolbachia* did not impact variability of fecundity.

Individual based population model

The overall pattern of the model runs (Figure 8) illustrates a pattern similar to that observed in the greenhouse and growth chamber experiments. In contrast to the analyses of the individual aphid data outside the model, there was a significant interaction effect between soybean variety and aphid strain (p-value was <0.001 for both the main effects and interaction in more than 99% of model experiments). The *Rag1* and *Rag 1* + *2* genotypes had a stronger impact than *Rag2*, and Bt1 strains are more strongly impacted by *Rag1*, *Rag1* + *2* and *Rag2* than are Bt3 strains. For the Bt1 strain, which does not have *Wolbachia*, *Arsenophonus* decreased fecundity on *Rag1* (100% of models significant at p < 0.05, diff = 720–402 = 315) and increased total fecundity on *Rag1* + *2* (87% of models significant at p < 0.05, diff = 864–616 = 248) (Figure 9A). *Arsenophonus* had no significant effect when Bt1 strain aphids are exposed to *Rag2* and *W82*.

For the Bt3 strain, neither *Wolbachia* nor *Arsenophonus* impacted fecundity on *Rag1*, however, *Arsenophonus* decreased fecundity on *Rag1* + *2* (87% of models significant at p < 0.05 (*A*–*W*+) vs. (*A*+*W*+), diff = 2,312–1,798 = 514) (Figure 9B). Fecundity of the Bt3 strain increased on Rag2 if both *Wolbachia* and *Arsenophonus* were present [80% of models were significant at p < 0.05 (*A*+*W*+) vs. (*A*–*W*–), diff = 4,449–3,593 = 853]. For the Bt3 strain when on W82, the presence of *Wolbachia* (whether alone or with *Arsenophonus*) resulted in higher fecundity than when *Wolbachia* was absent [100% (*A*+*W*+) vs. (*A*–*W*–) and 88% (*A*–*W*+) vs. (*A*–*W*–) models significant at p < 0.05, diff (*A*+*W*+) = 5,478–3,872 = 1,606, diff (*A*–*W*+) = 4,855–3,872 = 983].

Discussion

We did not detect differences in overall fecundity in *A. glycines* with or without *Arsenophonus* or *Wolbachia*, in experiments using whole plants or individual aphids, but did observe differences in patterns of fecundity of individual aphids on detached leaves. We also

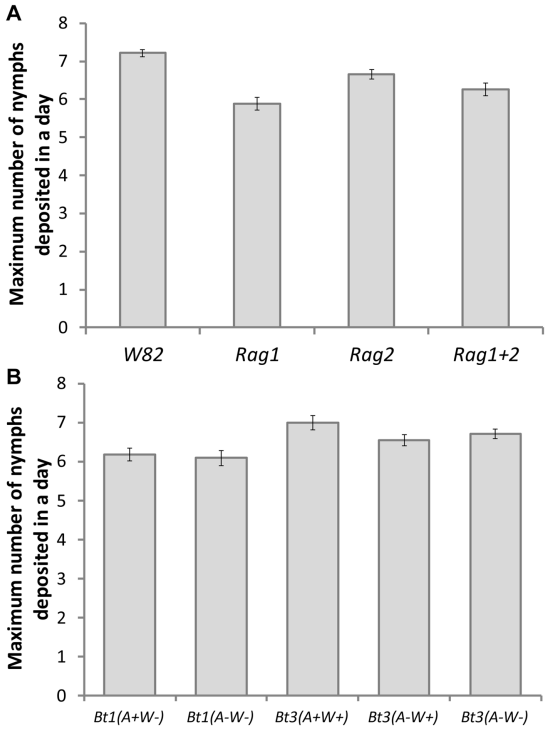

FIGURE 4
Aphid strain and soybean genotype affected maximum number of aphid nymphs deposited on detached leaves. Average number of the maximum number of nymphs deposited by an individual aphid in a single day: by genotype **(A)** and by aphid strain **(B)**. There were significant differences among genotypes (df = 3, $X^2 = 92.83$, $p < 0.001$) and aphid strains (df = 4, $X^2 = 46.79$, $p < 0.0001$). Using Bonferroni adjusted tests of specified contrasts of genotypes and strains ($\alpha = 0.0063$ see methods for more information), aphids had a higher maximum number of nymphs deposited in a day on the susceptible genotype (*W82*) than the other genotypes. Bt1(*A*+*W*–) was significantly lower than Bt3(*A*+*W*+) but not from Bt1(*A*–*W*–). Bt3(*A*+*W*+) was significantly higher than Bt3(*A*–*W*+) and Bt3(*A*–*W*–).

TABLE 1 Day nymphs were first deposited by aphid strain on soybean genotypes.

		Day first nymph deposited[a]			
Soybean genotype	Strain	Day 5	Day 6	Day 7	Average
W82	Bt1(*A*+*W*–)	8	4	0	5.3(±0.1)
	Bt1(*A*–*W*–)	12	0	0	5(±0)
	Bt3(*A*+*W*+)	11	1	0	5.1(±0.1)
	Bt3(*A*–*W*+)	12	0	0	5.2(±0.1)
	Bt3(*A*–*W*–)	10	3	0	5(±0)
Rag1	Bt1(*A*+*W*–)	0	8	1	6.1(±0.1)
	Bt1(*A*–*W*–)	6	4	0	5.4(±0.2)
	Bt3(*A*+*W*+)	6	5	1	5.6(±0.2)
	Bt3(*A*–*W*+)	7	5	0	5.6(±0.1)
	Bt3(*A*–*W*–)	5	7	0	5.4(±0.1)
Rag2	Bt1(*A*+*W*–)	2	10	0	5.8(±0.1)
	Bt1(*A*–*W*–)	9	1	0	5.1(±0.1)
	Bt3(*A*+*W*+)	9	3	0	5.3(±0.1)
	Bt3(*A*–*W*+)	11	1	0	5.3(±0.1)
	Bt3(*A*–*W*–)	9	3	0	5.1(±0.1)
Rag1 + 2	Bt1(*A*+*W*–)	4	7	0	5.6(±0.2)
	Bt1(*A*–*W*–)	0	8	4	6.3(±0.1)
	Bt3(*A*+*W*+)	7	5	0	5.4(±0.1)
	Bt3(*A*–*W*+)	7	5	0	5.5(±0.2)
	Bt3(*A*–*W*–)	6	6	0	5.4(±0.1)

Numbers in table represent the count of aphids that began depositing on a particular day of the experiment as well as the average.
[a]There was a significant difference in the day the first nymph was deposited, (Cochran–Mantel–Haenszel row mean scores differ df = 4, $\chi^2 = 25.23$, $p < 0.0001$).

observed differences in overall aphid fecundity when individual aphid data was used in simulations of whole plant experiments (Table 2, Figure 9). We were able to detect these differences in the simulations because measurements of individual aphids on detached leaves removed the impact of intraspecific competition and plant health which confounded the whole plant experiments.

On whole plants (Figure 1), Bt1 and Bt3 aphid strains produced levels of offspring matching those expected from previous published work; *Rag1* and *Rag1 + 2* plants reduced total aphid counts for all Bt1 and Bt3 strains, but *Rag2* plants only reduced counts of Bt1 strains, due to Bt3 being virulent on *Rag2* (Hill et al., 2010). As indicated earlier, there were no detectible differences due to the presence of bacterial symbionts when aphids were grown on whole plants.

The average and cumulative number of nymphs deposited for all Bt1 and Bt3 strains decreased when aphids were placed on resistant genotypes but were most pronounced for both strains when placed on *Rag1* and *Rag1 + 2* detached leaves. These results indicate that detached leaves of these resistant genotypes retained their resistance. As in the whole plant experiments, we were not able to determine differences in overall fecundity due to presence or absence of bacterial symbionts in overall fecundity of individual aphids on detached leaves, however, we were able to detect differences due to bacterial symbionts in simulations based on the individual plant study. Aphid counts in whole plant studies combine the impact of survival and fecundity of individual aphids, intraspecific competition, and the impact of aphid population size on plant health. In contrast, our observations of individual aphids on detached leaves permitted the separation of fecundity and survival patterns from the influence of competition or plant health. When the differences observed in individual aphids are combined through simulations, the individual differences were magnified, and this allowed the detection of differences among aphid populations and observed differences that exceeded the whole plant studies.

On detached leaves, secondary symbionts impacted the maximum number of nymphs deposited (Figure 4), the day the first nymph was deposited (Table 1) and may have delayed the peak deposition of aphids (Figure 5). However, the bacteria impacted Bt1 and Bt3 aphid strains differently (Table 2, Figure 9). *Arsenophonus* when together with *Wolbachia*, increased the maximum number of nymphs deposited by Bt3 strains. In Bt1, which does not have *Wolbachia*, there was not an increase. This increase with both *Arsenophonus* and *Wolbachia* present in max aphids deposited in a day may have resulted in the increased fecundity observed on *Rag2* for Bt3(*A*+*W*+) in the individual based model results. In addition, *Wolbachia* increased overall fecundity in the individual based models when Bt3 was reared on *W82*. In the

10.3389/fmicb.2023.1209595

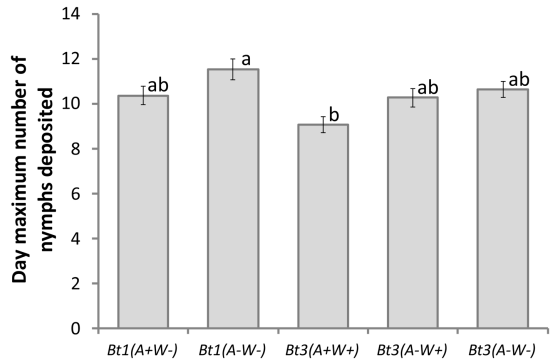

FIGURE 5
Aphid strain affected the day maximum number of aphid nymphs were deposited on detached leaves. Average day that the maximum number of nymphs were deposited by five aphid strains on four soybean genotypes (df = 4, $X^2 = 14.13$, $p = 0.0069$). Error bars are standard errors of the means. Means with the same letter are not significantly different using Tukey–Kramer *post hoc* comparisons ($p < 0.05$). Aphids that died before depositing nymphs were not included in the analysis. See Table 1 for sample size.

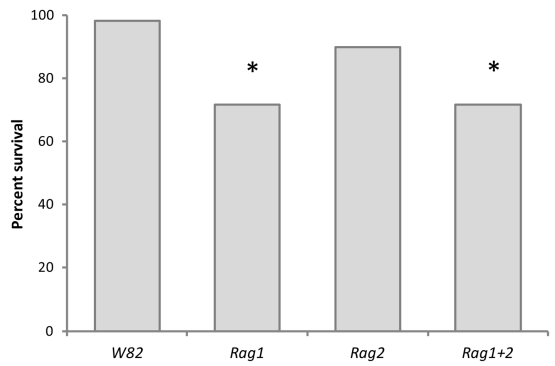

FIGURE 6
Resistant soybean genotypes decreased aphid survival on detached leaves. Percent aphid survival at day 14, cultured on leaves of four varieties of soybean (*W82*, *Rag1*, *Rag2*, *Rag1 + 2*). The percentages shown were calculated by combining all five strains of aphid used in the study [Bt1(*A+W–*), Bt1(*A–W–*), Bt3(*A+W+*), Bt3(*A–W+*), Bt3(*A–W–*)]. Asterisks indicate a significant difference ($p < 0.05$) from the susceptible *W82* soybean genotype. Aphids survived significantly better ($p < 0.05$) on the *W82* variety of soybean than on genotypes with *Rag1* or *Rag1 + 2* ($X^2 = 15.3293$, df = 3, $p = 0.0016$). There was not a significant difference between *W82* and *Rag2*.

Bt1 strains, the presence of *Arsenophonus* only impacted the first day of deposition, which was delayed when aphids were placed on *Rag1*, *Rag2*, and *W82*. When Bt1 aphids without *Arsenophonus* were reared on *Rag1 + 2*, first day of deposition was slightly delayed compared to the Bt1 strain with *Arsenophonus* (Table 1). In the individual based model, day of deposition was a probable cause for the decreased fecundity on *Rag1* and increased fecundity on *Rag1 + 2* for Bt1 aphids with *Arsenophonus*, compared to those without.

Our detached leaves study allowed us to better understand why Bt3 had higher total nymph deposition counts at the end of the study than Bt1. Similar low performance of Bt1 in comparison to Bt2 and Bt3 was also seen by Chirumamilla et al. (2014). In our experiment we determined that the difference was not due to higher mortality in Bt1, because survival of the two strains was not significantly different, but instead Bt3 starts aphid deposition earlier (Table 1) and deposits more nymphs during peak fecundity (Figure 4). Possible reasons for this difference may be genetic or other factors associated with being in culture longer than Bt3.

Fine scale observation across genotypes on detached leaves also helped us better understand how aphids respond to the different plant genotypes. Our whole plant study (Figure 1) as well as previous research has shown that all three resistant genotypes used in this experiment decrease aphid counts when compared to the susceptible genotype (*W82*) and is further confirmation that *Rag2* impacts Bt1 more than Bt3 (Hill et al., 2010).

Resistant plant genotypes decreased the maximum number of aphids deposited in a single day (Figure 4) as well as delaying the day the first nymph was deposited for both Bt1 and Bt3 strains with the possible exception of Bt3 reared on *Rag2* (Table 1). In addition, *Rag1* and *Rag1 + 2* lowered survival of all the soybean aphid strains used in the experiment (Figure 6).

Previous research has indicated that detached leaves of resistant soybean genotypes depress soybean aphid fecundity (Michel et al., 2010; Lagos-Kutz et al., 2019). Our research is a refinement of previous methods and indicates that detached leaves of the varieties used in this experiment retained levels of host resistance that impacted aphid fecundity in Bt1 and Bt3 aphids. Previous attempts at rearing aphids on detached leaves of biotype differential genotypes used methods that could have accelerated leaf senescence, resulting in decreased ability to mount host resistance modes of action. In our experiment, through direct illumination of plant leaves, frequent replacement of leaves, and the wrapping of the leaf petiole in moistened cotton, we were able to maintain healthy leaves throughout the experiment and the cultures for an extended period (18 days rather than 8 days).

One of the advantages of comparing results from whole plants and detached leaves is that the controlled observation made on detached leaves can compensate for some of the possible factors that negatively impact whole plant cage studies. The patterns observed on whole plants in greenhouses or growth chambers are the result of population dynamics (fecundity, intraspecific competition, survival) and host health and resistance. As was seen in the greenhouse experiments, plant health can be compromised in whole plant experiments as aphid populations increase. Poor host health then reduced aphid populations. This occurs on the hosts most likely to have rapid aphid growth thereby confounding plant health effects with aphid population growth. Individual based models remove this impact by removing intraspecific competition and removing host health effects by maintaining healthy leaves resulting in a closer approximation to the aphid intrinsic rate of increase. Combining individual data with individual based models of population growth therefore isolates the impact of fecundity and host resistance from intraspecific competition and host health. Moreover, the finer observations obtained through individual aphid studies on detached leaves provides fecundity curves necessary for individual based modeling of the evolution of virulence (O'Keefe and Antonovics, 2002; DeAngelis and Mooij, 2005; Schofield et al., 2005).

Previous work has used patterns of fecundity, such as those obtained through this research, in individual based modeling (DeAngelis and Mooij, 2005) to determine optimal refugia with transgenic crops to reduce the evolution of resistance in fall armyworms (Garcia et al., 2016) and pollen beetles (Stratonovitch et al., 2014); to reduce the evolution of pesticide resistance in mosquitoes (Barbosa

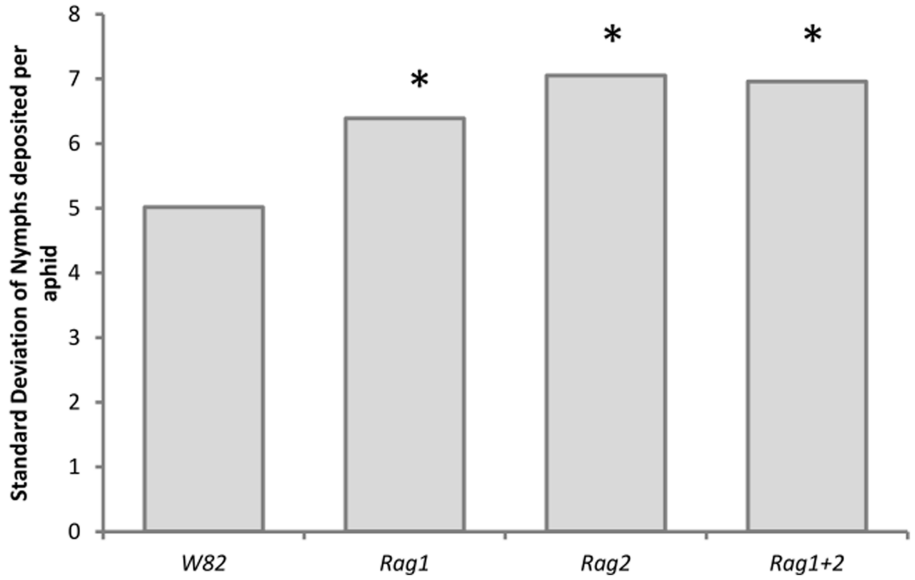

FIGURE 7
Resistant soybean genotypes increased variability of total fecundity per aphid on detached leaves. Standard deviation of the total number of nymphs deposited by aphids that survived to the end of the experiment (18 days). The standard deviation was calculated across all five strains for each plant genotype. There is a significant difference in the variation of nymphs deposited using model II ANOVA testing for significant difference of variation (df = 3, $p < 0.0001$). Asterisks indicate a significant difference ($p < 0.05$) from the *W82* soybean genotype. *W82* genotype was significantly less variable that *Rag1, Rag2* or *Rag1 + 2*.

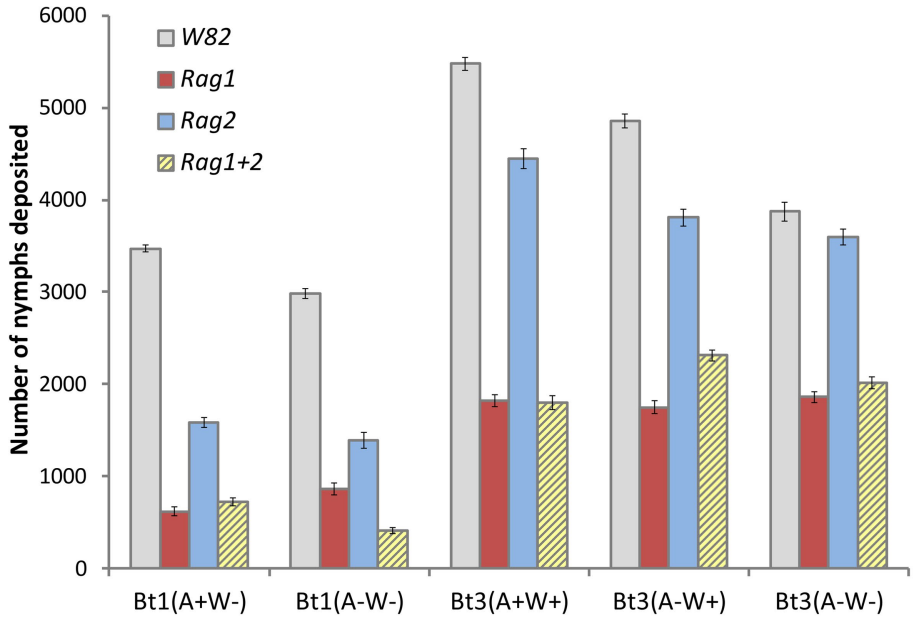

FIGURE 8
Simulations using individual leaf data found significant interactions similar to those in whole plant experiments. Average number of aphids per plant from simulations of whole plant experiment using individual leaf data. The study simulated five clonal strains of aphids [Bt1(*A*+*W*−), Bt1(*A*−*W*−), Bt3(*A*+*W*+), Bt3(*A*−*W*+), Bt3(*A*−*W*−)], grown on four genotypes of soybean (*W82*, *Rag1*, *Rag2*, *Rag1 + 2*) in each of 1,000 simulated experiments. The average represents the average of the average number of aphids per plant and error bars represent the average standard error. Using the same statistical method as used in the whole plant experiment, there was a significant interaction effect in more than 99% of the model runs.

et al., 2018); and maximize treatments for sea lice on farmed salmon (McEwan et al., 2015). These papers used, as a key parameter of these models, the rate of reproduction of individual organisms. The more detailed information provided by our group combined with other information on aphid movement patterns can result in more precise and better models predicting the evolution of virulence which in turn can be used in Integrated Pest Management (IPM) and resistant plant variety plans. This has been particularly important for increasing the longevity of genetically modified resistant crops including cotton and corn (Ives et al., 2017; Takahashi et al., 2017; Shrestha et al., 2018).

Plant Variety		Rag1		Rag1+2		Rag2		W82		Nymphs Deposited
	Bt1 Strain	(A+W-)	(A-W-)	(A+W-)	(A-W-)	(A+W-)	(A-W-)	(A+W-)	(A-W-)	
Rag1	(A+W-)		87%	37%	94%	100%	100%	100%	100%	616
	(A-W-)			47%	100%	100%	100%	100%	100%	864
Rag1+2	(A+W-)				100%	100%	100%	100%	100%	720
	(A-W-)					100%	100%	100%	100%	405
Rag2	(A+W-)						30%	100%	100%	1587
	(A-W-)							100%	100%	1389
W82	(A+W-)								32%	3471
	(A-W-)									2983

Plant Variety		Rag1			Rag1+2			Rag2			W82			Nymphs Deposited
	Bt3 Strain	(A+W+)	(A-W+)	(A-W-)	(A+W+)	(A-W+)	(A-W-)	(A+W+)	(A-W+)	(A-W-)	(A+W+)	(A-W+)	(A-W-)	
Rag1	(A+W+)		2%	1%	2%	82%	9%	100%	100%	100%	100%	100%	100%	1824
	(A-W+)			3%	1%	94%	28%	100%	100%	100%	100%	100%	100%	1749
	(A-W-)				1%	78%	4%	100%	100%	100%	100%	100%	100%	1858
Rag1+2	(A+W+)					86%	17%	100%	100%	100%	100%	100%	100%	1798
	(A-W+)						26%	100%	100%	100%	100%	100%	100%	2312
	(A-W-)							100%	100%	100%	100%	100%	100%	2011
Rag2	(A+W+)								37%	80%	81%	4%	28%	4446
	(A-W+)									1%	100%	94%	0%	3810
	(A-W-)										100%	99%	3%	3593
W82	(A+W+)											12%	100%	5478
	(A-W+)												88%	4855
	(A-W-)													3872

FIGURE 9
Proportion of model runs with significant differences ($p < 0.05$) among Bt1 (top) and Bt3 (bottom) biotype strains for all soybean varieties. Differences outside the diagonal, comparing results on the same soybean variety, are grayed out. Comparisons with a larger proportion of significant differences are purple/pink, those with a lower proportion are pale blue. Differences of 100% only occurred outside the diagonal and were left white.

TABLE 2 Significant measures of *Arsenophonus* and *Wolbachia* fecundity on soybean aphid reproduction by experiment.

Experiment	Measure	*Arsenophonus*	*Wolbachia*	*Arsenophonus* + *Wolbachia*
Detached/individual leaf				
	Maximum number of aphids deposited	↑ Bt3 increased (on all plant varieties)		
	Day first aphid deposited	↓Bt1 deposit later (on Rag1, Rag2, W82)		
individual based model				
	Bt1 effects	↓ decreased on Rag1, ↑ increased on Rag1 + 2		
	Bt3 effects	↓ decreased on Rag1 + 2	↑ increased on W82	↑ increased on Rag2

Only significant results are included in the table. Results from the whole plant study and some measures from the detached leaf/individual leaf study did not have significant effects and thus were not included in the table.

In the detached leaf experiment, all aphid strains had low variability in aphid fecundity across individuals on *W82* but higher variability on resistant genotypes (Figure 7). This is surprising given that the aphid strains used are inbred clonal laboratory strains and that the antibiotic-treated strains are parthenogenetic isofemale lines from which similar responses are expected. We hypothesize that this variable response to plant resistance may result from genetic, epigenetic or symbiont differences that can arise within a clonal line (Figueroa et al., 2018) and/or unequally expressed antibiosis in leaves. Genetic variability within clonal lines has potential for providing an avenue for the evolution of virulence in the soybean aphid. Moreover, this variability in iso-female parthenogenetic laboratory lines, points to the even higher potential for genetic diversity in sexually reproducing and outbred field populations. The high potential for the development of virulence has been observed in field populations of the soybean aphid (Wille and Hartman, 2009). High levels of genic and genotypic diversity have also been observed in the invasive population of *Myzus persicae* in Australia (Wilson et al., 2002). Our observations of range of response of genetic diversity in parthenogenetic clonal laboratory lines of the soybean aphid, as well

as previously published observations of the potential for the development of diversity in other clonal aphids (Blackman, 1979; Lushai et al., 2000; Wilson et al., 2002) should be considered when developing a strategy of how to best use resistant plant genotypes in the field for soybean aphid control.

This study shows that symbionts and plant genotypes impact soybean aphid population growth through multiple aspects of fecundity, and when combined result in significant changes in aphid population growth. In addition, host resistance impacts on fecundity that were difficult to observe when analyzing the detached leaf experiment data (Figure 2) were clear when this data was used in individual based population models (Figure 8).

Future work

The impact of *Arsenophonus* and *Wolbachia* on soybean aphid virulence on resistant soybean genotypes, when aphids and plants are grown in optimal conditions, is difficult to characterize because it is dependent on both the aphid strain and the plant genotype. As both this work and that of others indicate, costs, and benefits due to infections with secondary symbionts can be subtle and difficult to observe fully in the laboratory (Montllor et al., 2002; Koga et al., 2003; Russell and Moran, 2006; Weldon et al., 2013; Oliver et al., 2014; Zytynska and Weisser, 2016). Some of the difficulty arises from the fact that costs and benefits are not only aphid-strain dependent but can also vary among individuals within an aphid strain. It is therefore important that future studies, to detect the impact of facultative symbionts in the soybean aphid, be conducted at a fine scale using individual aphids and we would additionally suggest implementing simulations to identify the effects of host pest interactions on pest population dynamics.

Moreover the effect of *Wolbachia* and *Arsenophonus* in the soybean aphid may be more readily detected when the aphid and its host plant are exposed to stress such as (1) exposure to high and low temperatures, (2) poor plant nutrient status such as low iron, (3) toxin exposure including pesticides, and (4) plant chemistry of the overwintering hosts *Rhamnus cathartica, R. alnifolia* and possibly *Frangula alnus* (syn. *Rhamnus frangula*) (Voegtlin et al., 2004, 2005).

Data availability statement

The original contributions presented in the study are included in the article/Supplementary material, further inquiries can be directed to the corresponding authors.

Ethics statement

The manuscript presents research on animals that do not require ethical approval for their study.

Author contributions

RG, EPW, CBH, and GLH conceived the study. RG, EPW, CBH, RM, AF, AL, AKD, TKH, FNS-A, and MQN carried out the work of setting up experiments, microinjections, testing of aphids infection status, and collected the data. RG, EPW, and CBH analyzed data. EPW wrote the model. RG, CBH, and GLH secured funding. RG and EPW wrote the manuscript. All authors contributed to the article and approved the submitted version.

Funding

This work was supported by generous grants from the U.S. Mid-West farmers through the checkoff program funds from the United Soybean Board (USB), Illinois Soybean Association (ISA), and the North Central Soybean Research Program (NCSRP) to RG and GLH. Funding was also provided by USDA, Agricultural Research Service, Integrated Management of Soybean Pathogens and Pests, Accession number 432114 to GLH.

Acknowledgments

The authors thank Brian Diers and Troy Cary for providing soybean seeds. We also thank David Voegtlin for always being willing to share his vast knowledge of aphids and specifically soybean aphid plant-host associations. Jim Nardi for support and comments on the manuscript and Alfredo Ghezzi for technical support. Alvaro Hernandez, Leslie Benson and Chris Wright at the University of Illinois Keck Center for sequencing support. The first author thanks Geoffrey Levin for facilitating the installation of the incubators and Carol Augspurger for the generous use of her laboratory which made it possible to complete this work. This work is dedicated to the memory of Dr. Richard E. Joost who believed that basic research was essential to the advancement of agriculture and whose support made this work possible. This is contribution #1591 from the Institute of Environment at Florida International University.

Conflict of interest

The authors declare that the research was conducted in the absence of any commercial or financial relationships that could be construed as a potential conflict of interest.

Publisher's note

Supplementary material

The Supplementary material for this article can be found online at: https://www.frontiersin.org/articles/10.3389/fmicb.2023.1209595/full#supplementary-material

References

Agresti, A. (2002). *Categorical data analysis. Wiley Series in Probability and Statistics*. Hoboken, NJ: John Wiley & Sons.

Alt, J., and Ryan-Mahmutagic, M. (2013). Soybean aphid biotype 4 identified. *Crop Sci.* 53, 1491–1495. doi: 10.2135/cropsci2012.11.0672

Bahlai, C. A., van der Werf, W., O'Neal, M., Hemerik, L., and Landis, D. A. (2015). Shifts in dynamic regime of an invasive lady beetle are linked to the invasion and insecticidal management of its prey. *Ecol. Appl.* 25, 1807–1818. doi: 10.1890/14-2022.1

Bai, X., Zhang, W., Orantes, L., Jun, T.-H., Mittapalli, O., Mian, M. A. R., et al. (2010). Combining next-generation sequencing strategies for rapid molecular resource development from an invasive aphid species, Aphis glycines. *PLoS ONE* 5:e11370. doi: 10.1371/journal.pone.0011370

Bansal, R., Mian, M. A. R., and Michel, A. P. (2013). Microbiome diversity of Aphis glycines with extensive superinfection in native and invasive populations. *Environ. Microbiol. Rep.* 6, 57–69. doi: 10.1111/1758-2229.12108

Bansal, R., and Michel, A. (2015). "Molecular adaptations of aphid biotypes in overcoming host-plant resistance" in *Short views on insect genomics and proteomics*. eds. C. Raman, M. Goldsmith and T. Agunbiade (Cham: Springer), 75–93.

Barbosa, S., Kay, K., Chitnis, N., and Hastings, I. M. (2018). Modelling the impact of insecticide-based control interventions on the evolution of insecticide resistance and disease transmission. *Parasit. Vectors* 11:482. doi: 10.1186/s13071-018-3025-z

Barros, L. G., Avelino, B. B., da Silva, D. C. G., Ferreira, E. G. C., Castanho, F. M., Ferreira, M. E., et al. (2023). Mapping of a soybean rust resistance in PI 594756 at the Rpp 1 locus. *Mol. Breeding* 43:12. doi: 10.1007/s11032-023-01358-4

Bass, C., and Field, L. M. (2011). Gene amplification and insecticide resistance. *Pest Manag. Sci.* 67, 886–890. doi: 10.1002/ps.2189

Bass, C., Zimmer, C. T., Riveron, J. M., Wilding, C. S., Wondji, C. S., Kaussmann, M., et al. (2013). Gene amplification and microsatellite polymorphism underlie a recent insect host shift. *Proc. Natl. Acad. Sci. U. S. A.* 110, 19460–19465. doi: 10.1073/pnas.1314122110

Bensadia, F., Boudreault, S., Guay, J.-F., Michaud, D., and Cloutier, C. (2006). Aphid clonal resistance to a parasitoid fails under heat stress. *J. Insect Physiol.* 52, 146–157. doi: 10.1016/j.jinsphys.2005.09.011

Biere, A., and Tack, A. J. M. (2013). Evolutionary adaptation in three-way interactions between plants, microbes and arthropods. *Funct. Ecol.* 27, 646–660. doi: 10.1111/1365-2435.12096

Blackman, R. L. (1979). Stability and variation in aphid clonal lineages. *Biol. J. Linn. Soc.* 11, 259–277. doi: 10.1111/j.1095-8312.1979.tb00038.x

Blackman, R. L., and Eastop, V. F. (2000). *Aphids on the world's crops: an identification and information guide*. Wiley, New York.

Bressan, A. (2014). Emergence and evolution of *Arsenophonus* bacteria as insect-vectored plant pathogens. *Infect. Genet. Evol.* 22, 81–90. doi: 10.1016/j.meegid.2014.01.004

Bressan, A., Sémétey, O., Arneodo, J., Lherminier, J., and Boudon-Padieu, E. (2009). Vector transmission of a plant-pathogenic bacterium in the *Arsenophonus* clade sharing ecological traits with facultative insect endosymbionts. *Phytopathology* 99, 1289–1296. doi: 10.1094/PHYTO-99-11-1289

Buchner, P. (1965). "Aphids" in *Endosymbiosis of animals with plant microorganisms*. ed. P. Buchner (New York: Interscience), 297–332.

Casiraghi, M., Werren, J. H., Bazzocchi, C., Biserni, A., and Bandi, C. (2003). dnaA gene sequences from *Wolbachia pipientis* support subdivision into supergroups and provide no evidence for recombination in the lineages infecting nematodes. *Parassitologia* 45, 13–18.

Caspi-Fluger, A., and Zchori-Fein, E. (2010). Do plants and insects share the same symbionts? *Isr. J. Plant Sci.* 58, 113–119. doi: 10.1560/ijps.58.2.113

Chirumamilla, A., Hill, C. B., and Hartman, G. L. (2014). Stability of soybean aphid resistance in soybean across different temperatures. *Crop Sci.* 54, 2557–2563. doi: 10.2135/cropsci2014.05.0393

Clark, M. A., Baumann, L., Munson, M. A., Baumann, P., Campbell, B. C., Duffus, J. E., et al. (1992). The eubacterial endosymbionts of whiteflies (Homoptera: Aleyrodoidea) constitute a lineage distinct from the endosymbionts of aphids and mealybugs. *Curr. Microbiol.* 25, 119–123. doi: 10.1007/BF01570970

Darby, A. C., Choi, J.-H., Wilkes, T., Hughes, M. A., Werren, J. H., Hurst, G. D. D., et al. (2010). Characteristics of the genome of *Arsenophonus nasoniae*, son-killer bacterium of the wasp Nasonia. *Insect Mol. Biol.* 19, 75–89. doi: 10.1111/j.1365-2583.2009.00950.x

Davis, M. J., Ying, Z., Brunner, B. R., Pantoja, A., and Ferwerda, F. H. (1998). Rickettsial relative associated with papaya bunchy top disease. *Curr. Microbiol.* 36, 80–84. doi: 10.1007/s002849900283

DeAngelis, D. L., and Mooij, W. M. (2005). Individual-based modeling of ecological and evolutionary processes. *Annu. Rev. Ecol. Evol. Syst.* 36, 147–168. doi: 10.1146/annurev.ecolsys.36.102003.152644

Degnan, P. H., and Moran, N. A. (2007). Evolutionary genetics of a defensive facultative symbiont of insects: exchange of toxin-encoding bacteriophage. *Mol. Ecol.* 17, 916–929. doi: 10.1111/j.1365-294x.2007.03616.x

Di Prisco, G., Cavaliere, V., Annoscia, D., Varricchio, P., Caprio, E., Nazzi, F., et al. (2013). Neonicotinoid clothianidin adversely affects insect immunity and promotes replication of a viral pathogen in honey bees. *Proc. Natl. Acad. Sci. U. S. A.* 110, 18466–18471. doi: 10.1073/pnas.1314923110

Duron, O., Bouchon, D., Boutin, S., Bellamy, L., Zhou, L., Engelstädter, J., et al. (2008). The diversity of reproductive parasites among arthropods: *Wolbachia* do not walk alone. *BMC Biol.* 6:27. doi: 10.1186/1741-7007-6-27

Duron, O., Wilkes, T. E., and Hurst, G. D. D. (2010). Interspecific transmission of a male-killing bacterium on an ecological timescale. *Ecol. Lett.* 13, 1139–1148. doi: 10.1111/j.1461-0248.2010.01502.x

Elton, C. S. (2000). *The ecology of invasions by animals and plants*. University of Chicago Press, Chicago.

Fenn, K., and Blaxter, M. (2007). *Coexist, cooperate and thrive: Wolbachia as long-term symbionts of filarial nematodes*. Larger, Basel.

Ferrari, J., Darby, A. C., Daniell, T. J., Godfray, H. C. J., and Douglas, A. E. (2004). Linking the bacterial community in pea aphids with host-plant use and natural enemy resistance. *Ecol. Entomol.* 29, 60–65. doi: 10.1111/j.1365-2311.2004.00574.x

Feyereisen, R., Dermauw, W., and Van Leeuwen, T. (2015). Genotype to phenotype, the molecular and physiological dimensions of resistance in arthropods. *Pestic. Biochem. Physiol.* 121, 61–77. doi: 10.1016/j.pestbp.2015.01.004

Figueroa, C. C., Fuentes-Contreras, E., Molina-Montenegro, M. A., and Ramírez, C. C. (2018). Biological and genetic features of introduced aphid populations in agroecosystems. *Curr. Opin. Insect. Sci.* 26, 63–68. doi: 10.1016/j.cois.2018.01.004

Fox, C. M., Kim, K.-S., Cregan, P. B., Hill, C. B., Hartman, G. L., and Diers, B. W. (2014). Inheritance of soybean aphid resistance in 21 soybean plant introductions. *Theor. Appl. Genet.* 127, 43–50. doi: 10.1007/s00122-013-2199-1

Frago, E., Dicke, M., and Godfray, H. C. J. (2012). Insect symbionts as hidden players in insect-plant interactions. *Trends Ecol. Evol.* 27, 705–711. doi: 10.1016/j.tree.2012.08.013

Francis, F., Guillonneau, F., Leprince, P., De Pauw, E., Haubruge, E., Jia, L., et al. (2010). Tritrophic interactions among *Macrosiphum euphorbiae* aphids, their host plants, and endosymbionts: investigation by a proteomic approach. *J. Insect Physiol.* 56, 575–585. doi: 10.1016/j.jinsphys.2009.12.001

Fukatsu, T., and Ishikawa, H. (1992). A novel eukaryotic extracellular symbiont in an aphid, Astegopteryx styraci (Homoptera, Aphididae, Hormaphidinae). *J. Insect Physiol.* 38, 765–773. doi: 10.1016/0022-1910(92)90029-d

Garcia, A. G., Ferreira, C. P., Cônsoli, F. L., and Godoy, W. A. C. (2016). Predicting evolution of insect resistance to transgenic crops in within-field refuge configurations, based on larval movement. *Ecol. Complex.* 28, 94–103. doi: 10.1016/j.ecocom.2016.07.006

Gherna, R. L., Werren, J. H., Weisburg, W., Cote, R., Woese, C. R., Mandelco, L., et al. (1991). *Arsenophonus nasoniae* gen. Nov., sp. nov., the causative agent of the son-killer trait in the parasitic wasp Nasonia vitripennis. *Int. J. Syst. Bacteriol.* 41, 563–565. doi: 10.1099/00207713-41-4-563

Giordano, R., Donthu, R. K., Zimin, A. V., Julca Chavez, I. C., Gabaldon, T., van Munster, M., et al. (2020). Soybean aphid biotype 1 genome: insights into the invasive biology and adaptive evolution of a major agricultural pest. *Insect Biochem. Mol. Biol.* 120:103334. doi: 10.1016/j.ibmb.2020.103334

Hallett, R. H., Bahlai, C. A., Xue, Y., and Schaafsma, A. W. (2013). Incorporating natural enemy units into a dynamic action threshold for the soybean aphid, Aphis glycines (Homoptera: Aphididae). *Pest Manag. Sci.* 70, 879–888. doi: 10.1002/ps.3674

Hallmann, C. A., Foppen, R. P. B., van Turnhout, C. A. M., de Kroon, H., and Jongejans, E. (2014). Declines in insectivorous birds are associated with high neonicotinoid concentrations. *Nature* 511, 341–343. doi: 10.1038/nature13531

Hansen, A. K., Jeong, G., Paine, T. D., and Stouthamer, R. (2007). Frequency of secondary symbiont infection in an invasive psyllid relates to parasitism pressure on a geographic scale in California. *Appl. Environ. Microbiol.* 73, 7531–7535. doi: 10.1128/aem.01672-07

Hebert, S. L., Jia, L., and Goggin, F. L. (2007). Quantitative differences in aphid virulence and foliar symptom development on tomato plants carrying the mi resistance gene. *Environ. Entomol.* 36, 458–467. doi: 10.1093/ee/36.2.458

Heimpel, G. E., Yang, Y., Hill, J. D., and Ragsdale, D. W. (2013). Environmental consequences of invasive species: greenhouse gas emissions of insecticide use and the role of biological control in reducing emissions. *PLoS One* 8:e72293. doi: 10.1371/journal.pone.0072293

Henry, L. M., Peccoud, J., Simon, J.-C., Hadfield, J. D., Maiden, M. J. C., Ferrari, J., et al. (2013). Horizontally transmitted symbionts and host colonization of ecological niches. *Curr. Biol.* 30:183. doi: 10.1016/j.cub.2013.07.029

Hesler, L. S., Chiozza, M. V., O'Neal, M. E., Mac Intosh, G. C., Tilmon, K. J., Chandrasena, D. I., et al. (2013). Performance and prospects of rag genes for management of soybean aphid. *Entomol. Exp. Appl.* 147, 201–216. doi: 10.1111/eea.12073

Hill, C. B., Chirumamilla, A., and Hartman, G. L. (2012). Resistance and virulence in the soybean-Aphis glycines interaction. *Euphytica* 186, 635–646. doi: 10.1007/s10681-012-0695-z

Hill, C. B., Crull, L., Herman, T. K., Voegtlin, D. J., and Hartman, G. L. (2010). A new soybean aphid (Hemiptera: Aphididae) biotype identified. *J. Econ. Entomol.* 103, 509–515. doi: 10.1603/ec09179

Hill, C. B., Li, Y., and Hartman, G. L. (2004a). Resistance to the soybean aphid in soybean germplasm. *Crop Sci.* 44, 98–106. doi: 10.2135/cropsci2004.9800

Hill, C. B., Li, Y., and Hartman, G. L. (2004b). Resistance of glycine species and various cultivated legumes to the soybean aphid (Homoptera: Aphididae). *J. Econ. Entomol.* 97, 1071–1077. doi: 10.1603/0022-0493(2004)097[1071:ROGSAV]2.0.CO;2

Hill, C. B., Li, Y., and Hartman, G. L. (2006a). A single dominant gene for resistance to the soybean aphid in the soybean genotype Dowling. *Crop Sci.* 46, 1601–1605. doi: 10.2135/cropsci2005.11-0421

Hill, C. B., Li, Y., and Hartman, G. L. (2006b). Soybean aphid resistance in soybean Jackson is controlled by a single dominant gene. *Crop Sci.* 46, 1606–1608. doi: 10.2135/cropsci2005.11-0438

Huger, A. M., Skinner, S. W., and Werren, J. H. (1985). Bacterial infections associated with the son-killer trait in the parasitoid wasp Nasonia (= Mormoniella) vitripennis (Hymenoptera: Pteromalidae). *J. Invertebr. Pathol.* 46, 272–280. doi: 10.1016/0022-2011(85)90069-2

Hunt, D., Foottit, R., Gagnier, D., and Baute, T. (2003). First Canadian records of Aphis glycines (Hemiptera: Aphididae). *Can. Entomol.* 135, 879–881. doi: 10.4039/n03-027

Irwin, M. E., Kampmeier, G., and Weisser, W. (2007). "Aphid movement: process and consequences" in *Aphids as crop pests*. eds. H. Emden and R. Harrington (Wallingford: CABI), 153–186.

Irwin, M. E., Thresh, J. M., and Harrison, B. D. (1988). Long-range aerial dispersal of cereal aphids as virus vectors in North America. *Philos. Trans. R. Soc. London B Biol. Sci.* 321, 421–446. doi: 10.1098/rstb.1988.0101

Ives, A. R., Paull, C., Hulthen, A., Downes, S., Andow, D. A., Haygood, R., et al. (2017). Spatio-temporal variation in landscape composition may speed resistance evolution of pests to Bt crops. *PLoS One* 12:e0169167. doi: 10.1371/journal.pone.0169167

Johnson, K. D., O'Neal, M. E., Ragsdale, D. W., Difonzo, C. D., Swinton, S. M., Dixon, P. M., et al. (2009). Probability of cost-effective management of soybean Aphid (Hemiptera: Aphididae) in North America. *J. Econ. Entomol.* 102, 2101–2108. doi: 10.1603/029.102.0613

Jousselin, E., Cœur d'Acier, A., Vanlerberghe-Masutti, F., and Duron, O. (2013). Evolution and diversity of *Arsenophonus* endosymbionts in aphids. *Mol. Ecol.* 22, 260–270. doi: 10.1111/mec.12092

Kaur, R., Shropshire, J. D., Cross, K. L., Leigh, B., Mansueto, A. J., Stewart, V., et al. (2021). Living in the endosymbiotic world of *Wolbachia*: a centennial review. *Cell Host Microbe* 29, 879–893. doi: 10.1016/j.chom.2021.03.006

Kim, K.-S., Hill, C. B., Hartman, G. L., Mian, M. A. R., and Diers, B. W. (2008). Discovery of soybean aphid biotypes. *Crop Sci.* 48:923. doi: 10.2135/cropsci2007.08.0447

Kim, C. S., Schaible, G., Garrett, L., Lubowski, R., and Lee, D. (2008). Economic impacts of the U. S. soybean aphid infestation: a multi-regional competitive dynamic analysis. *Agric. Econ. Res. Rev.* 37, 227–242. doi: 10.1017/S1068280500003026

Koga, R., Tsuchida, T., and Fukatsu, T. (2003). Changing partners in an obligate symbiosis: a facultative endosymbiont can compensate for loss of the essential endosymbiont Buchnera in an aphid. *Proc. Biol. Sci.* 270, 2543–2550. doi: 10.1098/rspb.2003.2537

Lagos-Kutz, D., Pawlowski, M. L., Diers, B. W., Purandare, S. R., Tilmon, K. J., and Hartman, G. L. (2019). Virulence of soybean aphid, Aphis glycines (Hemiptera: Aphididae) clones on detached leaves and whole plants. *J. Kansas Entomol. Soc.* 92, 497–511. doi: 10.2317/0022-8567-92.3.497

Li, S.-J., Ahmed, M. Z., Lv, N., Shi, P.-Q., Wang, X.-M., Huang, J.-L., et al. (2017). Plantmediated horizontal transmission of *Wolbachia* between whiteflies. *ISME J.* 11, 1019–1028. doi: 10.1038/ismej.2016.164

Li, Y., Hill, C. B., and Hartman, G. L. (2004). Effect of three resistant soybean genotypes on the fecundity, mortality, and maturation of soybean aphid (Homoptera: Aphididae). *J. Econ. Entomol.* 97, 1106–1111. doi: 10.1093/jee/97.3.1106

Liu, S., Chougule, N. P., Vijayendran, D., and Bonning, B. C. (2012). Deep sequencing of the transcriptomes of soybean aphid and associated endosymbionts. *PLoS One* 7:e45161. doi: 10.1371/journal.pone.0045161

Liu, J., Wu, K., Hopper, K. R., and Zhao, K. (2004). Population dynamics of Aphis glycines (Homoptera: Aphididae) and its natural enemies in soybean in northern China. *Ann. Entomol. Soc. Am.* 97, 235–239. doi: 10.1603/0013-8746(2004)097[0235,pdoagh]2.0.co;2

Lough, T. J., and Lucas, W. J. (2006). Integrative plant biology: role of phloem long-distance macromolecular trafficking. *Annu. Rev. Plant Biol.* 57, 203–232. doi: 10.1146/annurev.arplant.56.032604.144145

Loxdale, H. D., Hardie, J., Halbert, S., Foottit, R., Kidd, N. A. C., and Carter, C. I. (1993). The relative importance of short- and long-range movement of flying aphids. *Biol. Rev.* 68, 291–311. doi: 10.1111/j.1469-185x.1993.tb00998.x

Łukasik, P., Dawid, M. A., Ferrari, J., and Godfray, H. C. J. (2013). The diversity and fitness effects of infection with facultative endosymbionts in the grain aphid, Sitobion avenae. *Oecologia* 173, 985–996. doi: 10.1007/s00442-013-2660-5

Łukasik, P., van Asch, M., Guo, H., Ferrari, J., Charles, J., and Godfray, H. (2012). Unrelated facultative endosymbionts protect aphids against a fungal pathogen. *Ecol. Lett.* 16, 214–218. doi: 10.1111/ele.12031

Lushai, G., Loxdale, H. D., and MaLean, N. (2000). Genetic diversity in clonal lineages. *J. Reprod. Dev.* 46, 21–22.

Mardorf, J. L., Fehr, W. R., and O'Neal, M. E. (2010). Agronomic and seed traits of soybean lines with the rag 1 gene for aphid resistance. *Crop Sci.* 50, 1891–1895. doi: 10.2135/cropsci2010.02.0079

Mathers, C. T. (2020). Improved genome assembly and annotation of the soybean aphid (Aphis glycines Matsumara). *G3 (Bethesda)* 10, 899–906. doi: 10.1534/g3.119.400954

McCarville, M. T., and O'Neal, M. E. (2012). Measuring the benefit of biological control for single gene and pyramided host plant resistance for Aphis glycines (Hemiptera: Aphididae) management. *J. Econ. Entomol.* 105, 1835–1843. doi: 10.1603/EC12043

McCarville, M. T., and O'Neal, M. E. (2013). Soybean aphid (Aphididae: Hemiptera) population growth as affected by host plant resistance and an insecticidal seed treatment. *J. Econ. Entomol.* 106, 1302–1309. doi: 10.1603/EC12495

McCarville, M. T., O'Neal, M. E., Potter, B. D., Tilmon, K. J., Cullen, E. M., McCornack, B. P., et al. (2014). One gene versus two: a regional study on the efficacy of single gene versus pyramided resistance for soybean aphid management. *J. Econ. Entomol.* 107, 1680–1687. doi: 10.1603/ec14047

McEwan, G. F., Groner, M. L., Fast, M. D., Gettinby, G., and Revie, C. W. (2015). Using agent-based modelling to predict the role of wild Refugia in the evolution of resistance of sea lice to Chemotherapeutants. *PLoS One* 10:e0139128. doi: 10.1371/journal.pone.0139128

Michel, A. P., Mian, M. A. R., Davila-Olivas, N. H., and Cañas, L. A. (2010). Detached leaf and whole plant assays for soybean aphid resistance: differential responses among resistance sources and biotypes. *J. Econ. Entomol.* 103, 949–957. doi: 10.1603/ec09337

Montllor, C. B., Maxmen, A., and Purcell, A. H. (2002). Facultative bacterial endosymbionts benefit pea aphids *Acyrthosiphon pisum* under heat stress. *Ecol. Entomol.* 27, 189–195. doi: 10.1046/j.1365-2311.2002.00393.x

Moran, N. A., Degnan, P. H., Santos, S. R., Dunbar, H. E., and Ochman, H. (2005). The players in a mutualistic symbiosis: insects, bacteria, viruses, and virulence genes. *Proc. Natl. Acad. Sci. U. S. A.* 102, 16919–16926. doi: 10.1073/pnas.0507029102

Moran, N. A., Munson, M. A., Baumann, P., and Ishikawa, H. (1993). A molecular clock in endosymbiotic bacteria is calibrated using the insect hosts. *Proc. R. Soc. Lond. Ser. B: Biol. Sci.* 253, 167–171. doi: 10.1098/rspb.1993.0098

Munson, M. A., Baumann, P., Clark, M. A., Baumann, L., Moran, N. A., Voegtlin, D. J., et al. (1991b). Evidence for the establishment of aphid-eubacterium endosymbiosis in an ancestor of four aphid families. *J. Bacteriol.* 173, 6321–6324. doi: 10.1128/jb.173.20.6321-6324.1991

Munson, M. A., Baumann, P., and Kinsey, M. G. (1991a). Buchnera gen. Nov. and *Buchnera aphidicola* sp. nov., a taxon consisting of the mycetocyte-associated, primary endosymbionts of aphids. *Int. J. Syst. Bacteriol.* 41, 566–568. doi: 10.1099/00207713-41-4-566

Myers, C., and Hill, E. (2014). Benefits of neonicotinoid seed treatments to soybean production. United States Environmental Protection Agency Memo. Available at: (https://www.epa.gov/sites/production/files/2014-10/documents/benefits_of_neonicotinoid_seed_treatments_to_soybean_production_2.pdf).

Natukunda, M. I., and MacIntosh, G. (2020). The resistant soybean-Aphis glycines interaction: current knowledge and prospects. *Front. Plant Sci.* 11:1223. doi: 10.3389/fpls.2020.01223

Neupane, S., Purintun, J. M., Mathew, F. M., Varenhorstm, A. J., and Nepal, M. P. (2019). Molecular basis of soybean resistance to soybean aphids and soybean cyst nematodes. *Plan. Theory* 8:374. doi: 10.3390/plants8100374

Nováková, E., Hypsa, V., and Moran, N. A. (2009). *Arsenophonus*, an emerging clade of intracellular symbionts with a broad host distribution. *BMC Microbiol.* 9:143. doi: 10.1186/1471-2180-9-143

O'Keefe, K. J., and Antonovics, J. (2002). Playing by different rules: the evolution of virulence in sterilizing pathogens. *Am. Nat.* 159, 597–605. doi: 10.1086/339990

Oliver, K. M., Campos, J., Moran, N. A., and Hunter, M. S. (2007). Population dynamics of defensive symbionts in aphids. *Proc. R. Soc. Lond. Ser. B: Biol. Sci.* 275, 293–299. doi: 10.1098/rspb.2007.1192

Oliver, K. M., Moran, N. A., and Hunter, M. S. (2005). Variation in resistance to parasitism in aphids is due to symbionts not host genotype. *Proc. Natl. Acad. Sci. U. S. A.* 102, 12795–12800. doi: 10.1073/pnas.0506131102

Oliver, K. M., Russell, J. A., Moran, N. A., and Hunter, M. S. (2003). Facultative bacterial symbionts in aphids confer resistance to parasitic wasps. *Proc. Natl. Acad. Sci. U. S. A.* 100, 1803–1807. doi: 10.1073/pnas.0335320100

Oliver, K. M., Smith, A. H., and Russell, J. A. (2014). Defensive symbiosis in the real world – advancing ecological studies of heritable, protective bacteria in aphids and beyond. *Funct. Ecol.* 28, 341–355. doi: 10.1111/1365-2435.12133

Pawlowski, M., Hill, C. B., Voegtlin, D. J., and Hartman, G. L. (2014). Soybean aphid intrabiotype variability based on colonization of specific soybean genotypes. *Insect Sci.* 22, 785–792. doi: 10.1111/1744-7917.12169

Perlman, S. J., Hunter, M. S., and Zchori-Fein, E. (2006). The emerging diversity of Rickettsia. *Proc. Biol. Sci.* 273, 2097–2106. doi: 10.1098/rspb.2006.3541

Ragsdale, D. W., Landis, D. A., Brodeur, J., Heimpel, G. E., and Desneux, N. (2011). Ecology and management of the soybean aphid in North America. *Annu. Rev. Entomol.* 56, 375–399. doi: 10.1146/annurev-ento-120709-144755

Ragsdale, D. W., Voegtlin, D. J., and O'Neil, R. J. (2004). Soybean aphid biology in North America. *Ann. Entomol. Soc. Am.* 97, 204–208. doi: 10.1093/aesa/97.2.204

Russell, C. W., Bouvaine, S., Newell, P. D., and Douglas, A. E. (2013). Shared metabolic pathways in a coevolved insect-bacterial symbiosis. *Appl. Environ. Microbiol.* 79, 6117–6123. doi: 10.1128/aem.01543-13

Russell, J. A., and Moran, N. A. (2006). Costs and benefits of symbiont infection in aphids: variation among symbionts and across temperatures. *Proc. Biol. Sci.* 273, 603–610. doi: 10.1098/rspb.2005.3348

Sánchez-Bayo, F. (2014). Environmental science. The trouble with neonicotinoids. *Science* 346, 806–807. doi: 10.1126/science.1259159

Sandström, J. P., Russell, J. A., White, J. P., and Moran, N. A. (2001). Independent origins and horizontal transfer of bacterial symbionts of aphids. *Mol. Ecol.* 10, 217–228. doi: 10.1046/j.1365-294x.2001.01189.x

Scarborough, C. L., Ferrari, J., and Godfray, H. C. (2005). Aphid protected from pathogen by endosymbiont. *Science* 310:1781. doi: 10.1126/science.1120180

Schofield, P., Chaplain, M., and Hubbard, S. (2005). Evolution of searching and life history characteristics in individual-based models of host-parasitoid-microbe associations. *J. Theor. Biol.* 237, 1–16. doi: 10.1016/j.jtbi.2005.03.025

Shrestha, R. B., Dunbar, M. W., French, B. W., and Gassmann, A. J. (2018). Effects of field history on resistance to Bt maize by western corn rootworm, *Diabrotica virgifera virgifera* LeConte (Coleoptera: Chrysomelidae). *PLoS One* 13:e0200156. doi: 10.1371/journal.pone.0200156

Smith, C. M., and Chuang, W. P. (2014). Plant resistance to aphid feeding: behavioral, physiological, genetic and molecular cues regulate aphid host selection and feeding. *Pest Manag. Sci.* 70, 528–540. doi: 10.1002/ps.3689

Song, F., and Swinton, S. M. (2009). Returns to integrated pest management research and outreach for soybean aphid. *J. Econ. Entomol.* 102, 2116–2125. doi: 10.1603/029.102.0615

Song, F., Swinton, S. M., DiFonzo, C., O'Neal, M., and Ragsdale, D. W. (2006). Profitability analysis of soybean aphid control treatments in three north central states. Michigan State University Department of Agricultural Economics. Available at: http://ageconsearch.umn.edu/bitstream/11489/1/sp06-24.pdf (Accessed April 8, 2023).

Stevens, L., Giordano, R., and Fialho, R. F. (2001). Male-killing, nematode infections, bacteriophage infection, and virulence of cytoplasmic bacteria in the genus *Wolbachia*. *Annu. Rev. Ecol. Syst.* 32, 519–545. doi: 10.1146/annurev.ecolsys.32.081501.114132

Stratonovitch, P., Elias, J., Denholm, I., Slater, R., and Semenov, M. A. (2014). An individual-based model of the evolution of pesticide resistance in heterogeneous environments: control of *Meligethes aeneus* population in oilseed rape crops. *PLoS One* 9:e115631. doi: 10.1371/journal.pone.0115631

Takahashi, D., Yamanaka, T., Sudo, M., and Andow, D. A. (2017). Is a larger refuge always better? Dispersal and dose in pesticide resistance evolution. *Evolution* 71, 1494–1503. doi: 10.1111/evo.13255

Tilmon, K. J., Hodgson, E. W., O'Neal, M. E., and Ragsdale, D. W. (2011). Biology of the soybean aphid, aphis glycines (Hemiptera: Aphididae) in the United States. *J. Integ. Pest Manag.* 2, 1–A7. doi: 10.1603/IPM10016

Tsuchida, T., Koga, R., and Fukatsu, T. (2004). Host plant specialization governed by facultative symbiont. *Science* 303:1989. doi: 10.1126/science.1094611

Tsuchida, T., Koga, R., Shibao, H., Matsumoto, T., and Fukatsu, T. (2002). Diversity and geographic distribution of secondary endosymbiotic bacteria in natural populations of the pea aphid, *Acyrthosiphon pisum*. *Mol. Ecol.* 11, 2123–2135. doi: 10.1046/j.1365-294x.2002.01606.x

Turgeon, R., and Wolf, S. (2009). Phloem transport: cellular pathways and molecular trafficking. *Annu. Rev. Plant Biol.* 60, 207–221. doi: 10.1146/annurev.arplant.043008.092045

Van Bel, A. J., and Gaupels, F. (2004). Pathogen-induced resistance and alarm signals in the phloem. *Mol. Plant Pathol.* 5, 495–504. doi: 10.1111/j.1364-3703.2004.00243.x

Van der Berg, H., Ankasah, D., Muhammad, A., Rusli, R., Widayanto, H. A., Wirasto, H. B., et al. (1997). Evaluating the role of predation in population fluctuations of the soybean aphid aphis glycines in farmers' fields in Indonesia. *J. Appl. Ecol.* 34, 971–984. doi: 10.2307/2405287

van der Wilk, F., Dullemans, A. M., Verbeek, M., and van den Heuvel, J. F. J. M. (1999). Isolation and characterization of APSE-1, a bacteriophage infecting the secondary endosymbiont of *Acyrthosiphon pisum*. *Virology* 262, 104–113. doi: 10.1006/viro.1999.9902

Venette, R. C., and Ragsdale, D. W. (2004). Assessing the invasion by soybean aphid (Homoptera: Aphididae): where will it end? *Ann. Entomol. Soc. Am.* 97, 219–226. doi: 10.1093/aesa/97.2.219

Voegtlin, D. J., O'Neil, R. J., and Graves, W. R. (2004). Tests of suitability of overwintering hosts of Aphis glycines: identification of a new host association with *Rhamnus alnifolia* L'Heritier. *Ann. Entomol. Soc. Am.* 97, 233–234. doi: 10.1603/0013-8746(2004)097[0233:TOSOOH]2.0.CO;2

Voegtlin, D. J., O'Neil, R. J., Graves, W. R., Lagos, D., and Yoo, H. J. S. (2005). Potential winter hosts of soybean aphid. *Ann. Entomol. Soc. Am.* 98, 690–693. doi: 10.1603/0013-8746(2005)098[0690:PWHOSA]2.0.CO;2

Vogel, K. J., and Moran, N. A. (2013). Functional and evolutionary analysis of the genome of an obligate fungal symbiont. *Genome Biol. Evol.* 5, 891–904. doi: 10.1093/gbe/evt054

Von Dohlen, C. D., and Moran, N. A. (2000). Molecular data supports a rapid radiation of aphids in the cretaceous and multiple origins of host alternation. *Biol. J. Linnean Soc.* 71, 689–717. doi: 10.1111/j.1095-8312.2000.tb01286.x

Wallin, J. R., and Loonan, D. V. (1971). Low-level jet winds, aphid vectors, local weather, and barley yellow dwarf virus outbreaks. *Phytopathology* 61, 1068–1070. doi: 10.1094/Phyto-61-1068

Wang, X., Fang, Y., Lin, Z., Zhang, L., and Wang, H. (1994). A study on the damage and economic threshold of the soybean aphid at the seedling stage. Plant Protection (Institute of Plant Protection, CAAS, China), 20, pp. 12–13. Available at: (https://core.ac.uk/download/pdf/84312646.pdf).

Weinert, L. A., Werren, J. H., Aebi, A., Stone, G. N., and Jiggins, F. M. (2009). Evolution and diversity of Rickettsia bacteria. *BMC Biol.* 7:6. doi: 10.1186/1741-7007-7-6

Weldon, S. R., Strand, M. R., and Oliver, K. M. (2013). Phage loss and the breakdown of a defensive symbiosis in aphids. *Proc. Biol. Sci.* 280:20122103. doi: 10.1098/rspb.2012.2103

Wenger, J. A., Cassone, B. J., Legeai, F., Johnston, J. S., Bansal, R., Yates, A. D., et al. (2020). Whole genome sequence of the soybean aphid, Aphis glycines. *Insect Biochem. Mol. Biol.* 123:102917. doi: 10.1016/j.ibmb.2017.01.005

Wenger, J. A., and Michel, A. P. (2013). Implementing an evolutionary framework for understanding genetic relationships of phenotypically defined insect biotypes in the invasive soybean aphid (Aphis glycines). *Evol. Appl.* 6, 1041–1053. doi: 10.1111/eva.12084

Werren, J. H., Baldo, L., and Clark, M. E. (2008). *Wolbachia*: master manipulators of invertebrate biology. *Nat. Rev. Microbiol.* 6, 741–751. doi: 10.1038/nrmicro1969

Werren, J. H., Skinner, S. W., and Huger, A. M. (1986). Male-killing bacteria in a parasitic wasp. *Science* 231, 990–992. doi: 10.1126/science.3945814

Wiarda, S. L., Fehr, W. R., and O'Neal, M. E. (2012). Soybean aphid (Hemiptera: Aphididae) development on soybean with rag 1 alone, Rag2 alone, and both genes combined. *J. Econ. Entomol.* 105, 252–258. doi: 10.1603/EC11020

Wille, B. D., and Hartman, G. L. (2009). Two species of symbiotic bacteria present in the soybean aphid (Hemiptera: Aphididae). *Environ. Entomol.* 38, 110–115. doi: 10.1603/022.038.0113

Wilson, A. C., Sunnucks, P., Blackman, R. L., and Hales, D. F. (2002). Microsatellite variation in cyclically parthenogenetic populations of *Myzus persicae* in South-Eastern Australia. *Heredity* 88, 258–266. doi: 10.1038/sj.hdy.6800037

Wu, Z., Schenk-Hamlin, D., Zhan, W., Ragsdale, D. W., and Heimpel, G. E. (2004). The soybean aphid in China: a historical review. *Ann. Entomol. Soc. Am.* 97, 209–218. doi: 10.1603/0013-8746(2004)097[0209:TSAICA]2.0.CO;2

Wulff, J. A., Buckman, K. A., Wu, K., Heimpel, G. E., and White, J. A. (2013). The endosymbiont *Arsenophonus* is widespread in soybean aphid, Aphis glycines, but does not provide protection from parasitoids or a fungal pathogen. *PLoS One* 8:e62145. doi: 10.1371/journal.pone.0062145

Wulff, J. A., and White, J. A. (2015). The endosymbiont *Arsenophonus* provides a general benefit to soybean aphid (Hemiptera: Aphididae) regardless of host plant resistance (rag). *Environ. Entomol.* 44, 574–581. doi: 10.1093/ee/nvv031

Zytynska, S. E., and Weisser, W. W. (2016). The natural occurrence of secondary bacterial symbionts in aphids. *Ecol. Entomol.* 41, 13–26. doi: 10.1111/een.12281

frontiers | Frontiers in Microbiology

TYPE Review
PUBLISHED 14 September 2023
DOI 10.3389/fmicb.2023.1244239

OPEN ACCESS

EDITED BY
Daisuke Kageyama,
National Agriculture and Food Research Organization (NARO), Japan

REVIEWED BY
Sonam Popli,
University of Toledo, United States
Vipin Rana,
University of Maryland, College Park, United States

*CORRESPONDENCE
Yifeng Li
✉ yifengli@gdaas.cn

RECEIVED 22 June 2023
ACCEPTED 24 August 2023
PUBLISHED 14 September 2023

CITATION
Guo Y, Shao J, Wu Y and Li Y (2023) Using *Wolbachia* to control rice planthopper populations: progress and challenges. *Front. Microbiol.* 14:1244239. doi: 10.3389/fmicb.2023.1244239

Using *Wolbachia* to control rice planthopper populations: progress and challenges

Yan Guo, Jiayi Shao, Yanxian Wu and Yifeng Li*

Guangdong Provincial Key Laboratory of High Technology for Plant Protection, Institute of Plant Protection, Guangdong Academy of Agricultural Sciences, Key Laboratory of Green Prevention and Control on Fruits and Vegetables in South China Ministry of Agriculture and Rural Affairs, Guangzhou, China

Wolbachia have been developed as a tool for protecting humans from mosquito populations and mosquito-borne diseases. The success of using *Wolbachia* relies on the facts that *Wolbachia* are maternally transmitted and that *Wolbachia*-induced cytoplasmic incompatibility provides a selective advantage to infected over uninfected females, ensuring that *Wolbachia* rapidly spread through the target pest population. Most transinfected *Wolbachia* exhibit a strong antiviral response in novel hosts, thus making it an extremely efficient technique. Although *Wolbachia* has only been used to control mosquitoes so far, great progress has been made in developing *Wolbachia*-based approaches to protect plants from rice pests and their associated diseases. Here, we synthesize the current knowledge about the important phenotypic effects of *Wolbachia* used to control mosquito populations and the literature on the interactions between *Wolbachia* and rice pest planthoppers. Our aim is to link findings from *Wolbachia*-mediated mosquito control programs to possible applications in planthoppers.

KEYWORDS

***Wolbachia*, mosquitoes, planthoppers, transmission, cytoplasmic incompatibility, pathogen inhibition**

Introduction

Wolbachia are a group of gram-negative bacteria that live inside invertebrate cells and have been successfully developed to control mosquitoes and mosquito-borne diseases by decreasing host population density or decreasing host virus transmission. Unlike chemical control approaches, which result in collateral destruction of beneficial insects, *Wolbachia*-mediated population control has proven to be an excellent vector-control agent because it targets a single species. Moreover, as the target population is suppressed, the chemical control approaches become less effective, while *Wolbachia*-mediated pest population control is more effective. Because of *Wolbachia* pervasiveness in nature and lack of genetic modification, *Wolbachia*-mediated control programs are accepted as environmentally friendly biocontrol strategies to control insect pest populations and disease vectors. To date, the *Wolbachia* control strategies successfully used have been limited to mosquitoes. There is a question of whether *Wolbachia* control strategies could be applied more broadly to other pest insects and insect-borne diseases.

Rice (*Oryza sativa*), cultivated extensively in the tropical and subtropical regions of the world, is the staple food for billions of people worldwide (Sarao et al., 2016). Rice planthoppers (Hemiptera: Delphacidae), the most destructive pests of rice, suck rice sap and oviposit in rice tissues, inducing a substantial threat to rice production. In addition to heavy infestations, rice planthoppers also act as vectors of major plant viruses, such as rice stripe virus, rice

black-streaked dwarf virus, rugged stunt virus, grassy stunt virus, and southern rice black-streaked dwarf virus (Hibino, 1996). Various strategies have been developed to control planthoppers. Among those strategies, spraying chemical insecticides is the main method used for controlling this pest. However, blanket application of insecticides has already induced planthopper resistance and disrupted the ecological balance of rice ecosystems in most rice planting countries. Thus, a more practical, economical and environmentally friendly strategy is urgently needed to control planthoppers and their associated diseases.

The success of *Wolbachia*-mediated mosquito control programs promotes similar strategies that could be applied to planthoppers. Here, we summarize the important properties of *Wolbachia* used for mosquito control, including stability transmission, host reproduction alteration, and pathogen inhibition. We also review the current knowledge about the interactions between *Wolbachia* and planthoppers and point out the similarities and differences in biology between mosquitoes and planthoppers to link findings from *Wolbachia*-mediated mosquito control programs to possible applications in planthoppers.

Wolbachia phenotypes

Wolbachia diversity

Wolbachia strains were first identified in the reproductive tissue of *Culex pipiens* in 1924 (Hertig and Wolbach, 1924). Since then, these bacteria have been found to infect approximately half of all arthropod species from terrestrial and aquatic environments, including nematodes, mites, spiders and all orders of insects (Weinert et al., 2015). *Wolbachia* formed a monophyletic group with other insect-associated microorganisms using 16S rRNA gene sequences. In recent decades, a large number of *Wolbachia* with close phylogenetic affinity have been revealed by PCR and sequencing techniques. Based on the variable gene *ftsZ*, *Wolbachia* from arthropods form two divergent clades; several different *Wolbachia strains* from filarial nematodes are assigned to two additional clades (Werren et al., 1995; Bandi et al., 1998). These clades have since been termed supergroups, which are used to describe the divergence of the *Wolbachia* group. In addition, *Wolbachia* surface protein (*wsp*) and *groEL* genes are used to distinguish the major phylogenetic subdivisions of *Wolbachia*. Due to extensive recombination and strong diversifying selection in the *wsp* gene, *wsp* should therefore be unsuitable for use alone for reliable *Wolbachia* strain characterization when trying to type and quantify strain diversity (Werren and Bartos, 2001; Baldo et al., 2005; Lo et al., 2007). Considering that a single-locus approach to strain characterization may be misleading, a multilocus sequence typing (MLST) system has been established to type *Wolbachia* strains using five standard housekeeping genes (*gatB, coxA, hcpA, fbpA, and ftsZ*) (Baldo et al., 2006). Based on the combination of alleles at a sample of housekeeping genes, the MLST approach defines a strain as a sequence type. This accurate strain typing system MLST using combinations of alleles as molecular markers to genotype strains is considered a universal and unambiguous tool for *Wolbachia* strain typing, molecular evolutionary, and population genetics studies (Baldo et al., 2006). Overall, the MLST system provides an excellent method for typing *Wolbachia* strains from diverse hosts and for discriminating among strains in the same host species (Baldo et al., 2006).

Wolbachia strains are subdivided into 17 supergroups from A to R, except for supergroup G, which is controversial (Baldo et al., 2006; Baldo and Werren, 2007; Wang et al., 2016; Zhao et al., 2021). The majority of *Wolbachia* strains found in insects belong to supergroups A and B. Most *Wolbachia* strains that infect arthropods are supergroups A, B, D, E, F, and H (Figure 1). As molecular biology techniques have developed, *Wolbachia* genome sequences are exploited to define genetic diversity and significant genes associated with altering host biology, as well as relationships between *Wolbachia* and hosts at the gene level (Kaur et al., 2021). To date, over 26 complete *Wolbachia* genomes have been published, and nearly 1,000 *Wolbachia* genomes from different arthropod and nematode species have been assembled (Scholz et al., 2020; Kaur et al., 2021). Our understanding of *Wolbachia* genetic diversity is still developing, which will help us to identify useful *Wolbachia* variants with desirable phenotypic effects for alternative *Wolbachia*-mediated population control strategies.

Wolbachia horizontal and vertical transmission

Numerous studies have shown that *Wolbachia* exists in diverse cells and somatic tissues of the host, such as the salivary gland, fat bodies, ovary, testis, midgut, and tegument (Dobson et al., 1999; Toomey et al., 2013). Although *Wolbachia* have been found in host somatic tissues, they exhibit strong reproductive tissue tropism in the host (Frydman et al., 2006; Fast et al., 2011; Toomey et al., 2013). *Wolbachia* are rarely or not transmitted by sperm, while they accumulate in developing spermatocytes of male hosts (Clark et al., 2002; Ijichi et al., 2002; Ju et al., 2017). In female hosts, *Wolbachia* enter ovaries and spread into developing oocytes, eventually dispersing within the offspring of the host (Kose and Karr, 1995; Ferree et al., 2005). Thus, *Wolbachia* is considered as an intracellular maternally transmitted bacterium. The unique ability of *Wolbachia* to invade host populations has rapidly promoted their exploration as a potential tool in the control of pests.

Wolbachia persist and disperse in arthropods and filarial nematodes that mostly depend on their horizontal and vertical transmission. *Wolbachia* can transfer from one species to another, that is, horizontal transmission (Figure 2A), though it has low transmission efficiency. Phylogenetic incongruence between *Wolbachia* and their hosts suggests that horizontal transmission of *Wolbachia* occurs frequently between many hosts (Baldo et al., 2006; Su et al., 2019). MLST analysis of *Wolbachia* and successful horizontal transfer of *Wolbachia* by microinjection have also provided evidence for horizontal transmission (Xi et al., 2005, 2006; Li et al., 2017; Zheng et al., 2019). As recorded, horizontal transmission of *Wolbachia* could occur by many pathways, such as feeding on common plants (Sintupachee et al., 2006; Le Clec'h et al., 2013; Li et al., 2017; Sanaei et al., 2023), parasitic wasps (Ahmed et al., 2015; Brown and Lloyd, 2015; Goya et al., 2022), parasitic mites (Houck et al., 1991; Jaenike et al., 2007; Gehrer and Vorburger, 2012), hybridization (Jiang et al., 2018; Su et al., 2019), and predation (Goodacre et al., 2006; Wang et al., 2010; Su et al., 2019). Although interspecific horizontal transmission inefficiently occurs, *Wolbachia* horizontal transmission is found in many insects, including rice planthoppers (Zhang et al., 2013), wasps (Huigens et al., 2004; Goya et al., 2022; Zhou et al., 2022), fruit flies (Turelli et al., 2018), trypetids (Schuler et al., 2013), psyllids

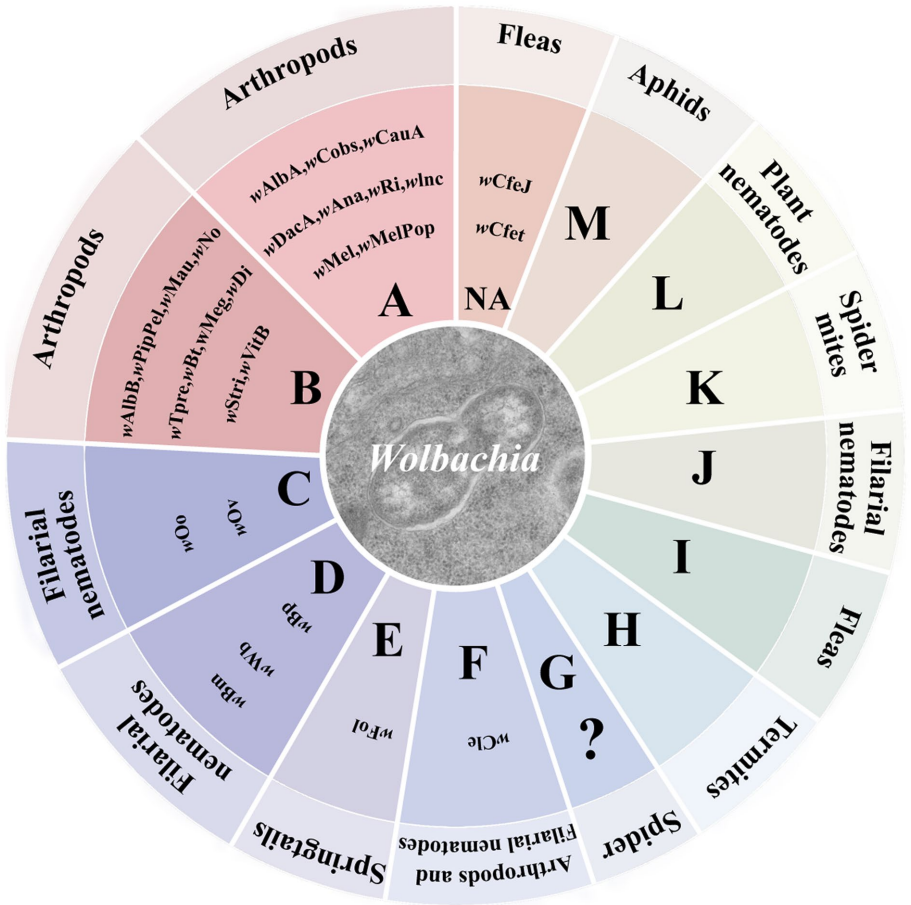

FIGURE 1
Wolbachia supergroups. *Wolbachia* strains are subdivided into different supergroups. Most *Wolbachia* supergroups are listed in the circle graph. Colors correspond to different patterns of *Wolbachia*-host associations across the supergroups. "?": controversial supergroup; NA, not annotated at supergroup level.

(Serbina et al., 2022), moths (Ahmed et al., 2016), ladybirds (Shaikevich and Romanov, 2023), mosquitoes (Shaikevich et al., 2019), mites (Su et al., 2019), butterflies (Ahmed et al., 2016; Zhao et al., 2021) and so forth.

Wolbachia can also vertically transmit from mother to offspring via the host egg cytoplasm (Figure 2B), which is considered the main pathway for infection transfer across hosts (Werren, 1997). Vertical transmission of symbionts in hosts is generally maternal and occurs through trans eggs and transovarial transmission (Rosen, 1988; Lequime et al., 2016). In *trans*-egg transmission, *Wolbachia* spread into eggs at the time of oviposition. In transovarial transmission, *Wolbachia* infect the germinal tissues and enter into the developing oocytes of the female host. When *Wolbachia* initially infect a new host, they need to reach the germinal tissues for successful transovarial transmission (Werren et al., 2008). *Wolbachia* transovarial transmission relies on the infection of developing oocytes, which results in nearly 100% infection of the host progeny (Lequime et al., 2016). Due to the difficultly of detecting trans-egg transmission *in vitro* and vivo, *Wolbachia* vertical transmission in the host is mostly focused on transovarial transmission. The factors that impact *Wolbachia* vertical transmission are complex and undistinguishable and are related to *Wolbachia* densities, interactions with other symbionts, and the ability of *Wolbachia* to migrate into the host oocyte.

Wolbachia vertical transmission has been intensively investigated in Diptera insects. *Drosophila* ovarioles are of the polytrophic meroistic type and divide into the terminal filament, germarium, and vitellarium from tip to pedicel (Szklarzewicz et al., 2007; Swiatoniowska et al., 2013; Szklarzewicz et al., 2013). The female germline stem cell niche (GSCN) is on the apical tip of the germarium, where germline stem cells divide asymmetrically, and one daughter cell exits the GSCN and forms the egg's germline (Fast et al., 2011). Germline cells divide and form egg chambers in the germarium and finally mature into eggs in the vitellarium. Observation research found an intense accumulation of *Wolbachia* in the GSCN and the somatic stem cell niche (SSCN), which is located at the germarium and supports somatic stem cells (Frydman et al., 2006; Fast et al., 2011). Further research showed that *Wolbachia* enter the ovaries of *Drosophila* from the anterior tip of the germarium (Martinez et al., 2014). After that, *Wolbachia* utilize the host actin cytoskeleton during oogenesis for efficient transmission and maintenance between *Drosophila* generations (Newton et al., 2015). Actin-inhibiting drugs significantly abrogate *Wolbachia* uptake in the host, indicating that the host actin cytoskeleton plays an important role in *Wolbachia* transmission (Ferree et al., 2005; Newton et al., 2015; Nevalainen et al., 2023).

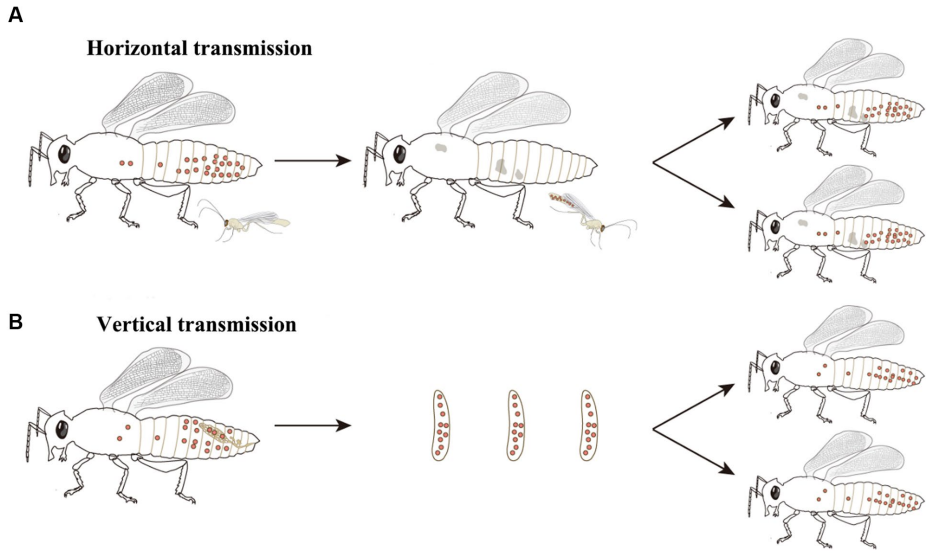

FIGURE 2
Wolbachia transmission. *Wolbachia* persist and disperse in hosts by horizontal and vertical transmission. **(A)** *Wolbachia* horizontally transmit from one species to another. The most common horizontal transmission of *Wolbachia* occurs by parasitic wasps. Parasitic wasps infect *Wolbachia* when they parasitize a *Wolbachia*-infected host, then transfer *Wolbachia* to new hosts when they parasitize closest species. **(B)** *Wolbachia* vertically transmit from mother to offspring. In female hosts, *Wolbachia* infect the germinal tissues, enter into the developing oocytes and be incorporated into the embryos, eventually dispersing within the offspring of host. Red dots: *Wolbachia*.

Wolbachia-induced cytoplasmic incompatibility

Wolbachia impact the ecology, evolution, and reproductive biology of their host species to increase their already widespread distribution. *Wolbachia* are best known for their effects on host reproduction, such as male killing, feminization, thelytokous parthenogenesis, and cytoplasmic incompatibility (CI) (Werren et al., 2008). In 1971, *Wolbachia* were first verified to be associated with CI, causing the embroys of hosts to perish, which occurs when males carrying *Wolbachia* mate with females that are uninfected or harboring different *Wolbachia* strains (Yen and Barr, 1971; Werren, 1997; Hoffmann, 2020). A range of negative fecundity effects or no effects associated with *Wolbachia* has been described, although the mechanisms responsible for those fitness effects are mostly unknown. Other *Wolbachia* strains exhibit strong positive fecundity effects on their host, including fecundity increases (Fast et al., 2011; Guo et al., 2018a).

How *Wolbachia* manipulate the reproduction of hosts, especially *Wolbachia*-induced CI, has attracted great attention in recent decades. Although the means by which *Wolbachia* mediate CI are currently unknown, there is a general consensus that *Wolbachia* modify sperm at an early stage of spermatogenesis, and a rescue activity takes place in the same *Wolbachia*-infected egg to reverse or neutralize the modification of sperm following fertilization (Werren, 1997; Xiao et al., 2021). Three different models have been proposed to account for the mechanisms of CI induction and rescue: the "lock-and-key," "slow-motion," and "titration-restitution" models (Figure 3; Poinsot et al., 2003). Moreover, *Wolbachia* genes involved in modification and rescue have been identified, which are collectively named *cifA* and *cifB*. The two genes are organized into an operon-like genetic element, which encodes the CifA and CifB proteins (Beckmann et al., 2017; LePage et al., 2017). To distinguish the CI-inducing modifications and CifA rescues viability, two types of functional models for CI have been proposed. In the host modification models, *Wolbachia* Cifs (CifA and CifB) modify the infected sperm, resulting in CI when the modified sperm fertilizes an uninfected egg (Kose and Karr, 1995; Werren, 1997; Bossan et al., 2011). In the "toxin-antidote" model, CifB disrupts the processing of paternally derived chromosomes or nuclease activity and then changes or delays paternal chromatin condensation and separation during the first zygotic mitosis (Tram and Sullivan, 2002). Even so, much remains to be learned about the actual molecular mechanisms of CI induction and rescue, which can help account for CI in insects infected with different *Wolbachia* strains.

The feature of *Wolbachia* inducing a conditional sterility CI in infected insects is important for pest and disease control. In recent years, CI has been successfully explored to control the mosquito population and mosquito-borne diseases through population suppression or population replacement approaches. In the population suppression approach, large numbers of *Wolbachia*-infected male mosquitoes are released into the field, and the male sterility induced by CI causes significant drops in mosquito number. In the population replacement strategy, both *Wolbachia*-infected male mosquitoes and infected female mosquitoes are released, which can suppress mosquito-borne diseases by decreasing host virus transmission. Overall, *Wolbachia*-induced CI is central to both population suppression and population replacement programs (Ross et al., 2019).

Wolbachia-induced pathogen inhibition

Reducing the infection or transmission of pathogens is another important property of *Wolbachia* used for pest and disease control. *Wolbachia* can inhibit RNA viral replication, which was initially

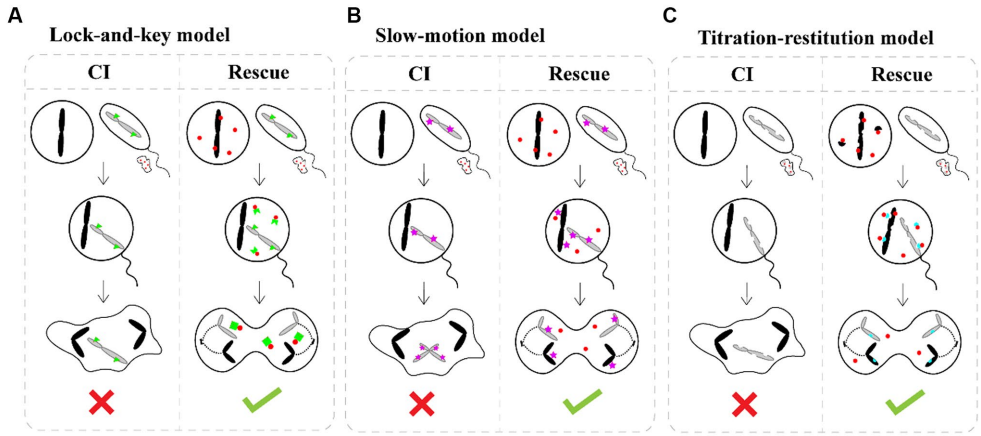

FIGURE 3
CI induction and rescue models. **(A)** The "lock-and-key" model. *Wolbachia* (red dots) produce a "lock" (green triangle) binding on paternal chromosomes. *Wolbachia* are shed with most of the cytoplasm as spermatogenesis. Cytoplasmic incompatibility occurs in crosses between infected males and uninfected female because the paternal material is "locked-in," while eggs infected by *Wolbachia* remain compatible after fertilization because *Wolbachia* produce a "key" in the egg which removes the lock. **(B)** The "slow-motion" model. *Wolbachia* (red dots) produce a slowing down factor (purple star) binding on paternal chromosomes. After that, *Wolbachia* are shed from the maturing spermatocyte. Embryonic mortality occurs in crosses between infected males and uninfected females because *Wolbachia* slow down paternal chromosomes movements during the first embryonic mitosis, which is rescued by the similar modification of maternal chromosomes when *Wolbachia* are present in the egg. **(C)** The "titration-restitution" model. *Wolbachia* (red dots) titrate out a protein (semicircles) of paternal and maternal chromosomes. The titrated protein of paternal chromosomes is expelled as *Wolbachia* are shed from the maturing spermatocyte. Cytoplasmic incompatibility occurs when sperm cell enters an uninfected egg due to lack of the host protein. Rescue occurs between two infected individuals, because the *Wolbachia* in eggs give back the host protein (blue semicircles) to maternal and paternal chromosomes.

discovered in *Drosophila melanogaster* (Hedges et al., 2008; Teixeira et al., 2008). Subsequently, *Wolbachia* were found to be broadly effective against mosquito-borne diseases such as Zika virus, chikungunya virus, dengue virus, yellow fever virus, and West Nile virus, making them less capable of transmitting infection to offspring and humans (Bian et al., 2013a; Ford et al., 2019). *Wolbachia* can also confer resistance against eukaryotic parasites (Bourtzis et al., 2014), providing a broad range of pathogen protection. Several studies have shown that the antiviral response is dramatically enhanced by *Wolbachia* newly transinfected to the host, although natural *Wolbachia*-infected mosquitoes are found to limit virus replication and transmission (Armbruster et al., 2003; Guo et al., 2022). Microinjection technology expands the entry of *Wolbachia* into new hosts. Once *Wolbachia* infects, *Wolbachia*-induced CI produces a frequency-dependent fitness advantage that can drive the spread of *Wolbachia* within new hosts (Sullivan, 2020). Data have further indicated that the extent of viral inhibition provided by transinfected *Wolbachia* depends on the *Wolbachia* variants, host species, virus and host-*Wolbachia*–virus interactions.

Wolbachia-induced pathogen inhibition is variable between related hosts and different *Wolbachia* strains in the same host, which is strongly linked to the density of *Wolbachia* in host tissues. In mosquitoes, virus inhibition correlates with higher *Wolbachia* density in the salivary glands, midgut, and ovaries. Unlike mosquitoes, high *Wolbachia* densities in the head, gut, and Malpighian tubules of *Drosophila* are thought to be important for virus inhibition (Osborne et al., 2012). It is widely believed that higher *Wolbachia* densities are important for effective antiviral behavior (Chrostek et al., 2013), and *Wolbachia* may confer virus inhibition by interfering with viral binding, entry into the cell, and RNA replication in the early stages (Schultz et al., 2018; Lu et al., 2020). Regardless of which pathway *Wolbachia* acts on, the production of progeny viruses from the same *Wolbachia*-infected cells is reduced, and virus dissemination and transmission are ultimately limited (Kaur et al., 2021). Interestingly, the varied extent of virus inhibition was also associated with viral dose. Recent data suggest that *w*Mel exhibits strong inhibition in high dengue dose mosquitoes, while inhibition appears lower or even increases virus transmission when the dengue dose is low (King et al., 2018).

Wolbachia-induced pathogen inhibition may be related to the upregulation of host innate immunity (Figure 4). This is evident from the inhibition caused by *Wolbachia* newly transferred to hosts (Moreira et al., 2009; Walker et al., 2011; Ant et al., 2018). In mosquitoes with transinfected *Wolbachia* strains, *Wolbachia* upregulate the expression of genes involved in innate defense pathways and then prime insect innate immunity to block pathogen replication (Bian et al., 2013b; Moretti et al., 2018). However, inhibition associated with native *Wolbachia* variants does not show an immune-priming phenotype but does confer antiviral activity (Mousson et al., 2012). These results suggest that innate immune priming may occur in hosts with newly transinfected *Wolbachia* variants or novel host-*Wolbachia* associations (Rances et al., 2012).

Another explanation for *Wolbachia* inhibiting virus replication is the competition for resources between viruses, *Wolbachia*, and the host cell (Figure 5). Viral replication and *Wolbachia* growth in the host are tightly regulated by cholesterol metabolism (Lin and Rikihisa, 2003). A recent study has shown that *Wolbachia* is unable to synthesize cholesterol *de novo* and that its replication is cholesterol dependent. Thus, cholesterol depletion of host cells by *Wolbachia* could directly interfere with virus replication in the same host (Rainey et al., 2014). In addition to cholesterol, iron homeostasis needs to be tightly regulated to enable viral replication and bacterial growth. In *Wolbachia*-infected mosquitoes, the iron-binding proteins transferrin and ferritin

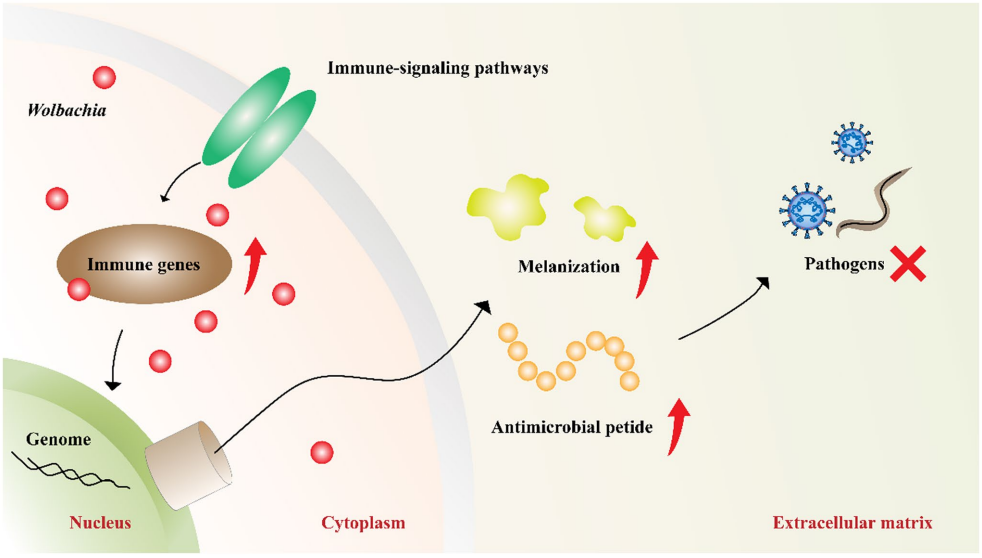

FIGURE 4
Wolbachia upregulate host innate immunity. *Wolbachia* enhance the synthesis of antimicrobial peptides and melanization by impacting the central genes of host immune-signaling pathways. The increased innate immunity partially accounts for *Wolbachia* inhibiting pathogens. Red dots: *Wolbachia*; red arrow: upregulation; red "X": inhibition.

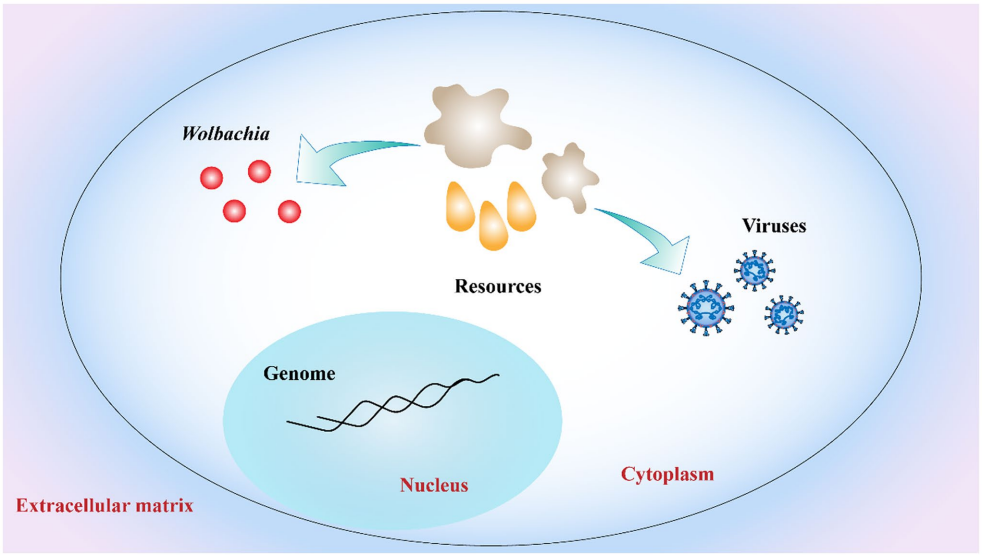

FIGURE 5
Competition for host cell resources. Both *Wolbachia* growth and virus replication rely on host cell resources. Resources depletion of host cells by *Wolbachia* interferes with virus replication in host limited cell resources. Red dots: *Wolbachia*; orange drop shapes and gray irregular shapes: host cell resources.

were upregulated, suggesting that *Wolbachia* regulated iron homeostasis (Kremer et al., 2009; Rances et al., 2012). However, this phenomenon is reversed when the host infect is infected with virus (Tchankouo-Nguetcheu et al., 2010). These experiments related to *Wolbachia*, antiviral activity and host cells are intriguing, clearly suggesting that host cell resources are important for both viral replication and *Wolbachia* growth. In summary, to develop alternative vector-control strategies, much remains to be learned concerning the mechanisms of *Wolbachia*-mediated pathogen inhibition.

Wolbachia in planthoppers

Wolbachia discovery in planthoppers

The small brown planthopper (*Laodelphax striatellus*; SBPH), brown planthopper (*Nilaparvata lugens*; BPH), and white-backed planthopper (*Sogatella furcifera*; WBPH) are the three serious and destructive pests of rice that directly cause 20 to 40% of crop loss globally each year (Yang and Zhang, 2016; Sullivan, 2020). *Wolbachia*

in SBPH were first discovered in 1992 using partial sequences of the ribosomal DNA (Rousset et al., 1992), and WBPH was reported to harbor the same *Wolbachia* strain *w*Stri in 2003 (Kittayapong et al., 2003). In contrast to SBPH and WBPH, BPH was found to be infected with a different *Wolbachia* strain, *w*Lug. There were significantly different infection statuses among the three planthoppers (Table 1). The infection rate of *Wolbachia* in SBPHs increased gradually according to the investigation data from 1982 to 1994 (Noda, 1984a; Hoshizaki and Shimada, 1995). A recent study indicated that nearly all SBPHs were infected by *Wolbachia* in the rice-growing regions of China (Zhang et al., 2013). In WBPH, the infection rate of *Wolbachia* is different between females and males; nearly 100% of females are infected with *Wolbachia*, while only half of males are infected (Li et al., 2020). BPH is naturally infected by the *Wolbachia* strain *w*Lug at a prevalence of only ~18%, showing the lowest infection frequency among the three planthoppers (Qu et al., 2013).

Wolbachia is located in multiple tissues of planthoppers, including somatic tissues, ovaries, and testes. The somatic localization of *Wolbachia* is thought to facilitate their horizontal transmission, which also indicates the complex interactions between *Wolbachia* and the host. The reproductive localization of *Wolbachia* is thought to facilitate their vertical transmission. *Wolbachia* exhibit high-efficiency vertical transmission in planthoppers, as they do in the model insect *Drosophila* (Nakamura et al., 2012; Guo et al., 2018b), which occurs only in female hosts. In contrast to *Drosophila* ovarioles, planthopper ovarioles are of the telotrophic meroistic type and consist of a terminal filament, tropharium, and vitellarium (Szklarzewicz et al., 2013; Guo et al., 2018b). A cluster of nurse cells connected to the central trophic core radially arranged in the anterior of the tropharium; previtellogenesis arranged on the base of the tropharium (Szklarzewicz et al., 2007). Developing oocytes arrange in the vitellarium, which connects the tropharium through nutritive cords (Szklarzewicz et al., 2007, 2013). *Wolbachia* bind to Vg outside the ovarioles and endocytose into the tropharium of planthoppers during the early phase of vitellogenesis (Guo et al., 2018b). *Wolbachia* in the tropharium enter the arrested oocyte and establish an early infection as the trophic core divides. In addition, *Wolbachia* in the nurse cells spread into the developing oocytes through the nutritive cords that are wide channels formed between nurse cells and establish stable inheritance in host generation (Guo et al., 2018b). *Wolbachia* behavior during host embryogenesis is also well characterized. Microscopic observations indicated that *Wolbachia* were mainly localized at the anterior part cells of the embryo in early embryogenesis and then migrated to the posterior region during late embryogenesis, where gonads were formed (Guo et al., 2019). Research related to *Wolbachia* transmission in host oogenesis and embryogenesis can partially explain how *Wolbachia* exhibit high vertical transmission in planthoppers.

Wolbachia functions in planthoppers

Wolbachia show different functions on three planthoppers (Table 1). Recent research has shown that *Wolbachia* provide beneficial effects to BPH. Egg production in *Wolbachia*-infected BPH females is higher than that in uninfected females. However, the longevity of *Wolbachia*-infected BPHs is shorter than that of uninfected BPHs, which may partially explain the high egg production and low prevalence of *Wolbachia* in wild BPH. Similar to BPH, *Wolbachia* also significantly increased the fecundity of SBPH, which may be associated with the high number of ovarioles that contain apoptotic nurse cells and mitotic germ cells (Guo et al., 2018b, 2020). In addition, *Wolbachia* affects the miRNA expression of SBPH to alter the expression of genes related to fecundity (Liu et al., 2019). Further experimental and genomic evidence demonstrated that *Wolbachia* increases the fecundity of BPH and SBPH females by synthesizing the essential nutrients biotin and riboflavin (Ju et al., 2020). In contrast, *Wolbachia* exhibit negative effects on WBPH; *Wolbachia*-infected females produce fewer eggs than *Wolbachia*-uninfected females (Li et al., 2022). Although many studies have focused on the interactions between *Wolbachia* and planthoppers, the mechanism of *Wolbachia*-mediated alterations in planthopper oogenesis has not yet been explored.

The CI phenotype in laboratory and wild SBPH populations was found in 1984 (Noda, 1984b). In 1992, the CI phenotype in SBPH was confirmed, which was caused by *Wolbachia w*Stri (Rousset et al., 1992). *w*Stri induced strong CI in SBPH, and the level of CI remained high regardless of the age of *Wolbachia*-infected males. There are no viable eggs from *Wolbachia*-infected SBPH females that mated with uninfected SBPH males. RNA-seq comparative analysis of *Wolbachia*-infected and uninfected SBPH shows that iLvE mediates branched-chain amino acid biosynthesis and may be associated with *Wolbachia*-induced CI (Ju et al., 2017). Knocking down iLvE expression in *Wolbachia*-uninfected SBPH males partially rescued fertility in crosses between these males and *Wolbachia*-infected females. Wild WBPH populations are infected by the same *Wolbachia w*Stri as SBPH are, while the level of CI in WBPH is very weak or even zero. However, a strong CI phenotype was expressed when WBPH was double-infected

TABLE 1 *Wolbachia* in small brown planthopper (SBPH), brown planthopper (BPH), and white-backed planthopper (WBPH).

	SPBH	BPH	WBPH
Wolbachia strain	*w*Stri	*w*Lug	*w*Stri
Infection frequency	100%	~18%	100% (female) ~50% (male)
Key features	Strong cytoplasmic incompatibility Maternal transmission Provide nutrients Increase fertility Increase resistance Protect against virus	Maternal transmission Provide nutrients Increase fertility Short lifespans Increase resistance	Weak cytoplasmic Incompatibility Maternal transmission Decrease fertility

with *Wolbachia* and *Cardinium* bacterium, indicating that *Wolbachia* may only play an auxiliary role in the CI of WBPH (Li et al., 2022). Interestingly, *Wolbachia* *w*Lug in wild BPH populations lacks the ability to induce CI. A recent study showed that BPH infected with *w*Stri by microinjection exhibited a high CI level, although the CI level was much lower than that in the original host SBPH (Gong et al., 2020).

In recent years, effects other than reproductive effects on planthoppers have received increasing attention. Studies have shown that *Wolbachia* of planthoppers increase resistance to insecticides, protect against some RNA viruses, and have other effects. In SBPH, *Wolbachia* *w*Stri is associated with increased resistance to the insecticide buprofezin, although there is no relationship between *Wolbachia* density and resistance (Li et al., 2020). BPH increased insecticide susceptibility and decreased detoxification metabolism when the density of *Wolbachia* was decreased by high temperature (Zhang et al., 2021). Further results indicated that *w*Lug orchestrates the detoxification metabolism of BPH via the CncC pathway to promote host insecticide resistance. In addition, *Wolbachia* wStri was recently shown to inhibit the growth of positive-sense RNA mosquito viruses, and the inhibition level was up to 99.9%. The presence of *w*Stri did not affect the growth of the negative-sense RNA viruses in the *Bunyaviridae* and *Rhabdoviridae* families (Schultz et al., 2018). *w*Stri in *Aades albopictus* cells has also been shown to repress ZIKV, and the inhibited stages of the ZIKV life cycle were identified to two distinct blocks, including reduction of ZIKV entry into cells and distraction viral genome replication in *Wolbachia*-infected cells. The addition of a cholesterol-lipid supplement partially rescued ZIKV entry in *w*Stri-infected cells but did not rescue viral replication, showing that viral entry is affected in a cholesterol-dependent manner (Schultz et al., 2018). *Wolbachia* *w*Stri has the ability to inhibit a wider variety of positive-sense RNA viruses, making it an attractive candidate for future vector-controlled approaches to limit viral infection and spread.

Opportunities and challenges

Wolbachia-based mosquito control strategies have been shown to be effective at limiting arbovirus disease spread in approximately 23 countries (Gong et al., 2023). Among them, over 8 countries have used *Wolbachia*-based mosquito population suppression strategies, which closely depend on *Wolbachia*-induced CI. The most important aspect of this strategy is that stable and heritable CI-induced *Wolbachia* infections should be established in target species. To control mosquitoes, adult sterile males with artificial *Wolbachia* infection have been released to mate with wild females. The eggs produced by these females are perishable, resulting in a target species population decline in a given period. However, the mass release of adult sterile males involves a potential risk of accidentally releasing fertile CI-induced *Wolbachia*-infected females. Insects are traditionally sterilized by radiation; combining *Wolbachia*-induced CI with the radiation sterilization technique can sterilize any residual females that are not removed from the released males using low-dose irradiation. Recent field trials indicated that the combination of *Wolbachia* and radiation sterilization resulted in a near elimination of mosquito populations (Zheng et al., 2019). Another efficient vector-control strategy is *Wolbachia*-based population replacement, which has been successfully used in 15 countries. The success of this strategy relies on two aspects of *Wolbachia*: pathogen inhibition and CI drive. Rather than releasing large numbers of *Wolbachia*-infected males to suppress insect populations, *Wolbachia*-infected females would be released to replace a wild uninfected population by a CI-based drive, reducing their vector competence and inhibiting arboviral disease (Kaur et al., 2021).

In recent years, great progress has been made in developing possible applications for protecting plants from planthoppers and their associated diseases. BPH is naturally infected with *Wolbachia* strain *w*Lug at a low prevalence that does not cause CI. Gong et al. (2020) established a *w*Stri-infected BPH line by withdrawing the embryo cytoplasm of SBPH and injecting it into the embryos of BPH. *w*Stri maintained perfect maternal transmission in the new host BPH. The *w*Stri-infected BPH exhibited near 100% CI, although it was slightly lower than that in its native host SBPH (Gong et al., 2020). The high level of CI and low fitness costs of *w*Stri-infected BPHs enable individuals infected with *w*Stri to rapidly invade BPH populations. Furthermore, *w*Stri-infected BPH dramatically reduced planthopper RRSV viral loads and viral transmission to rice plants. The viral load in *w*Stri-infected BPH decreased 75% relative to that in uninfected BPH (Gong et al., 2020). Otherwise, rice seedlings attacked by *w*Stri-infected BPH resulted in a dramatic 82% lower incidence of viral infection compared with that attacked by uninfected BPH (Gong et al., 2020). Above all, the *w*Stri strain appears to be well suited for the *Wolbachia*-based replacement strategy to control BPHs and their associated diseases, although much work still needs to be done before strategy implementation.

Possible *Wolbachia*-based population control applications for SBPH and WBPH are more complex than those for in BPH. SBPH and WBPH naturally carry *Wolbachia*, so double infections are needed for population replacement, whereas double infected strains or novel strains with native *Wolbachia* removed but carrying another variant added are needed for population suppression. First, a stable and heritable CI-induced *Wolbachia* infection line should be established by artificial transfection (Figure 6). Although embryonic microinjection technology significantly promotes *Wolbachia* transfection efficiency from donors to recipients, many problems remain, such as selecting useful *Wolbachia* variants, which have desirable phenotypic effects for alternative strategies and maintain stability in the longer term. Apart from native *Wolbachia*, new *Wolbachia* interactions with other endosymbionts and the complex microbiome could influence host fitness and indirectly affect *Wolbachia* invasion (Ross et al., 2019).

Host fitness cost is an important determinant in *Wolbachia*-based pest control strategies. The fitness of hosts is altered when hosts are infected with different *Wolbachia* strains. In general, natural *Wolbachia* infections are benign or even beneficial to the host, such as increasing fertility or lifespans as well as inhibiting the virus. In contrast, diverse negative effects on fitness are found when *Wolbachia* are transferred to novel hosts, depending on the *Wolbachia* strain and host. It is usually difficult to predict the fitness effects of *Wolbachia* on novel hosts because *Wolbachia* densities and tissue distributions dramatically change from native to novel hosts. Most negative effects are that *Wolbachia* transfections often reduce

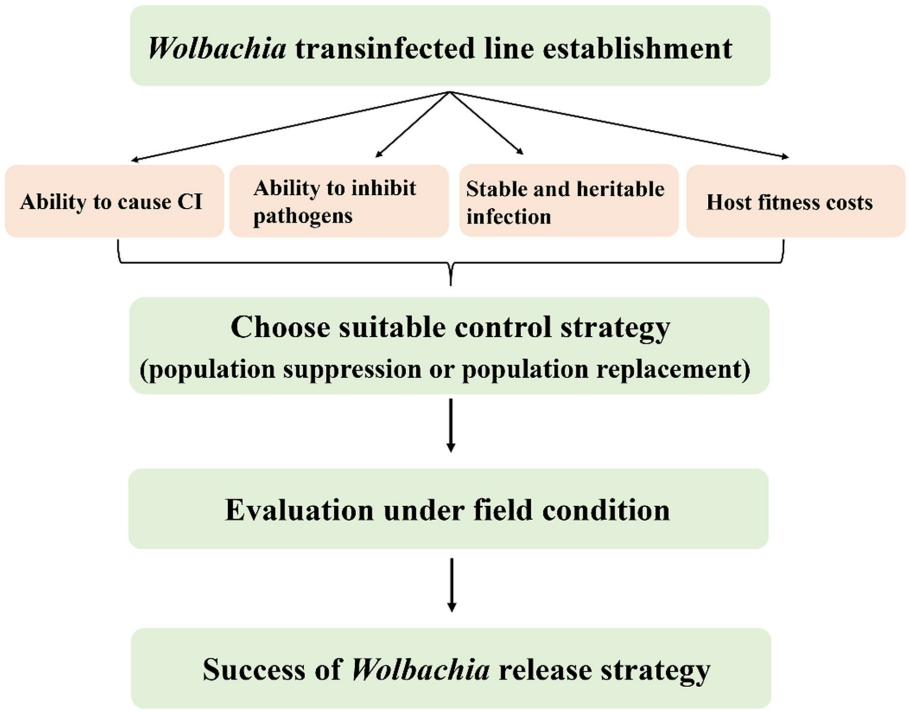

FIGURE 6
Properties of *Wolbachia* used for planthoppers control. The success of *Wolbachia*-based population control strategies relies on the important properties of *Wolbachia* including host reproduction alteration, pathogen inhibition, stability transmission and weak or no host fitness cost. CI, cytoplasmic incompatibility.

TABLE 2 *Wolbachia*-mediated mosquito control strategies and the possible strategy for planthoppers.

	Mosquitoes	Planthoppers
Native *Wolbachia*	Yes/No	Yes/No
Wolbachia transfection	Yes	Yes
Key features	Cytoplasmic incompatibility Maternal transmission Pathogen inhibition	Cytoplasmic incompatibility Maternal transmission Pathogen inhibition
Host fitness cost	No/Weak	Weak
Key biology of host	Females bite human and transmit virus Males feed plant juices	Both females and males destruct rice and transmit virus
Control strategies	Population suppression/population replacement	Population replacement

novel host fecundity or egg hatch, which may prevent transinfected *Wolbachia* establishment if they are too severe. The overall impact of *Wolbachia* infections on host fitness is often insufficiently estimated because it strongly depends on the environmental context. The fitness effects of *Wolbachia* observed in standard laboratory studies are only partial to estimate the dynamics of *Wolbachia* in natural populations.

Choose suitable *Wolbachia*-based population control strategies, population suppression or population replacement, which closely depend on the biology of the target pest. In mosquitoes, both males and females can feed on damaged and intact vegetative tissue, plant juices, damaged fruits, and homopterans, which act as an energy source for their physiological maintenance and locomotion. Only female mosquitoes bite animals or humans to take a blood meal, which is required for egg development. Therefore, there is no or little threat to animals or humans using *Wolbachia*-based mosquito suppression strategies by releasing adult sterile males. To efficiently reduce the prevalence of mosquito-borne diseases, *Wolbachia*-based replacement strategies were carried out by the release of *Wolbachia*-transinfected antiviral females or eggs. Nevertheless, both female and male planthoppers suck rice sap and transmit viral diseases, and there is no mature biotechnology or equipment for sex sorting to date. Hence, a population replacement strategy may be more suitable for controlling planthoppers than population suppression based on the current knowledge of interactions between *Wolbachia* and the host (Table 2). Moreover, the chosen

strategies should be evaluated under field conditions to demonstrate the possibility of their practical implementation in the future.

Author contributions

YG and YL wrote the manuscript. JS and YW performed the images processing. All authors contributed to the article and approved the submitted version.

Funding

This study was supported by the Research and Development program in key areas of Guangdong Province (Grant No. 2021B0707010010), the Special Fund for Scientific Innovation Strategy-Construction of High-Level Academy of Agriculture Science (Grant Nos. R2021YJ-YB2007 and 202117TD), and the National Natural Science Foundation of China (grant no. 31901879).

Acknowledgments

We thank ZhiHao Zheng of the Plant Protection Research Institute, Guangdong Academy of Agricultural Science, China for his thoughtful suggestions on the review.

Conflict of interest

The authors declare that the research was conducted in the absence of any commercial or financial relationships that could be construed as a potential conflict of interest.

Publisher's note

References

Ahmed, M. Z., Breinholt, J. W., and Kawahara, A. Y. (2016). Evidence for common horizontal transmission of *Wolbachia* among butterflies and moths. *BMC Evol. Biol.* 16:118. doi: 10.1186/s12862-016-0660-x

Ahmed, M. Z., Li, S. J., Xue, X., Yin, X. J., Ren, S. X., Jiggins, F. M., et al. (2015). The intracellular bacterium *Wolbachia* uses parasitoid wasps as phoretic vectors for efficient horizontal transmission. *PLoS Pathog.* 10:e1004672. doi: 10.1371/journal.ppat.1004672

Ant, T. H., Herd, C. S., Geoghegan, V., Hoffmann, A. A., and Sinkins, S. P. (2018). The *Wolbachia* strain wAu provides highly efficient virus transmission blocking in *Aedes aegypti*. *PLoS Pathog.* 14:e1006815. doi: 10.1371/journal.ppat.1006815

Armbruster, P., Damsky, W. E., Giordano, R., Birungi, J., Munstermann, L. E., and Conn, J. E. (2003). Infection of new- and old-world *Aedes albopictus* (Diptera: culicidae) by the intracellular parasite *Wolbachia*: implications for host mitochondrial DNA evolution. *J. Med. Entomol.* 40, 356–360. doi: 10.1603/0022-2585-40.3.356

Baldo, L., Hotopp, J. C. D., Jolley, K. A., Bordenstein, S. R., Biber, S. A., Choudhury, R. R., et al. (2006). Multilocus sequence typing system for the endosymbiont *Wolbachia pipientis*. *Appl. Environ. Microbiol.* 72, 7098–7110. doi: 10.1128/AEM.00731-06

Baldo, L., Lo, N., and Werren, J. H. (2005). Mosaic nature of the *Wolbachia* surface protein. *J. Bacteriol.* 187, 5406–5418. doi: 10.1128/jb.187.15.5406-5418.2005

Baldo, L., and Werren, J. H. (2007). Revisiting *Wolbachia* supergroup typing based on WSP: spurious lineages and discordance with MLST. *Curr. Microbiol.* 55, 81–87. doi: 10.1007/s00284-007-0055-8

Bandi, C., Anderson, T. J. C., Genchi, C., and Blaxter, M. L. (1998). Phylogeny of *Wolbachia* in filarial nematodes. *Proc. R. Soc. Lond. B Biol. Sci.* 265, 2407–2413. doi: 10.1098/rspb.1998.0591

Beckmann, J. F., Ronau, J. A., and Hochstrasser, M. (2017). A *Wolbachia* deubiquitylating enzyme induces cytoplasmic incompatibility. *Nat. Microbiol.* 2:17007. doi: 10.1038/nmicrobiol.2017.7

Bian, G., Joshi, D., Dong, Y., Lu, P., Zhou, G., Pan, X. L., et al. (2013b). *Wolbachia* invades *Anopheles stephensi* populations and induces refractoriness to plasmodium infection. *Science* 340, 748–751. doi: 10.1126/science.1236192

Bian, G., Zhou, G., Lu, P., and Xi, Z. Y. (2013a). Replacing a native *Wolbachia* with a novel strain results in an increase in endosymbiont load and resistance to dengue virus in a mosquito vector. *PLoS Negl. Trop. Dis.* 7:e2250. doi: 10.1371/journal.pntd.0002250

Bossan, B., Koehncke, A., and Hammerstein, P. (2011). A new model and method for understanding *Wolbachia*-induced cytoplasmic incompatibility. *PLoS One* 6:e19757. doi: 10.1371/journal.pone.0019757

Bourtzis, K., Dobson, S. L., Xi, Z. Y., Rasgon, J. L., Calvitti, M., Moreira, L. A., et al. (2014). Harnessing mosquito-*Wolbachia* symbiosis for vector and disease control. *Acta Trop.* 132, S150–S163. doi: 10.1016/j.actatropica.2013.11.004

Brown, A. N., and Lloyd, V. K. (2015). Evidence for horizontal transfer of *Wolbachia* by a *Drosophila* mite. *Exp. Appl. Acarol.* 66, 301–311. doi: 10.1007/s10493-015-9918-z

Chrostek, E., Marialva, M. S. P., Esteves, S. S., Weinert, L. A., Martinez, J., Jiggins, F. M., et al. (2013). *Wolbachia* variants induce differential protection to viruses in *Drosophila melanogaster*: a phenotypic and phylogenomic analysis. *PLoS Genet.* 9:e1003896. doi: 10.1371/journal.pgen.1003896

Clark, M. E., Veneti, Z., Bourtzis, K., and Karr, T. L. (2002). The distribution and proliferation of the intracellular bacteria *Wolbachia* during spermatogenesis in *Drosophila*. *Mech. Dev.* 111, 3–15. doi: 10.1016/s0925-4773(01)00594-9

Dobson, S. L., Bourtzis, K., Braig, H. R., Jones, B. F., Zhou, W., Rousset, F., et al. (1999). *Wolbachia* infections are distributed throughout insect somatic and germ line tissues. *Insect Biochem. Mol. Biol.* 29, 153–160. doi: 10.1016/s0965-1748(98)00119-2

Fast, E. M., Toomey, M. E., Panaram, K., Desjardins, D., Kolaczyk, E. D., and Frydman, H. M. (2011). *Wolbachia* enhance *Drosophila* stem cell proliferation and target the germline stem cell niche. *Science* 334, 990–992. doi: 10.1126/science.1209609

Ferree, P. M., Frydman, H. M., Li, J. M., Cao, J., Wieschaus, E., and Sullivan, W. (2005). *Wolbachia* utilizes host microtubules and dynein for anterior localization in the *Drosophila* oocyte. *PLoS Pathog.* 1:e14. doi: 10.1371/journal.ppat.0010014

Ford, S. A., Allen, S. L., Ohm, J. R., Sigle, L. T., Sebastian, A., Albert, I., et al. (2019). Selection on *Aedes aegypti* alters *Wolbachia*-mediated dengue virus blocking and fitness. *Nat. Microbiol.* 4, 1832–1839. doi: 10.1038/s41564-019-0533-3

Frydman, H. M., Li, J. M., Robson, D. N., and Wieschaus, E. (2006). Somatic stem cell niche tropism in *Wolbachia*. *Nature* 441, 509–512. doi: 10.1038/nature04756

Gehrer, L., and Vorburger, C. (2012). Parasitoids as vectors of facultative bacterial endosymbionts in aphids. *Biol. Lett.* 8, 613–615. doi: 10.1098/rsbl.2012.0144

Gong, J. T., Li, Y. J., Li, T. P., Liang, Y., Hu, L., Zhang, D. J., et al. (2020). Stable introduction of plant-virus-inhibiting *Wolbachia* into planthoppers for rice protection. *Curr. Biol.* 30, 4837–4845. doi: 10.1016/j.cub.2020.09.033

Gong, J. T., Li, T. P., Wang, M. K., and Hong, X. Y. (2023). *Wolbachia*-based strategies for control of agricultural pests. *Curr. Opin. Insect Sci.* 57:101039. doi: 10.1016/j.cois.2023.101039

Goodacre, S. L., Martin, O. Y., Thomas, C. F. G., and Hewitt, G. M. (2006). *Wolbachia* and other endosymbiont infections in spiders. *Mol. Ecol.* 15, 517–527. doi: 10.1111/j.1365-294X.2005.02802.x

Goya, L. F., Lanteri, A. A., Confalonieri, V. A., and Rodriguero, M. S. (2022). New host-parasitoid interactions in *Naupactus cervinus* (Coleoptera, Curculionidae) raise the question of Wolbachia horizontal transmission. *Symbiosis* 86, 325–336. doi: 10.1007/s13199-022-00838-z

Guo, Y., Gong, J. T., Mo, P. W., Huang, H. J., and Hong, X. Y. (2019). *Wolbachia* localization during *Laodelphax striatellus* embryogenesis. *J. Insect Physiol.* 116, 125–133. doi: 10.1016/j.jinsphys.2019.05.006

Guo, Y., Guo, J. T., and Li, Y. F. (2022). *Wolbachia* wPip blocks Zika virus transovarial transmission in *Aedes albopictus*. *Microbiol. Spectr.* 10:e0263321. doi: 10.1128/spectrum.02633-21

Guo, Y., Hoffmann, A. A., Xu, X. Q., Mo, P. W., Huang, H. J., Gong, J. T., et al. (2018b). Vertical transmission of Wolbachia is associated with host vitellogenin in *Laodelphax striatellus*. *Front. Microbiol.* 9:2016. doi: 10.3389/fmicb.2018.02016

Guo, Y., Hoffmann, A. A., Xu, X. Q., Zhang, X., Huang, H. J., Ju, J. F., et al. (2018a). Wolbachia-induced apoptosis associated with increased fecundity in *Laodelphax striatellus* (Hemiptera: Delphacidae). *Insect Mol. Biol.* 27, 796–807. doi: 10.1111/imb.12518

Guo, Y., Khan, J., Zheng, X. Y., and Wu, Y. (2020). Wolbachia increase germ cell mitosis to enhance the fecundity of *Laodelphax striatellus*. *Insect Biochem. Mol. Biol.* 127:103471. doi: 10.1016/j.ibmb.2020.103471

Hedges, L. M., Brownlie, J. C., O'Neill, S. L., and Johnson, K. N. (2008). Wolbachia and virus protection in insects. *Science* 322:702. doi: 10.1126/science.1162418

Hertig, M., and Wolbach, S. B. (1924). Studies on rickettsia-like micro-organisms in insects. *J. Med. Res.* 44, 329–374.7.

Hibino, H. (1996). Biology and epidemiology of rice viruses. *Annu. Rev. Phytopathol.* 34, 249–274. doi: 10.1146/annurev.phyto.34.1.249

Hoffmann, A. A. (2020). Wolbachia. *Curr. Biol.* 30, R1113–R1114. doi: 10.1016/j.cub.2020.08.039

Hoshizaki, S., and Shimada, T. (1995). PCR-based detection of Wolbachia, cytoplasmic incompatibility microorganisms, infected in natural populations of *Laodelphax striatellus* (Homoptera: Delphacidae) in Central Japan: has the distribution of Wolbachia spread recently? *Insect Mol. Biol.* 4, 237–243. doi: 10.1111/j.1365-2583.1995.tb00029.x

Houck, M. A., Clark, J. B., Peterson, K. R., and Kidwell, M. G. (1991). Possible horizontal transfer of Drosophila genes by the mite *Proctolaelaps regalis*. *Science* 253, 1125–1128. doi: 10.1126/science.1653453

Huigens, M. E., de Almeida, R. P., Boons, P. A. H., Luck, R. F., and Stouthamer, R. (2004). Natural interspecific and intraspecific horizontal transfer of parthenogenesis-inducing Wolbachia in *Trichogramma wasps*. *Proc. R. Soc. Lond. B Biol. Sci.* 271, 509–515. doi: 10.1098/rspb.2003.2640

Ijichi, N., Kondo, N., Matsumoto, R., Shimada, M., Ishikawa, H., and Fukatsu, T. (2002). Internal spatiotemporal population dynamics of infection with three Wolbachia strains in the adzuki bean beetle, *Callosobruchus chinensis* (Coleoptera: Bruchidae). *Appl. Environ. Microbiol.* 68, 4074–4080. doi: 10.1128/AEM.68.8.4074-4080.2002

Jaenike, J., Polak, M., Fiskin, A., Helou, M., and Minhas, M. (2007). Interspecific transmission of endosymbiotic Spiroplasma by mites. *Biol. Lett.* 3, 23–25. doi: 10.1098/rsbl.2006.0577

Jiang, W., Zhu, J., Wu, Y., Li, L., Li, Y., Ge, C., et al. (2018). Influence of *Wolbachia* infection on mitochondrial DNA variation in the genus Polytremis (Lepidoptera: Hesperiidae). *Mol. Phylogenet. Evol.* 129, 158–170. doi: 10.1016/j.ympev.2018.08.001

Ju, J. F., Bing, X. L., Zhao, D. S., Guo, Y., Xi, Z. Y., Hoffmann, A. A., et al. (2020). Wolbachia supplement biotin and riboflavin to enhance reproduction in planthoppers. *ISME J.* 14, 676–687. doi: 10.1038/s41396-019-0559-9

Ju, J. F., Hoffmann, A. A., Zhang, Y. K., Duan, X. Z., Guo, Y., Gong, J. T., et al. (2017). *Wolbachia*-induced loss of male fertility is likely related to branch chain amino acid biosynthesis and iLvE in *Laodelphax striatellus*. *Insect Biochem. Mol. Biol.* 85, 11–20. doi: 10.1016/j.ibmb.2017.04.002

Kaur, R., Shropshire, J. D., Cross, K. L., Leigh, B., Mansueto, A. J., Stewart, V., et al. (2021). Living in the endosymbiotic world of *Wolbachia*: a centennial review. *Cell Host Microbe* 29, 879–893. doi: 10.1016/j.chom.2021.03.006

King, J. G., Souto-Maior, C., Sartori, L. M., Maciel-de-Freitas, R., and Gomes, M. G. M. (2018). Variation in *Wolbachia* effects on *Aedes mosquitoes* as a determinant of invasiveness and vectorial capacity. *Nat. Commun.* 9:1483. doi: 10.1038/s41467-018-03981-8

Kittayapong, P., Jamnongluk, W., Thipaksorn, A., Milne, J. R., and Sindhusake, C. (2003). Wolbachia infection complexity among insects in the tropical rice-field community. *Mol. Ecol.* 12, 1049–1060. doi: 10.1046/j.1365-294X.2003.01793.x

Kose, H., and Karr, T. L. (1995). Organization of *Wolbachia pipientis* in the *Drosophila* fertilized egg and embryo revealed by an anti-*Wolbachia* monoclonal antibody. *Mech. Dev.* 51, 275–288. doi: 10.1016/0925-4773(95)00372-x

Kremer, N., Voronin, D., Charif, D., Mavingui, P., Mollereau, B., and Vavre, F. (2009). Wolbachia interferes with ferritin expression and iron metabolism in insects. *PLoS Pathog.* 5:e1000630. doi: 10.1371/journal.ppat.1000630

Le Clec'h, W., Chevalier, F. D., Genty, L., Bertaux, J., Bouchon, D., and Sicard, M. (2013). Cannibalism and predation as paths for horizontal passage of Wolbachia between terrestrial isopods. *PLoS One* 8:e60232. doi: 10.1371/journal.pone.0060232

LePage, D. P., Metcalf, J. A., Bordenstein, S. R., On, J., Perlmutter, J. I., Shropshire, J. D., et al. (2017). Prophage WO genes recapitulate and enhance *Wolbachia*-induced cytoplasmic incompatibility. *Nature* 543, 243–247. doi: 10.1038/nature21391

Lequime, S., Paul, R. E., and Lambrechts, L. (2016). Determinants of arbovirus vertical transmission in mosquitoes. *PLoS Pathog.* 12:e1005548. doi: 10.1371/journal.ppat.1005548

Li, S. J., Ahmed, M. Z., Lv, N., Shi, P. Q., Wang, X. M., Huang, J. L., et al. (2017). Plant-mediated horizontal transmission of Wolbachia between whiteflies. *ISME J.* 11, 1019–1028. doi: 10.1038/ismej.2016.164

Li, F., Li, P., Hua, H., Hou, M., and Wang, F. (2020). Diversity, tissue localization, and infection pattern of bacterial symbionts of the white-backed planthopper, *Sogatella furcifera* (Hemiptera: Delphacidae). *Microb. Ecol.* 79, 720–730. doi: 10.1007/s00248-019-01433-4

Li, T. P., Zhou, C. Y., Wang, M. K., Zha, S. S., Chen, J., Bing, X. L., et al. (2022). Endosymbionts reduce microbiome diversity and modify host metabolism and fecundity in the planthopper *Sogatella furcifera*. *Msystems* 7:e0151621. doi: 10.1128/msystems.01516-21

Lin, M. Q., and Rikihisa, Y. (2003). *Ehrlichia chaffeensis* and *Anaplasma phagocytophilum* lack genes for lipid a biosynthesis and incorporate cholesterol for their survival. *Infect. Immun.* 71, 5324–5331. doi: 10.1128/iai.71.9.5324-5331.2003

Liu, L., Zhang, K. J., Rong, X., Li, Y. W., and Liu, H. (2019). Identification of Wolbachia-responsive miRNAs in the small brown planthopper, *Laodelphax striatellus*. *Front. Physiol.* 10:928. doi: 10.3389/fphys.2019.00928

Lo, N., Paraskevopoulos, C., Bourtzis, K., O'Neill, S., Werren, J., Bordenstein, S., et al. (2007). Taxonomic status of the intracellular bacterium *Wolbachia pipientis*. *Int. J. Syst. Evol. Microbiol.* 57, 654–657. doi: 10.1099/ijs.0.64515-0

Lu, P., Sun, Q., Fu, P., Li, K., Liang, X., and Xi, Z. Y. (2020). *Wolbachia* inhibits binding of dengue and Zika viruses to mosquito cells. *Front. Microbiol.* 11:1750. doi: 10.3389/fmicb.2020.01750

Martinez, J., Longdon, B., Bauer, S., Chan, Y. S., Miller, W. J., Bourtzis, K., et al. (2014). Symbionts commonly provide broad spectrum resistance to viruses in insects: a comparative analysis of Wolbachia strains. *PLoS Pathog.* 10:e1004369. doi: 10.1371/journal.ppat.1004369

Moreira, L. A., Iturbe-Ormaetxe, I., Jeffery, J. A., Lu, G., Pyke, A. T., Hedges, L. M., et al. (2009). A *Wolbachia* symbiont in *Aedes aegypti* limits infection with dengue, chikungunya, and plasmodium. *Cells* 139, 1268–1278. doi: 10.1016/j.cell.2009.11.042

Moretti, R., Yen, P. S., Houe, V., Lampazzi, E., Desiderio, A., Failloux, A. B., et al. (2018). Combining Wolbachia-induced sterility and virus protection to fight *Aedes albopictus*-borne viruses. *PLoS Negl. Trop. Dis.* 12:e0006626. doi: 10.1371/journal.pntd.0006626

Mousson, L., Zouache, K., Arias-Goeta, C., Raquin, V., Mavingui, P., and Failloux, A. B. (2012). The native Wolbachia symbionts limit transmission of dengue virus in *Aedes albopictus*. *PLoS Negl. Trop. Dis.* 6:e1989. doi: 10.1371/journal.pntd.0001989

Nakamura, Y., Yukuhiro, F., Matsumura, M., and Noda, H. (2012). Cytoplasmic incompatibility involving Cardinium and Wolbachia in the white-backed planthopper *Sogatella furcifera* (Hemiptera: Delphacidae). *Appl. Entomol. Zool.* 47, 273–283. doi: 10.1007/s13355-012-0120-z

Nevalainen, L. B., Layton, E. M., and Newton, I. L. G. (2023). *Wolbachia* promotes its own uptake by host cells. *Infect. Immun.* 91:e0055722. doi: 10.1128/iai.00557-22

Newton, I. L., Savytskyy, O., and Sheehan, K. B. (2015). *Wolbachia* utilize host actin for efficient maternal transmission in *Drosophila melanogaster*. *PLoS Pathog.* 11:e1004798. doi: 10.1371/journal.ppat.1004798

Noda, H. (1984a). Cytoplasmic incompatibility in a rice planthopper. *J. Hered.* 75, 345–348.

Noda, H. (1984b). Cytoplasmic incompatibility in allopatric field populations of the small brown planthopper, *Laodelphax striatellus*. *Japan. Entomol. Exp. Appl.* 35, 263–267.

Osborne, S. E., Iturbe-Ormaetxe, I., Brownlie, J. C., O'Neill, S. L., and Johnson, K. N. (2012). Antiviral protection and the importance of Wolbachia density and tissue tropism in *Drosophila simulans*. *Appl. Environ. Microbiol.* 78, 6922–6929. doi: 10.1128/aem.01727-12

Poinsot, D., Charlat, S., and Mercot, H. (2003). On the mechanism of Wolbachia-induced cytoplasmic incompatibility: confronting the models with the facts. *BioEssays* 25, 259–265. doi: 10.1002/bies.10234

Qu, L. Y., Lou, Y. H., Fan, H. W., Ye, Y. X., Huang, H. J., Hu, M. Q., et al. (2013). Two endosymbiotic bacteria, *Wolbachia* and *Arsenophonus*, in the brown planthopper *Nilaparvata lugens*. *Symbiosis* 61, 47–53. doi: 10.1007/s13199-013-0256-9

Rainey, S. M., Shah, P., Kohl, A., and Dietrich, I. (2014). Understanding the Wolbachia-mediated inhibition of arboviruses in mosquitoes: progress and challenges. *J. Gen. Virol.* 95, 517–530. doi: 10.1099/vir.0.057422-0

Rances, E., Ye, Y. H., Woolfit, M., McGraw, E. A., and O'Neill, S. L. (2012). The relative importance of innate immune priming in *Wolbachia*-mediated dengue interference. *PLoS Pathog.* 8:e1002548. doi: 10.1371/journal.ppat.1002548

Rosen, L. (1988). Further observations on the mechanism of vertical transmission of flaviviruses by *Aedes mosquitoes*. *Am. J. Trop. Med. Hyg.* 39, 123–126. doi: 10.4269/ajtmh.1988.39.123

Ross, P. A., Turelli, M., and Hoffmann, A. A. (2019). Evolutionary ecology of *Wolbachia* releases for disease control. *Annu. Rev. Genet.* 53, 93–116. doi: 10.1146/annurev-genet-112618-043609

Rousset, F., Bouchon, D., Pintureau, B., Juchault, P., and Solignac, M. (1992). *Wolbachia* endosymbionts responsible for various alterations of sexuality in arthropods. *Proc. Natl. Acad. Sci. U. S. A.* 250, 91–98. doi: 10.1098/rspb.1992.0135

Sanaei, E., Albery, G. F., Yeoh, Y. K., Lin, Y. P., Cook, L. G., and Engelstadter, J. (2023). Host phylogeny and ecological associations best explain *Wolbachia* host shifts in scale insects. *Mol. Ecol.* 32, 2351–2363. doi: 10.1111/mec.16883

Sarao, P. S., Sahi, G. K., Neelam, K., Mangat, G. S., Patra, B. C., and Singh, K. (2016). Donors for resistance to brown planthopper *Nilaparvata lugens* (Stal) from wild rice species. *Rice Sci.* 23, 219–224. doi: 10.1016/j.rsci.2016.06.005

Scholz, M., Albanese, D., Tuohy, K., Donati, C., Segata, N., and Rota-Stabelli, O. (2020). Large scale genome reconstructions illuminate Wolbachia evolution. *Nat. Commun.* 11:5235. doi: 10.1038/s41467-020-19016-0

Schuler, H., Bertheau, C., Egan, S. P., Feder, J. L., Riegler, M., Schlick-Steiner, B. C., et al. (2013). Evidence for a recent horizontal transmission and spatial spread of Wolbachia from endemic *Rhagoletis cerasi* (Diptera: Tephritidae) to invasive *Rhagoletis cingulata* in Europe. *Mol. Ecol.* 22, 4101–4111. doi: 10.1111/mec.12362

Schultz, M. J., Tan, A. L., Gray, C. N., Isern, S., Michael, S. F., Frydman, H. M., et al. (2018). *Wolbachia* wStri blocks Zika virus growth at two independent stages of viral replication. *mBio* 9, e00738–e00718. doi: 10.1128/mBio.00738-18

Serbina, L. S., Gajski, D., Malenovsky, I., Corretto, E., Schuler, H., and Dittmer, J. (2022). *Wolbachia* infection dynamics in a natural population of the pear psyllid *Cacopsylla pyri* (Hemiptera: Psylloidea) across its seasonal generations. *Sci. Rep.* 12:16502. doi: 10.1038/s41598-022-20968-0

Shaikevich, E., Bogacheva, A., Rakova, V., Ganushkina, L., and Ilinsky, Y. (2019). Wolbachia symbionts in mosquitoes: intra- and intersupergroup recombinations, horizontal transmission and evolution. *Mol. Phylogenet. Evol.* 134, 24–34. doi: 10.1016/j.ympev.2019.01.020

Shaikevich, E., and Romanov, D. (2023). Symbiotic Wolbachia bacteria in coccinellid parasitoids: genetic diversity, horizontal transfer, and recombination. *Int. J. Microbiol.* 26, 269–280. doi: 10.1007/s10123-022-00295-0

Sintupachee, S., Milne, J. R., Poonchaisri, S., Baimai, V., and Kittayapong, P. (2006). Closely related *Wolbachia* strains within the pumpkin arthropod community and the potential for horizontal transmission via the plant. *Microb. Ecol.* 51, 294–301. doi: 10.1007/s00248-006-9036-x

Su, Q. H., Hu, G. W., Yun, Y. L., and Peng, Y. (2019). Horizontal transmission of *Wolbachia* in *Hylyphantes graminicola* is more likely via intraspecies than interspecies transfer. *Symbiosis* 79, 123–128. doi: 10.1007/s13199-019-00623-5

Sullivan, W. (2020). Vector control: *Wolbachia* expands its protective reach from humans to plants. *Curr. Biol.* 30, R1489–R1491. doi: 10.1016/j.cub.2020.11.005

Swiatoniowska, M., Ogorzalek, A., Golas, A., Michalik, A., and Szklarzewicz, T. (2013). Ultrastructure, distribution, and transovarial transmission of symbiotic microorganisms in *Nysius ericae* and *Nithecus jacobaeae* (Heteroptera: Lygaeidae: Orsillinae). *Protoplasma* 250, 325–332. doi: 10.1007/s00709-012-0416-4

Szklarzewicz, T., Jankowska, W., Łukasiewicz, K., and Szymańska, B. (2007). Structure of the ovaries and oogenesis in *Cixius nervosus* (Cixiidae), *Javesella pellucida* and *Conomelus anceps* (Delphacidae) (Insecta, Hemiptera, Fulgoromorpha). *Arthropod Struct. Dev.* 36, 199–207. doi: 10.1016/j.asd.2006.09.001

Szklarzewicz, T., Kalandyk-Kolodziejczyk, M., Kot, M., and Michalik, A. (2013). Ovary structure and transovarial transmission of endosymbiotic microorganisms in *Marchalina hellenica* (Insecta, Hemiptera, Coccomorpha: Marchalinidae). *Acta Zool.* 94, 184–192. doi: 10.1111/j.1463-6395.2011.00538.x

Tchankouo-Nguetcheu, S., Khun, H., Pincet, L., Roux, P., Bahut, M., Huerre, M., et al. (2010). Differential protein modulation in midguts of *Aedes aegypti* infected with chikungunya and dengue 2 viruses. *PLoS One* 5:e13149. doi: 10.1371/journal.pone.0013149

Teixeira, L., Ferreira, A., and Ashburner, M. (2008). The bacterial symbiont *Wolbachia* induces resistance to RNA viral infections in *Drosophila melanogaster*. *PLoS Biol.* 6, 2753–2763. doi: 10.1371/journal.pbio.1000002

Toomey, M. E., Panaram, K., Fast, E. M., Beatty, C., and Frydman, H. M. (2013). Evolutionarily conserved *Wolbachia*-encoded factors control pattern of stem-cell niche tropism in *Drosophila* ovaries and favor infection. *Proc. Natl. Acad. Sci. U. S. A.* 110, 10788–10793. doi: 10.1073/pnas.1301524110

Tram, U., and Sullivan, W. (2002). Role of delayed nuclear envelope breakdown and mitosis in *Wolbachia*-induced cytoplasmic incompatibility. *Science* 296, 1124–1126. doi: 10.1126/science.1070536

Turelli, M., Cooper, B. S., Richardson, K. M., Ginsberg, P. S., Peckenpaugh, B., Antelope, C. X., et al. (2018). Rapid global spread of wRi-like *Wolbachia* across multiple *Drosophila*. *Curr. Biol.* 28, 963–971. doi: 10.1016/j.cub.2018.02.015

Walker, T., Johnson, P., Moreira, L., Iturbe-Ormaetxe, I., Frentiu, F., McMeniman, C., et al. (2011). The wMel *Wolbachia* strain blocks dengue and invades caged *Aedes aegypti* populations. *Nature* 476:450. doi: 10.1038/nature10355

Wang, Z. Y., Deng, C., Yun, Y. L., Jian, C., and Peng, Y. (2010). Molecular detection and the phylogenetics of *Wolbachia* in Chinese spiders (Araneae). *J. Arachnol.* 38, 237–241. doi: 10.1636/joa_b09-69.1

Wang, G. H., Jia, L. Y., Xiao, J. H., and Huang, D. W. (2016). Discovery of a new Wolbachia supergroup in cave spider species and the lateral transfer of phage WO among distant hosts. *Infect. Genet. Evol.* 41, 1–7. doi: 10.1016/j.meegid.2016.03.015

Weinert, L. A., Araujo-Jnr, E. V., Ahmed, M. Z., and Welch, J. J. (2015). The incidence of bacterial endosymbionts in terrestrial arthropods. *Proc. R. Soc. Lond. B Biol. Sci.* 282:20150249. doi: 10.1098/rspb.2015.0249

Werren, J. H. (1997). Biology of Wolbachia. *Annu. Rev. Entomol.* 42, 587–609. doi: 10.1146/annurev.ento.42.1.587

Werren, J. H., Baldo, L., and Clark, M. E. (2008). *Wolbachia*: master manipulators of invertebrate biology. *Nat. Rev. Microbiol.* 6, 741–751. doi: 10.1038/nrmicro1969

Werren, J. H., and Bartos, J. D. (2001). Recombination in *Wolbachia*. *Curr. Biol.* 11, 431–435. doi: 10.1016/s0960-9822(01)00101-4

Werren, J. H., Zhang, W., and Guo, L. R. (1995). Evolution and phylogeny of *Wolbachia*: reproductive parasites of arthropods. *Proc. R. Soc. Lond. B Biol. Sci.* 261, 55–63. doi: 10.1098/rspb.1995.0117

Xi, Z. Y., Dean, J. L., Khoo, C., and Dobson, S. L. (2005). Generation of a novel *Wolbachia* infection in *Aedes albopictus* (Asian tiger mosquito) via embryonic microinjection. *Insect Biochem. Mol. Biol.* 35, 903–910. doi: 10.1016/j.ibmb.2005.03.015

Xi, Z. Y., Khoo, C. C. H., and Dobson, S. L. (2006). Interspecific transfer of *Wolbachia* into the mosquito disease vector *Aedes albopictus*. *Proc. R. Soc. Lond. B Biol. Sci.* 273, 1317–1322. doi: 10.1098/rspb.2005.3405

Xiao, Y., Chen, H., Wang, H., Zhang, M., Chen, X., Berk, J. M., et al. (2021). Structural and mechanistic insights into the complexes formed by *Wolbachia* cytoplasmic incompatibility factors. *Proc. Natl. Acad. Sci. U. S. A.* 118:e2107699118. doi: 10.1073/pnas.2107699118

Yang, L., and Zhang, W. (2016). Genetic and biochemical mechanisms of rice resistance to planthopper. *Plant Cell Rep.* 35, 1559–1572. doi: 10.1007/s00299-016-1962-6

Yen, J. H., and Barr, A. R. (1971). New hypothesis of the cause of cytoplasmic incompatibility in *Culex pipiens* L. *Nature* 232, 657–658. doi: 10.1038/232657a0

Zhang, Y., Cai, T., Ren, Z., Liu, Y., Yuan, M., Cai, Y., et al. (2021). Decline in symbiont-dependent host detoxification metabolism contributes to increased insecticide susceptibility of insects under high temperature. *ISME J.* 15, 3693–3703. doi: 10.1038/s41396-021-01046-1

Zhang, K. J., Han, X., and Hong, X. Y. (2013). Various infection status and molecular evidence for horizontal transmission and recombination of Wolbachia and Cardinium among rice planthoppers and related species. *Insect Sci.* 20, 329–344. doi: 10.1111/j.1744-7917.2012.01537.x

Zhao, Z., Zhu, J., Hoffmann, A. A., Cao, L., Shen, L., Fang, J., et al. (2021). Horizontal transmission and recombination of Wolbachia in the butterfly tribe Aeromachini Tutt, 1906 (Lepidoptera: Hesperiidae). G3-genes genomes. *Genetics* 11:jkab221. doi: 10.1093/g3journal/jkab221

Zheng, X. Y., Zhang, D. J., Li, Y. J., Yang, C., Wu, Y., Liang, X., et al. (2019). Incompatible and sterile insect techniques combined eliminate mosquitoes. *Nature* 572, 56–61. doi: 10.1038/s41586-019-1407-9

Zhou, J. C., Zhao, X., Huo, L. X., Shang, D., Dong, H., and Zhang, L. S. (2022). Wolbachia-driven memory loss in a parasitic wasp increases superparasitism to enhance horizontal transmission. *MBio* 13:e0236222. doi: 10.1128/mbio.02362-22

frontiers | Frontiers in Microbiology

TYPE Review
PUBLISHED 13 October 2023
DOI 10.3389/fmicb.2023.1267832

OPEN ACCESS

EDITED BY
Takema Fukatsu,
National Institute of Advanced Industrial Science and Technology (AIST), Japan

REVIEWED BY
Yunsheng Wang,
Hunan Agricultural University, China
Sonam Popli,
University of Toledo, United States

*CORRESPONDENCE
Giulio Petronio Petronio
✉ giulio.petroniopetronio@unimol.it

RECEIVED 27 July 2023
ACCEPTED 25 September 2023
PUBLISHED 13 October 2023

CITATION
Minwuyelet A, Petronio Petronio G, Yewhalaw D, Sciarretta A, Magnifico I, Nicolosi D, Di Marco R and Atenafu G (2023) Symbiotic *Wolbachia* in mosquitoes and its role in reducing the transmission of mosquito-borne diseases: updates and prospects. *Front. Microbiol.* 14:1267832. doi: 10.3389/fmicb.2023.1267832

Symbiotic *Wolbachia* in mosquitoes and its role in reducing the transmission of mosquito-borne diseases: updates and prospects

Awoke Minwuyelet[1], Giulio Petronio Petronio[2]*, Delenasaw Yewhalaw[3,4], Andrea Sciarretta[5], Irene Magnifico[2], Daria Nicolosi[6], Roberto Di Marco[2] and Getnet Atenafu[1]

[1]Department of Biology, College of Natural and Computational Sciences, Debre Markos University, Debre Markos, Ethiopia, [2]Department of Medicine and Health Sciences, University of Molise, Campobasso, Italy, [3]Tropical and Infectious Diseases Research Center, Jimma University, Jimma, Ethiopia, [4]Faculty of Health Sciences, School of Medical Laboratory Sciences, Jimma University, Jimma, Ethiopia, [5]Department of Agriculture, Environment and Food Sciences, Università degli Studi del Molise, Campobasso, Italy, [6]Department of Pharmaceutical and Health Sciences, Università degli Studi di Catania, Catania, Italy

Mosquito-borne diseases such as malaria, dengue fever, West Nile virus, chikungunya, Zika fever, and filariasis have the greatest health and economic impact. These mosquito-borne diseases are a major cause of morbidity and mortality in tropical and sub-tropical areas. Due to the lack of effective vector containment strategies, the prevalence and severity of these diseases are increasing in endemic regions. Nowadays, mosquito infection by the endosymbiotic *Wolbachia* represents a promising new bio-control strategy. Wild-infected mosquitoes had been developing cytoplasmic incompatibility (CI), phenotypic alterations, and nutrition competition with pathogens. These reduce adult vector lifespan, interfere with reproduction, inhibit other pathogen growth in the vector, and increase insecticide susceptibility of the vector. Wild, uninfected mosquitoes can also establish stable infections through trans-infection and have the advantage of adaptability through pathogen defense, thereby selectively infecting uninfected mosquitoes and spreading to the entire population. This review aimed to evaluate the role of the *Wolbachia* symbiont with the mosquitoes (*Aedes, Anopheles,* and *Culex*) in reducing mosquito-borne diseases. Global databases such as PubMed, Web of Sciences, Scopus, and pro-Quest were accessed to search for potentially relevant articles. We used keywords: *Wolbachia*, *Anopheles*, *Aedes*, *Culex*, and mosquito were used alone or in combination during the literature search. Data were extracted from 56 articles' texts, figures, and tables of the included article.

KEYWORDS

mosquito symbiont, *Wolbachia*, *Aedes*, *Anopheles*, *Culex*, mosquito, mosquito-borne diseases

1. Introduction

Due to their high adaptation capacity to various environments, mosquitoes have endured for millions of years (Couper et al., 2021). Different pathogenic, endosymbiont and symbiotic organisms have the ability to infect them. The main carriers of human pathogens are various species of mosquitoes from the genera *Aedes, Anopheles,* and *Culex*. Those mosquito genera are vectors of emerging and reemerging human diseases caused by pathogens, such as protozoan parasites, viruses, and nematodes (Iturbe-Ormaetxe et al., 2011).

Among the protozoan parasitic diseases, malaria is caused by different *Plasmodium* species. It is a life-threatening disease spread to humans by the bite of infected female *Anopheles* mosquitoes. According to the *World Health Organization* (WHO) report in 2022, globally, more than 3.2 billion people (almost half the world's population) are at risk of malaria; furthermore, 245 million malaria cases have been recorded, with a mortality of 0.6 million. Children are the most affected group of patients. Malaria is also a great burden from an economic point of view; $ 12 billion is lost per year in economic productivity in Africa alone (WHO, 2022).

Similarly, among mosquito-borne viral diseases, viruses belonging to the *Flaviviridae* family, such as *Dengue* virus, *Zika* virus, yellow fever virus, chikungunya virus, and *West Nile* virus, can be transmitted to humans by *Aedes aegypti* and *Ae. albopictus*.

About half of the world's population is at risk of dengue, which is estimated to infect 100–400 million people yearly. It is found in tropical and subtropical climates worldwide, mainly in urban and semi-urban areas (Leta et al., 2018). Likewise, West Nile fever is caused by an RNA virus, namely *West Nile* virus (WNV). The virus causes severe disease in birds, horses, and other mammals, but most human infections occur through the bite of infected mosquitoes. About 1 in 150 infected people develop neurological disease and die. It is common in Africa, Europe, the Middle East, North America, and Western Asia (Leta et al., 2018; CDC, 2023). In addition, Yellow fever is caused by an arbovirus and is transmitted to humans through the bites of infected *Aedes* and *Haemagogus* mosquitoes. It is a high-impact high-threat disease with the risk of cross-boundary transmission (Leta et al., 2018; WHO, 2023a).

Moreover, the Zika virus is transmitted to humans through the bites of infected mosquitoes, mainly *Ae. aegypti*, particularly in tropical regions. Zika virus infection clinical manifestation is similar to other arboviruses, with fever, skin rash, conjunctivitis, muscle and joint pain, fatigue, and headache (Leta et al., 2018; WHO, 2023b). On the other hand, Chikungunya fever is caused by an RNA virus belonging to the *alphavirus* genus, the *Togaviridae* family. Infection in humans occurs through the bite of infected female mosquitoes (commonly *Ae. aegypti* and *Ae. albopictus*). More than 2 million cases arise each year. The disease is now identified in more than 110 countries (Bettis et al., 2022).

Among nematode infections transmitted by mosquito vectors, filariasis is mainly caused by the filarial worm *Wuchereria bancrofti,* and less commonly *Brugia malayi* and *Brugia timori*. *Anopheles* is the main filariasis vector in Africa, however, in the Americas the main vector is *Culex*. It is also transmitted by the bite of infected *Aedes* and *Mansonia* species. Filariasis has been considered a neglected tropical disease. However, it is the second leading cause of permanent malformation and disability, next to leprosy worldwide. Lymphatic filariasis affects the lymphatic system and causes abnormal enlargement of body parts, which can cause pain, severe disability, and social stigma. It affects more than 120 million of people in 72 tropical and subtropical countries. Over 882 million people in 44 countries worldwide remain threatened by lymphatic filariasis and require preventive chemotherapy to stop the spread of this parasitic infection (Bizhani et al., 2021; WHO, 2021).

To reduce the threat and burden of these vector-borne diseases, insecticides have been widely used in the last many years. However, due to the frequent and prolonged use of insecticides to control insect disease vectors and pests of crops, mosquitoes developed resistance to several classes of insecticides. As a result, bacteria belonging to the *Wolbachia* genus have been proposed as potential candidates for mosquito-borne disease control strategies (van den Berg et al., 2021). A brief timeline of *Wolbachia* isolation, the impact of infection, and utilization as a prevention method is presented in Figure 1 (Werren and O'Neill, 1997; Carrington et al., 2011; Kamtchum-Tatuene et al., 2017; Dorigatti et al., 2018).

Wolbachia is a genus of Gram-negative, non-spore-forming, obligate intracellular parasitic bacteria that frequently infect mosquitoes. It is a member of the Alphaproteobacteria belonging to the Rickettsiales order. The bacterium was first isolated in 1924 by Hertig and Wolbach from the *Cx. pipiens* germlines (Hertig and Wolbach, 1924). Later in 1936, Hertig, designated it as *Wolbachia pipientis* (Hertig, 1936; Philip, 1956).

In the last two decades, different strains of *Wolbachia* were isolated and identified by genome sequencing: *Wolbachia* wAna, *Wolbachia* wSim, *Wolbachia* wMel, and *Wolbachia* wMoj from *Drosophila* species (Salzberg et al., 2005). Then different *Wolbachia* strains are grouped into two major phylogenetic lineages. More than 18 clades, ranging from A to R, have been identified, and almost all were isolated from arthropods (Landmann, 2019). The general distribution of *Wolbachia* strains and their associated supergroups in mosquitoes are summarized in Figure 2 (Inácio da Silva et al., 2021).

Besides mosquitoes, these intracellular bacteria selectively infect arthropods, nematodes, and other organisms but are harmless to humans (Osei-Poku et al., 2012). It forms endosymbiotic relationships that range from parasitism to mutualism (Zug and Hammerstein, 2012; Sullivan, 2017). Parasitism and mutualism are host, environment, temperature, and density-dependent induced by the same genetic machinery and shifted by selection (Bordenstein et al., 2009; Zug and Hammerstein, 2015; Rohrscheib et al., 2016). Parasitism persistently affects several hosts' biological indicators, such as physiology, immunity, and host development (Werren et al., 2008; Gutzwiller et al., 2015). The host's capacity for reproduction was also altered. Additionally, it makes arthropods sterile, and infertile, with reduced longevity, which strongly impacts male mosquitoes (Werren and Windsor, 2000; Ahmed et al., 2015; Sicard et al., 2019). On the other hand, mutualism provides resistance to viral pathogens or the provision of metabolites during host nutritional stress (Allman et al., 2020; Kaur et al., 2021).

Abbreviations: AMP, Antimicrobial peptides; CHIKV, Chikungunya virus; CI, Cytoplasmic incompatibility; DDT, Dichlorodiphenyltrichloroethane; DENV, Dengue Virus; IIT, Incompatible insect technique; IMM, Integrated mosquito management; NO, Nitric oxide; PCR, Polymerized chain reaction; RNA, Ribonucleic acid; ROS, Reactive oxygen species; SIT, Sterile insect technique.

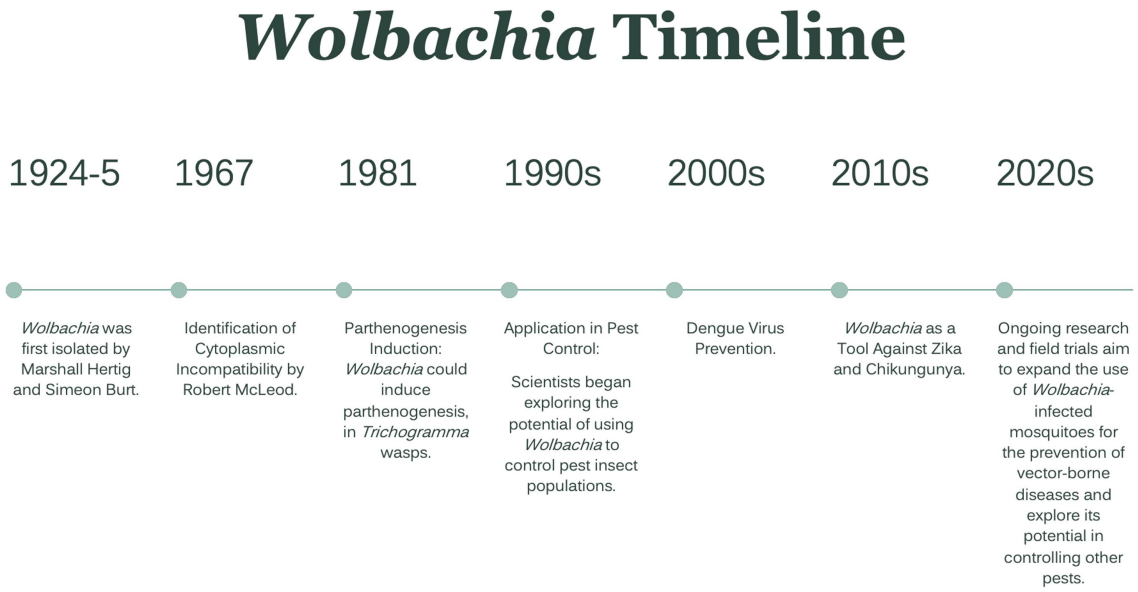

FIGURE 1
Wolbachia Timeline. From first isolation to ongoing research.

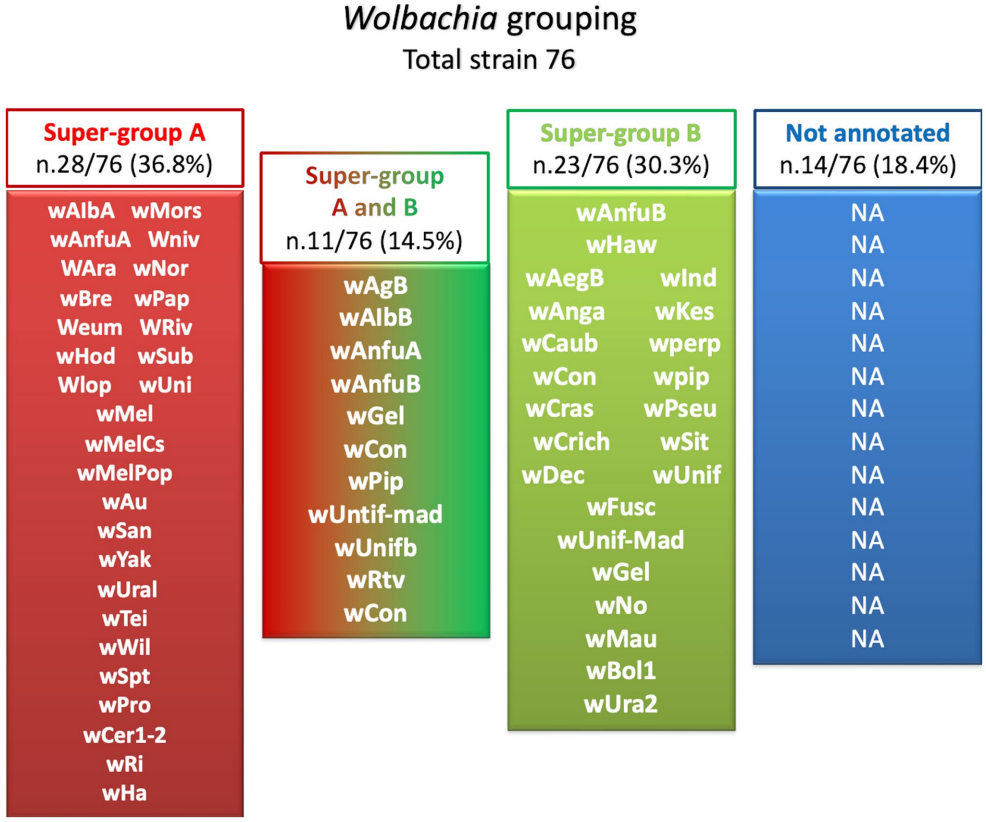

FIGURE 2
Wolbachia strains isolated from mosquito grouping. Of the 76 isolated *Wolbachia* strains, 28 (36.8%) belong to super-group A (Red), 23 strains (30.3%) are also grouped in super-group B (Green), 11 strains (14.5%) are also grouped under both A and B (Red and Green), while 14 (18.4%) were non annotated (Blue).

The bacterium has the ability to be transmitted vertically through insect eggs and spread horizontally across populations (Hedges et al., 2008; Zug and Hammerstein, 2012; Duron et al., 2015). A vertically transmitted *Wolbachia* is frequently found in the insect's endosymbionts, with a 28%–30% prevalence of naturally infected mosquitoes (Kittayapong et al., 2000; Dorigatti et al., 2018; Inácio da Silva et al., 2021). Furthermore, there are different types of symbiont transmission, from vertical (genetic) to horizontal (infectious), with horizontal transmission opting for parasitism. In contrast, vertically transmitted endosymbionts evolve toward reciprocity (Zug and Hammerstein, 2015) among naturally infected genera: *Aedes, Culex*, *Drosophila,* and other insect species (Osei-Poku et al., 2012; Sicard et al., 2019; Inácio da Silva et al., 2021) but not commonly reported in *Ae. aegypti* and *Anopheles* species.

Even though *Wolbachia* infection is transmitted between unrelated species, it spreads more quickly among related species. As a result, strains that naturally exist in mosquitoes are suitable for trans-infection into different vector species, enabling bacterial diffusion among mosquito populations (Turelli and Hoffmann, 1991).

Wolbachia-infected mosquitoes reduce mosquito-borne diseases by reducing competent mosquito populations or the vector's number of mosquitoes and/or pathogen replication (Yen and Failloux, 2020). This is due to CI stimulated by the dynamics of *Wolbachia* strains introduced into a mosquito population and immune modulation (Kambris et al., 2010), which are triggered to change the host's behavior and the pathogenic transmission effect (Sinkins et al., 2005; Hedges et al., 2008; Kambris et al., 2009, 2010; Dorigatti et al., 2018). This phenomenon reduces pathogen replication and disease transmissions by vectors to humans and/or animals.

In this review, we focused on assessing the role of *Wolbachia* infection in the genera *Aedes, Anopheles,* and *Culex* in reducing vector-borne diseases. Global electronic databases (PubMed, Web of Sciences, Scopus, and Pro-Quest) were used to search potentially relevant and most recent articles published from 2000 to 2022. *Wolbachia, Anopheles, Aedes, Culex*, and mosquito were used alone or in combination as a keyword during the literature search. The search was conducted from November 15th to December 12th, 2022. Papers were chosen according to topic pertinence; only research articles published in English and articles with all the required information were included in the review. Data were extracted from the included articles' texts, figures, and tables, of the included articles. Preliminary 946 articles were accessed, of which only 56 were used for review, as shown in Supplementary Figure S1 and Supplementary Table S1.

2. *Wolbachia* strain and mosquito infection

This study retrieved 56 original studies. Of these, 32 and 13 studies reported infection of *Aedes* and *Anopheles* species by *Wolbachia*. Other 11 original studies revealed infection in *Culex* species (Supplementary Figure S1 and Supplementary Table S1).

2.1. *Wolbachia* infection in *Aedes* species

The genus *Aedes* includes more than 950 species and is one of the most widespread mosquito genera in the world (Rogers, 2023). Among them, *Ae. aegypti* and *Ae. albopictus* are the most known biological vectors of vector-borne diseases (Brelsfoard and Dobson, 2011; Silva et al., 2017; Damiani et al., 2022) and are included in this study. These two main species are primarily responsible for spreading filariasis, dengue, yellow fever, chikungunya, West Nile Virus, and Zika fever, which can result in serious human diseases (Hoey, 2000; Brasil et al., 2016). These illnesses are a major public health problem resulting in millions of infections and thousands of fatalities yearly (Caragata et al., 2021).

Due to the disease's severity and the limitation of current prevention patterns, entomopathogenic bacteria have been explored to enhance current control measures and proposed as an effective strategy to reduce the increasing problem of vector-borne diseases (Turley et al., 2009; Mohanty et al., 2016; Yen and Failloux, 2020).

A recent molecular study by Li et al. (2023) in the Chinese province of Hainan revealed that the prevalence of *Wolbachia* was 86.7% from field-collected *Ae. albopictus* (Li et al., 2023). Another study conducted in eastern Thailand by Kittayapong et al. (2002) demonstrated the maternal transmission of *Wolbachia* from field-collected *Ae. albopictus* was nearly 100%. Wild infections also have efficient vertical transmission across host generations, essential for symbiosis. Even though there was no natural infection report of *Ae. aegypti* populations by *Wolbachia*, many studies indicated trans-infection techniques to infect non-wild infected mosquito populations (Turley et al., 2009; Walker et al., 2011; Jeffries and Walker, 2015; O'Neill, 2018; Ding et al., 2020; Liew et al., 2021). This technique established stable vertical transmission in *Ae. albopictus*, *Ae. aegypti* and *Anopheles* species (McMeniman et al., 2009; Iturbe-Ormaetxe et al., 2011; Calvitti et al., 2014).

2.1.1. *Wolbachia* infection and its effect on *Aedes* species

Wolbachia infection on *Aedes* is becoming an increasingly popular alternative candidate strategy for controlling vector-borne disease transmission (Brelsfoard and Dobson, 2011). According to research findings, infected females can successfully mate with infected and uninfected males and give live *Wolbachia*-positive offspring (Sinkins, 2004; O'Neill, 2018). On the other hand, when uninfected females mate with infected males, they produce non-viable eggs (Figure 3) (Charlat et al., 2001; Poinsot et al., 2003; Werren et al., 2008; Brelsfoard and Dobson, 2011; Beebe et al., 2021). As a result of male sperm infection, haploid cells do not effectively fuse with uninfected eggs, causing the failure of embryonic development or early embryonic death (Caragata et al., 2021). Other research findings pointed out that *Wolbachia*-infected male nutrition can be linked to reduced fertility and fecundity in mates (Islam and Dobson, 2006; Beebe et al., 2021). This disrupts the normal development of the zygote produced by infected males and uninfected females mating (Serbus et al., 2008).

The study conducted in Crevalcore, Italy by Puggioli et al. (2016) focused on using a specific *Ae. albopictus* line that was genetically modified to produce sterile males generated by introducing wPip in the ARwP line. The finding showed bidirectional reproductive barriers between infected and uninfected mosquitoes, meaning that when infected males mate with uninfected females or vice versa, the eggs produced fail to develop or hatch, thus leading to a reduction in the overall mosquito population (Puggioli et al., 2016). Similarly, the study conducted by Moretti et al. (2018) in Italy focused on a genetically manipulated line of *Ae. albopictus* mosquitoes using ARwP-M reduced

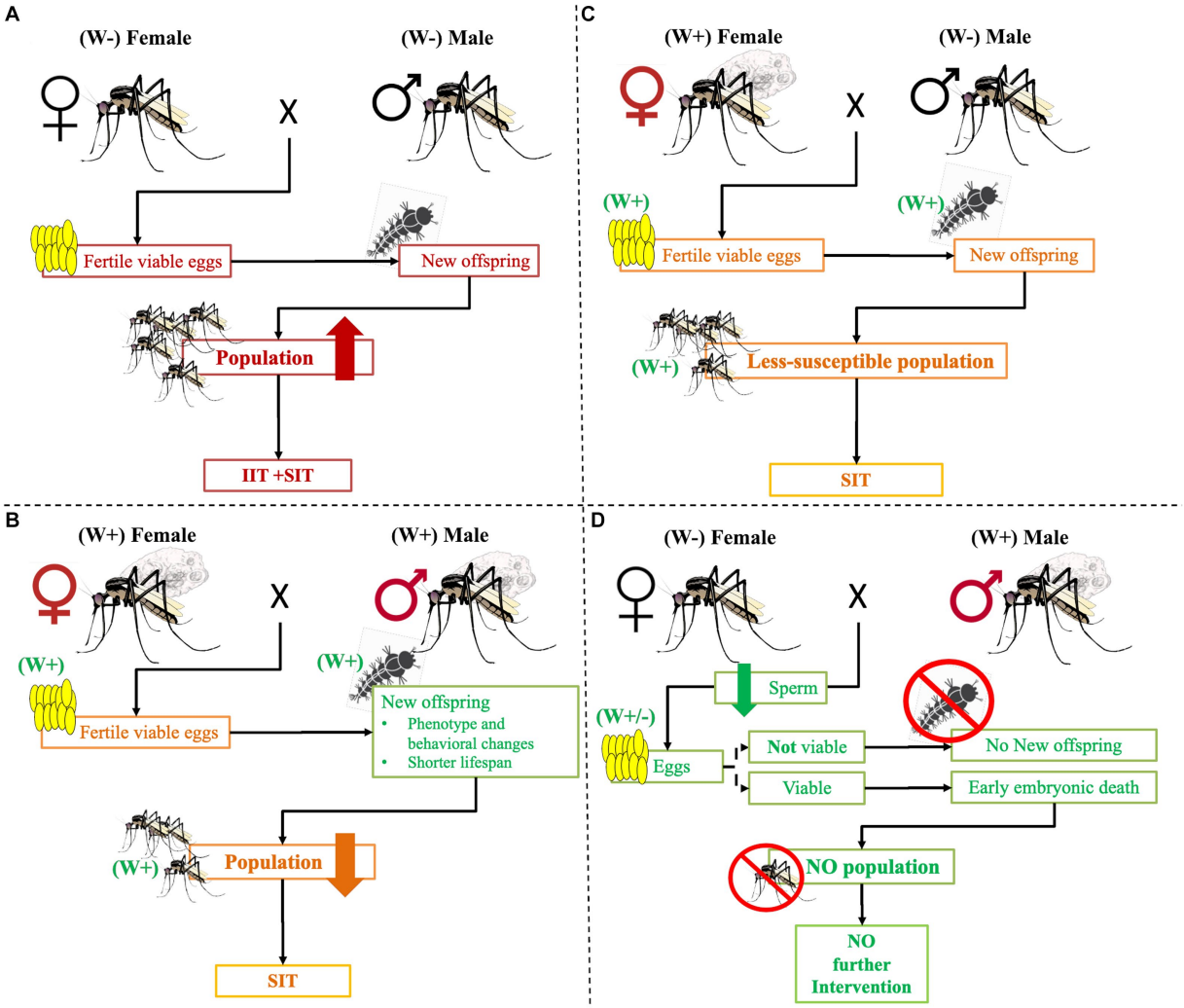

FIGURE 3
The possible crosses between *Wolbachia*-infected and/or uninfected mosquitos. Maternal transmission of *Wolbachia* effects. **(A)** When *Wolbachia* uninfected female and male mosquitoes mate, they will give a viable egg that will continue the next generation and disease transmission. To tackle it, intervention, IIT, and/or SIT are needed. Similarly, **(B)** when infected females and males mate, they produce infected viable eggs. However, the development of the offspring continues the phenotype, adult behaviors may change, the life span is short, and the population declines. As a result, no more diseases frequently occur, but intervention like SIT is still needed. **(C)** When infected females mate with uninfected males, they produce infected viable eggs that can grow but are less susceptible to developing pathogens and transmitting diseases. The adult life span may be short and may not effectively bite humans and other hosts. Nevertheless, control intervention such as SIT is needed. **(D)** When an uninfected female mating with an infected male, no more viable egg is produced or early embryonic death occurs in the new generation. As a result, no more intervention is needed. Key: W+: *Wolbachia* infected, W−: *Wolbachia* uninfected, ×: Mates.

Ae. albopictus populations. This suggested the introduction of a combined ARwP-M line, which carries wPip and wMel-induced sterility and virus protection to fight *Ae. Albopictus-borne* viruses. This could be a potential strategy for controlling *Ae. albopictus* populations and reducing the transmission of chikungunya and dengue viruses (Moretti et al., 2018).

Based on this, to reduce the *Ae. albopictus* population in the field, Zheng et al. (2019) used Incompatible Insect Technology (IIT), which utilizes sterilization with the maternally inherited endosymbiont *Wolbachia*, but the accidental release of females infected with the same strain of *Wolbachia* as the released males could comprise its effectiveness (Zheng et al., 2019). In this scenario, a study conducted in Nanyang, Singapore by Ong et al. (2022) reported that an IIT combined with a sterile insect technique (IIT-SIT) releasing X-ray irradiated *Wolbachia*-infected male mosquitoes resulted in a 98% reduction in *Ae. aegypti* populations also showed an 88% reduction in the incidence of dengue fever (Ong et al., 2022).

Likewise, an on-field trial performed in South Miami, United States, by Mains et al. (2019) showed the release of many infected *Ae. aegypti* males significantly reduced the egg-hatching rate in areas populated by infected males, consistent with the CI expectations. Similarly, the number of *Ae. aegypti* were significantly reduced in areas where infected males were getting infected compared to untreated areas, reducing the Zika virus burden (Mains et al., 2019). Moreover, the release of sterile or incompatible males resulted in the suppression of both wild-type and wMel-infected *Ae.aegypti*

populations, confirming the utility of bidirectional incompatibility in the field (Beebe et al., 2021) as demonstrated in northern Queensland, Australia by Beebe et al. (2021).

The main limitation of the IIT is releasing infected male mosquitos maternally inherited. To overcome this constraint, a combination strategy between IIT techniques and the Sterile Insect Technique (SIT) was also tested, whereby overwhelming numbers of sterile insects are released into the wild (Zheng et al., 2019; Villegas-Chim et al., 2022). SIT is a control method applied against agricultural pests as well as human disease vector populations, by providing the release of sterile or incompatible males (Werren et al., 2008). According to Iturbe-Ormaetxe et al. (2011), *Wolbachia* transinfection experiments are more successful when the donor and recipient organisms are closely related.

Likewise, Moreira et al. (2009a,b) and Bian et al. (2010) demonstrated that bacterial infection can occur in different body parts of *Ae.aegypti* like the midgut, fat body, brain, and salivary gland, with a high prevalence in the reproductive tissues, both ovaries and testicles (Bi and Wang, 2020). Another study conducted in Mexico by Mejia et al. (2022) found relatively greater *Wolbachia* densities in reproductive tissues than those in the somatic tissues (Mejia et al., 2022). This implies that reproductive parts infection can inhibit the vector fecundity and fertility.

Beyond the reproductive system, the brain also is a target for *Wolbachia* infection, affecting oviposition and host-seeking behavior. However, this condition does not alter the attraction of mosquitoes to the human odor (Wiwatanaratanabutr et al., 2010; Turley et al., 2014) but rather, the blood-feeding ability by affecting the proboscis's anatomy (Turley et al., 2009; Moreira et al., 2009a; Bian et al., 2010).

A study by Caragata et al. (2016a) demonstrated that *Wolbachia* infection can induce diet-nutritional stress in *Ae. aegypti* reducing vector susceptibility versus Dengue virus and the avian malarial parasite *Plasmodium gallinaceum*. Similarly, Geoghegan et al. (2017) found that infection alters lipid/cholesterol metabolism including differential cholesterol and lipid profiles (Geoghegan et al., 2017). These findings suggest a possible competition for nutrients between *Wolbachia* and other pathogens inhibiting replication and shortening vector life span.

According to De Oliveira et al. (2017), *Ae. albopictus* demonstrated greater competitive ability in a variety of laboratory settings. Its larvae outperformed *Ae. aegypti* (both infected and uninfected groups) in terms of development and performance index survival rate. *Wolbachia* boosted the larval survival rate of *Ae. aegypti.* This finding indicated that larval density greatly impacts the competition for nutrients in infected vectors (De Oliveira et al., 2017).

According to a study conducted by Islam and Dobson (2006) on the impact of *Wolbachia* on *Ae. albopictus,* uninfected larvae, had the best survival rate, partly because males infected with wAlbB or wAlbA had lower survival rates. Dutra et al. (2016), recorded similar results at Penn State Brazil and found that wMel infection of *Ae. aegypti* caused faster larval growth in males and females at greater densities but did not affect females living in less crowded settings (Dutra et al., 2016). While wMelPop infection of *Ae. aegypti* exhibited highly inhibitory effects of larval food level, the effect of strain alone was not significant, according to a different study conducted in Queensland, Australia by Kho et al. (2016). These differences may be due to bacterial density and host susceptibility. Thus a higher density causes more pronounced effects. For instance, *W. pipientis* strain wMelPop is known for shortening life spans when inserted into the main dengue vector *Ae. aegypti* (Thomas et al., 2011; Yeap et al., 2014) but not in *Ae. albopictus* (Mousson et al., 2010), as demonstrated by Wiwatanaratanabutr et al. (2010).

According to Ross et al. (2017) wMel and wMelPop-CLA infections of *Ae. aegypti* could not be transmitted to the next generation when mosquitoes were exposed to 26–37°C across all life stages. In contrast, under the same temperature range, an increase in infection density allowed the infection to be inherited from mother to offspring (Ross et al., 2017).

Besides vertical transmission, innate immune priming is also strain and density-dependent. Indeed, epithelial cells that are also involved in regulating innate immune responses to bacteria and parasites produce a significant number of reactive oxygen species and antimicrobial peptides (Ryu et al., 2010; Pircalabioru et al., 2016). In *Ae. aegypti,* an increased level of reactive oxygen compounds suppresses the replication of West Nile virus (Hussain et al., 2013), Dengue virus (Bian et al., 2010; Frentiu et al., 2014), Chikungunya virus (Aliota et al., 2016a), and Zika virus (Aliota et al., 2016b). Furthermore, it confers resistance to various ribonucleic acid (RNA) viruses and virus-induced death in flies, but it reduces adult vectorial capacity (Mohanty et al., 2016). Replication of West Nile virus is significantly reduced in the presence of *Wolbachia* by the alteration of GATA4 expression which inhibits virus assembly (Hussain et al., 2013). Those imply that *Wolbachia* infection has evolutionary, biological, and developmental impacts on mosquito vectors.

On the other hand, Quek et al. (2022) found that in the absence of *Wolbachia*, microfilariae quickly lose their capacity to develop in the mosquito vector because of their inability to break out of their shells and get through the gut wall. They also showed that the enzyme chitinase, essential for microfilariae to leave their shells, was low in *Wolbachia*-depleted microfilariae, preventing them from leaving their shells. When chitinase was added to *Wolbachia*-depleted microfilariae in a lab, they could break out of their shells just as well as the ones that were not treated. So, it looks like *Wolbachia* has a big role in the transmission of filariasis and suggests that anti-*Wolbachia* treatment mediates a more accelerated impact on the elimination of lymphatic filariasis (Quek et al., 2022).

2.2. *Wolbachia* infection in *Anopheles* mosquitoes

Among all retrieved articles in this review, 13 were on *Wolbachia* infection of *Anopheles* species (Supplementary Figure S1 and Supplementary Table S1). There are more than 460 recognized species in the genus *Anopheles. An. gambiae* and *An. funestus* are the most significant global malaria vectors (Sinka et al., 2012; Wiebe et al., 2017). Currently, *An.stepheni* is going to be the main concern for malaria transmission in Africa. The genus *Anopheles* is most well-known for conveying malaria but also transmits other diseases like filarial worms (Coetzee, 2020; Kientega et al., 2022).

The first recorded on-field infection of *Wolbachia* in *Anopheles* species was reported in Burkina Faso by Baldini et al. (2014) using 16S rRNA gene analysis from *An. gambiae* reproductive tissue. This study also isolated a new strain of *Wolbachia*, namely wAnga. Similarly, other research conducted in Senegal reported the first *Wolbachia* on-field infection in another species, namely *An.*

funestus, using the 16S rRNA gene and isolating new strains called wAnfu-A and wAnfu-B (Niang et al., 2018). In 2022 Waymire et al. detected *Wolbachia* haplotypes in wild *Anopheles stephensi* in eastern Ethiopia (Waymire et al., 2022). Despite this evidence, according to a phylogenies screening conducted in 2019 by Chrostek and Gerth on *Wolbachia* 16S rRNA presence in *An. gambiae* there is no congruence between host and symbiont phylogenies (Chrostek and Gerth, 2019).

2.2.1. *Wolbachia* infection and parasite development *Anopheles* species

Once the *Anopheles* infection is established, the inherent mechanism is similar to the *Aedes* and *Culex* species, as shown in Figure 2 (Hughes et al., 2011). However, the role of *Wolbachia* in inhibiting the malaria parasites in *Anopheles* mosquitoes is still not well-known (Straub et al., 2020), *In vitro* trans-infection of *An. gambiae* with wMelPop and wAlbB strains performed by Hughes et al. (2011) demonstrated the bacteria distributed throughout the fat body, head, sensory organs, and other tissues.

On the other hand, a study conducted in Pennsylvania, United States, by Hughes et al. (2012) found that the wAlbB strain significantly increases *P. berghei* oocyst levels in the infected *An. gambiae* midgut while wMelPop modestly suppresses oocyst levels. Another study from East Lansing, United States, by Joshi et al. (2014), reported that wAlbB infections of *An. stephensi* had reduced female fecundity and caused a minor decrease in male mating competitiveness. Later, Joshi et al. (2017) revealed wAlbB infection in *An. stephensi* led to a reduction in parasite numbers of up to 92% at the sporozoite stage and more than half at the oocyst stage. This finding implies that wAlbB strain infections can reduce the parasite density depending on the *Plasmodium* species and vector population. This evidence is in agreement with what was reported by Baldini et al. (2018) on natural *Wolbachia* infection in the malaria mosquito *Anopheles arab*iensis in Tanzania.

Another study conducted in Dangassa, Mali, by Gomes et al. (2017) found the *Wolbachia* infection in the field-collected *An. coluzzii* was positive for wAnga and revealed a significantly lower prevalence and intensity of *P. falciparum* sporozoite. Similarly, in Bobo-Dioulasso, Burkina Faso, Shaw et al. (2016) revealed that *Wolbachia* infections in natural *Anopheles* populations affect egg laying and negatively correlate with *Plasmodium* development. Finally, in 2020 Wong et al. reported that *Wolbachia* infection in *An. gambiae* is able to reduce the mosquito life span and provide resistance to pathogen infection (Wong et al., 2020).

2.3. *Wolbachia* infection in *Culex* species

Among all retrieved articles in this review, 11 have as subjects the epidemiology and infection of *Culex* species (Supplementary Table S1). The genus *Culex* has several species; however, *Cx. pipiens* and *Cx. quinquefasciatus,* reviewed in the selected studies, are vectors for various human diseases, such as arbovirus diseases like the *West Nile* virus, Japanese encephalitis, and filariasis (Harbach, 1985; Omar, 1996; Paramasivan et al., 2003).

The first *Wolbachia* infection in mosquitoes was reported from *Cx. pipiens* reproductive tissues by Hertig and Wolbach (1924). Later on, different studies showed that the prevalence of *Wolbachia* in this species ranges from 65% to 100% in field-collected females and nearly 100% in males (Karami et al., 2016; Bergman and Hesson, 2021).

2.3.1. *Wolbachia* infection and its effect on the *Culex* species

The mode of infection and its effect on *Culex* physiology is similar to *Aedes*. However, Hague et al. (2020) demonstrated that the infected host raises temperature preference. In contrast to the uninfected, most hosts infected with *Wolbachia* supergroup A prefer cooler temperatures than uninfected ones, On the other hand, supergroup B infected hosts prefer warmer temperatures (Hague et al., 2020). These findings suggest that *Wolbachia* infection-inducing host behavior's alterations facilitate bacterial replication and disease spread (Moreira et al., 2009b; Glaser and Meola, 2010; Caragata et al., 2016b). Interestingly similar evidence has not been reported for *Aedes* and *Anopheles*.

According to Atyame et al. (2011) a considerable amount of *Wolbachia* diversity can be generated within a single host species in a short time, and playing a key role in their evolution. Furthermore, a recent study by Zhang et al. (2020) clarified the immune system's role in *Cx. pipiens* infection, according to the author the competition for scarce nutrients may not be the primary cause of *Wolbachia*-mediated pathogen suppression, as evidenced by the fact that the presence of *Wolbachia per se* does not always alter pathogen infections. Instead, it is brought on by host immunological reactions (Zhang et al., 2020).

In vitro insecticide susceptibility studies by Berticat et al. (2002) and Duron et al. (2006) showed that the symbiotic maternally inherited *Wolbachia* affected *Cx. quinquefasciatus* and *Cx. pipiens* insecticide resistance depending on infection density and the type of insecticide used (Berticat et al., 2002; Duron et al., 2006). Therefore, a medium-density infection synergises with deltamethrin and other organophosphates, but not with Dichloro-diphenyl-trichloroethane (DDT) (Berticat et al., 2002; Duron et al., 2006; Shemshadian et al., 2021). Likewise, Echaubard et al. (2010) also reported that a medium-density infection in *Cx. pipiens* made the vector insecticide-susceptible whereas with a higher density infection caused insecticide-resistance. These results may partially explain the presence of high-density infections in pesticide-resistant mosquitoes in the field (Echaubard et al., 2010).

Similarly, *in vitro* infection with wPipSJ made *Cx. quinquefasciatus* less susceptible to entomopathogenic bacteria as demonstrated by Díaz-Nieto et al. (2021). These findings agree with on-field records, where *Cx. quinquefasciatus* infected by wPipSJ are more resistant to *Bacillus wiedmannii* var. *thuringiensis*, and *B. thuringiensis* subsp. israelensis, and *Lysinibacillus sphaericus* bacterial infections (Díaz-Nieto et al., 2021).

3. Discussion

Integrated Mosquito Management (IMM) strategies are currently the best option for reducing mosquito populations (CDC, 2020). This implementation is based on understanding mosquito biology, ecology, and mosquito pathogen interaction. Indeed, IMM programs employ several strategies, together with insecticides, such as larval breeding source reduction through community participation and biological control techniques like predatory fish and symbiotic bacteria (Dodson et al., 2017; CDC, 2020).

Currently, scientific evidence has underscored the appropriate use of the symbiotic bacteria *W. pipientis* as a new weapon in the fight against mosquitoes as vector-borne diseases. Compared to insecticide-based methods, it has the advantage of potentially being more cost-effective and environmentally friendly (Iturbe-Ormaetxe et al., 2011). In addition, *Wolbachia* infection density was positively correlated with insecticides, making this management strategy even more attractive (Berticat et al., 2002; Duron et al., 2006; Shemshadian et al., 2021). These suggest that reducing vector population and other pathogen replication in the host also increases the vectors' susceptibility to different insecticides.

When considering *Wolbachia* infection as a pathogen for inhibition and population reduction, factors such as strain, density, distribution, and infection frequency must be considered (Bian et al., 2010). The mechanism of *Wolbachia* infection to protect the host from pathogens is immune priming, in which symbiotic infection upregulates basal immune responses and primes insect defenses against subsequent pathogen infections (Ye et al., 2013). However, Hughes et al. (2012) reported that the wAlbB strain significantly increases *P. berghei* oocyst levels in the infected *An. gambiae*. These various effects imply that *Wolbachia* strains differ in their interactions with the host and/or pathogen, and these variations may be used to elucidate the molecular processes that prevent pathogen development in mosquitoes.

In addition to strain and density, the distribution of bacterial infections within the mosquito's body also significantly impacts mosquito population decline. Infection of the reproductive tract causes host reproductive failure due to CI (Li et al., 2023). Reproductively infected mosquitoes cannot produce viable offspring or transmit the bacteria to their offspring (Sinkins, 2004; O'Neill, 2018). On this basis, releasing *Wolbachia*-infected male mosquitoes into the field decreased the fecundity and the fertility of wild mosquito populations. *Wolbachia* Incompatible Insect Technology (IIT) performing this strategy has proven to be a promising method for eliminating invasive mosquito populations such as *Ae. aegypti* and *Ae. albopictus* and reducing the incidence of vector-borne diseases such as dengue, chikungunya, and Zika (Pagendam et al., 2020).

To enhance the effect of population reduction of mosquitoes in the human community, IIT can be combined with radiation-based SIT, which is rearing, sterilization, and release of large numbers of male mosquitoes to mate with fertile wild females, thereby reducing offspring production from the target population (Zheng et al., 2019; Chen et al., 2023). This further reinforces the dependence on strain type and density in infection vertical transmission.

Even though the release of *Wolbachia*-carrying mosquitoes into communities is not immediately stopping the epidemic, it leads to mosquito population declines over several months (Iturbe-Ormaetxe et al., 2011; Liew et al., 2021). These imply that *Wolbachia* influences the transmission effect when mosquitoes are exposed for an extended time to obtain the capacity of *Wolbachia* strains to infiltrate the uninfected mosquito population in the community.

Besides, before and during the implementation of releases of *Wolbachia*-infected mosquitoes for mosquito population suppression or replacement. It is important to keep engaging with the community and educating them to increase their understanding of this method, including clear and specific health risk assessment information (Sánchez-González et al., 2021). In addition to maintaining community support, programs should evaluate and monitor to determine how well they reduce the mosquito population (Sánchez-González et al., 2021; Villegas-Chim et al., 2022). Household perception surveys in different areas of Singapore provided a good understanding of public acceptance and sentiments toward using *Wolbachia-Aedes* technology (Liew et al., 2021). In addition, Texas and California in the United States, Thailand, Mexico, and Australia have released *Wolbachia*-infected mosquitoes and reported a significant drop in *Ae. aegypti* mosquitoes to control dengue, chikungunya, and Zika also gaining acceptance in the community (Wiwatanaratanabutr et al., 2010; Torres et al., 2020; Villegas-Chim et al., 2022).

The main difficulty with using *Wolbachia* for controlling vectors in the community is that the main vectors, like *Ae.aegypti* and *Anopheles* species, are not usually naturally infected. Trans-infection in the laboratory is necessary to ensure the bacterium is stably transmitted in these vector populations. In addition, culturing obligate intracellular bacteria is a challenge. Insect cells support *Wolbachia* growth, but culturing is long and difficult to manipulate cells. Modified Eagle's Minimum Essential Medium, Schneider's Insect Medium, Mitsuhashi-Maramorosch Insect Medium, and their one-to-one combinations are tested and effective for *Wolbachia* culture (Angeloni, 2021). Moreover, experts must transfer *Wolbachia's* strain into a new host once it grows in the cell culture.

4. Conclusion

Different *Wolbachia* species and strains have been isolated at different times. These different *Wolbachia* species and strains commonly infect and affect mosquito species differently. Once *Wolbachia*-infected mosquitoes release, they may reduce or prevent disease transmission through two mechanisms: (1) by reducing mosquito population density and/or survival rate; (2) by reducing the ability of mosquitoes to transmit diseases and/or pathogen replication or development. It causes the hosts' CI, phenotypic changes, and nutritional competition with other pathogens. These triggers reduce adult survivorship, inhibit mosquito reproduction, and prevent pathogen replication or development. *Wolbachia* infection from mosquitoes also sensitizes status to insecticides. Accordingly, *Wolbachia* can be used for biological control of mosquito-borne diseases, a public health problem in the tropical and sub-tropical world and some developed countries. *Wolbachia* reduces infection and transmission of diseases such as malaria, filariasis, dengue, chikungunya, yellow fever, zika, and West Nile fever.

Author contributions

AM: Conceptualization, Formal analysis, Writing – original draft, Writing – review & editing, Investigation, Validation, Visualization. GPP: Validation, Visualization, Writing – review & editing, Investigation, Supervision. DY: Validation, Writing – review & editing, Supervision. AS: Supervision, Validation, Writing – review & editing. IM: Writing – review & editing, Validation. DN: Validation, Writing – review & editing. RM: Supervision, Validation, Writing – review &

editing. GA: Supervision, Validation, Writing – review & editing, Conceptualization, Data curation.

Funding

The author(s) declare financial support was received for the research, authorship, and/or publication of this article.

Conflict of interest

The authors declare that the research was conducted in the absence of any commercial or financial relationships that could be construed as a potential conflict of interest.

Publisher's note

Supplementary material

The Supplementary material for this article can be found online at: https://www.frontiersin.org/articles/10.3389/fmicb.2023.1267832/full#supplementary-material

References

Ahmed, M., Li, S., Xue, X., Yin, X., Ren, S., Jiggins, F., et al. (2015). The intracellular bacterium *Wolbachia* uses parasitoid wasps as phoretic vectors for efficient horizontal transmission. *PLoS Pathog.* 11:e1004672. doi: 10.1371/journal.ppat.1004672

Aliota, M., Peinado, S., Velez, I., and Osorio, J. (2016b). The wMel strain of *Wolbachia* reduces transmission of Zika virus by *Aedes aegypti*. *Sci. Rep.* 6:28792. doi: 10.1038/srep28792

Aliota, M., Walker, E., Yepes, U., Dario Velez, I., Christensen, B., and Osorio, J. (2016a). The wMel strain of *Wolbachia* reduces transmission of chikungunya virus in *Aedes aegypt*. *PLoS Negl. Trop. Dis.* 10:e0004677. doi: 10.1371/journal.pntd.0004677

Allman, M., Fraser, J., Ritchie, S., Joubert, D., Simmons, C., and Flores, H. (2020). *Wolbachia*'s deleterious impact on *Aedes aegypti* egg development: the potential role of nutritional parasitism. *Insects* 11:735. doi: 10.3390/insects11110735

Angeloni, S. K. (2021). Optimization of *Wolbachia* culture conditions and purification of *Wolbachia*. California State University. Available at: http://hdl.handle.net/20.500.12680/fq978086r

Atyame, C. M., Delsuc, F., Pasteur, N., Weill, M., and Duron, O. (2011). Diversification of *Wolbachia* endosymbiont in the *Culex pipiens* mosquito. *Mol. Biol. Evol.* 28, 2761–2772. doi: 10.1093/molbev/msr083

Baldini, F., Rougé, J., Kreppel, K., Mkandawile, G., Mapua, S. A., Sikulu-Lord, M., et al. (2018). First report of natural *Wolbachia* infection in the malaria mosquito *Anopheles arabiensis* in Tanzania. *Parasit. Vectors* 11, 1–7. doi: 10.1186/s13071-018-3249-y

Baldini, F., Segata, N., Pompon, J., Marcenac, P., Robert Shaw, W., Dabiré, R., et al. (2014). Evidence of natural *Wolbachia* infections in field populations of *Anopheles gambiae*. *Nat. Commun.* 5:3985. doi: 10.1038/ncomms4985

Beebe, N., Pagendam, D., Trewin, B., Boomer, A., Bradford, M., Ford, A., et al. (2021). Releasing incompatible males drives strong suppression across populations of wild and *Wolbachia*-carrying *Aedes aegypti* in Australia. *Proc. Natl. Acad. Sci.* 118:e2106828118. doi: 10.1073/pnas.2106828118

Bergman, A., and Hesson, J. (2021). *Wolbachia* prevalence in the vector species *Culex pipiens* and *Culex torrentium* in a Sindbis virus-endemic region of Sweden. *Parasit. Vectors* 14:428. doi: 10.1186/s13071-021-04937-6

Berticat, C., Rousset, F., Raymond, M., Berthomieu, A., and Weill, M. (2002). High *Wolbachia* density in insecticide–resistant mosquitoes. *Proc. R. Soc. Lond. Ser. B Biol. Sci.* 269, 1413–1416. doi: 10.1098/rspb.2002.2022

Bettis, A. A., L'Azou Jackson, M., Yoon, I.-K., Breugelmans, J. G., Goios, A., Gubler, D. J., et al. (2022). The global epidemiology of chikungunya from 1999 to 2020: a systematic literature review to inform the development and introduction of vaccines. *PLoS Negl. Trop. Dis.* 16:e0010069. doi: 10.1371/journal.pntd.0010069

Bi, J., and Wang, Y. (2020). The effect of the endosymbiont *Wolbachia* on the behavior of insect hosts. *Insect Sci.* 27, 846–858. doi: 10.1111/1744-7917.12731

Bian, G., Xu, Y., Lu, P., Xie, Y., and Xi, Z. (2010). The endosymbiotic bacterium *Wolbachia* induces resistance to dengue virus in *Aedes aegypti*. *PLoS Pathog.* 6:e1000833. doi: 10.1371/journal.ppat.1000833

Bizhani, N., Hashemi Hafshejani, S., Mohammadi, N., Rezaei, M., and Rokni, M. B. (2021). Lymphatic filariasis in Asia: a systematic review and meta-analysis. *Parasitol. Res.* 120, 411–422. doi: 10.1007/s00436-020-06991-y

Bordenstein, S., Paraskevopoulos, C., Dunning Hotopp, J., Sapountzis, P., Lo, N. B. C., Bandi, C., et al. (2009). Parasitism and mutualism in *Wolbachia*: what the phylogenomic trees can and cannot say. *Mol. Biol. Evol.* 26, 231–241. doi: 10.1093/molbev/msn243

Brasil, P., Calvet, G., Siqueira, A., Wakimoto, M., de Sequeira, P. C., Nobre, A., et al. (2016). Zika virus outbreak in Rio de Janeiro, Brazil: clinical characterization, epidemiological and virological aspects. *PLoS Negl. Trop. Dis.* 10:e0004636. doi: 10.1371/journal.pntd.0004636

Brelsfoard, C., and Dobson, S. (2011). *Wolbachia* effects on host fitness and the influence of male aging on cytoplasmic incompatibility in *Aedes polynesiensis* (Diptera: Culicidae). *J. Med. Entomol.* 48, 1008–1015. doi: 10.1603/ME10202

Calvitti, M., Moretti, R., Lampazzi, E., Bellini, R., and Dobson, S. L. (2014). Characterization of a new *Aedes albopictus* (Diptera: Culicidae)-*Wolbachia pipientis* (Rickettsiales: Rickettsiaceae) symbiotic association generated by the artificial transfer of the w pip strain from *Culex pipiens* (Diptera: Culicidae). *J. Med. Entomol.* 47, 179–187. doi: 10.1603/me09140

Caragata, E., Dutra, H., and Moreira, L. (2016b). Exploiting intimate relationships: controlling mosquito-transmitted disease with *Wolbachia*. *Trends Parasitol.* 32, 207–218. doi: 10.1016/j.pt.2015.10.011

Caragata, E., Dutra, H., Sucupira, P., Ferreira, A., and Moreira, L. (2021). *Wolbachia* as translational science: controlling mosquito-borne pathogens. *Trends Parasitol.* 37, 1050–1067. doi: 10.1016/j.pt.2021.06.007

Caragata, E., Rezende, F., Simões, T., and Moreira, L. (2016a). Diet-induced nutritional stress and pathogen interference in *Wolbachia*-infected *Aedes aegypti*. *PLoS Negl. Trop. Dis.* 10:e0005158. doi: 10.1371/journal.pntd.0005158

Carrington, L. B., Lipkowitz, J. R., Hoffmann, A. A., and Turelli, M. (2011). A re-examination of *Wolbachia*-induced cytoplasmic incompatibility in California *Drosophila simulans*. *PLoS One* 6:e22565. doi: 10.1371/journal.pone.0022565

CDC. (2020). CENTR for diseases control and prevention 2020. Integrated Mosquito Management. Available at: https://www.cdc.gov/mosquitoes/mosquitocontrol/professionals/integrated-mosquito

CDC. (2023). Centers of diseases control and preventions 2023. West Nile Virus. Available at: https://www.cdc.gov/westnile/index.html

Charlat, S., Calmet, C., and Merçot, H. (2001). On the mod resc model and the evolution of *Wolbachia* compatibility types. *Genetics* 159, 1415–1422. doi: 10.1093/genetics/159.4.1415

Chen, C., Aldridge, R., Gibson, S., Kline, J., Aryaprema, V., Qualls, W., et al. (2023). Developing the radiation-based sterile insect technique (SIT) for controlling *Aedes aegypti*: identification of a sterilizing dose. *Pest Manag. Sci.* 79, 1175–1183. doi: 10.1002/ps.7303

Chrostek, E., and Gerth, M. (2019). Is *Anopheles gambiae* a natural host of *Wolbachia*? *MBio* 10, 10–1128. doi: 10.1128/mBio.00784-19

Coetzee, M. (2020). Key to the females of Afrotropical *Anopheles* mosquitoes (Diptera: Culicidae). *Malar. J.* 19, 1–20. doi: 10.1186/s12936-020-3144-9

Couper, L., Farner, J., Caldwell, J., Childs, M., Harris, M., Kirk, D., et al. (2021). How will mosquitoes adapt to climate warming? *elife* 10:e69630. doi: 10.7554/eLife.69630

Damiani, C., Cappelli, A., Comandatore, F., Montarsi, F., Serrao, A., Michelutti, A., et al. (2022). *Wolbachia* in *Aedes koreicus*: rare detections and possible implications. *Insects* 13:216. doi: 10.3390/insects13020216

De Oliveira, S., Villela, D., Dias, F., Moreira, L., and Maciel De Freitas, R. (2017). How does competition among wild type mosquitoes influence the performance of *Aedes aegypti* and dissemination of *Wolbachia pipientis*? *PLoS Negl. Trop. Dis.* 11:e0005947. doi: 10.1371/journal.pntd.0005947

Díaz-Nieto, L., Gil, M., Lazarte, J., Perotti, M., and Berón, C. (2021). *Culex quinquefasciatus* carrying *Wolbachia* is less susceptible to entomopathogenic bacteria. *Sci. Rep.* 11, 1–9. doi: 10.1038/s41598-020-80034-5

Ding, H., Yeo, H., and Puniamoorthy, N. (2020). *Wolbachia* infection in wild mosquitoes (Diptera: Culicidae): implications for transmission modes and host-endosymbiont associations in Singapore. *Parasit. Vectors* 13, 1–6. doi: 10.1186/s13071-020-04466-8

Dodson, B., Andrews, E., Turell, M., and Rasgon, J. (2017). *Wolbachia* effects on Rift Valley fever virus infection in *Culex tarsalis* mosquitoes. *PLoS Negl. Trop. Dis.* 11:e0006050. doi: 10.1371/journal.pntd.0006050

Dorigatti, I., Mccormack, C., Nedjati-Gilani, G., and Ferguson, N. (2018). Using *Wolbachia* for dengue control: insights from modelling. *Trends Parasitol.* 34, 102–113. doi: 10.1016/j.pt.2017.11.002

Duron, O., Labbé, P., Berticat, C., Rousset, F., Guillot, S., Raymond, M., et al. (2006). High *Wolbachia* density correlates with cost of infection for insecticide resistant *Culex pipiens* mosquitoes. *Evolution* 60, 303–314. doi: 10.1111/j.0014-3820.2006.tb01108.x

Duron, O., Noël, V., McCoy, K. D., Bonazzi, M., Sidi-Boumedine, K., Morel, O., et al. (2015). The recent evolution of a maternally-inherited endosymbiont of ticks led to the emergence of the Q fever pathogen, *Coxiella burnetii*. *PLoS Pathog.* 11:e1004892. doi: 10.1371/journal.ppat.1004892

Dutra, H., Lopes Da Silva, V., Da Rocha Fernandes, M., Logullo, C., Maciel-De-Freitas, R., and Moreira, L. (2016). The influence of larval competition on Brazilian *Wolbachia*-infected *Aedes aegypti* mosquitoes. *Parasit. Vectors* 9, 1–5. doi: 10.1186/s13071-016-1559-5

Echaubard, P., Duron, O., Agnew, P., Sidobre, C., Noël, V., Weill, M., et al. (2010). Rapid evolution of *Wolbachia* density in insecticide resistant *Culex pipiens*. *Heredity* 104, 15–19. doi: 10.1038/hdy.2009.100

Frentiu, F., Zakir, T., Walker, T., Popovici, J., Pyke, A., van den Hurk, A., et al. (2014). Limited dengue virus replication in field-collected *Aedes aegypti* mosquitoes infected with *Wolbachia*. *PLoS Negl. Trop. Dis.* 8:e2688. doi: 10.1371/journal.pntd.0002688

Geoghegan, V., Stainton, K., Rainey, S. M., Ant, T. H., Dowle, A. A., Larson, T., et al. (2017). Perturbed cholesterol and vesicular trafficking associated with dengue blocking in *Wolbachia*-infected *Aedes aegypti* cells. *Nat. Commun.* 8:526. doi: 10.1038/s41467-017-00610-8

Glaser, R., and Meola, M. (2010). The native *Wolbachia* endosymbionts of *Drosophila melanogaster* and *Culex quinquefasciatus* increase host resistance to West Nile virus infection. *PLoS One* 5:e11977. doi: 10.1371/journal.pone.0011977

Gomes, F., Hixson, B., Tyner, M., Ramirez, J., Canepa, G., Alves e Silva, T. L., et al. (2017). Effect of naturally occurring *Wolbachia* in *Anopheles gambiae* sl mosquitoes from Mali on *Plasmodium falciparum* malaria transmission. *Proc. Natl. Acad. Sci.* 114, 12566–12571. doi: 10.1073/pnas.1716181114

Gutzwiller, F., Carmo, C., Miller, D., Rice, D., Newton, I., Hawley, R., et al. (2015). Dynamics of *Wolbachia pipientis* gene expression across the *Drosophila melanogaster* life cycle. *G3* 5, 2843–2856. doi: 10.1534/g3.115.021931

Hague, M., Caldwell, C., and Cooper, B. (2020). Pervasive effects of *Wolbachia* on host temperature preference. *MBio* 11, e01768–e01720. doi: 10.1128/mBio.01768-20

Harbach, R. (1985). Pictorial keys to the genera of mosquitoes, subgenera of *Culex* and the species of *Culex* occurring in southwestern Asia and Egypt, with a note on the subgeneric placement of *Culex deserticola* (Diptera: Culicidae). *Mosq. Syst.* 17, 83–107.

Hedges, L., Brownlie, J., O'Neill, S., and Johnson, K. (2008). *Wolbachia* and virus protection in insects. *Science* 322:702. doi: 10.1126/science.1162418

Hertig, M. (1936). The rickettsia, *Wolbachia pipientis* and associated inclusions of the mosquito, *Culex pipiens*. *Parasitology* 28, 453–486. doi: 10.1017/S0031182000022666

Hertig, M., and Wolbach, S. (1924). Studies on Rickettsia-like micro-organisms in insects. *J. Med. Res.* 44, 329–374.7.

Hoey, J. (2000). West Nile fever in New York City. *CMAJ* 162:1036.

Hughes, G., Koga, R., Xue, P., Fukatsu, T., and Rasgon, J. (2011). *Wolbachia* infections are virulent and inhibit the human malaria parasite *Plasmodium falciparum* in *Anopheles gambiae*. *PLoS Pathog.* 7:e1002043. doi: 10.1371/journal.ppat.1002043

Hughes, G., Vega-Rodriguez, J., Xue, P., and Rasgon, J. (2012). *Wolbachia* strain wAlbB enhances infection by the rodent malaria parasite *Plasmodium berghei* in *Anopheles gambiae* mosquitoes. *Appl. Environ. Microbiol.* 78, 1491–1495. doi: 10.1128/AEM.06751-11

Hussain, M., Lu, G., Torres, S., Edmonds, J. H., Kay, B. H., Khromykh, A. A., et al. (2013). Effect of *Wolbachia* on replication of West Nile virus in a mosquito cell line and adult mosquitoes. *J. Virol.* 87, 851–858. doi: 10.1128/JVI.01837-12

Inácio Da Silva, L., Dezordi, F., Paiva, M., and Wallau, G. (2021). Systematic review of *Wolbachia* symbiont detection in mosquitoes: an entangled topic about methodological power and true symbiosis. *Pathogens* 10:39. doi: 10.3390/pathogens10010039

Islam, M., and Dobson, S. (2006). *Wolbachia* effects on *Aedes albopictus* (Diptera: Culicidae) immature survivorship and development. *J. Med. Entomol.* 43, 689–695. doi: 10.1603/0022-2585(2006)43[689:WEOAAD]2.0.CO;2

Iturbe-Ormaetxe, I., Walker, T., and O'neill, S. (2011). *Wolbachia* and the biological control of mosquito-borne disease. *EMBO Rep.* 12, 508–518. doi: 10.1038/embor.2011.84

Jeffries, C. L., and Walker, T. (2015). The potential use of *Wolbachia*-based mosquito biocontrol strategies for Japanese encephalitis. *PLoS Negl. Trop. Dis.* 9:e0003576. doi: 10.1371/journal.pntd.0003576

Joshi, D., Mcfadden, M., Bevins, D., Zhang, F., and Xi, Z. (2014). *Wolbachia* strain wAlbB confers both fitness costs and benefit on *Anopheles stephensi*. *Parasit. Vectors* 7, 1–9. doi: 10.1186/1756-3305-7-336

Joshi, D., Pan, X., McFadden, M. J., Bevins, D., Liang, X., Lu, P., et al. (2017). The maternally inheritable *Wolbachia* wAlbB induces refractoriness to *Plasmodium berghei* in *Anopheles stephensi*. *Front. Microbiol.* 8:366. doi: 10.3389/fmicb.2017.00366

Kambris, Z., Blagborough, A., Pinto, S., Blagrove, M., Godfray, H. C., Sinden, R. E., et al. (2010). *Wolbachia* stimulates immune gene expression and inhibits *Plasmodium* development in *Anopheles gambiae*. *PLoS Pathog.* 6:e1001143. doi: 10.1371/journal.ppat.1001143

Kambris, Z., Cook, P., Phuc, H., and Sinkins, S. (2009). Immune activation by life-shortening *Wolbachia* and reduced filarial competence in mosquitoes. *Science* 326, 134–136. doi: 10.1126/science.1177531

Kamtchum-Tatuene, J., Makepeace, B. L., Benjamin, L., Baylis, M., and Solomon, T. (2017). The potential role of *Wolbachia* in controlling the transmission of emerging human arboviral infections. *Curr. Opin. Infect. Dis.* 30, 108–116. doi: 10.1097/QCO.0000000000000342

Karami, M., Moosa-Kazemi, S., Oshaghi, M., Vatandoost, H., Sedaghat, M., Rajabnia, R., et al. (2016). *Wolbachia* endobacteria in natural populations of *Culex pipiens* of Iran and its phylogenetic congruence. *J. Arthropod. Borne Dis.* 10, 347–363.

Kaur, R., Shropshire, J., Cross, K., Leigh, B., Mansueto, A., Stewart, V., et al. (2021). Living in the endosymbiotic world of *Wolbachia*: a centennial review. *Cell Host Microbe* 29, 879–893. doi: 10.1016/j.chom.2021.03.006

Kho, E., Hugo, L., Lu, G., Smith, D., and Kay, B. (2016). Effects of larval nutrition on *Wolbachia*-based dengue virus interference in *Aedes aegypti* (Diptera: Culicidae). *J. Med. Entomol.* 53, 894–901. doi: 10.1093/jme/tjw029

Kientega, M., Kranjc, N., Traoré, N., Kaboré, H., Soma, D., Morianou, I., et al. (2022). Analysis of the genetic variation of the fruitless gene within the *Anopheles gambiae* (Diptera: Culicidae) complex populations in Africa. *Insects* 13:1048. doi: 10.3390/insects13111048

Kittayapong, P., Baimai, V., and O'neill, S. (2002). Field prevalence of *Wolbachia* in the mosquito vector *Aedes albopictus*. *Am. J. Trop. Med. Hyg.* 66, 108–111. doi: 10.4269/ajtmh.2002.66.108

Kittayapong, P., Baisley, K., Baimai, V., and O'Neill, S. (2000). Distribution and diversity of *Wolbachia* infections in Southeast Asian mosquitoes (Diptera: Culicidae). *J. Med. Entomol.* 37, 340–345. doi: 10.1093/jmedent/37.3.340

Landmann, F. (2019). The *Wolbachia* endosymbionts. *Microbiol. Spectr.* 7:7-2. doi: 10.1128/microbiolspec.BAI-0018-2019

Leta, S., Beyene, T., De Clercq, E., Amenu, K., Kraemer, M., and Revie, C. (2018). Global risk mapping for major diseases transmitted by *Aedes aegypti* and *Aedes albopictus*. *Int. J. Infect. Dis.* 67, 25–35. doi: 10.1016/j.ijid.2017.11.026

Li, Y., Sun, Y., Zou, J., Zhong, D., Liu, R., Zhu, C., et al. (2023). Characterizing the *Wolbachia* infection in field-collected Culicidae mosquitoes from Hainan Province, China. *Parasit. Vectors* 16, 1–2. doi: 10.1186/s13071-023-05719-y

Liew, C., Soh, L., Chen, I., and Ng, L. (2021). Public sentiments towards the use of *Wolbachia-Aedes* technology in Singapore. *BMC Public Health* 21, 1–2. doi: 10.1186/s12889-021-11380-w

Mains, J., Kelly, P., Dobson, K., Petrie, W., and Dobson, S. (2019). Localized control of *Aedes aegypti* (Diptera: Culicidae) in Miami, FL, via inundative releases of *Wolbachia*-infected male mosquitoes. *J. Med. Entomol.* 56, 1296–1303. doi: 10.1093/jme/tjz051

McMeniman, C. J., Lane, R., Cass, B., Fong, A., Sidhu, M., Wang, Y., et al. (2009). Stable introduction of a life-shortening *Wolbachia* infection into the mosquito *Aedes aegypti*. *Science* 323, 141–144. doi: 10.1126/science.1165326

Mejia, A., Dutra, H., Jones, M., Perera, R., and Mcgraw, E. (2022). Cross-tissue and generation predictability of relative *Wolbachia* densities in the mosquito *Aedes aegypti*. *Parasit. Vectors* 15, 1–10. doi: 10.1186/s13071-022-05231-9

Mohanty, I., Rath, A., Mahapatra, N., and Hazra, R. (2016). *Wolbachia*: a biological control strategy against arboviral diseases. *J. Vector Borne Dis.* 53, 199–207.

Moreira, L. A., Iturbe-Ormaetxe, I., Jeffery, J. A., Lu, G., Pyke, A. T., Hedges, L. M., et al. (2009a). A *Wolbachia* symbiont in *Aedes aegypti* limits infection with dengue, chikungunya, and plasmodium. *Cells* 139, 1268–1278. doi: 10.1016/j.cell.2009.11.042

Moreira, L., Saig, E., Turley, A., Ribeiro, J., O'neill, S., and Mcgraw, E. (2009b). Human probing behavior of *Aedes aegypti* when infected with a life-shortening strain of *Wolbachia*. *PLoS Negl. Trop. Dis.* 3:e568. doi: 10.1371/journal.pntd.0000568

Moretti, R., Yen, P., Houé, V., Lampazzi, E., Desiderio, A., Failloux, A., et al. (2018). Combining *Wolbachia*-induced sterility and virus protection to fight *Aedes albopictus*-borne viruses. *PLoS Negl. Trop. Dis.* 12:e0006626. doi: 10.1371/journal.pntd.0006626

Mousson, L., Martin, E., Zouache, K., Madec, Y., Mavingui, P., and Failloux, A. (2010). *Wolbachia* modulates chikungunya replication in *Aedes albopictus*. *Mol. Ecol.* 19, 1953–1964. doi: 10.1111/j.1365-294X.2010.04606.x

Niang, E., Bassene, H., Makoundou, P., Fenollar, F., Weill, M., and Mediannikov, O. (2018). First report of natural *Wolbachia* infection in wild *Anopheles funestus* population in Senegal. *Malar. J.* 17, 1–6. doi: 10.1186/s12936-018-2559-z

O'Neill, S. (2018). The use of *Wolbachia* by the world mosquito program to interrupt transmission of *Aedes aegypti* transmitted viruses. *Adv. Exp. Med. Biol.* 1062, 355–360. doi: 10.1007/978-981-10-8727-1_24

Omar, M. (1996). A survey of bancroftian filariasis among south-east Asian expatriate workers in Saudi Arabia. *Tropical Med. Int. Health* 1, 155–160. doi: 10.1111/j.1365-3156.1996.tb00021.x

Ong, J., Ho, S., Soh, S., Wong, Y., Ng, Y., Vasquez, K., et al. (2022). Assessing the efficacy of male *Wolbachia*-infected mosquito deployments to reduce dengue incidence in Singapore: study protocol for a cluster-randomized controlled trial. *Trials* 23:1023. doi: 10.1186/s13063-022-06976-5

Osei-Poku, J., Han, C., Mbogo, C., and Jiggins, F. (2012). Identification of *Wolbachia* strains in mosquito disease vectors. *PLoS One* 7:e49922. doi: 10.1371/journal.pone.0049922

Pagendam, D., Trewin, B., Snoad, N., Ritchie, S., Hoffmann, A., Staunton, K., et al. (2020). Modelling the *Wolbachia* incompatible insect technique: strategies for effective mosquito population elimination. *BMC Biol.* 18:161. doi: 10.1186/s12915-020-00887-0

Paramasivan, R., Mishra, A., and Mourya, D. (2003). West Nile virus: the Indian scenario. *Indian J. Med. Res.* 118:108.

Philip, C. (1956). Comments on the classification of the order Rickettsiales. *Can. J. Microbiol.* 2, 261–270. doi: 10.1139/m56-030

Pircalabioru, G., Aviello, G., Kubica, M., Zhdanov, A., Paclet, M., Brennan, L., et al. (2016). Defensive mutualism rescues NADPH oxidase inactivation in gut infection. *Cell Host Microbe* 19, 651–663. doi: 10.1016/j.chom.2016.04.007

Poinsot, D., Charlat, S., and Mercot, H. (2003). On the mechanism of *Wolbachia*-induced cytoplasmic incompatibility: confronting the models with the facts. *BioEssays* 25, 259–265. doi: 10.1002/bies.10234

Puggioli, A., Calvitti, M., Moretti, R., and Bellini, R. (2016). wPip *Wolbachia* contribution to *Aedes albopictus* SIT performance: advantages under intensive rearing. *Acta Trop.* 164, 473–481. doi: 10.1016/j.actatropica.2016.10.014

Quek, S., Cook, D., Wu, Y., Marriott, A., Steven, A., Johnston, K., et al. (2022). *Wolbachia* depletion blocks the transmission of lymphatic filariasis by preventing chitinase dependent parasite escheatment. *Proc. Natl. Acad. Sci.* 119:e2120003119. doi: 10.1073/pnas.2120003119

Rogers, K. (2023). Aedes. Encyclopedia Britannica. Available at: https://www.britannica.com/animal/Aedes.

Rohrscheib, C., Frentiu, F., Horn, E., Ritchie, F., van Swinderen, B., Weible, M., et al. (2016). Intensity of mutualism breakdown is determined by temperature, not amplification of *Wolbachia* genes. *PLoS Pathog.* 12:e1005888. doi: 10.1371/journal.ppat.1005888

Ross, P., Wiwatanaratanabutr, I., Axford, J., White, V., Endersby-Harshman, N., and Hoffmann, A. (2017). *Wolbachia* infections in *Aedes aegypti* differ markedly in their response to cyclical heat stress. *PLoS Pathog.* 13:e1006006. doi: 10.1371/journal.ppat.1006006

Ryu, J., Ha, E., and Lee, W. (2010). Innate immunity and gut–microbe mutualism in *Drosophila*. *Dev. Comp. Immunol.* 34, 369–376. doi: 10.1016/j.dci.2009.11.010

Salzberg, S., Hotopp, J., Delcher, A., Pop, M., Smith, D., Eisen, M., et al. (2005). Serendipitous discovery of *Wolbachia* genomes in multiple *Drosophila* species. *Genome Biol.* 6, 1–8. doi: 10.1186/gb-2005-6-3-r2

Sánchez-González, L., Adams, L., Saavedra, R., Little, E., Medina, N., Major, C., et al. (2021). Assessment of community support for *Wolbachia*-mediated population suppression as a control method for *Aedes aegypti* mosquitoes in a community cohort in Puerto Rico. *PLoS Negl. Trop. Dis.* 15:e0009966. doi: 10.1371/journal.pntd.0009966

Serbus, L., Casper-Lindley, C., Landmann, F., and Sullivan, W. (2008). The genetics and cell biology of *Wolbachia*-host interactions. *Annu. Rev. Genet.* 42, 683–707. doi: 10.1146/annurev.genet.41.110306.130354

Shaw, W., Marcenac, P., Childs, L., Buckee, C., Baldini, F., Sawadogo, S., et al. (2016). *Wolbachia* infections in natural *Anopheles* populations affect egg laying and negatively correlate with *Plasmodium* development. *Nat. Commun.* 7:11772. doi: 10.1038/ncomms11772

Shemshadian, A., Vatandoost, H., Oshaghi, M., Abai, M., and Djadid, N. (2021). Relationship between *Wolbachia* infection in *Culex quinquefasciatus* and its resistance to insecticide. *Heliyon* 7:e06749. doi: 10.1016/j.heliyon.2021.e06749

Sicard, M., Bonneau, M., and Weill, M. (2019). *Wolbachia* prevalence, diversity, and ability to induce cytoplasmic incompatibility in mosquitoes. *Curr. Opin. Insect Sci.* 34, 12–20. doi: 10.1016/j.cois.2019.02.005

Silva, J., Magalhães Alves, D., Bottino-Rojas, V., Pereira, T., Sorgine, M., Caragata, E., et al. (2017). *Wolbachia* and dengue virus infection in the mosquito *Aedes fluviatilis* (Diptera: Culicidae). *PLoS One* 12:e0181678. doi: 10.1371/journal.pone.0181678

Sinka, M., Bangs, M., Manguin, S., Rubio-Palis, Y., Chareonviriyaphap, T., Coetzee, M., et al. (2012). A global map of dominant malaria vectors. *Parasit. Vectors* 5:69. doi: 10.1186/1756-3305-5-69

Sinkins, S. (2004). *Wolbachia* and cytoplasmic incompatibility in mosquitoes. *Insect Biochem. Mol. Biol.* 34, 723–729. doi: 10.1016/j.ibmb.2004.03.025

Sinkins, S., Walker, T., Lynd, A., Steven, A., Makepeace, B., Godfray, H. C., et al. (2005). *Wolbachia* variability and host effects on crossing type in *Culex* mosquitoes. *Nature* 436, 257–260. doi: 10.1038/nature03629

Straub, T., Shaw, W., Marcenac, P., Sawadogo, S., Dabiré, R., Diabaté, A., et al. (2020). The *Anopheles coluzzii* microbiome and its interaction with the intracellular parasite *Wolbachia*. *Sci. Rep.* 10, 13847–13841. doi: 10.1038/s41598-020-70745-0

Sullivan, W. (2017). *Wolbachia*, bottled water, and the dark side of symbiosis. *Mol. Biol. Cell* 28, 2343–2346. doi: 10.1091/mbc.e17-02-0132

Thomas, P., Kenny, N., Eyles, D., Moreira, L., O'Neill, S., and Asgari, S. (2011). Infection with the wMel and wMelPop strains of *Wolbachia* leads to higher levels of melanization in the hemolymph of *Drosophila melanogaster*, *Drosophila simulans* and *Aedes aegypti*. *Dev. Comp. Immunol.* 35, 360–365. doi: 10.1016/j.dci.2010.11.007

Torres, R., Hernandez, E., Flores, V., Ramirez, J., and Joyce, A. (2020). *Wolbachia* in mosquitoes from the Central Valley of California, USA. *Parasit. Vectors* 13:558. doi: 10.1186/s13071-020-04429-z

Turelli, M., and Hoffmann, A. (1991). Rapid spread of an inherited incompatibility factor in California Drosophila. *Nature* 353, 440–442. doi: 10.1038/353440a0

Turley, A., Moreira, L., O'neill, S., and Mcgraw, E. (2009). *Wolbachia* infection reduces blood-feeding success in the dengue fever mosquito, *Aedes aegypti*. *PLoS Negl. Trop. Dis.* 3:e516. doi: 10.1371/journal.pntd.0000516

Turley, A., Smallegange, R., Takken, W., Zalucki, M., O'neill, S., and Mcgraw, E. (2014). *Wolbachia* infection does not alter attraction of the mosquito *Aedes* (Stegomyia) aegypti to human odours. *Med. Vet. Entomol.* 28, 457–460. doi: 10.1111/mve.12063

van den Berg, H., da Silva Bezerra, H. S., al-Eryani, S., Chanda, E., Nagpal, B. N., Knox, T. B., et al. (2021). Recent trends in global insecticide use for disease vector control and potential implications for resistance management. *Sci. Rep.* 11:23867. doi: 10.1038/s41598-021-03367-9

Villegas-Chim, J., Martin-Park, A., Puerta-Guardo, H., Eugenia Toledo-Romaní, M., Pavía-Ruz, N., Contreras-Perera, Y., et al. (2022). "Community engagement and social assessment for *Wolbachia*-based suppression of natural populations of *Aedes aegypti*: the Mexican experience" in *Mosquito research-recent advances in pathogen interactions, immunity, and vector control strategies*. eds. H. Puerta-Guardo and P. Manrique-Saide (London: Intechopen)

Walker, T. J. P. H., Johnson, P. H., Moreira, L. A., Iturbe-Ormaetxe, I., Frentiu, F. D., McMeniman, C. J., et al. (2011). The wMel *Wolbachia* strain blocks dengue and invades caged *Aedes aegypti* populations. *Nature* 476, 450–453. doi: 10.1038/nature10355

Waymire, E., Duddu, S., Yared, S., Getachew, D., Dengela, D., Bordenstein, S. R., et al. (2022). *Wolbachia* 16S rRNA haplotypes detected in wild *Anopheles stephensi* in eastern Ethiopia. *Parasit. Vectors* 15, 1–11. doi: 10.1186/s13071-022-05293-9

Werren, J., Baldo, L., and Clark, M. (2008). *Wolbachia*: master manipulators of invertebrate biology. *Nat. Rev. Microbiol.* 6, 741–751. doi: 10.1038/nrmicro1969

Werren, J. H., and O'Neill, S. L. (1997). "The evolution of heritable symbionts" in *Influential passengers: inherited microorganisms and arthropod reproduction*. eds. S. L. O'Neill, A. A. Hoffmann and J. H. Werren (Oxford: Oxford University Press)

Werren, J., and Windsor, D. (2000). *Wolbachia* infection frequencies in insects: evidence of a global equilibrium? *Proc. Biol. Sci.* 267, 1277–1285. doi: 10.1098/rspb.2000.1139

WHO. (2021). *Global programme to eliminate lymphatic filariasis: progress report, 2020*, World Health Organization Geneva

WHO. (2022). *World malaria report 2022*. World Health Organization Geneva

WHO. (2023a). Yellow fever. Available at: https://www.who.int/news-room/fact-sheets/detail/yellow-fever

WHO. (2023b). Zika virus disease. Available at: https://www.who.int/health-topics/zika-virus-disease#tab=tab_1

Wiebe, A., Longbottom, J., Gleave, K., Shearer, F., Sinka, M., Massey, N., et al. (2017). Geographical distributions of African malaria vector sibling species and evidence for insecticide resistance. *Malar. J.* 16, 85–80. doi: 10.1186/s12936-017-1734-y

Wiwatanaratanabutr, I., Allan, S., Linthicum, K., and Kittayapong, P. (2010). Strain-specific differences in mating, oviposition, and host-seeking behavior between *Wolbachia*-infected and uninfected *Aedes albopictus*. *J. Am. Mosq. Control Assoc.* 26, 265–273. doi: 10.2987/09-5937.1

Wong, M. L., Liew, J. W. K., Wong, W. K., Pramasivan, S., Mohamed Hassan, N., Wan Sulaiman, W. Y., et al. (2020). Natural *Wolbachia* infection in field-collected Anopheles and other mosquito species from Malaysia. *Parasit. Vectors* 13, 1–15. doi: 10.1186/s13071-020-04277-x

Ye, Y, Woolfit, M, Rancès, E, and O'Neill, S, McGraw E. (2013). *Wolbachia*-associated bacterial protection in the mosquito *Aedes aegypti*. *PLoS Negl. Trop. Dis.*, 7,:e2362, doi: 10.1371/journal.pntd.0002362

Yeap, H. L., Axford, J. K., Popovici, J., Endersby, N. M., Iturbe-Ormaetxe, I., Ritchie, S. A., et al. (2014). Assessing quality of life-shortening *Wolbachia*-infected *Aedes aegypti* mosquitoes in the field based on capture rates and morphometric assessments. *Parasit. Vectors* 7, 58–13. doi: 10.1186/1756-3305-7-58

Yen, P., and Failloux, A. (2020). A review: *Wolbachia*-based population replacement for mosquito control shares common points with genetically modified control approaches. *Pathogens* 9:404. doi: 10.3390/pathogens9050404

Zhang, D., Wang, Y., He, K., Yang, Q., Gong, M., Ji, M., et al. (2020). *Wolbachia* limits pathogen infections through induction of host innate immune responses. *PLoS One* 15:e0226736. doi: 10.1371/journal.pone.0226736

Zheng, X., Zhang, D., Li, Y., Yang, C., Wu, Y., Liang, X., et al. (2019). Incompatible and sterile insect techniques combined eliminate mosquitoes. *Nature* 572, 56–61. doi: 10.1038/s41586-019-1407-9

Zug, R., and Hammerstein, P. (2012). Still a host of hosts for *Wolbachia*: analysis of recent data suggests that 40% of terrestrial arthropod species are infected. *PLoS One* 7:e38544. doi: 10.1371/journal.pone.0038544

Zug, R., and Hammerstein, P. (2015). Bad guys turned nice? A critical assessment of *Wolbachia* mutualisms in arthropod hosts. *Biol. Rev.* 90, 89–111. doi: 10.1111/brv.12098

frontiers | Frontiers in Microbiology

TYPE Original Research
PUBLISHED 01 February 2024
DOI 10.3389/fmicb.2024.1346068

OPEN ACCESS

EDITED BY
Zhiyong Li,
Shanghai Jiao Tong University, China

REVIEWED BY
Rodrigo Morchón García,
University of Salamanca, Spain
Takahiro Hosokawa,
Kyushu University, Japan

*CORRESPONDENCE
Joseph D. Turner
✉ joseph.turner@lstmed.ac.uk

†PRESENT ADDRESSES
Nicolas Pionnier,
Department of Life Sciences, Faculty of Science and Engineering, Manchester Metropolitan University, Manchester, United Kingdom

Denis Voronin,
Systems Genomics Section, Laboratory of Parasitic Diseases, NIAID, NIH, Bethesda, MD, United States

Ghaith Aljayyoussi,
Boehringer Ingelheim Pharma GmbH & Co. KG Drug Discovery Sciences, Ingelheim am Rhein, Germany

RECEIVED 28 November 2023
ACCEPTED 02 January 2024
PUBLISHED 01 February 2024

CITATION
Hegde S, Marriott AE, Pionnier N, Steven A, Bulman C, Gunderson E, Vogel I, Koschel M, Ehrens A, Lustigman S, Voronin D, Tricoche N, Hoerauf A, Hübner MP, Sakanari J, Aljayyoussi G, Gusovsky F, Dagley J, Hong DW, O'Neill P, Ward SA, Taylor MJ and Turner JD (2024) Combinations of the azaquinazoline anti-*Wolbachia* agent, AWZ1066S, with benzimidazole anthelmintics synergise to mediate sub-seven-day sterilising and curative efficacies in experimental models of filariasis. *Front. Microbiol.* 15:1346068. doi: 10.3389/fmicb.2024.1346068

Combinations of the azaquinazoline anti-*Wolbachia* agent, AWZ1066S, with benzimidazole anthelmintics synergise to mediate sub-seven-day sterilising and curative efficacies in experimental models of filariasis

Shrilakshmi Hegde[1], Amy E. Marriott[1], Nicolas Pionnier[1†], Andrew Steven[1], Christina Bulman[2], Emma Gunderson[2], Ian Vogel[2], Marianne Koschel[3], Alexandra Ehrens[3], Sara Lustigman[4], Denis Voronin[4†], Nancy Tricoche[4], Achim Hoerauf[3,5], Marc P. Hübner[3,5], Judy Sakanari[2], Ghaith Aljayyoussi[1†], Fabian Gusovsky[6], Jessica Dagley[1], David W. Hong[7], Paul O'Neill[7], Steven A. Ward[1], Mark J. Taylor[1] and Joseph D. Turner[1*]

[1]Department of Tropical Disease Biology, Centre for Drugs and Diagnostics, Centre for Neglected Tropical Diseases, Liverpool School of Tropical Medicine, Liverpool, United Kingdom, [2]Department of Pharmaceutical Chemistry, University of California, San Francisco, San Francisco, CA, Unites States, [3]Department of Immunology and Parasitology, Institute for Medical Microbiology, University Hospital Bonn, Bonn, Germany, [4]Laboratory of Molecular Parasitology, Lindsley F. Kimball Research Institute, New York Blood Center, New York, NY, Unites States, [5]German Center for Infection Research (DZIF), Partner Site Bonn-Cologne, Bonn, Germany, [6]Eisai Co., Ltd., Tokyo, Japan, [7]Department of Chemistry, University of Liverpool, Liverpool, United Kingdom

Lymphatic filariasis and onchocerciasis are two major neglected tropical diseases that are responsible for causing severe disability in 50 million people worldwide, whilst veterinary filariasis (heartworm) is a potentially lethal parasitic infection of companion animals. There is an urgent need for safe, short-course curative (macrofilaricidal) drugs to eliminate these debilitating parasite infections. We investigated combination treatments of the novel anti-*Wolbachia* azaquinazoline small molecule, AWZ1066S, with benzimidazole drugs (albendazole or oxfendazole) in up to four different rodent filariasis infection models: *Brugia malayi*—CB.17 SCID mice, *B. malayi*—Mongolian gerbils, *B. pahangi*—Mongolian gerbils, and *Litomosoides sigmodontis*—Mongolian gerbils. Combination treatments synergised to elicit threshold (>90%) *Wolbachia* depletion from female worms in 5 days of treatment, using 2-fold lower dose-exposures of AWZ1066S than monotherapy. Short-course lowered dose AWZ1066S-albendazole combination treatments also delivered partial adulticidal activities and/or long-lasting inhibition of embryogenesis, resulting in complete transmission blockade in *B. pahangi* and *L. sigmodontis* gerbil models. We determined that short-course AWZ1066S-albendazole co-treatment significantly augmented the depletion of *Wolbachia* populations within both germline and hypodermal tissues of *B. malayi* female worms and

in hypodermal tissues in male worms, indicating that anti-*Wolbachia* synergy is not limited to targeting female embryonic tissues. Our data provides pre-clinical proof-of-concept that sub-seven-day combinations of rapid-acting novel anti-*Wolbachia* agents with benzimidazole anthelmintics are a promising curative and transmission-blocking drug treatment strategy for filarial diseases of medical and veterinary importance.

KEYWORDS

lymphatic filariasis, *Wolbachia*, onchocerciasis, AWZ1066S, benzimidazole, macrofilaricidal drugs, anti-*Wolbachia* drugs

Introduction

Filariasis is a serious risk to health and economic prosperity in low- and middle-income countries. Lymphatic filariasis (LF) is a mosquito-transmitted disease caused by filarial nematode parasites *Wuchereria bancrofti*, *Brugia malayi*, or *Brugia timori* and results in debilitating pathologies, including severe lymphoedema in 36 million individuals, with further 800 million individuals estimated at risk of getting infected (Local Burden of Disease Neglected Tropical Diseases Control, 2020; WHO, 2020). Brugian filariasis reservoir infections in cats and dogs further jeopardise its elimination efforts in Asia (Nochot et al., 2019; Mallawarachchi et al., 2021), whilst the related veterinary filaria, *Dirofilaria immitis,* is the cause of heartworm disease in these companion animals and, along with *D. repens,* is a zoonotic risk to human health (Simon et al., 2017). Curative treatments of dogs are based on the arsenical drug, melarsomine, which requires a complex long-term treatment strategy in dogs with intensive veterinary management due to the risk of serious inflammatory side effects. There is no established cure for heartworm in cats (Turner et al., 2020). Onchocerciasis, caused by *Onchocerca volvulus,* is transmitted by blackflies and is the cause of skin and ocular disease (river blindness) in 14 million people.

Current efforts to eliminate human filariasis as a public health problem have focused on mass drug administration (MDA) with the established anthelmintics Ivermectin (IVM), Albendazole (ABZ), and Diethylcarbamazine (DEC) (Crump, 2017; Gyapong et al., 2018). These drugs act directly against the infective microfilarial stage or temporarily disrupt embryogenesis in the case of ABZ to remove microfilariae (mf) from circulation or skin, with the aim of breaking the transmission cycle. Because adult filarial nematode infections are chronic, and MDA drugs have negligible or low levels of curative activity against adult parasites, this strategy requires annual administrations, with high population coverage, for up to 15 years to achieve elimination. Additionally, treatment with IVM is unsuitable for patients co-infected with eye worm (*Loa loa*) and harbouring high *L. loa* mf loads due to severe life-threatening post-treatment reactions caused by the rapid microfilaricidal effect of IVM on *L. loa* mf (Gardon et al., 1997). Although MDA has successfully achieved LF elimination in some countries, the strategy has been less effective in achieving expected outcomes in India and sub-Saharan African countries (except for Togo and Malawi) (Sodahlon et al., 2013; WHO, 2019; Modi et al., 2021). Whilst onchocerciasis has been certified as eliminated from Colombia, Ecuador, Guatemala, and Mexico following biannual IVM treatment, no country in sub-Saharan Africa has yet achieved elimination despite intensive IVM MDA deployment as a front-line control and elimination strategy since 1995 (Lakwo et al., 2020; WHO, 2022). Therefore, there is a demand for new short-course drug treatments that are macrofilaricidal and can be safely employed in *L. loa* endemic regions in Africa to accelerate the elimination of human filariasis (WHO, 2020). Short-course macrofilaricides avoiding toxic or inflammatory side effects would be equally valuable in the management of veterinary/zoonotic filariasis in cats and dogs.

The causative agents of LF, onchocerciasis, and heartworm contain the endosymbiont *Wolbachia* (Slatko et al., 2010). This mutualism is essential for normal biological function, including larval development, embryogenesis, and survival, in filarial worms (Turner et al., 2020). *Wolbachia* provides an essential source of nucleotides as well as haem, riboflavin (vitamin B2), and FAD (flavin adenine dinucleotide) (Foster et al., 2005; Wu et al., 2009; Li and Carlow, 2012). *Wolbachia* occupies two distinct intra-cellular niches within filarial tissues, the hypodermal chord syncytium and the female germline, where they spread via host cell division. The germline is seeded with *Wolbachia* via infection from the hypodermal population during early fourth-stage larval development. *Wolbachia* subsequently localises in the embryonic stem cell niche by mitotic segregation (Landmann et al., 2012). Effective antibiotic depletion of *Wolbachia* induces rapid apoptosis of eggs and developing embryos, spreading to trigger apoptosis in somatic tissues of uterine mf and culminating in cessation of mf production (Landmann et al., 2011). Sterilisation of female filariae post-*Wolbachia* removal appears irreversible because in doxycycline LF and onchocerciasis clinical trials, patients remain free of mf, and excerpted *Onchocerca* female worms are devoid of uterine embryonic contents for more than 2 years post-treatment (Hoerauf et al., 2008). Removal of *Wolbachia* from hypodermal chords does not trigger widespread apoptosis at this tissue site but manifests in a more gradual decline in both female and male adult longevity, reducing life-span from 10–15 years to 18–24 months, as determined in doxycycline clinical trials (Taylor et al., 2005; Hoerauf et al., 2008).

A key advantage of a drug targeting *Wolbachia* in filariasis is that the gradual depletion of mf from blood or skin post-embryogenesis blockade avoids the inflammatory adverse reactions

experienced following rapid-acting microfilaricidal treatments, particularly in *L. loa* co-infection (Haarbrink et al., 2000; Ehrens et al., 2022). An administration of doxycycline (DOX) for treating onchocerciasis in areas of *L. loa* co-endemicity has been shown to be well-tolerated (Turner et al., 2010). Doxycycline is also effective in curing circulating mf stages in brugian zoonotic filariasis and is a proven curative treatment in heartworm disease, which avoids melarsomine-like acute adverse events due to the slow-kill mode of action (Kramer et al., 2018; Nochot et al., 2019).

Because protracted doxycycline regimens of 4–5 weeks are required to mediate both sterilising and curative outcomes in LF and onchocerciasis, and because of contraindications in children and during pregnancy, new rapid-acting drugs targeting *Wolbachia* have been developed (Johnston et al., 2021). These new drugs address a target product profile of a new curative drug for onchocerciasis, which requires ideally ≤7 days of oral dosing and is ready to be advanced into clinical testing (Specht and Kaminsky, 2022). To identify novel anti-*Wolbachia* candidates, we screened 10,000 compounds using a *Wolbachia*-infected *Aedes albopictus* cell line (Clare et al., 2015; Johnston et al., 2017). From this screening, we identified and developed the first-in-class azaquinazoline, AWZ1066S (Hong et al., 2019), as a candidate anti-*Wolbachia* macrofilaricide.

We have previously demonstrated that the standard anthelmintic benzimidazole drug, albendazole, can synergise with registered antibiotics to deplete *Wolbachia* in rodent models of *B. malayi*. The drug could reduce the number of required daily treatment exposures to overcome a minimum, clinically relevant threshold of 90% *Wolbachia* depletion in female worms, mediate a block of mf production, and accelerate macrofilaricidal activity (Turner et al., 2017). In this study, we explore the extent to which combining the novel anti-*Wolbachia* azaquinazoline, AWZ1066S, with albendazole or the veterinary benzimidazole, oxfendazole (OXF), being repurposed for human use (Gonzalez et al., 2019), may reduce the treatment regimen and exposure time-frame necessary to deliver threshold efficacies in rodent models of filariasis. We further report the tissue-level tropisms during anti-*Wolbachia* depletion synergy when combining AWZ1066S with benzimidazoles.

Materials and methods

Drugs preparation

DOX, OXF, and ABZ were obtained from Sigma Aldrich (Dorset, UK) as dry powders. Prior to treatment, they were resuspended in the appropriate vehicle (DOX in distilled water, ABZ and OXF in 0.5% carboxymethyl cellulose, 0.5% benzyl alcohol, 0.4% Tween 80, and 0.9% NaCl). AWZ1066S, synthesised by Eisai Co., Ltd. (Tokyo, Japan), was provided as a dried powder and stored at 4°C. It was resuspended prior to treatment in a vehicle comprised of 55% PEG300, 25% Propylene glycol, and 20% water.

B. malayi in vivo infection studies

CB.17 male severe-combined immunodeficiency (SCID) mice were purchased from Charles River (Harlow, UK). They were housed in individually ventilated cages with a HEPA-filtered air system at the University of Liverpool Biological Services Unit (UoL BSU). The mice experienced 12:12 h light:dark cycles and had access to food and water *ad libitum*. Mice were weighed before dosing, and their weight was monitored weekly following dosing to observe any decline in welfare. Male Mongolian gerbils (*Meriones ungiculatus*) were bred and maintained at UoL BSU. Animal procedures were approved by the Animal Welfare and Ethics Review Boards (AWERB) of Liverpool School of Tropical Medicine and the University of Liverpool and undertaken in accordance with UK home office licencing approval. The *B. malayi* life cycle (TRS sub-periodic human isolate) was maintained at LSTM and UoL BSU by serial passage between Mongolian gerbils and *Aedes aegypti* (Liverpool filarial susceptible strain). *B. malayi* infections in CB.17 SCID mice and gerbils were done as described previously (Turner et al., 2017; Bakowski et al., 2019; Hong et al., 2019). CB.17 SCID mice (aged 6–10 weeks) were inoculated intraperitoneally with 100 *B. malayi* third-stage (L3) larvae. Mice were weighed, and 100 μl oral drug doses were adjusted accordingly (±8 μl for each 1 g weight change from 25 g). Groups of 4–12 mice received assigned drug treatment by oral gavage commencing 6 weeks after inoculation (Figure 1A). Mice received either 100 or 150 mg/kg of AWZ1066S for 5 days two times daily (*bid*—bis in die) alone or in combination with 5 mg/kg ABZ or OXF *bid* for 5 days. Separate control groups of ABZ or OXF alone were also included, where animals received 5 mg/kg bi-daily dosing for 5 days. Sham animals only received vehicle treatment. DOX treatment with 25 mg/kg *bid* for 42 days was also included, which has been previously reported to deplete *Wolbachia* levels > 90% (Turner et al., 2017). To match the same frequency and volume of dosing between the groups, animals without additional ABZ treatment received a corresponding volume of the ABZ-vehicle and animals without AWZ1066S dosing received a matching volume of AWZ1066S-vehicle. Mice were necropsied at 6–7 weeks after commencement of treatment by rising concentration CO_2 asphyxiation. Death was confirmed by exsanguination via cardiac puncture (Home office schedule 1 procedure). *B. malayi* adults and mf were recovered by peritoneal washing. Individual motile parasites were enumerated by microscopy and kept frozen at −20°C until further molecular analysis.

B. pahangi in vivo infection studies

Male Mongolian gerbils (*Meriones unguiculatus*) aged 5–7 weeks were purchased from Charles River International (Massachusetts, USA). The study was carried out at the University of California, San Francisco and all animal procedures were approved by the University of California, San Francisco Institutional Animal Care and Use Committee (IACUC) (approvals: AN109629-03 and AN173847-02) and adhered to the guidelines set forth in the NIH guide for the care and use of laboratory animals and the USDA animal care policies. Gerbils

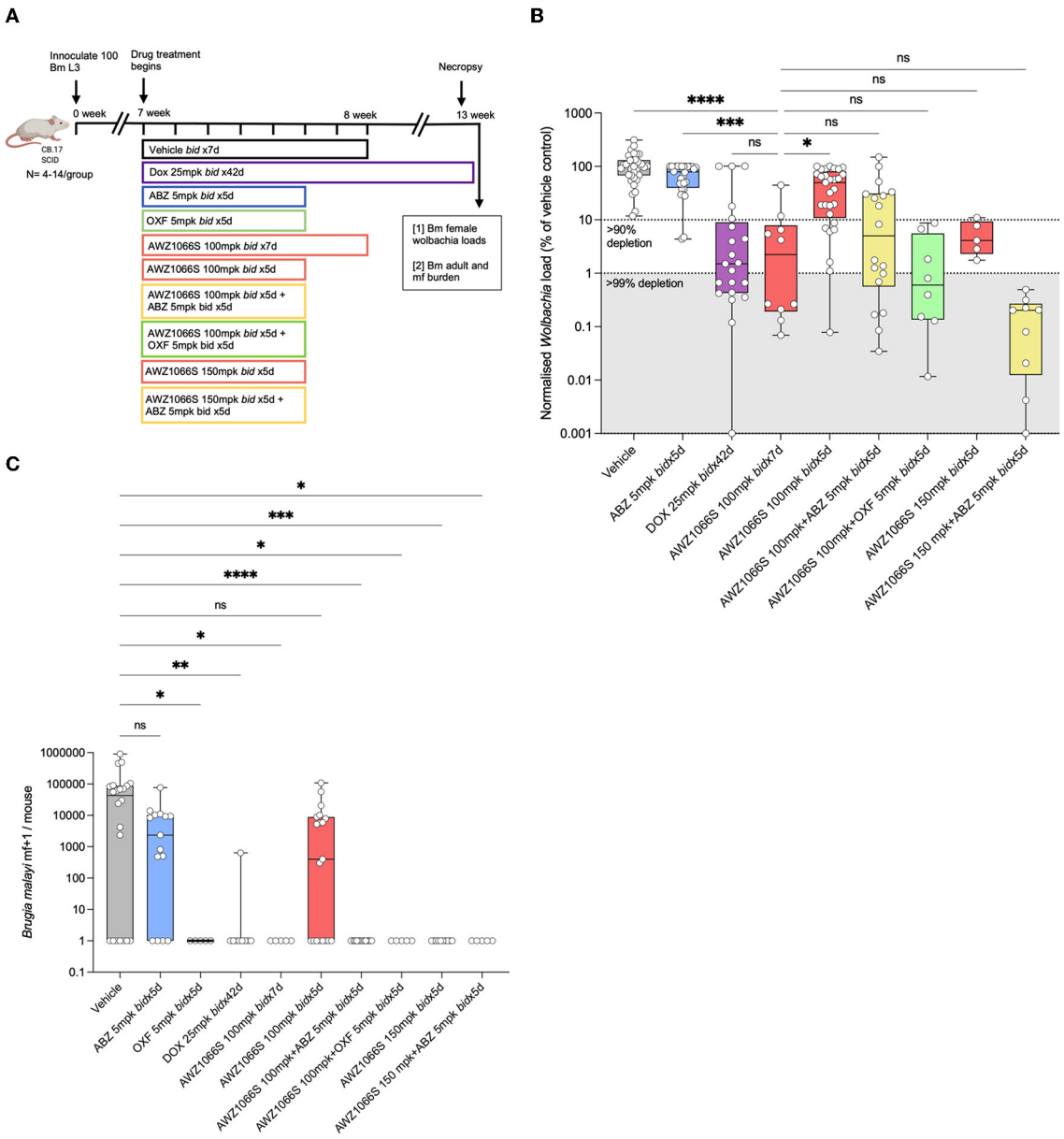

FIGURE 1
Five-day co-administration of AWZ1066S with albendazole or oxfendazole enhances filarial *Wolbachia* depletion and blocks mf production in female *B. malayi*. **(A)** Schematic of experimental design. **(B)** *Wolbachia* titres in female *B. malayi* measured by qPCR of the single copy *Wolbachia* gene, wsp. normalised percentage *Wolbachia* load compared to the median vehicle control level is plotted. **(C)** mf loads per mouse. Box and whiskers represent min/max median and interquartile range with individual plots overlayed. Significance is indicated ns, $p < 0.05$*, $p < 0.01$**, $p < 0.001$***, and $p < 0.0001$**** calculated by the Kruskal-Wallis test with Dunn's multiple comparisons. Data is derived from $n = 5–6$ mice/group from between one and four individual experiments, combined. ns, not significant.

were injected intraperitoneally (IP) with 200 *B. pahangi* L3 as described elsewhere (Gunderson et al., 2020; Hubner et al., 2020a). Twenty-four weeks post-infection, the gerbils were treated with either 50 or 100 mg/kg AWZ1066S alone or in combination with ABZ twice daily by oral gavage. ABZ was used at a 10 mg/kg bi-daily dose equilibrated to match systemic exposure of the active metabolite, ABZ-sulfoxide, as standard human 400 mg dosing in gerbils. Sham animals only received vehicle treatment. Another control group for ABZ alone was also included, where animals were treated with 10 mg/kg ABZ two times daily. To ensure that all animals are treated with the same frequency and volume, the groups without additional ABZ treatment received a corresponding volume of the ABZ-vehicle and groups without AWZ1066S dosing received a matching volume of AWZ1066S-vehicle. Animals were euthanised 19 weeks following the primary treatment (43 weeks post-infection), and the parasites were collected from the peritoneal cavity. The recovered adult worms were sexed under a dissecting microscope, counted, and kept frozen until

further downstream molecular analysis. Mf in the peritoneal cavity were quantified by mixing peritoneal wash 9:1 (v/v) with 0.04% methylene blue:water and counted under an inverted microscope.

To quantify the number of mf shed after overnight culture *in vitro*, individual female worms from control and different treatment groups were cultured in RPMI medium containing 10% FBS, 2x penicillin and streptomycin at 37°C and 5% CO_2 overnight. The next day, the number of mf released from each female was quantified by counting under the microscope.

L. sigmondontis in vivo infection studies

Female Mongolian gerbils (*M. unguiculatus*) were purchased from Janvier Labs (Saint-Berthevin, France) and housed in individually ventilated cages with access to food and water *ad libitum* at the Institute of Medical Microbiology, Immunology and Parasitology, University Hospital Bonn, Germany. Housing conditions and all study procedures were performed according to the European Union animal welfare guidelines and the State Office for Nature, Environment and Consumer Protection, Cologne, Germany (AZ 84-02.04.2015.A507). *L. sigmondontis* infections in gerbils were carried out as described before (Hubner et al., 2019a,b, 2020b). Briefly, 9-week-old female jirds were naturally infected by exposure to mites *(Ornithonyssus bacoti)* containing *L. sigmodontis* L3 larvae. The treatment started 14 weeks post-infection, and animals received different doses of either AWZ1066S (25, 50, or 100 mg/kg) alone or in combination with 10 mg/kg Albendazole two times a day by oral gavage. Control groups were treated with ABZ alone (10 mg/kg, 5 d, *bid*) or vehicle alone (Sham). To match the dosing volume and frequency, animals that received a single drug dose also received vehicle treatment corresponding to the second drug. Peripheral mf levels were quantified before treatment (12 wpi) and every other week after treatment (2, 4, 6, 8, 10, 12, 14, and 17 wpt) by microscopy. Necropsy was performed 17 weeks post-treatment start. Mf was quantified by counting under the microscope from pleural lavage after diluting 10 µl of peripheral blood in 190 µl Hinkelmann solution (0.5% eosin Y, 0.5% phenol, 0.185% formaldehyde in water). If there were <50 mf in 10 µl, the sample was centrifuged at 400 g for 5 min, the supernatant was discarded, and the pellet was resuspended and completely transferred to a microscope slide for counting. Adult worms were extracted from the thoracic cavity and peritoneum. Isolated worms were sorted according to their sex, separated and individually frozen for subsequent *Wolbachia* analysis.

Embryogram from adult worms was done as described elsewhere (Ziewer et al., 2012; Risch et al., 2023). Briefly, worms were fixed using 4% formaldehyde for 24 h and then stored in 60% ethanol until analysis. Single female worms were homogenised in 80 µl PBS and 20 µl Hinkelmann solution [0.5% (wt/vol) eosin Y, 0.5% (wt/vol) phenol (both from Merck) and 0.185% (vol/vol) formaldehyde (Sigma-Aldrich) in deionised water] was added. Ten microlitre of serially diluted worm homogenate were analysed by microscopy, and the numbers of the embryonic stages like "egg," "morula," "pretzel," and "stretched mf" per female adult worm were calculated. For undiluted samples that did not contain any embryonal stages, the homogenate was centrifuged at 400 g for 5 min, and the pellet was resuspended in 10 µl and analysed by microscopy. If embryonal stages were present, five intact female worms were analysed per gerbil. The analyses were performed as previously described (Ziewer et al., 2012).

Molecular assays

Genomic DNA was isolated from frozen worms using the DNeasy blood and tissue kit (QIAGEN, Manchester, UK) for *L. sigmodontis* via the QIAamp DND mini kit (QIAGEN, Hilden, Germany) as per the manufacturer's instructions. For *B. malayi* and *B. pahangi* infections, the single-copy *Wolbachia* gene *wsp* was measured using qPCR as previously described (Halliday et al., 2014; Sharma et al., 2016). For *L. sigmodontis* infection, *Wolbachia* numbers were quantified by qPCR using the single-copy LsFtsZ gene as previously described (Schiefer et al., 2012, 2020).

Fluorescent *in-situ* hybridisation and microscopy analysis

Wolbachia detection using FISH staining was carried out as described before (Dodson et al., 2014; Walker et al., 2021) with some modifications. Frozen whole worms were fixed overnight at 4°C in ethanol and 1x PBS (1:1). Worms were incubated for 5 min at 4°C in 4% paraformaldehyde in 1X PBS and washed in 1x PBS two times. Worms were then incubated for 10 min at 37°C with a 10 µg/ml pepsin solution and washed two times in 1X PBS. Hybridisation was conducted in dark conditions at 37°C for overnight, with 100 µl of hybridisation buffer [50% formamide, 5xSSC, 200 g/L dextran sulphate, 250 mg/L poly(A), 250 mg/L salmon sperm DNA, 250 mg/L tRNA, 0.1 M dithiothreitol (DTT), and 0.5 × Denhardt's solution] containing *Wolbachia* specific 16S rRNA probes W1:/5ATTO590N/AATCCGGCCGARC CGACCC, and W2:/5ATTO590N/CTTCTGTGAGTACCGTCAT TATC. After hybridisation, worms were washed in 100 µl of washing buffer (hybridisation buffer without probes) at 37°C for 15 min. Subsequently, two washes in 1X SSC buffer with 10 mm DTT and two washes in 0.1X SSC buffer with 10 mm DTT were performed, followed by one wash in 1X PBS at room temperature. Finally, samples were mounted in Vectashield anti-fading medium with DAPI (Vector Laboratories, London, UK), stored at 4°C overnight, and then observed using a laser scanning confocal microscope (Zeiss, Cambridge, UK). No-probe controls were also included as negative controls.

For quantification of *Wolbachia* intensity, five random pictures were taken from the distal ovary and hypodermal chords from each worm. A minimum of three worms from each treatment group were imaged unless specified. *Wolbachia* intensity was measured using the ROI method in a defined unit area by ImageJ/FiJi software (https://imagej.nih.gov/ij/).

Pharmacokinetic studies and bioanalysis

Pharmacokinetic studies were conducted to determine the drug concentrations of 10 mg/kg ABZ and 50 mg/kg AWZ1066S administered orally as monotherapies or in combination for 5 days from the *L. sigmodontis* infection model in jirds. This was done to ensure that drug exposures after combination therapies were in line with those observed in the previous rich PK studies during mono therapies (Turner et al., 2017; Hong et al., 2019). For sparse PK analysis, 8 μL blood samples were collected at 0.5, 1, 3, 6, and 24 h after first dosing vena saphena and were immediately transferred to DBS cards (Whatman 903 Protein saver card, Sigma-Aldrich, Germany). The whole blood concentration of AWZ1066S was quantified at WuXi Apptech (Couvet, Switzerland) using liquid chromatography and mass spectroscopy on a UPLC (ultrahigh-pressure liquid chromatography) as described elsewhere (Hong et al., 2019; Turner et al., 2017).

Statistical analysis

The continuous variables of *wsp* copy numbers (in *B. malayi* and *B. pahangi*), *LsFtsZ* copy numbers, peripheral mf numbers, adult parasite counts, and embryo counts in *L. sigmodontis* did not satisfy the assumption of normal distribution by D'Agostino and Pearson omnibus tests. Statistical significance was assessed using GraphPad Prism (version 9.5.1) by Kruskal–Wallis 1-way- ANOVA tests followed by Dunn's multiple comparisons *post-hoc* test to compare three or more groups. Significant differences in *Wolbachia* signal intensity in *B. malayi* hypodermal chords and ovarian tissue following drug treatments were analysed using 2-way-ANOVA followed by Šídák's multiple comparisons *post-hoc* test.

Results

Five-day co-administration of AWZ1066S with albendazole or oxfendazole enhances filarial *Wolbachia* depletion and blocks mf production

AWZ1066S is a first-in-class azaquinazoline anti-*Wolbachia* small molecule that can deliver >90% *Wolbachia* depletion following 7-day oral exposures in pre-clinical animal models compared to 4–6 weeks needed to achieve the same level of depletion by DOX (Turner et al., 2017; Hong et al., 2019). In a CB.17 SCID mouse model of brugian filariasis (Halliday et al., 2014), we previously defined a dose of 100 mg/kg given two times daily (*bid*) for seven days as minimally effective in driving >90% depletions in adult female *Wolbachia* loads and knock-on disruption of embryogenesis leading to prevention of mf production (Hong et al., 2019). To test whether albendazole (ABZ) could synergise with AWZ1066S to boost *Wolbachia* depletion, we treated *B. malayi*-infected CB.17 SCID mice with AWZ1066S alone or in combination with ABZ two times daily for 5 days (Figure 1A). Bi-daily 25 mg/kg DOX treatment (matching 100 mg daily dosing in humans) (Sharma et al., 2016) for 6 weeks was used as a reference control that resulted in 99.3% median *Wolbachia* depletion in female *B. malayi* compared to vehicle (Figures 1B, C). ABZ treatment at 5 mg/kg two times daily for 5 days [bioequivalent to 400 mg standard daily dosing in humans (Turner et al., 2017)] did not significantly alter *Wolbachia* loads. AWZ1066S 100 mg/kg bi-daily dosing for 7 days resulted in an expected >90% *Wolbachia* efficacy (median 97.8% depletion). When we reduced this regimen to 5 bi-daily cycles of 100 mg/kg, this was significantly less effective at depleting *Wolbachia* in female *B. malayi* (a 51.4% reduction, Kruskal-Wallis 1-way-ANOVA $p < 0.0001$, Dunn's *post-hoc* test $p < 0.05$ vs. AWZ1066S 100 mg/kg *bid* x7). However, co-administration of 5 mg/kg ABZ with 100 mg/kg of AWZ1066S for 5 days rescued this regimen in terms of mediating a >90% significant reduction in *Wolbachia* levels (98.8% median depletion) which was equipotent compared with a 7-day dosing (Figure 1B). We further tested whether oxfendazole (OXF), another benzimidazole drug with improved oral bioavailability, could also mediate synergy when co-administered with AWZ1066S. We observed low or absent adult *B. malayi* worm burdens and mf in oxfendazole-treated animals (Figure 1C; Supplementary Table S1), consistent with direct macrofilaricidal activity defined in other filariasis research models (Hubner et al., 2020b). In surviving worms, combined bi-daily dosing of 5 mg/kg OXF with 100 mg/kg AWZ1066S for 5 days also enhanced the level of *Wolbachia* depletion efficacy to >99%, demonstrating synergy is not specific to ABZ but rather consistent with a class-wide effect of benzimidazole co-administration (Figure 1B). When we co-administered elevated 150 mg/kg bi-daily doses of AWZ1066S for 5 days, we could achieve a potency boost of 96 vs. 51.4% median *Wolbachia* depletions. When co-dosed with ABZ, this efficacy increased to 99.8% depletion, further illustrating the synergistic potential of ABZ co-administration.

The transmission-blocking impact of combination synergy was examined by enumerating the total numbers of *B. malayi* mf within the peritoneal cavity of infected SCID mice (Figure 1C). In vehicle control animals, 7/22 infections were mf negative (32%), and the median yield of mf/mouse was 4.3×10^4. ABZ had reduced but not prevented mf accumulations in the majority of mice (4/15 mice mf-, median 0.5×10^4), and mf production was not significantly different from vehicle control levels. Six-week bi-daily DOX or 7-day AWZ1066S at 100 mg/kg significantly prevented mf release, whereby 8/9 and 5/5 mice were mf negative, respectively (Kruskal-Wallis 1-way-ANOVA $p < 0.0001$, Dunn's *post-hoc* tests $p = 0.0005$ and $p = 0.0092$, respectively). The reduced 5-day bi-daily dosing of AWZ1066S at 100 mg/kg failed to block mf release in the majority of mice treated (8/19 mice mf-, median yield of 0.04×10^4), and mf production in this treatment group was not significantly different to those in the vehicle control group. Comparatively, when ABZ or OXF was added to this regimen as a combination, mf production was completely blocked (15/15 and 5/5 mice, Dunn's *post-hoc* tests, $p < 0.0001$ and $p = 0.003$, respectively). The elevated 150 mg/kg dose of AWZ1066S two times-daily for 5 days achieved a complete block of mf production regardless of whether ABZ was co-dosed (7/7 and 5/5 mice, Dunn's *post-hoc* tests, $p < 0.0001$ & $p = 0.003$, respectively). There was no significant difference in total adult worm burden among the control and treatment groups (Supplementary Table S1). In summary, our data

demonstrates it is feasible to mediate >90% *Wolbachia* depletion and block mf production from female *B. malayi* worms following sub-seven-day dosing of AWZ1066S. Combinations with either benzimidazole, ABZ, or OXF synergise to reduce the dose exposure of AWZ1066S necessary to mediate these threshold anti-*Wolbachia* and sterilising activities.

Five-day combinations with albendazole reduce the dose exposure of AWZ1066S necessary to deliver long-term anti-*Wolbachia* anti-filarial activities

To confirm that the "rescue" effect of co-treating lowered 5-day doses of AWZ1066S with benzimidazoles was not unique to *B. malayi* and to verify the persistence of efficacy in terms of potential recrudescence of *Wolbachia* and resumption of mf production, we utilised long-term models of lymphatic filariasis in gerbils. The *B. pahangi* infection model was used to test the effect of AWZ1066S and ABZ combination on *Wolbachia* depletion in mature, fecund female worms. We infected *Meriones unguiculatus* Mongolian gerbils with *B. pahangi* L3, and following 24 weeks of infection, gerbils were treated bi-daily with different concentrations of AWZ1066S either alone or in combination with 10 mg/kg ABZ two times daily (Figure 2A). This dose of ABZ was determined to be bio-equivalent to SCID mouse dosing at 5 mg/kg (Supplementary Figure S1) and thus aligned with 400 mg daily exposures in humans (Shenoy et al., 2002; Turner et al., 2017; Ceballos et al., 2018). Gerbils were necropsied after a long washout period of 17 weeks (Figure 2A). The quantification of *wsp* copies in female worms by qPCR confirmed the SCID mouse model data in *B. malayi,* that a bi-daily treatment of 100 mg/kg AWZ1066S as a monotherapy for 7 days was sufficient to result in >99% reduction in *Wolbachia* titres in adult female worms, whereas a 5-day ABZ monotherapy did not have any anti-*Wolbachia* efficacy (Figure 2B). In this model, *B. pahangi* females were more sensitive to the anti-*Wolbachia* effect of 5-day bi-daily AWZ1066S at 100 mg/kg two times daily than in the *B. malayi* SCID model (Figure 1). This regimen resulted in >99.9% *Wolbachia* depletion irrespective of ABZ co-dosing, which was statistically non-inferior to the corresponding 7-day AWZ1066S regimen (Figure 2B). However, when we de-escalated a 5-day dosing of bi-daily AWZ1066S to 50 mg/kg, monotherapy mediated <90% *Wolbachia* depletion, which was inferior to a 7-day 100 mg/kg dosing (82.7% median depletion, Kruskal-Wallis 1-way-ANOVA $p < 0.0001$, Dunn's *post-hoc* test $p = 0.015$). The co-administration of 10 mg/kg ABZ for 5 days with this sub-optimal regimen induced synergy in anti-*Wolbachia* efficacy within female *B. pahangi* whereby *Wolbachia* was depleted in all worms to >99%, which was non-inferior to 7-day bi-daily dosing of AWZ1066S with 100 mg/kg (Figure 2B). Further, reducing the regimen of AWZ1066S to 25 mg/kg bi-daily for 5 days in combination with ABZ was inferior to the 7-day bi-daily 100 mg/kg regimen of AWZ1066S in terms of anti-*Wolbachia* efficacy (Dunn's *post-hoc* test $p < 0.0001$), although this combination treatment still mediated a shift in *Wolbachia* depletions compared to the 25 mg/kg 5-day bi-daily AWZ1066S monotherapy (77.9 vs. 0% median depletion).

The impact of *Wolbachia* depletions on embryogenesis and mf production was measured by enumerating the total numbers of mf in gerbils following a 17-week washout of drug treatments. *B. pahangi* mf had accumulated in vehicle control animals to a median level of 1.2×10^6. The 7-day 100 mg/kg bi-daily regimen of AWZ1066S positive control had resulted in a median 99.7% significant depletion in peritoneal mf compared with vehicle controls (Kruskal-Wallis 1-Way-ANOVA $p < 0.0001$, Dunn's *post-hoc* test $p < 0.001$) which were also statistically superior to a median 63% reduction in peritoneal mf mediated by ABZ treatment for 5 days (Figure 2C). All 100–50 mg/kg 5-day AWZ1066S treatments and combinations were statistically non-inferior to the 7-day high dose of AWZ1066S in terms of reducing the numbers of mf to >99%. The impact of combination synergy was, however, observable at the lowest dose of AWZ1066S tested, whereby monotherapy for 5 days two times daily did not significantly lower mf yields compared with vehicle levels and thus was statistically inferior to the 7-day 100 mg/kg dosing (1.5% median reduction, Dunn's *post-hoc* test $p < 0.0001$). Combining this low AWZ1066S dose with ABZ reverted mf depletion levels to, on average, 73.5%, which was non-inferior to high dose efficacy.

Because of the longevity of lymphatic filarial mf (60–100 weeks half-life) (Eberhard, 1986), and because we had commenced treatments after the establishment of fecund infections, residual low levels of mf recorded within treated gerbils may reflect the presence of mf released prior to *Wolbachia* depletions and knock-on block of embryogenesis. Therefore, we also enumerated mf released *ex vivo* from live female *B. pahangi* cultured overnight following their isolation from gerbils treated with AWZ1066S and ABZ combinations (Figure 2D). Vehicle control-treated female worms released a median of 2,600 mf overnight, with a minority of 14/45 worms non-productive in mf release (31%). ABZ treatment reduced the median level of mf released to 300 but with a similar number of unproductive female worms (25/55; 45%). Comparatively, the high-dose 100 mg/kg 7 bi-daily regimen of AWZ1066S had significantly prevented mf release in 83% (15/18) of female worms in culture (Kruskal-Wallis 1-Way-ANOVA $p < 0.0001$, Dunn's *post-hoc* test $p < 0.001$ and $p < 0.05$ vs. vehicle and ABZ treatment groups, respectively). Between 83–95% of *B. pahangi* worms assayed were unproductive in releasing mf in 100–50 mg/kg AWZ1066S 5-day treatment groups, irrespective of ABZ co-dosing. However, when reducing the *in vivo* dose exposure of AWZ1066S to 25 mg/kg bi-daily for 7 days, only a minority of female worms assayed (9/28, 32%) were unproductive in mf release, which was significantly inferior to the mf blocking activity of 7-day 100 mg/kg AWZ1066S (Dunn's *post-hoc* test $p < 0.01$). Co-dosing this inferior regimen of AWZ1066S with ABZ blocked mf production within 64% of female worms in culture (14/22).

There were no significant differences in total adult, female or male worm burdens between groups at 18 weeks post-treatment, and recoveries in vehicle controls were highly variable (median 72 worms per gerbil, range 16–121, Figures 2E–G). However, both 7-day and 5-day 100 mg/kg bi-daily AWZ1066S dosing had resulted in a trend towards lower adult burdens (60.8 and 45.3% median reductions, respectively), whilst gerbils receiving lowered doses of

10.3389/fmicb.2024.1346068

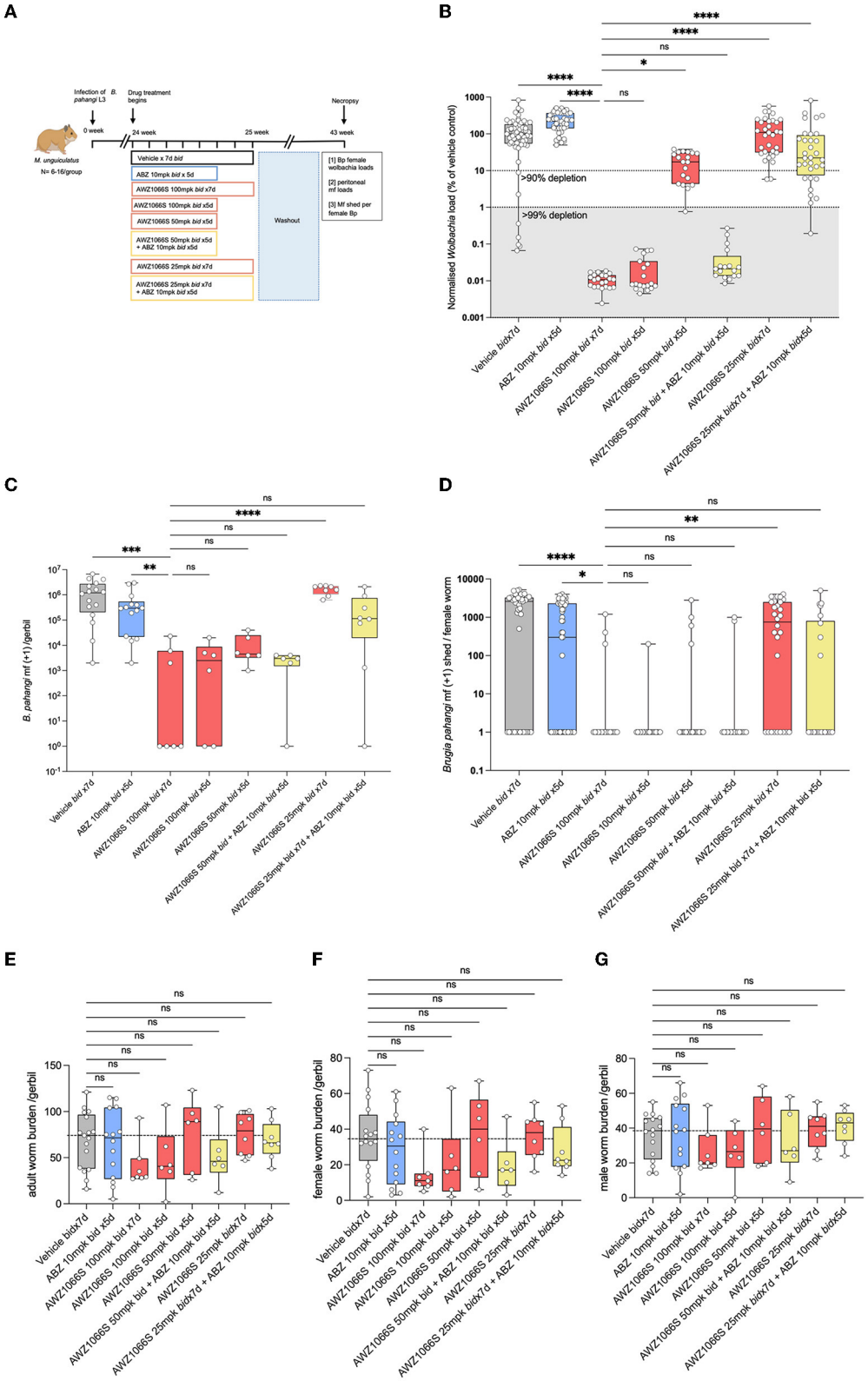

FIGURE 2
Synergistic depletion of *Wolbachia* and mf blockade in female *B. pahangi* after low-dose 5-day AWZ1066S and ABZ combination therapy. **(A)** Schematic representation of the experimental design; **(B)** *Wolbachia* numbers in individual female *B. pahangi* measured by qPCR for the single copy *Wolbachia* gene wsp; **(C)** the total number of mf recovered from gerbil peritonea; and **(D)** the number of mf shed from individual female worms cultured overnight. Enumeration of total **(E)**, female **(F)**, and male **(G)** adult worm burdens at end-point. Box and whiskers indicate min/max, median, and interquartile range with individual data overlayed. Significance is indicated: ns, $p < 0.05$*, $p < 0.01$**, $p < 0.001$***, and $p < 0.0001$**** calculated by the Kruskal-Wallis test with Dunn's multiple comparisons. Data is derived from $n = 6–8$ gerbils/group from two individual experiments combined. ns, not significant.

AWZ1066S were more similar to vehicle control levels with the exception of 50 mg/kg combined with ABZ, which resulted in a 37.8% median reduction.

We then utilised an *L. sigmodontis* infection model to further assess the impact of co-administration of ABZ with low-dose titrations of AWZ1066S in *Wolbachia* depletion and embryogenesis inhibition. In this rodent-adapted filarial infection model, mf produced from fecund infections migrate from the adult thoracic cavity infection site and establish long-term parasitaemias. We had previously defined that 50 mg/kg AWZ1066S two times daily for 7 days was sufficient to deplete *Wolbachia* >99% and remove mf from circulation in this model (Hong et al., 2019). Following 12 weeks of infection, *M. unguiculatus* gerbils were treated at or below this reference dose of AWZ1066S as a monotherapy or in combination with 10 mg/kg ABZ. The effects of treatment were evaluated following a long washout period of 16 weeks (Figure 3A). The AWZ1066S 50 mg/kg bi-daily 7-day regimen mediated the predicted >99% depletion of *Wolbachia* within *L. sigmodontis* female adults, whereas ABZ monotherapy was not efficacious (Kruskal-Wallis 1-way-ANOVA $p < 0.0001$, Dunn's *post-hoc* test $p < 0.0001$; Figure 3B). Lowering the dose time-frame of 50 mg/kg of AWZ1066S to 5 days was equally >99% efficacious in *Wolbachia* depletions, irrespective of ABZ co-dosing (Figure 3B). However, 25 mg/kg AWZ1066S alone mediated a 35% median reduction in *Wolbachia,* which was inferior to the 7-day 50 mg/kg dosing (Dunn's *post-hoc* test $p < 0.0001$). Yet, the co-administration of ABZ with 25 mg/kg AWZ1066S rescued *Wolbachia* depletion efficacy to a >99% median level (Figure 3B).

From the point of treatment, we assessed peripheral blood *L. sigmodontis* microfilaraemias every 2 weeks. In vehicle controls, peripheral microfilaraemias remained constant over the post-treatment time period, at a median range of between 941 and 785 mf/10μl blood (Figure 3C). The reference 7-day bi-daily 50 mg/kg dose of AWZ1066S gradually lowered mf in the blood and, at 17-week post-treatment, all gerbils were amicrofilaraemic (Kruskal-Wallis 1-way-ANOVA $p < 0.0001$, Dunn's *post-hoc* test $p < 0.01$; Figure 3D). ABZ monotherapy did not deplete mf from peripheral circulation and was inferior to the AWZ1066S 7-day dosing (Dunn's *post-hoc* test $p < 0.05$). Lowering the dose time-frame of 50 mg/kg AWZ1066S to 5 days was equally 100% efficacious in the gradual clearance of mf from circulation, irrespective of ABZ co-dosing. However, lowering the 5-day dosage of AWZ1066S to 25 mg/kg bi-daily was insufficient to mediate clearance of mf from circulation ($p < 0.01$ compared with the 7-day 50 mg/kg dosing; Figure 3D). ABZ co-administration at this dose level resulted in complete efficacy in the gradual removal of mf from the blood of infected gerbils (Figures 3C, D). Embryograms of uterine content in *L. sigmodontis* female worms at 17 weeks post-treatment confirmed that whilst ABZ monotherapy alone had no significant impact in embryogenic stages *in uteri,* co-dosing had significantly augmented the otherwise sub-optimal embryotoxic activity of 7-day bi-daily 25 mg/kg AWZ1066S (Figures 3E–H).

L. sigmodontis adult worm burdens were significantly reduced following the AWZ1066S 50 mg/kg regimen dose for 7 days (a 79% median reduction compared with vehicle controls, range 52–83%, Kruskal-Wallis 1-Way-ANOVA $p = 0.0001$, Dunn's *post-hoc* test $p < 0.05$; Figure 3I). Of the reduced 5-day regimens, only the combination of 50 mg/kg AWZ1066S with ABZ mediated a similar, significant 88% reduction in adult worm burden (range 66–97%, Dunn's *post-hoc* test $p < 0.05$; Figure 3I). Both female and male worm burdens were significantly reduced following this 5-day combination drug exposure (Figures 3J, K).

The exposure profiles of AWZ1066S were measured over 24 h post-first dose at 1, 3, 5, or 24 h in groups of 3 *L. sigmodontis*-infected gerbils receiving 50 or 25 mg/kg AWZ1066S with or without ABZ co-administrations (Figure 4A). The area under the curve (AUC_{0-24h}) of AWZ1066S was dose proportional, and both AUCs and peak plasma levels (C_{max}) were similar in gerbils receiving either monotherapy or ABZ combination (Figure 4B). When adjusting to the 50 mg/kg dose and combining data ($n = 6$ gerbils per group), co-dosing of ABZ did not cause any significant alteration in AWZ1066S blood concentration at any time-point measured (Figure 4C), indicating a lack of drug-drug interaction. Combined, these data demonstrate that ABZ can augment the anti-*Wolbachia* activity of sub-optimal, low-dose 5-day exposures of the investigational drug AWZ1066S, with concomitant long-term significant impacts on complete transmission blockade and partial adulticidal activities.

AWZ1066S-ABZ combination augments *Wolbachia* depletions within uterine and hypodermal chords

Filarial *Wolbachia* resides in two different tissues in female *B. malayi*—the hypodermal chord syncytium and female germline (Taylor and Hoerauf, 1999; Taylor et al., 1999; Landmann et al., 2010). To understand the initial dynamics of AWZ1066S monotherapy or in combination with ABZ treatment on distinct *Wolbachia* tissue populations, we used a *B. malayi* infection model in *M. unguiculatus* gerbils. Adult parasites were recovered after 2 weeks of drug treatment with either 50 mg/kg *bid* AWZ1066S alone or in combination with 10 mg/kg ABZ for 5 days. Vehicle and 10 mg/kg ABZ control groups were also included (Figure 5A). Using previously established FISH staining with *Wolbachia*-specific 16S rRNA probes (Walker et al., 2021; Marriott et al., 2023), we visualised and quantified *Wolbachia* loads both in hypodermal chords and ovaries in female worms from control and different drug treatment groups. Previous studies have shown that the ovaries have the highest density of germline *Wolbachia* populations (Bakowski et al., 2019) and are also the only tissue site in mature adult worms containing proliferating cells (Foray et al., 2018); thus, they serve as an ideal tissue to compare against hypodermal chords. Via measuring *Wolbachia* fluorescent signal intensity from randomly selected fields of view, AWZ1066S monotherapy resulted in a significant 83% mean depletion in ovaries (2-way-ANOVA $p < 0.0001$, Šídák's multiple comparisons *post-hoc* test $p < 0.0001$ vs. vehicle; Figures 5B–D) whereas only a non-significant average 35% depletion was observed in hypodermal chords compared to the respective tissues in vehicle-treated worms. ABZ alone had a non-significant mean 59% effect on *Wolbachia* levels in ovaries and no impact on *Wolbachia* levels in hypodermal chords. The effect of ABZ combination therapy with AWZ1066S was the

10.3389/fmicb.2024.1346068

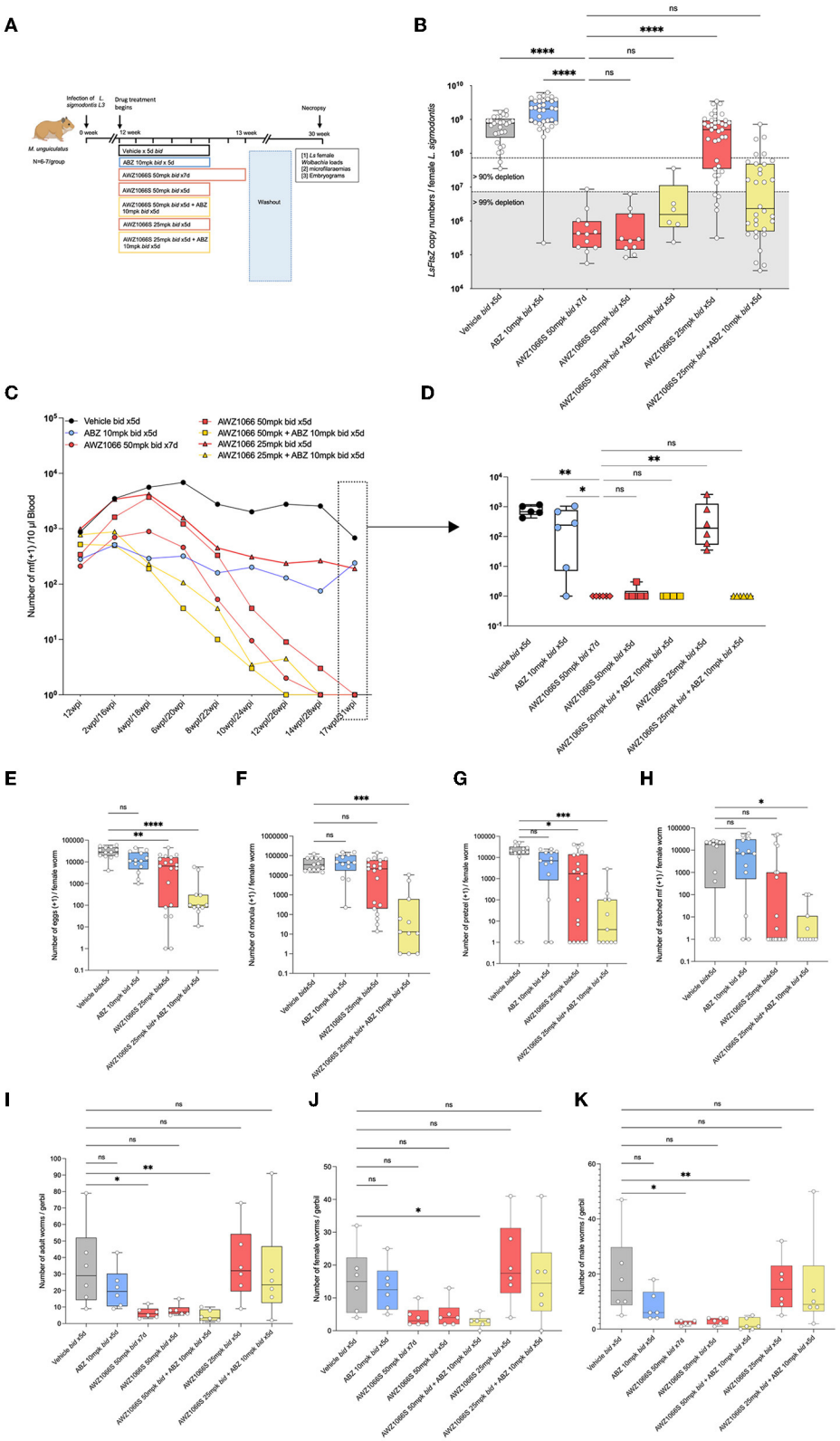

FIGURE 3
Synergistic depletion of *Wolbachia* in female *L. sigmodontis*, clearance of mf from circulation and adulticidal activity after a low-dose 5-day AWZ1066S and ABZ combination therapy. **(A)** Schematic representation of experimental design. **(B)** *Wolbachia* numbers in individual female *L. sigmodontis* measured by qPCR for the single copy *Wolbachia* gene, ftsz. **(C)** Time course of median microfilaraemias per group following drug treatment. **(D)** Comparison of microfilaraemias at end-point. **(E)** Embryogram enumeration of eggs. **(F)** Early-stage morulae. **(G)** Pretzel-stage coiled mf. **(H)** Stretched mf from uteri of female *L. sigmodontis* at end-point. **(I)** Total numbers, **(J)** female, and **(K)** male *L. sigmodontis* adults at end-point. Box and whiskers indicate min/max, median and interquartile range with individual data overlayed. Significance is indicated ns, $p < 0.05$*, $p < 0.01$**, $p < 0.001$***, and $p < 0.0001$**** calculated by the Kruskal-Wallis test with Dunn's multiple comparisons. Data is derived from $n = 7–8$ gerbils/group from a single experiment. ns, not significant.

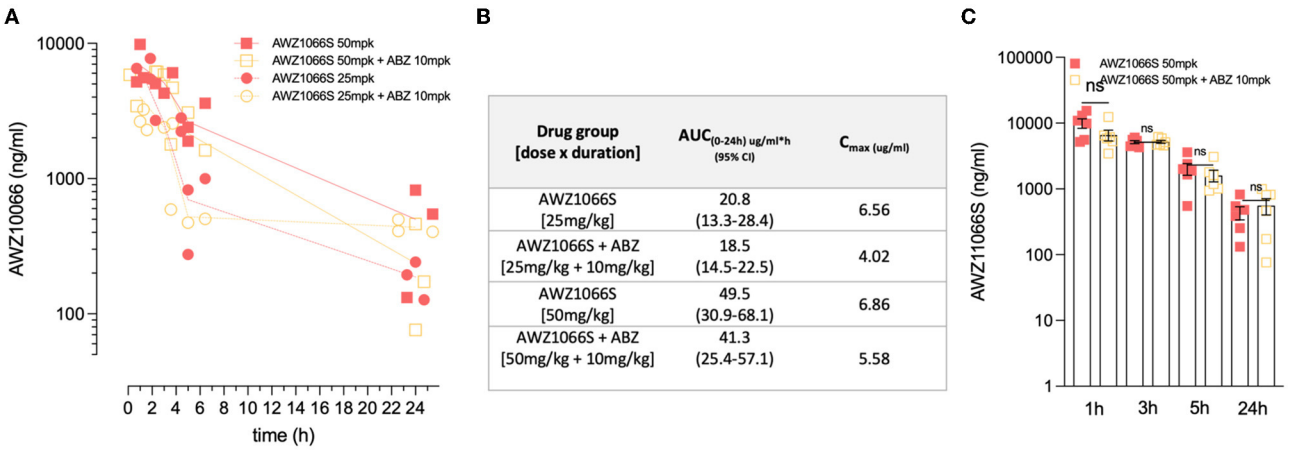

Drug group [dose x duration]	$AUC_{(0\text{-}24h)}$ ug/ml*h (95% CI)	C_{max} (ug/ml)
AWZ1066S [25mg/kg]	20.8 (13.3-28.4)	6.56
AWZ1066S + ABZ [25mg/kg + 10mg/kg]	18.5 (14.5-22.5)	4.02
AWZ1066S [50mg/kg]	49.5 (30.9-68.1)	6.86
AWZ1066S + ABZ [50mg/kg + 10mg/kg]	41.3 (25.4-57.1)	5.58

FIGURE 4
ABZ co-dosing does not significantly alter AWZ1066S drug exposure profiles. **(A)** AWZ1066S blood concentrations. **(B)** Summary PK parameters over 24 h in indicated groups. **(C)** Combined AWZ1066S blood exposure data adjusted to 50 mg/kg (assuming linearity with or without ABZ co-dosing). No significant (ns) differences when compared to Student's *t*-test. Data from individual gerbils and time-points are plotted from groups of 3–6 gerbils. Bars and error bars represent mean ± SEM.

augmentation of a significant 88.5% depletion of *Wolbachia* within both hypodermal chord and ovarian populations ($p < 0.0001$, Figures 5B–D). We then examined *Wolbachia* depletion levels in male *B. pahangi* following short-course exposures of AWZ1066S ± ABZ (Figure 5E), whereby effects would be limited to the hypodermis. Whilst ABZ only had no impact on male *Wolbachia* loads, treatment of AWZ1066S at 50 mg/kg bi-daily for 5 days in combination with ABZ reduced the median *Wolbachia* depletion level from 84.8 to 92.3% (both statistically significant vs. vehicle; Kruskal-Wallis 1-way-ANOVA $p < 0.0001$, Dunn's *post-hoc* tests $p < 0.0001$). When further de-escalating the dose of AWZ1066S to 25 mg/kg two times daily, only the combination with ABZ mediated a significant 85.1% median *Wolbachia* depletion (Dunn's *post-hoc* test $p < 0.0001$ vs. vehicle; Figure 5E). Together, these data demonstrate that whilst the germline population is more sensitive to depletion by low-dose, short-course AWZ1066S treatments, ABZ can augment the depletion of nematode *Wolbachia* residing within both germline and hypodermal tissues.

Discussion

We report a pharmacological synergy between the first-in-class azaquinazoline anti-*Wolbachia* small molecule, AWZ1066S, and anthelmintic benzimidazoles (albendazole, oxfendazole), in targeting *Wolbachia* within filarial worms in multiple rodent infection models. The resulting combination treatment delivers minimal effective exposure durations of 5 days whilst concomitantly decreasing the systemic exposure of AWZ1066S by ~2-fold necessary to achieve at least 90% *Wolbachia* depletion, a clinically determined minimum threshold for delivering slow-cure macrofilaricidal activity in lymphatic filariasis (Johnston et al., 2021).

The data in our study confirms the profound *Wolbachia* depletion from filarial tissues by AWZ1066S. AWZ1066S is a unique narrow-spectrum anti-*Wolbachia* compound with no general antibiotic properties and rapid bactericidal kinetics, achieving near maximal clearance of nematode *Wolbachia in vitro* following exposure of 1 day vs. 6 days required for tetracyclines, rifamycins, and fluoroquinolones (Hong et al., 2019; Johnston et al., 2021). We have previously established that regimens between 100 and 50 mg/kg two times daily for 7 days are efficacious in delivering a threshold >90% anti-*Wolbachia* activity against *B. malayi* immature adults in SCID mice and *L. sigmodontis* in gerbils, respectively, leading to total block of mf production via embryostasis. In addition, we determined that via depletion of *Wolbachia* in the mf-stage, AWZ1066S can also block the development of *Brugia* in the mosquito vector via a deficit in *Wolbachia,* inhibition of mf chitinase production and failure to exsheath in the insect midgut (Quek et al., 2022). Most recently, we have determined 90% anti-*Wolbachia* activity of AWZ1066S against developing larvae of the veterinary filaria, *Dirofilaria immitis,* following 2-day exposures *in vivo,* extending the potential use-case of this new class of anti-*Wolbachia* therapeutic from human to veterinary medicine (Turner et al., 2020; Marriott et al., 2023). In this study, compared with a 100 mg per day human equivalent dose exposure of doxycycline (Sharma et al., 2016), which requires 6 weeks in a SCID model of brugian filariasis to mediate >90% anti-*Wolbachia* activity, we further established the minimum AWZ1066S dose time frame of 5 days which could sustainably deplete *Wolbachia* to a similar or >99% threshold when sufficient bi-daily dose-exposures were applied against mature *B. pahangi* in gerbils (Figures 1, 2). We further corroborated a minimum >90% anti-*Wolbachia* effect in a complementary *L. sigmodontis* gerbil model with a 50 mg/kg 5-day bi-daily regimen. Extending our prior data (Hong et al., 2019), we also confirmed no rebound of *Wolbachia* with these minimum 5-day bi-daily dose AWZ1066S regimens up to 18 weeks post-treatment in both models (Figure 3). These 5-day monotherapeutic doses led to a complete cessation of mf production in 95% of mature fecund female *Brugia*

10.3389/fmicb.2024.1346068

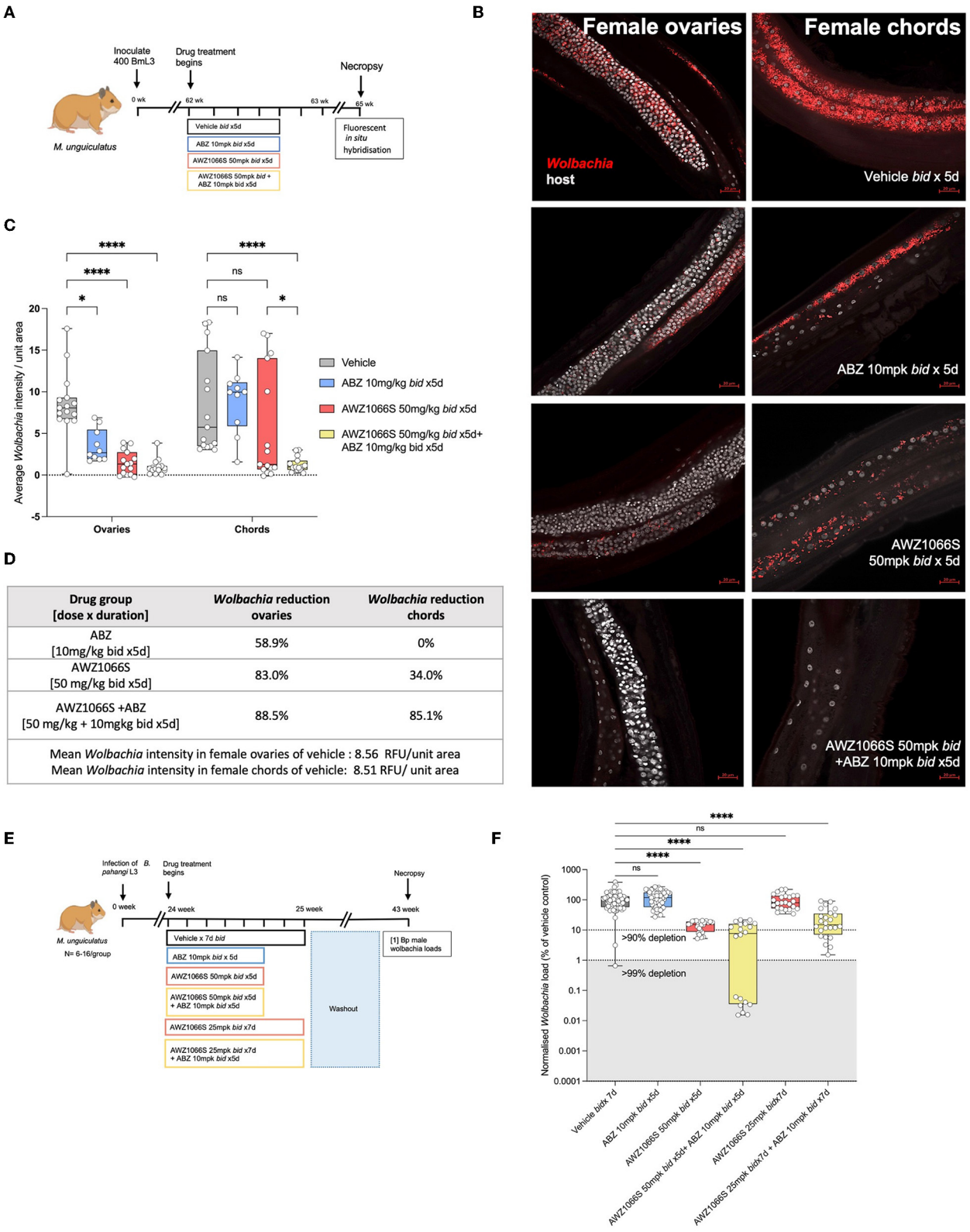

Drug group [dose x duration]	*Wolbachia* reduction ovaries	*Wolbachia* reduction chords
ABZ [10mg/kg bid x5d]	58.9%	0%
AWZ1066S [50 mg/kg bid x5d]	83.0%	34.0%
AWZ1066S +ABZ [50 mg/kg + 10mgkg bid x5d]	88.5%	85.1%
Mean *Wolbachia* intensity in female ovaries of vehicle : 8.56 RFU/unit area Mean *Wolbachia* intensity in female chords of vehicle: 8.51 RFU/ unit area		

FIGURE 5
Treatment of AWZ1066S with ABZ synergistically targets both uterine and hypodermal chord *Wolbachia*. **(A)** Schematic representation of experimental design. **(B)** Representative FISH photomicrographs using *Wolbachia* (red) specific probes against 16S rRNA gene. Bars −20 μm. **(C)** Morphometric analysis of FISH signal intensity. Data plotted is *Wolbachia* intensity per field of view from three individual worms combined. Bars represent mean *Wolbachia* intensity ± SEM. Significance is indicated $p < 0.05$*, $p < 0.0001$**** calculated by 2-way-Anova with Šídák's multiple comparisons *post-hoc* test. **(D)** Table summarising *Wolbachia* depletion in ovarian and hypodermal chord populations. **(E)** Experimental design and **(F)** *Wolbachia* loads in male *B. pahangi* following *in vivo* exposure to indicated doses of AWZ1066S ± ABZ. Box and whiskers indicate min/max, median and interquartile range with individual data overlayed. Significance is indicated $p < 0.0001$**** calculated by the Kruskal-Wallis test with Dunn's multiple comparisons. Data is derived from $n = 7–8$ gerbils/group from a single experiment. ns, not significant.

pahangi assayed whilst delivering a gradual and complete clearance of *L. sigmodontis* mf from the circulation, mediated via block of embryogenesis (Figures 2, 3). Importantly, in these long-term models, we could also begin to discern significant macrofilaricidal activity, with reduced adult worm burdens following treatment compared with vehicle controls (Figure 3). Typically, 12 months is a minimum necessary time frame for induction of significant macrofilaricidal activity following the loss of the endosymbiont via 6-week doxycycline therapy in clinical LF trials, judged by loss of ultrasonograph "filarial dance sign" in intra-lymphatic worm nests (Debrah et al., 2006). However, we have previously reported that high-dose rifampicin, when combined with ABZ to augment *Wolbachia* depletions, can begin to affect adult worm burdens in as short as 6 weeks following treatment in a SCID mouse model of brugian filariasis (Aljayyoussi et al., 2017; Turner et al., 2017). The accelerated AWZ1066S-mediated macrofilaricidal activity after 18 weeks might, therefore, reflect the rapid *Wolbachia* kill kinetics of this azaquinazoline agent compared with registered antibiotics.

Our data reinforces that *Wolbachia* is an exquisitely selective drug target whereby it contributes towards multiple fundamental biological processes underpinning the obligatory mutualism with its filarial host. *Wolbachia* is postulated to provide a source of nucleotides and micronutrients (including flavin adenine dinucleotide, haem and riboflavin) to meet the metabolic demands of filariae, particularly in periods of rapid growth, as gene pathways intact in the symbiont are either insufficient or lacking in *Wolbachia* containing filarial worms (Slatko et al., 2010).

Other cell biology processes that *Wolbachia* is implicated in regulating across nematode and insect hosts include oxidative stress, autophagy and apoptosis (Landmann et al., 2011; Voronin et al., 2012; Gill et al., 2014). *Wolbachia* localises in two major tissues within filariae—the hypodermal chord syncytium and the female germline (Slatko et al., 2010; Taylor et al., 2012). A rapid manifestation of antibiotic depletion of endobacteria from the female filarial germline is a widespread apoptosis spreading from *Wolbachia*-containing germline cells to non-Wolbachia-containing somatic tissues of developing embryos and mf (Landmann et al., 2011). More recent evidence from spatiotemporal microscopy studies suggests antibiotic *Wolbachia* removal from the female germline initiates a dysregulation of stem cell proliferation, leading to a significant diminution and disorganisation of the ovary mitotic zone, which precedes widespread apoptosis of embryos leading to sterility (Foray et al., 2018). In comparison, rapid apoptosis is not a tissue-specific feature following depletion of hypodermal *Wolbachia.* It is thus postulated that permanent clearance of the hypodermal *Wolbachia* population leads to a deficit of nutrient sources for prolonged survival in the adult filarial parasitic niche (Slatko et al., 2010; Landmann et al., 2011). An alternate hypothesis, supported by cellular changes in white blood cell composition, localisation and granulocyte-released effector molecules surrounding adult *Onchocerca* post-*Wolbachia* removal, is that endobacterial titres aid the parasite subversion of an otherwise complex, attritional anti-parasite host immune response (Hansen et al., 2011; Tamarozzi et al., 2016). This spatially and temporally segregated impact of *Wolbachia* removal from distinct filarial tissue sites may explain why lowered-dose doxycycline exposures in LF clinical trials lead to an irreversible block of embryogenesis but not significant macrofilaricidal activity (Turner et al., 2006). Consistent with a hypothesis that reproductive tissues are a more sensitive site for drug-mediated *Wolbachia* clearance, in this study, we observed that sub-optimal dosing of AWZ1066S monotherapy mediated more consistent *Wolbachia* depletions in ovaries than in those of the lateral chords (Figure 5). Contrasting depletion levels by lowered dose exposures of anti-*Wolbachia* drugs in different filarial tissues may reflect effect site pharmacokinetics (i.e., local drug penetration or drug detoxification) or that the *Wolbachia* residing in the reproductive tissues are intrinsically more sensitive to drug activity, potentially via virtue of higher division rate and metabolic activity. Recent dual RNAseq analysis of *Wolbachia* gene transcription in the hypodermal vs. the ovarian population within *B. malayi* indicates a relatively harsher environment in the former location, reflected by upregulation of bacterial stress response proteins, which may impinge on endobacterial growth (Chevignon et al., 2021).

Upon combining humanised dose exposures of ABZ equivalent to standard 400 mg dosing (Turner et al., 2017) or matching doses of the veterinary OXF, which has higher systemic exposure and is being repurposed for human helminth indications (Lanusse et al., 1995; Gokbulut et al., 2007; Bach et al., 2020; Ehrens et al., 2022; Risch et al., 2023), we could demonstrate a pharmacological synergy of otherwise sub-optimal doses of AWZ1066S given alone for 5 days. The impact of ABZ "rescue" meant these otherwise ~2-fold sub-optimal 5-day doses could recapitulate profound sterilising and partial macrofilaricidal activities in the rodent models and washout periods tested. This indicates synergy is likely consistent across the benzimidazole anthelmintic class. The classical mode of action of benzimidazole drugs, including the active metabolite of ABZ (ABZ-sulphoxide) and OXF, is via capping the alpha β-tubulin subunit to prevent microtubule polymerisation in helminth parasites (Oxberry et al., 2001). Benzimidazole-mediated β-tubulin polymerisation inhibition results in two major deleterious consequences—disruption of cell proliferation leading to apoptosis (Zhang et al., 2017) and defective uptake and transport of energy stores leading to parasite starvation (Lacey, 1990; Keiser and Utzinger, 2010; Chai et al., 2021). In tissue-dwelling filarial nematodes, probably related to low systemic exposures of ABZ compared with gut-dwelling helminths, drug effects are typically transient and non-lethal to adult filariae but lead to temporary disruption of embryogenesis in female adult worms (Cardenas et al., 2010), which is manifest by a gradual, partial reduction in mf in circulation (Awadzi et al., 1991; Klion et al., 1993). The mechanism by which ABZ or OXF can synergise anti-*Wolbachia* drug efficacies with AWZ1066S or other anti-*Wolbachia* agents remains to be resolved. In this study, we found that human equivalent, physiologically relevant dosing of ABZ up to 5 days as monotherapy had no long-term effect on *Wolbachia* abundance *per se* in three different filarial infection models (assayed between 6 and 18 weeks following exposure). Intracellular bacteria are known to utilise the host cytoskeleton system for inter- and intracellular locomotion. For instance, in *Drosophila* cells, *Wolbachia* can also undergo horizontal cell-to-cell transfer (White et al., 2017). Intracellularly, *Wolbachia* resides in host Golgi-related vesicles (Cho et al., 2011), and microtubules play a crucial role in the formation, maintenance, and intracellular locomotion of these

vesicles (Cole et al., 1996; Wu et al., 2016). Hence, disruption of microtubule structure by benzimidazole drugs may limit the division and spread of residual surviving *Wolbachia* within the host cell post-removal of AWZ1066S and/or might induce a more bacteriostatic environment augmenting AWZ1066S targeting during dual exposures of drugs.

A further related hypothesis we examined was that synergy in *Wolbachia* depletion exerted by ABZ was targeted specifically to prevent germline cell proliferation and inhibit residual surviving *Wolbachia* spread between germline cells post-drug removal. Whilst long-term, ABZ monotherapy did not adversely affect total endobacterial titres, at 2 weeks post-exposure, we could discern a partial reduction in ovarian *Wolbachia* by microscopy analysis, suggesting a temporary tissue-specific impact of ABZ. Our theory of synergy operating exclusively at the level of the germline was initially corroborated by prior observations that reduced dose exposures of minocycline and rifampicin could lead to enhanced endobacterial depletions in female but not male worms, enumerated from whole worms by PCR (Turner et al., 2017). However, in our spatial FISH microscopy studies reported here, we could resolve significant synergism in both uterine and hypodermal populations of female *B. malayi* with AWZ1066S + ABZ combinations, and we could also discern that AWZ1066S + ABZ could mediate a long-term synergistic depletion of the hypodermal population in male *B. pahangi* (Figure 5). Thus, we confirm ABZ-mediated synergistic hypodermal *Wolbachia* depletion is also demonstrable, which may depend on exposure level, exposure time-frame, drug physiochemical properties aiding penetration and inherent kill-kinetic of the anti-*Wolbachia* agent being combined.

In prior work, we first defined a synergy between registered antibiotics (minocycline or rifampicin) and ABZ at the level of anti-*Wolbachia* efficacy, as well as mf production and accelerated curative efficacy (Turner et al., 2017). Clinically, it has also been demonstrated that ABZ-doxycycline combinations can reduce the dose time frame (from 4 to 3 weeks) for effective *Wolbachia* clearance and embryostatic activity in onchocerciasis (Klarmann-Schulz et al., 2017). Our data herein demonstrates that synergy is also operable when combined with a novel azaquinazoline anti-*Wolbachia* class of drug, and thus benzimidazoles may be a universal synergist that can be applied with new bespoke anti-*Wolbachia* compounds in development (Clare et al., 2019; Johnston et al., 2021) or repurposed antibiotics to lower doses and reduce total exposure periods in line with challenging 7-day dosing requirements for the treatment of LF and onchocerciasis. Beyond human medicine, combinations of azaquinazoline candidates or other rapid-acting novel anti-*Wolbachia* agents with registered benzimidazole drugs may provide new therapeutic options for curing veterinary/zoonotic infections such as *B. malayi* and *D. immitis* infections of cats and dogs.

Data availability statement

The original contributions presented in the study are included in the article/Supplementary material, further inquiries can be directed to the corresponding author.

Ethics statement

The animal study was approved by *B. malayi* infection procedures in mice and gerbils were approved by the Animal Welfare and Ethics Review Boards (AWERB) of Liverpool School of Tropical Medicine and University of Liverpool and undertaken in accordance with UK home office licencing approval. *B. pahangi* infection procedures in gerbils were approved by the University of California, San Francisco Institutional Animal Care and Use Committee (IACUC) (approvals: AN109629-03 and AN173847-02) and adhered to the guidelines set forth in the NIH guide for the care and use of laboratory animals and the USDA animal care policies. *L. sigmodontis* study procedures were performed according to the European union animal welfare guidelines and the state office for nature, environment and consumer protection, Cologne, Germany (AZ 84-02.04.2015.A507). The study was conducted in accordance with the local legislation and institutional requirements.

Author contributions

SH: Formal analysis, Investigation, Methodology, Visualisation, Writing—original draft, Writing—review & editing. AM: Formal analysis, Investigation, Methodology, Writing—review & editing. NP: Formal analysis, Investigation, Methodology, Writing—review & editing. AS: Formal analysis, Investigation, Methodology, Writing—review & editing. CB: Formal analysis, Investigation, Methodology, Writing—review & editing. EG: Formal analysis, Investigation, Methodology, Writing—review & editing. IV: Formal analysis, Investigation, Methodology, Writing—review & editing. MK: Formal analysis, Investigation, Methodology, Writing—review & editing. AE: Formal analysis, Investigation, Methodology, Writing—review & editing. SL: Formal analysis, Investigation, Methodology, Writing—review & editing. DV: Formal analysis, Investigation, Methodology, Visualisation, Writing—review & editing. NT: Formal analysis, Investigation, Methodology, Writing—review & editing. AH: Conceptualisation, Formal analysis, Funding acquisition, Supervision, Writing—review & editing. MH: Conceptualisation, Formal analysis, Funding acquisition, Supervision, Writing—review & editing. JS: Conceptualisation, Formal analysis, Funding acquisition, Supervision, Writing—review & editing. GA: Formal analysis, Investigation, Methodology, Writing—review & editing. FG: Conceptualisation, Funding acquisition, Resources, Supervision, Writing—review & editing. JD: Methodology, Writing—review & editing. DH: Conceptualisation, Formal analysis, Funding acquisition, Investigation, Methodology, Supervision, Writing—review & editing. PO'N: Conceptualisation, Funding acquisition, Supervision, Writing—review & editing. SW: Conceptualisation, Funding acquisition, Supervision, Writing—review & editing. MT: Conceptualisation, Funding acquisition, Supervision, Writing—review & editing. JT: Conceptualisation, Formal analysis, Funding acquisition, Methodology, Supervision, Visualisation, Writing—original draft, Writing—review & editing.

Funding

The author(s) declare financial support was received for the research, authorship, and/or publication of this

article. This work was supported by the MRC DPFS award MR/R025401/1, Confidence in Concept Tropical Infectious Disease Consortium award MC_PC_19045, a Bill and Melinda Gates Foundation (BMGF) award (OPP1119043), a Global Health Innovative Technology (G-HIT) Fund grant (RFP-2019), and a Wellcome Trust Institutional Translational Partnership Award (2195760/Z/19/Z, internal award reference - iTPA2212) to JT, MT, FG, SW, PO'N, and DH. Further support was provided by a Bill & Melinda Gates Foundation Grant (OPP1017584) awarded to SL and JS and (OPP1134310) to AH and MH. AH and MH were also funded under Germany's Excellence Strategy—EXC2151-390873048. AH and MH are members of the German Center for Infection Research (DZIF). MH received funding from the German Center for Infection Research (TTU 09.701).

Acknowledgments

The authors would like to thank Dr. Brenda Beerntsen, University of Missouri-Columbia, for supplying the *Brugia pahangi* L3 and K. C. Lim, Chris Franklin, and Mona Luo, UC San Francisco, for their assistance on the animal study.

Conflict of interest

FG was employed by Eisai Co., Ltd., Tokyo, Japan.

The remaining authors declare the research was conducted in the absence of any commercial or financial relationships that could be construed as a potential conflict of interest.

The author(s) declared that they were an editorial board member of Frontiers, at the time of submission. This had no impact on the peer review process and the final decision.

Publisher's note

Supplementary material

The Supplementary Material for this article can be found online at: https://www.frontiersin.org/articles/10.3389/fmicb.2024.1346068/full#supplementary-material

References

Aljayyoussi, G., Tyrer, H. E., Ford, L., Sjoberg, H., Pionnier, N., Waterhouse, D., et al. (2017). Short-course, high-dose rifampicin achieves *Wolbachia* depletion predictive of curative outcomes in preclinical models of lymphatic filariasis and onchocerciasis. *Sci. Rep.* 7:210. doi: 10.1038/s41598-017-00322-5

Awadzi, K., Hero, M., Opoku, O., Buttner, D. W., and Gilles, H. M. (1991). The chemotherapy of onchocerciasis. XV. Studies with albendazole. *Trop. Med. Parasitol.* 42, 356–360.

Bach, T., Galbiati, S., Kennedy, J. K., Deye, G., Nomicos, E. Y. H., Codd, E. E., et al. (2020). Pharmacokinetics, safety, and tolerability of oxfendazole in healthy adults in an open-label phase 1 multiple ascending dose and food effect study. *Antimicrob. Agents Chemother.* 64, e01018-20. doi: 10.1128/AAC.01018-20

Bakowski, M. A., Shiroodi, R. K., Liu, R., Olejniczak, J., Yang, B., Gagaring, K., et al. (2019). Discovery of short-course anti*wolbachia*l quinazolines for elimination of filarial worm infections. *Sci. Transl. Med.* 11:aav3523. doi: 10.1126/scitranslmed.aav3523

Cardenas, M. Q., Oliveira-Menezes, A., and Lanfredi, R. M. (2010). Effects of albendazole on Litomosoides chagasfilhoi (Nematoda: Filarioidea) females *in vivo*. *Parasitol. Res.* 107, 817–826. doi: 10.1007/s00436-010-1934-7

Ceballos, L., Krolewiecki, A., Juarez, M., Moreno, L., Schaer, F., Alvarez, L. I., et al. (2018). Assessment of serum pharmacokinetics and urinary excretion of albendazole and its metabolites in human volunteers. *PLoS Negl. Trop. Dis.* 12:e0005945. doi: 10.1371/journal.pntd.0005945

Chai, J. Y., Jung, B. K., and Hong, S. J. (2021). Albendazole and mebendazole as anti-parasitic and anti-cancer agents: an update. *Kor. J. Parasitol.* 59, 189–225. doi: 10.3347/kjp.2021.59.3.189

Chevignon, G., Foray, V., Perez-Jimenez, M. M., Libro, S., Chung, M., Foster, J. M., et al. (2021). Dual RNAseq analyses at soma and germline levels reveal evolutionary innovations in the elephantiasis-agent Brugia malayi, and adaptation of its *Wolbachia* endosymbionts. *PLoS Negl. Trop. Dis.* 15:e0008935. doi: 10.1371/journal.pntd.0008935

Cho, K. O., Kim, G. W., and Lee, O. K. (2011). *Wolbachia* bacteria reside in host Golgi-related vesicles whose position is regulated by polarity proteins. *PLoS ONE* 6:e22703. doi: 10.1371/journal.pone.0022703

Clare, R. H., Bardelle, C., Harper, P., Hong, W. D., Borjesson, U., Johnston, K. L., et al. (2019). Industrial scale high-throughput screening delivers multiple fast acting macrofilaricides. *Nat. Commun.* 10:11. doi: 10.1038/s41467-018-07826-2

Clare, R. H., Cook, D. A., Johnston, K. L., Ford, L., Ward, S. A., Taylor, M. J., et al. (2015). Development and validation of a high-throughput anti-*Wolbachia* whole-cell screen: a route to macrofilaricidal drugs against onchocerciasis and lymphatic filariasis. *J. Biomol. Screen.* 20, 64–69. doi: 10.1177/1087057114551518

Cole, N. B., Sciaky, N., Marotta, A., Song, J., and Lippincott-Schwartz, J. (1996). Golgi dispersal during microtubule disruption: regeneration of Golgi stacks at peripheral endoplasmic reticulum exit sites. *Mol. Biol. Cell.* 7, 631–650. doi: 10.1091/mbc.7.4.631

Crump, A. (2017). Ivermectin: enigmatic multifaceted 'wonder' drug continues to surprise and exceed expectations. *J. Antibiot.* 70, 495–505. doi: 10.1038/ja.2017.11

Debrah, A. Y., Mand, S., Specht, S., Marfo-Debrekyei, Y., Batsa, L., Pfarr, K., et al. (2006). Doxycycline reduces plasma VEGF-C/sVEGFR-3 and improves pathology in lymphatic filariasis. *PLoS Pathog.* 2:e92. doi: 10.1371/journal.ppat.0020092

Dodson, B. L., Hughes, G. L., Paul, O., Matacchiero, A. C., Kramer, L. D., Rasgon, J. L., et al. (2014). *Wolbachia* enhances West Nile virus (WNV) infection in the mosquito Culex tarsalis. *PLoS Negl. Trop. Dis.* 8:e2965. doi: 10.1371/journal.pntd.0002965

Eberhard, M. L. (1986). Longevity of microfilariae following removal of the adult worms. *Trop. Med. Parasitol.* 37, 361–363.

Ehrens, A., Hoerauf, A., and Hubner, M. P. (2022). Current perspective of new anti-*Wolbachia*l and direct-acting macrofilaricidal drugs as treatment strategies for human filariasis. *GMS Infect. Dis.* 10:Doc02. doi: 10.3205/id000079

Foray, V., Perez-Jimenez, M. M., Fattouh, N., and Landmann, F. (2018). *Wolbachia* control stem cell behavior and stimulate germline proliferation in filarial nematodes. *Dev. Cell.* 45, 198–211.e3. doi: 10.1016/j.devcel.2018.03.017

Foster, J., Ganatra, M., Kamal, I., Ware, J., Makarova, K., Ivanova, N., et al. (2005). The *Wolbachia* genome of *Brugia malayi*: endosymbiont evolution within a human pathogenic nematode. *PLoS Biol.* 3:e121. doi: 10.1371/journal.pbio.0030121

Gardon, J., Gardon-Wendel, N., Demanga, N., Kamgno, J., Chippaux, J. P., Boussinesq, M., et al. (1997). Serious reactions after mass treatment of onchocerciasis with ivermectin in an area endemic for *Loa loa* infection. *Lancet* 350, 18–22. doi: 10.1016/S0140-6736(96)11094-1

Gill, A. C., Darby, A. C., and Makepeace, B. L. (2014). Iron necessity: the secret of *Wolbachia*'s success? *PLoS Negl. Trop. Dis.* 8:e3224. doi: 10.1371/journal.pntd.0003224

Gokbulut, C., Bilgili, A., Hanedan, B., and McKellar, Q. A. (2007). Comparative plasma disposition of fenbendazole, oxfendazole and albendazole in dogs. *Vet. Parasitol.* 148, 279–287. doi: 10.1016/j.vetpar.2007.06.028

Gonzalez, A. E., Codd, E. E., Horton, J., Garcia, H. H., and Gilman, R. H. (2019). Oxfendazole: a promising agent for the treatment and control of helminth infections in humans. *Exp. Rev. Anti Infect. Ther*. 17, 51–56. doi: 10.1080/14787210.2018.1555241

Gunderson, E. L., Vogel, I., Chappell, L., Bulman, C. A., Lim, K. C., Luo, M., et al. (2020). The endosymbiont *Wolbachia* rebounds following antibiotic treatment. *PLoS Pathog*. 16:e1008623. doi: 10.1371/journal.ppat.1008623

Gyapong, J. O., Owusu, I. O., da-Costa Vroom, F. B., Mensah, E. O., and Gyapong, M. (2018). Elimination of lymphatic filariasis: current perspectives on mass drug administration. *Res. Rep. Trop. Med*. 9, 25–33. doi: 10.2147/RRTM.S125204

Haarbrink, M., Abadi, G. K., Buurman, W. A., Dentener, M. A., Terhell, A. J., Yazdanbakhsh, M., et al. (2000). Strong association of interleukin-6 and lipopolysaccharide-binding protein with severity of adverse reactions after diethylcarbamazine treatment of microfilaremic patients. *J. Infect. Dis*. 182, 564–569. doi: 10.1086/315735

Halliday, A., Guimaraes, A. F., Tyrer, H. E., Metuge, H. M., Patrick, C. N., Arnaud, K. O., et al. (2014). A murine macrofilaricide pre-clinical screening model for onchocerciasis and lymphatic filariasis. *Parasit. Vect*. 7:472. doi: 10.1186/s13071-014-0472-z

Hansen, R. D., Trees, A. J., Bah, G. S., Hetzel, U., Martin, C., Bain, O., et al. (2011). A worm's best friend: recruitment of neutrophils by *Wolbachia* confounds eosinophil degranulation against the filarial nematode Onchocerca ochengi. *Proc. Biol. Sci*. 278, 2293–2302. doi: 10.1098/rspb.2010.2367

Hoerauf, A., Specht, S., Buttner, M., Pfarr, K., Mand, S., Fimmers, R., et al. (2008). *Wolbachia* endobacteria depletion by doxycycline as antifilarial therapy has macrofilaricidal activity in onchocerciasis: a randomized placebo-controlled study. *Med. Microbiol. Immunol*. 197, 295–311. doi: 10.1007/s00430-007-0062-1

Hong, W. D., Benayoud, F., Nixon, G. L., Ford, L., Johnston, K. L., Clare, R. H., et al. (2019). AWZ1066S, a highly specific anti-*Wolbachia* drug candidate for a short-course treatment of filariasis. *Proc. Natl. Acad. Sci. U. S. A*. 116, 1414–1419. doi: 10.1073/pnas.1816585116

Hubner, M. P., Ehrens, A., Koschel, M., Dubben, B., Lenz, F., Frohberger, S. J., et al. (2019a). Macrofilaricidal efficacy of single and repeated oral and subcutaneous doses of flubendazole in *Litomosoides sigmodontis* infected jirds. *PLoS Negl. Trop. Dis*. 13:e0006320. doi: 10.1371/journal.pntd.0006320

Hubner, M. P., Gunderson, E., Vogel, I., Bulman, C. A., Lim, K. C., Koschel, M., et al. (2020a). Short-course quinazoline drug treatments are effective in the *Litomosoides sigmodontis* and *Brugia pahangi* jird models. *Int. J. Parasitol. Drugs Drug Resist*. 12, 18–27. doi: 10.1016/j.ijpddr.2019.12.001

Hubner, M. P., Koschel, M., Struever, D., Nikolov, V., Frohberger, S. J., Ehrens, A., et al. (2019b). *In vivo* kinetics of *Wolbachia* depletion by ABBV-4083 in *L. sigmodontis* adult worms and microfilariae. *PLoS Negl. Trop. Dis*. 13:e0007636. doi: 10.1371/journal.pntd.0007636

Hubner, M. P., Martin, C., Specht, S., Koschel, M., Dubben, B., Frohberger, S. J., et al. (2020b). Oxfendazole mediates macrofilaricidal efficacy against the filarial nematode *Litomosoides sigmodontis in vivo* and inhibits *Onchocerca* spec. motility *in vitro*. *PLoS Negl. Trop. Dis*. 14:e0008427. doi: 10.1371/journal.pntd.0008427

Johnston, K. L., Cook, D. A. N., Berry, N. G., David Hong, W., Clare, R. H., Goddard, M., et al. (2017). Identification and prioritization of novel anti-*Wolbachia* chemotypes from screening a 10,000-compound diversity library. *Sci. Adv*. 3:eaao1551. doi: 10.1126/sciadv.aao1551

Johnston, K. L., Hong, W. D., Turner, J. D., O'Neill, P. M., Ward, S. A., Taylor, M. J., et al. (2021). Anti-*Wolbachia* drugs for filariasis. *Trends Parasitol*. 37, 1068–1081. doi: 10.1016/j.pt.2021.06.004

Keiser, J., and Utzinger, J. (2010). The drugs we have and the drugs we need against major helminth infections. *Adv. Parasitol*. 73, 197–230. doi: 10.1016/S0065-308X(10)73008-6

Klarmann-Schulz, U., Specht, S., Debrah, A. Y., Batsa, L., Ayisi-Boateng, N. K., Osei-Mensah, J., et al. (2017). Comparison of doxycycline, minocycline, doxycycline plus albendazole and albendazole alone in their efficacy against onchocerciasis in a randomized, open-label, pilot trial. *PLoS Negl. Trop. Dis*. 11:e0005156. doi: 10.1371/journal.pntd.0005156

Klion, A. D., Massougbodji, A., Horton, J., Ekoue, S., Lanmasso, T., Ahouissou, N. L., et al. (1993). Albendazole in human loiasis: results of a double-blind, placebo-controlled trial. *J. Infect. Dis*. 168, 202–206. doi: 10.1093/infdis/168.1.202

Kramer, L., Crosara, S., Gnudi, G., Genchi, M., Mangia, C., Viglietti, A., et al. (2018). *Wolbachia*, doxycycline and macrocyclic lactones: new prospects in the treatment of canine heartworm disease. *Vet. Parasitol*. 254, 95–97. doi: 10.1016/j.vetpar.2018.03.005

Lacey, E. (1990). Mode of action of benzimidazoles. *Parasitol. Today* 6, 112–115. doi: 10.1016/0169-4758(90)90227-U

Lakwo, T., Oguttu, D., Ukety, T., Post, R., and Bakajika, D. (2020). Onchocerciasis elimination: progress and challenges. *Res. Rep. Trop. Med*. 11, 81–95. doi: 10.2147/RRTM.S224364

Landmann, F., Bain, O., Martin, C., Uni, S., Taylor, M. J., Sullivan, W., et al. (2012). Both asymmetric mitotic segregation and cell-to-cell invasion are required for stable germline transmission of *Wolbachia* in filarial nematodes. *Biol. Open* 1, 536–547. doi: 10.1242/bio.2012737

Landmann, F., Foster, J. M., Slatko, B., and Sullivan, W. (2010). Asymmetric *Wolbachia* segregation during early Brugia malayi embryogenesis determines its distribution in adult host tissues. *PLoS Negl. Trop. Dis*. 4:e758. doi: 10.1371/journal.pntd.0000758

Landmann, F., Voronin, D., Sullivan, W., and Taylor, M. J. (2011). Anti-filarial activity of antibiotic therapy is due to extensive apoptosis after *Wolbachia* depletion from filarial nematodes. *PLoS Pathog*. 7, e1002351. doi: 10.1371/journal.ppat.1002351

Lanusse, C. E., Gascon, L. H., and Prichard, R. K. (1995). Comparative plasma disposition kinetics of albendazole, fenbendazole, oxfendazole and their metabolites in adult sheep. *J. Vet. Pharmacol. Ther*. 18, 196–203. doi: 10.1111/j.1365-2885.1995.tb00578.x

Li, Z., and Carlow, C. K. (2012). Characterization of transcription factors that regulate the type IV secretion system and riboflavin biosynthesis in *Wolbachia* of *Brugia malayi*. *PLoS ONE* 7, e51597. doi: 10.1371/journal.pone.0051597

Local Burden of Disease Neglected Tropical Diseases Control (2020). The global distribution of lymphatic filariasis, 2000-18: a geospatial analysis. *Lancet Glob. Health* 8, e1186–e1194. doi: 10.1016/S2214-109X(20)30286-2

Mallawarachchi, C. H., Chandrasena, T., Withanage, G. P., Premarathna, R., Mallawarachchi, S., Gunawardane, N. Y., et al. (2021). Molecular characterization of a reemergent *Brugia malayi* parasite in Sri Lanka, suggestive of a novel strain. *Biomed. Res. Int*. 2021:9926101. doi: 10.1155/2021/9926101

Marriott, A. E., Dagley, J. L., Hegde, S., Steven, A., Fricks, C., DiCosty, U., et al. (2023). Dirofilariasis mouse models for heartworm preclinical research. *Front. Microbiol*. 14:1208301. doi: 10.3389/fmicb.2023.1208301

Modi, A., Vaishnav, K. G., Kothiya, K., and Alexander, N. (2021). Lymphatic filariasis elimination endgame in an urban Indian setting: the roles of surveillance and residual microfilaremia after mass drug administration. *Infect. Dis. Poverty* 10:73. doi: 10.1186/s40249-021-00856-x

Nochot, H., Loimek, S., Priyavoravong, P., Wongkamchai, S., and Sarasombath, P. T. (2019). Therapeutic efficacy of doxycycline in domestic cats naturally infected with *Brugia malayi* in field condition. *Exp. Parasitol*. 200, 73–78. doi: 10.1016/j.exppara.2019.03.016

Oxberry, M. E., Gear, T. G., and Prichard, R. K. (2001). Assessment of benzimidazole binding to individual recombinant tubulin isotypes from *Haemonchus contortus*. *Parasitology* 122 (Pt 6), 683–687. doi: 10.1017/S0031182001007788

Quek, S., Cook, D. A. N., Wu, Y., Marriott, A. E., Steven, A., Johnston, K. L., et al. (2022). *Wolbachia* depletion blocks transmission of lymphatic filariasis by preventing chitinase-dependent parasite exsheathment. *Proc. Natl. Acad. Sci. U. S. A*. 119:e2120003119. doi: 10.1073/pnas.2120003119

Risch, F., Scheunemann, J. F., Reichwald, J. J., Lenz, B., Ehrens, A., Gal, J., et al. (2023). The efficacy of the benzimidazoles oxfendazole and flubendazole against *Litomosoides sigmodontis* is dependent on the adaptive and innate immune system. *Front. Microbiol*. 14:1213143. doi: 10.3389/fmicb.2023.1213143

Schiefer, A., Hubner, M. P., Krome, A., Lammer, C., Ehrens, A., Aden, T., et al. (2020). Corallopyronin A for short-course anti-*wolbachial*, macrofilaricidal treatment of filarial infections. *PLoS Negl. Trop. Dis*. 14:e0008930. doi: 10.1371/journal.pntd.0008930

Schiefer, A., Schmitz, A., Schaberle, T. F., Specht, S., Lammer, C., Johnston, K. L., et al. (2012). Corallopyronin A specifically targets and depletes essential obligate *Wolbachia* endobacteria from filarial nematodes *in vivo*. *J. Infect. Dis*. 206, 249–257. doi: 10.1093/infdis/jis341

Sharma, R., Al Jayoussi, G., Tyrer, H. E., Gamble, J., Hayward, L., Guimaraes, A. F., et al. (2016). Minocycline as a re-purposed anti-*Wolbachia* macrofilaricide: superiority compared with doxycycline regimens in a murine infection model of human lymphatic filariasis. *Sci. Rep*. 6:23458. doi: 10.1038/srep23458

Shenoy, R. K., Suma, T. K., John, A., Arun, S. R., Kumaraswami, V., Fleckenstein, L. L., et al. (2002). The pharmacokinetics, safety and tolerability of the co-administration of diethylcarbamazine and albendazole. *Ann. Trop. Med. Parasitol*. 96, 603–614. doi: 10.1179/00034980212500 1663

Simon, F., Gonzalez-Miguel, J., Diosdado, A., Gomez, P. J., Morchon, R., Kartashev, V., et al. (2017). The complexity of zoonotic filariasis episystem and its consequences: a multidisciplinary view. *Biomed. Res. Int*. 2017:6436130. doi: 10.1155/2017/6436130

Slatko, B. E., Taylor, M. J., and Foster, J. M. (2010). The *Wolbachia* endosymbiont as an anti-filarial nematode target. *Symbiosis* 51, 55–65. doi: 10.1007/s13199-010-0067-1

Sodahlon, Y. K., Dorkenoo, A. M., Morgah, K., Nabiliou, K., Agbo, K., Miller, R., et al. (2013). A success story: Togo is moving toward becoming the first sub-Saharan African nation to eliminate lymphatic filariasis through mass drug administration and countrywide morbidity alleviation. *PLoS Negl. Trop. Dis*. 7:e2080. doi: 10.1371/journal.pntd.0002080

Specht, S., and Kaminsky, R. (2022). "Product profiles for new drugs against human and animal filariasis," in *Human and Animal Filariasis: Landscape, Challenges, and Control*, eds R. Kaminsky, and T. G. Geary (Weinheim: Wiley-VCH), 45–66.

Tamarozzi, F., Turner, J. D., Pionnier, N., Midgley, A., Guimaraes, A. F., Johnston, K. L., et al. (2016). *Wolbachia* endosymbionts induce neutrophil extracellular trap formation in human onchocerciasis. *Sci. Rep*. 6:35559. doi: 10.1038/srep35559

Taylor, M., Mediannikov, O., Raoult, D., and Greub, G. (2012). Endosymbiotic bacteria associated with nematodes, ticks and amoebae. *FEMS Immunol. Med. Microbiol.* 64, 21–31. doi: 10.1111/j.1574-695X.2011.00916.x

Taylor, M. J., Bilo, K., Cross, H. F., Archer, J. P., and Underwood, A. P. (1999). 16S rDNA phylogeny and ultrastructural characterization of *Wolbachia* intracellular bacteria of the filarial nematodes *Brugia malayi*, *B. pahangi*, and *Wuchereria bancrofti*. *Exp. Parasitol.* 91, 356–361. doi: 10.1006/expr.1998.4383

Taylor, M. J., and Hoerauf, A. (1999). *Wolbachia* bacteria of filarial nematodes. *Parasitol. Today* 15, 437–442. doi: 10.1016/S0169-4758(99)01533-1

Taylor, M. J., Makunde, W. H., McGarry, H. F., Turner, J. D., Mand, S., Hoerauf, A., et al. (2005). Macrofilaricidal activity after doxycycline treatment of *Wuchereria bancrofti*: a double-blind, randomised placebo-controlled trial. *Lancet* 365, 2116–2121. doi: 10.1016/S0140-6736(05)66591-9

Turner, J. D., Mand, S., Debrah, A. Y., Muehlfeld, J., Pfarr, K., McGarry, H. F., et al. (2006). A randomized, double-blind clinical trial of a 3-week course of doxycycline plus albendazole and ivermectin for the treatment of Wuchereria bancrofti infection. *Clin. Infect. Dis.* 42, 1081–1089. doi: 10.1086/501351

Turner, J. D., Marriott, A. E., Hong, D., Ward, P. O. N., Taylor, S. A., Novel, M. J., et al. (2020). anti-*Wolbachia* drugs, a new approach in the treatment and prevention of veterinary filariasis? *Vet. Parasitol.* 279:109057. doi: 10.1016/j.vetpar.2020.109057

Turner, J. D., Sharma, R., Al Jayoussi, G., Tyrer, H. E., Gamble, J., Hayward, L., et al. (2017). Albendazole and antibiotics synergize to deliver short-course anti-*Wolbachia* curative treatments in preclinical models of filariasis. *Proc. Natl. Acad. Sci. U. S. A.* 114, E9712–E21. doi: 10.1073/pnas.1710845114

Turner, J. D., Tendongfor, N., Esum, M., Johnston, K. L., Langley, R. S., Ford, L., et al. (2010). Macrofilaricidal activity after doxycycline only treatment of *Onchocerca volvulus* in an area of *Loa loa* co-endemicity: a randomized controlled trial. *PLoS Negl. Trop. Dis.* 4:e660. doi: 10.1371/journal.pntd.0000660

Voronin, D., Cook, D. A., Steven, A., and Taylor, M. J. (2012). Autophagy regulates *Wolbachia* populations across diverse symbiotic associations. *Proc. Natl. Acad. Sci. U. S. A.* 109, E1638–E1646. doi: 10.1073/pnas.1203519109

Walker, T., Quek, S., Jeffries, C. L., Bandibabone, J., Dhokiya, V., Bamou, R., et al. (2021). Stable high-density and maternally inherited *Wolbachia* infections in *Anopheles moucheti* and *Anopheles demeilloni* mosquitoes. *Curr. Biol.* 31, 2310–20.e5. doi: 10.1016/j.cub.2021.03.056

White, P. M., Pietri, J. E., Debec, A., Russell, S., Patel, B., Sullivan, W., et al. (2017). Mechanisms of horizontal cell-to-cell transfer of *Wolbachia* spp. in *Drosophila melanogaster*. *Appl. Environ. Microbiol.* 83, e03425-16. doi: 10.1128/AEM.03425-16

WHO (2019). *Global Programme to Eliminate Lymphatic Filariasis: Progress Report.* Geneva: World Health Organization.

WHO (2020). *Ending the Neglect to Attain the Sustainable Development Goals: A Road Map for Neglected Tropical Diseases 2021–2030*. Geneva: World Health Organization, Licence: CC BY-NC-SA 30 IGO.

WHO (2022). Elimination of human onchocerciasis: progress report, 2021. *Wkly. Epidemiol. Rec.* 97, 591–598.

Wu, B., Novelli, J., Foster, J., Vaisvila, R., Conway, L., Ingram, J., et al. (2009). The heme biosynthetic pathway of the obligate *Wolbachia* endosymbiont of *Brugia malayi* as a potential anti-filarial drug target. *PLoS Negl. Trop. Dis.* 3:e475. doi: 10.1371/journal.pntd.0000475

Wu, J., de Heus, C., Liu, Q., Bouchet, B. P., Noordstra, I., Jiang, K., et al. (2016). Molecular pathway of microtubule organization at the golgi apparatus. *Dev. Cell.* 39, 44–60. doi: 10.1016/j.devcel.2016.08.009

Zhang, X., Zhao, J., Gao, X., Pei, D., and Gao, C. (2017). Anthelmintic drug albendazole arrests human gastric cancer cells at the mitotic phase and induces apoptosis. *Exp. Ther. Med.* 13, 595–603. doi: 10.3892/etm.2016.3992

Ziewer, S., Hubner, M. P., Dubben, B., Hoffmann, W. H., Bain, O., Martin, C., et al. (2012). Immunization with *L. sigmodontis* microfilariae reduces peripheral microfilaraemia after challenge infection by inhibition of filarial embryogenesis. *PLoS Negl. Trop. Dis.* 6:e1558. doi: 10.1371/journal.pntd.0001558

frontiers | Frontiers in Microbiology

TYPE Original Research
PUBLISHED 06 February 2024
DOI 10.3389/fmicb.2024.1304401

OPEN ACCESS

EDITED BY
Didier Bouchon,
University of Poitiers, France

REVIEWED BY
Sarah Bordenstein,
The Pennsylvania State University (PSU), United States
Mathieu Sicard,
Université Montpellier 2, France

*CORRESPONDENCE
Hiroki Ando
✉ ando.hiroki.m4@f.gifu-u.ac.jp

RECEIVED 29 September 2023
ACCEPTED 12 January 2024
PUBLISHED 06 February 2024

CITATION
Pramono AK, Hidayanti AK, Tagami Y and Ando H (2024) Bacterial community and genome analysis of cytoplasmic incompatibility-inducing *Wolbachia* in American serpentine leafminer, *Liriomyza trifolii*.
Front. Microbiol. 15:1304401.
doi: 10.3389/fmicb.2024.1304401

Bacterial community and genome analysis of cytoplasmic incompatibility-inducing *Wolbachia* in American serpentine leafminer, *Liriomyza trifolii*

Ajeng K. Pramono[1], Ardhiani K. Hidayanti[2,3], Yohsuke Tagami[4] and Hiroki Ando[1,5]*

[1]Laboratory of Phage Biologics, Graduate School of Medicine, Gifu University, Gifu, Japan, [2]School of Biological Environment, The United Graduate School of Agricultural Science, Gifu University, Gifu, Japan, [3]School of Life Sciences and Technology, Institut Teknologi Bandung (ITB), Bandung, Indonesia, [4]Laboratory of Applied Entomology, Faculty of Agriculture, Shizuoka University, Shizuoka, Japan, [5]Center for One Medicine Innovative Translational Research (COMIT), Gifu University, Gifu, Japan

Liriomyza trifolii, an agricultural pest, is occasionally infected by *Wolbachia*. A *Wolbachia* strain present in *Liriomyza trifolii* is associated with cytoplasmic incompatibility (CI) effects, leading to the death of embryos resulting from incompatible crosses between antibiotic-treated or naturally *Wolbachia*-free strain females and *Wolbachia*-infected males. In this study, high-throughput sequencing of hypervariable rRNA genes was employed to characterize the bacterial community in *Wolbachia*-infected *L. trifolii* without antibiotic treatment. The analysis revealed that *Wolbachia* dominates the bacterial community in *L. trifolii*, with minor presence of *Acinetobacter*, *Pseudomonas*, and *Limnobacter*. To elucidate the genetic basis of the CI phenotype, metagenomic sequencing was also conducted to assemble the genome of the *Wolbachia* strain. The draft-genome of the *Wolbachia* strain *w*Ltri was 1.35 Mbp with 34% GC content and contained 1,487 predicted genes. Notably, within the *w*Ltri genome, there are three distinct types of cytoplasmic incompatibility factor (*cif*) genes: Type I, Type III, and Type V *cifA;B*. These genes are likely responsible for inducing the strong cytoplasmic incompatibility observed in *L. trifolii*.

KEYWORDS

***Wolbachia*, *Liriomyza trifolii*, CIF, cytoplasmic incompatibility factor, phage WO**

1 Introduction

Wolbachia are intracellular symbiont bacteria (Phylum: Pseudomonadota, Class: Alphaproteobacteria) found in various terrestrial arthropods and nematodes. About 20–66% of both animal taxa are infected by *Wolbachia* (Hilgenboecker et al., 2008; Gomes et al., 2022). The maternally inherited endosymbiotic *Wolbachia* can manipulate the reproduction of their hosts, using several mechanisms, including cytoplasmic incompatibility (CI), male killing, parthenogenesis, and feminization (Correa and Ballard,

2016). CI causes offspring death when an infected male mates with an uninfected female, while the mating of infected females with the same *Wolbachia* strain produces viable offspring either way (Yen and Barr, 1973; Shropshire et al., 2020). The degree of CI induction can vary significantly between different *Wolbachia* strains, with some strains causing no reproductive manipulation or CI, such as *w*Au in *Drosophila simulans* and *w*Mau in *D. mauritiana*, while others can cause weak CI as in *w*Yak of *D. yakuba*, or complete CI that affects all embryos in *w*Pip of *Culex pipiens* complex species (Laven, 1967; Hoffmann et al., 1996; Meany et al., 2019; Beckmann et al., 2021). CI induced by *Wolbachia* can be a useful technique for controlling insect populations. The use of CI-*Wolbachia* has been effective in controlling the mosquito vector-borne diseases population, reducing the transmission of disease in the health sector, and can be considered in the agricultural sector through incompatible insect technique (IIT) to control insect pests (Laven, 1967; Hidayanti et al., 2022).

Cytoplasmic incompatibility is a two-sided phenomenon, involving a form of "modification" in sperm and a corresponding "rescue" mechanism occurring within the eggs (Hurst, 1991). The CI effect in *Wolbachia* is mainly attributed to a class of genes known as cytoplasmic incompatibility factor (*cif*) genes, which forms the molecular basis of CI (Beckmann et al., 2017, 2019; Le Page et al., 2017). The *cif* genes, *cifA* and *cifB*, usually occur in an operon, but unpaired and fragmented *cif* genes are also found in some strains (Martinez et al., 2021). In addition, multiple pair's amplification and diversification of *cif* genes have been reported to contribute to CI diversity in *w*Pip from the mosquito *Culex pipiens* (Bonneau et al., 2018a,b). The *cif* gene products are categorized into Type I–V based on their protein domain similarity (Lindsey et al., 2018; Martinez et al., 2021). Cif proteins with deubiquitinase activity are sometimes referred to as Cid, while Cif proteins with DNase activity are sometimes referred to as Cin (Beckmann et al., 2017). The affinity between CidA–CidB, and CinA–CinB, have been confirmed (Beckmann et al., 2017; Chen et al., 2019). Furthermore, co-expressing *cifA*/*cifB* transgenes in *Drosophila melanogaster* also mimics the embryonic defects, a feature of CI that results in embryo death (Le Page et al., 2017; Chen et al., 2019), while transgenic expression of *cifB* alone induces CI in *Anopheles gambiae* (Adams et al., 2021). Besides, transgenic expression of a single *cifA* gene can rescue defects in egg-hatch rates and growth defects induced by CifB in yeast (Shropshire et al., 2018; Adams et al., 2021).

Liriomyza trifolii (Diptera: Agromyzidae), a polyphagous leafminer insect is a significant invasive pest of agricultural vegetable and ornamental plants (Kang et al., 2009; Zhang et al., 2017). *Wolbachia* infection is prevalent in *Liriomyza* species in Japan and the Indo-Pacific region, with 30–80% of the population being positive for the infection (Xu et al., 2021). *Wolbachia*-infected *L. trifolii* exhibited strong CI phenotype, resulting in very few eggs hatching from the crossing between infected males with naturally *Wolbachia*-free or antibiotic-treated females (Tagami et al., 2006a). The *Wolbachia* strain found in *L. trifolii* has been assigned to Supergroup B, in contrast to the majority of *Wolbachia* strains identified in Diptera, which belong to Supergroup A (Scholz et al., 2020). Unfortunately, the low completeness of the initial genome has hindered the identification of *cif* genes and other important gene markers, such as the *Wolbachia* surface protein gene *wsp* (Braig and Zhou, 1998) and the five housekeeping genes (*gatB*, *coxA*, *hcpA*, *ftsZ*, and *fbpA*) used in the *Wolbachia* multilocus strain typing (MLST) methodology (Baldo et al., 2006).

In this study, we surveyed the bacterial community in *L. trifolii* to explore its microbiome, and sequenced, assembled, and analyzed the genome of its *Wolbachia* to investigate the putative genetic basis of the strong CI effect on its insect host. We additionally provided a detailed description of the newly assembled genome through phylogenetic and comparative genome analysis. This involved the identification of *cif* genes and the prophage region to further characterize the strains in comparison to other closely related *Wolbachia* genomes.

2 Materials and methods

2.1 Insect rearing, sample collection, and DNA extraction

Liriomyza trifolii were provided by Applied Entomology Laboratory, Faculty of Agriculture, Shizuoka University. The flies were isolated in Hamamatsu, Shizuoka, Japan in 1991, and maintained on the leaves of kidney bean plants in a 34 cm (width) × 35 cm (length) × 34 cm (height) cage with light–dark regime (16:8) at 23°C (Tagami et al., 2006a; Hidayanti et al., 2022).

Total genomic DNA was extracted from *L. trifolii* using Qiagen DNeasy Blood and Tissue Kit, following the manufacturer's instruction (Qiagen, Hilden, Germany), with slight modifications. Adults insects ($n = 30–50$) were crushed in 50 µL ATL buffer with a motorized pestle (Power Masher II; Nippi, Tokyo, Japan); 130 µL of ATL buffer, and 20 µL proteinase-K (20 mg/mL) were added to the homogenate and incubated in a 56°C dry bath incubator (Major Science, Taiwan) for 2–3 h; 200 µL of buffer AL and 200 µL of 99.5% ethanol were added following incubation at 56°C; to maximize DNA yield, the DNA was eluted in 50 µL of buffer AE. DNA yield and purity were verified with a Nanodrop 1000 spectrophotometer (Thermo Fisher Scientific, Waltham, MA, United States). The extracted DNA was aliquoted for sequencing and cloning of 16S rRNA gene and the *Wolbachia* surface protein (*wsp*) gene, and metagenomic library construction for next-generation sequencing (NGS).

2.2 High-throughput and sanger amplicon sequencing

2.2.1 High-throughput 16S rRNA amplicon sequencing

The total DNA from *L. trifolii* was amplified using primers to target the hypervariable V3–V4 regions of the 16S rRNA gene, which includes Illumina adaptor sequences (in triplicate), using these primers: Forward Primer (5′-TCGTCGGCAGCGTCAGATGTGTATAAGAGACAGCCTACGGGNGGCWGCAG-3′) and Reverse Primer (5′-GTCTCGTGGGCTCGGAGATGTGTATAAGAGACAGGACTACHVGGGTATCTAATCC-3′). The amplicon classification was also confirmed with the near-full-length 16S rRNA gene clones sequencing, amplified using primers 27F-mix (5'-AGRGTTTGATYMTGGCTCAG-3′) and 1492R (5'-GGHTACCTTGTTACGACTT-3′) (Hongoh et al., 2007).

The high-throughput amplicon sequencing analysis was performed using the QIIME2-2021.4 platform (Bolyen et al., 2019). Adapter and primer sequences were removed using the following options: --p-front-f CCTACGGGNGGCWGCAG --p-front-r GACTACHVGGGTATCTAATCC. The reads were trimmed, denoised, paired, and dereplicated with the built-in dada2 algorithm (Callahan et al., 2016). The amplicon sequence variants (ASVs) were taxonomically classified using the q2-feature-classifier, which had been trained for V3–V4 regions of 16S rRNA (Bokulich et al., 2018).

2.2.2 *Wolbachia* amplicon sequencing

The presence of *Wolbachia* was detected using *Wolbachia* surface protein (*wsp*) gene primers (wsp81F: 5'-TGGTCCAATA AGTGATGAAGAAAC-3′ and wsp691R: 5'-AAAAATTAAA CGCTACTCCA-3′) (Braig and Zhou, 1998). The *wsp* amplicons were cloned and sequenced to confirm whether the *Wolbachia* strain in the current sample was identical to the previously detected *Wolbachia* associated with strong cytoplasmic incompatibility in *L. trifolii* (Tagami et al., 2006a). The alignment of the *wsp* sequences was also performed with the previously sequenced *wsp* from the *Wolbachia* survey in Japan and Indo-pacific region (Xu et al., 2021).

2.3 *Wolbachia* shotgun sequencing, genome assembly and bioinformatics analyses

The *Wolbachia* draft genome was obtained by preparing a shotgun metagenome library with an Illumina DNA prep kit, which was then sequenced using the MiSeq Reagent Kit v2 and v3. The metagenomic sequencing reads were filtered based on base quality (Q20) and length (>50 bp). Next, the filtered reads were paired and assembled using MEGAHIT (Li et al., 2015) and only contigs longer than 1,000 bp were retained for further analysis. A custom database of *Wolbachia* genomes was utilized to identify *Wolbachia* contigs based on nucleotide similarity using blastn (Altschul et al., 1990). Scaffolds were created using Codon Code Aligner (v. 9.0.1, Codon Code Corporation) and Mauve Contig Mover (MCM) (Rissman et al., 2009), followed by manual inspection and visualization in Geneious Prime 2022.1.1. Genome completeness was determined by the presence of single-copy genes of Proteobacteria (proteobacteria_odb10) using BUSCO 5.2.2 (Manni et al., 2021). Average Nucleotide Identity (ANI) was calculated using FastANI tool (Jain et al., 2018). Annotation of coding regions, RNA genes, and other genomic features was done through the RAST-tk pipeline (Aziz et al., 2008). The prophage region was automatically detected using PHASTER (Arndt et al., 2016) and subsequently refined manually based on similarity searches against prophage region in the *Wolbachia* of *Ischnura elegans*, the largest *Wolbachia* genome assembled from the Darwin Tree of Life biodiversity genomics project (Vancaester and Blaxter, 2023). Identification of Gene Transfer Agents (GTAs) was also performed through sequence similarity searched against RcGTA in *Rhodobacter capsulatus* and a putative GTA in *w*Mel. The sequence similarity searches were conducted using the BLAST suite against the nr database (https://www.ncbi.nlm.nih.gov/), a custom *Wolbachia* genome database (Supplementary Table S1; Pascar and Chandler, 2018), or specific genes as otherwise mentioned.

2.4 Phylogenomic analysis

A phylogenetic tree of *Wolbachia* was created from concatenated 40 single copy orthologous genes, aligned with MAFFT 7.402 (Katoh and Standley, 2013). The trees were generated with 1,000 bootstraps using Maximum Likelihood method and JTT matrix-based model in MEGAX (Kumar et al., 2018). For the CI genes phylogeny, the *cifA* and *cifB* homologs were identified and constructed as previously described (Martinez et al., 2021). To clarify the origin of the large terminase (*terL*) in *w*Meg, an unrooted *terL* phylogenetic tree was constructed using identified homologs from reference genomes. These homologs were retrieved through nucleotide similarity searches, using the following sequences as queries: the *terL* sequences downstream of the Type III *cifA;B* in *w*Meg (CP021120.1), and the previously identified *terL* sequences in WORiC (CP001391.1; sr1WO), WORiA (CP001391.1; sr2WO), WOMelB (AE017196.1; sr3WO), as well as WOFol2 (CP015510.2; sr4WO).

2.5 Protein domain prediction

The *cif* genes were translated into amino acid then queried individually using HHpred (https://toolkit.tuebingen.mpg.de/hhpred/; Söding et al., 2005) with defaults parameters against the following databases: PDB_mmCIF70_24_Oct, SCOPe70_2.08, Pfam-A_v36, SMART_v6.0, PHROGs_v4, TIGRFAMs_v15.0, and COG_KOG_v1.0.

3 Results

3.1 Microbiome of *Liriomyza trifolii*

The *Wolbachia* strains in the current study was identical to the strain associated with strong CI in *L. trifolii* in the previous study (Tagami et al., 2006a). The identity was confirmed using a partial *wsp* gene which was amplified, cloned, and Sanger-sequenced ($n = 24$). The *wsp* gene is commonly used as an indicator of *Wolbachia* infection in insects. There are at least three *wsp* alleles have been identified in *Wolbachia* in *L. trifolii*, *w*LtriA, *w*LsatA, and *w*LsatD. All clones from the sample were identical to the *w*LsatD-type allele, hereafter referred to as *w*Ltri.

High-throughput sequencing of the hypervariable region of the 16S rRNA gene was also performed to gain insights into the bacterial community present in *L. trifolii* without the antibiotic treatment. A total of 533,982 V3–V4 amplicon reads were quality-filtered, de-noised, and merged into 176,493 functional sequences. These sequences were de-replicated into 161 ASVs, in which 28 ASVs accounted for more than 80% of the total reads. Each of these ASVs were classified into taxa; in contrast to operational taxonomic unit (OTU)-based clustering, different ASVs could be classified into the same taxon.

The bacterial community in *L. trifolii* was largely dominated by Pseudomonadota (synonym, Proteobacteria) members, accounting for 96% of the total ASVs, with a minor presence of Actinobacteria,

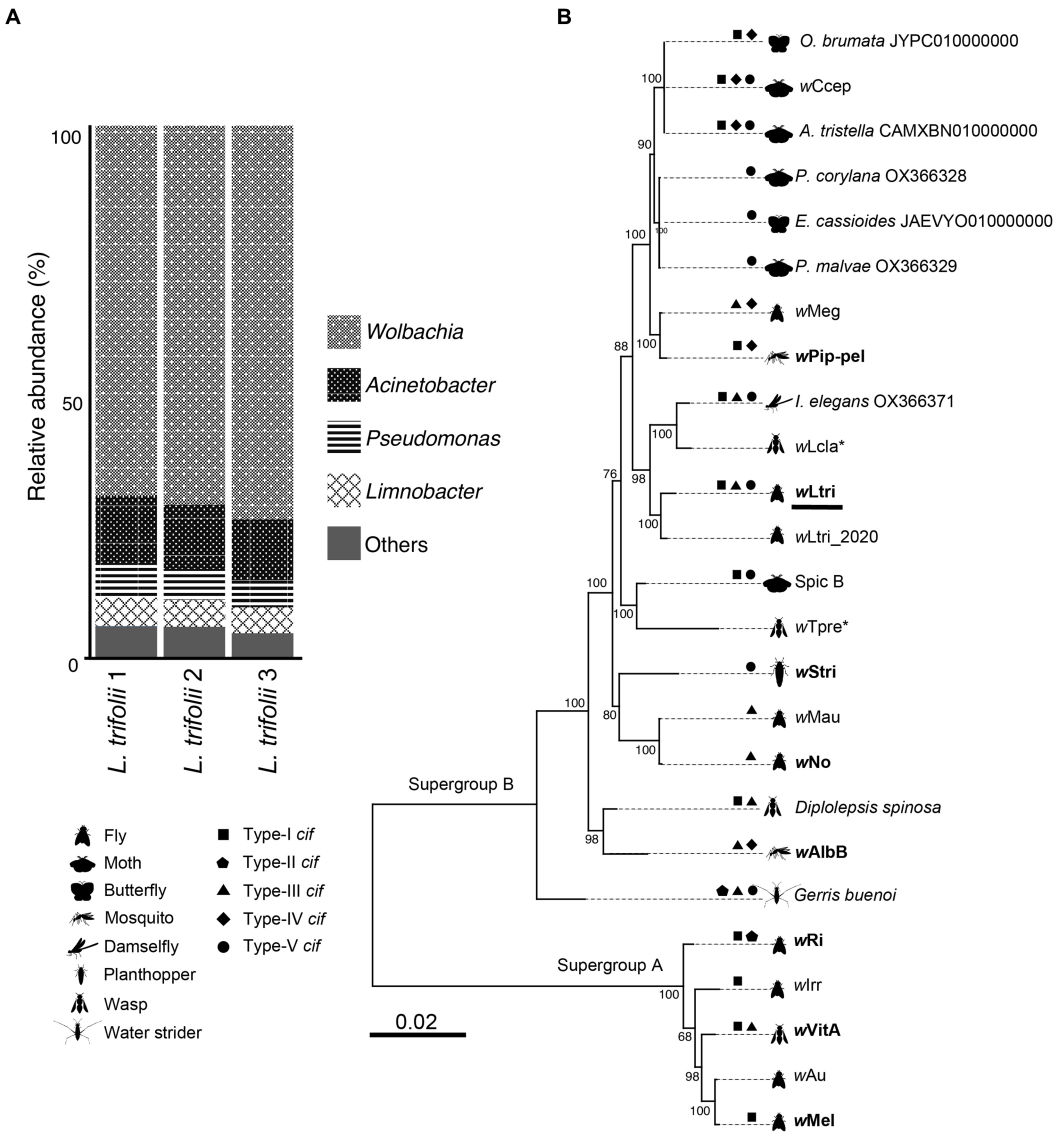

FIGURE 1
(A) Prokaryote composition in *Liriomyza trifolii* at the genus level in triplicate. **(B)** Phylogeny of 25 strains of *Wolbachia*. The tree was constructed based on nucleotide sequences of 40 single-copy orthologous genes. The *Wolbachia* strains that are reported to cause CI are presented in boldface, while the parthenogenesis-inducing strains are marked with an asterisk. The *w*Ltri from this current study is underlined.

Bacteroidota, and Firmicutes. Among the identified genera, *Wolbachia* was the most abundant taxon (Figure 1A), with the representative ASV exhibiting an identical sequence to that of CI-inducing *Wolbachia* strains which infect a rice moth, *Corcyra cephalonica* (wCcep), as well as *Wolbachia* strains derived from other moths, such as *Agriphila tristella*, *Erebia cassioides*, and *Operophtera brumata*. The cloning and sequencing of an almost full-length 16S gene confirmed this finding. Likewise, ASVs from *Acinetobacter* and *Pseudomonas* were detected and matched to the 16S rRNA sequences recovered from metagenomic assembled contigs. These genera have been consistently reported to co-exist with *Wolbachia* in both wild and laboratory-reared mosquitoes, including *Culex* and *Aedes* (Beier et al., 1996; Pidiyar et al., 2002, 2004; Lindh et al., 2005; Zouache et al., 2009a,b; Minard et al., 2013; Schrieke et al., 2021; Rau et al., 2022).

3.2 The genome of *w*Ltri, the *Wolbachia* strain in *Liriomyza trifolii*

A total of 15,421,862,646 high-quality bases were assembled using MEGAHIT into contigs. A contig covering the entire *L. trifolii* mitochondrial sequence was identified, and it exhibited 99.1% nucleotide similarity to *L. trifolii* GU327644. A total of 435 contigs originating from *Wolbachia* were identified using BLASTN searches against a custom database (Supplementary Table S1) and further validated via manual inspection. The *w*Ltri contigs were reordered using Mauve Contig Mover (MCM) to create a draft genome (Figure 2). The genome comparison analysis also included a previously sequenced *L. trifolii*, which contains 443 contigs of *Wolbachia*, assembled using a similar short-read sequencing technology and genome assembler, referred to as *w*Ltri_2020 hereinafter (Vicoso and

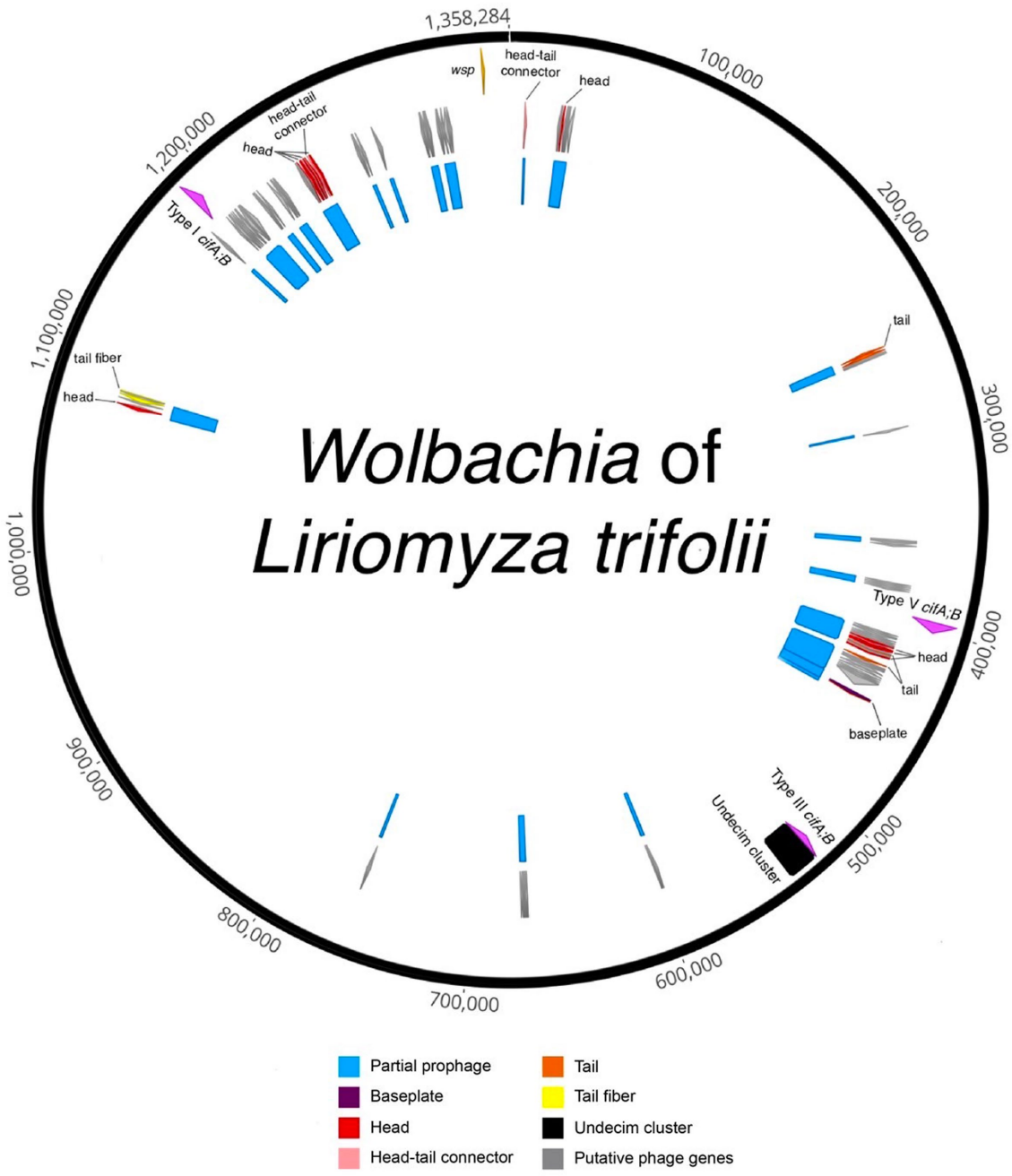

FIGURE 2
Circularized draft genome annotation of the *Wolbachia* of *Liriomyza trifolii*. Partial prophage regions are indicated in blue, representing regions with incomplete prophage regions predicted by PHASTER and/or parts of prophage WO in the *Wolbachia* of *Ischnura elegans*. Structural genes are denoted in red (head), pink (head-tail connector), purple (baseplate), orange (tail), and yellow (tail fiber), while gray signifies putative phage genes, encompassing genes found in phages but with unknown functions. The Undecim cluster is depicted in black. The *cif* genes are highlighted in fuchsia, and the *Wolbachia* surface protein (*wsp*) gene is represented in light orange.

Bachtrog, 2015; Scholz et al., 2020). The Average Nucleotide Identity score between *w*Ltri draft genome and wLtri_NCBI was 98.1%. The completeness of the *w*Ltri genome based on BUSCO (proteobacteria_odb10) was 80.3%, which represents a typical value for complete *Wolbachia* genomes (Sinha et al., 2019), while the completeness of *w*Ltri_2020 was only 31.6%. The assembly size of *w*Ltri was 1,358,284 bp, which was longer than that of *w*Ltri_2020 (879,722 bp). The genome of *w*Ltri contained 1,487 coding sequences (CDSs), along with 5S, 23S, and 16S rRNA, and 34 tRNA genes, while *w*Ltri_2020 had fewer CDSs ($n = 1,206$) and an incomplete set of rRNA genes (Table 1).

Based on the maximum likelihood phylogenetic tree of single-copy genes, the newly sequenced *w*Ltri belongs to the Supergroup B and it clustered with *w*Ltri_2020, which infects the same host species, *L. trifolii* (Figure 1B). *Wolbachia* of Supergroup B is commonly found in Lepidopteran hosts, with only a few instances identified in Dipteran

TABLE 1 Comparison of assembly status and genome characteristics among *Wolbachia* strains.

Wolbachia strain	Insect host	Total length (bp)	Contigs	GC%	CDSs	tRNAs	rRNAs	BUSCO score*	Reference
*w*Ltri	*Liriomyza trifolii*	1,358,284	435	34.0	1,487	34	3	80.3	This study
*w*Ltri_2020	*Liriomyza trifolii*	817,747	443	33.5	1,206	18	1	31.6	Scholz et al. (2020)
*w*Meg	*Chrysomya megacephala*	1,376,868	1	34.0	1,242	34	3	85.5	Unpublished (2019)
*w*Pip-pel	*Culex quinquefasciatus*	1,482,455	1	34.2	1,373	34	3	86.3	Klasson et al. (2008)
*w*VitA	*Nasonia vitripennis*	1,325,529	142	32.3	1,325	34	3	83.9	Newton et al. (2016)
*w*Di	*Diaphorina citri* Kuwayama	1,528,786	1	34.1	1,394	34	3	80.6	Neupane et al. (2022)

*Based on proteobacteria_odb10. CDS, Coding sequence.

hosts (Meany et al., 2019; Scholz et al., 2020; Vancaester and Blaxter, 2023). Within the Supergroup B clade, *w*Ltri formed a monophyletic group with *Wolbachia* strains that infect other arthropods, such as damselflies (*I. elegans*) and wasps (*Leptopilina clavipes*), rather than with strains infecting flies, such as *w*Mau of *Drosophila mauritiana* and *w*No of *Drosophila simulans* (Figure 1B). To further investigate the relationship between *w*Ltri and *Wolbachia* strains in wasps, a phylogenetic tree was constructed using *wsp* genes (Supplementary Figure S1). The analysis included a parasitoid wasp, *Hemiptarsenus varicornis*, found near the initial *L. trifolii* sampling location (Tagami et al., 2006b). Although the *wsp* gene undergoes rapid evolution, the *wsp* gene derived from *w*Ltri consistently clustered with the *wsp* amplified from wasps *H. varicornis* and *Trichogramma pretiosum* (wTpre).

3.3 Prophage regions in *w*Ltri

In the case of *w*Ltri, prophage sequences were analyzed using the PHASTER tool and sequence homology to previously known prophage WO to identify incomplete prophage regions with a combined size of 98.9 Kb (Figure 2). Prophage regions were also identified using nucleotide similarity searches against *Wovirus*, which includes WO phages, from a newly proposed family, Symbioviridae. The *Wovirus* was further subclassified into four groups, sr1WO, sr2WO, sr3WO, and sr4WO, based on gene synteny in the phage core module and serine-recombinase nucleotide identity (Bordenstein and Bordenstein, 2022). A BLASTN search using these recombinases revealed fragments in wLtri with 84 and 88% nucleotide similarity to sr1WO and sr3WO, respectively.

Our analysis also revealed the presence of a set of 11 conserved genes, known as Undecim Cluster, in *w*Ltri genome. This cluster is part of the EAM of Phage WO, which is commonly found in sr3WO and is occasionally present in sr4WO and WO-like islands (Bordenstein and Bordenstein, 2022). The EAM in *w*Ltri displays a module synteny similar to that of the WO-like island in WOAlbB3, *w*No, WOMau2, and *w*VitA, where it also comprises *cifA* and *cifB* genes (Bordenstein and Bordenstein, 2022). Notably, the *cif* genes found in these WO-like islands belong to Type III *cifA;B*, unlike in sr3WO, which mostly includes Type I *cifA;B*.

Interestingly, in *w*Meg, downstream of Undecim cluster—Type III *cifA;B*, a large terminase gene (*terL*) was identified (Supplementary Figure S2A). The gene is commonly used as a prophage marker due to its high degree of conservation and ubiquity across phage genomes. To determine whether the *terL* was originated from a Phage WO carrying the Type III *cifA;B*, the intergenic region between the *cif* genes and *terL* was aligned with other *Wolbachia* which possessed same type of *cif* genes in the reference genomes, including *w*Ltri. The intergenic region (1,113 bp) displayed potential shared synteny (Supplementary Figure S2B), revealing distinct partitioning into two segments: a left portion (L; 554 bp) downstream of the Undecim cluster—*cif* genes, and a right portion (R; 559 bp) upstream of *terL*. While both segments were occasionally repeated in some of the reference genomes, they were never co-occurred, except in *w*Meg (Supplementary Figure S2C; Supplementary Tables S2, S3).

The L was found adjacent to *cif* genes and/or the Undecim Cluster in the genomes that possess it. In the *Wolbachia* of *I. elegans*, the L was identified in two locations: the first near a partial Undecim Cluster—*cif* genes, and the second near an incomplete Undecim Cluster without *cif* genes in a different location (Supplementary Table S2). In *w*Irr, the L was associated with IS256, while in the *Wolbachia* of *Erebia cassioides* and *Leptopilina clavipes*, *w*Lcla, it was associated with IS110 family transposase (Supplementary Table S2). Conversely, the R was found in more location within the genomes, often at breakpoints, and was associated with IS982, IS5, and IS630 (Supplementary Figure S3; Supplementary Table S3).

In the *Wolbachia* genome, a terminase gene may also have been derived from Gene Transfer Agents (GTAs). BLAST searches (TBLASTN, BLASTN) using the amino acid and nucleotide sequences of a terminase-like protein (RCAP_rcc01683) from RcGTA, a well-studied GTA in *Rhodobacter capsulatus*, as queries against the *Wolbachia* reference genomes and *w*Ltri, did not yield any significant matches. However, when a terminase from the putative GTA in *w*Mel (WD_1016; AE017196) was used as a query, it revealed matches within the reference genomes (Supplementary Table S4). Notably, these findings included the *terL* which was located downstream of the WO-like island in *w*Meg, revealing 82% nucleotide and 83% amino

acid similarities, respectively. In addition, a phylogenetic tree constructed using homologs of *terL* from *w*Meg and prophage WO revealed that they belong to two distinct clades, which further divided into a sub-clade that separates Supergroup A from Supergroup B (Supplementary Figure S2C).

3.4 Cytoplasmic incompatibility genes

*w*Ltri has three phylogenetically distinct *cifA*–*cifB* gene pairs which belong to Type I, III, and V (Figure 3A). The *w*Ltri Type I showed moderate to low amino acid similarity to the CifA (63–68%) and CifB (48–51%) of the experimentally validated CI-inducing *Wolbachia* strains *w*Mel and *w*Pip, respectively. The Type V also showed moderate and low amino acid similarity of 57 and 20% to the CifA–CifB proteins of *w*Stri, respectively. On the other hand, *w*Ltri Type III showed high amino acid similarity (98%) to CifA and CifB of CI-inducing *w*No. Furthermore, the *w*Ltri Type III was the only gene pair located within the EAM of WO-like islands, adjacent to an Undecim cluster.

In *w*Ltri CifA, four protein domains were identified (Figure 3B). The first two were the Ribon-helix–helix Protein (RHH domain) and Prefoldin, found in the Type I CifA of *w*Ltri. Despite a low probability of homology (probability 22–31%), these domains were also found in functional CifAs (CidA). However, the CifA of *w*Ltri lacks Serine/Threonine phosphatase 2A and DUF3243, which are present in *w*Pip and *w*Mel, respectively. Additionally, the Puf superfamily RNA-binding protein (Type III) was identified in both *w*Ltri and *w*No. Lastly, the DUF 5662 (Type V) was found in *w*Ltri but not in *w*Stri Type V CifA, which contains the Puf superfamily. In *w*Ltri CifB, three protein domains were identified (Figure 3B). The PD-(D/E)XK nuclease superfamily was consistently found in all *w*Ltri CifB with a high probability (>96%). Furthermore, the Type I exhibited the presence of a deubiquitinase domain DUB (probability 96%), while the Type V contained an OTU-like cysteine protease (probability 99%).

4 Discussion

This study represents the first survey of the bacterial community of the American Serpentine Leafminer fly, *L. trifolii*, in Japan. Using 16S rRNA high-throughput amplicon sequencing, it revealed *Wolbachia* as the most abundant bacterium in *L. trifolii*. The genome of the *Wolbachia* strain, *w*Ltri, had never been assembled with high completeness before. This *w*Ltri assembly represents the most complete genome sequence of a cytoplasmic-inducing *Wolbachia* of *L. trifolii*. Another available *Wolbachia* genome from *L. trifolii*, *w*Ltri_2020, is a binning of 443 contigs with only 31.6% BUSCO completeness (Vicoso and Bachtrog, 2015; Scholz et al., 2020). *w*Ltri_2020 was not included in some of the analyses in this study as it contains only partial genome information. We have also determined that *w*Ltri was the main endosymbiont of *L. trifolii*, using16S rRNA gene amplicon sequencing and metagenomic data.

Unlike the majority of *Wolbachia* strains found in Dipteran hosts, which belong to Supergroup A, *w*Ltri is classified under Supergroup B. The phylogeny of supergroup A and B have been found to be incongruent with those of their hosts, due to frequent horizontal transmission of *Wolbachia* strains across diverse host species (Raychoudhury et al., 2009; Wang et al., 2020). Insect parasitoids have been proposed as a means of facilitating this horizontal transmission of endosymbionts when infected and uninfected parasitoid wasps develop within the same host insect (Huigens et al., 2000, 2004; Ahmed et al., 2015). *Liriomyza trifolii* is also susceptible to parasitoid wasps, with approximately 24 species of leafminer parasitoids identified in Japan (Arakaki and Kinjo, 1998). Among these wasps, a *wsp* sequence from *H.* var*icornis*, found near the original sampling location of *L. trifolii*, formed a clade with that of *w*Ltri. However, due to the limited availability of *wsp* sequences from other parasitoids, it was the only sequence included in the analysis. This limitation is attributed to the lower prevalence of *Wolbachia* infection in leafminer parasitoids compared to *Liriomyza*, in which among the surveyed 15 leafminer parasitoid species, only *H.* var*icornis* was infected with *Wolbachia* (Tagami et al., 2006b). Besides, the migration of leafminers *Liriomyza* from another country (Abe, 2017) may potentially introduce endosymbiont transfer between the established *Liriomyza* and the invasive species. Therefore, additional research is needed to comprehensively understand the potential role of *Liriomyza* parasitoids and the impact of invasive *Liriomyza* on the horizontal transmission of *Wolbachia* strains.

Wolbachia is well known for inducing CI in many insects, including *L. trifolii* (Tagami et al., 2006a). Recent studies have shown that the proteins which are responsible for CI, CifA and CifB, can be classified into Types I–V (Martinez et al., 2021). In the genome of *w*Ltri, three sets of *cifA;B* genes—Types I, III, and V—were identified. Notably, the genes encoding Type I and Type V CifB in *w*Ltri were shorter, exhibiting low protein similarity to functional Cif in *w*Pip, *w*Mel, *w*No, and *w*Stri. Typically, *cifB* often accumulates more mutations before *cifA*, rendering the gene non-functional before being eliminated from the genome (Martinez et al., 2021). However, in *w*Ltri, although the genes were shorter, the predicted gene products containing domains commonly found in Type I CifB, such as PD-(D/E)XK nuclease superfamily and DUB, remained recognizable. The Type V CifB in *w*Ltri was also considerably shorter than that of *w*Stri, a *Wolbachia* strain in *Laodelphax striatellus*. This difference is not unexpected due to the greater diversity of protein domains in Type V CifB compared to other types, encompassing domains such as the C-terminal domain of Latrotoxin, those involved in protein–protein interactions (tetratricopeptide and ankyrin repeats), and a protease domain (OTU-like cysteine protease) (Martinez et al., 2021). However, in *w*Ltri, only the latter and a PD-(D/E)XK were present. In contrast, the Type III *cifA;B* of *w*Ltri appeared highly conserved, sharing adjacent gene synteny with CI-inducing *Wolbachia* strains like *w*No, which exclusively contains Type III *cifA;B* genes.

The amplification-diversification of functional *cif* genes and the cumulative presence of these genes have been associated with cytoplasmic incompatibility (CI) strength (Le Page et al., 2017; Bonneau et al., 2018b). In the genome of *Wolbachia* in *Culex pipiens* *w*Pip, variations and copy numbers of *cif* genes (*cidA*, *cidB*) are identified and the expression of these multiple *cid* gene variants in males may account for differences in CI cellular phenotypes (Bonneau et al., 2018a,b). Furthermore, *w*Mel, a *Wolbachia* strain with only one copy of these genes exhibits a weak CI phenotype, whereas strains with two or three copies of the genes, such as *w*Ri and *w*Ha, showed a strong CI effects (Le Page et al., 2017). The facts that *w*Ltri causes strong CI in *L. trifolii* (Tagami et al., 2006a) and its genome harbored

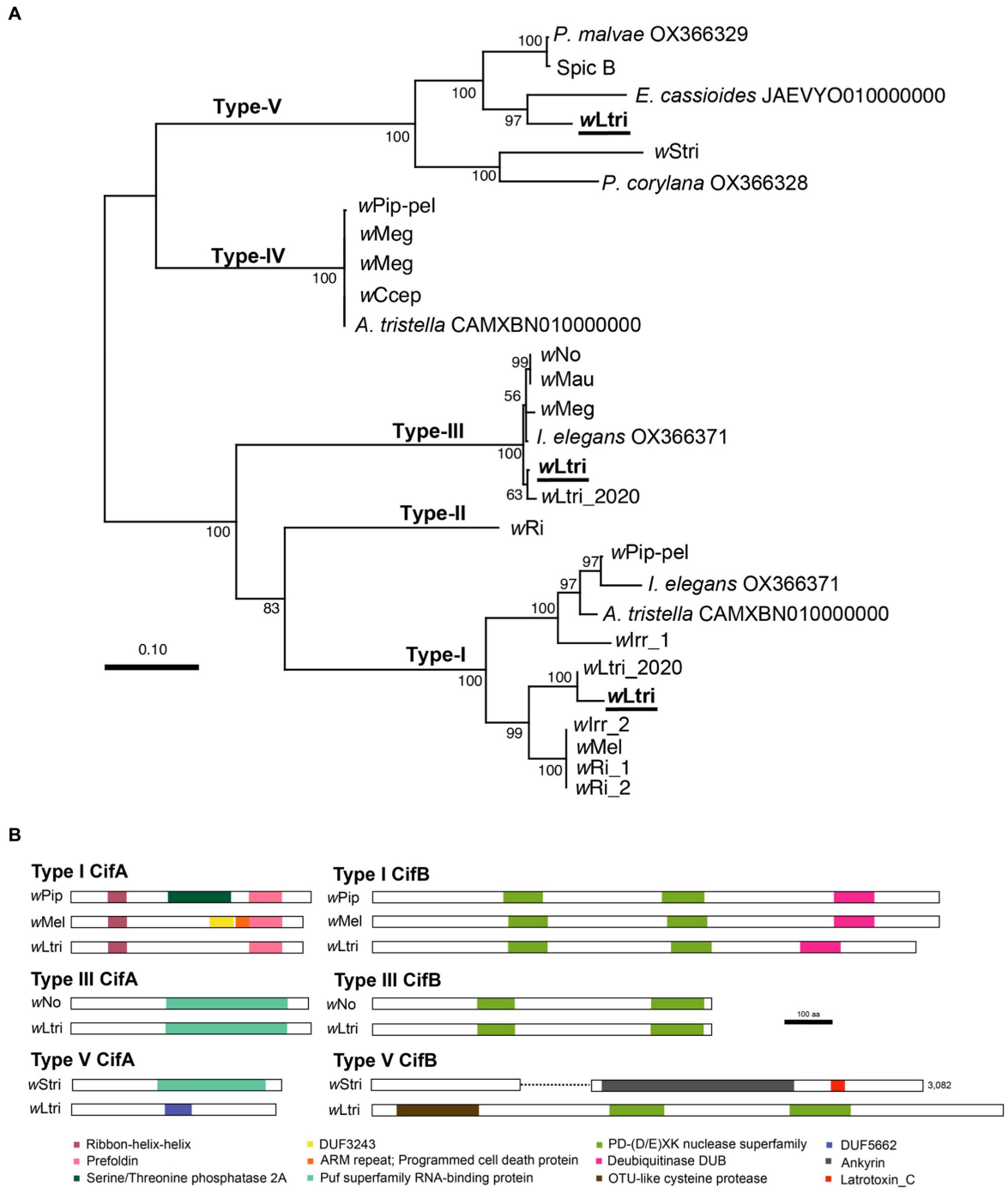

FIGURE 3
(A) Maximum likelihood tree of concatenated *cifA* and *cifB* nucleotide sequences. Partially sequenced *cif* homologs were excluded. Bootstrap values were estimated from 1,000 replicates. **(B)** Representative structures of Cif proteins with predicted domains. The *w*Stri type V CifB has a length of 3,082 amino acids. To accommodate presentation constraints, it was shortened without eliminating any identifiable domains.

three sets of *cifA–cifB* genes, might supported this correlation. Ultimately it is necessary to confirm that these *cif* gene products interact with each other through performing an *in vitro* pull-down study, which demonstrates the specific binding of functional cognate protein pairs (CifA and CifB). Afterward, to determine the individual gene activity, transgenic expression of a single *cif* gene can be conducted, allowing for the assessment of whether a gene alone can induce CI or whether other *cif* genes or factors are necessary for the CI to occur (Beckmann et al., 2017; Le Page et al., 2017; Adams et al., 2021; Horard et al., 2022).

The *w*Ltri Type III *cifA;B* are located adjacent to a conserved set of 11 genes, collectively known as the Undecim Cluster, which constitutes a eukaryotic association module (EAM) within phage WO. Phage WO, a bacteriophage that infects intracellular *Wolbachia*, faces the challenge of 2-fold barriers: the eukaryotic cell membrane and the intracellular bacterial cell membranes. Consequently, it

frequently carries an EAM containing genes that exhibit eukaryotic-like functions and origins, which have the potential to influence host-*Wolbachia* interactions (Bordenstein and Bordenstein, 2022). After infection, the phage WO that integrates its genetic material into the *Wolbachia* genome refer as putative prophage WO. Although it is thought that no complete prophage WO has been identified in *w*Ltri, the genes surrounding the *cif*s exhibit module synteny akin to that of the WO-like island found in *w*No, *w*Mau, and *w*AlbB. These WO-like Islands are considered defective prophages, likely stemming from an ancestral prophage WO genome, which has since undergone domestication by the bacterial host or is undergoing degradation and elimination from the chromosome (Bordenstein and Bordenstein, 2022).

The WO-like island of *w*Ltri also exhibits module synteny with that of *w*Meg, a *Wolbachia* strain found in the blowfly *Chrysomya megacephala*, which is commonly associated with carrion and other decaying materials in human environments (Badenhorst and Villet, 2018). This similarity extends to the intergenic region between their Type III *cifA;B* and *terL*. However, the *terL* was distinct from the known *terL* genes of phage WO. Within *Wolbachia* genomes, *terL* is not exclusively associated with prophage WO but is also linked to Gene Transfer Agents (GTAs), which are virus-like structures responsible for packaging and transferring prokaryotic DNA between donor and recipient prokaryotic cells (Lang and Beatty, 2000; Lang et al., 2017; Bordenstein and Bordenstein, 2022). Although the *terL* in *w*Meg exhibited low nucleotide sequence similarity to a terminase-like gene in RcGTA of *R. capsulatus*, it demonstrated higher similarities to a terminase found in a putative GTA from *w*Mel (AE017196). This observation suggests that the *terL* in *w*Meg might be a component of GTAs within *Wolbachia* genomes. Furthermore, the *terL* homologs formed a distinct clade, separating them from other *terL* genes within the prophage WO region, suggests that the *terL* genes in *w*Meg and prophage WO have different evolutionary origins. This clade further branched into sub-clades that distinguished Supergroups A and B, consistent with previous finding that *terL* genes within putative GTAs in *Wolbachia* genomes can effectively differentiate between these Supergroups (Bordenstein and Bordenstein, 2022).

Regarding the potential synteny of the intergenic region between the *cif* genes and *terL* in the *Wolbachia* genomes, it appears to involve at least two "genomic scars" resulting from ancestral transposition events associated with IS256, IS110, IS982, IS5, and IS630. In *w*Meg, an ancient phage WO carrying Type III *cifA;B* might had integrated its genome into or near a GTA sequence. Subsequently, the GTA and the prophage WO may have deteriorated over time, or transposition events could have joined the breakpoints near the *cif* genes and *terL*, ultimately leading to the genetic remnants that are presently observed. Given that the intergenic sequences were frequently located in the vicinity of breakpoints in *w*Ltri and other *Wolbachia* genomes, the observed similarities in this region are likely a consequence of the latter phenomenon.

In summary, our bacterial community survey indicates that *Wolbachia* is the main endosymbiont in *L. trifolii*, alongside minor occurrences of *Acinetobacter*, *Pseudomonas*, and *Limnobacter*. The *Wolbachia* strain in *L. trifolii*, *w*Ltri, possesses three distinct types of cytoplasmic incompatibility factor (*cif*) genes: Type I, Type III, and Type V *cifA;B*. The diversification and cumulative presence of these genes may contribute to the strong CI effects observed in *L. trifolii*.

Data availability statement

The data presented in the study are deposited in the DNA Data Bank of Japan (DDBJ) repository, accession number DRA017213 (https://ddbj.nig.ac.jp/resource/bioproject/PRJDB16160).

Ethics statement

The manuscript presents research on animals that do not require ethical approval for their study.

Author contributions

AP: Conceptualization, Data curation, Investigation, Validation, Writing – original draft, Writing – review & editing. AH: Conceptualization, Investigation, Writing – original draft, Writing – review & editing. YT: Funding acquisition, Project administration, Supervision, Writing – original draft, Writing – review & editing. HA: Funding acquisition, Project administration, Supervision, Writing – original draft, Writing – review & editing.

Funding

The author(s) declare financial support was received for the research, authorship, and/or publication of this article. This research was partly funded by a grant from the Japan Society for the Promotion of Science (JSPS) KAKENHI to HA (Grant Numbers: 20H03723, 15K21770) and YT (Grant Number: JP419K06069).

Conflict of interest

The authors declare that the research was conducted in the absence of any commercial or financial relationships that could be construed as a potential conflict of interest.

The author(s) declared that they were an editorial board member of Frontiers, at the time of submission. This had no impact on the peer review process and the final decision.

Publisher's note

Supplementary material

The Supplementary material for this article can be found online at: https://www.frontiersin.org/articles/10.3389/fmicb.2024.1304401/full#supplementary-material

References

Abe, Y. (2017). Invasion of Japan by exotic leafminers *Liriomyza* spp. (Diptera: Agromyzidae) and its consequences. *Appl. Entomol. Zool.* 52, 175–182. doi: 10.1007/s13355-017-0486-z

Adams, K. L., Abernathy, D. G., Willett, B. C., Selland, E. K., Itoe, M. A., and Catteruccia, F. (2021). *Wolbachia cifB* induces cytoplasmic incompatibility in the malaria mosquito vector. *Nat. Microbiol.* 6, 1575–1582. doi: 10.1038/s41564-021-00998-6

Ahmed, M. Z., Li, S. J., Xue, X., Yin, X. J., Ren, S. X., Jiggins, F. M., et al. (2015). The intracellular bacterium *Wolbachia* uses parasitoid wasps as phoretic vectors for efficient horizontal transmission. *PLoS Pathog.* 10:e1004672. doi: 10.1371/journal.ppat.1004672

Altschul, S. F., Gish, W., Miller, W., Myers, E. W., and Lipman, D. J. (1990). Basic local alignment search tool. *J. Mol. Biol.* 215, 403–410. doi: 10.1016/S0022-2836(05)80360-2

Arakaki, N., and Kinjo, K. (1998). Notes on the parasitoid fauna of the serpentine leafminer *Liriomyza trifolii* (burgess) (Diptera: Agromyzidae) in Okinawa, southern Japan. *Appl. Entomol. Zool.* 33, 577–581. doi: 10.1303/aez.33.577

Arndt, D., Grant, J. R., Marcu, A., Sajed, T., Pon, A., Liang, Y., et al. (2016). PHASTER: a better, faster version of the PHAST phage search tool. *Nucleic Acids Res.* 44, W16–W21. doi: 10.1093/nar/gkw387

Aziz, R. K., Bartels, D., Best, A. A., DeJongh, M., Disz, T., Edwards, R. A., et al. (2008). The RAST server: rapid annotations using subsystems technology. *BMC Genomics* 9:75. doi: 10.1186/1471-2164-9-75

Badenhorst, R., and Villet, M. H. (2018). The uses of *Chrysomya megacephala* (Fabricius, 1794) (Diptera: Calliphoridae) in forensic entomology. *Forens. Sci. Res.* 3, 2–15. doi: 10.1080/20961790.2018.1426136

Baldo, L., Dunning Hotopp, J. C., Jolley, K. A., Bordenstein, S. R., Biber, S. A., Choudhury, R. R., et al. (2006). Multilocus sequence typing system for the endosymbiont *Wolbachia pipientis*. *Appl. Environ. Microbiol.* 72, 7098–7110. doi: 10.1128/AEM.00731-06

Beckmann, J. F., Bonneau, M., Chen, H., Hochstrasser, M., Poinsot, D., Merçot, H., et al. (2019). The toxin–antidote model of cytoplasmic incompatibility: genetics and evolutionary implications. *Trends Genet.* 35, 175–185. doi: 10.1016/j.tig.2018.12.004

Beckmann, J. F., Ronau, J. A., and Hochstrasser, M. (2017). A *Wolbachia* deubiquitylating enzyme induces cytoplasmic incompatibility. *Nat. Microbiol.* 2:17007. doi: 10.1038/nmicrobiol.2017.7

Beckmann, J. F., Van Vaerenberghe, K., Akwa, D. E., and Cooper, B. S. (2021). A single mutation weakens symbiont-induced reproductive manipulation through reductions in deubiquitylation efficiency. *Proc. Natl. Acad. Sci.* 118:e2113271118. doi: 10.1073/pnas.2113271118

Beier, J. C., Pumpuni, C. B., Demaio, J., and Kent, M. (1996). The midgut bacterial Flora of wild *Aedes triseriatus*, *Culex pipiens*, and *Psorophora columbiae* mosquitoes. *Am. J. Trop. Med. Hyg.* 54, 219–223. doi: 10.4269/ajtmh.1996.54.219

Bokulich, N. A., Kaehler, B. D., Rideout, J. R., Dillon, M., Bolyen, E., Knight, R., et al. (2018). Optimizing taxonomic classification of marker-gene amplicon sequences with QIIME 2's q2-feature-classifier plugin. *Microbiome* 6:90. doi: 10.1186/s40168-018-0470-z

Bolyen, E., Rideout, J. R., Dillon, M. R., Bokulich, N. A., Abnet, C. C., Al-Ghalith, G. A., et al. (2019). Reproducible, interactive, scalable and extensible microbiome data science using QIIME 2. *Nat. Biotechnol.* 37, 852–857. doi: 10.1038/s41587-019-0209-9

Bonneau, M., Atyame, C., Beji, M., Justy, F., Cohen-Gonsaud, M., Sicard, M., et al. (2018a). *Culex pipiens* crossing type diversity is governed by an amplified and polymorphic operon of *Wolbachia*. *Nat. Commun.* 9:319. doi: 10.1038/s41467-017-02749-w

Bonneau, M., Landmann, F., Labbé, P., Justy, F., Weill, M., and Sicard, M. (2018b). The cellular phenotype of cytoplasmic incompatibility in *Culex pipiens* in the light of cidB diversity. *PLoS Pathog.* 14:e1007364. doi: 10.1371/journal.ppat.1007364

Bordenstein, S. R., and Bordenstein, S. R. (2022). Widespread phages of endosymbionts: phage WO genomics and the proposed taxonomic classification of Symbioviridae. *PLoS Genet.* 18:e1010227. doi: 10.1371/journal.pgen.1010227

Braig, H. R., and Zhou, W., Dobson, S.'L. & O'Neill, S. L. (1998). Cloning and characterization of a gene encoding the major surface protein of the bacterial endosymbiont *Wolbachia pipientis*. *J. Bacteriol.* 180:2373–2378. doi: 10.1128/JB

Callahan, B. J., McMurdie, P. J., Rosen, M. J., Han, A. W., Johnson, A. J. A., and Holmes, S. P. (2016). DADA2: high-resolution sample inference from Illumina amplicon data. *Nat. Methods* 13, 581–583. doi: 10.1038/nmeth.3869

Chen, H., Ronau, J. A., Beckmann, J. F., and Hochstrasser, M. (2019). A *Wolbachia* nuclease and its binding partner provide a distinct mechanism for cytoplasmic incompatibility. *Proc. Natl. Acad. Sci. U. S. A.* 116, 22314–22321. doi: 10.1073/pnas.1914571116

Correa, C. C., and Ballard, J. W. O. (2016). *Wolbachia* associations with insects: winning or losing against a master manipulator. *Front. Ecol. Evol.* 3:153. doi: 10.3389/fevo.2015.00153

Gomes, T. M. F. F., Wallau, G. L., and Loreto, E. L. S. (2022). Multiple long-range host shifts of major *Wolbachia* supergroups infecting arthropods. *Sci. Rep.* 12:8131. doi: 10.1038/s41598-022-12299-x

Hidayanti, A. K., Gazali, A., and Tagami, Y. (2022). Effect of quorum sensing inducers and inhibitors on cytoplasmic incompatibility induced by *Wolbachia* (Rickettsiales: Anaplasmataceae) in American serpentine Leafminer (Diptera: Agromyzidae): potential tool for the incompatible insect technique. *J. Insect Sci.* 22:8. doi: 10.1093/jisesa/ieab106

Hilgenboecker, K., Hammerstein, P., Schlattmann, P., Telschow, A., and Werren, J. H. (2008). How many species are infected with *Wolb–chia*?—a statistical analysis of current data. *FEMS Microbiol. Lett.* 281, 215–220. doi: 10.1111/j.1574-6968.2008.01110.x

Hoffmann, A. A., Clancy, D., and Duncan, J. (1996). Naturally-occurring *Wolbachia* infection in *Drosophila simulans* that does not cause cytoplasmic incompatibility. *Heredity* 76, 1–8. doi: 10.1038/hdy.1996.1

Hongoh, Y., Sato, T., Dolan, M. F., Noda, S., Ui, S., Kudo, T., et al. (2007). The motility symbiont of the termite gut flagellate *Caduceia versatilis* is a member of the "*Synergistes*" group. *Appl. Environ. Microbiol.* 73, 6270–6276. doi: 10.1128/AEM.00750-07

Horard, B., Terretaz, K., Gosselin-Grenet, A. S., Sobry, H., Sicard, M., Landmann, F., et al. (2022). Paternal transmission of the Wolbachia CidB toxin underlies cytoplasmic incompatibility. *Curr. Biol.* 32, 1319–1331.e5. doi: 10.1016/j.cub.2022.01.052

Huigens, M. E., de Almeida, R. P., Boons, P. A., Luck, R. F., and Stouthamer, R. (2004). Natural interspecific and intraspecific horizontal transfer of parthenogenesis-inducing *Wolbachia* in *Trichogramma* wasps. *Proc. R. Soc. B Biol. Sci.* 271, 509–515. doi: 10.1098/rspb.2003.2640

Huigens, M. E., Luck, R. F., Klaassen, R. H., Maas, M. F., Timmermans, M. J., and Stouthamer, R. (2000). Infectious parthenogenesis. *Nature* 405, 178–179. doi: 10.1038/35012066

Hurst, L. D. (1991). The evolution of cytoplasmic incompatibility or when spite can be successful. *J. Theor. Biol.* 148, 269–277. doi: 10.1016/s0022-5193(05)80344-3

Jain, C., Rodriguez-R, L. M., Phillippy, A. M., Konstantinidis, K. T., and Aluru, S. (2018). High throughput ANI analysis of 90K prokaryotic genomes reveals clear species boundaries. *Nat. Commun.* 9:5114. doi: 10.1038/s41467-018-07641-9

Kang, L., Chen, B., Wei, J.-N., and Liu, T.-X. (2009). Roles of thermal adaptation and chemical ecology in *Liriomyza* distribution and control. *Annu. Rev. Entomol.* 54, 127–145. doi: 10.1146/annurev.ento.54.110807.090507

Katoh, K., and Standley, D. M. (2013). MAFFT multiple sequence alignment software version 7: improvements in performance and usability. *Mol. Biol. Evol.* 30, 772–780. doi: 10.1093/molbev/mst010

Klasson, L., Walker, T., Sebaihia, M., Sanders, M. J., Quail, M. A., and Lord, A. (2008). Genome evolution of Wolbachia strain wPip from the Culex pipiens group. *Molecular biology and evolution*, 25, 1877–1887. doi: 10.1093/molbev/msn133

Kumar, S., Stecher, G., Li, M., Knyaz, C., and Tamura, K. (2018). MEGA X: molecular evolutionary genetics analysis across computing platforms. *Mol. Biol. Evol.* 35, 1547–1549. doi: 10.1093/molbev/msy096

Lang, A. S., and Beatty, J. T. (2000). Genetic analysis of a bacterial genetic exchange element: the gene transfer agent of *Rhodobacter capsulatus*. *Proc. Natl. Acad. Sci. U. S. A.* 97, 859–864. doi: 10.1073/pnas.97.2.859

Lang, A. S., Westbye, A. B., and Beatty, J. T. (2017). The distribution, evolution, and roles of gene transfer agents in prokaryotic genetic exchange. *Annu. Rev. Virol.* 4, 87–104. doi: 10.1146/annurev-virology-101416-041624

Laven, H. (1967). Eradication of Culex pipiens fatigans through cytoplasmic incompatibility. *Nature* 216, 383–384. doi: 10.1038/216383a0

Le Page, D. P., Metcalf, J. A., Bordenstein, S. R., On, J., Perlmutter, J. I., Shropshire, J. D., et al. (2017). Prophage WO genes recapitulate and enhance *Wolbachia*-induced cytoplasmic incompatibility. *Nature* 543, 243–247. doi: 10.1038/nature21391

Li, D., Liu, C.-M., Luo, R., Sadakane, K., and Lam, T.-W. (2015). MEGAHIT: an ultra-fast single-node solution for large and complex metagenomics assembly via succinct *de Bruijn* graph. *Bioinformatics* 31, 1674–1676. doi: 10.1093/bioinformatics/btv033

Lindh, J. M., Terenius, O., and Faye, I. (2005). 16S rRNA gene-based identification of midgut Bacteria from field-caught *Anopheles gambiae* Sensu Lato and *A. funestus* mosquitoes reveals new species related to known insect symbionts. *Appl. Environ. Microbiol.* 71, 7217–7223. doi: 10.1128/AEM.71.11.7217-7223.2005

Lindsey, A. R. I., Rice, D. W., Bordenstein, S. R., Brooks, A. W., Bordenstein, S. R., and Newton, I. L. G. (2018). Evolutionary genetics of cytoplasmic incompatibility genes *cifA* and *cifB* in prophage WO of *Wolbachia*. *Genome Biol. Evol.* 10, 434–451. doi: 10.1093/gbe/evy012

Manni, M., Berkeley, M. R., Seppey, M., and Zdobnov, E. M. (2021). BUSCO: assessing genomic data quality and beyond. *Curr. Protoc.* 1:e323. doi: 10.1002/cpz1.323

Martinez, J., Klasson, L., Welch, J. J., and Jiggins, F. M. (2021). Life and death of selfish genes: comparative genomics reveals the dynamic evolution of cytoplasmic incompatibility. *Mol. Biol. Evol.* 38, 2–15. doi: 10.1093/molbev/msaa209

Meany, M. K., Conner, W. R., Richter, S. V., Bailey, J. A., Turelli, M., and Cooper, B. S. (2019). Loss of cytoplasmic incompatibility and minimal fecundity effects explain

relatively low *Wolbachia* frequencies in *Drosophila mauritiana*. *Evolution* 73, 1278–1295. doi: 10.1111/evo.13745

Minard, G., Tran, F. H., Raharimalala, F. N., Hellard, E., Ravelonandro, P., Mavingui, P., et al. (2013). Prevalence, genomic and metabolic profiles of *Acinetobacter* and *Asaia* associated with field-caught *Aedes albopictus* from Madagascar. *FEMS Microbiol. Ecol.* 83, 63–73. doi: 10.1111/j.1574-6941.2012.01455.x

Neupane, S., Bonilla, S. I., Manalo, A. M., and Pelz-Stelinski, K. S. (2022). Complete de novo assembly of *Wolbachia* endosymbiont of *Diaphorina citri* Kuwayama (Hemiptera: Liviidae) using long-read genome sequencing. *Sci. Rep.* 16:125. doi: 10.1038/s41598-021-03184-0

Newton, I. L., Clark, M. E., Kent, B. N., Bordenstein, S. R., Qu, J., Richards, S., et al. (2016). Comparative genomics of two closely related *Wolbachia* with different reproductive effects on hosts. *Genome Biol. Evol.* 8, 1526–1542. doi: 10.1093/gbe/evw096

Pascar, J., and Chandler, C. H. (2018). A bioinformatics approach to identifying *Wolbachia* infections in arthropods. *PeerJ* 6:e5486. doi: 10.7717/peerj.5486

Pidiyar, V. J., Jangid, K., Patole, M. S., and Shouche, Y. S. (2004). Studies on cultured and uncultured microbiota of wild *Culex quinquefasciatus* mosquito midgut based on 16s ribosomal RNA gene analysis. *Am. J. Trop. Med. Hyg.* 70, 597–603. doi: 10.4269/ajtmh.2004.70.597

Pidiyar, V., Kaznowski, A., Narayan, N. B., Patole, M., and Shouche, Y. S. (2002). *Aeromonas culicicola* sp. nov., from the midgut of *Culex quinquefasciatus*. *Int. J. Syst. Evol. Microbiol.* 52, 1723–1728. doi: 10.1099/00207713-52-5-1723

Rau, J., Werner, D., Beer, M., Höper, D., and Kampen, H. (2022). The microbial RNA metagenome of *Aedes albopictus* (Diptera: Culicidae) from Germany. *Parasitol. Res.* 121, 2587–2599. doi: 10.1007/s00436-022-07576-7

Raychoudhury, R., Baldo, L., Oliveira, D. C. S. G., and Werren, J. H. (2009). Modes of acquisition of *Wolbachia*: horizontal transfer, hybrid introgression, and codivergence in the *Nasonia* species complex. *Evolution* 63, 165–183. doi: 10.1111/j.1558-5646.2008.00533.x

Rissman, A. I., Mau, B., Biehl, B. S., Darling, A. E., Glasner, J. D., and Perna, N. T. (2009). Reordering contigs of draft genomes using the mauve aligner. *Bioinformatics* 25, 2071–2073. doi: 10.1093/bioinformatics/btp356

Scholz, M., Albanese, D., Tuohy, K., Donati, C., Segata, N., and Rota-Stabelli, O. (2020). Large scale genome reconstructions illuminate *Wolbachia* evolution. *Nat. Commun.* 11:5235. doi: 10.1038/s41467-020-19016-0

Schrieke, H., Maignien, L., Constancias, F., Trigodet, F., Chakloute, S., Rakotoarivony, I., et al. (2021). The mosquito microbiome includes habitat-specific but rare symbionts. *Comput. Struct. Biotechnol. J.* 20, 410–420. doi: 10.1016/j.csbj.2021.12.019

Shropshire, J. D., Leigh, B., and Bordenstein, S. R. (2020). Symbiont-mediated cytoplasmic incompatibility: what have we learned in 50 years? *elife* 9, 1–36. doi: 10.7554/ELIFE.61989

Shropshire, J. D., On, J., Layton, E. M., Zhou, H., and Bordenstein, S. R. (2018). One prophage WO gene rescues cytoplasmic incompatibility in *Drosophila melanogaster*. *Proc. Natl. Acad. Sci. U. S. A.* 115, 4987–4991. doi: 10.1073/pnas.1800650115

Sinha, A., Li, Z., Sun, L., Carlow, C. K. S., and Cordaux, R. (2019). Complete genome sequence of the *Wolbachia* wAlbB endosymbiont of *Aedes albopictus*. *Genome Biol. Evol.* 11, 706–720. doi: 10.1093/gbe/evz025

Söding, J., Biegert, A., and Lupas, A. N. (2005). The HHpred interactive server for protein homology detection and structure prediction. *Nucleic Acids Res.* 33, W244–W248. doi: 10.1093/nar/gki408

Tagami, Y., Doi, M., Sugiyama, K., Tatara, A., and Saito, T. (2006a). *Wolbachia*-induced cytoplasmic incompatibility in *Liriomyza trifolii* and its possible use as a tool in insect pest control. *Biol. Control* 38, 205–209. doi: 10.1016/j.biocontrol.2006.03.008

Tagami, Y., Doi, M., Sugiyama, K., Tatara, A., and Saito, T. (2006b). Survey of leafminers and their parasitoids to find endosymbionts for improvement of biological control. *Biol. Control* 38, 210–216. doi: 10.1016/j.biocontrol.2006.01.015

Vancaester, E., and Blaxter, M. (2023). Phylogenomic analysis of *Wolbachia* genomes from the Darwin tree of life biodiversity genomics project. *PLoS Biol.* 21. doi: 10.1371/journal.pbio.3001972

Vicoso, B., and Bachtrog, D. (2015). Numerous transitions of sex chromosomes in Diptera. *PLoS Biol.* 13:e1002078. doi: 10.1371/journal.pbio.1002078

Wang, X., Xiong, X., Cao, W., Zhang, C., Werren, J. H., and Wang, X. (2020). Phylogenomic analysis of *Wolbachia* strains reveals patterns of genome evolution and recombination. *Genome Biol. Evol.* 12, 2508–2520. doi: 10.1093/GBE/EVAA219

Xu, X., Ridland, P. M., Umina, P. A., Gill, A., Ross, P. A., Pirtle, E., et al. (2021). High incidence of related *Wolbachia* across unrelated leaf-mining diptera. *Insects* 12:788. doi: 10.3390/insects12090788

Yen, J. H., and Barr, A. R. (1973). The etiological agent of cytoplasmic incompatibility in *Culex pipiens*. *J. Invertebr. Pathol.* 22, 242–250. doi: 10.1016/0022-2011(73)90141-9

Zhang, X. R., Xing, Z. L., Lei, Z. R., and Gao, Y. L. (2017). Recent status of the invasive Leafminer *Liriomyza trifolii* in China. *Southwest. Entomol* 42, 301–304. doi: 10.3958/059.042.0130

Zouache, K., Voronin, D., Tran-Van, V., and Mavingui, P. (2009a). Composition of bacterial communities associated with natural and laboratory populations of *Asobara tabida* infected with *Wolbachia*. *Appl. Environ. Microbiol.* 75, 3755–3764. doi: 10.1128/AEM.02964-08

Zouache, K., Voronin, D., Tran-Van, V., Mousson, L., Failloux, A.-B., and Mavingui, P. (2009b). Persistent *Wolbachia* and cultivable Bacteria infection in the reproductive and somatic tissues of the mosquito vector *Aedes albopictus*. *PLoS One* 4:e6388. doi: 10.1371/journal.pone.0006388

frontiers | Frontiers in Microbiology

TYPE Original Research
PUBLISHED 15 February 2024
DOI 10.3389/fmicb.2024.1352378

OPEN ACCESS

EDITED BY
George Tsiamis,
University of Patras, Greece

REVIEWED BY
Shrivardhan Dheeman,
MVN University, India
Margaret Thairu,
University of Wisconsin-Madison,
United States

*CORRESPONDENCE
Lindsey J. Cantin
lcantin@neb.com

RECEIVED 08 December 2023
ACCEPTED 05 February 2024
PUBLISHED 15 February 2024

CITATION
Cantin LJ, Dunning Hotopp JC and Foster JM (2024) Improved metagenome assemblies through selective enrichment of bacterial genomic DNA from eukaryotic host genomic DNA using ATAC-seq. *Front. Microbiol.* 15:1352378. doi: 10.3389/fmicb.2024.1352378

Improved metagenome assemblies through selective enrichment of bacterial genomic DNA from eukaryotic host genomic DNA using ATAC-seq

Lindsey J. Cantin[1]*, Julie C. Dunning Hotopp[2] and Jeremy M. Foster[1]

[1]Biochemistry and Microbiology Division, New England BioLabs, Ipswich, MA, United States, [2]Institute for Genome Sciences, University of Maryland School of Medicine, Baltimore, MD, United States

Genomics can be used to study the complex relationships between hosts and their microbiota. Many bacteria cannot be cultured in the laboratory, making it difficult to obtain adequate amounts of bacterial DNA and to limit host DNA contamination for the construction of metagenome-assembled genomes (MAGs). For example, *Wolbachia* is a genus of exclusively obligate intracellular bacteria that live in a wide range of arthropods and some nematodes. While *Wolbachia* endosymbionts are frequently described as facultative reproductive parasites in arthropods, the bacteria are obligate mutualistic endosymbionts of filarial worms. Here, we achieve 50-fold enrichment of bacterial sequences using ATAC-seq (Assay for Transposase-Accessible Chromatin using sequencing) with *Brugia malayi* nematodes, containing *Wolbachia* (*w*Bm). ATAC-seq uses the Tn5 transposase to cut and attach Illumina sequencing adapters to accessible DNA lacking histones, typically thought to be open chromatin. Bacterial and mitochondrial DNA in the lysates are also cut preferentially since they lack histones, leading to the enrichment of these sequences. The benefits of this include minimal tissue input (<1 mg of tissue), a quick protocol (<4 h), low sequencing costs, less bias, correct assembly of lateral gene transfers and no prior sequence knowledge required. We assembled the *w*Bm genome with as few as 1 million Illumina short paired-end reads with >97% coverage of the published genome, compared to only 12% coverage with the standard gDNA libraries. We found significant bacterial sequence enrichment that facilitated genome assembly in previously published ATAC-seq data sets from human cells infected with *Mycobacterium tuberculosis* and *C. elegans* contaminated with their food source, the OP50 strain of *E. coli*. These results demonstrate the feasibility and benefits of using ATAC-seq to easily obtain bacterial genomes to aid in symbiosis, infectious disease, and microbiome research.

KEYWORDS

genome assembly, bacterial symbiont, *Wolbachia*, ATAC-seq, filariasis, epigenetics, metagenome assembled genomes

1 Introduction

Many symbiotic bacteria remain uncultured and may even be impossible to culture in the absence of the host (Ashton et al., 2003; Hongoh, 2010; Xie et al., 2019; Masson and Lemaitre, 2020). Genomics and metagenomics have long been used to study these bacteria through the analysis of the host and microbiota genome sequences. The creation of what are now called metagenome assembled genomes (MAGs) from host genome sequencing data was demonstrated for *Wolbachia* endosymbionts in the *Drosophila* genome sequencing projects (Salzberg et al., 2005).

Bacterial endosymbionts can live within eukaryotic hosts long-term, resulting in mutualistic, commensal, and parasitic relationships. In mutualistic relationships, both species benefit from their interactions. The microbial symbionts often provide metabolites from pathways absent in the eukaryotic host, while the host provides a nutrient rich environment for their resident bacteria (Douglas, 2014). For example, the human gut microbiome consists of trillions of bacteria, with many of them metabolizing nutrients from food components nondigestible by the host and protecting their host from pathogen invasion (Bäckhed et al., 2005; Bull and Plummer, 2014). Nitrogen fixing bacteria are common symbionts of plants, animals, fungi and protists where they increase the bioavailability of nitrogen for the eukaryotic host (Kneip et al., 2007).

In parasitic relationships, the bacteria will usually benefit at the expense of the eukaryotic host by causing disease or disrupting normal biological processes during their replication in the host (Balloux and van Dorp, 2017). The pathogenic bacterium *Mycobacterium tuberculosis* (*M. tb*) is an intracellular parasite that lives in macrophages in the respiratory system of mammalian hosts. The host provides a safe niche for bacterial replication in a tissue that allows the bacteria to spread through air droplets. The infection can lead to fibrosis and necrosis of the host's lung tissue (Smith, 2003).

Wolbachia endosymbionts are some of the most abundant intracellular bacteria and are present in almost 60% of all arthropod species and some nematode species (Hilgenboecker et al., 2008). *Wolbachia* endosymbionts are maternally transmitted and live in the reproductive tissues of their host. In insects, the bacteria were first studied as reproductive parasites that act through male killing, feminization, parthenogenesis and cytoplasmic incompatibility (Werren, 1997; Chen et al., 2020). More recently, *Wolbachia* has been found to provide protection to arthropods from other pathogens, such as RNA viruses (Hedges et al., 2008; Ye et al., 2013; Drew et al., 2021). This demonstrates the complex relationships between hosts and their symbionts and how there is a continuum between parasitism and mutualism that can often be context dependent.

Wolbachia is also present in many filarial nematodes as an obligate mutualistic endosymbiont, meaning the worms cannot survive without the bacteria and the bacteria cannot live outside of the worms (Mclaren et al., 1975; Sironi et al., 1995; Bandi et al., 1998, 2001; Quek et al., 2022). Filarial nematodes are insect-borne parasites that cause filariasis, one of the leading causes of morbidity in the world. *Brugia malayi* (*B. malayi*) and *Wuchereria bancrofti* are the predominant species that cause lymphatic filariasis, which can lead to elephantiasis and disfigurement. Onchocerciasis, caused by *Onchocerca volvulus*, can result in visual impairment (WHO, 1995; WHO, 2019; Medeiros et al., 2021). Various combinations of ivermectin, diethylcarbamazine, and albendazole have been used to prevent filarial infections, but these drugs cannot treat established infections (Campbell, 1991; Richards et al., 2001; Mackenzie et al., 2002; Molyneux et al., 2003). Antibiotics, such as doxycycline and rifampicin, kill the endosymbiotic bacteria, leading to the eventual death of the adult worms (Taylor et al., 2005; Bazzocchi et al., 2008; Hoerauf et al., 2008; Specht et al., 2008; Supali et al., 2008; Coulibaly et al., 2009; Mand et al., 2009; Wanji et al., 2009; Johnston et al., 2014; Aljayyoussi et al., 2017). Therefore, anti-*Wolbachia* therapy is a promising avenue for the treatment and eradication of filariasis (Clare et al., 2019; Taylor et al., 2019; Johnston et al., 2021). The *Wolbachia* reside in the lateral cords in both sexes of adult worms but are also found in the ovaries and embryos of adult females (Kozek, 1977; McGarry et al., 2004; Landmann et al., 2010). The bacteria are required for the development, reproduction, and long-term survival of adult worms. It is likely that *Wolbachia* provide necessary metabolites from biological pathways that are incomplete or absent in the nematode genomes. These may include heme, riboflavin, nucleotide synthesis, and additional ATP for the host (Foster et al., 2005; Wu et al., 2009; Darby et al., 2012; Li and Carlow, 2012; Luck et al., 2016; Grote et al., 2017). In return, the worms may provide essential amino acids to the bacteria.

Sequences from *Wolbachia* and other bacterial symbionts have been found in eukaryotic host genomes, as a result of lateral gene transfer (LGT) (Hotopp et al., 2007; Ioannidis et al., 2013; Sieber et al., 2017). Nuclear *Wolbachia* transfers (*nuwts*) are found in over 80% of insect and nematode species infected with the bacteria. In *B. malayi*, there are hundreds of these *nuwts*, with over 10.6% of the *w*Bm genome integrated into the host nuclear genome. While many bacterial LGT sequences have deteriorated in host genomes, some of these transfers appear to be functional with actively transcribed protein coding genes across a wide range of eukaryotic species (Gladyshev et al., 2008; Acuña et al., 2012; Husnik et al., 2013; Ioannidis et al., 2013; Sieber et al., 2017).

To study the complex co-evolution between eukaryotes and their symbionts, it is necessary to obtain genome sequences from both species. In filarial endosymbionts, these genomes can be used to identify new drug targets. In other symbionts, the genomes can be used to identify novel molecular pathways related to their persistent infections and biological outcomes in eukaryotic hosts. Yet sequencing the genomes of intracellular bacteria is difficult because many cannot be cultured outside of the host or eukaryotic cell lines due to genome reduction (Wade, 2002; Fenollar et al., 2003; Foster et al., 2005; McCutcheon, 2010; Almeida et al., 2019). Even for bacteria with a high multiplicity of infection, the larger host genome results in substantial host DNA contamination and low relative levels of bacterial sequences. Field and clinical specimens can be limited, making it difficult to use standard sequencing methods with low sample input. Deep metagenomic sequencing can be used to assemble symbiont genomes, however this can be expensive and still may not result in sufficient bacterial sequences for *de novo* assembly. *Nuwts* and LGTs from the bacterial genomes can also be difficult to assemble if the sequencing depth is similar between species in a metagenomic sample. Techniques have been developed to enrich for bacterial DNA, particularly with *Wolbachia*, including pulsed-field gel purification (Sun et al., 2001; Foster et al., 2004; Wu et al., 2004; Foster et al., 2005), fluorescence-activated cell sorting (Thompson et al., 2013; Dam et al., 2020) and oligonucleotide probe hybridization (Kent et al., 2011; Melnikov et al., 2011; Geniez et al., 2012; Lefoulon et al., 2019). Unfortunately, these protocols are time consuming, require specialized equipment, require *a*

priori knowledge of antibodies or sequences for probes, require expensive reagents, and/or require large quantities of input material.

Here, we present a novel application of ATAC-seq (Assay for Transposase-Accessible Chromatin using sequencing) for bacterial sequence enrichment to facilitate *de novo* genome assembly. Typically, ATAC-seq uses the Tn5 transposase to selectively cut and ligate sequencing adapters to accessible eukaryotic chromatin regions free of histones (Buenrostro et al., 2013). This leads to the enrichment of those "open" regions during sequencing, as the remaining majority of the genome is inaccessible to the transposase. Mitochondria and bacteria do not contain histones resulting in uniform Tn5 cutting across their genome. As a proof of principle, we performed ATAC-seq on *B. malayi* worms and show *de novo* genome assembly of the *Wolbachia* (*w*Bm) endosymbiont. Similar enrichment of bacterial sequences in published ATAC-seq datasets in human cells infected with *Mycobacterium M.tb* (Pacis et al., 2015) and *C. elegans* with *E. coli* strain OP50 contamination (Daugherty et al., 2017) enabled *de novo* assemblies of these bacterial genomes. This bacterial enrichment method should improve species identification and *de novo* metagenome assembly for a variety of host-associated microbiota.

2 Materials and methods

2.1 Tissue collection

Live adult *B. malayi* females and males were shipped overnight from the NIH-NIAID Research Reagent Resource Center (FR3) at the University of Georgia (Michalski et al., 2011). Upon arrival, the worms were transferred to prewarmed 37°C RPMI 1640 containing 10% heat inactivated fetal bovine serum (Thermo Fisher Scientific), 2 mM L-glutamine, 5 g/L glucose, 100 ug/mL streptomycin, 100 U/mL penicillin and 250 ng/mL amphotericin (Millipore Sigma) and incubated overnight at 37°C with 5% CO_2. The worms were sorted into groups of 3 by sex and rinsed two times in 1X PBS. All liquid was removed, and the worms were frozen in 1.5 mL LoBind tubes with liquid nitrogen. All samples were stored at −80°C.

2.2 Nuclei isolation and *Wolbachia* immunostaining

The presence of *Wolbachia* cells in nuclei isolations were assessed using immunostaining for the *Wolbachia* surface protein (WSP). Three frozen adult female worms were placed on ice for 5 min prior to Dounce homogenization in 0.5 mL chilled 1X homogenization buffer (320 mM sucrose), 0.1 mM EDTA, 0.1% NP40 substitute (Millipore Sigma), 5 mM $CaCl_2$, 3 mM Mg $(Ac)_2$, 10 mM Tris pH 7.8, 167 µM β-mercaptoethanol, 1X protease inhibitor cocktail (Millipore Sigma) in water. Lysates were filtered through 200 µm then 40 µm filters to remove large tissue fragments and cuticle fragments, while retaining released nuclei and bacterial cells. The nuclei were pelleted by centrifugation at 500 x g for 10 min. The pellet was resuspended in 4 mL nuclei extraction buffer (10 mM Hepes pH 7.4, 1.5 mM $MgCl_2$, 10 mM KCl, 1X protease inhibitor cocktail and 0.2% NP40 substitute) (Neely and Bao, 2019). The samples were split into 1 mL aliquots and added to poly-L-ornithine-treated (Millipore Sigma) glass cover slips (Thermo Fisher Scientific) by centrifugation at 500 x g at 4°C in a 12 well cell culture plate. The coverslips with adhered nuclei were fixed using 10% formalin for 10 min. The coverslips were washed 3 times with 1X PBS for 10 min and then blocked for 30 min in blocking buffer (0.5% BSA in 1X PBS). The Anti-*Wolbachia* surface protein (WSP) antibody (BEI resources) was diluted 1:1000 in blocking buffer and placed on the coverslips overnight at 4°C. To remove excess antibody, the coverslips were washed 3 times in 1X PBS with 0.05% Tween-20 for 10 min. A goat anti-mouse IgG conjugated with Alexa Fluor 488 (Abcam) was used as secondary antibody to localize WSP. All subsequent steps were performed in the dark. The antibody was diluted 1:2000 in blocking buffer and placed on the coverslips for 1 h at room temperature. The nuclei were washed 3 times with 0.05% Tween-20 in 1X PBS for 5 min and then washed an additional 2 times in 1X PBS. Coverslips were placed upside down on to a glass microscope slide with a droplet of Prolong Gold Antifade Mount with DAPI (Thermo Fisher Scientific). The nuclei were imaged using a Zeiss LSM 880 confocal microscope. The channel images were pseudo colored and stacked using ImageJ (Fiji v2.1.0).

2.3 Nuclei isolation and ATAC-seq library preparation and sequencing

The Omni-ATAC-seq protocol (Corces et al., 2017) was adapted for fresh frozen nematodes. All steps were performed on ice unless noted otherwise. We prepared 2 biological replicates for each sex, with each replicate containing a pool of 3 worms. The frozen male and female worm samples were Dounce homogenized in 1X homogenization buffer (recipe in previous section) separately. The lysates were sequentially filtered through 70 µm, 40 µm and 20 µm filters, removing worm cuticles and undisrupted embryos. Nuclei were pelleted by spinning at 500 x g for 10 min in a fixed angle centrifuge at 4°C. After removing the supernatant, the pellet was resuspended in 1 mL ATAC Resuspension buffer (10 mM Tris–HCl pH 7.4, 10 mM NaCl, 3 mM $MgCl_2$, 0.1% Tween-20) and pelleted again. The supernatant was completely removed, and the pellets were each resuspended in transposition mix containing 25 µL 2X tagmentation buffer (Diagenode), 2.5 µL loaded tagmentase (Diagenode), 16.5 µL 1X PBS, 0.5 µL 1% digitonin, 0.5 µL 10% Tween-20, and 5 µL ultrapure water. The samples were incubated at 37°C for 30 min at 1000 rpm in a thermomixer (Eppendorf). The tagmented DNA was cleaned up using the Monarch PCR and DNA Cleanup Kit (New England BioLabs) and eluted in 20 µL of ultrapure water. The libraries were indexed and amplified with 10 PCR cycles using unique dual indexes (Diagenode) and NEBNext High-Fidelity 2X PCR Master Mix (New England BioLabs). The libraries were size selected using consecutive AMPure XP bead (Beckman Coulter) clean ups by removing fragments bound to 0.5X beads and then keeping fragments bound to 1.0X beads. The samples were pooled and sequenced on a single flow cell of the Illumina NextSeq 550 to a depth of at least 20 million reads per library.

2.4 Genomic DNA library preparation and sequencing

Two biological replicates of genomic DNA (gDNA) from 10 adult female *B. malayi* worms were extracted using the Monarch High

Molecular Weight DNA Extraction Kit for Tissue (New England BioLabs) using the standard protocol. DNA was run on a Pippin Pulse gel (Sage Science) and had an average length of 100 kb. The genomic DNA libraries were made following the Nextera DNA Library Prep Kit protocol (Illumina), starting with 50 ng of DNA. Replicate 1 was tagmented for 5 min and replicate 2 was tagmented for 15 min with 5 µL TDE1 at 55°C in the thermomixer. The reaction was cleaned using the Monarch PCR and DNA Cleanup kit. The libraries were indexed and amplified using Nextera dual indexes (Illumina) and NEBNext High-Fidelity 2X PCR Master Mix with 10 PCR cycles. Excess adapters and primers were removed by cleaning up with 1.5X AMPure XP beads (Beckman Coulter). The samples were pooled at equal concentrations and sequenced on a single flow cell of the Illumina NextSeq 550 to a depth of at least 20 million reads per library.

2.5 ATAC-seq analyses

Default options for each analysis tool were used unless noted otherwise. The paired-end reads from all libraries were trimmed to remove remaining adapter sequences and low quality bases using Cutadapt (v1.16) (Martin, 2011) with the –paired and –nextera options. The read quality was assessed using FastQC (v0.11.9) (Andrews, 2023). Some reads may map with equal quality to both the *w*Bm and *B. malayi* genomes as a result of *nuwt* sequences. Therefore, we aligned all of the trimmed reads to both the reference *B. malayi* chromosomes (GCF_000002995.4) and the *w*Bm genome (AE017321.1) separately and calculated the mapping percentages using Bowtie2 (version 2.4.5) (Langmead and Salzberg, 2012). To identify which reads map to both genomes, we first used "Samtools view -F 4 | cut -f 1" (v1.15.1) (Li et al., 2009) to extract mapped read names from each of the BAM files. The Unix "comm" command was then used to find the read names shared between the *w*Bm and *B. malayi* mapped BAM files for each library. The proportion of shared reads was calculated by counting the number of common read names and dividing that by the total number of reads in each library. We retained the shared mapped reads in their respective BAM files for further analyses. Picard (v2.27.5) (Broadinstitute/picard Broad institute, 2023) was used to calculate the insert size (CollectInsertSzeMetrics) and to mark PCR duplicates (MarkDuplicates) in the BAM files. We used Deeptools (v3.5.1) (Ramírez et al., 2014) to make BigWig files (BamCoverage) of the ATAC-seq and gDNA libraries for visualization in IGV (v2.11.9) (Thorvaldsdóttir et al., 2013) and to calculate the sequencing depth (plotCoverage) for reads aligned to the *B. malayi* nuclear and *Wolbachia* chromosomes. We called peaks in the ATAC-seq samples aligned to the *B. malayi* nuclear chromosomes using MACS2 (v2.2.7.1) (Zhang et al., 2008) with an FDR cutoff for 0.05. ATAC-seq peaks that overlap with *nuwt* regions in the *B. malayi* genome were removed using Bedtools intersect (v2.30.0) (Quinlan and Hall, 2010), as we cannot determine if the reads originate from *B. malayi* or *Wolbachia* DNA. The BAM and filtered peak files were loaded into R using Diffbind (v3.4.11) (Stark and Brown, 2023) to create a read count matrix across all ATAC-seq samples for each peak region. This count matrix in Diffbind was then used to calculate the FRiP (fraction of reads in peaks) and Pearson correlation between replicates. We used ChIPseeker (v1.30.3) (Yu et al., 2015) to annotate ATAC-seq peaks to genomic features, with promoters calculated as 1 kb up and downstream of the first base in the gene model.

2.6 *Wolbachia de novo* genome assembly and assessment

Trimmed reads for female ATAC-seq and gDNA libraries were randomly downsampled to 10 million, 1 million, 500 thousand and 100 thousand total reads using Seqtk subseq (v1.3) (Li, 2023). We used SPAdes (v3.15.4) (Nurk et al., 2017; Prjibelski et al., 2020) to make metagenomic assemblies from the downsampled libraries with the "meta" setting. We mapped the reads from each library back to its respective assembly to obtain sequencing depth for each contig. Each assembly was aligned to the NCBI Nucleotide (NT) database (v5) containing *Wolbachia* genomes and to the *B. malayi* genome (GCF_000002995.4) using BLASTN (v2.13.0) (Altschul et al., 1990; Camacho et al., 2009). Blobtoolkit (v3.2.7) (Laetsch and Blaxter, 2017; Challis et al., 2020) was used to visualize and bin the ATAC-seq and gDNA assemblies (with 10 million input reads) by BLAST results, sequence coverage and GC content. Using the Blobtoolkit viewer, we filtered the gDNA and ATAC-seq assemblies using multiple metrics. First, all contigs with a length less than 500 bp were removed, as these are difficult to bin correctly (Strous et al., 2012; Gurevich et al., 2013; Vosloo et al., 2021). For the gDNA assembly, the contigs that aligned to bacterial sequences with BLASTN were kept to bin *Wolbachia* contigs. With the ATAC-seq assembly, all contigs with over 1,000X coverage were kept to isolate *Wolbachia* contigs from nematode sequences. The few remaining *B. malayi* (rRNA regions) and mitochondrial contigs were also removed based on BLAST results. Quast (v5.2.0) (Gurevich et al., 2013) was used to assess the genome qualities, with the published *w*Bm genome (AE017321.1) and annotation used as a reference (Foster et al., 2005). With Quast, we identified the percentage of the genome assembled, misassembles, mismatches, N50, genome features, and contig number. BUSCO (v5.4.2) (Simão et al., 2015; Manni et al., 2021) with the bacteria odb10 database was also used within QUAST to assess genome completeness, comparing the gene content between the *w*Bm reference and our new assemblies. We then used D-genies (v1.5.0) (Cabanettes and Klopp, 2018; Li, 2018) with Minimap2 alignment to visualize the alignment of our binned assemblies and the reference genome. BLASTN was used to map the binned assemblies to the reference *w*Bm genome using output format 6. Columns 1, 7 and 8 were kept, creating a bed file to view the coordinates of gaps in our new assemblies using IGV. GenMap (v1.3.0) (Pockrandt et al., 2020) was used to identify repeats in the reference genome, by calculating the mappability of each region using 75 bp k-mers, the same length as our sequencing reads. Using Bedtools intersect (v2.30.0) (Quinlan and Hall, 2010), we found overlaps between the gaps in our new assemblies and the repeat regions of the reference genome. Bedtools intersect was also used to calculate overlap between mismatches and SNPs (identified with QUAST) with *nuwts* in the *w*Bm genome. The repeat length, score and assembly status were visualized using ggplot2 (Valero-Mora, 2010).

2.7 Genome assembly with published ATAC-seq data

SRA-toolkit (v2.11.1) was used to download ATAC-seq runs from *C. elegans* (SRR5000677) (Daugherty et al., 2017) and human dendritic cells infected with *M. tb* (SRR1725731) (Pacis et al., 2015). The raw

reads were trimmed with Cutadapt as described above (Section 2.5). We used Kraken2 (v2.1.3) (Wood et al., 2019) to classify the trimmed reads by taxonomy. The reads were then assembled with Spades as described above (Section 2.6). The trimmed reads were mapped back to the new assemblies using Bowtie2 to calculate sequencing depth. The assemblies were aligned to the NCBI NT database using BLASTN. The assemblies, coverage files and BLASTN results were visualized with Blobtoolkit.

3 Results

3.1 Prescence of *Wolbachia* cells after nuclei isolation

ATAC-sequencing using the Tn5 transposase was performed on adult *B. malayi*, containing *Wolbachia* endosymbionts. Nuclei isolation is the first step in ATAC-seq library preparation. *Wolbachia* presence after cell membrane lysis was confirmed with immunofluorescent staining. *Wolbachia* cells were stained using the anti-WSP antibody, while *B. malayi* nuclei were stained with DAPI. Intact *Wolbachia* cells can be seen amongst the nematode nuclei, confirming that *Wolbachia* DNA will be present during ATAC-sequencing (Figure 1).

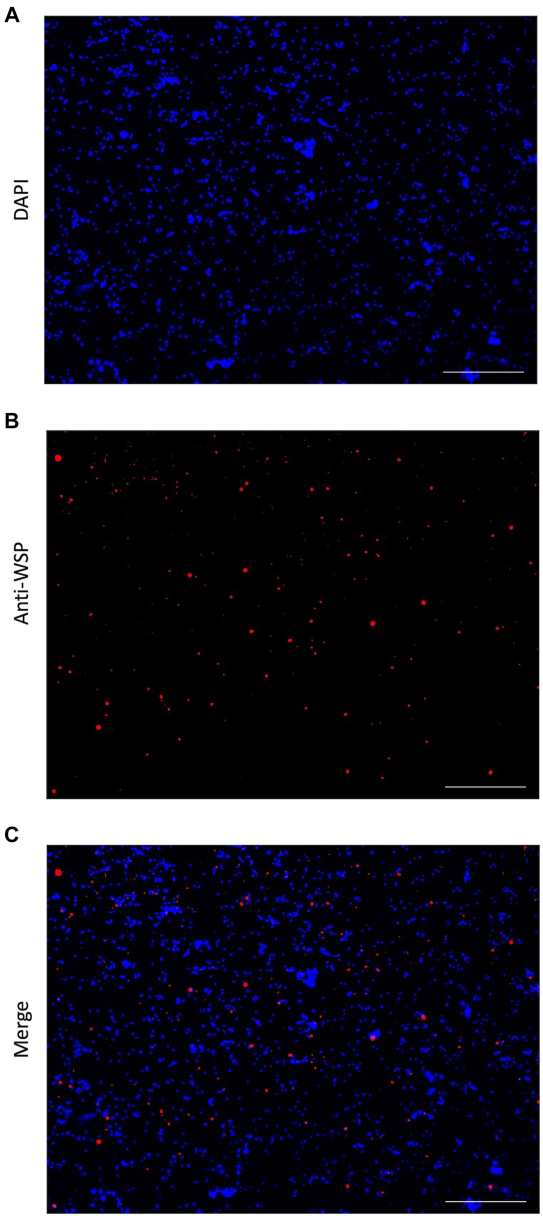

FIGURE 1
Immunofluorescent detection of *Wolbachia*. **(A)** DAPI stain (blue) of isolated *Brugia malayi* nuclei. **(B)** Anti-WSP detection in the nuclei isolation using an anti-mouse IgG secondary antibody conjugated with Alexa Fluor 488 (pseudo colored red). **(C)** Merged image, showing the presence of *Wolbachia* cells in *Brugia malayi* nuclei extraction. All images at 40X, Scale = 100 μm.

3.2 *Brugia malayi* chromatin accessibility

ATAC-seq and gDNA libraries were aligned to both the *B. malayi* and *Wolbachia* genomes. Both libraries had an average insert size of 100 bp (Supplementary Figure S1). The Tn5 transposase cuts and attaches sequencing adapters to DNA that is not surrounded by histones. Since bacterial genomes do not contain histones, we expected an enrichment of *Wolbachia* reads in ATAC-seq libraries. We found that at least 60% of reads mapped to the *Wolbachia* genome in the adult female ATAC-seq libraries, while only 1.19% of reads were from the bacteria in the standard gDNA libraries (Figure 2; Supplementary Table S1). This represents an over 50-fold enrichment of bacterial reads when transposase library preparation is used on samples containing intact chromatin. 23.27% of reads map only to the *B. malayi* nuclear and mitochondrial chromosomes in the ATAC-seq library, with 96% of reads mapping to these chromosomes in the gDNA library. A small proportion of reads map to both the *B. malayi* nuclear and *w*Bm chromosomes. These most likely represent reads mapping to *nuwts*, as these sequences are found in both species. There is a higher number of these dual-mapped reads in the ATAC-seq library. The bulk of these reads are likely originating from *Wolbachia*, as a result of the overall enrichment of the bacterial sequences. The remaining reads are unassigned or map to the gerbil genome, which is the laboratory host for the nematode.

When mapped on the *B. malayi* nuclear genome, ATAC-seq reads pile up in distinct regions called peaks, while gDNA reads map relatively uniformly across the chromosomes (Figure 3A). The ATAC-seq peaks correspond to open chromatin regions where transcription factors can bind the DNA and actively regulate gene expression. Many peaks are shared across males and females. However, some peaks can only be found in one sample type, resulting in a unique chromatin landscape dependent on the nematode sex. The read coverage distribution was calculated for ATAC-seq and gDNA reads mapped to the *B. malayi* chromosomes (Supplementary Figure S2). The gDNA libraries have a bell-shaped coverage distribution curve, with an average depth of 25 reads. Both the male and female ATAC-seq libraries have an L shaped coverage distribution curve with an average depth of 16.8 and 9.7 reads, respectively. This means that the gDNA libraries have a more uniform coverage across all of the *B. malayi* chromosomes, while most genomic regions have little to no coverage in the ATAC-seq samples, as expected.

Using Pearson correlation, we find that biological ATAC-seq replicates cluster together, showing the reproducibility of our data with this optimized ATAC-seq method (Figure 3B). The clustering also shows that males and females have global differences in the

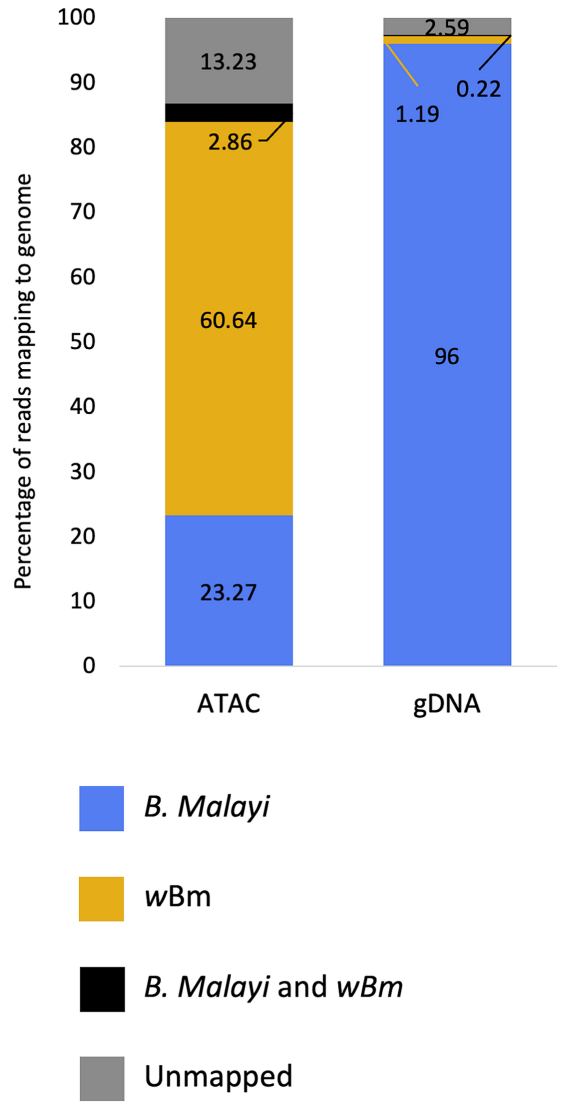

FIGURE 2
Mapping statistics of ATAC-seq and gDNA libraries from *Brugia malayi* samples containing *Wolbachia*. The proportion of reads mapping to the *Brugia malayi* and mitochondrial chromosomes only is shown blue. The proportion of reads mapping to the *Wolbachia* genome only is shown in yellow. The proportion of reads that multi-map to both the *Brugia malayi* and *w*Bm chromosomes are shown in black. Reads that are unmapped are shown in grey.

chromatin accessibility. The ATAC-seq peaks were assigned to genomic features using the *B. malayi* genome annotation (Figure 3C). Promoter regions (defined as 1 kb up- and downstream of the first base in the gene model) had the greatest number of peaks at 46.2%. Distal intergenic regions, which generally correspond to enhancers, have 27.3% of the peaks. The other 26.5% of peaks fall in genic regions, including untranslated regions, exons, and introns. An enrichment of peaks at promoter regions has been observed in other ATAC-seq datasets. In mammals, around 10–25% of peaks are found in promoter regions (Chung et al., 2018; Yan et al., 2020). *Drosophila melanogaster* data is more similar to *B. malayi*, where 40–50% of peaks are found in promoters (Santiago et al., 2021; Dhall et al., 2023).

3.3 Enrichment of *Wolbachia* reads in *Brugia malayi* ATAC-seq

As mentioned in the previous section, there was an enrichment of *Wolbachia* reads in the ATAC-seq libraries compared to the gDNA libraries. We found that the read coverage is almost uniform across the *Wolbachia* genome in all of the libraries, with much higher sequencing depth in the ATAC-seq libraries (Figure 4A). The average coverage distribution across the *Wolbachia* genome was calculated for all libraries (Figures 4B,C). The gDNA libraries had a bell-shaped distribution, with an average depth of 29.5 reads, similar to that observed for the nematode chromosomes (Figure 4B; Supplementary Figure S2). The male and female ATAC-seq libraries also had a bell-shaped distribution, with an average read depth of 1856.6 and 1991 reads, respectively (Figure 4C). The sequencing depth and coverage from the ATAC-seq libraries is much higher in the *Wolbachia* chromosome than in the *B. malayi* chromosomes (Supplementary Figure S2). There are some regions with higher read depth in the *w*Bm genome with both library preparation methods, however, these regions have different coordinates in the ATAC-seq and gDNA libraries. There is a slight GC (guanine + cytosine) bias in the ATAC-seq libraries, leading to higher read coverage in genomic regions with higher GC content (Supplementary Figure S3). The gDNA libraries have an increase in sequencing depth over *nuwts*, with almost twice as many average reads compared to regions that have not been transferred to the *B. malayi* nuclear genome (Supplementary Table S2). ATAC-seq libraries have uniform depth between *nuwts* and the rest of the *w*Bm genome. Therefore, reads from *B. malayi nuwts* artificially increase read depth in gDNA libraries, while they do not appear to have any effects on ATAC-seq mapping. This means that ATAC-seq reads mapping to the *nuwts* in the *w*Bm genome most likely originate from *Wolbachia*. There is a similar distribution of reads mapping to the *w*Bm and *B. malayi* chromosomes in the adult male and adult female ATAC-seq samples (Supplementary Table S1). While the larger females contain an overall higher number of *Wolbachia*, the ratio of *Wolbachia* cells to nematode nuclei appear to be similar between the two sexes (McGarry et al., 2004). Additionally, the *Wolbachia* containing embryos were removed during nuclei isolation, resulting in a loss of the embryonic *Wolbachia* DNA in the female libraries. Therefore, it is unsurprising that the adult female samples do not have a significantly higher proportion of *Wolbachia* reads than the adult males.

3.4 *Wolbachia de novo* genome assembly

Metagenomic assemblies for female ATAC-seq and gDNA libraries were created using metaSpades(Nurk et al., 2017) from 10 million randomly subsampled reads. We used Blobtools to visualize and bin our assemblies based on GC content, BLASTN alignment, and sequencing depth (Figure 5) (Laetsch and Blaxter, 2017; Challis et al., 2020). The plots show each contig represented as a circle, where the size represents the length of the contig, and the color represents the BLAST results. GC content and read coverage are represented on the x and y-axis, respectively. In both the ATAC-seq and gDNA assemblies, the contigs cannot be binned by GC content, as both the *B. malayi* and *Wolbachia* genomes are AT rich with similar GC

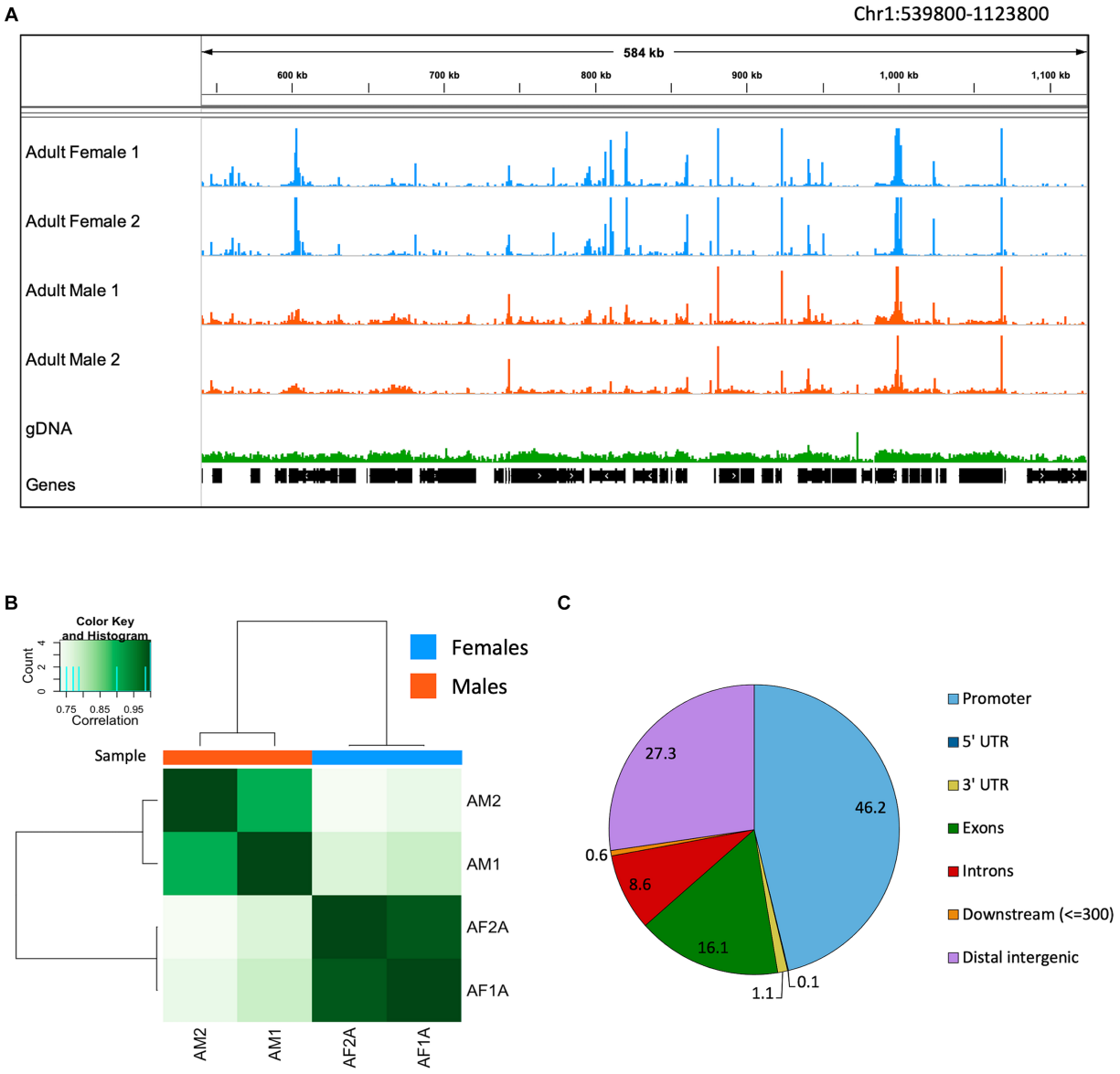

FIGURE 3
Brugia malayi chromatin accessibility. **(A)** IGV trace showing an example of ATAC-seq and gDNA read alignments in *Brugia malayi* Chr1. Adult female ATAC-seq replicates are shown in blue, adult males in orange and gDNA in green. Genes are shown in black. The scale for the ATAC-seq libraries is 0–1,500 and 0–500 for gDNA. **(B)** Heatmap showing the Pearson correlation between ATAC-seq samples. Dark colors correspond to higher correlation coefficients. **(C)** Pie chart showing proportion of ATAC-seq peaks mapped to each genomic feature.

percentages (25 and 34%, respectively) (Foster et al., 2005; Tracey et al., 2020). In the ATAC-seq assembly, the contigs can be binned by both coverage and BLAST results alone (Figure 5A). A combination of the two can be used to remove the few remaining *B. malayi* contigs from the coverage binning method. The contigs assigned to *B. malayi* with high coverage contain the ribosomal RNA (rRNA) tandem repeat, which appears to be completely open in *B. malayi* chr2 (Supplementary Figure S4), and the complete mitochondrial chromosome, which located outside of the nucleus and does not contain histones (Supplementary Figure S4). The gDNA assembly cannot be binned using coverage, as there is uniform coverage throughout both *B. malayi* and *Wolbachia* chromosomes (Figure 5B). Therefore, the contigs from the ATAC-seq assembly were binned using a coverage cutoff of 1,000, with the *B. malayi* mitochondria and rRNA tandem repeats removed, while the contigs from the gDNA assembly were binned by BLAST results only.

We end up with a more complete and correct assembly using ATAC-seq libraries compared to the gDNA library (Table 1; Figure 6). The ATAC-seq assembly has 56 contigs that align to the *w*Bm genome, covering over 97% of the reference (Figure 6A). The gDNA assembly still covers 96% of the *w*Bm genome, however the assembly is much more fragmented with 333 contigs aligning to the reference (Figure 6B). The ATAC-seq assembly has larger contigs, resulting in a much higher N50 value compared to the gDNA assembly, with 37,139 bp versus 7,533 bp, respectively (Table 1). The gDNA library has 9 misassemblies, including inversions, relocations, and translocations, while the ATAC-seq assembly has none. Additionally, the DNA from both the gDNA and ATAC-seq libraries were derived from the same

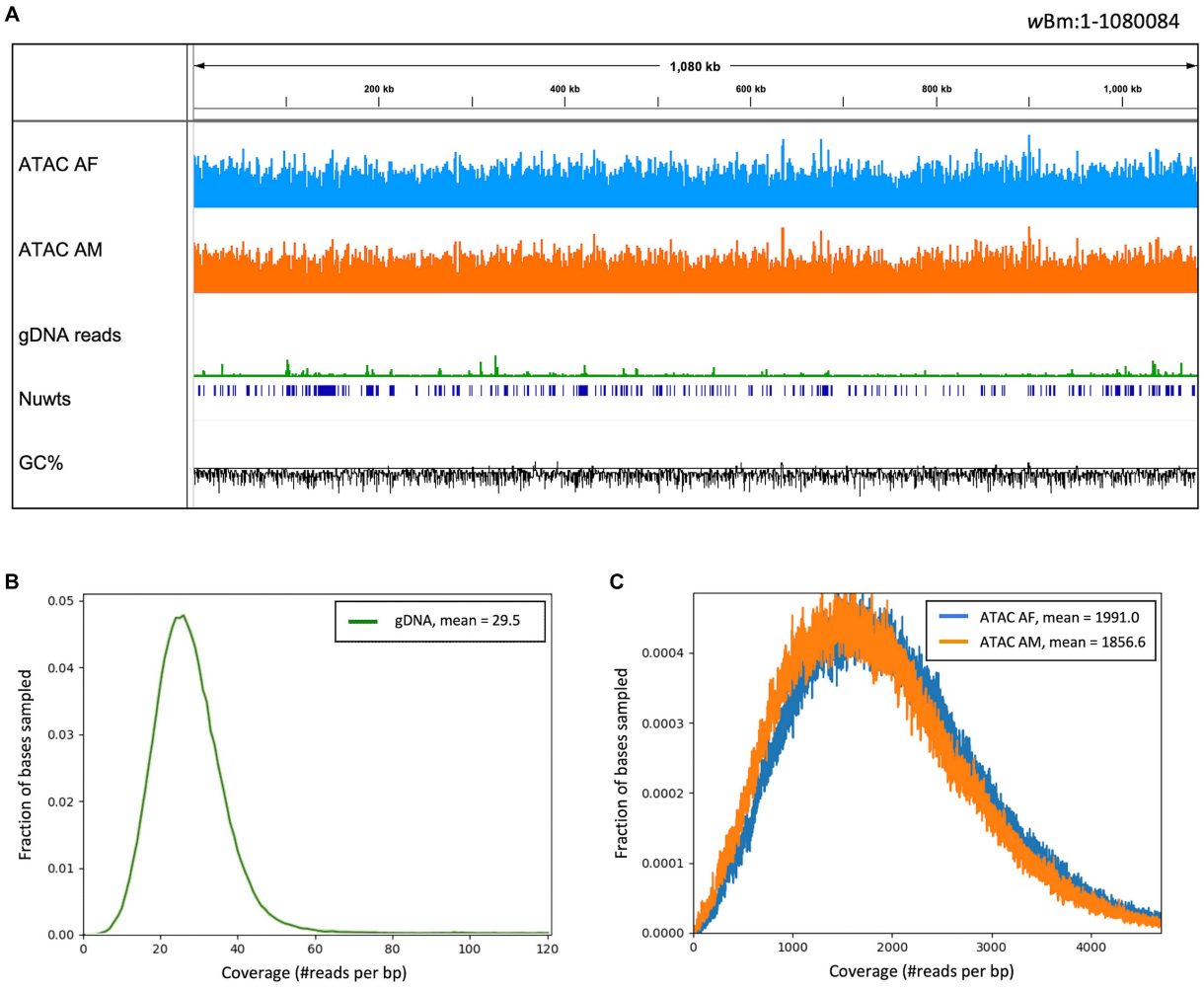

FIGURE 4
Read coverage across the *Wolbachia* genome. **(A)** IGV trace showing read alignment across the *w*Bm genome. ATAC-seq library tracks have a scale of 0–7,500 reads and the gDNA track has a scale of 1,000 reads per 50 bp bin. The nuclear transfer origins are shown in dark blue. GC fraction is shown in black with a scale of 0–1 with the solid black line representing 0.5. **(B)** Distribution of gDNA read depth across the *w*Bm genome, with an average depth of 29.5. **(C)** Distribution of ATAC-seq read depth across the *w*Bm genome. The female library has an average depth of 1991 reads and the male library has an average depth of 1856.6 reads. Colors correspond to sample type with female ATAC-seq in blue, male ATAC-seq in orange and gDNA in green. 100,000 bases were randomly sampled across the *w*Bm reference genome for **(B,C)**.

batch of worms yet the gDNA library has 308 nucleotides that do not match the *w*Bm reference genome and the ATAC-seq library only has one nucleotide change. 87.4% of the nucleotide mismatches in the gDNA assembly fall within *nuwts* and are most likely the result of nucleotide changes in the host nuclear genome. The ATAC-seq mismatch falls outside of *nuwts* and is either a real nucleotide change or is the result of a PCR error.

Although we had an average sequencing depth of almost 2000X, there are still some gaps present in the ATAC-seq assembly. To determine whether the gaps are from repetitive regions or low read coverage, we first identified repeats in the *w*Bm reference genome. These regions may be more difficult to assemble with short read sequencing. Repeat scores of the genomic sequences were calculated by taking the inverse of the mappability score (1 – m, where m = mappability). We mapped our ATAC-seq contigs onto the reference genome to identify the coordinates of our gaps and compared this to the sequencing coverage and repetitive regions (Supplementary Figure S5A). The gaps overlap with the repeats and are not correlated with read coverage and depth. However, not all repeats resulted in gaps in the assembly. When the repeats were plotted by repeat score and repeat length, we found that repeats longer than 163 bps were not assembled, except for two repeats with lengths of 557 and 584 bps (Supplementary Figure S5B). Therefore, gaps are generally caused by repeats significantly longer than our average fragment size and are not a result of low read coverage.

3.5 *De novo* genome assembly with decreasing starting sequencing reads

Deep sequencing of samples containing endosymbionts has been previously used to assemble unculturable bacterial genomes (Kumar and Blaxter, 2011; Mackelprang et al., 2011). These datasets contain hundreds of millions of reads, resulting in high sequencing and computational costs. We were able to obtain a high-quality assembly using only 10 million reads from our ATAC-seq dataset. Here,

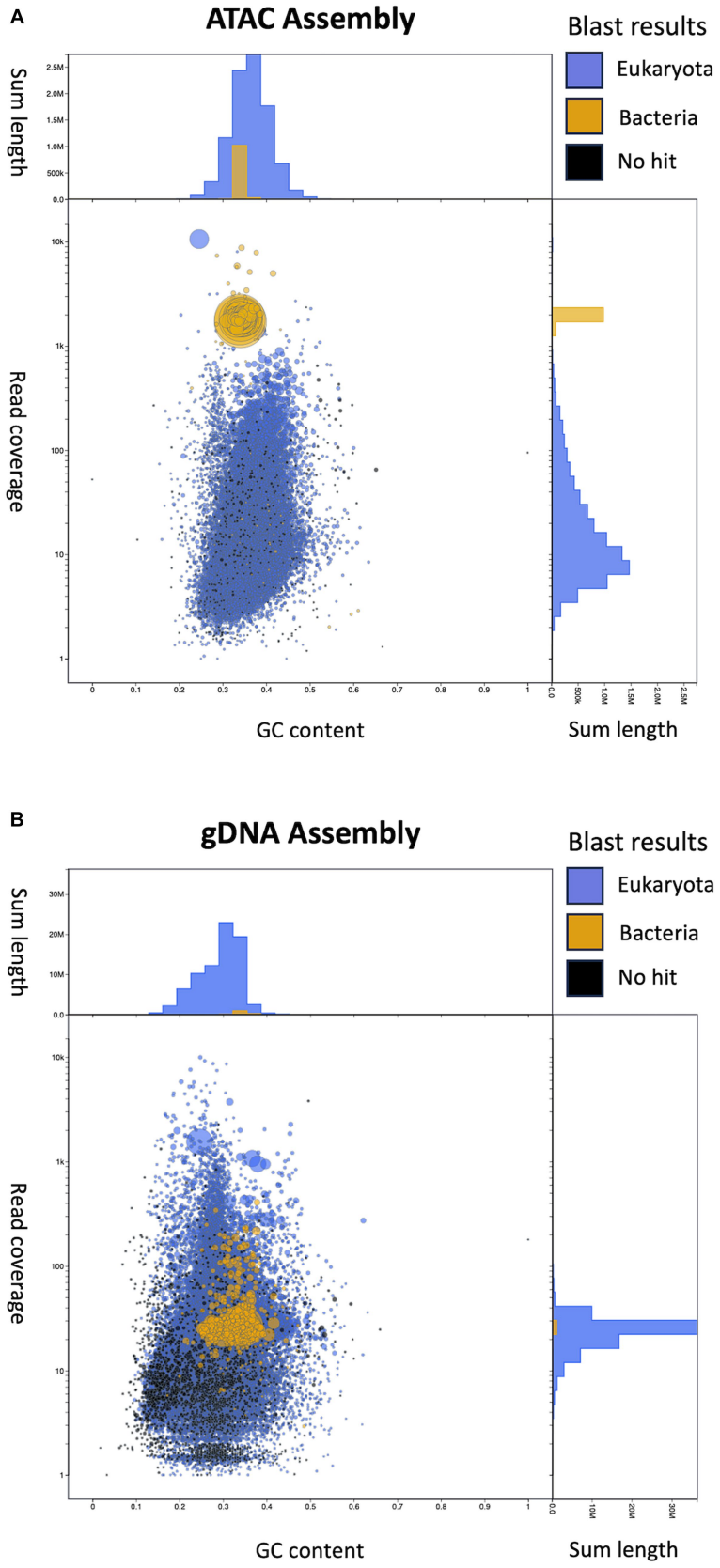

FIGURE 5
Visualization of assemblies using Blobtools. **(A)** Blobtools plot showing Female ATAC-seq *de novo* assembly. **(B)** Blobtools plot showing gDNA *de novo* assembly. In both plots, contigs are represented by circles, where the size corresponds to the length of the contig. The color of the circles displays the BLAST results, where blue contigs match eukaryotic sequences, yellow contigs match bacterial sequences and black contigs do not match to any

(Continued)

FIGURE 5 (Continued)
sequences in the NCBI Nucleotide database. The *x*-axis is the GC content of the contigs. The *y*-axis is the coverage of the contigs, after the starting reads are mapped back onto the new assemblies. The *y*-axis labels are the actual values, while the distance between tick marks is on a $\log_{10}$ scale. The length of the contigs is summed by GC content bins (top of each plot) and by converge bins (right of each plot).

TABLE 1 Genome quality statistics for the new assemblies calculated using QUAST.

Assembly	Genome fraction	# of contigs	Largest contig	N50	Misassemblies	Mismatches
ATAC-seq	97.4%	56	106,937	37,139	0	1
gDNA	96.0%	333	35,983	7,533	9	308

we further subsampled the starting read numbers to determine how many reads are necessary for *Wolbachia* genome assembly using both ATAC-seq and standard gDNA methods. The original ATAC-seq and gDNA libraries were randomly downsampled to 20, 10, 1, 0.5, 0.25 and 0.1 million total reads. These libraries with decreasing read numbers were then assembled using metaSpades (Nurk et al., 2017), as described in the previous section.

The metagenomic assemblies were evaluated and compared to the *w*Bm reference genome using QUAST (Gurevich et al., 2013). We determined the length of each new assembly and compared it to that of the reference genome (Figure 7A). The gDNA assemblies created with 20 and 10 million starting reads resulted in an over assembly of the *Wolbachia* genome, indicating sequences are either inappropriately duplicated or *B. malayi* sequences are incorrectly added into the bacterial assembly because of *nuwts*. The gDNA assembly created with 1 million reads is much shorter than the reference, meaning there is not enough sequencing coverage to assemble the bacterial genome. The ATAC-seq genomes made with 20, 10, 1 and 0.5 million reads are all assembled to a similar length as the reference. The ATAC-seq data does not have the issue with over assembly when higher numbers of starting reads are used, likey because of increased correct reads originating from *Wolbachia* cells and little to no reads from the *B. malayi nuwts*. Even at 250 thousand reads, the ATAC-seq assembly results in an almost complete genome but with a larger number of contigs.

Another important aspect of genome quality is the presence of genomic features, such as genes. We identified the number of genomic features found in our new assemblies and compared these values to the *w*Bm reference annotation which has 804 genomic features (Foster et al., 2005) (Figure 7B). The ATAC-seq assemblies with 10 and 20 million reads both have 787 genomic features assembled, while the genome from 1 million reads has slightly fewer with 779. The gDNA assembly with 20 million reads has only 730 genomic features, despite having a longer genome length. The genes present in the gDNA assemblies drop down to 677 with 10 million reads and only 6 genes assembled with 1 million starting reads. Therefore, the use of ATAC-seq for bacterial symbiont assembly results in higher quality genomes and requires a lower number of reads, resulting in less expensive sequencing costs.

3.6 Bacterial enrichment in published ATAC-seq datasets

Having determined that ATAC-seq performs efficiently as a bacterial sequence enrichment method for *B. malayi* and *Wolbachia*, we wanted to determine if this method works across diverse bacteria and eukaryote pairs using published ATAC-seq datasets (Pacis et al., 2015; Daugherty et al., 2017) (Supplementary Figure S6). Daugherty et al., published an ATAC-seq dataset in *C. elegans* across life cycle stages (Daugherty et al., 2017). We focused on the young adult sample (SRR5000677), as the nematodes at this life cycle stage consume OP50 *E. coli* as their primary food source. The dataset had 82.8% of total reads originating from *E. coli* DNA, with only 16.5% of reads mapping to *C. elegans*. Pacis et al., identified open chromatin in human dendritic cells (DCs) infected with *M. tb* using ATAC-seq (Pacis et al., 2015). The study used 5 *M. tb* cells per individual human DC. When taking into account the length of their respective genomes and the 5:1 ratio of bacterial to eukaryotic cells, we would expect 0.6% of the reads to originate from bacterial DNA if no enrichment method is used. This dataset (SRR1725731) contains 31.8% bacterial reads and 67.4% human reads. This results in a 50-fold enrichment of bacteria sequences over the expected value, similar to the enrichment we report here for *B. malayi* and *Wolbachia*. We created *de novo* assemblies from these datasets to obtain OP50 and *M. tb* genomes using metaSpades (Nurk et al., 2017). Similar to the ATAC-seq *Wolbachia* assemblies, we found higher read coverage on the bacterial contigs (Figure 8). These results demonstrate the bacterial sequence enrichment capabilities of ATAC-seq for bacteria with large genomes over 4 million bps.

4 Discussion

Sequencing of symbiont genomes is important in order to study complex co-evolution between species, including parasitic, mutualistic and obligate relationships (Moran et al., 2000; Wernegreen, 2002; McCutcheon and Moran, 2012). Here, we present a new use for ATAC-sequencing as a method of bacterial sequence enrichment for metagenome assembly. We used *B. malayi* containing the endosymbiotic bacteria *Wolbachia* as a proof of principal for *de novo* genome assembly. There is over 50-fold enrichment of bacterial sequences in our ATAC-seq datasets compared to that of the standard gDNA libraries. This is a result of the lack of histones in the bacteria. The Tn5 transposase is able to cut the bacterial DNA uniformly, whereas only a small fraction of eukaryotic chromatin is cut corresponding to regions where no nucleosomes are present. Therefore, only a small proportion of the *B. malayi* genome is sequenced, while the whole *Wolbachia* genome is sequenced at high levels. Future ATAC-seq datasets containing a mixture of prokaryotic and eukaryotic organisms will determine if this method can be used to quantify the ratio of bacterial cells and host cells present within a sample.

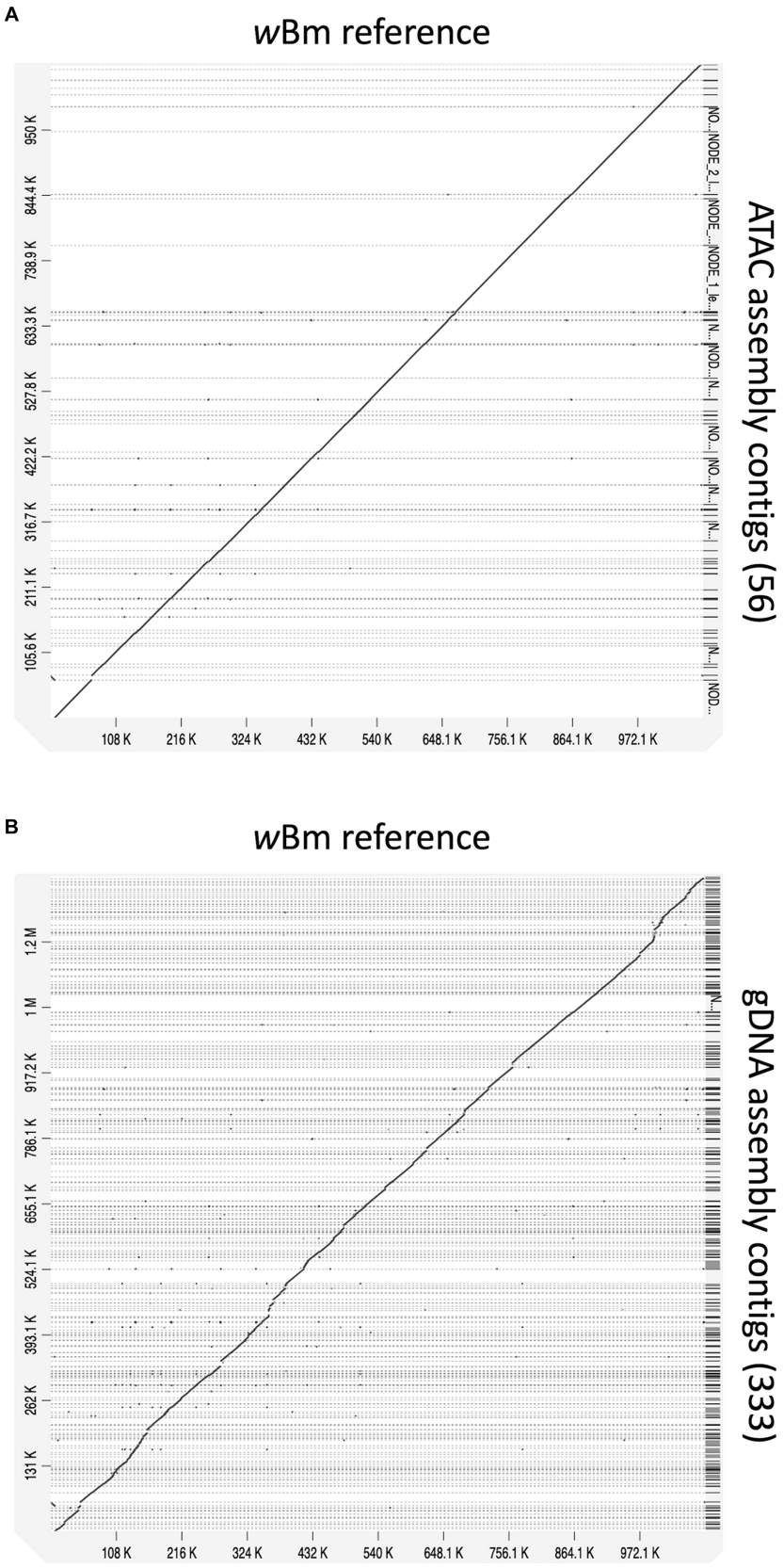

FIGURE 6
Alignments of new assemblies to the *w*Bm reference genome. **(A)** ATAC-seq assembly with 56 contigs mapping to the *w*Bm reference genome. **(B)** gDNA assembly with 333 contigs mapping to the *w*Bm reference genome. The genomes were aligned using minimap2 and the dot plots were created with D-genies. All contigs are sorted based on the coordinates of the reference genome. Grey dashed lines represent contig boundaries.

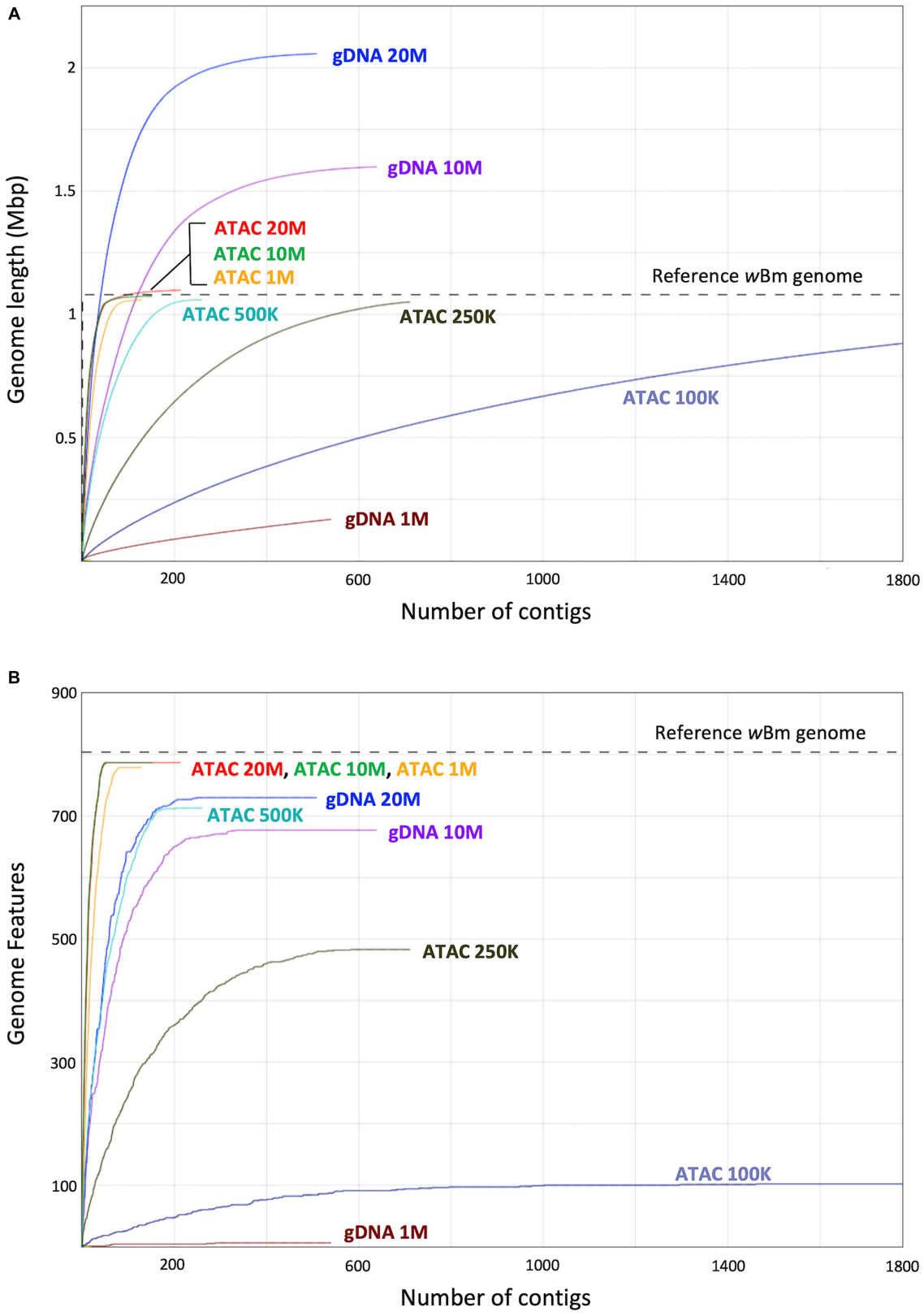

FIGURE 7
Genome length and genomic feature calculations from assemblies with decreasing input reads. **(A)** Graph showing the length of assemblies with decreasing starting reads compared to the *w*Bm reference genome. The *x*-axis represents the number of contigs, and the y-axis represents the sum length of the contigs in millions of base pairs. **(B)** Graph showing the number of genomic features (genes) found in each assembly compared to that of the *w*Bm reference genome. The *x*-axis represents the number of contigs, and the *y*-axis represents the sum of the genomic features assembled. The color of the line represents the assembly. In both panels the grey dotted line corresponds to the corresponding value in the *w*Bm reference genome.

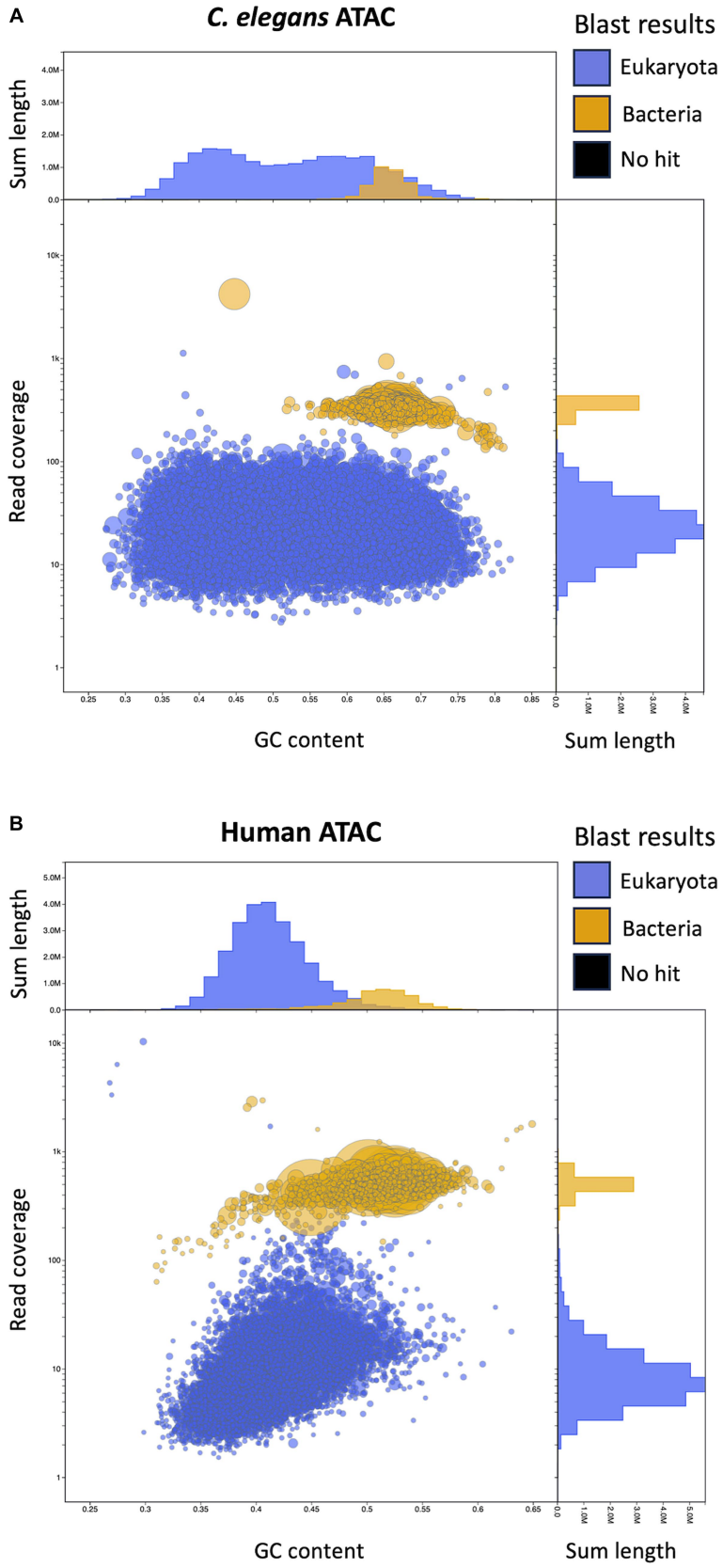

FIGURE 8
Visualization of *C. elegans* with *E. coli* and Human with *M. tb* ATAC-seq assemblies with Blobtools. **(A)** Blobtools plot showing *de novo* genome assembly from published *C. elegans* ATAC-seq data contaminated with OP50 *E. coli*. **(B)** Blobtools plot showing *de novo* genome assembly with published ATAC-seq data from human DCs infected with *M. tb*. Further details for the plot organization are described in the Figure 5 legend.

When mapped to the *B. malayi* nuclear chromosomes, the ATAC-seq reads pile up in peaks, corresponding to the accessible regions of the genome. The chromatin structure is unique across adult males and females, which may lead to their specialized gene expression. The peaks are highly enriched in gene promoters, with a proportion of 46.2%. This enrichment is higher than what is typically observed in mammals (Chung et al., 2018; Yan et al., 2020). Similar to *B. malayi*, nearly 50% of peaks fall in promoter regions in *Drosophila melanogaster* (Santiago et al., 2021; Dhall et al., 2023). There appears to be a smaller proportion of enhancers in nematodes and arthropods when compared to mammals, which may relate to their smaller genomes.

With the high proportion of reads mapping to the *Wolbachia* chromosome, we hypothesized that ATAC-seq could be an efficient sequencing method for *de novo* genome assembly of bacterial endosymbionts. We assembled genomes from both the ATAC-seq and gDNA libraries using metaSpades and performed quality assessment using Blobtools and QUAST (Gurevich et al., 2013; Laetsch and Blaxter, 2017; Nurk et al., 2017). The ATAC-seq assembly can be binned into *Wolbachia* and *B. malayi* contigs by read coverage alone, meaning a reference genome is not required to separate out the bacterial genome. This method can be useful when working with samples that contain unknown bacterial species. The ATAC-seq assembly is also higher quality than gDNA assembly across every metric measured, including contig number, N50, misassemblies, and nucleotide mismatches. The gDNA genome is over assembled, meaning that sequences are inappropriately incorporated into the assembly. This results in a longer length and an increased number of misassemblies. Additionally, the gDNA assembly has over 300 incorrect nucleotide changes compared to just one in the ATAC assembly. The gDNA assembly seems to be affected by *nuwt* sequences from the *B. malayi* nuclear genome, as these chromosomes have similar sequencing depth to the *w*Bm genome. Therefore, the assembler cannot determine which sequence is correct for the *Wolbachia* assembly, resulting in *B. malayi* sequence incorporation. The ATAC-seq assembly does not have this issue, as there is significantly more sequencing depth over the regions transferred as nuwts originating from the *Wolbachia*, resulting in incorporation of the correct bacterial sequences. ATAC-seq shows vast improvement on assembly with symbiotic species which have experienced lateral gene transfer. Additionally, with ATAC-seq assembly, as few as 1 million starting reads can be used, while maintaining high quality of the resulting genome, including total length, low contig number and a high proportion of assembled genes. This aspect of ATAC-seq allows for lower sequencing and computational costs when compared to standard deep sequencing methods.

One drawback to the ATAC-seq enrichment method is the use of short read sequencing. Longer reads cannot be used, as enrichment involves the cutting of the histone free DNA. Despite high read coverage across the entire *Wolbachia* genome, we still have some gaps between contigs, specifically in highly repetitive regions. Repeats significantly longer than our fragment sizes could not be assembled, regardless of coverage depth. While ATAC-seq can still be used for high quality *de novo* genome assembly, it will also be useful for bacterial population genomics or SNP analysis, where short read sequencing is commonly used in combination with a long-read based reference genome (Joseph and Read, 2010; Epstein et al., 2012; Cornejo et al., 2013). Optimization of the ATAC-seq protocol, such as enzyme dilution, or lower Tn5 temperature and incubation time, may allow for longer reads. The ATAC-seq libraries also show more of a GC bias than the gDNA libraries. Therefore, ATAC-seq appears to be more sensitive to PCR bias with increasing PCR cycles (Benjamini and Speed, 2012). In future experiments, a lower number of cycles can be used, as we obtained a high yield from the ATAC libraries using 10 cycles.

Many comparative genomics studies are from field and clinical samples, where the starting material is limited, and the bacteria are unculturable outside of the host. An additional advantage to ATAC-seq, beyond bacterial sequence enrichment, is low sample input requirements. ATAC-seq can be performed on as little as 500 total cells with less than a day of library preparation time (Grandi et al., 2022).

Finally, ATAC-seq bacterial enrichment can be used beyond *Wolbachia* genome assembly. Bacterial enrichment was found in two previously published ATAC-seq datasets in *C. elegans* and human DCs (Pacis et al., 2015; Daugherty et al., 2017). Over 80% of reads from the *C. elegans* library originated from their food source, OP50 *E.coli*. In human DCs ATAC-seq data, there was also a 50-fold enrichment of *M. tb* sequences, similar to what we observed in our *B. malayi* and *Wolbachia* dataset. We were able to perform *de novo* assembly on the *C. elegan* and human libraries, resulting in bacterial genomes around 4 million base pairs long. These results show the utility of ATAC-seq enrichment across a wide variety of samples containing both eukaryotes and bacteria.

5 Conclusion

ATAC-seq provides a novel enrichment method for unculturable endosymbiotic bacterial sequences and can improve metagenome assembled genomes. We assembled higher quality genomes using ATAC-seq compared to standard gDNA sequencing, with as few as 1 million starting reads. Lateral gene transfer is common between closely associated bacterial endosymbionts and their eukaryotic hosts. ATAC-seq is able to correctly assemble these sequences that have been transferred to the host nuclear genome, while standard gDNA sequencing results in incorporation of incorrect sequences due to similar sequencing coverage of the bacteria and host. Compared to other symbiont sequencing methods, ATAC-seq requires a very low amount of starting material and sequencing depth. One of the main benefits of this method is the ability to enrich, sequence, assemble and bin contigs from unknown bacterial species, as no reference genome is required. ATAC-seq bacterial sequence enrichment will be beneficial for studying the complex relationships between bacteria and eukaryotes in symbiosis, infectious disease, agriculture, and microbiome research.

Data availability statement

The datasets presented in this study can be found in online repositories. The names of the repository/repositories and accession number(s) can be found at: https://www.ncbi.nlm.nih.gov/, PRJNA1043224 https://figshare.com/, doi:10.6084/m9.figshare.24703149.v1 https://figshare.com/, doi:10.6084/m9.figshare.24701145.

v1 https://figshare.com/, doi:10.6084/m9.figshare.24702282.v1 https://figshare.com/, doi:10.6084/m9.figshare.24702858.v1.

Author contributions

LC: Conceptualization, Formal analysis, Investigation, Methodology, Visualization, Writing – original draft, Writing – review & editing. JD: Funding acquisition, Supervision, Writing – review & editing. JF: Conceptualization, Funding acquisition, Supervision, Writing – review & editing.

Funding

The author(s) declare financial support was received for the research, authorship, and/or publication of this article. Research and salaries were funded by New England BioLabs and by federal funds from the National Institute of Allergy and Infectious Diseases, National Institute of Health, Department of Health and Human Services under grant number U19AI110820.

Acknowledgments

We thank New England BioLabs for supporting parasitology research, particularly Thomas Evans, Salvatore Russello and the late Donald Comb. We would also like to thank the NEB sequencing core. Finally, we acknowledge the Filariasis Research reagent Resource Center for supplying the nematodes used in this study.

Conflict of interest

The authors declare that the research was conducted in the absence of any commercial or financial relationships that could be construed as a potential conflict of interest.

Publisher's note

Supplementary material

The Supplementary material for this article can be found online at: https://www.frontiersin.org/articles/10.3389/fmicb.2024.1352378/full#supplementary-material

References

Acuña, R., Padilla, B. E., Flórez-Ramos, C. P., Rubio, J. D., Herrera, J. C., Benavides, P., et al. (2012). Adaptive horizontal transfer of a bacterial gene to an invasive insect pest of coffee. *Proc. Natl. Acad. Sci. USA* 109, 4197–4202. doi: 10.1073/pnas.1121190109

Aljayyoussi, G., Tyrer, H. E., Ford, L., Sjoberg, H., Pionnier, N., Waterhouse, D., et al. (2017). Short-course, high-dose rifampicin achieves Wolbachia depletion predictive of curative outcomes in preclinical models of lymphatic Filariasis and onchocerciasis. *Sci. Rep.* 7:210. doi: 10.1038/s41598-017-00322-5

Almeida, A., Mitchell, A. L., Boland, M., Forster, S. C., Gloor, G. B., Tarkowska, A., et al. (2019). A new genomic blueprint of the human gut microbiota. *Nature* 568, 499–504. doi: 10.1038/s41586-019-0965-1

Altschul, S. F., Gish, W., Miller, W., Myers, E. W., and Lipman, D. J. (1990). Basic local alignment search tool. *J. Mol. Biol.* 215, 403–410. doi: 10.1016/S0022-2836(05)80360-2

Andrews, S. FastQC. (2023). Available at: https://github.com/s-andrews/FastQC (Accessed October 31, 2023).

Ashton, M., Rosado, W., Govind, N. S., and Tosteson, T. R. (2003). Culturable and nonculturable bacterial symbionts in the toxic benthic dinoflagellate *Ostreopsis lenticularis*. *Toxicon* 42, 419–424. doi: 10.1016/S0041-0101(03)00174-0

Bäckhed, F., Ley, R. E., Sonnenburg, J. L., Peterson, D. A., and Gordon, J. I. (2005). Host-bacterial mutualism in the human intestine. *Science* 307, 1915–1920. doi: 10.1126/science.1104816

Balloux, F., and van Dorp, L. (2017). Q&a: what are pathogens, and what have they done to and for us? *BMC Biol.* 15:91. doi: 10.1186/s12915-017-0433-z

Bandi, C., Anderson, T. J., Genchi, C., and Blaxter, M. L. (1998). Phylogeny of Wolbachia in filarial nematodes. *Proc. R. Soc. B Biol. Sci.* 265, 2407–2413. doi: 10.1098/rspb.1998.0591

Bandi, C., Trees, A. J., and Brattig, N. W. (2001). Wolbachia in filarial nematodes: evolutionary aspects and implications for the pathogenesis and treatment of filarial diseases. *Vet. Parasitol.* 98, 215–238. doi: 10.1016/S0304-4017(01)00432-0

Bazzocchi, C., Mortarino, M., Grandi, G., Kramer, L. H., Genchi, C., Bandi, C., et al. (2008). Combined ivermectin and doxycycline treatment has microfilaricidal and adulticidal activity against Dirofilaria immitis in experimentally infected dogs. *Int. J. Parasitol.* 38, 1401–1410. doi: 10.1016/j.ijpara.2008.03.002

Benjamini, Y., and Speed, T. P. (2012). Summarizing and correcting the GC content bias in high-throughput sequencing. *Nucleic Acids Res.* 40:e72. doi: 10.1093/nar/gks001

Broadinstitute/picard Broad institute; (2023). Available at: https://github.com/broadinstitute/picard (Accessed October 31, 2023).

Buenrostro, J. D., Giresi, P. G., Zaba, L. C., Chang, H. Y., and Greenleaf, W. J. (2013). Transposition of native chromatin for fast and sensitive epigenomic profiling of open chromatin, DNA-binding proteins and nucleosome position. *Nat. Meth.* 10, 1213–1218. doi: 10.1038/nmeth.2688

Bull, M. J., and Plummer, N. T. (2014). Part 1: the human gut microbiome in health and disease. *Integr Med Clin J.* 13, 17–22.

Cabanettes, F., and Klopp, C. (2018). D-GENIES: dot plot large genomes in an interactive, efficient and simple way. *PeerJ.* 6:e4958. doi: 10.7717/peerj.4958

Camacho, C., Coulouris, G., Avagyan, V., Ma, N., Papadopoulos, J., Bealer, K., et al. (2009). BLAST+: architecture and applications. *BMC Bioinform.* 10:421. doi: 10.1186/1471-2105-10-421

Campbell, W. C. (1991). Ivermectin as an antiparasitic agent for use in humans. *Ann. Rev. Microbiol.* 45, 445–474. doi: 10.1146/annurev.mi.45.100191.002305

Challis, R, Richards, E, Rajan, J, Cochrane, G, and Blaxter, M. BlobToolKit – interactive quality assessment of genome assemblies. *G3 Genes Genomes Genetics.* (2020); 10:1361–74. doi: 10.1534/g3.119.400908

Chen, H., Zhang, M., and Hochstrasser, M. (2020). The biochemistry of cytoplasmic incompatibility caused by endosymbiotic Bacteria. *Genes* 11:852. doi: 10.3390/genes11080852

Chung, M, Teigen, L, Libro, S, Bromley, RE, Kumar, N, Sadzewicz, L, et al. (2018). Multispecies transcriptomics data set of Brugia malayi, its Wolbachia endosymbiont wBm, and *Aedes aegypti* across the B. Malayi life cycle. *Microbiol. Res. Announc.* 7:e01306-18.

Clare, R. H., Bardelle, C., Harper, P., Hong, W. D., Börjesson, U., Johnston, K. L., et al. (2019). Industrial scale high-throughput screening delivers multiple fast acting macrofilaricides. *Nat. Commun.* 10:11. doi: 10.1038/s41467-018-07826-2

Corces, M. R., Trevino, A. E., Hamilton, E. G., Greenside, P. G., Sinnott-Armstrong, N. A., Vesuna, S., et al. (2017). An improved ATAC-seq protocol reduces background and enables interrogation of frozen tissues. *Nat. Meth.* 14, 959–962. doi: 10.1038/nmeth.4396

Cornejo, O. E., Lefébure, T., Pavinski Bitar, P. D., Lang, P., Richards, V. P., Eilertson, K., et al. (2013). Evolutionary and population genomics of the cavity causing Bacteria *Streptococcus mutans*. *Mol. Biol. Evol.* 30, 881–893. doi: 10.1093/molbev/mss278

Coulibaly, Y. I., Dembele, B., Diallo, A. A., Lipner, E. M., Doumbia, S. S., Coulibaly, S. Y., et al. (2009). A randomized trial of doxycycline for Mansonella perstans infection. *N. Engl. J. Med.* 361, 1448–1458. doi: 10.1056/NEJMoa0900863

Dam, H. T., Vollmers, J., Sobol, M. S., Cabezas, A., and Kaster, A. K. (2020). Targeted cell sorting combined with single cell genomics captures low abundant microbial dark matter with higher sensitivity than metagenomics. *Front Microbiol* 11, 11:1377. doi: 10.3389/fmicb.2020.01377

Darby, A. C., Armstrong, S. D., Bah, G. S., Kaur, G., Hughes, M. A., Kay, S. M., et al. (2012). Analysis of gene expression from the Wolbachia genome of a filarial nematode supports both metabolic and defensive roles within the symbiosis. *Genome Res.* 22, 2467–2477. doi: 10.1101/gr.138420.112

Daugherty, A. C., Yeo, R. W., Buenrostro, J. D., Greenleaf, W. J., Kundaje, A., and Brunet, A. (2017). Chromatin accessibility dynamics reveal novel functional enhancers in *C. elegans*. *Genome Res.* 27, 2096–2107. doi: 10.1101/gr.226233.117

Dhall, J. K., Kasturacharya, N., Pandit, A., and Cp, L. (2023). Optimized protocol for assay for transposase-accessible chromatin by sequencing (ATAC-seq) from *Drosophila melanogaster* brain tissue. *STAR Protoc.* 4:102153. doi: 10.1016/j.xpro.2023.102153

Douglas, A. E. (2014). Symbiosis as a general principle in eukaryotic evolution. *Cold Spring Harb. Perspect. Biol.* 6:a016113. doi: 10.1101/cshperspect.a016113

Drew, G. C., Stevens, E. J., and King, K. C. (2021). Microbial evolution and transitions along the parasite–mutualist continuum. *Nat. Rev. Microbiol.* 19, 623–638. doi: 10.1038/s41579-021-00550-7

Epstein, B., Branca, A., Mudge, J., Bharti, A. K., Briskine, R., Farmer, A. D., et al. (2012). Population genomics of the Facultatively mutualistic Bacteria Sinorhizobium meliloti and *S. medicae*. *PLoS Genet.* 8:e1002868. doi: 10.1371/journal.pgen.1002868

Fenollar, F., La Scola, B., Inokuma, H., Dumler, J. S., Taylor, M. J., and Raoult, D. (2003). Culture and phenotypic characterization of a *Wolbachia pipientis* isolate. *J. Clin. Microbiol.* 41, 5434–5441. doi: 10.1128/JCM.41.12.5434-5441.2003

Foster, J., Ganatra, M., Kamal, I., Ware, J., Makarova, K., Ivanova, N., et al. (2005). The Wolbachia genome of Brugia malayi: endosymbiont evolution within a human pathogenic nematode. *PLoS Biol.* 3:e121. doi: 10.1371/journal.pbio.0030121

Foster, J. M., Kumar, S., Ganatra, M. B., Kamal, I. H., Ware, J., Ingram, J., et al. (2004). Construction of bacterial artificial chromosome libraries from the parasitic nematode *Brugia malayi* and physical mapping of the genome of its *Wolbachia* endosymbiont. *Int. J. Parasitol.* 34, 733–746. doi: 10.1016/j.ijpara.2004.02.001

Geniez, S., Foster, J. M., Kumar, S., Moumen, B., LeProust, E., Hardy, O., et al. (2012). Targeted genome enrichment for efficient purification of endosymbiont DNA from host DNA. *Symbiosis Phila Pa.* 58, 201–207. doi: 10.1007/s13199-012-0215-x

Gladyshev, E. A., Meselson, M., and Arkhipova, I. R. (2008). Massive Horizontal Gene Transfer in Bdelloid Rotifers. *Science* 320, 1210–1213. doi: 10.1126/science.1156407

Grandi, F. C., Modi, H., Kampman, L., and Corces, M. R. (2022). Chromatin accessibility profiling by ATAC-seq. *Nat. Protoc.* 17, 1518–1552. doi: 10.1038/s41596-022-00692-9

Grote, A., Voronin, D., Ding, T., Twaddle, A., Unnasch, T. R., Lustigman, S., et al. (2017). Defining Brugia malayi and Wolbachia symbiosis by stage-specific dual RNA-seq. *PLoS Negl. Trop. Dis.* 11:e0005357. doi: 10.1371/journal.pntd.0005357

Gurevich, A., Saveliev, V., Vyahhi, N., and Tesler, G. (2013). QUAST: quality assessment tool for genome assemblies. *Bioinformatics* 29, 1072–1075. doi: 10.1093/bioinformatics/btt086

Hedges, L. M., Brownlie, J. C., O'Neill, S. L., and Johnson, K. N. (2008). Wolbachia and virus protection in insects. *Science* 322:702. doi: 10.1126/science.1162418

Hilgenboecker, K., Hammerstein, P., Schlattmann, P., Telschow, A., and Werren, J. H. (2008). How many species are infected with Wolbachia? – a statistical analysis of current data. *FEMS Microbiol. Lett.* 281, 215–220. doi: 10.1111/j.1574-6968.2008.01110.x

Hoerauf, A., Specht, S., Büttner, M., Pfarr, K., Mand, S., Fimmers, R., et al. (2008). Wolbachia endobacteria depletion by doxycycline as antifilarial therapy has macrofilaricidal activity in onchocerciasis: a randomized placebo-controlled study. *Med. Microbiol. Immunol.* 197, 295–311. doi: 10.1007/s00430-007-0062-1

Hongoh, Y. (2010). Diversity and genomes of uncultured microbial symbionts in the termite gut. *Biosci. Biotechnol. Biochem.* 74, 1145–1151. doi: 10.1271/bbb.100094

Hotopp, J. C. D., Clark, M. E., Oliveira, D. C. S. G., Foster, J. M., Fischer, P., Torres, M. C. M., et al. (2007). Widespread lateral gene transfer from intracellular Bacteria to multicellular eukaryotes. *Science* 317, 1753–1756. doi: 10.1126/science.1142490

Husnik, F., Nikoh, N., Koga, R., Ross, L., Duncan, R. P., Fujie, M., et al. (2013). Horizontal gene transfer from diverse Bacteria to an insect genome enables a tripartite nested mealybug Symbiosis. *Cell* 153, 1567–1578. doi: 10.1016/j.cell.2013.05.040

Ioannidis, P., Johnston, K. L., Riley, D. R., Kumar, N., White, J. R., Olarte, K. T., et al. (2013). Extensively duplicated and transcriptionally active recent lateral gene transfer from a bacterial Wolbachia endosymbiont to its host filarial nematode Brugia malayi. *BMC Genom.* 14:639. doi: 10.1186/1471-2164-14-639

Johnston, K. L., Ford, L., Umareddy, I., Townson, S., Specht, S., Pfarr, K., et al. (2014). Repurposing of approved drugs from the human pharmacopoeia to target Wolbachia endosymbionts of onchocerciasis and lymphatic filariasis. *Int. J. Parasitol. Drugs Drug Resist.* 4, 278–286. doi: 10.1016/j.ijpddr.2014.09.001

Johnston, K. L., Hong, W. D., Turner, J. D., O'Neill, P. M., Ward, S. A., and Taylor, M. J. (2021). Anti-Wolbachia drugs for filariasis. *Trends Parasitol.* 37, 1068–1081. doi: 10.1016/j.pt.2021.06.004

Joseph, S. J., and Read, T. D. (2010). Bacterial population genomics and infectious disease diagnostics. *Trends Biotechnol.* 28, 611–618. doi: 10.1016/j.tibtech.2010.09.001

Kent, B. N., Salichos, L., Gibbons, J. G., Rokas, A., Newton, I. L. G., Clark, M. E., et al. (2011). Complete bacteriophage transfer in a bacterial endosymbiont (Wolbachia) determined by targeted genome capture. *Genome Biol. Evol.* 3, 209–218. doi: 10.1093/gbe/evr007

Kneip, C., Lockhart, P., Voß, C., and Maier, U. G. (2007). Nitrogen fixation in eukaryotes – new models for symbiosis. *BMC Evol. Biol.* 7:55. doi: 10.1186/1471-2148-7-55

Kozek, W. J. (1977). Transovarially-transmitted intracellular microorganisms in adult and larval stages of Brugia malayi. *J. Parasitol.* 63, 992–1000. doi: 10.2307/3279832

Kumar, S., and Blaxter, M. L. (2011). Simultaneous genome sequencing of symbionts and their hosts. *Symbiosis* 55, 119–126. doi: 10.1007/s13199-012-0154-6

Laetsch, DR, and Blaxter, ML. BlobTools: interrogation of genome assemblies. F1000 Research; (2017) 6:1287. Available at: https://f1000research.com/articles/6-1287 (Accessed October 31, 2023).

Landmann, F., Foster, J. M., Slatko, B., and Sullivan, W. (2010). Asymmetric Wolbachia segregation during early Brugia malayi embryogenesis determines its distribution in adult host tissues. *PLoS Negl. Trop. Dis.* 4:e758. doi: 10.1371/journal.pntd.0000758

Langmead, B., and Salzberg, S. L. (2012). Fast gapped-read alignment with bowtie 2. *Nat. Methods* 9, 357–359. doi: 10.1038/nmeth.1923

Lefoulon, E., Vaisman, N., Frydman, H. M., Sun, L., Voland, L., Foster, J. M., et al. (2019). Large enriched fragment targeted sequencing (LEFT-SEQ) applied to capture of Wolbachia genomes. *Sci. Rep.* 9:5939. doi: 10.1038/s41598-019-42454-w

Li, H. (2018). Minimap2: pairwise alignment for nucleotide sequences. *Bioinformatics* 34, 3094–3100. doi: 10.1093/bioinformatics/bty191

Li, H. *lh3/seqtk*. (2023). Available at: https://github.com/lh3/seqtk (Accessed October 31, 2023).

Li, Z., and Carlow, C. K. S. (2012). Characterization of transcription factors that regulate the type IV secretion system and riboflavin biosynthesis in *Wolbachia* of *Brugia malayi*. *PLoS One* 7:e51597. doi: 10.1371/journal.pone.0051597

Li, H., Handsaker, B., Wysoker, A., Fennell, T., Ruan, J., Homer, N., et al. (2009). The sequence alignment/map format and SAMtools. *Bioinformatics* 25, 2078–2079. doi: 10.1093/bioinformatics/btp352

Luck, A. N., Yuan, X., Voronin, D., Slatko, B. E., Hamza, I., and Foster, J. M. (2016). Heme acquisition in the parasitic filarial nematode *Brugia malayi*. *FASEB J.* 30, 3501–3514. doi: 10.1096/fj.201600603R

Mackelprang, R., Waldrop, M. P., DeAngelis, K. M., David, M. M., Chavarria, K. L., Blazewicz, S. J., et al. (2011). Metagenomic analysis of a permafrost microbial community reveals a rapid response to thaw. *Nature* 480, 368–371. doi: 10.1038/nature10576

Mackenzie, C. D., Malecela, M., Mueller, I., and Homeida, M. A. (2002). "Approaches to the control and elimination of the clinically important filarial diseases" in *The Filaria* (Boston, MA: Springer), 155–165.

Mand, S., Pfarr, K., Sahoo, P. K., Satapathy, A. K., Specht, S., Klarmann, U., et al. (2009). Macrofilaricidal activity and amelioration of lymphatic pathology in Bancroftian Filariasis after 3 weeks of doxycycline followed by single-dose Diethylcarbamazine. *Am. J. Trop. Med. Hyg.* 81, 702–711. doi: 10.4269/ajtmh.2009.09-0155

Manni, M., Berkeley, M. R., Seppey, M., and Zdobnov, E. M. (2021). BUSCO: assessing genomic data quality and beyond. *Curr Protoc.* 1:e323. doi: 10.1002/cpz1.323

Martin, M. (2011). Cutadapt removes adapter sequences from high-throughput sequencing reads. *EMBnet.journal.* 17, 10–12. doi: 10.14806/ej.17.1.200

Masson, F., and Lemaitre, B. (2020). Growing Ungrowable Bacteria: overview and perspectives on insect symbiont Culturability. *Microbiol. Mol. Biol. Rev.* 84, e00089–20. doi: 10.1128/mmbr.00089-20

McCutcheon, J. P. (2010). The bacterial essence of tiny symbiont genomes. *Curr. Opin. Microbiol.* 13, 73–78. doi: 10.1016/j.mib.2009.12.002

McCutcheon, J. P., and Moran, N. A. (2012). Extreme genome reduction in symbiotic bacteria. *Nat. Rev. Microbiol.* 10, 13–26. doi: 10.1038/nrmicro2670

McGarry, H. F., Egerton, G. L., and Taylor, M. J. (2004). Population dynamics of Wolbachia bacterial endosymbionts in Brugia malayi. *Mol. Biochem. Parasitol.* 135, 57–67. doi: 10.1016/j.molbiopara.2004.01.006

Mclaren, D. J., Worms, M. J., Laurence, B. R., and Simpson, M. G. (1975). Micro-organisms in filarial larvae (Nematoda). *Trans. R. Soc. Trop. Med. Hyg.* 69, 509–514. doi: 10.1016/0035-9203(75)90110-8

Medeiros, ZM, AVB, Vieira, Xavier, AT, GSN, Bezerra, de FC, Lopes M, Bonfim, CV, et al. Lymphatic Filariasis: a systematic review on morbidity and its repercussions in countries in the Americas. *Int. J. Environ. Res. Public Health*. (2021); 19:316. doi: 10.3390/ijerph19010316

Melnikov, A., Galinsky, K., Rogov, P., Fennell, T., Van Tyne, D., Russ, C., et al. (2011). Hybrid selection for sequencing pathogen genomes from clinical samples. *Genome Biol.* 12:R73. doi: 10.1186/gb-2011-12-8-r73

Michalski, ML, Griffiths, KG, Williams, SA, Kaplan, RM, and Moorhead, AR. The NIH-NIAID Filariasis research reagent resource center. M Knight, *PLoS Negl. Trop. Dis.* (2011). 5:e1261. doi: 10.1371/journal.pntd.0001261

Molyneux, D. H., Bradley, M., Hoerauf, A., Kyelem, D., and Taylor, M. J. (2003). Mass drug treatment for lymphatic filariasis and onchocerciasis. *Trends Parasitol.* 19, 516–522. doi: 10.1016/j.pt.2003.09.004

Moran, N. A., Wernegreen, J. J., Moran, N. A., and Wernegreen, J. J. (2000). Lifestyle evolution in symbiotic bacteria: insights from genomics. *Trends Ecol. Evol.* 15, 321–326. doi: 10.1016/S0169-5347(00)01902-9

Neely, A. E., and Bao, X. (2019). Nuclei isolation staining (NIS) method for imaging chromatin-associated proteins in difficult cell types. *Curr. Protoc. Cell Biol.* 84:e94. doi: 10.1002/cpcb.94

Nurk, S., Meleshko, D., Korobeynikov, A., and Pevzner, P. A. (2017). metaSPAdes: a new versatile metagenomic assembler. *Genome Res.* 27, 824–834. doi: 10.1101/gr.213959.116

Pacis, A., Tailleux, L., Morin, A. M., Lambourne, J., MacIsaac, J. L., Yotova, V., et al. (2015). Bacterial infection remodels the DNA methylation landscape of human dendritic cells. *Genome Res.* 25, 1801–1811. doi: 10.1101/gr.192005.115

Pockrandt, C., Alzamel, M., Iliopoulos, C. S., and Reinert, K. (2020). GenMap: ultra-fast computation of genome mappability. *Bioinformatics* 36, 3687–3692. doi: 10.1093/bioinformatics/btaa222

Prjibelski, A., Antipov, D., Meleshko, D., Lapidus, A., and Korobeynikov, A. (2020). Using SPAdes De novo assembler. *Curr Protoc Bioinform.* 70:e102. doi: 10.1002/cpbi.102

Quek, S., Cook, D. A. N., Wu, Y., Marriott, A. E., Steven, A., Johnston, K. L., et al. (2022). Wolbachia depletion blocks transmission of lymphatic filariasis by preventing chitinase-dependent parasite exsheathment. *Proc. Natl. Acad. Sci.* 119:e2120003119. doi: 10.1073/pnas.2120003119

Quinlan, A. R., and Hall, I. M. (2010). BEDTools: a flexible suite of utilities for comparing genomic features. *Bioinformatics* 26, 841–842. doi: 10.1093/bioinformatics/btq033

Ramírez, F., Dündar, F., Diehl, S., Grüning, B. A., and Manke, T. (2014). deepTools: a flexible platform for exploring deep-sequencing data. *Nucleic Acids Res.* 42, W187–W191. doi: 10.1093/nar/gku365

Richards, F. O., Boatin, B., Sauerbrey, M., and Sékétéli, A. (2001). Control of onchocerciasis today: status and challenges. *Trends Parasitol.* 17, 558–563. doi: 10.1016/S1471-4922(01)02112-2

Salzberg, S. L., Hotopp, J. C. D., Delcher, A. L., Pop, M., Smith, D. R., Eisen, M. B., et al. (2005). Serendipitous discovery of Wolbachia genomes in multiple Drosophilaspecies. *Genome Biol.* 6:R23. doi: 10.1186/gb-2005-6-3-r23

Santiago, I. J., Zhang, D., Saras, A., Pontillo, N., Xu, C., Chen, X., et al. (2021). Drosophila Fezf functions as a transcriptional repressor to direct layer-specific synaptic connectivity in the fly visual system. *Proc. Natl. Acad. Sci. USA* 118:e2025530118. doi: 10.1073/pnas.2025530118

Sieber, K. B., Bromley, R. E., and Dunning Hotopp, J. C. (2017). Lateral gene transfer between prokaryotes and eukaryotes. *Exp. Cell Res.* 358, 421–426. doi: 10.1016/j.yexcr.2017.02.009

Simão, F. A., Waterhouse, R. M., Ioannidis, P., Kriventseva, E. V., and Zdobnov, E. M. (2015). BUSCO: assessing genome assembly and annotation completeness with single-copy orthologs. *Bioinformatics* 31, 3210–3212. doi: 10.1093/bioinformatics/btv351

Sironi, M., Bandi, C., Sacchi, L., Sacco, B. D., Damiani, G., and Genchi, C. (1995). Molecular evidence for a close relative of the arthropod endosymbiont Wolbachia in a filarial worm. *Mol. Biochem. Parasitol.* 74, 223–227. doi: 10.1016/0166-6851(95)02494-8

Smith, I. (2003). *Mycobacterium tuberculosis* pathogenesis and molecular determinants of virulence. *Clin. Microbiol. Rev.* 16, 463–496. doi: 10.1128/CMR.16.3.463-496.2003

Specht, S., Mand, S., Marfo-Debrekyei, Y., Debrah, A. Y., Konadu, P., Adjei, O., et al. (2008). Efficacy of 2- and 4-week rifampicin treatment on the Wolbachia of Onchocerca volvulus. *Parasitol. Res.* 103, 1303–1309. doi: 10.1007/s00436-008-1133-y

Stark, R, and Brown, G. DiffBind: differential binding analysis of ChIP-Seq peak data. Bioconductor version: Release (3.18); (2023) 1–75. Available at: https://bioconductor.org/packages/DiffBind/ (Accessed October 31, 2023).

Strous, M., Kraft, B., Bisdorf, R., and Tegetmeyer, H. (2012). The binning of metagenomic Contigs for microbial physiology of mixed cultures. *Front. Microbiol.* 3:410. doi: 10.3389/fmicb.2012.00410

Sun, L. V., Foster, J. M., Tzertzinis, G., Ono, M., Bandi, C., Slatko, B. E., et al. (2001). Determination of Wolbachia genome size by pulsed-field gel electrophoresis. *J. Bacteriol.* 183, 2219–2225. doi: 10.1128/JB.183.7.2219-2225.2001

Supali, T., Djuardi, Y., Pfarr, K. M., Wibowo, H., Taylor, M. J., Hoerauf, A., et al. (2008). Doxycycline treatment of Brugia malayi—infected persons reduces Microfilaremia and adverse reactions after Diethylcarbamazine and Albendazole treatment. *Clin. Infect. Dis.* 46, 1385–1393. doi: 10.1086/586753

Taylor, M. J., Bandi, C., and Hoerauf, A. (2005). Wolbachia bacterial endosymbionts of filarial nematodes. *Adv. Parasitol.* 60, 245–284. doi: 10.1016/S0065-308X(05)60004-8

Taylor, M. J., von Geldern, T. W., Ford, L., Hübner, M. P., Marsh, K., Johnston, K. L., et al. (2019). Preclinical development of an oral anti-Wolbachia macrolide drug for the treatment of lymphatic filariasis and onchocerciasis. *Sci. Transl. Med.* 11:eaau2086. doi: 10.1126/scitranslmed.aau2086

Thompson, A., Bench, S., Carter, B., and Zehr, J. (2013). "Chapter three - coupling FACS and genomic methods for the characterization of uncultivated symbionts" in *Methods in enzymology*. ed. D. L. EF (Academic Press), 45–60.

Thorvaldsdóttir, H., Robinson, J. T., and Mesirov, J. P. (2013). Integrative genomics viewer (IGV): high-performance genomics data visualization and exploration. *Brief. Bioinform.* 14, 178–192. doi: 10.1093/bib/bbs017

Tracey, A., Foster, J. M., Paulini, M., Grote, A., Mattick, J., Tsai, Y. C., et al. (2020). Nearly complete genome sequence of Brugia malayi strain FR3. *Microbiol. Res. Announc.* 9, e00154–e00120. doi: 10.1128/MRA.00154-20

Valero-Mora, P. M. (2010). ggplot2: elegant graphics for data analysis. *J. Stat. Softw.* 35, 1–3. doi: 10.18637/jss.v035.b01

Vosloo, S., Huo, L., Anderson, C. L., Dai, Z., Sevillano, M., and Pinto, A. (2021). Evaluating de novo assembly and binning strategies for time series drinking water metagenomes. *Microbiol. Spectr.* 9, e01434–e01421. doi: 10.1128/Spectrum.01434-21

Wade, W. (2002). Unculturable bacteria—the uncharacterized organisms that cause oral infections. *J. R. Soc. Med.* 95, 81–83. doi: 10.1177/014107680209500207

Wanji, S., Tendongfor, N., Nji, T., Esum, M., Che, J. N., Nkwescheu, A., et al. (2009). Community-directed delivery of doxycycline for the treatment of onchocerciasis in areas of co-endemicity with loiasis in Cameroon. *Parasit. Vectors* 2:39. doi: 10.1186/1756-3305-2-39

Wernegreen, J. J. (2002). Genome evolution in bacterial endosymbionts of insects. *Nat. Rev. Genet.* 3, 850–861. doi: 10.1038/nrg931

Werren, J. H. (1997). Biology of Wolbachia. *Annu. Rev. Entomol.* 42, 587–609. doi: 10.1146/annurev.ento.42.1.587

WHO (2019). Global programme to eliminate lymphatic filariasis: progress report, 2018. *Wkly Epidemiol. Rec.* 94, 457–470.

WHO. Onchocerciasis and its control: Report of a WHO expert committee on onchocerciasis control. World Health Organization; (1995). Available at: https://iris.who.int/handle/10665/37346 (Accessed October 24, 2023).

Wood, D. E., Lu, J., and Langmead, B. (2019). Improved metagenomic analysis with kraken 2. *Genome Biol.* 20:257. doi: 10.1186/s13059-019-1891-0

Wu, B., Novelli, J., Foster, J., Vaisvila, R., Conway, L., Ingram, J., et al. (2009). The Heme biosynthetic pathway of the obligate Wolbachia endosymbiont of Brugia malayi as a potential anti-filarial drug target. *PLoS Negl. Trop. Dis.* 3:e475. doi: 10.1371/journal.pntd.0000475

Wu, M., Sun, L. V., Vamathevan, J., Riegler, M., Deboy, R., Brownlie, J. C., et al. (2004). Phylogenomics of the reproductive parasite *Wolbachia pipientis* wMel: a streamlined genome overrun by Mobile genetic elements. *PLoS Biol.* 2:e69. doi: 10.1371/journal.pbio.0020069

Xie, S., Lan, Y., Sun, C., and Shao, Y. (2019). Insect microbial symbionts as a novel source for biotechnology. *World J. Microbiol. Biotechnol.* 35:25. doi: 10.1007/s11274-019-2599-8

Yan, F., Powell, D. R., Curtis, D. J., and Wong, N. C. (2020). From reads to insight: a hitchhiker's guide to ATAC-seq data analysis. *Genome Biol.* 21:22. doi: 10.1186/s13059-020-1929-3

Ye, Y. H., Woolfit, M., Rancès, E., O'Neill, S. L., and McGraw, E. A. (2013). Wolbachia-associated bacterial protection in the mosquito *Aedes aegypti*. *PLoS Negl. Trop. Dis.* 7:e2362. doi: 10.1371/journal.pntd.0002362

Yu, G., Wang, L. G., and He, Q. Y. (2015). ChIPseeker: an R/Bioconductor package for ChIP peak annotation, comparison and visualization. *Bioinformatics* 31, 2382–2383. doi: 10.1093/bioinformatics/btv145

Zhang, Y., Liu, T., Meyer, C. A., Eeckhoute, J., Johnson, D. S., Bernstein, B. E., et al. (2008). Model-based analysis of ChIP-Seq (MACS). *Genome Biol.* 9:R137. doi: 10.1186/gb-2008-9-9-r137

frontiers | Frontiers in Microbiology

TYPE Original Research
PUBLISHED 25 March 2024
DOI 10.3389/fmicb.2024.1364009

OPEN ACCESS

EDITED BY
Takema Fukatsu,
National Institute of Advanced Industrial Science and Technology (AIST), Japan

REVIEWED BY
Xiao-Li Bing,
Nanjing Agricultural University, China
Habib Ali,
Khwaja Fareed University of Engineering and Information Technology (KFUEIT), Pakistan

*CORRESPONDENCE
Laura Renee Serbus
✉ Lserbus@fiu.edu

†These authors have contributed equally to this work

RECEIVED 01 January 2024
ACCEPTED 29 February 2024
PUBLISHED 25 March 2024

CITATION
Sharmin Z, Samarah H, Aldaya Bourricaudy R, Ochoa L and Serbus LR (2024) Cross-validation of chemical and genetic disruption approaches to inform host cellular effects on *Wolbachia* abundance in *Drosophila*. *Front. Microbiol.* 15:1364009. doi: 10.3389/fmicb.2024.1364009

Cross-validation of chemical and genetic disruption approaches to inform host cellular effects on *Wolbachia* abundance in *Drosophila*

Zinat Sharmin[1,2], Hani Samarah[1,2], Rafael Aldaya Bourricaudy[1,2†], Laura Ochoa[2,3†] and Laura Renee Serbus[1,2,3*]

[1]Department of Biological Sciences, Florida International University, Miami, FL, United States, [2]Biomolecular Sciences Institute, Florida International University, Miami, FL, United States, [3]Department of Chemistry and Biochemistry, Florida International University, Miami, FL, United States

Introduction: Endosymbiotic *Wolbachia* bacteria are widespread in nature, present in half of all insect species. The success of *Wolbachia* is supported by a commensal lifestyle. Unlike bacterial pathogens that overreplicate and harm host cells, *Wolbachia* infections have a relatively innocuous intracellular lifestyle. This raises important questions about how *Wolbachia* infection is regulated. Little is known about how *Wolbachia* abundance is controlled at an organismal scale.

Methods: This study demonstrates methodology for rigorous identification of cellular processes that affect whole-body *Wolbachia* abundance, as indicated by absolute counts of the *Wolbachia surface protein* (*wsp*) gene.

Results: Candidate pathways, associated with well-described infection scenarios, were identified. *Wolbachia*-infected fruit flies were exposed to small molecule inhibitors known for targeting those same pathways. Sequential tests in *D. melanogaster* and *D. simulans* yielded a subset of chemical inhibitors that significantly affected whole-body *Wolbachia* abundance, including the Wnt pathway disruptor, IWR-1 and the mTOR pathway inhibitor, Rapamycin. The implicated pathways were genetically retested for effects in *D. melanogaster*, using inducible RNAi expression driven by constitutive as well as chemically-induced somatic GAL4 expression. Genetic disruptions of *armadillo*, *tor,* and *ATG6* significantly affected whole-body *Wolbachia* abundance.

Discussion: As such, the data corroborate reagent targeting and pathway relevance to whole-body *Wolbachia* infection. The results also implicate Wnt and mTOR regulation of autophagy as important for regulation of *Wolbachia* titer.

KEYWORDS

***Wolbachia*, *Drosophila*, titer, Wnt, mTOR, autophagy, endosymbiosis, commensalism**

Introduction

Resident intracellular microbes, referred to as endosymbionts, are widespread in nature. Endosymbiotic microbes are commonly thought of as mutualists, in which the interaction between host and microbe benefits both partners of the symbiosis. However, endosymbionts can also exhibit relatively inert (commensal) or detrimental (parasitic) interactions with a host organism. Evidence suggests that some commensal and/or mutualistic microbes are descendants of formerly parasitic ancestors (Sachs et al., 2014). Other endosymbionts have been found to

exhibit context-dependent plasticity in their symbiotic interactions, as seen in *Salmonella*, which is carried innocuously by chickens, but causes severe infection in humans (Foley et al., 2013). To account for this diversity, intracellular bacteria are now described in terms of a symbiotic spectrum, ranging from mutualistic to parasitic (Lewis, 1985).

For any endosymbiont, high infection prevalence in host populations is the mark of success. Members of the *Wolbachia* genus are naturally widespread bacterial endosymbionts, carried in certain lineages of mites, crustaceans, nematodes and in about 50% of all insect species (Sazama et al., 2019). *Wolbachia* are often described as reproductive parasites because some strains induce parthenogenesis, male-killing, feminization or cytoplasmic incompatibility, which ultimately favor the success of infected females (Werren et al., 2008). In other instances, *Wolbachia* have been found to serve as mutualists, by sustaining host viability and reproduction (Taylor et al., 2005; Pannebakker et al., 2007; Landmann et al., 2011), as well as by repelling harmful viral infections in the host (Hedges et al., 2008; Teixeira et al., 2008; Cogni et al., 2021). Due to absence of evident benefits or detriments, *Wolbachia* infections can often be described as commensal. The *Wolbachia*-host symbiosis thus provides a new and valuable perspective for investigating, defining, and understanding the cellular basis of commensalism.

To date, *Wolbachia* studies have shared an interest in understanding how endosymbiont amount (titer) is specified within tissue culture cells, dissected host tissues, and whole organisms. *Wolbachia* titer has been assessed as a function of various host/strain combinations as well as in response to host age, crowding, temperature, diet, genetic background, microbiota, and chemical exposure (Hoffmann et al., 1998; Veneti et al., 2004; Unckless et al., 2009; Wiwatanaratanabutr and Kittayapong, 2009; Voronin et al., 2012; Ali et al., 2019; López-Madrigal and Duarte, 2019). A patchwork of cytological and qPCR-based methods have been used across assessments of *Wolbachia* abundance *in vivo*, with shared recognition that cellular processes interacting with *Wolbachia* may also affect *Wolbachia* abundance within the host (López-Madrigal and Duarte, 2019). The field is now in a position to investigate more broadly how *Wolbachia*-host interactions inform mechanisms of infection.

Fundamental questions remain regarding the involvement of host cellular processes in endosymbiotic infection. It is not clear whether signaling pathways relevant to *Wolbachia* infection have been fully identified, nor which relays of those relays affect *in vivo Wolbachia* titer most strongly. It also remains unclear what mechanistic attributes distinguish commensal infections from detrimental scenarios. To this end, this study asked whether *Wolbachia* titer is affected by the same host cellular pathways as commonly studied bacterial infections. 14 candidate host pathways and processes were tested, using complementary chemical and genetic tools. Whole-body *Wolbachia* abundance was assessed by real-time qPCR, to determine absolute counts of the *Wolbachia surface protein* (*wsp*) gene. This work yielded a subset of host functions for further pursuit, with implications for the basis of commensalism.

Materials and methods

Drosophila stocks and maintenance

Two fly strains were used in this study. Preliminary screening was performed using *Drosophila melanogaster* of the genotype *w*; *Sp/Cyo*; *Sb/TM6B* carrying the endogenous *w*Mel *Wolbachia* strain (Serbus and Sullivan, 2007; Christensen et al., 2016). *Drosophila simulans (D. sim)* infected with the endogenous *Wolbachia riverside* (*w*Ri) strain were used for further analyses (Hoffmann et al., 1990; Serbus and Sullivan, 2007). GAL4 lines sourced from the Bloomington Drosophila Stock Center (BDSC) were also used to drive RNAi expression. Constitutive somatic expression was driven by the Actin5C-GAL4 driver *w; P{Act5C-GAL4-w}E1/Cyo* (BDSC# 25374) and the daughterless-GAL4 driver *w; P{w+, GMR12B08-GAL4}attP2* (BDSC# 48489). Mifepristone-induced gene expression was driven by the GeneSwitch-GAL4 driver *yw {hs-FLP}; {w+, UAS-GFP}; {w+, Act5C-GS-GAL4}/TM6B, Tb* (BDSC #9431).

Fruit flies were maintained in plastic bottles/vials containing standard fly food media. The recipe was derived from Bloomington Drosophila Stock Center as described previously (Christensen et al., 2016). The flies were raised in an Invictus *Drosophila* incubator at 25°C, under standard 12:12 h light–dark cycle. For the experiments, "0-day old" flies were collected and kept on standard fly food medium for 2 days. The flies were then used for drug treatments in vials or within a plate assay format as described previously (Christensen et al., 2019). Only female flies were used for the plate-based screening experiments, to reduce possible variation in population behavior per well.

Chemical food preparation

Two or more chemicals were used to alter the functionality of each of the candidate host processes pursued in this study. Where possible, compounds with opposite effects on the process of interest were included, such as the microtubule-depolymerizing drug, colchicine, and the microtubule-stabilizing drug, taxol, as well as the phospholipase C (PLC) inhibitor, U73122, and the PLC activator, 3-M3MFBS. The final list included a total of 37 candidate compounds (Supplementary Table S1). All the drugs were dissolved in DMSO. Most stock solutions, including rifampicin, were prepared in advance as 10 mM solutions, aliquoted, and stored at −20°C. Rapamycin was ordered as a 5 mM solution in DMSO, also stored at −20°C. Light-sensitive drugs were stored in the dark.

Immediately before use, chemical stocks were thawed and diluted 100X into fly food that had been re-melted, then cooled. Control vials, prepared in parallel with the chemical treatment vials, were treated with equivalent amounts of DMSO alone. In all cases, the final concentration of DMSO in food was capped at 1%. For the chemical screen, a minimum of 10 mL drug food was prepared per condition, to be further dispensed in approximately 1 mL amounts per treatment well. For drug lethality tests and *GS-GAL4* induction experiments that were carried out in vials, food containing control DMSO and DMSO-solubilized compounds was prepared in larger volumes, to be dispensed into vials as 5 mL final amounts. After pouring, plates and vials were cooled and solidified in the fume hood, with foil wrappings used to protect light-sensitive compounds. Treatment vials were stored in Ziplock bags at 4°C as needed.

For the chemical screen,10 female flies were transferred to each treatment well. A DMSO-solubilized rifampicin control was also run on every qPCR plate to confirm the ongoing capacity of *Wolbachia* to respond to compound treatments. After 3 days of chemical feeding, pools of 5 female flies were removed from each treatment well and

processed as a group for *wsp* quantification using real-time qPCR. For the vial-based experiments that assessed drug lethality, flies were incubated in groups of 12, 6 females and 6 males per vial, with viability scored every 3 days. Flies were transferred to new treatment vials at day 6, using vials from the 4°C fridge that had been re-warmed. For vial-based experiments using DMSO and mifepristone, flies were incubated on treatment food in groups of 15 females and 5 males. Flies were transferred to new treatment vials every 3 days, using DMSO and mifepristone vials from the 4°C fridge that had been re-warmed. After 14 days of feeding were completed (Haselton et al., 2010; Serbus et al., 2015), pools of 5 female flies were removed from each vial and processed as a group for *wsp* quantification using real-time qPCR.

Genetic manipulations

To incorporate *Wolbachia* into GAL4 driver lines, the driver males were crossed to virgin females of the genotype *w*; *Sp/Cyo*; *Sb/TM6B,* carrying the *w*Mel *Wolbachia* strain (Christensen et al., 2016), which in this study is referred to as DB *w*Mel. F1 progeny were backcrossed to the parental lines to establish *Wolbachia*-infected driver stocks, with the same genotypes as the originally uninfected lines.

Genetic disruptions were achieved using VALIUM20 transgenic RNAi lines which depend on short hairpin RNA, also known as artificial microRNAs, to trigger gene silencing in both somatic and germline cells (Ni et al., 2011). Each host pathway was tested by two different UAS-shRNA responder lines (Supplementary Table S2), selected in accord with pathways targeted by "hit" compounds from the chemical screen. To generate RNAi-expressing flies, *w*Mel-infected virgin females were selected from freshly emerging bottles of each GAL4 driver stock. These females were crossed to males that carried responder UAS (upstream activating sequence) elements adjacent to a promoter that drives shRNA production (Ni et al., 2011). The parent flies were removed from the vials after 3–4 days of mating. Emerging F1 flies were collected in daily cohorts and aged for 5 days. The F1s that carried the GAL4 driver and the UAS responder were identified by phenotypic markers and separated within each cohort. Control siblings that contained either the GAL4 or UAS responder, but not both, were collected when available. In some cases, a separate control set was also generated in parallel by outcrossing *Wolbachia*-infected driver females to Oregon R (OreR) males. In all cases, control and treatment groups were generated and processed in parallel for *wsp* quantification.

DNA extraction and qPCR for whole-body *Wolbachia* quantification

Real-time qPCR was used to assess whole-body *Wolbachia* abundance, using the candidate gene *wsp* as a proxy for *Wolbachia* genomes per sample. Because *Wolbachia* reportedly carry one genome per bacterial cell (McGarry et al., 2004), resulting genome counts are expected to represent *Wolbachia* abundance per sample. DNA was extracted from pools of 5 female flies as per established methods (Christensen et al., 2019). Absolute measurements of the *wsp* gene from the extracted DNA samples were compared against reference plasmid standards, specifically a PGEM-T vector carrying a 160 bp PCR-amplified fragment of the *wsp* gene (Christensen et al., 2016). Real-time qPCR was carried out on a Bio-Rad CFX96 Connect Optics Module Real-Time System. Absolute *wsp* copy numbers were obtained by comparing cycle threshold (Ct) values to the standard curve generated from the plasmid standard. The *wsp* amplification primers were: Fwd 5' CATTGGTGTTGGTGTTGGTG 3′ and Rev. 5' ACCGAAATAACGAGCTCCAG 3′, used at 5 µM (Christensen et al., 2016).

Data display and analyses

Graphical displays showing "normalized" *wsp* counts as a scatter plot were created for display purposes only. To generate such graphs, median *wsp* counts for the DMSO controls per replicate were identified, then compared to the median *wsp* count of the entire dataset. A scaling factor was then identified and applied to each replicate, to normalize the median *wsp* value for the DMSO control and all associated experimental data. The raw absolute count data are available for review as needed (Supplementary material S1). Statistical analyses were conducted on raw (non-normalized) data within each experimental replicate for all experiments. Statistics appropriate to data normality and homogeneity were identified and applied as previously (Christensen et al., 2019). Power analysis was performed with an alpha set at 0.05 using a MATLAB-based data sub-sampling program, designed by Dr. Philip K. Stoddard. This program has the advantage that analyses can be customized to the statistical test appropriate to each dataset (Christensen et al., 2019). All statistical analysis worksheets for each experiment performed are also available (Supplementary material S1).

Results

Identifying and targeting candidate host processes relevant to bacterial infection

A literature search was first conducted to assess how intracellular bacterial abundance is regulated in commonly studied bacterial infections. After assessing 52 species from 17 genera, 26 bacterial species were identified, for which host gene/pathway effects on density regulation had been discussed (Supplementary Table S3). Of these, the literature highlighted 14 host mechanisms that altered the intracellular abundance of multiple bacterial classes (Supplementary Table S4; Supplementary material S2). Because these mechanisms were identified as more commonly involved in host–microbe interactions, they were prioritized for testing in the *Wolbachia-Drosophila* endosymbiosis model. Candidate compounds known to target each process were selected, with two or more compounds identified for testing each of the 14 classes of host targets. This culminated in the selection of 37 total candidate compounds to test for effects on whole-body *Wolbachia* titer (Table 1).

Host-directed small molecules alter *wsp* abundance in adult *Drosophila* hosts

The impact of the candidate compounds on whole-body *Wolbachia* titer was screened by absolute quantification of *wsp* by

10.3389/fmicb.2024.1364009

real-time qPCR (Kim et al., 2008; Serbus et al., 2012; Markstein et al., 2014; Christensen et al., 2019). *D. melanogaster* flies, carrying the endogenous *w*Mel *Wolbachia* strain, termed DB *w*Mel, were exposed for 3 days to food supplemented with DMSO-solubilized drugs or DMSO alone as a control. Treatments were initially tested for impact on whole-body *wsp* across two independent plate replicates. Those treatments which significantly changed *wsp* abundance in both plates were identified as preliminary hits. Of 37 chemicals tested, the primary screen identified 16 compounds were identified as meeting this criterion. These preliminary hit compounds were re-tested for reproducibility in a third plate replicate. 11 compounds were reconfirmed as hits, implicating a total of 9 host pathways and processes (Figure 1A). Most "hit" compounds elicited an increase in whole-body *wsp* abundance, with median values ranging 6–57% higher than the control ($p < 0.001$–0.036, $n = 6$ per plate replicate). The only exception was bortezomib, which reduced *wsp* to 48–71% of the DMSO control ($p < 0.001$, $n = 6$ amplifications per plate replicate) (Figure 1A; Table 2).

To investigate a role for candidate processes across systems, the hits from DB *w*Mel were retested against the *D. simulans* (Dsim) model, which naturally carries the *w*Ri *Wolbachia* strain. The Dsim *w*Ri re-screen identified a subset of 6 compounds that significantly affected whole-body *wsp* counts across 3 plate replicates (Figure 1B). 5 compounds increased whole-body *wsp* abundance to 15–52% higher than the DMSO control (*p*-value range: <0.001–0.041, $n = 6$ per plate replicate). These hits were associated with host Imd signaling, Calcium signaling, Ras/mTOR signaling, and Wnt signaling functions. By contrast, the proteasome inhibitor bortezomib continued to reduce *wsp* counts to 56–69% of the DMSO control ($p < 0.001$, $n = 6$ amplifications per plate replicate) (Figure 1B; Table 2).

To further investigate why some chemical treatments increase *wsp* counts, but others suppress *wsp,* a lethality assay was conducted. Flies were exposed to each of the "hit" compounds for a 12-day period. Bortezomib induced high lethality by the 6-day exposure timepoint for both DB *w*Mel and Dsim *w*Ri (Figures 2A,C). Thus, it is possible that *wsp* reductions by bortezomib reflect a *Wolbachia* response to toxic host conditions. However, flies exposed to all other "hit" compounds exhibited viability profiles comparable to DMSO controls, as per the example of IWR-1 (Figures 2B,D) (Supplementary Figure S1). Because the non-lethal "hit" compounds were all shown to elevate *wsp* counts, these results suggest that functions of multiple host pathways normally reduce whole-body *Wolbachia* loads.

Constitutive RNAi disruptions corroborate a subset of host pathway effects on *wsp*

To confirm the basis for host cellular effects on whole-body *Wolbachia* titer, genetic disruption experiments were performed, focusing on the pathways dually implicated by chemical screening of DB *w*Mel and Dsim *w*Ri. We used the GAL4::UAS system in *D. melanogaster*, which enables directed manipulation of gene expression (Brand and Perrimon, 1993; Duffy, 2002). In this case, the GAL4::UAS system was set to drive expression of short hairpin RNAi suppress the corresponding gene product (Perrimon et al., 2010; Ni et al., 2011; Perkins et al., 2015). The *w*Mel strain was crossed into well-established GAL4 driver lines that drive constitutive whole-body expression, including the reputedly "strong" Actin5C-GAL4 driver

TABLE 1 Screening targets and chemical tools.

Candidate host processes	Drug name	Drug effect
Cell cycle modulation	Flavopiridol	CDK inhibitor
	Roscovitine	CDK inhibitor
	Sodium butyrate	HDAC inhibitor
Cytoskeleton-based transport	Colchicine	Microtubule destabilizer
	Cytochalasin D	F-actin destabilizer
	Taxol	Microtubule stabilizer
Ubiquitin-proteasome system	Bortezomib	Proteasome inhibitor
	Epoxomicin	Proteasome inhibitor
Mitochondrial/ Antioxidant	Butylated hydroxytoluene	Antioxidant
	L-Glutathione	Antioxidant
	MitoBloCK-6	Mitochondrial import inhibitor
	Niclosamide	Pink1 activator
	Resveratrol	Cox-1 inhibitor
Apoptotic pathway	ABT-199	Bcl-2 inhibitor
	Apoptosis inhibitor	Caspase 3 inhibitor
	Caspase 8 inhibitor	Caspase 8 inhibitor
Imd pathway	CAY10512	NF κ B inhibitor
	SC76741	NF κ B inhibitor
GPCR signaling	Caffeine	cAMP phosphodiesterase inhibitor
	SQ22536	Adenylyl cyclase inhibitor
Phospholipase-related	M-3M3FBS	Phospholipase C activator
	U73122	Phospholipase C inhibitor
Calcium signaling	Nicardipine HCl	L-type voltage-dependent calcium channel inhibitor
	Verapamil	L-type calcium channel blocker
Ras/mTOR pathway	Erlotinib HCl	EGFR inhibitor
	Trametinib	MEK inhibitor
	Rapamycin	mTOR inhibitor
	Wortmanin	PI3 kinase inhibitor
Nitric oxide synthase	L-NAME	Nitric oxide synthetase inhibitor
	Methylxanthine	cAMP and cGMP phosphodiesterase inhibitor
	Sildenafil citrate	cGMP phosphodiesterase inhibitor
Jak–Stat signaling	Ruxolitinib	JAK 1/2 inhibitor
	SH-4-54	STAT2 inhibitor
Wnt pathway	IWR-1	AXIN inhibitor
	Ly090314	GSK-3 inhibitor
Kinase modulator	Pyrvinium pamoate	Akt inhibitor
	Staurosporine	PKC inhibitor

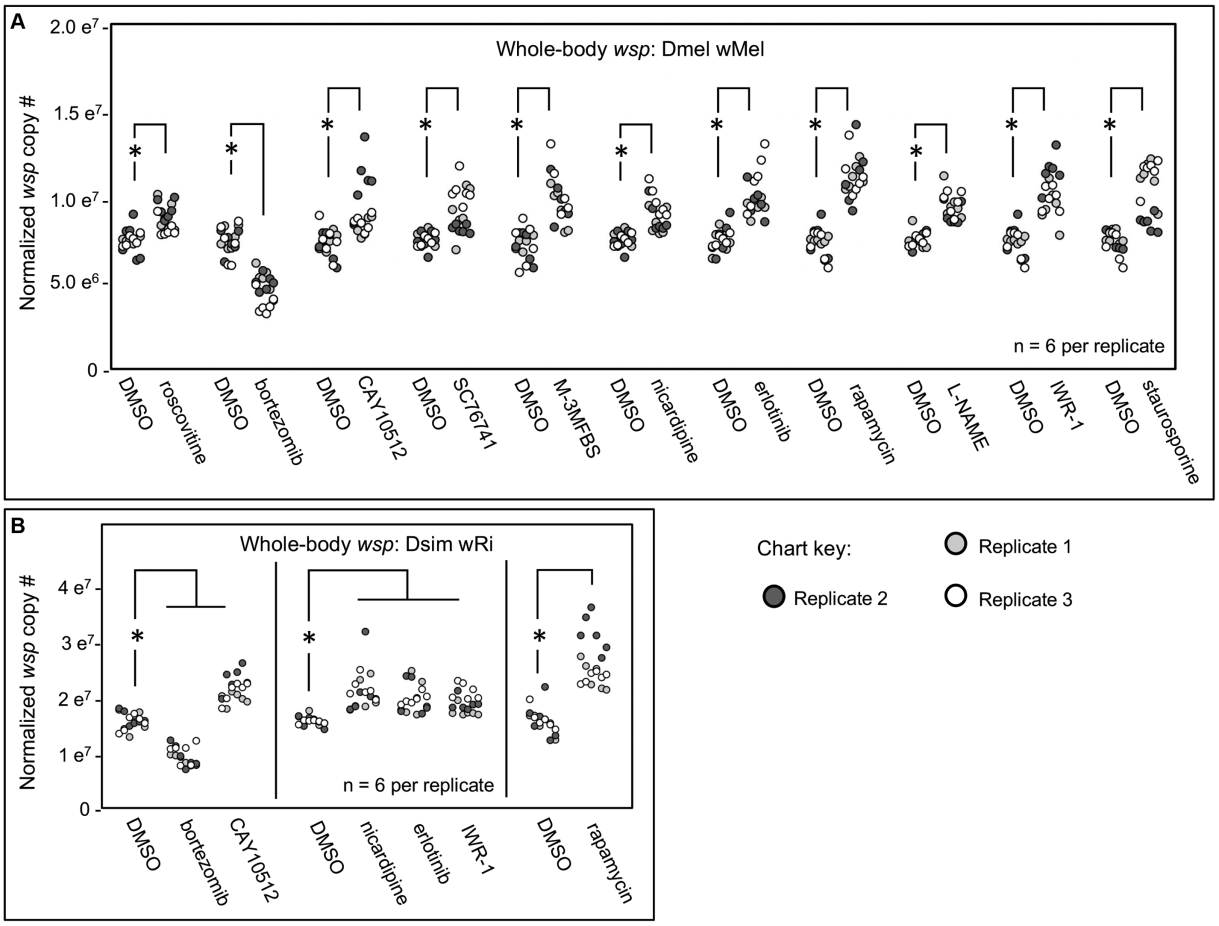

FIGURE 1
Whole body *wsp* abundance in response to chemical treatments. Display shows DMSO controls normalized across replicates, and the corresponding drug treatment data scaled accordingly. **(A)** Chemical treatment effects on whole-body *wsp* abundance in Dmel *w*Mel. **(B)** Chemical treatment effects on whole-body *wsp* abundance in Dsim *w*Ri. Significance was set at * $p < 0.05$, and is displayed only for conditions where all replicates met this standard.

(*Act-5C*), and the "milder" daughterless-GAL4 driver (*da-GAL4*) (Supplementary Table S5). Few to no F1 progeny were recovered that carried *Act5C-GAL4* as well as *UAS-shRNA* chromosomes, indicating lethality for such genetic combinations. However, crossing the *UAS-shRNA* lines to *da-GAL4* (Serbus et al., 2015) yielded ample RNAi-expressing F1 progeny for analysis.

No changes in *wsp* abundance were detected in response to constitutive shRNA disruption of Calcium signaling by knockdown of L-type calcium channels encoded by *Ca-alpha1D* and *Cac*. Inconsistent effects on *wsp* abundance were associated with disruptions to the Imd pathway by knockdown of NF-kappa-B/*Rel*, and the Rel activator, *Tak1*. Similar inconsistencies were observed for knockdown of the Wnt pathway gene, *shaggy (sgg)* gene (Supplementary material S1).

Constitutive shRNA disruption of the Wnt pathway gene *armadillo (arm)* yielded positive effects, increasing median whole-body *wsp* counts to 9–15% above the OreR-outcrossed control (*p*-value range: <0.001–0.034, $n = 6$ per plate replicate) (Figure 3). A significant *wsp* increase was also detected for the Ras/mTOR pathway, with *tor* disruption flies exhibiting higher whole-body *wsp* counts at 23–31% above both sibling controls and OreR-outcrossed controls ($p < 0.001$, $n = 6$ per plate replicate) (Figure 3). Ras/mTOR signaling was also retested by knockdown of the *Epidermal Growth Factor Receptor (EGFR)*. Compared to OreR-outcrossed controls, *EGFR* knockdowns did not consistently affect *wsp* abundance measurements. However, in comparison to sibling controls, EGFR disruption yielded a 35–44% increase in median *wsp* counts (*p*-value range: <0.001–0.002, $n = 6$ per plate replicate) (Figure 3). Thus, detection of *wsp* responses to EGFR disruption may be context-dependent.

To confirm an effect of Wnt and Ras/mTOR pathways on *Wolbachia,* the most consistent outcomes from the *da-GAL4::UAS-shRNA* experiments were retested. *Arm* RNAi elicited a 16–50% increase in median *wsp* abundance over the OreR-outcrossed control ($p < 0.001$, $n = 18$) (Figure 4A). Power analysis indicated the *arm* RNAi outcome to be robust ($\beta < 0.003$ at $n \geq 12$; total $n = 18$) (Figure 4B). *tor* RNAi triggered a 38–39% increase in *wsp* abundance as compared to OreR-outcrossed controls ($p < 0.001$, $n = 18$) (Figure 4C), a finding also well-supported by power analysis ($\beta < 0.002$ at $n \geq 4$; total $n = 18$) (Figure 4D). Taken together, these data indicate that constitutive RNAi disruption of Wnt and Ras/mTOR signaling increases whole-body *Wolbachia* titer.

TABLE 2 Chemical screen outcomes: comparing Dmel *w* Mel hits to Dsim *w* Ri results.

Host cellular process	Drug name	*p*-value range for Dmel *w*Mel	*p*-value range for Dsim *w*Ri	Hit in both systems?
Cell cycle modulation	Roscovitine	0.003–0.009	0.006–0.283	No
Ubiquitin-proteasome system	Bortezomib	<0.001 (all)	<0.001 (all)	Yes
Imd pathway	CAY10512	0.001–0.036	<0.001–0.001	Yes
	SC76741	<0.001–0.022	0.171–0.936	No
Phospholipase-related	M-3M3FBS	0.002–0.004	0.009–0.840	No
Calcium signaling	Nicardipine HCl	<0.001–0.016	<0.001–0.006	Yes
Ras/mTOR pathway	Erlotinib HCl	<0.001–0.002	<0.001–0.024	Yes
	Rapamycin	<0.001–0.001	<0.001 (all)	Yes
Nitric oxide synthase	L-NAME	<0.001–0.002	0.001–0.056	No
Wnt pathway	IWR-1	<0.001–0.001	<0.001–0.041	Yes
Kinase modulator	Staurosprine	0.002–0.006	0.003–0.061	No

Adult-induced RNAi disruptions provide further context for host effects on *wsp*

An intrinsic limitation of certain genetic disruption approaches, like constitutive RNAi induction, is that cumulative disruption effects could occur. To confirm ongoing Wnt and mTOR pathway effects on whole-body *wsp* abundance, "Gene-switch" GAL4 driver flies were used to induce GAL4 activity in adult flies. The Gene-switch version of GAL4 carries an inhibitory domain that blocks GAL4 function, until a de-repressor compound, mifepristone, is added (Roman et al., 2001). Because trial experiments on mifepristone identified low-power but potentially significant effects on *wsp* (Supplementary Figure S2), all *GS-GAL4* experiments were carried out with multiple controls. Flies carrying *GS-GAL4::UAS-shRNA* genotypes were always compared to non-expressing siblings, with half of the flies DMSO-treated, and the other half exposed to DMSO-solubilized mifepristone.

In tests of *arm* and *tor* RNAi knockdowns, no significant *wsp* abundance differences were observed between the DMSO-treated flies and mifepristone-treated flies that were incapable of RNAi expression (Figures 5A,B). However, mifepristone-fed flies that were capable of shRNA expression did show significant differences in their *wsp* counts. In the case of *GS-GAL4::arm-shRNA*, the mifepristone-treated flies exhibited reduced *wsp* counts, down to 45–71% of all other conditions tested in parallel (*p*-value range: <0.001–0.033, $n = 9$) (Figure 5A). By contrast, mifepristone-treated *GS-GAL4::tor-shRNA* flies carried 81–184% more *wsp* than all other conditions run in parallel (*p*-value range: <0.001–0.031, $n = 9$) (Figure 5B). These results confirm ongoing *Wolbachia* sensitivity to Wnt and mTOR disruption in adult hosts. Unlike the da-GAL4 data, the GS-GAL4 results notably show that Wnt and mTOR exert opposing effects on *Wolbachia* titer. This highlights a functional difference between constitutive and adult-specific disruptions of the Wnt pathway with respect to regulation of *Wolbachia* titer in adult insects.

One way to reconcile effects of *arm* and *tor* disruptions on *wsp* abundance is to consider the possibility that both may affect a consensus target relevant to *Wolbachia*. Literature indicates that Wnt signaling can suppress autophagy onset via multiple routes (Pérez-Plasencia et al., 2020), including through down-regulation of *Beclin-1*, also known as *ATG6* (Tao et al., 2017). mTORC1 is also known to inhibit ATG6 by suppressing the ATG6 activator, ULK1 (Hill et al., 2019). To test the effect of *ATG6* on whole-body *Wolbachia* titer, the *GS-GAL4::ATG6-shRNA* flies were generated. The mifepristone-fed, RNAi-expressing condition exhibit 67–173% higher *wsp* levels than non-expressing mifepristone-fed siblings and DMSO-fed flies of equivalent genotype (*p*-value range: <0.001–0.045, $n = 9$) (Figure 5C). These data suggest that *ATG6* normally suppresses whole-body *wsp* abundance, consistent with autophagy as a general suppressor of *Wolbachia* titer (Voronin et al., 2012; Strunov et al., 2022). Implications for Wnt and mTORC1 pathway interaction with autophagy are discussed below.

Discussion

This study explored the basis for endosymbiosis by inipvestigating the effect of candidate host processes on *Wolbachia* titer in two different host-strain combinations. To identify consensus cellular effects on whole-body *wsp* counts, candidate compounds were screened against DB *w*Mel and Dsim *w*Ri systems. This was followed by constitutive as well as inducible genetic disruptions in DB *w*Mel to further verify effects of the drug-implicated pathways on *wsp* abundance. The amenability of *Drosophila* to mechanistic cross-validation in this rigorous capacity has opened a series of questions and opportunities, while also informing on the mechanisms of endosymbiont titer control.

After identifying infection-related pathways of potential interest from the literature, a candidate drug screen was performed to test these pathways. *Wolbachia* titer responses were assessed via absolute quantification of the *wsp* gene from whole insect samples. This is a targeted approach, relative to prior comprehensive screens of *Wolbachia*-host interactions in *Drosophila* tissue culture cells (White et al., 2017; Grobler et al., 2018). The organism-centered approach provides a unique advantage in detecting system-level, endogenous responses, with measurements inclusive of bacterial relocation events within the organism (Landmann et al., 2012; White et al., 2017). Detection of an organismal titer change is also a stringent requirement because *Wolbachia* infection is carried in a variety of tissues (Heddi et al., 1999; Bian et al., 2013; Ali et al., 2018; Schneider et al., 2018; Kaur et al., 2020), and it cannot be assumed that host manipulation

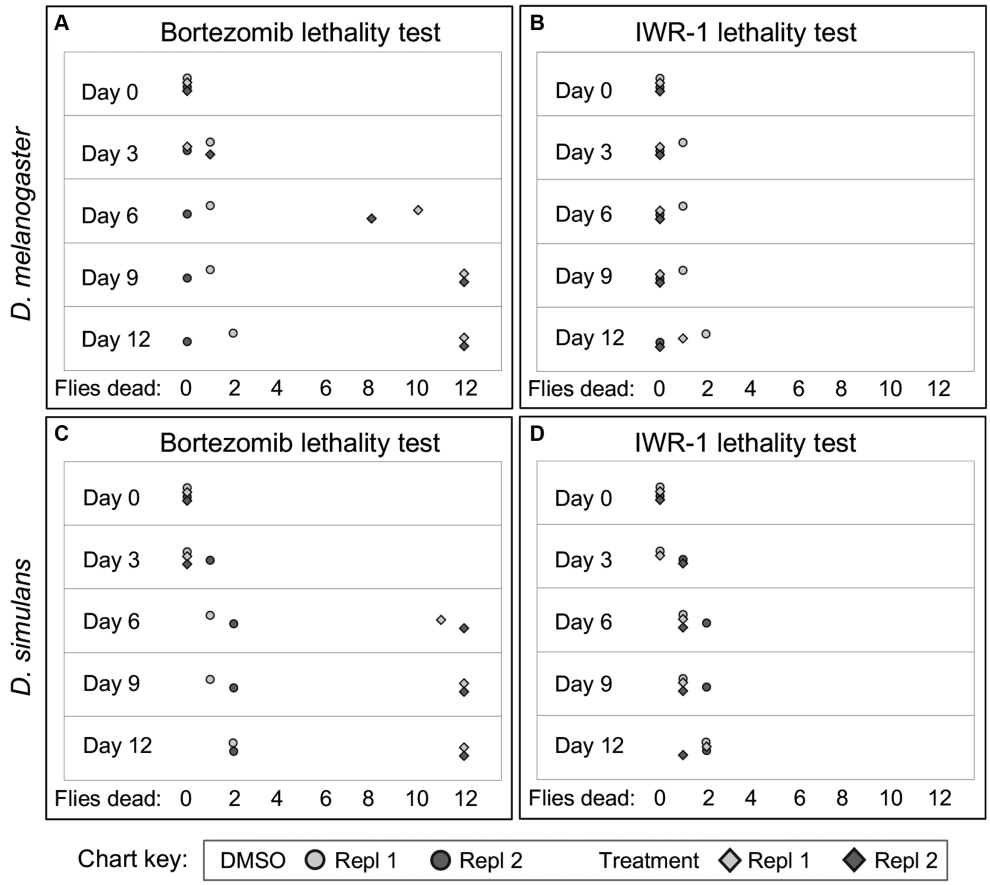

FIGURE 2
Example figure showing lethality data for bortezomib and IWR-1 compounds in *D. melanogaster* and *D. simulans*. **(A–D)** Depict the lethality effects two representative compounds, bortezomib **(A,C)** and IWR-1 **(B,D)**, on *D. melanogaster* and *D. simulans*. Each panel shows the number of dead flies at different time points (days) following exposure across two independent replicates. Circles: Control groups treated with 1% DMSO vehicle only. Diamonds: Experimental groups treated with bortezomib **(A,C)** or IWR-1 **(B,D)**.

will elicit uniform titer change across all tissues. Treatments yielding mild or contradictory outcomes at the tissue level will not be detected as hits by this method. Starting with a chemical screen provides an additional advantage in helping to narrow down the range of pathways for follow-up genetic testing, which as shown here, requires calibration at the level of tool selection, sample size, experiment duration, and controls required. Absolute counts by real-time qPCR are indispensible for the success of such analyses, to mitigate artifacts attributable to variable host ploidy, which may not always be foreseeable across tissues, systems, organism age, and nutritional conditions (Christensen et al., 2019; Ren et al., 2020).

This study emphasized pursuit of host pathways that are associated with commonly studied bacterial infections, as a springboard to delve deeper into processes which may also be involved in commensal *Wolbachia* infection. The cellular microbiology literature yielded a range of interesting host-side effects on bacterial genera such as *Coxiella, Legionella, Brucella, Rickettsia*, *Ehrlichia, Chlamydia*, and *Ehrlichia* (Rikihisa et al., 1995; Kessler et al., 2012; Czyż et al., 2014; Luo et al., 2016), for which host Calcium and Wnt signaling promotes bacterial proliferation. Another example is the Epidermal Growth Factor Receptor (EGFR) signaling pathway, which has been implicated in promoting host cell invasion by pathogens like *Salmonella* and *Neisseria* (Galán et al., 1992; Slanina et al., 2014). Other processes, such as the mTOR/autophagy pathway, have been shown to exert differential density effects depending on the bacterial strain. For example, mTOR signaling disruptions reduce intracellular loads for *Ehrlichia* (Luo et al., 2017), *Chlamydia, Listeria* (Derré et al., 2007), and *Salmonella* (Birmingham et al., 2006), but increase titers for *Anaplasma* and *Rickettsia* (Niu et al., 2008; Bechelli et al., 2018). Recurrent titer-related effects for host cellular processes on unrelated bacterial taxa invoke the possibility of generalized infection roles for host cellular pathways, and thus of potential interest in endosymbiosis as well (Supplementary Table S4) (Porter and Sullivan, 2023).

The candidate chemical screen yielded 11 compounds that consistently altered whole-body *wsp* levels in DB *w*Mel, 6 of which repeated the effect in Dsim *w*Ri. The "hit" compounds that were identified reflect roles for the Imd pathway, Calcium signaling, the Ras/mTOR pathway, and the Wnt pathway (Table 2), prioritizing these pathways for genetic follow-up experiments. The basis for a reduction in compound "hits" between DB *w*Mel to Dsim *w*Ri is inconclusive at this time. Some of the compounds may also have differential bioavailability, bioactivity and perdurance across systems, among other possibilities.

A notable aspect of the consensus, non-lethal hit compounds in both systems is that they all significantly increased *wsp* counts. Elevated *Wolbachia* titer has previously been observed in response to

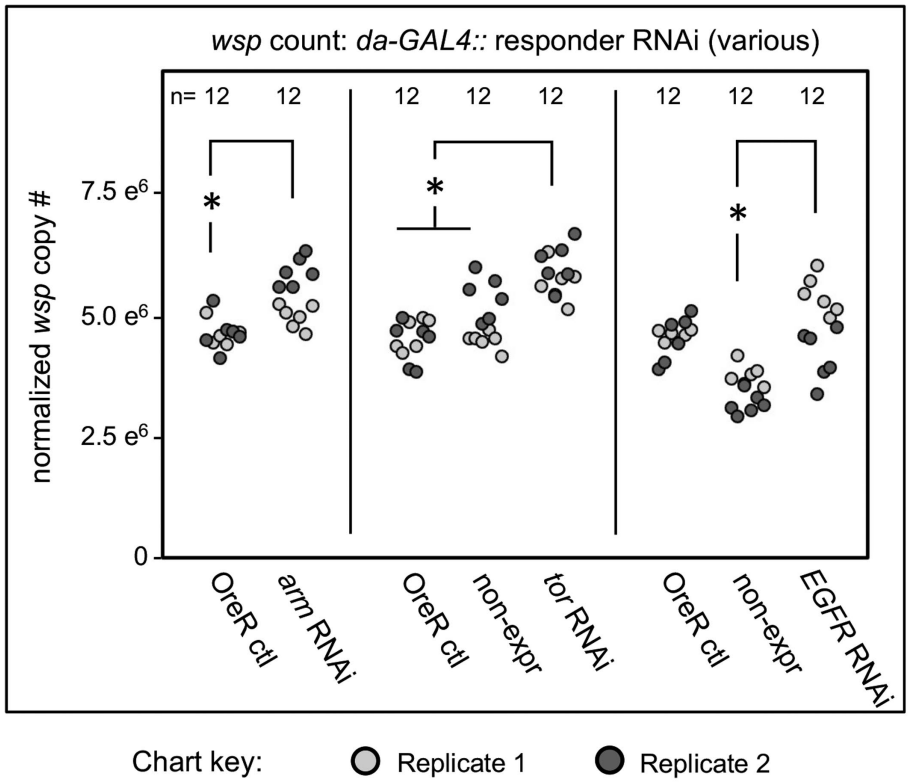

FIGURE 3
Whole body *wsp* abundance in control vs. *da-GALA:UAS-RNAi* knockdown flies. Oregon-R outcross controls are included throughout, and non-expressing sibling controls are shown where available. Display shows OreR controls normalized across replicates, and the corresponding conditions scaled accordingly. Panel shows data from 2 independent biological replicates. RNAi-expressing conditions shown from left to right are: *armadillo*, *tor*, and *EGFR* Significance was set at * $p < 0.05$, and is displayed only for conditions where all replicates met this standard.

ribosome disruption, for example (Grobler et al., 2018). Perhaps *Wolbachia* suppression by a suite of host cellular processes is relieved by disruption to host functional networks, allowing a favorable shift in *Wolbachia* life cycle dynamics. It is reasonable to consider commensalism as an artifact of endosymbiont genome reduction, with virulence factors eliminated over time (Metcalf et al., 2014; Sachs et al., 2014; Latorre and Manzano-Marín, 2017). The findings of this study suggest that for *Wolbachia,* commensalism is further supported by ongoing containment of endosymbiont population by the host, consistent with a view that commensalism is not necessarily free of conflict (Keeling and McCutcheon, 2017).

This study used complementary genetic approaches to cross-validate pathways implicated as *Wolbachia*-related by the chemical screen. Genetic corroboration of the host pathway functions is not always possible, as internal redundancies may render certain knockdowns ineffective. Developmental tolerance limits may also preclude analysis of the strongest knockdown effects, as when Actin5C-GAL4 was used in this study. Regardless of this, RNAi disruptions to host *arm* and *tor* genes affected whole-body *wsp* levels consistently and significantly. Dual effects of Wnt and mTOR disruptions on *Wolbachia* titer are consistent with literature connecting these signaling inputs to regulation of autophagy (Figure 6). There is a robust literature on antimicrobial functions of autophagy (Moy and Cherry, 2013), with reports of insects succumbing to pathogen infection when genes like ATG6 have been disrupted (Edosa et al., 2020).

Autophagy has been discussed previously as a regulator of endosymbiont titer, with functional effects dependent on the system used (Supplementary Table S6). Of the factors analyzed in this study, the one most immediate to the process of autophagy is ATG6 (Su et al., 2020). Thus, ATG6 suppression by RNAi would be expected to down-regulate autophagy. RNAi knockdowns of ATG6 yielded *Wolbachia* titer elevation, suggesting a model in which autophagy normally suppresses *Wolbachia* titer (Figure 6). This outcome is consistent with past results from others reporting that somatic autophagy antagonizes somatic *Wolbachia* titer (Voronin et al., 2012; Strunov et al., 2022).

The literature has also shown that the Wnt pathway affects autophagy regulation. In the absence of Wnt ligand, GSK-3 promotes autophagy activity by activating ULK1 (Ryu et al., 2021) as well as by suppressing Arm (Aros et al., 2021), which is a negative regulator of autophagy (Petherick et al., 2013; Feng et al., 2023) (Figure 6). Notably, GSK-3 works in a complex together with AXIN to suppress Arm (Ikeda et al., 1998), therefore AXIN disruption by IWR-1 should disrupt that function, with an indirect consequence of down-regulating autophagy, and allowing *Wolbachia* titer to increase. Tests of IWR-1 in this study yielded consistent *Wolbachia* titer elevation in both *D. melanogaster* and *D. simulans*. This finding is in accord with autophagy as a suppressor of whole-body *Wolbachia* abundance.

There is at least some complexity in Wnt pathway effects on whole-body *Wolbachia* titer. Because the GSK-3/AXIN complex antagonizes Arm in the Wnt pathway (Aros et al., 2021), Arm

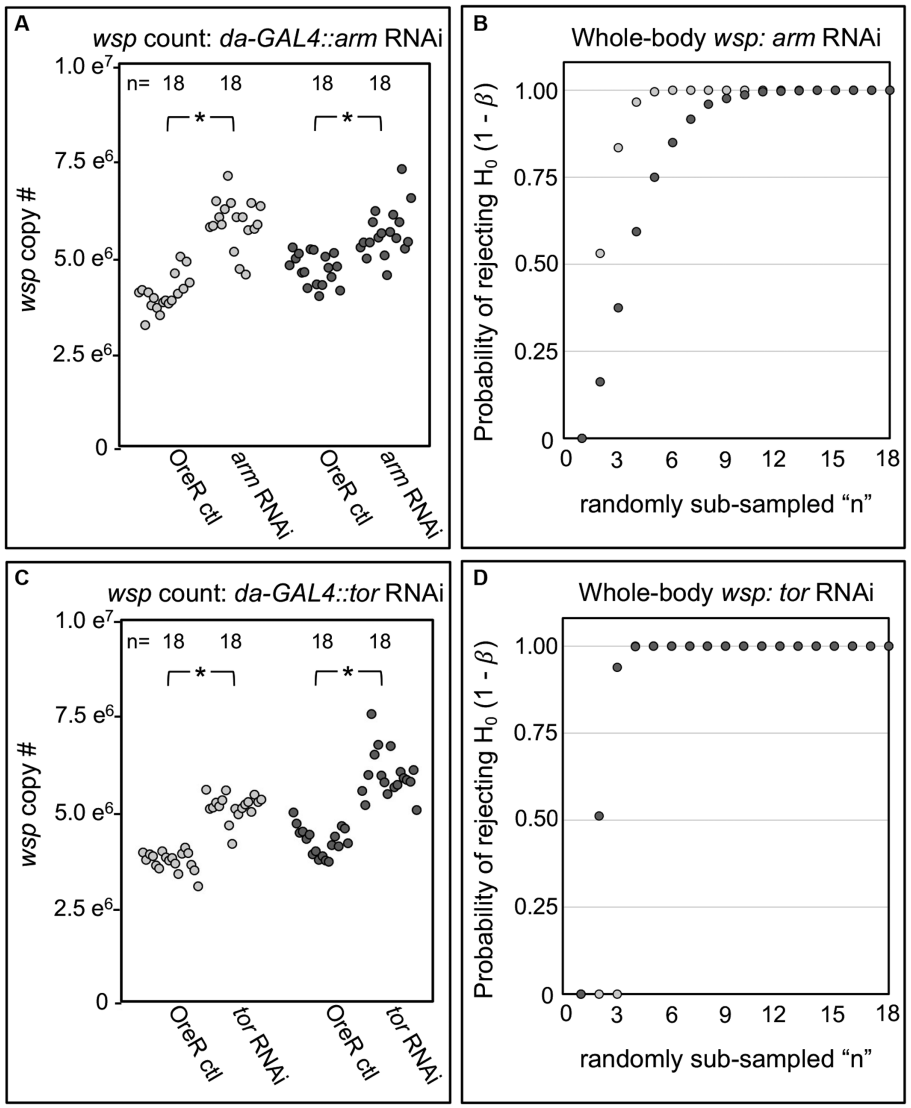

FIGURE 4
Whole body *wsp* abundance in control vs. *da-GAL4::UAS-RNAi* knockdown flies. Panels show data from 2 independent biological replicates. **(A)** Whole-body *wsp* abundance in *arm*-RNAi conditions. **(B)** Power analysis, testing the likelihood of significance as a function of sample size in **(A)**. **(C)** Whole-body *wsp* abundance in *tor*-RNAi conditions. **(D)** Power analysis, testing the likelihood of significance in **(C)**. Significance was set at * $p < 0.05$.

disruption would be expected to show the opposite results from an AXIN disruption. Meaning, since IWR-1 caused a titer increase, genetic disruptions in *arm* would be expected to prompt a titer decrease. From a mechanistic standpoint, this scenario would also make sense. It has been shown that Arm can suppress autophagy (Petherick et al., 2013; Feng et al., 2023) (Figure 6), so autophagy functions should increase when Arm RNAi is expressed, resulting in *Wolbachia* titer reduction. In this study, *Wolbachia* titer decreased in the induced *GS-GAL4:: Arm-shRNA* conditions. However, the constitutive *da-GAL4:: Arm-shRNA* treatment yielded a titer increase, not decrease. This disparity may be due to constitutive da-GAL4 disruption eliciting a cumulative, lifelong effect, with the possibility of involvement by other compensatory pathways. By contrast, the induction of GS-GAL4 in adults is uncoupled from earlier developmental events and may provide a more focused view of host pathway effects on *Wolbachia* titer in adult insects.

The mTOR pathway is well-known for regulation of autophagy. The mTORC1 complex has been shown to down-regulate autophagy through suppression of ULK1 (Yamamoto et al., 2023), as well as through suppression of GSK3 (Papadopoli et al., 2021) which would otherwise promote ULK1 function (Ryu et al., 2021) (Figure 6). In an alternate scenario, mTORC1 has the opposite regulatory effect, by inhibiting Wnt signaling at the level of the receptor, shutting down its function (Zeng et al., 2018). In that case, GSK3 would remain free to perform the complementary functions of activating ULK1 (Ryu et al., 2021) while also preventing Arm from suppressing ULK1 function (Petherick et al., 2013; Feng et al., 2023) (Figure 6). With this range of possibility, mTOR effects on autophagy function could go either way.

All mTORC1 disruptions in this study yielded a whole-body *Wolbachia* titer increase, regardless of the experimental system or type of manipulation tool used. This robust set of results is also compatible with the possibility of autophagy suppression of *Wolbachia*. If true, the

10.3389/fmicb.2024.1364009

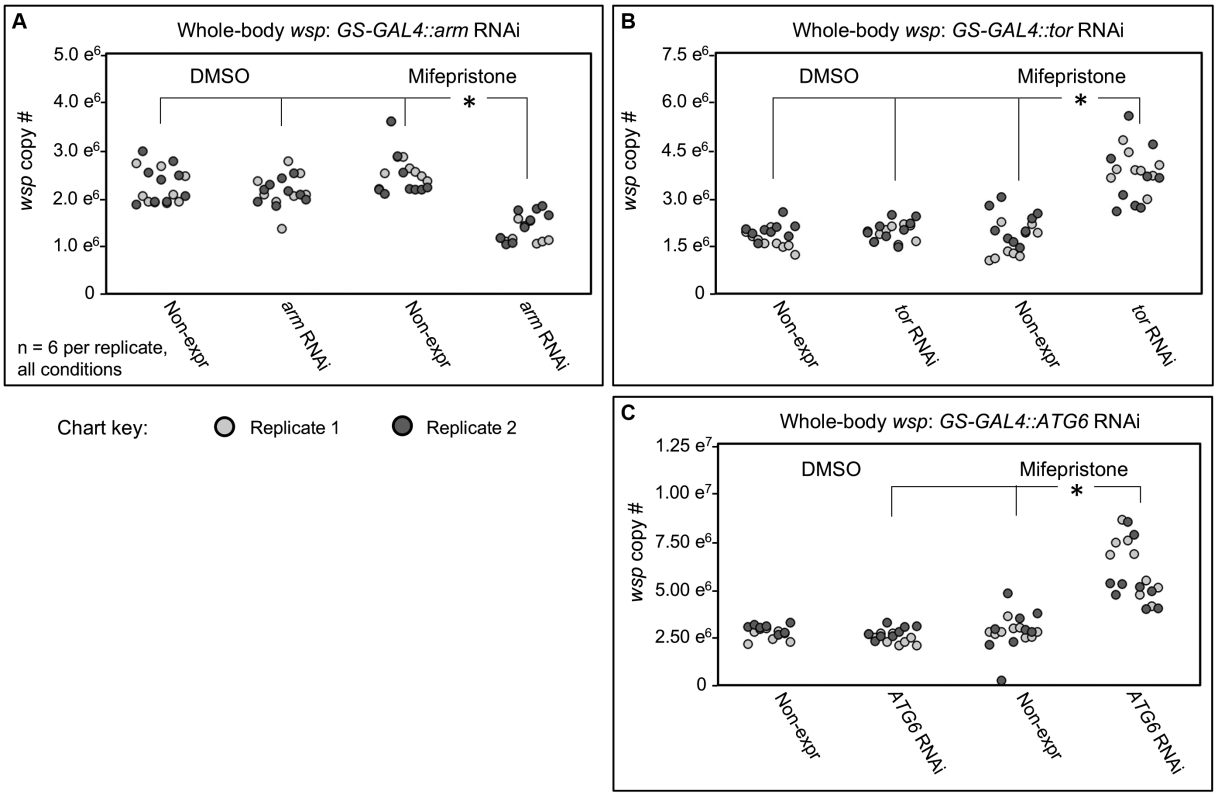

FIGURE 5
Whole body *wsp* abundance in control vs. *GS-GAL4::UAS-RNAi* knockdown flies. Flies capable of dsRNA expression were compared against non-expressing siblings, in the presence of DMSO or Mifepristone dissolved into DMSO. Genetic disruptions tested: **(A)** *arm* RNAi, **(B)** *tor* RNAi, **(C)** *ATG6* RNAi. Data out of range for **(C)**: 3 outliers for the Non-expressing DMSO condition at 2.01×10^7, 2.54×10^7, 2.064×10^7, and 1 outlier for the ATG6 RNAi DMSO condition at 2.28×10^7. Significance was set at * $p < 0.05$, and is displayed only for conditions where all replicates met this standard.

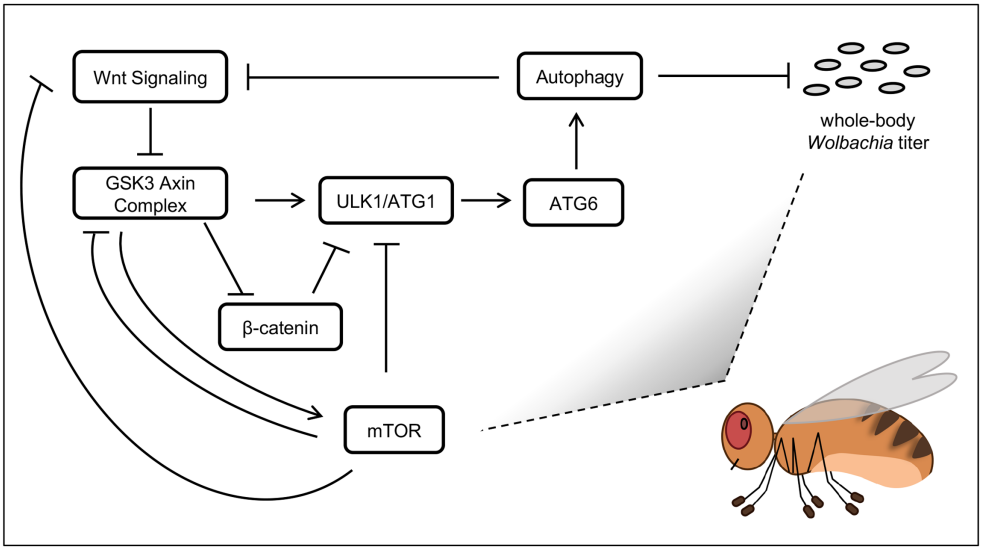

FIGURE 6
Models of host effects on whole-body *Wolbachia* titer. Pathway functions are displayed as per field literature. Boxes: host functions. Grey ovals: *Wolbachia* bacteria.

implication would be that under normal conditions, mTORC1 function emphasizes suppression of Wnt receptor activity relative to other autophagy-related targets, to promoting autophagy and indirectly, *Wolbachia* titer suppression. This model comes with a grain of salt, as signaling processes can be complex. The reported finding that autophagy can down-regulate Wnt signaling (Pérez-Plasencia

et al., 2020) is just one example of the nuance that may be involved (Figure 6). Future studies will be needed to elucidate how signaling and autophagy initiation affect *Wolbachia* and other microbial endosymbionts.

Data availability statement

The original contributions presented in the study are included in the article/Supplementary material, further inquiries can be directed to the corresponding author.

Ethics statement

The animal study was approved by FIU Institutional Biosafety Committee (IBC). The study was conducted in accordance with the local legislation and institutional requirements.

Author contributions

ZS: Conceptualization, Data curation, Methodology, Supervision, Validation, Visualization, Writing – original draft, Writing – review & editing, Formal analysis, Investigation. HS: Conceptualization, Data curation, Formal analysis, Investigation, Methodology, Supervision, Validation, Visualization, Writing – review & editing. RB: Conceptualization, Data curation, Formal analysis, Investigation, Methodology, Validation, Visualization, Writing – review & editing. LO: Conceptualization, Data curation, Formal analysis, Investigation, Methodology, Validation, Visualization, Writing – review & editing. LS: Conceptualization, Data curation, Methodology, Validation, Visualization, Writing – review & editing, Funding acquisition, Project administration, Resources, Software, Supervision, Writing – original draft.

Funding

The author(s) declare financial support was received for the research, authorship, and/or publication of this article. Support for this project was provided by startup funds from Florida International University (Academic Affairs) and a research grant awarded by the National Science Foundation (IOS-1656811).

Acknowledgments

Funding for this project came from FIU Academic Affairs and the NSF Division of Integrated Organismal Systems (#1656811). We thank Steen Christensen, Moises Camacho, Anthony Bellantuono, AJM Zehadee Momtaz, Erasmo Perera and FIU Biological Sciences for helpful discussions and logistical support. We also thank the University Graduate School, the College of Arts, Sciences and Education, the Biological Sciences Graduate program, the Transdisciplinary Biomolecular and Biomedical Sciences program, the Honors College and the Biology Honors Program at FIU for supporting our students.

Conflict of interest

The authors declare that the research was conducted in the absence of any commercial or financial relationships that could be construed as a potential conflict of interest.

Publisher's note

Supplementary material

The Supplementary material for this article can be found online at: https://www.frontiersin.org/articles/10.3389/fmicb.2024.1364009/full#supplementary-material

References

Ali, H., Muhammad, A., Islam, S. U., Islam, W., and Hou, Y. (2018). A novel bacterial symbiont association in the hispid beetle, *Octodonta nipae* (Coleoptera: Chrysomelidae), their dynamics and phylogeny. *Microb. Pathog.* 118, 378–386. doi: 10.1016/j.micpath.2018.03.046

Ali, H., Muhammad, A., Sanda, N. B., Huang, Y., and Hou, Y. (2019). Pyrosequencing uncovers a shift in bacterial communities across life stages of *Octodonta nipae* (Coleoptera: Chrysomelidae). *Front. Microbiol.* 10:466. doi: 10.3389/fmicb.2019.00466

Aros, C. J., Pantoja, C. J., and Gomperts, B. N. (2021). Wnt signaling in lung development, regeneration, and disease progression. *Commun. Biol.* 4:601. doi: 10.1038/s42003-021-02118-w

Bechelli, J., Vergara, L., Smalley, C., Buzhdygan, T. P., Bender, S., Zhang, W., et al. (2018). Atg5 supports *Rickettsia australis* infection in macrophages in vitro and in vivo. *Infect. Immun.* 87:e00651-18. doi: 10.1128/IAI.00651-18

Bian, G., Joshi, D., Dong, Y., Lu, P., Zhou, G., Pan, X., et al. (2013). Wolbachia invades Anopheles stephensi populations and induces refractoriness to plasmodium infection. *Science (New York, N.Y.)* 340, 748–751. doi: 10.1126/science.1236192

Birmingham, C. L., Smith, A. C., Bakowski, M. A., Yoshimori, T., and Brumell, J. H. (2006). Autophagy controls Salmonella infection in response to damage to the Salmonella-containing vacuole. *J. Biol. Chem.* 281, 11374–11383. doi: 10.1074/jbc.M509157200

Brand, A. H., and Perrimon, N. (1993). Targeted gene expression as a means of altering cell fates and generating dominant phenotypes. *Development* 118, 401–415. doi: 10.1242/dev.118.2.401

Christensen, S., Camacho, M., Sharmin, Z., Momtaz, A. J. M. Z., Perez, L., Navarro, G., et al. (2019). Quantitative methods for assessing local and bodywide contributions to Wolbachia titer in maternal germline cells of Drosophila. *BMC Microbiol.* 19:206. doi: 10.1186/s12866-019-1579-3

Christensen, S., Pérez Dulzaides, R., Hedrick, V. E., Momtaz, A. J. M. Z., Nakayasu, E. S., Paul, L. N., et al. (2016). Wolbachia endosymbionts modify Drosophila ovary protein levels in a context-dependent manner. *Appl. Environ. Microbiol.* 82, 5354–5363. doi: 10.1128/AEM.01255-16

Cogni, R., Ding, S. D., Pimentel, A. C., Day, J. P., and Jiggins, F. M. (2021). Wolbachia reduces virus infection in a natural population of Drosophila. *Commun. Biol.* 4:1327. doi: 10.1038/s42003-021-02838-z

Czyż, D. M., Potluri, L.-P., Jain-Gupta, N., Riley, S. P., Martinez, J. J., Steck, T. L., et al. (2014). Host-Directed Antimicrobial Drugs with Broad- 51 Spectrum Efficacy against Intracellular Bacterial Pathogens. *MBio*, 5. doi: 10.1128/mBio.01534-14

Derré, I., Pypaert, M., Dautry-Varsat, A., and Agaisse, H. (2007). RNAi screen in Drosophila cells reveals the involvement of the tom complex in Chlamydia infection. *PLoS Pathog.* 3, 1446–1458. doi: 10.1371/journal.ppat.0030155

Duffy, J. B. (2002). GAL4 system in Drosophila: a fly geneticist's Swiss army knife. *Genesis* 34, 1–15. doi: 10.1002/gene.10150

Edosa, T. T., Jo, Y. H., Keshavarz, M., Park, K. B., Cho, J. H., Bae, Y. M., et al. (2020). TmAtg6 plays an important role in anti-microbial defense against *Listeria monocytogenes* in the mealworm, *Tenebrio molitor*. *Int. J. Mol. Sci.* 21:1232. doi: 10.3390/ijms21041232

Feng, X., Sun, D., Li, Y., Zhang, J., Liu, S., Zhang, D., et al (2023). Local membrane source gathering by p62 body drives autophagosome formation. *Nature Communications* 14, 7338. doi: 10.1038/s41467-023-42829-8

Foley, S. L., Johnson, T. J., Ricke, S. C., Nayak, R., and Danzeisen, J. (2013). Salmonella pathogenicity and host adaptation in chicken-associated Serovars. *Microbiol. Mol. Biol. Rev.* 77, 582–607. doi: 10.1128/MMBR.00015-13

Galán, J. E., Pace, J., and Hayman, M. J. (1992). Involvement of the epidermal growth factor receptor in the invasion of cultured mammalian cells by *Salmonella typhimurium*. *Nature* 357, 588–589. doi: 10.1038/357588a0

Grobler, Y., Yun, C. Y., Kahler, D. J., Bergman, C. M., Lee, H., Oliver, B., et al. (2018). Whole genome screen reveals a novel relationship between Wolbachia levels and Drosophila host translation. *PLoS Pathog.* 14:e1007445. doi: 10.1371/journal.ppat.1007445

Haselton, A., Sharmin, E., Schrader, J., Sah, M., Poon, P., and Fridell, Y.-W. C. (2010). Partial ablation of adult Drosophila insulin-producing neurons modulates glucose homeostasis and extends life span without insulin resistance. *Cell Cycle* 9, 3063–3071. doi: 10.4161/cc.9.15.12458

Heddi, A., Grenier, A. M., Khatchadourian, C., Charles, H., and Nardon, P. (1999). Four intracellular genomes direct weevil biology: nuclear, mitochondrial, principal endosymbiont, and Wolbachia. *Proc. Natl. Acad. Sci. USA* 96, 6814–6819. doi: 10.1073/pnas.96.12.6814

Hedges, L. M., Brownlie, J. C., O'Neill, S. L., and Johnson, K. N. (2008). Wolbachia and virus protection in insects. *Science (New York, N.Y.)* 322:702. doi: 10.1126/science.1162418

Hill, S. M., Wrobel, L., and Rubinsztein, D. C. (2019). Post-translational modifications of Beclin 1 provide multiple strategies for autophagy regulation. *Cell Death Differ.* 26, 617–629. doi: 10.1038/s41418-018-0254-9

Hoffmann, A. A., Hercus, M., and Dagher, H. (1998). Population dynamics of the Wolbachia infection causing cytoplasmic incompatibility in *Drosophila melanogaster*. *Genetics* 148, 221–231. doi: 10.1093/genetics/148.1.221

Hoffmann, A. A., Turelli, M., and Harshman, L. G. (1990). Factors affecting the distribution of cytoplasmic incompatibility in *Drosophila simulans*. *Genetics* 126, 933–948. doi: 10.1093/genetics/126.4.933

Ikeda, S., Kishida, S., Yamamoto, H., Murai, H., Koyama, S., and Kikuchi, A. (1998). Axin, a negative regulator of the Wnt signaling pathway, forms a complex with GSK-3beta and beta-catenin and promotes GSK-3beta-dependent phosphorylation of beta-catenin. *EMBO J.* 17, 1371–1384. doi: 10.1093/emboj/17.5.1371

Kaur, R., Martinez, J., Rota-Stabelli, O., Jiggins, F. M., and Miller, W. J. (2020). Age, tissue, genotype and virus infection regulate Wolbachia levels in Drosophila. *Mol. Ecol.* 29, 2063–2079. doi: 10.1111/mec.15462

Keeling, P. J., and McCutcheon, J. P. (2017). Endosymbiosis: the feeling is not mutual. *J. Theor. Biol.* 434, 75–79. doi: 10.1016/j.jtbi.2017.06.008

Kessler, M., Zielecki, J., Thieck, O., Mollenkopf, H.-J., Fotopoulou, C., and Meyer, T. F. (2012). Chlamydia trachomatis disturbs epithelial tissue homeostasis in fallopian tubes via paracrine Wnt signaling. *The American Journal of Pathology*, 180, 186–198. doi: 10.1016/j.ajpath.2011.09.015

Kim, B. H., Yin, C.-H., Guo, Q., Bach, E. A., Lee, H., Sandoval, C., et al. (2008). A small molecule compound identified through a cell-based screening inhibits JAK/STAT pathway signaling in human cancer cells. *Molecular Cancer Therapeutics*, 7, 2672–2680. doi: 10.1158/1535-7163.MCT-08-0309

Landmann, F., Bain, O., Martin, C., Uni, S., Taylor, M. J., and Sullivan, W. (2012). Both asymmetric mitotic segregation and cell-to-cell invasion are required for stable germline transmission of Wolbachia in filarial nematodes. *Biol. Open* 1, 536–547. doi: 10.1242/bio.2012737

Landmann, F., Voronin, D., Sullivan, W., and Taylor, M. J. (2011). Anti-filarial activity of antibiotic therapy is due to extensive apoptosis after Wolbachia depletion from filarial nematodes. *PLoS Pathog.* 7:e1002351. doi: 10.1371/journal.ppat.1002351

Latorre, A., and Manzano-Marín, A. (2017). Dissecting genome reduction and trait loss in insect endosymbionts. *Ann. N. Y. Acad. Sci.* 1389, 52–75. doi: 10.1111/nyas.13222

Lewis, D. (1985). "Symbiosis and mutualism: crisp concepts and soggy semantics" in *The biology of mutualism: ecology and evolution*. ed. D. H. Boucher (London: Oxford University Press).

López-Madrigal, S., and Duarte, E. H. (2019). Titer regulation in arthropod-Wolbachia symbioses. *FEMS Microbiol. Lett.* 366:fnz232. doi: 10.1093/femsle/fnz232

Luo, T., Dunphy, P. S., Lina, T. T., and McBride, J. W. (2016). Ehrlichia chaffeensis exploits canonical and noncanonical host Wnt signaling pathways to stimulate phagocytosis and Promote Intracellular Survival. *Infection and Immunity*, 84, 686–700. doi: 10.1128/IAI.01289-15

Luo, T., Dunphy, P. S., and McBride, J. W. (2017). *Ehrlichia chaffeensis* tandem repeat effector targets differentially influence infection. *Front. Cell. Infect. Microbiol.* 7:178. doi: 10.3389/fcimb.2017.00178

Markstein, M., Dettorre, S., Cho, J., Neumuller, R. A., Craig-Muller, S., and Perrimon, N. (2014). Systematic screen of chemotherapeutics in Drosophila stem cell tumors. *Proceedings of the National Academy of Sciences*, 111, 4530–4535. doi: 10.1073/pnas.1401160111

McGarry, H. F., Egerton, G. L., and Taylor, M. J. (2004). Population dynamics of Wolbachia bacterial endosymbionts in Brugia malayi. *Mol. Biochem. Parasitol.* 135, 57–67. doi: 10.1016/j.molbiopara.2004.01.006

Metcalf, J. A., Jo, M., Bordenstein, S. R., Jaenike, J., and Bordenstein, S. R. (2014). Recent genome reduction of Wolbachia in *Drosophila recens* targets phage WO and narrows candidates for reproductive parasitism. *PeerJ* 2:e529. doi: 10.7717/peerj.529

Moy, R. H., and Cherry, S. (2013). Antimicrobial autophagy: a conserved innate immune response in Drosophila. *J. Innate Immun.* 5, 444–455. doi: 10.1159/000350326

Ni, J.-Q., Zhou, R., Czech, B., Liu, L.-P., Holderbaum, L., Yang-Zhou, D., et al. (2011). A genome-scale shRNA resource for transgenic RNAi in Drosophila. *Nat. Methods* 8, 405–407. doi: 10.1038/nmeth.1592

Niu, H., Yamaguchi, M., and Rikihisa, Y. (2008). Subversion of cellular autophagy by *Anaplasma phagocytophilum*. *Cell. Microbiol.* 10, 593–605. doi: 10.1111/j.1462-5822.2007.01068.x

Pannebakker, B. A., Loppin, B., Elemans, C. P. H., Humblot, L., and Vavre, F. (2007). Parasitic inhibition of cell death facilitates symbiosis. *Proc. Natl. Acad. Sci. USA* 104, 213–215. doi: 10.1073/pnas.0607845104

Papadopoli, D., Pollak, M., and Topisirovic, I. (2021). The role of GSK3 in metabolic pathway perturbations in cancer. *Biochim. Biophys. Acta, Mol. Cell Res.* 1868:119059. doi: 10.1016/j.bbamcr.2021.119059

Pérez-Plasencia, C., López-Urrutia, E., García-Castillo, V., Trujano-Camacho, S., López-Camarillo, C., and Campos-Parra, A. D. (2020). Interplay between autophagy and Wnt/β-catenin signaling in Cancer: therapeutic potential through drug repositioning. *Front. Oncol.* 10:1037. doi: 10.3389/fonc.2020.01037

Perkins, L. A., Holderbaum, L., Tao, R., Hu, Y., Sopko, R., McCall, K., et al. (2015). The transgenic RNAi project at Harvard Medical School: resources and validation. *Genetics* 201, 843–852. doi: 10.1534/genetics.115.180208

Perrimon, N., Ni, J.-Q., and Perkins, L. (2010). In vivo RNAi: today and tomorrow. *Cold Spring Harb. Perspect. Biol.* 2:a003640. doi: 10.1101/cshperspect.a003640

Petherick, K. J., Williams, A. C., Lane, J. D., Ordóñez-Morán, P., Huelsken, J., Collard, T. J., et al. (2013). Autolysosomal β-catenin degradation regulates Wnt-autophagy-p62 crosstalk. *EMBO J.* 32, 1903–1916. doi: 10.1038/emboj.2013.123

Porter, J., and Sullivan, W. (2023). The cellular lives of Wolbachia. *Nat. Rev. Microbiol.* 21, 750–766. doi: 10.1038/s41579-023-00918-x

Ren, D., Song, J., Ni, M., Kang, L., and Guo, W. (2020). Regulatory mechanisms of cell polyploidy in insects. *Front. Cell Dev. Biol.* 8:361. doi: 10.3389/fcell.2020.00361

Rikihisa, Y., Zhang, Y., and Park, J. (1995). Role of Ca2 and calmodulin in ehrlichial infection in macrophages. *Infection and Immunity*, 63, 2310–2316.

Roman, G., Endo, K., Zong, L., and Davis, R. L. (2001). P{switch}, a system for spatial and temporal control of gene expression in *Drosophila melanogaster*. *Proc. Natl. Acad. Sci.* 98, 12602–12607. doi: 10.1073/pnas.221303998

Ryu, H. Y., Kim, L. E., Jeong, H., Yeo, B. K., Lee, J. W., Nam, H., et al. (2021). GSK3B induces autophagy by phosphorylating ULK1. *Exp. Mol. Med.* 53, 369–383. doi: 10.1038/s12276-021-00570-6

Sachs, J. L., Skophammer, R. G., Bansal, N., and Stajich, J. E. (2014). Evolutionary origins and diversification of proteobacterial mutualists. *Proc. R. Soc. B Biol. Sci.* 281:20132146. doi: 10.1098/rspb.2013.2146

Sazama, E. J., Ouellette, S. P., and Wesner, J. S. (2019). Bacterial endosymbionts are common among, but not necessarily within, Insect Species. *Environ. Entomol.* 48, 127–133. doi: 10.1093/ee/nvy188

Serbus, L. R., Landmann, F., Bray, W. M., White, P. M., Ruybal, J., Lokey, R. S., et al. (2012). A cell-based screen reveals that the albendazole metabolite, albendazole sulfone, targets Wolbachia. *PLoS Pathogens*, 8, e1002922. doi: 10.1371/journal.ppat.1002922255

Schneider, D. I., Parker, A. G., Abd-Alla, A. M., and Miller, W. J. (2018). High-sensitivity detection of cryptic Wolbachia in the African tsetse fly (Glossina spp.). *BMC Microbiol.* 18:140. doi: 10.1186/s12866-018-1291-8

Serbus, L. R., and Sullivan, W. (2007). A cellular basis for Wolbachia recruitment to the host germline. *PLoS Pathog.* 3:e190. doi: 10.1371/journal.ppat.0030190

Serbus, L. R., White, P. M., Silva, J. P., Rabe, A., Teixeira, L., Albertson, R., et al. (2015). The impact of host diet on Wolbachia titer in Drosophila. *PLoS Pathog.* 11:e1004777. doi: 10.1371/journal.ppat.1004777

Slanina, H., Mündlein, S., Hebling, S., and Schubert-Unkmeir, A. (2014). Role of epidermal growth factor receptor signaling in the interaction of *Neisseria meningitidis* with endothelial cells. *Infect. Immun.* 82, 1243–1255. doi: 10.1128/IAI.01346-13

Strunov, A., Schmidt, K., Kapun, M., and Miller, W. J. (2022). Restriction of Wolbachia Bacteria in early embryogenesis of Neotropical Drosophila species via endoplasmic reticulum-mediated autophagy. *MBio* 13:e0386321. doi: 10.1128/mbio.03863-21

Su, T., Li, X., Yang, M., Shao, Q., Zhao, Y., Ma, C., et al. (2020). Autophagy: An intracellular degradation pathway regulating plant survival and stress response. *Frontiers Plant Science*, 11, 164. doi: 10.3389/fpls.2020.00164

Tao, H., Chen, F., Liu, H., Hu, Y., Wang, Y., and Li, H. (2017). Wnt/β-catenin signaling pathway activation reverses gemcitabine resistance by attenuating Beclin1-mediated autophagy in the MG63 human osteosarcoma cell line. *Mol. Med. Rep.* 16, 1701–1706. doi: 10.3892/mmr.2017.6828

Taylor, M. J., Bandi, C., and Hoerauf, A. (2005). Wolbachia bacterial endosymbionts of filarial nematodes. *Adv. Parasitol.* 60, 245–284. doi: 10.1016/S0065-308X(05)60004-8

Teixeira, L., Ferreira, A., and Ashburner, M. (2008). The bacterial symbiont Wolbachia induces resistance to RNA viral infections in *Drosophila melanogaster*. *PLoS Biol.* 6:e2. doi: 10.1371/journal.pbio.1000002

Unckless, R. L., Boelio, L. M., Herren, J. K., and Jaenike, J. (2009). Wolbachia as populations within individual insects: causes and consequences of density variation in natural populations. *Proc. Biol. Sci.* 276, 2805–2811. doi: 10.1098/rspb.2009.0287

Veneti, Z., Clark, M. E., Karr, T. L., Savakis, C., and Bourtzis, K. (2004). Heads or tails: host-parasite interactions in the Drosophila-Wolbachia system. *Appl. Environ. Microbiol.* 70, 5366–5372. doi: 10.1128/AEM.70.9.5366-5372.2004

Voronin, D., Cook, D. A. N., Steven, A., and Taylor, M. J. (2012). Autophagy regulates Wolbachia populations across diverse symbiotic associations. *Proc. Natl. Acad. Sci.* 109, E1638–E1646. doi: 10.1073/pnas.1203519109

Werren, J. H., Baldo, L., and Clark, M. E. (2008). Wolbachia: master manipulators of invertebrate biology. *Nat. Rev. Microbiol.* 6, 741–751. doi: 10.1038/nrmicro1969

White, P. M., Pietri, J. E., Debec, A., Russell, S., Patel, B., and Sullivan, W. (2017). Mechanisms of horizontal cell-to-cell transfer of Wolbachia spp. in *Drosophila melanogaster*. *Appl. Environ. Microbiol.* 83:e03425-16. doi: 10.1128/AEM.03425-16

White, P. M., Serbus, L. R., Debec, A., Codina, A., Bray, W., Guichet, A., et al. (2017). Reliance of Wolbachia on high rates of host proteolysis revealed by a genome-wide RNAi screen of Drosophila cells. *Genetics* 205, 1473–1488. doi: 10.1534/genetics.116.198903

Wiwatanaratanabutr, I., and Kittayapong, P. (2009). Effects of crowding and temperature on Wolbachia infection density among life cycle stages of *Aedes albopictus*. *J. Invertebr. Pathol.* 102, 220–224. doi: 10.1016/j.jip.2009.08.009

Yamamoto, H., Zhang, S., and Mizushima, N. (2023). Autophagy genes in biology and disease. *Nat. Rev. Genet.* 24, 382–400. doi: 10.1038/s41576-022-00562-w

Zeng, H., Lu, B., Zamponi, R., Yang, Z., Wetzel, K., Loureiro, J., et al. (2018). mTORC1 signaling suppresses Wnt/β-catenin signaling through DVL- dependent regulation of Wnt receptor FZD level. *Proc. Natl. Acad. Sci. USA* 115, E10362–E10369. doi: 10.1073/pnas.1808575115

frontiers | Frontiers in Microbiology

TYPE Original Research
PUBLISHED 07 May 2024
DOI 10.3389/fmicb.2024.1386458

OPEN ACCESS

EDITED BY
Yuval Gottlieb,
Hebrew University of Jerusalem, Israel

REVIEWED BY
Jeremy Foster,
New England Biolabs, United States
Habib Ali,
Khwaja Fareed University of Engineering and Information Technology (KFUEIT), Pakistan
Xiao-Li Bing,
Nanjing Agricultural University, China

*CORRESPONDENCE
Marius Poulain
✉ marius.poulain@outlook.fr
Anna Zaidman-Rémy
✉ anna.zaidman@insa-lyon.fr
Natacha Kremer
✉ natacha.kremer@cnrs.fr

RECEIVED 15 February 2024
ACCEPTED 12 April 2024
PUBLISHED 07 May 2024

CITATION
Poulain M, Rosinski E, Henri H, Balmand S, Delignette-Muller M-L, Heddi A, Lasseur R, Vavre F, Zaidman-Rémy A and Kremer N (2024) Development, feeding, and sex shape the relative quantity of the nutritional obligatory symbiont *Wolbachia* in bed bugs.
Front. Microbiol. 15:1386458.
doi: 10.3389/fmicb.2024.1386458

Development, feeding, and sex shape the relative quantity of the nutritional obligatory symbiont *Wolbachia* in bed bugs

Marius Poulain[1,2,3]*, Elodie Rosinski[1], Hélène Henri[1], Séverine Balmand[2], Marie-Laure Delignette-Muller[1], Abdelaziz Heddi[2], Romain Lasseur[3], Fabrice Vavre[1], Anna Zaidman-Rémy[2,4]* and Natacha Kremer[1]*

[1]Université Lyon 1, CNRS, VetAgroSup, Laboratoire de Biométrie et Biologie Evolutive, UMR 5558, Villeurbanne, France, [2]INSA Lyon, INRAE, BF2I, UMR203, Villeurbanne, France, [3]Izinovation SAS, Lyon, France, [4]Institut Universitaire de France, Paris, France

The common bed bug, *Cimex lectularius*, is a hemipteran insect that feeds only on blood, and whose bites cause public health issues. Due to globalization and resistance to insecticides, this pest has undergone a significant and global resurgence in recent decades. Blood is an unbalanced diet, lacking notably sufficient B vitamins. Like all strict hematophagous arthropods, bed bugs host a nutritional symbiont supplying B vitamins. In *C. lectularius*, this nutritional symbiont is the intracellular bacterium *Wolbachia* (*w*Cle). It is located in specific symbiotic organs, the bacteriomes, as well as in ovaries. Experimental depletion of *w*Cle has been shown to result in longer nymphal development and lower fecundity. These phenotypes were rescued by B vitamin supplementation. Understanding the interaction between *w*Cle and the bed bug may help to develop new pest control methods targeting the disruption of this symbiotic interaction. The objective of this work was thus to quantify accurately the density of *w*Cle over the life cycle of the host and to describe potential associated morphological changes in the bacteriome. We also sought to determine the impact of sex, feeding status, and aging on the bacterial population dynamics. We showed that the relative quantity of *w*Cle continuously increases during bed bug development, while the relative size of the bacteriome remains stable. We also showed that adult females harbor more *w*Cle than males and that *w*Cle relative quantity decreases slightly in adults with age, except in weekly-fed males. These results are discussed in the context of bed bug ecology and will help to define critical points of the symbiotic interaction during the bed bug life cycle.

KEYWORDS

***Cimex lectularius*, *Wolbachia*, nutritional symbiosis, host-symbiont interaction, bacterial growth dynamics, development, bacteriome**

1 Introduction

Bed bugs have undergone a major and worldwide resurgence in the number of infestations during the last decades (Doggett and Lee, 2023) due to globalization (Štefka et al., 2022), urbanization (Hwang et al., 2005), and selection of insecticide resistance (Dang et al., 2017). Bed bugs are mainly found in habitats associated with humans (Parola and Izri, 2020):

individual or collective housing, habitats linked to tourism (e.g., hotels, seasonal rentals) or health (e.g., hospitals, retirement homes), but also places associated with culture (e.g., movie theaters) or transportation (e.g., trains). Bites lead to itchy lesions and rashes, and infestations can cause sleep disturbances, psychological distress, and stigma (Doggett et al., 2012). Thus, bed bugs are a growing health and socio-economic burden requiring new, alternative methods to insecticides to control their populations.

The common bed bug, *Cimex lectularius,* is a strict hematophagous pest insect. This hemimetabolous insect undergoes five nymphal stages before the final molt to adulthood. Each instar requires a blood meal to proceed to the molting in 1 week, and both sexes bite at the adult stage. Like other strict hematophagous insects or species living on a nutritionally unbalanced diet (Janson et al., 2008; Rio et al., 2017; Duron and Gottlieb, 2020), bed bugs have evolved a long-term association with endosymbionts providing essentials nutrients that they lack in their diet, notably sufficient B vitamins. As far as known, *C. lectularius* microbiota is composed of one to three endosymbionts, one of them being an obligate nutritional symbiont. The obligate endosymbiont is *Wolbachia* (*w*Cle) (Sakamoto and Rasgon, 2006) and provides two essential B vitamins (i.e., biotin and riboflavin) (Hosokawa et al., 2010; Nikoh et al., 2014; Hickin et al., 2022). The experimental depletion of *w*Cle results in a decrease in the number of laid eggs, a decrease in hatching rate, an increase in nymphal development, and a smaller adult size (Chang, 1974; Hosokawa et al., 2010; Hickin et al., 2022). The two facultative endosymbionts are a γ-proteobacterial endosymbiont (Hypša and Aksoy, 1997; Hosokawa et al., 2010) of the Symbiopectobacterium family, known as *BEV*-like, for "Bacterial symbiont of *Euscelidius variegatus*" (Degnan et al., 2011; Nadal-Jimenez et al., 2022) and a torix *Rickettsia* (Potts et al., 2020; Thongprem et al., 2020; Pilgrim et al., 2021). Little is known about these facultative endosymbionts, but their effect on fitness appears limited (Hosokawa et al., 2010; Thongprem et al., 2020). All three endosymbionts are present in the ovaries, which ensure their vertical transmission through eggs (Hosokawa et al., 2010; Thongprem et al., 2020). Endosymbionts are also observed in specialized host cells called bacteriocytes. These cells form oblong-shaped organs, the bacteriomes, which are localized on the left and right side of the insect, between the fourth and fifth abdominal tergites (Hertig and Wolbach, 1924; Chang and Musgrave, 1973; Hosokawa et al., 2010; Thongprem et al., 2020).

Disrupting the nutritional symbiosis with the obligate endosymbiont *w*Cle could therefore be a promising control method, for instance by inducing a break-down in symbiosis or a stop in metabolic supplementation. To develop such a control strategy, it is essential to understand the dynamics of *w*Cle throughout the insect development, and as a function of sex and feeding. Previous studies have reported the presence of *w*Cle in the eggs, the first instars, and in the adults of both sexes (Hosokawa et al., 2010; Thongprem et al., 2020). *w*Cle relative quantity was shown to be higher in the fifth instar stage than in the first nymphal stage and to decrease in adult females starved for at least 21 days (Fisher et al., 2018). These results raise the question of the impact of development and natural aging (independent of starvation), but also of the dynamics of *w*Cle in males. Here, we thus present a detailed characterization of the interaction between *C. lectularius* and its nutritional obligatory endosymbiont *w*Cle using cohorts. We describe the dynamics of *w*Cle load in *C. lectularius*, and the effect of feeding, at all nymphal stages. We also document the development of the bacteriome during nymphal development. Finally, we quantify the evolution of the relative quantity of *w*Cle after adult emergence and specifically test the impacts of sex, aging, and starvation on the relative quantity of *w*Cle in adults.

2 Methods

2.1 Insects, feeding and rearing

The "F4" strain of *C. lectularius* was sampled in London (UK) in 2008 (Thongprem et al., 2020). Isofemale lines were created immediately after sampling and were reared on human blood in Oliver Otti's lab (Dresden, Germany) until 2021. For our experiments, we used three of these isofemale lines, provided by O. Otti: F4-V1, F4-V6, and F4-V48. These lines were confirmed by PCR to be negative for torix *Rickettsia* and are positive for *BEV*-like. We fed bed bugs on the Hemotek® system with human blood provided by the *Etablissement Français du Sang* [blood group: O or A with 17 IU.mL Sodium Heparin (BD Vacutainer); temperature: 36.5 ± 0.5°C; membrane: parafilm®]. Colonies were maintained in round plastic jars containing corrugated cardboard harborage shelters (41 mm × 30 mm), at 24°C, 60% relative humidity, and with a photoperiod of 12 L:12D.

2.2 Cohort generation and sampling for bacterial dynamics in nymphs

Couples from either F4-V1, F4-V6, and F4-V48 lines were fed weekly on 1 mL of human blood for 30 min. The cohorts were generated as follows: fed couples were isolated in 24-well plates to mate and oviposit for 5 days, then males were removed. After 2 weeks, females were removed, and nymphs were gathered in round plastic jars containing corrugated cardboard harborage shelters. For each cohort and each nymphal stage, unfed (UF) nymphs (1 to 3 nymphs per cohort) were sampled from the first nymphs hatched (#1 in Supplementary Figure S1) and the remaining nymphs were fed. Nymphs that did not feed were discarded. Sampling was completed at each nymphal stage by collecting nymphs one-day post-feeding (1DPF, #2 in Supplementary Figure S1), and five-days post-feeding (5DPF, #3 in Supplementary Figure S1). Molting to the next instar occurred 1 week after the last meal; nymphs that did not molt were discarded, and samplings were performed (UF, 1DPF, 5DPF) as described previously for the following stages (second, third, fourth, and fifth instar). Bed bugs were frozen immediately after collection and kept at −20°C until DNA extraction. A total of 168 nymphs were sampled, originating from 6 cohorts (1 F4-V1, 2 F4-V6, and 3 F4-V48).

2.3 Cohort generation and sampling for bacterial dynamics in adults

Nymphs at the fifth instar were taken from either F4-V1, F4-V6, and F4-V48 lines and were fed on 1 mL of human blood for 30 min. To quantify *Wolbachia* density over the nymph-to-adult transition, 5DPF fifth instars were sampled for both sexes, the sex being determined at that stage by a combination of approaches described

previously in Langer et al. (2020). One week after the fifth instar feeding, residual nymphs were discarded.

To determine the effect of sex, feeding, and aging on *Wolbachia* density, 1DPF male and female adults were sampled, and populations were divided equally into two round plastic jars. One jar was fed weekly (condition: weekly feeding), while the other one was not fed (condition: starvation after feeding on day 1). Each week, for 4 weeks, males and females of both jars were sampled at the date corresponding to 1DPF for the fed population (Supplementary Figure S2). Bed bugs were frozen immediately after collection and kept at −20°C until DNA extraction. A total of 146 fifth instars and adults were sampled, originating from 6 cohorts (1 F4-V1, 2 F4-V6, and 3 F4-V48).

2.4 DNA extraction

DNA was extracted using the MACHEREY-NAGEL NucleoSpin® 96 Tissue kit, following the protocol for genomic DNA from tissue, except for small individuals (i.e., from first to third instars). Small instar samples were placed in 0.2-mL tubes with three 1.5-mm stainless steel beads while large instar samples were placed in 2-mL tubes with one 5-mm diameter bead. All samples were left for 15 min at −80°C before being ground with a Tissue Lyzer (Retsch, Qiagen) for 2 min at 20 Hz. The following steps of the protocol followed the supplier's recommendations, except for the small individuals. Indeed, for small individuals, the volume of lysis and wash buffers was divided by 3 compared to the recommendations and compared to the samples considered as large (i.e., from the fourth nymphal stage to the adult stage). For all samples, pre-lysis was carried out for 2 h at 56°C, washes were performed under vacuum, while elution was performed by centrifugation at 5600 g for 2 min with 100 µL of elution buffer. Eluted DNA was stored at −20°C until qPCR quantification.

2.5 Detection of symbionts using PCR amplification

Conventional PCR was used to verify the presence/absence of symbionts. The *w*Cle 16S rRNA gene [INT2F, INT2R; 136 bp (Sakamoto and Rasgon, 2006)], the *γ-proteobacteria* 16S rRNA gene [BEV_F, BEV_R; 420 bp (Hosokawa et al., 2010)], the torix *Rickettsia gltA* gene [RiGltA405_F, RiGltA1193_R; 786 bp (Pilgrim et al., 2017)], and the *C. lectularius* ribosomal protein (*RPL18*) gene [RPL18F, RPL18R; 137 bp (Fisher et al., 2018)] were PCR-amplified as follows on a subset of unfed fifth instars ($n = 10$) and on one control sample known to be infected by the three symbionts. A 25-µL reaction containing 2.5 µL 10X DreamTaq® Green Buffer, 0.5 µL of dNTP (10 µM), 0.1 µL of DreamTaq® DNA Polymerase (5 U/µL), 0.5 µL of each primer set (10 µM) (primer sequences in Supplementary Table S1), and 2 µL of template DNA (previously diluted to 1/20) was prepared. All PCR reactions were performed in a Bio-Rad C1000 Touch™ thermal cycler with the following program: an initial denaturation step at 95°C for 5 min, followed by 35 cycles of 95°C for 30 s, Tm °C for 30 s and 72°C for 1 min. A final extension step of 72°C for 5 min was included. To visualize the amplicons, 5 µL of the PCR products were electrophoresed at 100 mV for 25 min (TBE 0.5X, 1% agarose, 0.5% BIOTIUM GelRed® Nucleic Acid Gel Stain).

2.6 *Wolbachia* quantification using real-time PCR

A real-time quantitative PCR (qPCR) duplex assay targeting the *w*Cle-*16S* rDNA and the bed bug *RPL18* gene was used to obtain relative quantification of *w*Cle in each bed bug. The 10-µL reaction mix contained 5 µL SsoAdvanced™ Universal Probe Supermix (Bio-Rad), 500 nM of each forward and reverse primer, 300 nM of each probe, and 2 µL of extracted DNA previously diluted to 1/20. We used primers and probes previously described (Supplementary Table S1). The probes were provided by IDT DNA Technologies and included two quenchers, Iowa Black® at the 3′ end, and another internal quencher called ZEN™. Each probe also had a specific fluorophore at the 5' end, FAM for *w*Cle, and HEX for the *RPL18* gene of *C. lectularius*. Real-time qPCR was performed in QuantStudio 6 Flex™ (Applied Biosystems) with the following program: an initial denaturation step at 95°C for 30 s, followed by 40 cycles of 95°C for 10 s, 60°C for 30 s and 72°C for 30 s. The qPCR assay efficiency (primer efficiency in Supplementary Table S1) was determined and confirmed in every run by constructing a standard curve using serial dilutions of a purified and quantified amplicon of each target. In addition, the specificity and absence of inhibitors in the samples were assessed upstream using dilutions of DNA extracts produced under the same conditions.

2.7 Statistical analysis of the relative quantity of *Wolbachia*

Each qPCR measurement was made in duplicate. Values for which the delta of quantification cycles (Cq) between replicates was greater than 0.5 cycles or the values of Cq were higher than 35 cycles were discarded [*w*Cle-16S: 7.14% discarded ($n = 12$), RPL18: 5.36% discarded ($n = 9$; 8 in common with *w*Cle-16S)]. Most of these discarded samples were young nymphal stages (71.42% of discarded are first instars).

The relative quantity (RQ) of *Wolbachia* within the insect was calculated based on equation one of Pfaffl (2001) where the ratio between the quantity of insect gene (reference) and *w*Cle gene (target) relied on the PCR efficiency (E) and the number of Cq:

$$RQ = \frac{\mathbf{E}reference^{\mathbf{Cq}reference}}{\mathbf{E}target^{\mathbf{Cq}target}}$$

We used the R software (version 4.1.0) for all analyses (R Core Team, 2024) and the ggplot2 R package (version 3.4.4) for all plots (Wickham, 2016). To test the effect of different factors (i.e., development, feeding, sex) and their interactions on relative *w*Cle quantities, we analyzed $\log_{10}$-transformed data using a linear mixed effect model with the lme4 R package (Bates et al., 2015).

For nymphal (N) samples, we tested the following model: lmer [$\log_{10}$(RQ) ~ Age_N + Feeding_State + Age_N:Feeding_State + (1|Cohort)], where Age_N is a quantitative variable associated to nymphal development (weeks), Feeding_State is a qualitative factor associated to blood feeding status (UF/1DPF/5DPF), and Cohort is a random factor linked to replicate sampling (A to F). Unfed (UF) first instars are considered as references in the model.

For adult (A) samples, because the feeding factor varies only after the adult's first blood meal, we first tested on fifth instars 5DPF and adults 7DPF of both sexes ($n = 26$) the effect of development (fifth instar to adult) on the relative quantity in *w*Cle in both sexes, with the following model: lmer [$\log_{10}$(RQ) ~ Age + Sex + Sex:Age + (1|Cohort)], using the fifth instar females as reference. We then tested on adults only the effect of aging, blood feeding, and sex, with the following model: lmer [$\log_{10}$(RQ) ~ Age_A + Sex + Feeding:Age_A + Sex:Age_A + Feeding:Sex:Age_A + (1|Cohort)], using the weekly fed-first week females as reference. Age and Age_A are quantitative variables associated with development and aging, respectively; Sex is a qualitative factor (female, male); Feeding is a qualitative factor associated to blood feeding status (fed, unfed), whose dynamics depends on the aging/duration of starvation; and Cohort is a random factor linked to replicate sampling (G to L).

Normality and homoscedasticity were checked graphically on residuals for each fitted model. Residuals were also checked for homogeneity of variance. Statistics for global effects of factors and their interactions are reported in Supplementary Tables S2, S4, S5. Model coefficients are reported with their mean ± confidence intervals (0.95). Interaction effects can be interpreted as an additive effect compared with the reference. Because calculating *p*-values from linear mixed effect model is complex and subject to controversy (Wasserstein and Lazar, 2016; Wasserstein et al., 2019), p-values estimated using the lmerTest R package (Kuznetsova et al., 2017) are only specified in Supplementary Tables S2, S4, S5.

2.8 *Wolbachia* localization using Fluorescence *In situ* Hybridization (FISH)

We documented the localization of *w*Cle for each nymphal stage after molting (10 nymphs per instar) in the F4-V48 line, using the FISH technique (Thongprem et al., 2020). Tissues were dissected in 1X PBS and preserved immediately in Carnoy solution (chloroform: ethanol: glacial acetic acid = 6:3:1) overnight. All samples were cleared by incubation in 6% H_2O_2 in ethanol until the body was transparent, i.e., for at least 24 h for first and second instars, and up to 5 weeks for third to fifth instars. We then used a tungsten micro-needle to make micropores in the nymph cuticle to allow the fluorescence probes to diffuse through the cuticle during the hybridization step. The samples were hybridized by incubating the tissues overnight in a hybridization buffer (20 mM Tris–HCl pH 8.0, 0.9 M NaCl, 0.01% Sodium dodecyl sulfate 30% formamide) with 10 pmol/mL of rRNA specific probes for *w*Cle (Hosokawa et al., 2010; probe sequences in Supplementary Table S1). After incubation, tissues were washed in buffer (0.3 M NaCl, 0.03 M sodium citrate, 0.01% sodium dodecyl sulfate) and mounted onto a slide using fluoro Gel with DABCO (Electron Microscopy Science) as a mounting medium. Slides were then observed under Leica THUNDER Imager 3D Assay epifluorescence microscope.

2.9 Evolution of bacteriome size over development

Length of bacteriome and thorax were measured on ImageJ 1.53c (Schneider et al., 2012) taking the maximum length (L_b) and width (W_b) of both bacteriomes, and the length (L_p) and width (W_p) at the middle of the pronotum. Relative bacteriome sizes were calculated by the ratio between pronotum estimated area ($L_p \times W_p$) and the mean estimated area ($\pi \times (1/2)\ L_b \times (1/2)\ W_b$) of both bacteriomes. We used the R software (version 4.1.0) for all analyses and plots (R Core Team, 2024).

To test the effect of age on absolute area of the bacteriome, we analyzed data using a Linear Model (LM). We tested the following model: lm ($\log_{10}$(Mean_area_bact) ~ Stage), where Stage is a qualitative factor associated to nymphal development (first to fifth instar) and Mean_area_bact is the mean of the estimated area of both bacteriomes in a nymph.

To test the effect of the age on the relative area of the bacteriome, we analyzed data using the following model: lm (Mean_ratio_area ~ Stage), where Mean_ratio_area is the mean of the estimated area of both bacteriomes relatively to the estimated area of the thorax in the nymph.

Normality and homoscedasticity were checked graphically on residuals for each fitted model. Residuals were checked for homogeneity of variance. LM statistics were given for global effects of factors. To compare the means of either the area or the relative size of the bacteriome between stages, we performed post-hoc Tukey tests (see Supplementary Table S3 for the complete output of each model).

2.10 Characterization of cryofixed bacteriomes using electro-microscopy (EM)

We performed the following manipulations at the *Centre Technologique des Microstructures* (CTμ, Université Claude Bernard Lyon 1, France). To avoid losing the samples during the procedure, bacteriomes of fifth instar females were dissected in PBS together with the proximal ovary and the surrounding cuticula. Samples were placed into specimen carriers previously covered with 0.5% lecithin in chloroform. Carriers were directly loaded into the HPM100 high pressure freezer and fast frozen. After freezing, samples were placed into a Leica EM AFS II Freeze substitution machine and incubated at -90°C for 30 h in substitution buffer (1% osmium tetroxide, 0.25% uranyl acetate, 0.5% glutaraldehyde, 1.5% H_2O in acetone) and then gradually heated to -30°C (+5°C/h) and maintained at that temperature for 24 h. Samples were washed with -30°C cold acetone and then gradually heated to 20°C (+10°C/h). Samples were placed in 25% Epon™ (Epoxy substitute embedding medium kit from Sigma-Aldrich®) in acetone for 3 h, 50% Epon™ in acetone for 17 h, 75% Epon™ in acetone for 3 h, then in three different baths of pure Epon™ for a total of 24 h. Infiltration and embedding in 1.7% benzyl dimethyl amine in Epon™ resin were performed during 4 days at 60°C.

Sectioning was performed on Leica EM UC7 ultramicrotome using a diamond knife (Diatome) and mounted on uncoated copper grids. Ultra-thin sections (70 nm) for Transmission Electro-microscopy (TEM) were observed at 120 keV using a JEOL 1400 electron microscope. Electron micrographs of standard sections were taken with GATAN DigitalMicrograph software (Pleasanton, CA) and further analyzed using ImageJ 1.53c.

3 Results

3.1 The relative quantity of *w*Cle increases exponentially over nymphal development

To analyze the dynamics of the obligatory endosymbiont *w*Cle during nymphal development, we measured by qPCR duplex assay the relative quantity of *w*Cle in 157 nymphs at different stages of development. *w*Cle quantity was below the level of detection in 2.55% of the samples ($n = 4$), which were all first instars. We tested the effect of development and feeding status on *w*Cle relative quantity on the remaining 153 samples, considering the variability observed between cohorts as a random effect in the model (Supplementary Figure S3).

The $\log_{10}$-transformed relative quantity of *w*Cle linearly increased with age (Figure 1) with a slope equal to 0.68 ± 0.11 (confidence interval at 0.95), equivalent to an increase by 4.68 of the relative quantity of *w*Cle at each nymphal stage; the $\log_{10}$-transformed absolute quantity of *w*Cle, as measured by quantification of its *16S* rDNA, increased ~2 times more strongly than that of the bed bug gene *RPL18* genes (Supplementary Figure S4). This result confirms an increase in the *w*Cle quantity relative to the number of host cells over nymphal development.

The blood feeding status also impacted the relative *w*Cle quantity, with an increase of 0.73 ± 0.45 on $\log_{10}$-transformed relative quantity (i.e., equivalent to an increase by 5.37 of the relative quantity) between unfed and 5DPF (Days Post Feeding) nymphs. This positive impact of blood feeding on the *w*Cle relative quantity dimmed as the nymph was growing (see interaction Age_N*Feeding State 5DPF Figure 1B).

3.2 The relative size of the bacteriome remains stable during nymphal development

To determine if the increase in *w*Cle relative quantity is associated with a change in the bacteriome shape or an over-growth of endosymbiont within the bacteriome, we performed Fluorescence *In situ* Hybridization (FISH) using probes targeting the endosymbiont 16S rRNA. *w*Cle was detected in bacteriomes of each sex at all instars during nymphal development (Figures 2A–F). All the bacteriocytes observed within a bacteriome were infected, and their cytoplasm was packed with *w*Cle (Figures 2A–E; Supplementary Figure S5). TEM observation performed on fifth instar females confirmed that *w*Cle exhibits a three-layer membrane presumably composed of the two membranes of the symbiont and an individual vacuolar membrane of insect origin similar to what has been described 50 years ago (Chang and Musgrave, 1973) (Figure 2G).

To determine if the increase in *w*Cle relative quantity is associated with an increase in symbiotic organ size, we measured the size of the bacteriome in 39 nymphs ($n = 6$–10/stage). While the bacteriome absolute area doubled at each stage between the first and fourth instars (Figure 2H), its relative area to the thorax remained unchanged between the different developmental stages (Figure 2I).

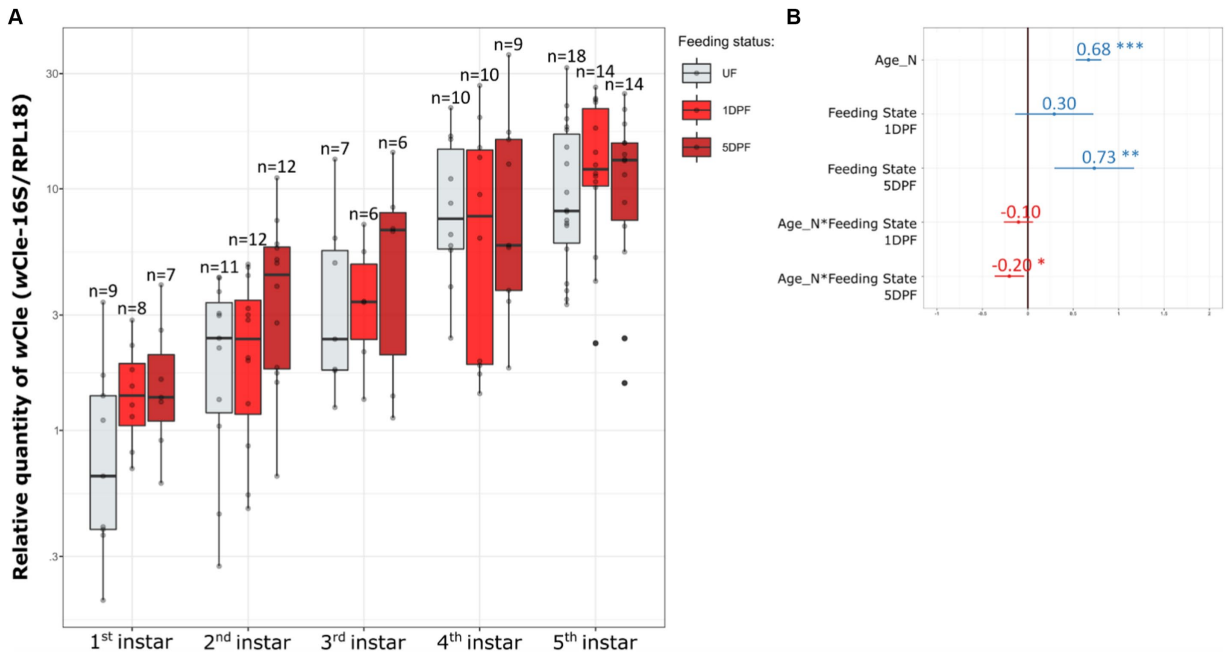

FIGURE 1
Dynamics of the *w*Cle relative quantity in nymphal bed bugs over development and associated statistics. **(A)** *w*Cle relative quantities of unfed (UF) newly molted nymphs, 1-day post-feeding nymphs (1DPF), and 5-day post-feeding nymphs (5DPF) are represented as boxplots for each nymphal instar. Each boxplot represents n = 6–18 individual nymphs (1 to 3 sampled nymphs per cohort). **(B)** Resume statistics of the mixed model $\log_{10}(RQ) \sim Age\_N + Feeding\_State + Age\_N{:}Feeding\_State + (1|Cohort)$, where Age_N is a quantitative factor (number of weeks) and Feeding_State a qualitative factor (UF, 1DPF, 5DPF, with UF set as reference). Estimate values and their associated confidence intervals are indicated on the panel (blue when positive effect, red when negative effect). As example for this analysis: $\log_{10}(RQ)$ increases by 0.68 ± 0.11 each week for UF individuals, $\log_{10}(RQ)$ increases by 0.73 ± 0.45 between the UF reference and 5DPF, and $\log_{10}(RQ)$ increases by 0.68–0.20 = 0.48 each week for 5DPF individuals. For detailed statistics, see Supplementary Table S2.

10.3389/fmicb.2024.1386458

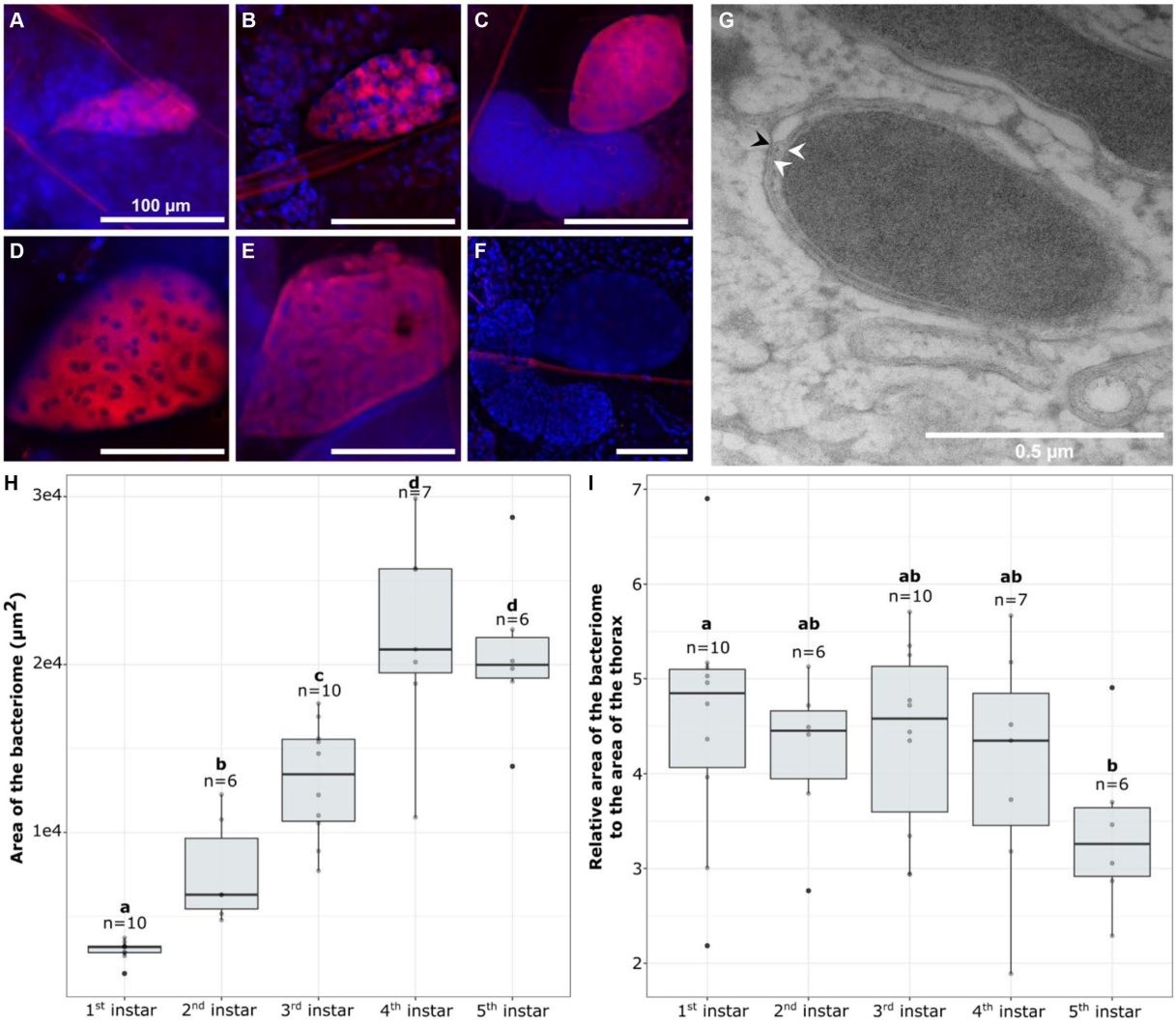

FIGURE 2
Visualization of the bacteriome and endosymbiont dynamics over bed bug development. **(A–F)** FISH visualization of *w*Cle in bacteriomes **(A)** first instar; **(B)** second instar; **(C)** third instar; **(D)** fourth instar; **(E)** fifth instar; **(F)** Negative control (without probe) of a third instar bacteriome. In red: *w*Cle; in blue: bacteriocyte nuclei (DAPI). Scale bars: 100 µm. **(G)** TEM of *w*Cle in a fifth instar female. White arrows show the two inner membranes of the endosymbiont, while the black one shows the peripheric third vacuolar membrane. **(H,I)** Dynamics of the bacterial size over development: **(H)** absolute area or **(I)** relative area of the bacteriome at each nymphal instar (first to fifth). Each boxplot represents $n = 6–10$ individual nymphs (F4-V48 line). Boxplots sharing the same letter are not significantly different (*t*-test, $p > 0.05$). For statistics, see Supplementary Table S3.

3.3 The dynamics of *w*Cle is positively impacted by feeding in males but not in females

We first aimed to determine whether the increase in *Wolbachia* relative quantity during nymphal development persists after the last molt (Figures 3A–D). We thus measured the relative quantity of *w*Cle in fifth instars (5DPF) and newly emerged adults (7DPF) a few days after feeding (data used symbolized by * on Figure 3C (females) and Figure 3D (males); statistics: Figure 3E). We showed a significant increase with development, as $\log_{10}$(RQ) of adult females increased by 0.63 ± 0.42 (equivalent to an increase by 4.57 of the relative quantity) compared to their fifth instar counterparts. No significant effect of sex on bacterial relative quantity was detected in this developmental window.

We then focused on adults and determined the effect of sex, aging, and feeding on the relative quantity of *w*Cle. We chose a weekly feeding protocol to mimic the natural feeding rate of bed bugs (Reinhardt and Siva-Jothy, 2007; Saveer et al., 2021). We thus measured the relative quantity of *w*Cle weekly during 28 days after emergence, in weekly fed or starved adults of each sex (total = 119 adults) and analyzed data using a global statistical model (Figure 3F). The relative quantity of *w*Cle slightly decreased with age in females for both feeding conditions (slope on $\log_{10}$-transformed data = −0.11 equivalent to a decrease of 0.78 each week; Figures 3A,C). In males, while the relative quantity of *w*Cle also decreased with time in starved males (slope on $\log_{10}$-transformed data = 0.16–0.28 = −0.12, equivalent to a decrease of 0.76 each week; Figure 3D), it increased with time in weekly-fed males (slope on $\log_{10}$-transformed data = 0.27–0.11 = 0.16, equivalent to an increase of 1.44 each week; Figure 3B), showing

10.3389/fmicb.2024.1386458

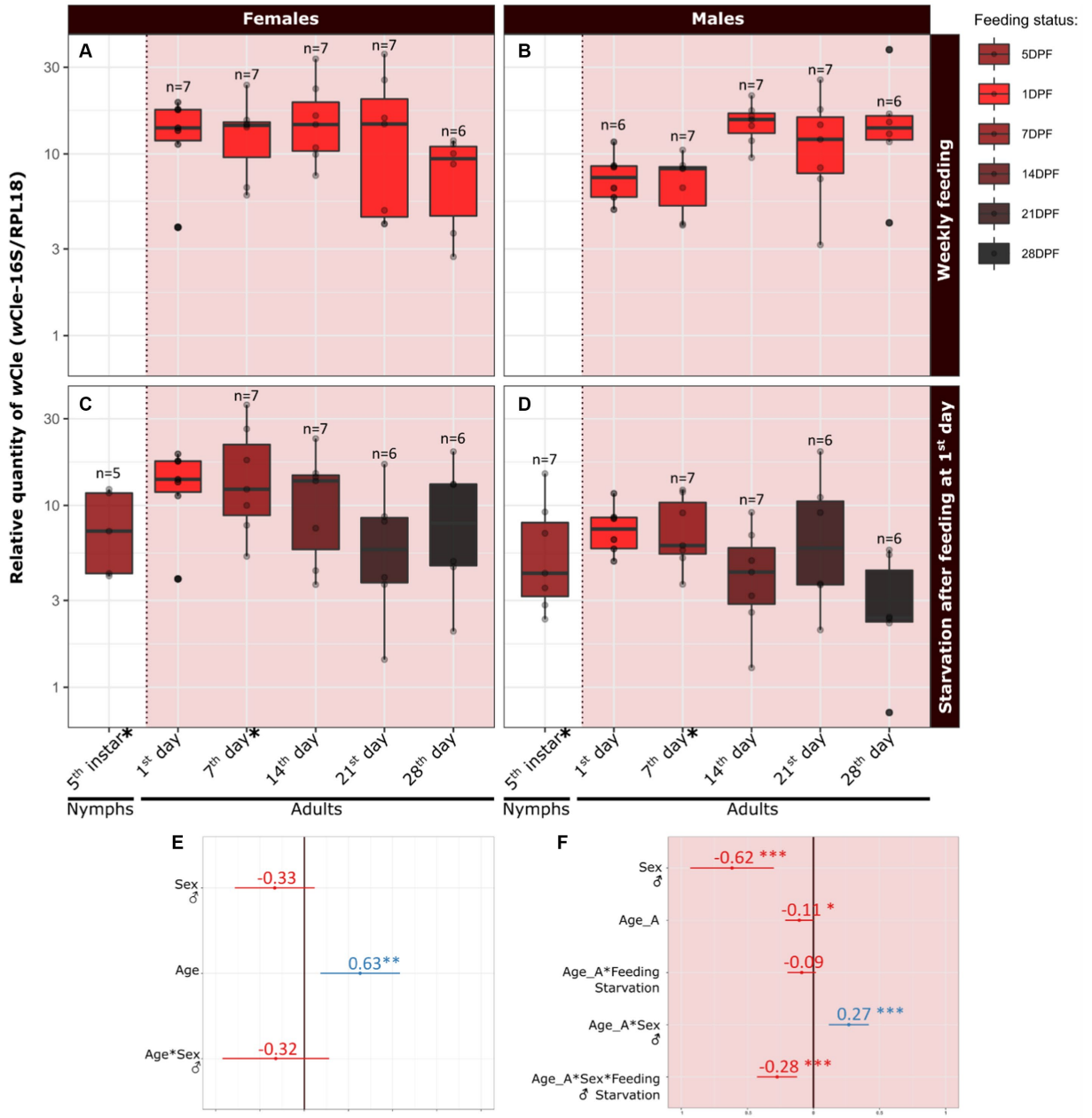

FIGURE 3
Dynamics of the relative quantity of *w*Cle from the fifth instar to adulthood, and during 5 weeks of adulthood. Concerning the relative quantity dynamics during last metamorphosis (i.e., between fifth instar (5DPF) and adulthood (7DPF) according to sex), the dataset used is marked with an asterisk on panels C and D. This first dataset was analyzed using a linear mixed model: $\log_{10}$(RQ) ~ Age + Sex + Sex:Age + (1|Cohort), where Age is a quantitative factor (weeks) and Sex a qualitative factor (female, male; female set as reference). Resume statistics are indicated on panel **(E)** Concerning the relative quantity dynamics in adult bed bugs according to sex, aging and feeding, the dataset used is presented in the red squares on the right of the dashed lines: relative quantity of *w*Cle in **(A)** females and **(B)** males fed every week (collection: 1DPF), or in **(C)** females and **(D)** males starved after the first-week meal (collected concomitantly with fed individuals). This latter dataset was analyzed using a linear mixed model $\log_{10}$(RQ) ~ Age_A + Sex + Feeding:Age_A + Sex:Age_A + Feeding:Sex:Age_A + (1|Cohort), where Age_A is a quantitative factor (weeks), Sex a qualitative factor (female set as reference) and Feeding is a qualitative factor (weekly fed, starved; weekly fed set as reference). Resume statistics are indicated on panel **(F)**. Each boxplot represents $n = 6–7$ individuals. Estimate values and their associated confidence intervals are indicated on panels **E** and **F**, respectively for each statistical analysis (blue when positive effect, red when negative effect). For detailed statistics, see Supplementary Tables S4, S5.

complex interactions between sex, age, and feeding conditions. Overall, males had nevertheless significantly less *w*Cle than females, as $\log_{10}$(RQ) of males was 0.62 ± 0.31 times less the one of females (equivalent to a 4,2-fold difference in relative quantity, Figures 3A–D,F). The $\log_{10}$-transformed absolute quantities of *Wolbachia* showed similar patterns (Supplementary Figure S6).

4 Discussion

In this study, we described the dynamics of *w*Cle, a nutritional obligatory symbiont of bed bugs. We observed that: (a) the largest increase in relative *w*Cle quantity occurred during the nymphal development; (b) this increase was exponential and positively impacted by the development of nymphal instars and the feeding status; (c) the size of the bacteriome increased isometrically with the development of the nymph; (d) except for continuously fed males, *w*Cle relative quantity decreased slightly during the first 4 weeks of adulthood, independently of the feeding status.

This study shows that the increase in *w*Cle relative quantity was exponential over nymphal development. Once adulthood was reached, *w*Cle relative quantity started to slightly decrease, except in weekly-fed males. These data complete and corroborate the results obtained by Fisher et al. (2018), which showed that *w*Cle relative quantity was higher in the fifth nymphal stage than in the first nymphal stage, but did not precisely quantify the dynamic between these two instars. Their data indicated an increase of ~1.6-fold in *w*Cle relative quantity between the end of the first instar and the start of the fifth instar in Jersey City and Harold Harlan strains. The increase was stronger in our F4 strain, with a ~6.4-fold increase in relative quantity. In the adult stage, our data confirm the decrease they reported in starved females. However, a stronger tendency was observed in Fisher et al.'s work, as titers in three-week starved females approached the low titer observed in first instars, while in our study, the decrease in the *w*Cle titer in four-week starved females only approached the titer measured in fifth instars. Fisher et al. (2018) observed that one of their two strains retained more *w*Cle through starvation than the other. One possible explanation could be differences in the way strains respond to starvation, as we used here the F4 strain (Thongprem et al., 2020) that is different from the strains used in the work of Fisher et al. (2018).

In this study, the increase in *w*Cle relative quantity in nymphs is associated with an increase in the absolute bacteriome size, but not in its relative size. These observations suggest an increase in the number of bacteria in each bacteriome and could result from two non-exclusive mechanisms: an increase in the bacteriocyte number, or an increase in the bacteriocyte size. The respective contribution of these two alternatives is difficult to evaluate in a species such as the bed bug. Indeed, bacteriocytes form very cohesive bacteriomes and it would require dissociating the organ in order to count and measure bacteriocytes. An increase in endosymbiont relative quantity from egg to adult stage (i.e., along nymphal, larval or pupal stages, depending on the insects) has been reported in several other nutritional endosymbiotic associations, such as the tsetse fly *Glossinidia glossina*/*Wigglesworthia glossinidia* (Rio et al., 2006), the cereal weevil *Sitophilus oryzae*/*Sodalis pierantonius* (Vigneron et al., 2014), or the pea aphid *Acyrtosiphon pisum*/*Buchnera aphidicola* (Simonet et al., 2016). In the pea aphid and the weevil, this increase was associated with a change in the number of the bacteriocytes or bacteriomes. In the *A. pisum*/*B. aphidicola* association, where bacteriocytes do not group into a cohesive bacteriome (Buchner, 1965; Douglas, 1989), the increase in the endosymbiont load during development was shown to correlate with both an increase in the quantity and in the size of bacteriocytes (Simonet et al., 2016, 2018). While bacteriocyte mitotic activity has not yet been reported, bacteriocyte enlargement and polyploidy has been proposed in several models to participate to bacteriome growth (Koch, 1959; Douglas, 1989; Moran et al., 1998; Baumann et al., 2006; Orr-Weaver, 2015; Alarcón et al., 2022; Nozaki and Shigenobu, 2022). Further experiments are needed to analyze the precise cellular mechanism of bacteriome growth in the bed bug. Alternatively, the increase in bacterial relative density could be linked to an increase in bacterial load in ovaries during development. To go further, it would be interesting to perform individual bacterial quantifications in bacteriomes and ovaries/testis. Unfortunately, it is technically very difficult to sex bed bugs and dissect bacteriomes in the early nymphal stages.

We noticed that blood intake had a positive effect (after 5 DPF) on the *w*Cle relative quantity in nymphs. This could indicate that blood ingestion brings profuse nutritional elements for *w*Cle proliferation. Based on this and previous works (Hosokawa et al., 2010; Nikoh et al., 2014; Hickin et al., 2022), the following succession of critical steps in the interaction could be considered: i) blood ingestion allows the increase in bacterial load, ii) this increase allows higher provision of B vitamins by the host, iii) the host molt once a critical threshold in B vitamin is reached, one week post blood-feeding. However, measuring the dynamic of *w*Cle in week-starved nymphs will be required to demonstrate that it is indeed the blood ingestion that enhances the developmental increase in *w*Cle, and that it is not simply due to aging. In the strict hematophagous hemipteran *Rhodnius prolixus*, the blood-meal stimulates the molt through humoral factors and neuronal signals generated by stretch receptors in the gut (Adams, 1999; Lange et al., 2022). Hence, another possibility would be that blood feeding in bedbugs impacts both the insect hormonal signaling regulating the molt and the bacterial load, coordinating an increase in bacterial quantity with the molting process.

After the increase in the *w*Cle relative quantity in nymphs up to adult emergence, its decrease in both weekly fed and starved females is intriguing. The decrease observed in starved females does not reach the first instar's quantity of *w*Cle like in Fisher et al. (2018). Because *w*Cle-synthetized B vitamins are necessary for fecundity and egg viability, we could expect either an increase or at least a steadiness in *w*Cle relative quantity in sexually mature fed females [i.e., ~5 days post emergence (Mellanby, 1939; Johnson, 1941; Davis, 1964)]. While the same pattern was observed between starved adults and weekly fed females, the slow decrease of *w*Cle could have different origins. In starved adults, nutritional scarcity could prevent the allocation of sufficient resources to endosymbiont growth or maintenance. Additionally, nutritional stress could trigger active mechanisms of endosymbiont elimination, including recycling of the symbionts for nutritive needs. For example, starved adults could engage in *w*Cle lysis by autophagy to retrieve nutrients through endosymbiont digestion during periods of nutritional scarcity. This process, known as wolbophagy, drives the elimination of the few damaged *Wolbachia* in healthy cells under stress conditions, and has been described in *Drosophila* (Deehan et al., 2021; Hargitai et al., 2022) but not in *Wolbachia*-nutritional endosymbioses. Drastic endosymbiont clearance by autophagy has been described in several associations, such as in some aphids (Hinde, 1971), the whitefly (Wang et al., 2022), or the carpenter ant (Gonçalves et al., 2020). This phenomenon is particularly exemplified in cereal weevils where the endosymbiont *S. pierantonius* grows dynamically during early adulthood, and provides essential amino acids for the host cuticle synthesis (Vigneron et al., 2014; Dell'Aglio et al., 2023). However, these gut-associated endosymbionts are eliminated through apoptotic and autophagic

mechanisms, starting 1 week after adult emergence, when the cuticle is fully synthetized and functional (Vigneron et al., 2014). The moderate decrease in *w*Cle quantity we observed along 4 weeks of adulthood in the bed bug could be the result of a moderate and progressive wolbophagy, which does not exclude a more drastic elimination later in the life cycle. To note, the mechanisms of transfer of nutrients from the endosymbionts to the host, especially B vitamins, remain unidentified so far in the bed bug-*w*Cle association, and could themselves rely on moderate wolbophagy, allowing the host to maintain a *w*Cle population while "harvesting" the B vitamins from the endosymbionts accordingly to its physiological needs.

Surprisingly, the weekly fed females also present a slow decrease of *w*Cle in the 4 weeks of observation, despite having abundant nutritional resources. However, this apparent abundance of nutritional resources must be put in perspective of their physiological needs. Indeed, weekly blood-feeding increases the mating rate (Mellanby, 1939; Johnson, 1941; Saveer et al., 2021). Mating is traumatic in bed bugs (Stutt and Siva-Jothy, 2001; Reinhardt et al., 2003; Reinhardt and Siva-Jothy, 2007); a high mating rate can thus enhance their induced immunity (Siva-jothy et al., 2019) and potentially impact *w*Cle density regulation. Weekly blood-feeding also increases the number of laid eggs (Mellanby, 1939; Johnson, 1941; Saveer et al., 2021). This increased reproductive activity (mating and egg production) of weekly-fed females likely requires a higher metabolic investment that could constrain the resource allocation to the endosymbionts despite the recurrent host feeding. Finally, a part of *w*Cle could be "lost" in the vertical transmission to the eggs. Counting the number of laid eggs per female and correlating them with the remaining quantity of endosymbionts in the mother's ovaries could be a way to confirm the potential "loss" of *w*Cle quantity by the mothers to the benefit of the transmission to progeny.

We also analyzed the *w*Cle dynamics in males, which had not been previously studied. Surprisingly, after emergence, weekly-fed males exhibited an increasing dynamics of *w*Cle relative quantity that contrasts with the decrease in *w*Cle quantities observed in starved males, but also in starved or weekly-fed females. This increasing quantity in weekly fed males is even more intriguing in males, in which the impact of an elimination of *w*Cle has a very limited effect on life history traits, such as the thorax size (Hickin et al., 2022). One hypothesis to explain the contrasting dynamics between weekly fed females and males could be that, while they both have access to food, they do likely not have similar metabolic needs, given the very costly investment the females make in reproduction. Therefore, *w*Cle could maintain and proliferate more effectively in weekly-fed males due to a higher availability of metabolic resources in these individuals.

Altogether, our main hypothesis to explain the regulation of *w*Cle behind the observed dynamics in adults would be that, in nutritional abundance conditions like weekly feeding, *w*Cle can proliferate to fulfill the host's needs. In contrast, during critical steps of host development, when the host's metabolic needs are higher (i.e., mating, starvation, egg formation), the symbiotic cost is in detriment of *w*Cle, whose quantity decreases. This decrease in quantity could be the result of either a decrease in proliferation due to nutritional scarcity, or an active recycling of endosymbionts by the host for example by wolbophagy. However, as described in other symbiotic associations, regulation of both *w*Cle location and load could also involve active immune mechanisms such as production of reactive oxygen species (ROS) (Pan et al., 2012; Zug and Hammerstein, 2015) or antimicrobial peptides (AMP) (Login et al., 2011) by the host.

5 Conclusion

This work shows a dynamics of *w*Cle that is positively impacted by blood ingestion during nymphal stages and in the adult males. This description of the dynamics of *w*Cle along the life cycle of its host allows to unveil that feeding is a critical step in the interaction, which should be considered in future research to pinpoint the best stages to decipher the molecular dialog between partners and envision the development of new symbiocides.

Data availability statement

The raw data supporting the conclusions of this article will be made available by the authors, without undue reservation. Access to raw data and scripts: https://zenodo.org/records/10817678.

Ethics statement

The manuscript presents research on animals that do not require ethical approval for their study.

Author contributions

MP: Data curation, Formal analysis, Investigation, Methodology, Writing – original draft, Writing – review & editing. ER: Resources, Writing – review & editing. HH: Data curation, Methodology, Writing – review & editing, Investigation. SB: Methodology, Visualization, Writing – review & editing, Investigation. M-LD-M: Methodology, Writing – review & editing. AH: Conceptualization, Funding acquisition, Writing – review & editing. RL: Funding acquisition, Project administration, Supervision, Writing – review & editing. FV: Conceptualization, Funding acquisition, Project administration, Supervision, Validation, Writing – original draft, Writing – review & editing. AZ-R: Conceptualization, Funding acquisition, Project administration, Supervision, Validation, Writing – original draft, Writing – review & editing, Methodology. NK: Conceptualization, Formal analysis, Funding acquisition, Project administration, Supervision, Validation, Writing – original draft, Writing – review & editing, Data curation, Methodology.

Funding

The author(s) declare financial support was received for the research, authorship, and/or publication of this article. This work was funded by the CIFRE contract n°2019/1626, the Pack Ambition Recherche Rhone-Alpes SymBed (20 009583 01), the ANR PRC FBI (ANR-21-CE35-0011), the Scientific Breakthrough Project Micro-be-have (Microbial impact on insect behavior) of Université de Lyon within the program 'Investissements d'Avenir' (ANR-11-IDEX-0007; ANR-16-IDEX-0005), and the Institut Universitaire de France (AZ-R, junior member).

Acknowledgments

We thank Oliver Otti for providing us bed bugs. We thank the Symbiotron platform from the FR3728 BioEEnViS (and especially Angelo Jacquet) and the Equipex+ InfectioTron (ANR-21-ESRE-0023) for facilities and equipment for rearing and experimentation on bed bugs. TEM imaging was performed at Centre Technologique des Microstructures EZUS LYON - Université Claude Bernard Lyon1 (CTμ), and we thank Lucie Geay for the ultra-thin sectioning of the tissues. We thank the members of MP thesis comity (Olivier Duron, Delphine Destoumieux-Garzon and François Leulier) for fruitful discussions.

Conflict of interest

MP and RL were employed by Izinovation SAS, a company working on protection against invasive species, pests, pathogens and in the field of plant health.

The remaining authors declare that the research was conducted in the absence of any commercial or financial relationships that could be construed as a potential conflict of interest.

Publisher's note

All claims expressed in this article are solely those of the authors and do not necessarily represent those of their affiliated organizations, or those of the publisher, the editors and the reviewers. Any product that may be evaluated in this article, or claim that may be made by its manufacturer, is not guaranteed or endorsed by the publisher.

Supplementary material

The Supplementary material for this article can be found online at: https://www.frontiersin.org/articles/10.3389/fmicb.2024.1386458/full#supplementary-material

References

Adams, T. S. (1999). Hematophagy and hormone release. *Ann. Entomol. Soc. Am.* 92, 1–13. doi: 10.1093/aesa/92.1.1

Alarcón, M. E., Polo, P. G., Akyüz, S. N., and Rafiqi, A. M. (2022). Evolution and ontogeny of bacteriocytes in insects. *Front. Physiol.* 13:1034066. doi: 10.3389/fphys.2022.1034066

Bates, D., Mächler, M., Bolker, B., and Walker, S. (2015). Fitting linear mixed-effects models using lme4. *J. Stat. Softw.* 67, 1–48. doi: 10.18637/jss.v067.i01

Baumann, P., Moran, N. A., and Baumann, L. (2006). "Bacteriocyte-associated endosymbionts of insects" in *The Prokaryotes*. eds. M. Dworkin, S. Falkow, E. Rosenberg, K. -H. Schleifer and E. Stackebrandt (New York, NY: Springer)

Buchner, P. (1965) *Endosymbiosis of animals with plant microorganisms*. Inderscience Publishers. Geneva

Chang, K. P. (1974). Effects of elevated temperature on the mycetome and symbiotes of the bed bug *Cimex lectularius* (Heteroptera). *J. Invertebr. Pathol.* 23, 333–340. doi: 10.1016/0022-2011(74)90098-6

Chang, K. P., and Musgrave, A. J. (1973). Morphology, histochemistry, and ultrastructure of mycetome and its rickettsial symbiotes in *Cimex lectularius* L. *Can. J. Microbiol.* 19, 1075–1081. doi: 10.1139/m73-171

Dang, K., Doggett, S. L., Veera Singham, G., and Lee, C. Y. (2017). Insecticide resistance and resistance mechanisms in bed bugs, Cimex spp. (Hemiptera: Cimicidae). *Parasit. Vectors* 10, 1–31. doi: 10.1186/s13071-017-2232-3

Davis, N. T. (1964). Studies of the reproductive physiology of Cimicidae (Hemiptera)-I. Fecundation and egg maturation. *J. Insect Physiol.* 10, 947–963. doi: 10.1016/0022-1910(64)90083-6

Deehan, M., Lin, W., Blum, B., Emili, A., and Frydman, H. (2021). Intracellular density of wolbachia is mediated by host autophagy and the bacterial cytoplasmic incompatibility gene cifb in a cell type-dependent manner in *drosophila melanogaster*. *MBio* 12, 1–19. doi: 10.1128/mBio.02205-20

Degnan, P. H., Bittleston, L. S., Hansen, A. K., Sabree, Z. L., Moran, N. A., and Almeida, R. P. P. (2011). Origin and examination of a leafhopper facultative endosymbiont. *Curr. Microbiol.* 62, 1565–1572. doi: 10.1007/s00284-011-9893-5

Dell'Aglio, E., Lacotte, V., Peignier, S., Rahioui, I., Benzaoui, F., Vallier, A., et al. (2023). Weevil carbohydrate intake triggers endosymbiont proliferation: a trade-off between host benefit and endosymbiont burden. *MBio* 14, 1–14. doi: 10.1128/mbio.03333-22

Doggett, S. L., Dwyer, D. E., Peñas, P. F., and Russell, R. C. (2012). Bed bugs: clinical relevance and control options. *Clin. Microbiol. Rev.* 25, 164–192. doi: 10.1128/CMR.05015-11

Doggett, S. L., and Lee, C. Y. (2023). Historical and contemporary control options against bed bugs, Cimex spp. *Annu. Rev. Entomol.* 68, 169–190. doi: 10.1146/annurev-ento-120220-015010

Douglas, A. E. (1989). Mycetocyte symbiosis in insects. *Biol. Rev.* 64, 409–434. doi: 10.1111/j.1469-185X.1989.tb00682.x

Duron, O., and Gottlieb, Y. (2020). Convergence of nutritional symbioses in obligate blood feeders. *Trends Parasitol.* 36, 816–825. doi: 10.1016/j.pt.2020.07.007

Fisher, M. L., Watson, D. W., Osborne, J. A., Mochizuki, H., Breen, M., and Schal, C. (2018). Growth kinetics of endosymbiont Wolbachia in the common bed bug, *Cimex lectularius*. *Sci. Rep.* 8, 11444–11449. doi: 10.1038/s41598-018-29682-2

Gonçalves, W. G., Fernandes, K. M., Silva, A. P. A., Gonçalves, D. G., Fiaz, M., and Serrão, J. E. (2020). Ultrastructure of the Bacteriocytes in the midgut of the carpenter ant *Camponotus rufipes*: endosymbiont control by autophagy. *Microsc. Microanal.* 26, 1236–1244. doi: 10.1017/S1431927620024484

Hargitai, D., Kenéz, L., al-Lami, M., Szenczi, G., Lőrincz, P., and Juhász, G. (2022). Autophagy controls Wolbachia infection upon bacterial damage and in aging *Drosophila*. *Front. Cell Dev. Biol.* 10:976882. doi: 10.3389/fcell.2022.976882

Hertig, M., and Wolbach, S. B. (1924). Studies on Rickettsia-like micro-organisms in insects. *J. Med. Res.* 44, 329–374.7.

Hickin, M. L., Kakumanu, M. L., and Schal, C. (2022). Effects of Wolbachia elimination and B-vitamin supplementation on bed bug development and reproduction. *Sci. Rep.* 12, 10270–10214. doi: 10.1038/s41598-022-14505-2

Hinde, R. (1971). The control of the mycetome symbiotes of the aphids *Brevicoryne brassicae* Myzus persicae, and Macrosiphum rosae. *J. Insect Physiol.* 17, 1791–1800. doi: 10.1016/0022-1910(71)90076-X

Hosokawa, T., Koga, R., Kikuchi, Y., Meng, X. Y., and Fukatsu, T. (2010). Wolbachia as a bacteriocyte-associated nutritional mutualist. *PNAS* 107, 769–774. doi: 10.1073/pnas.0911476107

Hwang, S. W., Svoboda, T. J., de Jong, I. J., Kabasele, K. J., and Gogosis, E. (2005). Bed bug infestations in an urban environment. *Emerg. Infect. Dis.* 11, 533–538. doi: 10.3201/eid1104.041126

Hypša, V., and Aksoy, S. (1997). Phylogenetic characterization of two transovarially transmitted endosymbionts of the bedbug *Cimex lectularius* (Heteroptera: Cimicidae). *Insect Mol. Biol.* 6, 301–304. doi: 10.1046/j.1365-2583.1997.00178.x

Janson, E. M., Stireman, J. O., Singer, M. S., and Abbot, P. (2008). Phytophagous insect-microbe mutualisms and adaptive evolutionary diversification. *Evolution* 62, 997–1012. doi: 10.1111/j.1558-5646.2008.00348.x

Johnson, C. G. (1941). The ecology of the bed-bug, *cimex lectularius* L., in Britain: report on research, 1935–1940. *J. Hyg.* 41, 345–461. doi: 10.1017/S0022172400012560

Koch, A. (1959). Intracellular symbiosis in insects. *Ann. Rev. Microbiol.* 14, 121–140. doi: 10.1146/annurev.mi.14.100160.001005

Kuznetsova, A., Brockhoff, P. B., and Christensen, R. H. B. (2017). lmerTest package: tests in linear mixed effects models. *J. Stat. Softw.* 82, 1–26. doi: 10.18637/JSS.V082.I13

Lange, A. B., Leyria, J., and Orchard, I. (2022). The hormonal and neural control of egg production in the historically important model insect, *Rhodnius prolixus*: a review, with new insights in this post-genomic era. *Gen. Comp. Endocrinol.* 321-322:114030. doi: 10.1016/j.ygcen.2022.114030

Langer, L., Froschauer, C., and Reinhardt, K. (2020). Sex differences in bedbug nymphs, *Cimex lectularius*. *J. Appl. Entomol.* 144, 838–843. doi: 10.1111/jen.12823

Login, F. H., Balmand, S., Vallier, A., Vincent-Monégat, C., Vigneron, A., Weiss-Gayet, M., et al. (2011). Antimicrobial peptides keep insect endosymbionts under control (method). *Science* 334, 362–365. doi: 10.1126/science.1209728

Mellanby, K. (1939). Fertilization and egg production in the bed-bug, *Cimex lectularius* L. *Parasitology* 31, 193–199. doi: 10.1017/S0031182000012750

Moran, N. A., Telang, A., and Smith, M. (1998). Symbionts of insects, a variety of insect groups harbor ancient prokaryotic endosymbionts. *Bioscience* 48, 295–304. doi: 10.1007/0-387-30741-9_16

Nadal-Jimenez, P., Siozios, S., Halliday, N., Cámara, M., and Hurst, G. D. D. (2022). *Symbiopectobacterium purcellii*, gen. Nov., sp. nov., isolated from the leafhopper *Empoasca decipiens*. *Int. J. Syst. Evol. Microbiol.* 72, 1–13. doi: 10.1099/ijsem.0.005440

Nikoh, N., Hosokawa, T., Moriyama, M., Oshima, K., Hattori, M., and Fukatsu, T. (2014). Evolutionary origin of insect-Wolbachia nutritional mutualism. *Proc. Natl. Acad. Sci.* 111, 10257–10262. doi: 10.1073/pnas.1409284111

Nozaki, T., and Shigenobu, S. (2022). Ploidy dynamics in aphid host cells harboring bacterial symbionts. *Sci. Rep.* 12, 9111–9112. doi: 10.1038/s41598-022-12836-8

Orr-Weaver, T. L. (2015). When bigger is better: the role of polyploidy in organogenesis. *Trends Genet.* 31, 307–315. doi: 10.1016/j.tig.2015.03.011

Pan, X., Zhou, G., Wu, J., Bian, G., Lu, P., Raikhel, A. S., et al. (2012). Wolbachia induces reactive oxygen species (ROS)-dependent activation of the toll pathway to control dengue virus in the mosquito *Aedes aegypti*. *Proc. Natl. Acad. Sci. USA* 109, E23–E31. doi: 10.1073/pnas.1116932108

Parola, P., and Izri, A. (2020). Clinical Practice: Clinical Practice. *N. Engl. J. Med.* 382, 2230–2237. doi: 10.1056/NEJMcp1905840

Pfaffl, M. W. (2001). A new mathematical model for relative quantification in real-time RT–PCR. *Nucleic Acids Res.* 29, 45e–445e. doi: 10.1093/nar/29.9.e45

Pilgrim, J., Ander, M., Garros, C., Baylis, M., Hurst, G. D. D., and Siozios, S. (2017). Torix group Rickettsia are widespread in Culicoides biting midges (Diptera: Ceratopogonidae), reach high frequency and carry unique genomic features. *Environ. Microbiol.* 19, 4238–4255. doi: 10.1111/1462-2920.13887

Pilgrim, J., Thongprem, P., Davison, H. R., Siozios, S., Baylis, M., Zakharov, E. V., et al. (2021). Torix Rickettsia are widespread in arthropods and reflect a neglected symbiosis. *GigaScience* 10, 1–19. doi: 10.1093/gigascience/giab021

Potts, R., Molina, I., Sheele, J. M., and Pietri, J. E. (2020). Molecular detection of Rickettsia infection in field-collected bed bugs. *New Microbes New Infect.* 34:100646. doi: 10.1016/j.nmni.2019.100646

R Core Team (2024). R: a language and environment for statistical computing. Available at: (https://www.R-project.org/).

Reinhardt, K., Naylor, R., and Siva-Jothy, M. T. (2003). Reducing a cost of traumatic insemination: female bedbugs evolve a unique organ. *Proc. R. Soc. B Biol. Sci.* 270, 2371–2375. doi: 10.1098/rspb.2003.2515

Reinhardt, K., and Siva-Jothy, M. T. (2007). Biology of the bed bugs (Cimicidae). *Annu. Rev. Entomol.* 52, 351–374. doi: 10.1146/annurev.ento.52.040306.133913

Rio, R. V. M., Attardo, G. M., and Weiss, B. L. (2017). Grandeur alliances: symbiont metabolic integration and obligate arthropod hematophagy. *Physiol. Behav.* 176, 139–148. doi: 10.1016/j.pt.2016.05.002.Grandeur

Rio, R. V. M., Wu, Y. N., Filardo, G., and Aksoy, S. (2006). Dynamics of multiple symbiont density regulation during host development: tsetse fly and its microbial flora. *Proc. R. Soc. B Biol. Sci.* 273, 805–814. doi: 10.1098/rspb.2005.3399

Sakamoto, J. M., and Rasgon, J. L. (2006). Geographic distribution of Wolbachia infections in *Cimex lectularius* (Heteroptera: Cimicidae). *J. Med. Entomol.* 43, 696–700. doi: 10.1603/0022-2585(2006)43[696:GDOWII]2.0.CO;2

Saveer, A. M., DeVries, Z., Santangelo, R. G., and Schal, C. (2021). Mating and starvation modulate feeding and host-seeking responses in female bed bugs, Cimex lectularius. *Sci. Rep.* 11:1915. doi: 10.1038/s41598-021-81271-y

Schneider, C. A., Rasband, W. S., and Eliceiri, K. W. (2012). NIH image to ImageJ: 25 years of image analysis. *Nat. Methods* 9, 671–675. doi: 10.1038/nmeth.2089

Simonet, P., Duport, G., Gaget, K., Weiss-Gayet, M., Colella, S., Febvay, G., et al. (2016). Direct flow cytometry measurements reveal a fine-tuning of symbiotic cell dynamics according to the host developmental needs in aphid symbiosis. *Sci. Rep.* 6:19967. doi: 10.1038/srep19967

Simonet, P., Gaget, K., Balmand, S., Ribeiro Lopes, M., Parisot, N., Buhler, K., et al. (2018). Bacteriocyte cell death in the pea aphid / Buchnera symbiotic system. *PNAS* 115, E1819–E1828. doi: 10.1073/pnas.1720237115

Siva-jothy, M. T., Zhong, W., Naylor, R., Heaton, L., Hentley, W., and Harney, E. (2019). Female bed bugs (*Cimex lectularius* L) anticipate the immunological consequences of traumatic insemination via feeding cues. *PNAS* 116, 14682–14687. doi: 10.1073/pnas.1904539116

Štefka, J., Votýpka, J., Lukeš, J., and Balvín, O. (2022). Cimex lectularius and *Cimex hemipterus* (bed bugs). *Trends Parasitol.* 38, 919–920. doi: 10.1016/j.pt.2022.04.006

Stutt, A. D., and Siva-Jothy, M. T. (2001). Traumatic insemination and sexual conflict in the bed bug *Cimex lectularius*. *Proc. Natl. Acad. Sci. USA* 98, 5683–5687. doi: 10.1073/pnas.101440698

Thongprem, P., Evison, S. E. F., Hurst, G. D. D., and Otti, O. (2020). Transmission, tropism, and biological impacts of Torix Rickettsia in the common bed bug *Cimex lectularius* (Hemiptera: Cimicidae). *Front. Microbiol.* 11:608763. doi: 10.3389/fmicb.2020.608763

Vigneron, A., Masson, F., Vallier, A., Balmand, S., Rey, M., Vincent-Monégat, C., et al. (2014). Insects recycle endosymbionts when the benefit is over. *Curr. Biol.* 24, 2267–2273. doi: 10.1016/j.cub.2014.07.065

Wang, Y., Li, C., Yan, J.-Y., Wang, T.-Y., Yao, Y.-L., Ren, F.-R., et al. (2022). Autophagy regulates white fl y-symbiont metabolic interactions. *Appl. Environ. Microbiol.* 88, 1–19. doi: 10.1128/AEM.02089-21

Wasserstein, R. L., and Lazar, N. A. (2016). The ASA statement on p-values: context, process, and purpose. *Am. Stat.* 70, 129–133. doi: 10.1080/00031305.2016.1154108

Wasserstein, R. L., Schirm, A. L., and Lazar, N. A. (2019). Moving to a world beyond "p < 0.05". *Am. Stat.* 73, 1–19. doi: 10.1080/00031305.2019.1583913

Wickham, H. (2016). ggplot2 elegant graphics for data analysis. Available at: http://www.springer.com/series/6991

Zug, R., and Hammerstein, P. (2015). Wolbachia and the insect immune system: what reactive oxygen species can tell us about the mechanisms of Wolbachia-host interactions. *Front. Microbiol.* 6:1201. doi: 10.3389/fmicb.2015.01201

frontiers | Frontiers in Microbiology

TYPE Original Research
PUBLISHED 20 May 2024
DOI 10.3389/fmicb.2024.1418032

OPEN ACCESS

EDITED BY
Takema Fukatsu,
National Institute of Advanced Industrial Science and Technology (AIST), Japan

REVIEWED BY
Kenneth Pfarr,
University Hospital Bonn, Germany
Yunsheng Wang,
Hunan Agricultural University, China

*CORRESPONDENCE
Lindsey J. Cantin
✉ lcantin@neb.com

RECEIVED 15 April 2024
ACCEPTED 06 May 2024
PUBLISHED 20 May 2024

CITATION
Cantin LJ, Gregory V, Blum LN and Foster JM (2024) Dual RNA-seq in filarial nematodes and *Wolbachia* endosymbionts using RNase H based ribosomal RNA depletion. *Front. Microbiol.* 15:1418032. doi: 10.3389/fmicb.2024.1418032

Dual RNA-seq in filarial nematodes and *Wolbachia* endosymbionts using RNase H based ribosomal RNA depletion

Lindsey J. Cantin[1]*, Vanessa Gregory[1], Laura N. Blum[2] and Jeremy M. Foster[1]

[1]Biochemistry and Microbiology Division, New England BioLabs, Ipswich, MA, United States, [2]Applications and Product Development, New England BioLabs, Ipswich, MA, United States

Lymphatic filariasis is caused by parasitic nematodes and is a leading cause of disability worldwide. Many filarial worms contain the bacterium *Wolbachia* as an obligate endosymbiont. RNA sequencing is a common technique used to study their molecular relationships and to identify potential drug targets against the nematode and bacteria. Ribosomal RNA (rRNA) is the most abundant RNA species, accounting for 80–90% of the RNA in a sample. To reduce sequencing costs, it is necessary to remove ribosomal reads through poly-A enrichment or ribosomal depletion. Bacterial RNA does not contain a poly-A tail, making it difficult to sequence both the nematode and *Wolbachia* from the same library preparation using standard poly-A selection. Ribosomal depletion can utilize species-specific oligonucleotide probes to remove rRNA through pull-down or degradation methods. While species-specific probes are commercially available for many commonly studied model organisms, there are currently limited depletion options for filarial parasites. Here, we performed total RNA sequencing from *Brugia malayi* containing the *Wolbachia* symbiont (*w*Bm) and designed ssDNA depletion probes against their rRNA sequences. We compared the total RNA library to poly-A enriched, Terminator 5′-Phosphate-Dependent Exonuclease treated, NEBNext Human/Bacteria rRNA depleted and our custom nematode probe depleted libraries. The custom nematode depletion library had the lowest percentage of ribosomal reads across all methods, with a 300-fold decrease in rRNA when compared to the total RNA library. The nematode depletion libraries also contained the highest percentage of *Wolbachia* mRNA reads, resulting in a 16–1,000-fold increase in bacterial reads compared to the other enrichment and depletion methods. Finally, we found that the *Brugia malayi* depletion probes can remove rRNA from the filarial worm *Dirofilaria immitis* and the majority of rRNA from the more distantly related free living nematode *Caenorhabditis elegans*. These custom filarial probes will allow for future dual RNA-seq experiments between nematodes and their bacterial symbionts from a single sequencing library.

KEYWORDS

filariasis, *Wolbachia*, dual RNA sequencing, symbiosis, RNA enrichment, ribosomal depletion

1 Introduction

Filariasis is an infectious disease caused by parasitic nematodes. The disease is one of the leading causes of disability worldwide, with an estimated 2 billion people at risk of infection in the tropical and sub-tropical regions of Africa, Asia, and South America (Taylor et al., 2010; Bhalla et al., 2013). Filarial parasites are transmitted through blood feeding insect vectors and can infect both humans and animals (Chandy et al., 2011). The pathology of the disease, from host preference to disease outcomes, is determined by the filarial species present. Lymphatic filariasis can lead to elephantiasis and disfigurement, which is caused by *Brugia malayi* (*B. malayi*) and *Wuchereria bancrofti* infections in humans (World Health Organization, 2019; Medeiros et al., 2021). Subcutaneous filariasis is caused by *Loa loa*, *Onchocerca volvulus*, and *Mansonella streptocerca* infections and can lead to skin issues and blindness (WHO Expert Committee on Onchocerciasis Control, 1993; Boussinesq, 2006; Mediannikov and Ranque, 2018). *Dirofilaria immitis* (*D. immitis*), also known as heartworm, is a filarial nematode that primarily infects canid species, leading to lung and heart damage (Simón et al., 2012; Anvari et al., 2020). Combinations of albendazole, ivermectin, and diethylcarbamazine are used to control the spread of the disease by targeting microfilariae (Campbell, 1991; Richards et al., 2001; Mackenzie et al., 2002; Molyneux et al., 2003). However, drugs that kill adult stages are necessary to treat active infections, as the worms can survive long-term in the vertebrate hosts.

The majority of filarial nematodes contain *Wolbachia* as an obligate intracellular bacterial symbiont at all stages of their life cycle (Mclaren et al., 1975; Sironi et al., 1995; Bandi et al., 1998, 2001; Quek et al., 2022). *Wolbachia* are critical to the development, reproduction, and long-term survival of adult nematodes, most likely by providing metabolites from biological pathways absent in the worms (Foster et al., 2005; Wu et al., 2009; Darby et al., 2012; Li and Carlow, 2012; Luck et al., 2016). However, the molecular basis for this symbiosis is still poorly understood. Anti-*Wolbachia* treatments with antibiotics, such as doxycycline and rifampicin, are a promising strategy for filariasis eradication by sterilizing and killing adult worms (Taylor et al., 2005, 2019; Bazzocchi et al., 2008; Hoerauf et al., 2008; Specht et al., 2008; Supali et al., 2008; Coulibaly et al., 2009; Mand et al., 2009; Wanji et al., 2009; Johnston et al., 2014, 2021; Aljayyoussi et al., 2017; Clare et al., 2019). Gene expression analysis for both the nematode and the bacteria during different life-cycle stages can help to identify the biological relationship between them and to determine putative drug targets.

RNA-sequencing is a powerful approach that can be used to identify and quantify genes expressed under certain conditions or throughout the life cycle (Wang et al., 2009; Hrdlickova et al., 2017). Ribosomal RNA (rRNA) makes up between 80 and 90% of total RNA in a cell (Zhao et al., 2018; Deng et al., 2022). Therefore, rRNA must be removed prior to sequencing to analyze the smaller fraction of messenger RNA (mRNA) and non-coding RNAs (ncRNA) involved in interesting cellular functions. Typically, rRNA is removed during library preparation using Poly(A) enrichment or ribosomal depletion methods (Sultan et al., 2014; Zhao et al., 2014; Schuierer et al., 2017). Poly(A) enrichment is commonly used when studying eukaryotes by selecting for RNA species containing a poly(A) tail, usually mRNA and some ncRNAs, while removing all others, including rRNA. However, poly(A) tails are mostly absent from bacterial RNAs, resulting in a loss of all bacterial signal from libraries prepared with this method (Prezza et al., 2020; Xiang et al., 2022).

Ribosomal depletion can be used to remove only the rRNA, allowing for eukaryotic mRNA, bacterial mRNA, and ncRNA to all be sequenced within the same library. Ribosomal depletion typically requires sequence specific probes for either the pulldown or targeted degradation of rRNA (Adiconis et al., 2013; Wahl et al., 2022). Commonly studied model organisms, such as mouse, rat, human and bacteria, have commercially available kits for ribosomal depletion. There are limited depletion options for filarial nematodes and other *Wolbachia* containing hosts, preventing dual RNA-sequencing of the hosts and bacterial endosymbionts together (Kumar et al., 2012, 2016; Grote et al., 2017; Chung et al., 2019). 5′ phosphate dependent exonucleases, such as Terminator and Xrn1, have also been used to selectively degrade large rRNA molecules containing a 5′ monophosphate (He et al., 2010; Kang et al., 2011; Grote et al., 2017; Wangsanuwat et al., 2020). However, this method does not remove the 5S rRNA and is greatly affected by the secondary structure of RNAs, lowering its efficiency and increasing off-target effects compared to probe-based depletion.

Here, we present ribosomal depletion probes for *B. malayi* and its *Wolbachia* endosymbiont, *w*Bm, to perform dual RNA-seq. We also provide a proof of principal for the updated publicly available NEBNext Custom RNA Depletion design tool (https://depletion-design.neb.com), incorporating a clustering step to remove redundancy in the probe set. We compared libraries prepared with our custom filarial nematode depletion probes and RNase H digestion to RNA-seq libraries prepared with no treatment (total RNA), poly(A) enrichment, 5′ phosphate dependent exonuclease digestion, and commercially available NEBNext rRNA depletion with a combination of probes designed for Human/Mouse/Rat and Bacteria. We find almost complete rRNA removal and an increase in *Wolbachia* mRNA reads with the *B. malayi* specific probes, improving upon results seen with the other methods mentioned above. The custom depletion probes were also tested for their ability to remove rRNA from total RNA of the closely related filarial nematode *D. immitis* and the distantly related free-living nematode *Caenorhabditis elegans* (*C. elegans*). We found an almost 70% reduction in rRNA reads in the *C. elegans* library and an over 99% reduction in the *D. immitis* library, showing that this custom probe design can be used as a pan-filariae ribosomal depletion method for dual RNA-seq with their *Wolbachia* endosymbionts.

2 Materials and methods

2.1 *B. malayi* tissue collection

Thirty live adult *B. malayi* females were received from the NIH-NIAID Research Reagent Resource Center (FR3, Athens, GA; Michalski et al., 2011). Immediately after arrival, the worms were placed at 37°C with 5% CO_2 in freshly prepared RPMI 1640 media containing 10% heat inactivated fetal bovine serum (Thermo Fisher Scientific, Waltham, MA), 2 mM L-glutamine, 5 g/L glucose, 100 ug/mL streptomycin, 100 U/mL penicillin and 250 ng/mL amphotericin (Millipore Sigma, Burlington, MA). The worms were

incubated overnight for a minimum of 16 h. The worms were sorted into groups of 3 and washed twice with 1X PBS. All washes were removed, and the worms were snap frozen in liquid nitrogen and stored in 1.5 mL LoBind tubes at −80°C.

2.2 *D. immitis* tissue collection

Five live adult female *D. immitis* were shipped overnight from the FR3. Upon arrival, the worms were rinsed two times in 1X PBS. All liquid was removed. The worms were placed individually in 1.5 mL DNA LoBind tubes and flash frozen in liquid nitrogen. The samples were stored at −80°C until future use.

2.3 *C. elegans* tissue collection

N2 strain *C. elegans* nematodes were maintained on 10 cm Nematode Growth Medium (NGM) agar plates seeded with OP50 *E. coli* (Chaudhuri et al., 2011). Once the plate was starved, the worms were recovered by rinsing the plates with 10 mL of M9 buffer (22 mM KH_2PO_4, 42 mM Na_2HPO_4, 86 mM NaCl) and transferring the liquid containing the worms to a 15 mL conical tube. The worms were pelleted by spinning at 400 × *g* for 5 min. To wash the worm pellet, the supernatant was removed and another 10 mL of M9 buffer was added to the tube to resuspend the pellet. The worms were washed a total of 5 times. After the final spin, 9 mL of the supernatant was discarded. The worm pellet was resuspended in the remaining buffer and transferred to a 1.5 mL DNA LoBind tube. The tube was spun at 400 × *g* for 5 min and the supernatant was removed. The *C. elegans* pellet was flash frozen in liquid nitrogen and stored at −80°C until future use.

2.4 Total RNA extraction, sequencing, and analysis

Total RNA was extracted separately from individual aliquots for each nematode species, including *B. malayi* (three adult female worms), *C. elegans* (worm pellet from a starved 10 cm plate, mixed sex), and *D. immitis* (one adult female worm). For each sample, 0.5 mL of TRIzol (Thermo Fisher Scientific, Waltham, MA) was added to the 1.5 mL LoBind tube containing the frozen tissue. The tissue and TRIzol mix were then moved to a sterile 2 mL Dounce Homogenizer. The nematodes were homogenized using 10 strokes of the A pestle and 10–20 strokes of the B pestle. The samples were incubated at room temperature for 5 min. We added 100 μL of chloroform to each sample and mixed by manually shaking for 10 s. After an additional 3-min incubation at room temperature, the aqueous and organic phases were separated by spinning at 12,000 × *g* for 15 min at 4°C. The upper clear aqueous phase containing the RNA was transferred to a clean 1.5 mL DNA LoBind tube. The volume in each tube was measured with a P1000 pipette and an equal volume of >95% ethanol was added. We used the Monarch Total RNA Miniprep Kit (New England BioLabs, Ipswich, MA) to complete the cleanup of the RNA, using the total RNA purification from TRIzol-extracted samples protocol as described, with the inclusion of the optional DNase I treatment. RNA quality was measured by running 1 μL of the purified RNA sample on a Bioanalyzer using the RNA 6000 pico kit (Agilent, Santa Clara, CA) with the Eukaryote Total RNA Pico Series II assay. All RNA used for further experiments had an RNA Integrity Number (RIN) of 8 or above.

Total RNA-seq libraries for each species were prepared using the NEBNext Ultra II RNA Library Prep Kit for Illumina (New England BioLabs, Ipswich, MA) using the manufacturer's instructions. We had three technical replicates for *B. malayi* and one replicate for the *D. immitis* and *C. elegans* samples. Briefly, RNA samples containing 10 ng of total RNA were fragmented for 15 min at 94°C prior to first and second strand synthesis. The cDNA was purified with 1.8X NEBNext Sample Purification Beads. The cDNA ends were repaired and ligated to Illumina adapters diluted 25-fold. After adapter ligation, the USER enzyme was used to selectively degrade the second cDNA strand, allowing for directional RNA-seq. The libraries were amplified by PCR using NEBNext Multiplex Oligos for Illumina (Dual Index Primers Set 1; New England BioLabs, Ipswich, MA), with a total of 10 cycles. The libraries were purified a final time using 0.9X NEBNext Sample Purification Beads and 1 uL was run on the Bioanalyzer using the High Sensitivity DNA Kit (Agilent, Santa Clara, CA) for validation and quantification. The libraries were pooled and sequenced on a single flow cell of the Illumina NextSeq 550 at a depth of at least 40 million paired-end reads per sample.

Each analysis tool used default options unless otherwise noted. The FASTQ reads were trimmed to remove adapter sequences with the –paired option using Cutadapt (v1.16; Martin, 2011). The quality of each library after trimming was calculated using FastQC (v0.11.9; Andrews, 2023). The trimmed reads were aligned to the genome for each respective species using HISAT2 (v2.1.0; Kim et al., 2019) with the –fr –rna-strandedness RF and -k 30 options. The trimmed reads were mapped to their reference genome, using the *B. malayi*-4.0 (GCA_000002995.5), ICBAS_JMDir_1.0 (GCA_024305405.1), and WBcel235 (GCA_000002985.3) genomes for *B. malayi*, *D. immitis*, and *C. elegans* reads, respectively. The SAM alignment files were converted to BAM files, keeping only the primary alignments and mapped reads using Samtools view -b -F 260 (v1.15.1; Li et al., 2009). Samtools view was also used to down-sample to 40 million paired reads per library. BamCoverage from deepTools (v3.5.1; Ramírez et al., 2014) was used to create bedGraph files with 50 base pair (bp) bins, skipping all 0 values. Bedtools (v2.29.2; Quinlan and Hall, 2010) merge with the options "-d 1 -c 4 -o sum" was used to combine the bedGraph bins directly beside one another. To identify rRNA regions with a high number of aligned sequencing reads, we kept all genomic regions with >1,000 reads. The regions were aligned to the nucleotide (nt) database using BLASTN (v2.13.0; Altschul et al., 1990; Camacho et al., 2009), to identify high coverage regions that match available rRNA sequences. A bed file was created for each species containing the genomic coordinates for regions that match rRNA sequences with BLAST and any genes that were assigned as rRNA in the reference annotation. The genomic sequences of these regions, representing the putative rRNA sequences, were obtained using the reference genomes and Bedtools getfasta. The *B. malayi* rRNA sequences were used to design custom rRNA depletion probes.

2.5 Ribosomal RNA probe design

Putative ribosomal RNA sequences from *B. malayi* and *w*Bm were fed into the NEBNext Custom RNA Depletion Design Tool (https://depletion-design.neb.com), a public tool which utilizes ChipD to select candidate probes at each position based on predicted melting temperature (Dufour et al., 2010). The result is a set of probes which closely tile the reference sequences. The initial probe set ($n = 2{,}020$) was clustered to collapse highly similar probes using vsearch where pairwise similarity was defined by (*number of matching columns*)/(*the shortest sequence length*; –cluster_fast –iddef 0 –qmask none; Rognes et al., 2016).

Several similarity thresholds (50, 60, and 70%) were evaluated before selecting the probe set clustered at 60% similarity ($n = 377$). This similarity threshold was chosen because it had ample tiling over all rRNA sequences, with the additional advantage of being synthesized in a single oligo pool (max per pool = 384 oligos). Candidate probe sets were aligned back to the putative rRNA sequences with bbmap (v39.06; https://sourceforge.net/projects/bbmap) to assess coverage. Probe efficacy was predicted *in silico* using bbduk to partition undepleted RNA reads by whether they had high k-mer similarity to the probe set or not. The selected probe set had high similarity to 88.69% of RNA reads, compared to 88.73% for the unclustered output. Following the development of this method, the NEBNext Custom RNA Depletion Design Tool was updated to include a clustering option to support the use of the tool with less well-characterized organisms. We ordered an oligo pool from IDT (Coralville, IA) containing the 377 *B. malayi* rRNA depletion probes at a concentration of 50 pmol/oligo. The oligo pool was resuspended in 25 μL of 10 mM Tris, 0.1 mM EDTA, at pH 7.5 (2 μM per probe final concentration) and stored at −20°C until future use.

2.6 RNA enrichment and sequencing

The total RNA, described in Section 2.4, was used to make *B. malayi* RNA libraries prepared with various ribosomal depletion methods. We used 10 ng of total RNA as the starting material for each library. One sample was treated with Terminator 5′-Phosphate-Dependant Exonuclease (Biosearch Technologies, Teddington, UK) using the manufacturer's standard procedure with Reaction Buffer A. The sample was incubated at 30°C for 60 min and the reaction was terminated by adding 1 μL of 100 mM EDTA. The sample was purified using the Monarch RNA Cleanup Kit (50 ug; New England BioLabs, Ipswich, MA), with a final elution of 6 μL.

We also tested different probe sets for RNase H based ribosomal depletion. The NEBNext rRNA Depletion Kit v2 for Human/Mouse/Rat in combination with the NEBNext rRNA depletion probes for bacteria (both from New England BioLabs, Ipswich, MA) were used to deplete the rRNA from *B. malayi* total RNA. We diluted 10 ng of RNA in nuclease-free water to final volume of 9 μL. We added 2 μL of the probe hybridization buffer, 2 μL of the human/mouse/rat v2 rRNA depletion solution and 2 μL of the bacteria rRNA depletion solution. The sample was then treated following the manufacturer's instructions. Briefly, the probes were annealed to the rRNA by incubating at 95°C for 2 min followed by a ramp down to 22°C at a rate of 0.1°C per second. The sample was then treated with RNase H for 30 min at 50°C to degrade the RNA in the RNA/DNA hybrids, followed by a DNase I incubation for 30 min at 37°C. The remaining RNA was purified using 1.8X of the NEBNext RNA Sample Purification Beads and eluted in 7 μL of nuclease-free water.

For the third RNA depletion method, we tested our custom *B. malayi* probe design with three technical replicates. We added 2 μL of our custom oligo pool, described in Section 2.5, to 2 μL of Hybridization Buffer from the NEBNext RNA Depletion Core Reagent Set (New England BioLabs, Ipswich, MA) per replicate. The hybridization mix was then added to 10 ng of total *B. malayi* RNA in 11 μL of nuclease-free water. The samples were then treated following manufacturer's instructions and as described above. We also used the custom *B. malayi* probes on *C. elegans* and *D. immitis* total RNA to test efficacy across nematode species. Both of these libraries started with 10 ng of total RNA, described in Section 2.4, and followed the same RNase H protocol described above using the NEBNext RNA Depletion Core Reagent Set.

Five μL from each elution for all three depletion methods, including the *C. elegans* and *D. immitis* samples, were taken into library preparation using the NEBNext Ultra II RNA Library Prep Kit for Illumina, following the same methods described in Section 2.4. All seven depletion libraries were pooled and sequenced using the Illumina NextSeq 550 to a depth of at least 40 million paired-end reads.

2.7 RNA-seq analysis

We used default settings for all analysis tools unless noted otherwise. All *B. malayi* RNA-seq libraries, including the 3 total (untreated), Terminator, Human/Mouse/Rat/Bacteria depleted, 3 custom depleted, and a publicly available Poly(A) enriched library (SRR3111490; Chung et al., 2019), were trimmed using Cutadapt (v1.16; Martin, 2011) with the –paired option and aligned to the *B. malayi*-4.0 (GCA_000002995.5) reference genome, containing the *Wolbachia* endosymbiont (*w*Bm) chromosome, using HISAT2 (v2.1.0; Kim et al., 2019) with the "–fr –rna-strandedness RF and -k 30" options. Samtools view (v1.15.1; Li et al., 2009) -b -F 260 was used on each alignment file to convert to a BAM file and remove all non-primary alignments and unmapped reads. As each library has a different number of sequencing reads, the BAM files were subsampled to 40 million reads each by dividing 40,000,000 by the total number of reads and using this value as the downsampling factor with the -s option. To visualize the read alignments, we used bamCoverage from DeepTools (v3.5.1; Ramírez et al., 2014) to make bigwig files from the filtered BAMs with 50 bp bins and normalization using counts per million (CPM). The bigwig files were visualized using IGV (v2.11.9; Thorvaldsdóttir et al., 2013).

RSeQC (v2.6.4.3; Wang et al., 2012) geneBody_coverage.py was used to visualize the distribution of reads across gene bodies to determine if there is a 5′ or 3′ bias with different depletion methods. FeatureCounts (v2.0.1; Liao et al., 2014) was used to count the number of reads over annotated genomic regions, including protein coding, non-coding and ribosomal genes, with the "-s 2

–primary -t gene -g 'gene_id"' options set. An additional column was added to the count output files, where each gene id was matched to the assigned "gene_biotype" from the annotation file. The sum of the reads assigned to each gene type was calculated and then divided by the total number of reads to quantify the proportion of reads mapped to rRNA, protein coding, ncRNA, or unannotated regions. The feature count files were also used to plot the correlation between the gene counts for the total vs. the custom depletion libraries. Fragments per million (FPM) was calculated for all three replicates for each library type by first taking the sum of all reads in each sample divided by 1 million to obtain the scaling factor, unique to each individual replicate. The counts for each gene were divided by the scaling factor and the average FPM was calculated for the total and custom depletion replicate libraries, separately. The log10 of the average FPMs was taken and visualized using ggplot2 (Valero-Mora, 2010). Correlations between the custom probe library and the Poly(A) or Terminator library were performed using the same methods, without averaging the Poly(A) and Terminator counts, as only one replicate was used.

Samtools view -L was used to identify which reads mapped to the *w*Bm chromosome using bed files for the whole chromosome and for just the *w*Bm rRNA regions. The reads mapping to the *w*Bm rRNA genes were subtracted from the total number of reads mapping to the whole chromosome, where the remaining reads correspond to *Wolbachia* reads mapping to genes of interest.

To analyze the rRNA depletion capacity of our custom probes on different nematode species, the *C. elegans* and *D. immitis* total and custom depletion libraries were compared. The same trimming, alignment, filtering and downsampling methods were used with their respective reference genomes: WBcel235 (GCA_000002985.3) for *C. elegans* and ICBAS_JMDir_1.0 (GCA_024305405.1) for *D. immitis*. BamCoverage was also used to make bigWig files with 50 bp bins and CPM normalization for visualization in the IGV browser. Samtools view -L was used to count reads mapping to the rRNA region bed files described in Section 2.4.

3 Results

3.1 RNA enrichment methods

We tested various RNA-seq enrichment and depletion methods in three nematode species, two of which contain *Wolbachia* as a bacterial endosymbiont. The different library preparation methods should result in sequencing of distinct RNA species (Figure 1, Table 1). Sequencing of *B. malayi* total untreated RNA should result in 80–95% ribosomal sequences, with a small number of mRNA, ncRNA, and bacterial sequences (Figure 1A). This would require large amounts of deep sequencing data to quantitatively study the protein coding gene expression. Poly(A) enrichment is one of the most commonly used methods for eukaryotic RNA-sequencing. This usually involves using Oligo(d)T beads to bind and pull-down the poly(A) tail of certain types of RNA molecules, including mRNA and some types of ncRNA, while removing all rRNA and bacterial RNAs (Figure 1B). However, poly(A) enrichment will remove all bacterial sequences.

TABLE 1 Expected sequencing outcomes from RNA enrichment and depletion methods.

Library preparation	RNA species	Bacterial mRNA
Total (no depletion)	mRNA, ncRNA, and all rRNA	+
Poly(A)	mRNA	-
Terminator exonuclease	mRNA, ncRNA, and 5S rRNA	+
Ribosomal depletion	mRNA and ncRNA	+

The removal of rRNA should enable the user to sequence all ncRNAs and mRNAs, from both eukaryotic and bacteria together in one sequencing library. This can be done using species specific depletion probes or with a phosphate-dependent exonuclease. Here, we tested Terminator 5′-Phosphate Dependent Exonuclease treatment prior to library preparation, which should remove all large rRNA molecules, while retaining mRNA, ncRNA and 5S rRNA, from both the nematodes and *Wolbachia* (Figure 1C). Species specific depletion probes can be designed to remove certain RNA molecules from the total RNA pool based on their nucleotide sequence. Here, we used DNA probes and RNase H to selectively degrade RNA molecules within an RNA/DNA hybrid (Figure 1D). When using DNA probes with sequences complementary to rRNA, we expect to sequence mRNA and ncRNA from both eukaryotes and bacteria. Comparing the sequencing outcomes of these library preparation methods allowed us to determine the most efficient technique for dual RNA-sequencing in samples containing both eukaryotic and prokaryotic RNAs.

3.2 Ribosomal depletion in *B. malayi*

We extracted high quality total RNA from *B. malayi* with an RNA Integrity of 9.2 (Supplementary Figure 1A). Two distinct peaks can be seen in the Bioanalyzer trace representing the abundant 18S and 28S rRNAs. After depletion with the custom (Nema) probe set, we observed a significant reduction in the ribosomal peaks (Supplementary Figure 1B). We prepared and sequenced five *B. malayi* RNA-seq libraries using the methods mentioned above. After sequencing, we aligned our reads to the *B. malayi* reference genome (Foster et al., 2020). The read coverage was mapped over annotated genes. No significant 5′ or 3′ bias was observed in any of our libraries, as the quality of the starting total RNA was high (Supplementary Figure 1C), although, the Terminator library has a slight 5′ bias.

There are a sizeable number of reads mapping to the ribosomal tandem repeat genes in the total RNA sample (Figure 2A). The Terminator library also has a pile up of reads over this region. However, there is a slightly different pattern of read peaks, as some of these regions have been depleted. The NEBNext Human/Mouse/Rat/Bacterial depletion probes remove a large portion of the rRNA reads, leaving 400–600 bp regions undepleted. The Poly(A) and Nema probes both remove almost all of the ribosomal reads. When we observe the read alignments at a

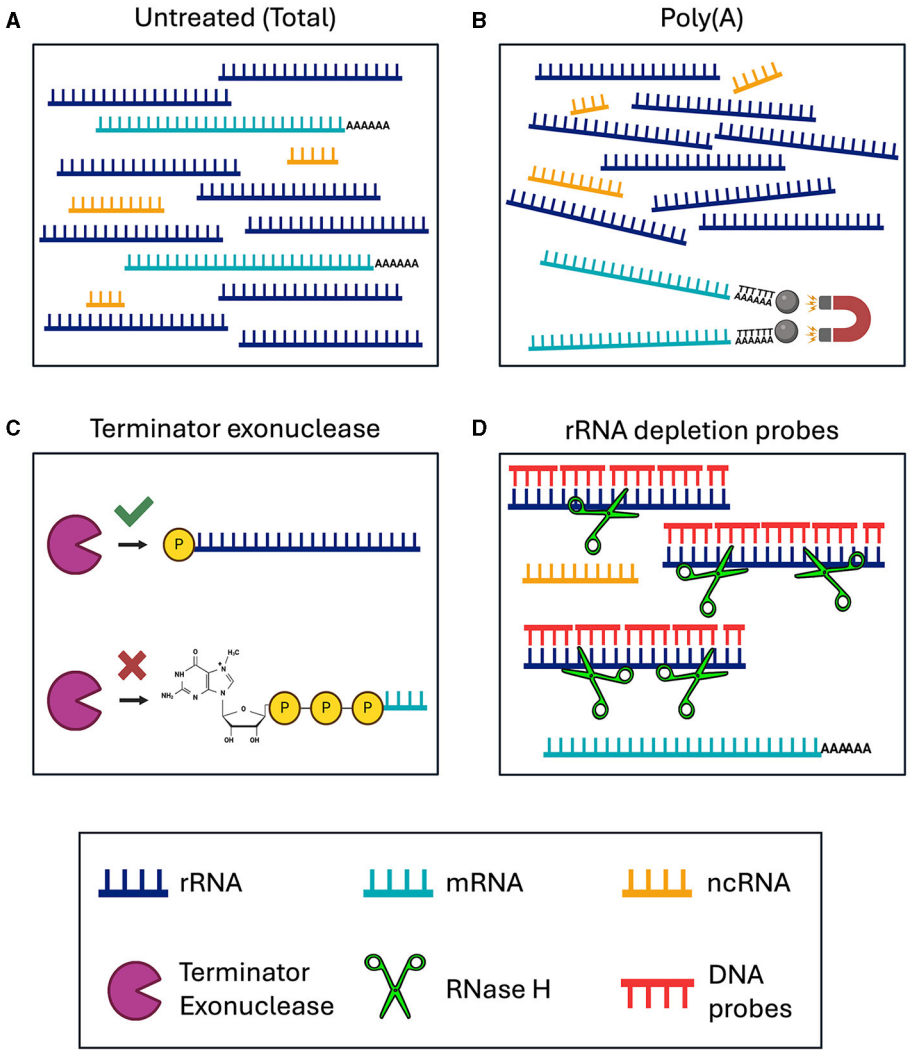

FIGURE 1
Schematic of RNA enrichment and depletion strategies tested in this study. **(A)** Total RNA sequencing. **(B)** Poly(A) enrichment with magnetic d(T) beads. **(C)** Terminator 5′ Phosphate Dependent Exonuclease treatment. **(D)** RNase H-based ribosomal depletion using sequence specific DNA probes. RNA species are color-coded with rRNA in dark blue, mRNA in teal, and ncRNA in yellow. The Terminator exonuclease is shown in purple, RNase H in green and DNA probes in red.

smaller scale, we can see reads aligned to protein coding genes surrounding the tandem repeat in every sample besides the total RNA (Figure 2B). However, the Nema probes and Poly(A) libraries have the highest level of mRNA signal. Additionally, we find virtually no reads aligned to the rRNA genes in the Nema probes library, while there appears to be some rRNA carryover in the Poly(A) library.

Each read was assigned to a genomic feature using the *B. malayi* reference genome annotation. We quantified the proportion of reads that map to each feature type for each library preparation method (Figure 2C). All annotated genes, besides protein coding and rRNA genes, were considered non-coding genes. Unannotated reads refer to those mapped to regions that do not contain any known genomic features. RNA-seq experiments often aim to study protein coding (mRNA) or non-coding (ncRNA) gene expression. Around 81% of reads in the total library mapped to rRNA genes, which makes the large majority of the reads unusable for downstream analyses. The Poly(A) library had 1.2% of reads mapping to rRNA and almost no reads mapping to ncRNAs. Unsurprisingly, this results in a substantial increase in mRNA reads. Therefore, Poly(A) enrichment is very useful for studying protein coding genes but will not allow for the study of ncRNAs. The Terminator library still had 33% of reads mapping to rRNA and an increase in reads mapping to unannotated regions, with only 32% of reads mapping to protein coding genes. The Human/Mouse/Rat/Bacteria depletion library had 27% of reads mapping to rRNA genes. While this value is significantly lower than in the total RNA library, there are still a large number of rRNAs that need to be removed when using probes designed for distantly related species. The Nema depletion library had the lowest number of rRNA reads at 0.23%. Notably, this value was even lower than the number of rRNA reads found in the Poly(A) depletion library. In this case, the RNase H method is 5 times more efficient at reducing rRNA carryover than using d(T) magnetic

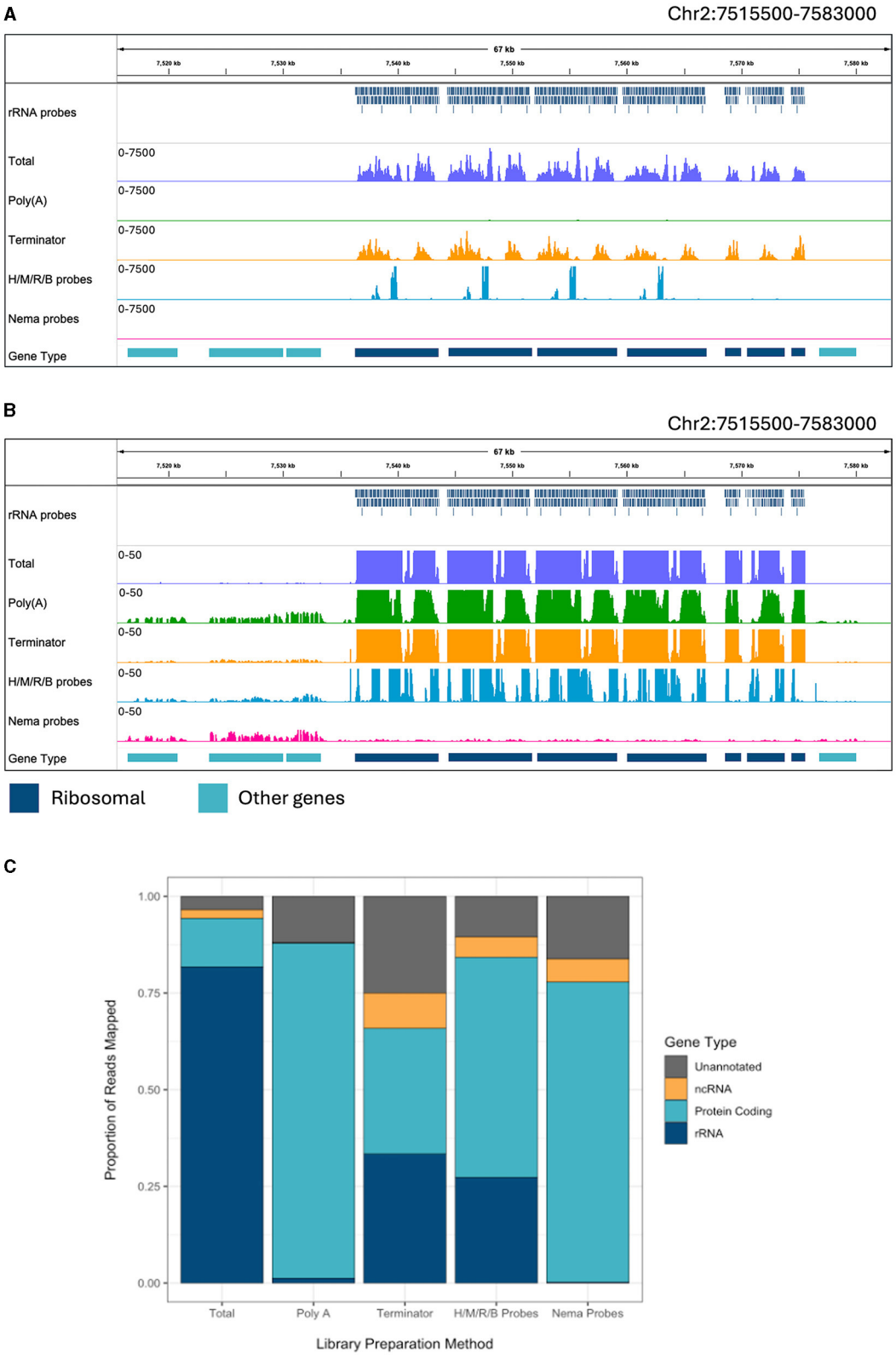

FIGURE 2
Ribosomal depletion across library preparation methods in *B. malayi*. **(A)** IGV trace showing the custom probes and RNA-seq libraries mapped to the ribosomal tandem repeat region on *B. malayi* Chr2. All BAM coverage files were normalized using CPM in 50 bp bins and shown at a scale of 0–7,500 reads. Protein coding gene annotations are shown in teal and ribosomal gene annotations are shown in dark blue. **(B)** IGV trace showing the same genomic region and coverage files as **(A)** with a scale of 0–50 reads. **(C)** Proportion of reads mapped to each gene annotation type, with unannotated regions in gray, non-coding genes in yellow, protein coding genes in teal. H/M/R/B probes = library made with NEBNext Human/Mouse/Rat rRNA depletion kit combined with the NEBNext Bacteria rRNA depletion probes.

beads. The Nema depletion library also had 6% of reads mapping to ncRNA genes, allowing for the examination of these less studied but functionally important RNA species.

3.3 Enrichment of *w*Bm RNA-seq reads after ribosomal depletion

The Nema depletion probes allow for a more comprehensive analysis of *B. malayi* gene expression. Next, we wanted to determine if this method can also be used to enhance studies of *Wolbachia* gene expression. The *B. malayi* reference genome contains the *w*Bm chromosome. When looking at the reads mapping to the bacteria, we find many reads mapping to rRNA genes in the total and Terminator libraries (Figure 3A). The Terminator enzyme does not appear to have any effective degradation of the bacterial rRNA. When looking at a smaller scale, we observe some rRNA reads present in the Poly(A) library as well (Figure 3B). The Nema depletion library has virtually no reads mapping to the rRNA regions but does contain expression signals in surrounding protein coding genes. Finally, the Human/Mouse/Rat/Bacteria depletion probes do remove the *w*Bm rRNAs, but this does not appear to increase the number of mRNA reads present.

We extracted all reads that mapped to the *w*Bm chromosome from each library. The reads were classified as either rRNA or other *Wolbachia* genes, representing the protein coding and non-coding genes. The proportion of reads mapping to either gene type was compared across libraries (Supplementary Figure 2). The total, Poly(A), and Terminator libraries had over 98% of *Wolbachia* reads mapping to ribosomal genes. Both probe depletion libraries had the opposite proportion, with over 99% of reads mapping outside of the rRNA genes. Next, we determined the percentage of reads mapping to the *w*Bm chromosome out of all the reads within each library (Figure 3C). The total and Terminator libraries had the highest number of *Wolbachia* reads, with around 2 and 3%, respectively. However, these reads do not provide useful information about *Wolbachia* biology as they are primarily rRNA. The Human/Mouse/Rat/Bacteria depletion library had only 0.07% of total reads mapped to *Wolbachia*. The low number of overall *Wolbachia* reads using this method does not allow for accurate quantification of bacterial gene expression. Finally, the Nema depletion library had around 1% of all reads mapping to *Wolbachia*, with almost all of the reads mapping outside of rRNA regions. These data show that the custom filarial nematode depletion probes are the best option for performing rRNA depletion for dual RNA-seq between the worms and their bacterial endosymbiont.

3.4 Correlation of gene expression between nema depletion and total RNA-seq

We investigated the effect of library preparation method on individual gene counts. All gene counts were normalized by calculating the number of fragments per million mapped fragments (FPM). The genes were not normalized for length, as we directly compared the same genes across enrichment and depletion methods. We plotted the Log_{10}(FPM) of each annotated gene for the Total and Nema depleted libraries (Figure 4). All gene types, excluding rRNAs, generally had higher read counts in the Nema deplete library. As expected, most rRNA genes had between 100 and 300 times more gene counts in the Total library and no rRNA genes had higher read counts in the Nema depleted sample.

There are some protein coding and non-coding genes that appear to have slightly higher read counts in the Total library. We investigated these genes to ensure that they were not being depleted as a result of off target probe binding. We found no evidence of sequence similarity between these genes and the rRNA probes, as the probe sequences do not map to their genome regions *in silico*. Most genes, such as Bm15518, have the same distribution of reads across the gene body, but with slightly lower coverage in the Nema library (Supplementary Figure 3A). This could be the result of technical artifacts during library preparation and sequencing, as many of these genes had variable gene counts across technical replicates. Bm9361 was the only gene where the distribution of reads differed across the gene body (Supplementary Figure 3B). In the Nema deplete library, a 200 nucleotide sequence around the 3′ end of the gene appears to be depleted. This may represent an off-target effect of the probe set. However, the overwhelming majority of genes have higher gene counts in the Nema deplete library, without any off-target probe binding.

We also compared the Nema depletion library gene counts to those of the Poly(A) and Terminator libraries. The Nema depletion and Poly(A) libraries had similar levels of protein coding gene expression (Supplementary Figure 4A). The Poly(A) library had higher counts in most rRNA genes, almost zero reads in *Wolbachia* genes and minimal reads in most ncRNA genes. The non-coding genes with similar counts in the Poly(A) and Nema depletion libraries probably represent the ncRNAs that contain a poly(A) tail. The Terminator library has higher counts in all rRNA genes, with less enrichment of protein coding and *Wolbachia* genes (Supplementary Figure 4B). There is an enrichment of a small subset of non-coding and protein coding genes in the Terminator library. This could be the result of technical artifacts from sequencing or biological artifacts as a result of their cap or secondary structures.

3.5 Ribosomal depletion in other nematode species

C. elegans is a commonly studied model organism in clade V of the nematode phylum (Parkinson et al., 2004). *D. immitis* is a more closely related filarial parasite in the same group, clade III, as *B. malayi*. It is estimated that clades III and V separated over 300 million years ago (Xie et al., 2022). We determined the efficiency of the depletion probes designed with *B. malayi* sequences on these other nematode species. Total and Nema depleted libraries were made with RNA from each species. The libraries were aligned to their species' respective reference genomes, along with the *B. malayi* probe sequences. We observed read and probe alignments over the annotated rRNA genes. In *C. elegans*, the probes have a patchy alignment to the rRNA genes, with many gaps present (Figure 5A). We still see rRNA depletion, however there are two distinct regions, of 500 and 250 bps, where the probes do not align

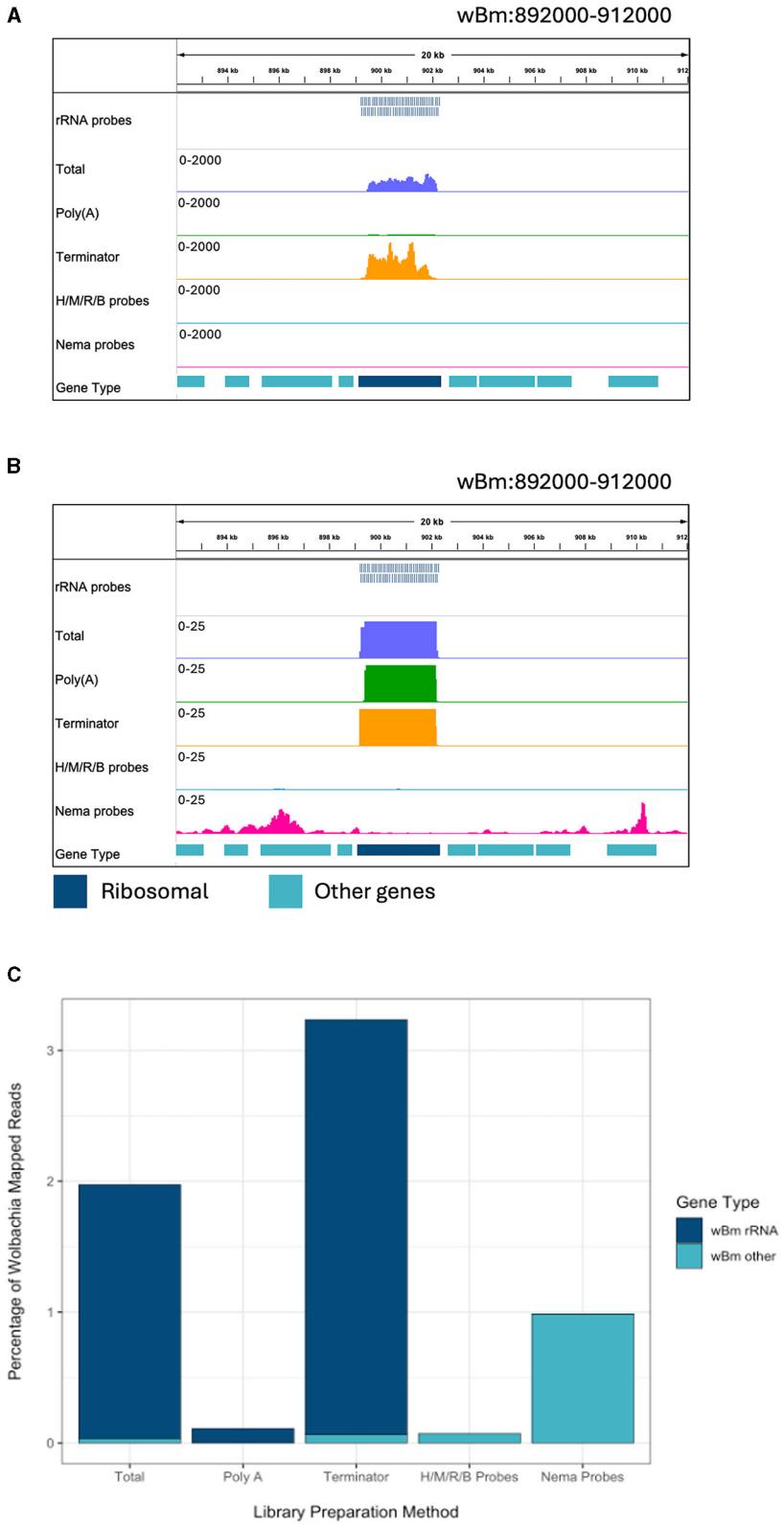

FIGURE 3
Ribosomal depletion across library preparation methods in *w*Bm. **(A)** IGV trace showing the custom probes and RNA-seq libraries aligned to an rRNA annotated region in the *w*Bm chromosome. All BAM coverage files were normalized using CPM in 50 bp bins. The scale is set to 0–2,000 reads. Protein coding gene annotations are shown in teal and ribosomal gene annotations are shown in dark blue. **(B)** IGV trace showing the same regions and tracks as **(A)**, with a scale of 0–25 reads. **(C)** Percentage of reads mapped to the *w*Bm chromosome from all mapped reads in each library. Reads mapped to rRNA genes are shown in dark blue and reads mapped to all other regions of the *w*Bm chromosome are shown in teal. H/M/R/B probes = library made with NEBNext Human/Mouse/Rat rRNA depletion kit combined with the NEBNext Bacteria rRNA depletion probes.

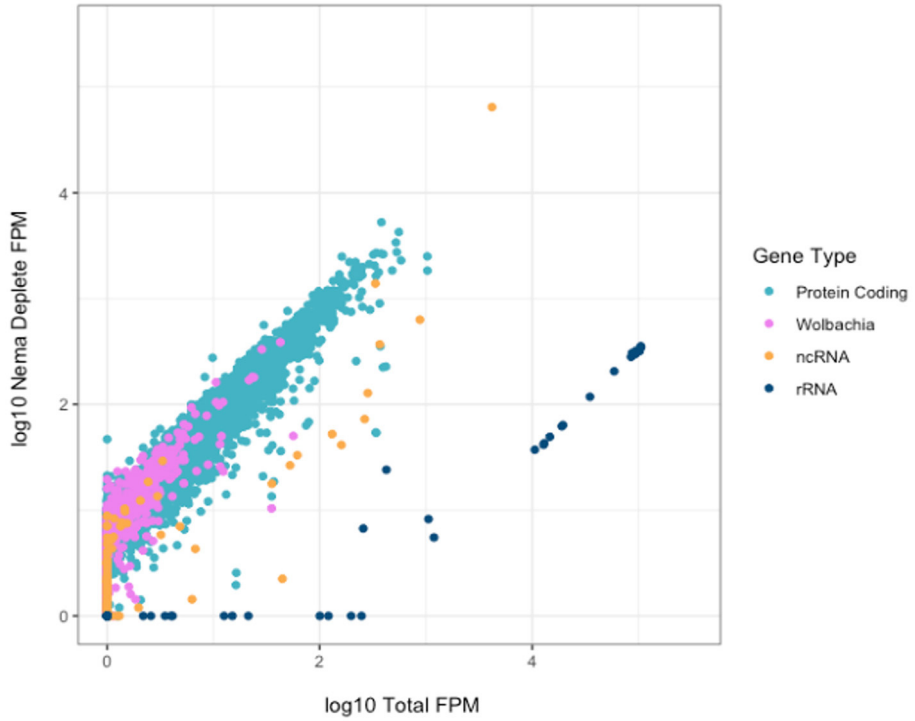

FIGURE 4
Correlation of gene counts between *B. malayi* Total and Nema depletion libraries. Plot showing the log10 FPM gene counts for the total (x-axis) and custom probe depleted (y-axis) libraries, with rRNA genes in dark blue, protein coding genes in teal, non-coding RNAs in yellow and *Wolbachia* non-rRNA genes in pink.

and the rRNA is not depleted. The probes have better alignment to the *D. immitis* rRNA genes and almost all rRNA appears to be removed in the Nema depleted library (Figure 5B). When observing read alignment over protein coding genes, we find an increase in reads for the Nema depleted libraries in both species (Supplementary Figures 5A, B).

We quantified the proportion of reads aligning to rRNA gene annotations from each library (Figure 5C). All reads mapping to ribosomal genes were called rRNA and the remaining mapped reads were classified as other. The *C. elegans* total RNA library had 92.9% of reads mapped to rRNA, with only 7.1% of reads mapped to other genes. The Nema depletion library had 29.5% of reads mapping to rRNA and 70.5% mapped to other regions, indicating that the *B. malayi* probes are not as effective at removing these sequences in this distantly related nematode species. In the *D. immitis* total library, 83% of reads mapped to annotated rRNA genes, with 17% mapping to other genes. The Nema depletion library had only 0.3% of reads mapping to rRNA regions and 99.7% mapping to other regions. The *B. malayi* rRNA probes efficiently removed these sequences at a similar rate across both filarial species. This probe design can most likely work as a pan-filarial nematode ribosomal depletion method.

4 Discussion

Enrichment and depletion methods in RNA-sequencing are important for studying biologically interesting gene expression in species across life cycle stages and conditions. Here, we presented ribosomal depletion strategies to study filarial parasites and their endosymbiotic bacteria. We tested poly(A) enrichment, Terminator exonuclease depletion, and species-specific probe depletion, including commercially available and custom probes, on nematode total RNA samples. The custom probes were designed against the *B. malayi* and *w*Bm ribosomal sequences using the NEBNext Custom RNA Depletion design tool, resulting in 377 non-redundant oligo sequences. We obtained complete removal of rRNA using these probes in *B. malayi* samples, which was a significant improvement compared to all other methods tested. There was less rRNA contamination with this RNase H-based method when compared to poly(A) bead enrichment. We found that the probes have negligible off-target effects on other gene sequences. The Terminator enzyme is advertised as a method to remove large rRNA sequences. While we did observe a reduction in the rRNA reads, over 30% of reads still mapped to ribosomal genes.

The Terminator method also appears to enrich and deplete certain protein coding and non-coding genes. Commercially available 5′ Phosphate-dependent exonucleases have been shown to be affected by the secondary structure of RNA. This method also had a slight 5′ sequencing bias when compared to the other library preparation methods (Supplementary Figure 1C). These data show that probe based ribosomal depletion methods should be preferred over current 5′ Phosphate-dependent exonuclease methods.

The NEBNext Human/Mouse/Rat probes combined with the NEBNext Bacteria probes also removed a large proportion of ribosomal reads. However, there were specific regions of

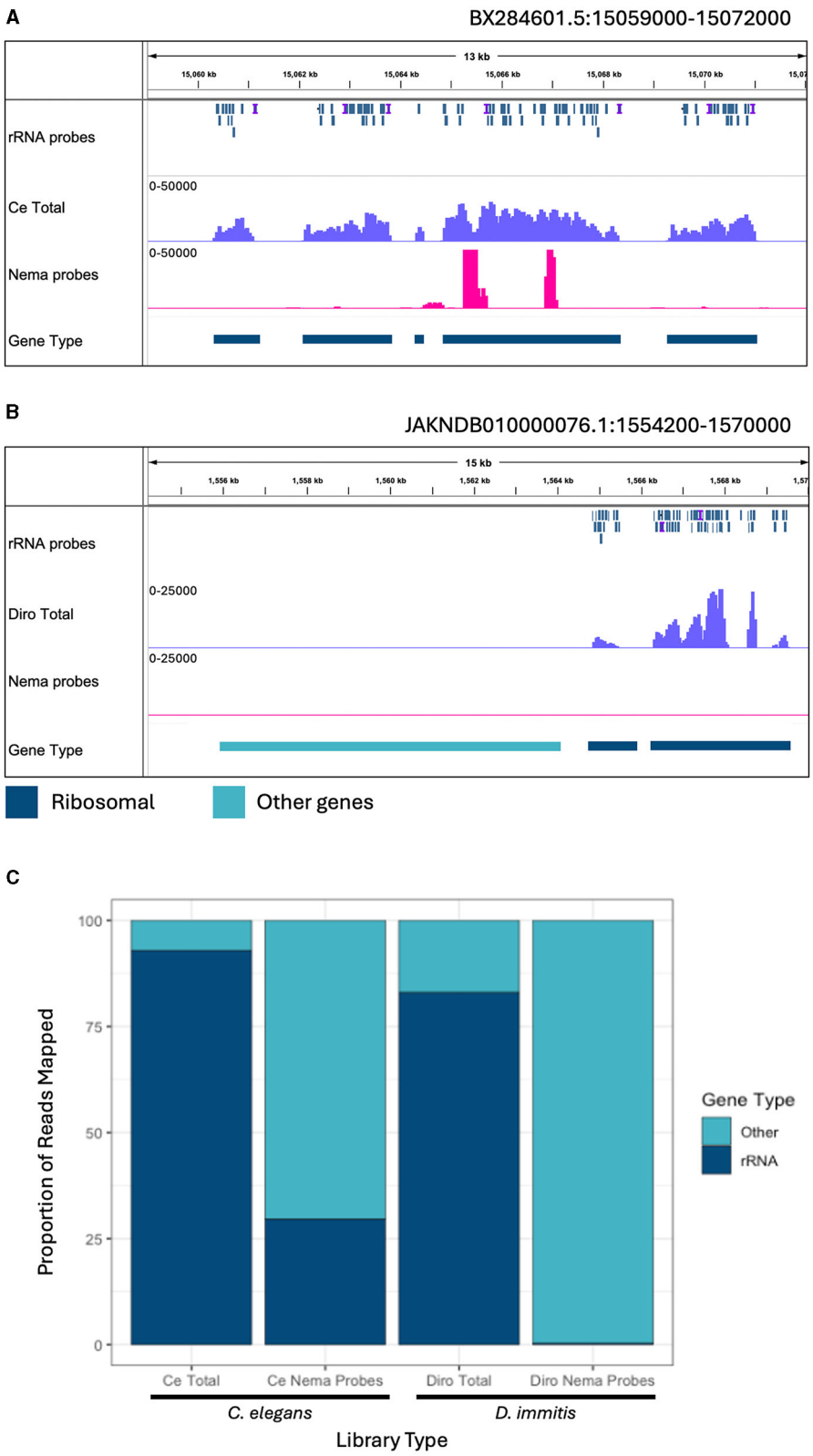

FIGURE 5
Ribosomal depletion with *B. malayi* custom depletion probes in other nematode species. **(A)** IGV track showing probe mapping in the *C. elegans* genome over ribosomal genes. Additional tracks include BAM coverage files normalized using CPM showing *C. elegans* total RNA (blue) and Nema depletion (pink) libraries at a scale of 0–50,000 reads. **(B)** IGV track showing probe mapping in the *D. immitis* genome over ribosomal genes. Additional tracks show BAM coverage files normalized using CPM of the *D. immitis* total RNA (blue) and Nema depletion (pink) libraries at a scale of 0–25,000. Protein coding gene annotations are shown in teal and rRNA annotations are shown in dark blue. **(C)** Proportion of reads mapping to ribosomal genes vs. other genomic regions in the *C. elegans* and *D. immitis* total and Nema depletion libraries. Reads mapping to ribosomal genes are represented in dark blue. Reads mapping to other genomic regions are shown in teal.

these genes that were not removed, leaving 30% of reads in rRNA genes. These regions likely correspond to sequences that have diverged significantly over time between vertebrates and nematodes. The addition of the Bacteria probes did efficiently remove the *Wolbachia* rRNAs.

The custom probes allowed for sequencing of non-coding and bacterial RNAs alongside the protein-coding RNAs. One limitation of this method is the necessity of an annotated reference genome or a total RNA-seq library to identify the abundant sequences. However, the nema depletion was the only method that resulted in abundant levels of *Wolbachia* sequences, not including rRNA reads. Therefore, this method can be used for dual RNA-seq studies in filarial nematodes containing *Wolbachia*. Sequencing both the eukaryotic and prokaryotic sequences in the same library will help to avoid technical artifacts and batch effects that could arise across *B. malayi* and *Wolbachia* libraries that must otherwise be prepared separately, using different methods. Additionally, these probes can be used to enrich for only *Wolbachia* sequences by combining rRNA depletion with poly(A) depletion. The probe-based rRNA depletion can also help to improve reference genome annotations of non-coding genes, as many of these sequences are removed when commonly used poly(A) enrichment is performed. This library preparation method is helpful in situations where the RNA is of low quality. Degraded RNAs are difficult to sequence using either poly(A) enrichment or Terminator depletion, as these methods rely on intact 3′ and 5′ ends, respectively. The probes are designed to bind over all regions of the rRNA, therefore those sequences can be removed even if the whole RNA molecule is fragmented.

The custom *B. malayi* probes did not completely remove rRNAs from the distantly related *C. elegans* samples. A small number of additional probes could be added to the pool to increase efficiency. However, the *B. malayi* probes were able to completely remove rRNAs from *D. immitis* samples. *B. malayi* and *D. immitis* are in distinct groups in the Filarioidea superfamily (Small et al., 2014). Therefore, we expect that these probes can be used as a high-quality ribosomal depletion method across all filarial parasites and facilitate efficient dual RNA-seq of those species harboring the *Wolbachia* endosymbiont.

Data availability statement

The datasets presented in this study can be found in online repositories. The names of the repository/repositories and accession number(s) can be found at: https://www.ncbi.nlm.nih.gov/, PRJNA1100530.

Ethics statement

The manuscript presents research on animals that do not require ethical approval for their study.

Author contributions

LC: Writing – review & editing, Writing – original draft, Visualization, Validation, Supervision, Methodology, Investigation, Formal analysis, Data curation, Conceptualization. VG: Writing – review & editing, Writing – original draft, Visualization, Methodology, Investigation, Formal analysis, Data curation. LB: Writing – review & editing, Writing – original draft, Software, Methodology, Formal analysis, Conceptualization. JF: Writing – review & editing, Writing – original draft, Supervision, Funding acquisition, Conceptualization.

Funding

The author(s) declare that no financial support was received for the research, authorship, and/or publication of this article.

Acknowledgments

We thank New England BioLabs for supporting parasitology research and the summer student internship program, particularly Thomas Evans, Salvatore Russello, and the late Donald Comb. We would also like to thank the NEB sequencing core for processing the samples. Finally, we acknowledge the Filariasis Research Reagent Resource Center for supplying the filarial nematodes used in this study.

Conflict of interest

LC, VG, LB, and JF were employed by New England BioLabs.

The reviewer KP declared a past collaboration with the author JF to the handling editor.

Publisher's note

Supplementary material

The Supplementary Material for this article can be found online at: https://www.frontiersin.org/articles/10.3389/fmicb.2024.1418032/full#supplementary-material

References

Adiconis, X., Borges-Rivera, D., Satija, R., DeLuca, D. S., Busby, M. A., Berlin, A. M., et al. (2013). Comparative analysis of RNA sequencing methods for degraded or low-input samples. *Nat. Methods* 10, 623–629. doi: 10.1038/nmeth.2483

Aljayyoussi, G., Tyrer, H. E., Ford, L., Sjoberg, H., Pionnier, N., Waterhouse, D., et al. (2017). Short-course, high-dose rifampicin achieves *Wolbachia* depletion predictive of curative outcomes in preclinical models of lymphatic

filariasis and onchocerciasis. *Sci. Rep*. 7:210. doi: 10.1038/s41598-017-00322-5

Altschul, S. F., Gish, W., Miller, W., Myers, E. W., and Lipman, D. J. (1990). Basic local alignment search tool. *J. Mol. Biol*. 215, 403–410. doi: 10.1016/S0022-2836(05)80360-2

Andrews, S. (2023). *FastQC*. Available online at: https://github.com/s-andrews/FastQC (accessed October 31, 2023).

Anvari, D., Narouei, E., Daryani, A., Sarvi, S., Moosazadeh, M., Ziaei Hezarjaribi, H., et al. (2020). The global status of *Dirofilaria immitis* in dogs: a systematic review and meta-analysis based on published articles. *Res. Vet. Sci*. 131, 104–116. doi: 10.1016/j.rvsc.2020.04.002

Bandi, C., Anderson, T. J., Genchi, C., and Blaxter, M. L. (1998). Phylogeny of *Wolbachia* in filarial nematodes. *Proc. R Soc. B Biol. Sci*. 265, 2407–2413. doi: 10.1098/rspb.1998.0591

Bandi, C., Trees, A. J., and Brattig, N. W. (2001). *Wolbachia* in filarial nematodes: evolutionary aspects and implications for the pathogenesis and treatment of filarial diseases. *Vet. Parasitol*. 98, 215–238. doi: 10.1016/S0304-4017(01)00432-0

Bazzocchi, C., Mortarino, M., Grandi, G., Kramer, L. H., Genchi, C., Bandi, C., et al. (2008). Combined ivermectin and doxycycline treatment has microfilaricidal and adulticidal activity against *Dirofilaria immitis* in experimentally infected dogs. *Int. J. Parasitol*. 38, 1401–1410. doi: 10.1016/j.ijpara.2008.03.002

Bhalla, D., Dumas, M., and Preux, P. M. (2013). "Chapter 18—neurological manifestations of filarial infections," in *Handbook of Clinical Neurology*, eds. H. H. Garcia, H. B. Tanowitz, and O. H. Del Brutto (Elsevier), 235–242. Available online at: https://www.sciencedirect.com/science/article/pii/B9780444534903000182 (accessed March 25, 2024).

Boussinesq, M. (2006). Loiasis. *Ann. Trop. Med. Parasitol*. 100, 715–731. doi: 10.1179/136485906X112194

Camacho, C., Coulouris, G., Avagyan, V., Ma, N., Papadopoulos, J., Bealer, K., et al. (2009). BLAST+: architecture and applications. *BMC Bioinform*. 10:421. doi: 10.1186/1471-2105-10-421

Campbell, W. C. (1991). Ivermectin as an antiparasitic agent for use in humans. *Annu. Rev. Microbiol*. 45, 445–474. doi: 10.1146/annurev.mi.45.100191.002305

Chandy, A., Thakur, A. S., Singh, M. P., and Manigauha, A. (2011). A review of neglected tropical diseases: filariasis. *Asian Pac. J. Trop. Med*. 4, 581–586. doi: 10.1016/S1995-7645(11)60150-8

Chaudhuri, J., Parihar, M., and Pires-daSilva, A. (2011). An introduction to worm lab: from culturing worms to mutagenesis. *J. Vis. Exp*. 47:2293. doi: 10.3791/2293

Chung, M., Teigen, L. E., Libro, S., Bromley, R. E., Olley, D., Kumar, N., et al. (2019). Drug repurposing of bromodomain inhibitors as potential novel therapeutic leads for lymphatic filariasis guided by multispecies transcriptomics. *mSystems* 4:19. doi: 10.1128/mSystems.00596-19

Clare, R. H., Bardelle, C., Harper, P., Hong, W. D., Börjesson, U., Johnston, K. L., et al. (2019). Industrial scale high-throughput screening delivers multiple fast acting macrofilaricides. *Nat. Commun*. 10:11. doi: 10.1038/s41467-018-07826-2

Coulibaly, Y. I., Dembele, B., Diallo, A. A., Lipner, E. M., Doumbia, S. S., Coulibaly, S. Y., et al. (2009). A randomized trial of doxycycline for *Mansonella perstans* infection. *N. Engl. J. Med*. 361, 1448–1458. doi: 10.1056/NEJMoa0900863

Darby, A. C., Armstrong, S. D., Bah, G. S., Kaur, G., Hughes, M. A., Kay, S. M., et al. (2012). Analysis of gene expression from the *Wolbachia* genome of a filarial nematode supports both metabolic and defensive roles within the symbiosis. *Genome Res*. 22, 2467–2477. doi: 10.1101/gr.138420.112

Deng, Z. L., Münch, P. C., Mreches, R., and McHardy, A. C. (2022). Rapid and accurate identification of ribosomal RNA sequences via deep learning. *Nucl. Acids Res*. 50:e60. doi: 10.1093/nar/gkac112

Dufour, Y. S., Wesenberg, G. E., Tritt, A. J., Glasner, J. D., Perna, N. T., Mitchell, J. C., et al. (2010). chipD: a web tool to design oligonucleotide probes for high-density tiling arrays. *Nucl. Acids Res*. 38, W321–W325. doi: 10.1093/nar/gkq517

Foster, J., Ganatra, M., Kamal, I., Ware, J., Makarova, K., Ivanova, N., et al. (2005). The *Wolbachia* genome of *Brugia malayi*: endosymbiont evolution within a human pathogenic nematode. *PLoS Biol*. 3:e121. doi: 10.1371/journal.pbio.0030121

Foster, J. M., Grote, A., Mattick, J., Tracey, A., Tsai, Y. C., Chung, M., et al. (2020). Sex chromosome evolution in parasitic nematodes of humans. *Nat. Commun*. 11:1964. doi: 10.1038/s41467-020-15654-6

Grote, A., Voronin, D., Ding, T., Twaddle, A., Unnasch, T. R., Lustigman, S., et al. (2017). Defining *Brugia malayi* and *Wolbachia* symbiosis by stage-specific dual RNA-seq. *PLoS Negl. Trop. Dis*. 11:e0005357. doi: 10.1371/journal.pntd.0005357

He, S., Wurtzel, O., Singh, K., Froula, J. L., Yilmaz, S., Tringe, S. G., et al. (2010). Validation of two ribosomal RNA removal methods for microbial metatranscriptomics. *Nat. Methods* 7, 807–812. doi: 10.1038/nmeth.1507

Hoerauf, A., Specht, S., Büttner, M., Pfarr, K., Mand, S., Fimmers, R., et al. (2008). *Wolbachia* endobacteria depletion by doxycycline as antifilarial therapy has macrofilaricidal activity in onchocerciasis: a randomized placebo-controlled study. *Med. Microbiol. Immunol*. 197, 295–311. doi: 10.1007/s00430-007-0062-1

Hrdlickova, R., Toloue, M., and Tian, B. (2017). RNA-seq methods for transcriptome analysis. *WIREs RNA* 8:e1364. doi: 10.1002/wrna.1364

Johnston, K. L., Ford, L., Umareddy, I., Townson, S., Specht, S., Pfarr, K., et al. (2014). Repurposing of approved drugs from the human pharmacopoeia to target *Wolbachia* endosymbionts of onchocerciasis and lymphatic filariasis. *Int. J. Parasitol. Drugs Drug Resist*. 4, 278–286. doi: 10.1016/j.ijpddr.2014.09.001

Johnston, K. L., Hong, W. D., Turner, J. D., O'Neill, P. M., Ward, S. A., and Taylor, M. J. (2021). Anti-*Wolbachia* drugs for filariasis. *Trends Parasitol*. 37, 1068–1081. doi: 10.1016/j.pt.2021.06.004

Kang, Y., Norris, M. H., Zarzycki-Siek, J., Nierman, W. C., Donachie, S. P., and Hoang, T. T. (2011). Transcript amplification from single bacterium for transcriptome analysis. *Genome Res*. 21, 925–935. doi: 10.1101/gr.116103.110

Kim, D., Paggi, J. M., Park, C., Bennett, C., and Salzberg, S. L. (2019). Graph-based genome alignment and genotyping with HISAT2 and HISAT-genotype. *Nat. Biotechnol*. 37, 907–915. doi: 10.1038/s41587-019-0201-4

Kumar, N., Creasy, T., Sun, Y., Flowers, M., Tallon, L. J., and Dunning Hotopp, J. C. (2012). Efficient subtraction of insect rRNA prior to transcriptome analysis of *Wolbachia-Drosophila* lateral gene transfer. *BMC Res. Not*. 5:230. doi: 10.1186/1756-0500-5-230

Kumar, N., Lin, M., Zhao, X., Ott, S., Santana-Cruz, I., Daugherty, S., et al. (2016). Efficient enrichment of bacterial mRNA from host-bacteria total RNA samples. *Sci. Rep*. 6:34850. doi: 10.1038/srep34850

Li, H., Handsaker, B., Wysoker, A., Fennell, T., Ruan, J., Homer, N., et al. (2009). The sequence alignment/map format and SAMtools. *Bioinformatics* 25, 2078–2079. doi: 10.1093/bioinformatics/btp352

Li, Z., and Carlow, C. K. S. (2012). Characterization of transcription factors that regulate the type IV secretion system and riboflavin biosynthesis in *Wolbachia* of *Brugia malayi*. *PLoS ONE* 7:e51597. doi: 10.1371/journal.pone.0051597

Liao, Y., Smyth, G. K., and Shi, W. (2014). featureCounts: an efficient general purpose program for assigning sequence reads to genomic features. *Bioinformatics* 30, 923–930. doi: 10.1093/bioinformatics/btt656

Luck, A. N., Yuan, X., Voronin, D., Slatko, B. E., Hamza, I., and Foster, J. M. (2016). Heme acquisition in the parasitic filarial nematode *Brugia malayi*. *FASEB J*. 30, 3501–3514. doi: 10.1096/fj.201600603R

Mackenzie, C. D., Malecela, M., Mueller, I., and Homeida, M. A. (2002). "Approaches to the control and elimination of the clinically important filarial diseases," in *The Filaria* (Boston, MA: Springer), 155–165. Available online at: https://link.springer.com/chapter/10.1007/0-306-47661-4_13 (accessed October 24, 2023).

Mand, S., Pfarr, K., Sahoo, P. K., Satapathy, A. K., Specht, S., Klarmann, U., et al. (2009). Macrofilaricidal activity and amelioration of lymphatic pathology in bancroftian filariasis after 3 weeks of doxycycline followed by single-dose diethylcarbamazine. *Am. J. Trop. Med. Hyg*. 81, 702–711. doi: 10.4269/ajtmh.2009.09-0155

Martin, M. (2011). Cutadapt removes adapter sequences from high-throughput sequencing reads. *EMBnet.j* 17, 10–12. doi: 10.14806/ej.17.1.200

Mclaren, D. J., Worms, M. J., Laurence, B. R., and Simpson, M. G. (1975). Micro-organisms in filarial larvae (Nematoda). *Trans. R Soc. Trop. Med. Hyg*. 69, 509–514. doi: 10.1016/0035-9203(75)90110-8

Medeiros, Z. M., Vieira, A. V. B., Xavier, A. T., Bezerra, G. S. N., Lopes, M. d. F. C., Bonfim, C. V., et al. (2021). Lymphatic filariasis: a systematic review on morbidity and its repercussions in countries in the Americas. *Int. J. Environ. Res. Publ. Health* 19:316. doi: 10.3390/ijerph19010316

Mediannikov, O., and Ranque, S. (2018). Mansonellosis, the most neglected human filariasis. *N. Microb. N. Infect*. 26, S19–S22. doi: 10.1016/j.nmni.2018.08.016

Michalski, M. L., Griffiths, K. G., Williams, S. A., Kaplan, R. M., and Moorhead, A. R. (2011). The NIH-NIAID filariasis research reagent resource center. *PLoS Negl. Trop. Dis*. 5:e1261. doi: 10.1371/journal.pntd.0001261

Molyneux, D. H., Bradley, M., Hoerauf, A., Kyelem, D., and Taylor, M. J. (2003). Mass drug treatment for lymphatic filariasis and onchocerciasis. *Trends Parasitol*. 19, 516–522. doi: 10.1016/j.pt.2003.09.004

Parkinson, J., Mitreva, M., Whitton, C., Thomson, M., Daub, J., Martin, J., et al. (2004). A transcriptomic analysis of the phylum Nematoda. *Nat. Genet*. 36, 1259–1267. doi: 10.1038/ng1472

Prezza, G., Heckel, T., Dietrich, S., Homberger, C., Westermann, A. J., and Vogel, J. (2020). Improved bacterial RNA-seq by Cas9-based depletion of ribosomal RNA reads. *RNA* 26, 1069–1078. doi: 10.1261/rna.075945.120

Quek, S., Cook, D. A. N., Wu, Y., Marriott, A. E., Steven, A., Johnston, K. L., et al. (2022). *Wolbachia* depletion blocks transmission of lymphatic filariasis by preventing chitinase-dependent parasite exsheathment. *Proc. Natl. Acad. Sci. U. S. A*. 119:e2120003119. doi: 10.1073/pnas.2120003119

Quinlan, A. R., and Hall, I. M. (2010). BEDTools: a flexible suite of utilities for comparing genomic features. *Bioinformatics* 26, 841–842. doi: 10.1093/bioinformatics/btq033

Ramírez, F., Dündar, F., Diehl, S., Grüning, B. A., and Manke, T. (2014). deepTools: a flexible platform for exploring deep-sequencing data. *Nucl. Acids Res*. 42, W187–W191. doi: 10.1093/nar/gku365

Richards, F. O., Boatin, B., Sauerbrey, M., and Sékétéli, A. (2001). Control of onchocerciasis today: status and challenges. *Trends Parasitol*. 17, 558–563. doi: 10.1016/S1471-4922(01)02112-2

Rognes, T., Flouri, T., Nichols, B., Quince, C., and Mahé F. (2016). VSEARCH: a versatile open source tool for metagenomics. *PeerJ* 4:e2584. doi: 10.7717/peerj.2584

Schuierer, S., Carbone, W., Knehr, J., Petitjean, V., Fernandez, A., Sultan, M., et al. (2017). A comprehensive assessment of RNA-seq protocols for degraded and low-quantity samples. *BMC Genomics* 18:442. doi: 10.1186/s12864-017-3827-y

Simón, F., Siles-Lucas, M., Morchón, R., González-Miguel, J., Mellado, I., Carretón, E., et al. (2012). Human and animal dirofilariasis: the emergence of a zoonotic mosaic. *Clin. Microbiol. Rev*. 25, 507–544. doi: 10.1128/CMR.00012-12

Sironi, M., Bandi, C., Sacchi, L., Sacco, B. D., Damiani, G., and Genchi, C. (1995). Molecular evidence for a close relative of the arthropod endosymbiont *Wolbachia* in a filarial worm. *Mol. Biochem. Parasitol*. 74, 223–227. doi: 10.1016/0166-6851(95)02494-8

Small, S. T., Tisch, D. J., and Zimmerman, P. A. (2014). Molecular epidemiology, phylogeny and evolution of the filarial nematode *Wuchereria bancrofti*. *Infect. Genet. Evol. J. Mol. Epidemiol. Evol. Genet. Infect. Dis*. 2014, 33–43. doi: 10.1016/j.meegid.2014.08.018

Specht, S., Mand, S., Marfo-Debrekyei, Y., Debrah, A. Y., Konadu, P., Adjei, O., et al. (2008). Efficacy of 2- and 4-week rifampicin treatment on the *Wolbachia* of *Onchocerca volvulus*. *Parasitol. Res*. 103, 1303–1309. doi: 10.1007/s00436-008-1133-y

Sultan, M., Amstislavskiy, V., Risch, T., Schuette, M., Dökel, S., Ralser, M., et al. (2014). Influence of RNA extraction methods and library selection schemes on RNA-seq data. *BMC Genomics* 15:675. doi: 10.1186/1471-2164-15-675

Supali, T., Djuardi, Y., Pfarr, K. M., Wibowo, H., Taylor, M. J., Hoerauf, A., et al. (2008). Doxycycline treatment of *Brugia malayi*-infected persons reduces microfilaremia and adverse reactions after diethylcarbamazine and albendazole treatment. *Clin. Infect. Dis*. 46, 1385–1393. doi: 10.1086/586753

Taylor, M. J., Bandi, C., and Hoerauf, A. (2005). *Wolbachia* bacterial endosymbionts of filarial nematodes. *Adv. Parasitol*. 60, 245–284. doi: 10.1016/S0065-308X(05)60004-8

Taylor, M. J., Hoerauf, A., and Bockarie, M. (2010). Lymphatic filariasis and onchocerciasis. *Lancet* 376, 1175–1185. doi: 10.1016/S0140-6736(10)60586-7

Taylor, M. J., von Geldern, T. W., Ford, L., Hübner, M. P., Marsh, K., Johnston, K. L., et al. (2019). Preclinical development of an oral anti-*Wolbachia* macrolide drug for the treatment of lymphatic filariasis and onchocerciasis. *Sci. Transl. Med*. 11:eaau2086. doi: 10.1126/scitranslmed.aau2086

Thorvaldsdóttir, H., Robinson, J. T., and Mesirov, J. P. (2013). Integrative Genomics Viewer (IGV): high-performance genomics data visualization and exploration. *Brief Bioinform*. 14, 178–192. doi: 10.1093/bib/bbs017

Valero-Mora, P. M. (2010). ggplot2: elegant graphics for data analysis. *J. Stat. Softw*. 35, 1–3. doi: 10.18637/jss.v035.b01

Wahl, A., Huptas, C., and Neuhaus, K. (2022). Comparison of rRNA depletion methods for efficient bacterial mRNA sequencing. *Sci. Rep*. 12:5765. doi: 10.1038/s41598-022-09710-y

Wang, L., Wang, S., and Li, W. (2012). RSeQC: quality control of RNA-seq experiments. *Bioinformatics* 28, 2184–2185. doi: 10.1093/bioinformatics/bts356

Wang, Z., Gerstein, M., and Snyder, M. (2009). RNA-Seq: a revolutionary tool for transcriptomics. *Nat. Rev. Genet*. 10, 57–63. doi: 10.1038/nrg2484

Wangsanuwat, C., Heom, K. A., Liu, E., O'Malley, M. A., and Dey, S. S. (2020). Efficient and cost-effective bacterial mRNA sequencing from low input samples through ribosomal RNA depletion. *BMC Genomics* 21:717. doi: 10.1186/s12864-020-07134-4

Wanji, S., Tendongfor, N., Nji, T., Esum, M., Che, J. N., Nkwescheu, A., et al. (2009). Community-directed delivery of doxycycline for the treatment of onchocerciasis in areas of co-endemicity with loiasis in Cameroon. *Parasit. Vect*. 2:39. doi: 10.1186/1756-3305-2-39

WHO Expert Committee on Onchocerciasis Control (1993). *Onchocerciasis and Its Control: Report of a WHO Expert Committee on Onchocerciasis Control*. Geneva: World Health Organization. Available online at: https://iris.who.int/handle/10665/37346 (accessed October 24, 2023).

World Health Organization (2019). Global programme to eliminate lymphatic filariasis: progress report, 2018. *Wkly Epidemiol. Rec*. 94, 457–470.

Wu, B., Novelli, J., Foster, J., Vaisvila, R., Conway, L., Ingram, J., et al. (2009). The heme biosynthetic pathway of the obligate *Wolbachia* endosymbiont of *Brugia malayi* as a potential anti-filarial drug target. *PLoS Negl. Trop. Dis*. 3:e475. doi: 10.1371/journal.pntd.0000475

Xiang, X., Poli, D., Degnan, B. M., and Degnan, S. M. (2022). Ribosomal RNA-depletion provides an efficient method for successful dual RNA-seq expression profiling of a marine sponge holobiont. *Mar. Biotechnol*. 24, 722–732. doi: 10.1007/s10126-022-10138-8

Xie, Y., Wang, S., Wu, S., Gao, S., Meng, Q., Wang, C., et al. (2022). Genome of the giant panda roundworm illuminates its host shift and parasitic adaptation. *Genom. Proteom. Bioinformat*. 20, 366–381. doi: 10.1016/j.gpb.2021.08.002

Zhao, S., Zhang, Y., Gamini, R., Zhang, B., and von Schack, D. (2018). Evaluation of two main RNA-seq approaches for gene quantification in clinical RNA sequencing: polyA+ selection versus rRNA depletion. *Sci. Rep*. 8:4781. doi: 10.1038/s41598-018-23226-4

Zhao, W., He, X., Hoadley, K. A., Parker, J. S., Hayes, D. N., and Perou, C. M. (2014). Comparison of RNA-Seq by poly (A) capture, ribosomal RNA depletion, and DNA microarray for expression profiling. *BMC Genomics* 15:419. doi: 10.1186/1471-2164-15-419

frontiers | Frontiers in Microbiology

TYPE Original Research
PUBLISHED 05 June 2024
DOI 10.3389/fmicb.2024.1380647

OPEN ACCESS

EDITED BY
George Tsiamis,
University of Patras, Greece

REVIEWED BY
Emilie Lefoulon,
The Pennsylvania State University (PSU), United States
Naima Bel Mokhtar,
University of Patras, Greece

*CORRESPONDENCE
Ioannis Eleftherianos
ioannise@gwu.edu

†These authors have contributed equally to this work

RECEIVED 01 February 2024
ACCEPTED 22 May 2024
PUBLISHED 05 June 2024

CITATION
Tafesh-Edwards G, Kyza Karavioti M, Markollari K, Bunnell D, Chtarbanova S and Eleftherianos I (2024) *Wolbachia* endosymbionts in *Drosophila* regulate the resistance to Zika virus infection in a sex dependent manner.
Front. Microbiol. 15:1380647.
doi: 10.3389/fmicb.2024.1380647

Wolbachia endosymbionts in *Drosophila* regulate the resistance to Zika virus infection in a sex dependent manner

Ghada Tafesh-Edwards[1†], Margarita Kyza Karavioti[1†], Klea Markollari[1], Dean Bunnell[2], Stanislava Chtarbanova[2] and Ioannis Eleftherianos[1*]

[1]Infection and Innate Immunity Laboratory, Department of Biological Sciences, The George Washington University, Washington, DC, United States, [2]Department of Biological Sciences, The University of Alabama, Tuscaloosa, AL, United States

Drosophila melanogaster has been used extensively for dissecting the genetic and functional bases of host innate antiviral immunity and virus-induced pathology. Previous studies have shown that the presence of *Wolbachia* endosymbionts in *D. melanogaster* confers resistance to infection by certain viral pathogens. Zika virus is an important vector-borne pathogen that has recently expanded its range due to the wide geographical distribution of the mosquito vector. Here, we describe the effect of *Wolbachia* on the immune response of *D. melanogaster* adult flies following Zika virus infection. First, we show that the presence of *Wolbachia* endosymbionts promotes the longevity of uninfected *D. melanogaster* wild type adults and increases the survival response of flies following Zika virus injection. We find that the latter effect is more pronounced in females rather than in males. Then, we show that the presence of *Wolbachia* regulates Zika virus replication during Zika virus infection of female flies. In addition, we demonstrate that the antimicrobial peptide-encoding gene *Drosocin* and the sole Jun N-terminal kinase-specific MAPK phosphatase *Puckered* are upregulated in female adult flies, whereas the immune and stress response gene *TotM* is upregulated in male individuals. Finally, we find that the activity of RNA interference and Toll signaling remain unaffected in Zika virus-infected female and male adults containing *Wolbachia* compared to flies lacking the endosymbionts. Our results reveal that *Wolbachia* endosymbionts in *D. melanogaster* affect innate immune signaling activity in a sex-specific manner, which in turn influences host resistance to Zika virus infection. This information contributes to a better understanding of the complex interrelationship between insects, their endosymbiotic bacteria, and viral infection. Interpreting these processes will help us design more effective approaches for controlling insect vectors of infectious disease.

KEYWORDS

Zika virus, *Drosophila melanogaster*, *Wolbachia*, innate immunity, infection, immune signaling

Introduction

Symbiotic interactions between microbes and animals are common in nature. The role of symbionts in providing nutrients missing in the diets of various animals has been known for many years. Such symbionts are particularly common in insects, perhaps because most insects are specialist herbivores and plants are frequently poor-quality food for animals; the essential elements that the animals lack can be provided by symbiotic microbes. In many cases, the association has become so close that the microbial partner (usually a bacterium) lives within cells in the host's body (it is then said to be an endosymbiont), is maternally transmitted from one host generation to another, and is never found in the free-living condition (Dale and Moran, 2006). Although such relationships have been most commonly studied with respect to nutritional effects on the host, there can be other benefits. For example, endosymbiotic bacteria may protect their hosts from parasites or pathogens (Brownlie and Johnson, 2009; Eleftherianos et al., 2013). The most widespread and widely studied endosymbionts are *Wolbachia*, which are harbored by more than half of all insect species and are able to manipulate the reproductive properties of their hosts, while in other hosts such as bedbugs or nematodes they can act as nutritional mutualists (Pietri et al., 2016; Landmann, 2019; Bi and Wang, 2020; Newton and Rice, 2020).

Wolbachia are Gram-negative obligate intracellular Alphaproteobacteria bacteria that are found in the germline and somatic tissues of most arthropod species, and they are transmitted maternally from infected mothers (Porter and Sullivan, 2023). Also, they establish an endosymbiotic relationship with several insect species, including *D. melanogaster* (Kaur et al., 2021). In fruit flies, *Wolbachia pipientis* endosymbionts modulate diverse biological processes, such as reproduction, nutrition, development, and longevity, offering many benefits to the host (Iturbe-Ormaetxe and O'Neill, 2007). Research on *Wolbachia* has important implications for understanding the molecular and functional bases of bacterial symbiosis, and also produces significant information on the regulation of host–microbe interactions which can be potentially used in translational applications in agriculture and biomedicine (Yen and Failloux, 2020; Edenborough et al., 2021; Araújo et al., 2022).

One of the crucial roles of *Wolbachia* in insects is the immune protection against certain viral pathogens known as a pathogen-blocking effect, which is probably attributed to the activation of host immunity or competition with virus for cellular resources (Pimentel et al., 2021). It was originally demonstrated that the presence of *Wolbachia* in *D. melanogaster* increases resistance to infection by three insect RNA viruses (Drosophila C virus, Nora virus and Flock House virus) but not to infection by a DNA virus (Insect Iridescent Virus 6) (Hedges et al., 2008; Teixeira et al., 2008). *Wolbachia*-mediated antiviral protection in *Drosophila* species has been demonstrated for a number of different *Wolbachia* strains (Martinez et al., 2014, 2017). For example, when dengue viruses are injected into *D. melanogaster*, virus accumulation is significantly reduced in the presence of the non-virulent *Wolbachia* strain wMel and the life-shortening strain wMelPop-CLA (Rancès et al., 2012). Interestingly, Toll and Immune deficiency (Imd) pathways are not required for expression of the dengue virus-blocking phenotype in the *Drosophila* host and *Wolbachia* endosymbionts do not interact with the Toll pathway-mediated resistance to viral oral infection (Rancès et al., 2013; Ferreira et al., 2014). However, *Wolbachia* decreases the biodiversity of the gut microbiota without changing the total microbial load, and altering the gut microbiota composition with antibiotic treatment increases *Wolbachia* density without boosting the resistance against *Drosophila* C Virus (DCV) (Simhadri et al., 2017; Ye et al., 2017). In terms of systemic viral infection, extracellular signal-regulated kinases (ERK) signaling activity increases in the presence of *Wolbachia* without affecting the protection of the host to systemic infection with DCV (Wong et al., 2016). When *D. melanogaster* adults are maintained on cholesterol-enriched diets and they contain the *Wolbachia* strains wMelPop and wMelCS, the flies exhibit reduced pathogen blocking and higher viral copy number compared to flies grown on standard diet (Caragata et al., 2013). Subsequent studies further revealed that stable transinfection of *D. melanogaster* with highly protective *Wolbachia* strains is not necessarily associated with general immune activation (Chrostek et al., 2014). Although DCV infection causes increased sleep in *D. melanogaster* females than in males flies, the presence of *Wolbachia* does not affect this behavioral response (Vale and Jardine, 2015). *Wolbachia* can suppress the evolution of *D. melanogaster* resistance genes because in the presence of the endosymbiotic bacteria, the resistant allele of *pastrel-a* gene, which has a major effect on resistance to DCV, is at a lower frequency than in the symbiont-free individuals (Martinez et al., 2016).

Zika virus is a vector-borne flavivirus that has become a significant threat to human health. The disease was originally limited to African countries, however, Zika virus cases have been reported in other parts of the world, such as Brazil and Malaysia (Plourde and Bloch, 2016). The *Flaviviridae* family comprises several notable viruses, including dengue virus and yellow fever virus, all of which are transmitted primarily through mosquito vectors and can cause significant public health concerns (Gubler et al., 2017). The connection between *D. melanogaster* and Zika virus lies in the use of fruit flies as a model organism to study Zika virus pathogenesis and the host innate immune response against flaviviruses. By introducing Zika virus into adult *D. melanogaster*, it is possible to identify important genes and pathways involved in the host response to viral infection, providing valuable information on host-virus interactions and the underlying antiviral mechanisms (Tafesh-Edwards and Eleftherianos, 2020a). For example, a recent study in which *Drosophila* flies were subjected to injection with Zika virus has demonstrated activation of the Imd pathway in the brain (Liu et al., 2018). More precisely, *Diptericin* (read-out of Imd signaling), but not *Drosomycin* (read-out of Toll signaling), is upregulated in the heads of Zika virus-infected flies, and this result is not observed in fly null mutants for the transcription factor Relish. In addition, the *Drosophila* Imd pathway in the fly brain appears to be required to restrict Zika virus infection in this tissue (Lye and Chtarbanova, 2018). Zika virus infection induces antiviral autophagy in the brain, a process that is Relish-dependent (Liu et al., 2018). The fly ortholog of the mammalian polyubiquitin-binding scaffold protein p62, the autophagy cargo receptor Ref(2)P, which is a known restriction factor for natural viral pathogens of the fly such as the *Drosophila* Sigma virus (Contamine et al., 1989; Longdon et al., 2010), is also directed against Zika virus in the brain, because its knockdown increases the rate of Zika virus replication in fly heads (Liu et al., 2018), and protection against Zika virus is not dependent on RNAi in the fly brain (Liu et al., 2018). However, we have recently shown that *Dicer2* loss-of-function mutant flies have increased sensitivity to Zika virus injection into the thorax and exhibit higher viral loads (Harsh et al., 2018).

Activation of the Imd pathway triggers signaling through the adaptor IMD protein and various caspases and kinases, resulting in the induction of c-Jun N-terminal kinase (Jnk) signaling, which forms one of the two functional branches of the Imd pathway (Sluss et al., 1996; Chen et al., 2002). Although the role of Jnk signaling in the regulation of the immune response against bacterial pathogens through modulating the expression of antimicrobial peptides and maintaining host homeostasis is well documented (Tafesh-Edwards and Eleftherianos, 2020b), its participation in the immune response of the fly against viral infections is lagging. Intriguingly, the Jnk pathway has a broad antiviral function against dengue, Zika, and chikungunya viruses, which is mediated by the complement system and apoptosis in the *Aedes aegypti* salivary glands (Chowdhury et al., 2020).

The contribution of Janus kinase–signal transducer and activator of transcription (Jak/Stat) signaling to the *D. melanogaster* antiviral immune response is virus specific (Tafesh-Edwards and Eleftherianos, 2020a). Although the Jak/Stat pathway can be induced by RNA viruses, such as DCV, Cricket Paralysis Virus (CrPV), Flock House Virus (FHV), and *Drosophila* X Virus (DXV), it is only required for resistance against the two Dicistroviruses, DCV and CrPV (Dostert et al., 2005; Myllymäki and Rämet, 2014; Chow and Kagan, 2018; Huang et al., 2023). Also, we have previously documented that Zika virus infection induces negative regulation of Jak/Stat signaling, and Zika virus non-structural protein 4A (NS4A) interacts with Jak/Stat signaling components (Harsh et al., 2020).

Here we explored the role of *Wolbachia* endosymbionts in the *D. melanogaster* immune response against Zika virus infection. For this, we tested the survival ability of wild type adult flies carrying *Wolbachia* endosymbionts during Zika virus infection and the viral replication in these individuals. We also assessed whether the presence of *Wolbachia* alters the innate immune signaling activity upon challenge with Zika virus. First, we find a positive correlation between the survival ability of female and male *D. melanogaster* following Zika virus infection and the presence of *Wolbachia* endosymbionts. Then, we show that females lacking *Wolbachia* have a higher Zika viral load than females carrying *Wolbachia*, which implies the participation of *Wolbachia* in resistance to Zika virus infection. Effects on fly survival and Zika virus load could be attributed to changes in the regulation of innate immune signaling, as females containing *Wolbachia* have increased Imd pathway activity and males containing *Wolbachia* have increased Jak/Stat pathway activity. This information is vital because it provides valuable insights into the interconnection between bacterial endosymbiosis in insects, viral pathogenesis, and host defense mechanisms. Similar research can contribute toward development of approaches for the management of vectors of infectious diseases.

Materials and methods

Fly stocks

Two natural Canton-S lines of *D. melanogaster* containing or lacking *Wolbachia pipientis* (strain *w*Mel) were used in all experiments. Flies were reared on ready-made fly food (LabExpress, Ann Arbor, MI, United States) supplemented with yeast (Carolina Biological Supply, Burlington, NC, United States). All vials were maintained in an incubator at 25°C and 12 h light/12 h dark photoperiod cycle. Both *D. melanogaster* lines were amplified for experimentation by transferring adult flies to fresh vials every third day. Female and male flies were selected from the same generation and randomly assigned to experimental groups.

Zika virus stocks

Stocks of Zika virus strain MR766 were maintained and amplified as described before (Harsh et al., 2018).

Fly longevity experiments

Ten male and 10 female Canton-S newly eclosed *D. melanogaster* adult flies carrying or lacking *Wolbachia* endosymbionts, were kept in separate vials containing fly food at 25°C and a 12:12-h light:dark photoperiod cycle. Observations were held at 24-h intervals to record fly survival over a 100-day period. All flies were transferred to fresh vials every 3 days. The experiment was repeated five times with three replicates for each experimental treatment. In total, 150 female and 150 male flies were used in the longevity experiments.

Fly survival experiments

Ten female and 10 male 3–5 days old flies of the two Canton-S lines carrying or lacking *Wolbachia* endosymbionts were first anesthetized with carbon dioxide for a few seconds and then injected into the thorax with 100 nL of a Zika virus solution (11,000 PFU/fly) in PBS (pH 7.5) using a Nanojector apparatus (Nanoject III Programmable Nanoliter Injector, Drummond Scientific, Broomall, PA, United States). Flies injected with 100 nL of PBS served as negative controls. Virus-infected and control flies were maintained in vials with fly food at 25°C and they were transferred to fresh vials every third day for the duration of the survival experiment. Survival results were estimated at 24-h intervals for up to 25 days. Three independent experiments were conducted, and each experiment included three replicates for each experimental condition.

Gene expression analysis

Ten female and 10 male Canton-S 3–5 days old flies containing or lacking *Wolbachia* were injected with either Zika virus or PBS only (negative control), as described above, and at 4 days post-injection were collected and stored at −80°C. A pool of 10 flies was homogenized using plastic pestles and RNA isolation was carried out using TRIzol (Invitrogen, Waltham, MA, United States) according to the manufacturer's protocol, followed by complementary DNA (cDNA) synthesis using the AB High-Capacity cDNA Reverse Transcription Kit (Fisher Scientific, Hampton, NH). Zika virus load and immune gene expression were estimated using Zika virus gene-specific primers and *D. melanogaster* gene-specific primers, respectively (Table 1). Gene expression analysis was assessed using quantitative Real Time PCR (qRT-PCR) and two technical replicates per treatment on a CFX96 Real-Time PCR detection system (Bio-Rad

10.3389/fmicb.2024.1380647

TABLE 1 Primer sequences used for quantitative PCR.

Gene	Accession number	Pathway	Forward primer (5′ to 3′)	Reverse primer (3′ to 5′)
Ago-2	CG7439	RNAi	CCGGAAGTGACTGTGACAGATCG	CCTCCACGCACTGCATTGCTCG
Basket	CG5680	Jnk	GACAGCTCAGCACCAACACT	GCTTGGCATGGGTTACATTT
Defensin	CG1385	Toll	CGCATAGAAGCGAGCCACATG	CGCATAGAAGCGAGCCACATG
Drosocin	CG10816	Imd	TTCACCATCGTTTTCCTGCT	AGCTTGAGCCAGGTGATCCT
Dicer-2	CG6493	RNAi	GTATGGCGATAGTGTGACTGCGAC	GCAGCTTGTTCCGCAGCAATATAGC
Diptericin	CG10794	Imd	TGCGCAATCGCTTCTAC	GTGGAGTGGGCTTCATG
Drosomycin	CG10810	Toll	TGAGAACCTTTTCCAATATGATG	CCAGGACCACCAGCAT
Puckered	CG7850	Jnk	GGCCTACAAGCTGGTGAAAG	AGTTCAGATTGGGCGAGATG
TotA	CG31509	Jak/Stat	GAAGATCGTGAGGCTGACAAC	GTCCTGGGCGTTTTTGATAA
TotM	CG14027	Jak/Stat	GCTGGGAAAGGTAAATGCTG	AGGCGCTGTTTTTCTGTGAC
RpL32	CG7939	–	GATGACCATCCGCCCAGCA	CGGACCGACAGCTGCTTGGC
ZIKV NS5	055839	–	CCTTGGATTCTTGAACGAGGA	AGAGCTTCATTCTCCAGATCAA

Laboratories, Hercules, CA). Cycle conditions were 95°C for 2 min, 40 repetitions of 95°C for 15 s, 61°C for 30 s, 95°C for 15 s, 65°C for 5 s, and 95°C for 5 s. Quantitative RT-PCR experiments were repeated three times with each experiment consisting of three biological replicates and two technical replicates per condition. In total, 360 female and 360 male flies were used in the gene expression analysis experiments.

Statistical analysis

All data were processed using the GraphPad Prism5 software. Results from the longevity and survival experiments were statistically analyzed using a log-rank (Mantel-Cox) test and a chi-square test for pairwise comparison between each experimental group and the control group. Results from the gene expression analyses were conducted using a one-way analysis of variance (ANOVA) as well as a Tukey *post-hoc* test. Fold changes were estimated using the $2^{-\Delta\Delta C}{}_{T}$ method and *Ribosomal protein L32* (*RpL32*) as the housekeeping gene (Livak and Schmittgen, 2001; Schmittgen and Livak, 2008). PBS control treatments were used as a baseline for comparison in differential expression analysis. *p*-values less than 0.05 were considered significantly different. All error bars represent standard error of mean and all figures were generated using the GraphPad Prism5 software.

Results

Presence of *Wolbachia* prolongs the lifespan of *Drosophila melanogaster* Canton-S flies

We first assessed changes in longevity between *D. melanogaster* Canton-S male and female adult flies carrying or lacking *Wolbachia* endosymbionts. We found that female flies containing *Wolbachia* had a maximum lifespan of 91 days, whereas female individuals lacking *Wolbachia* had a maximum lifespan of 61 days, indicating a significant difference in longevity depending on the presence of the endosymbionts (Figure 1A). We also found that males containing *Wolbachia* had a maximum lifespan of 98 days, which was significantly longer compared to males without *Wolbachia* whose maximum lifespan was 61 days (Figure 1B). We further observed a significant difference in lifespan between males and females carrying *Wolbachia,* indicating a difference in longevity between the two sexes in the presence of the endosymbiont (Figure 1C), but not in its absence (Figure 1D). These results indicate that the presence of *Wolbachia* endosymbionts extends the longevity of *D. melanogaster* female and male wild type adult flies.

Drosophila melanogaster Canton-S females carrying *Wolbachia* have increased survival response to Zika virus infection

Next, we investigated the survival ability of *D. melanogaster* carrying and lacking *Wolbachia* endosymbionts following Zika virus infection through intrathoracic injection. We found that the presence of *Wolbachia* had a protective effect on female flies and the difference in survival compared to females lacking *Wolbachia* was significant (Figure 2A). However, we observed that males without *Wolbachia* were more sensitive compared to males carrying the endosymbionts, but the difference was not statistically significant (Figure 2B). We also found that males containing *Wolbachia* exhibited a significant better survival rate compared to their female counterparts (Figure 2C). Finally, there was a statistically significant difference in survival between males lacking *Wolbachia* and their corresponding female individuals (Figure 2D). Together, these results suggest that *Wolbachia* endosymbionts promote the survival of *D. melanogaster* adult female flies upon infection with Zika virus.

Presence of *Wolbachia* in *Drosophila melanogaster* Canton-S females regulates Zika virus replication

We then examined whether the presence of *Wolbachia* in *D. melanogaster* female and male adult flies affects Zika virus load. For this, we used gene-specific primers to estimate the expression of Zika virus *NS5* methyltransferase, which encodes both the viral

10.3389/fmicb.2024.1380647

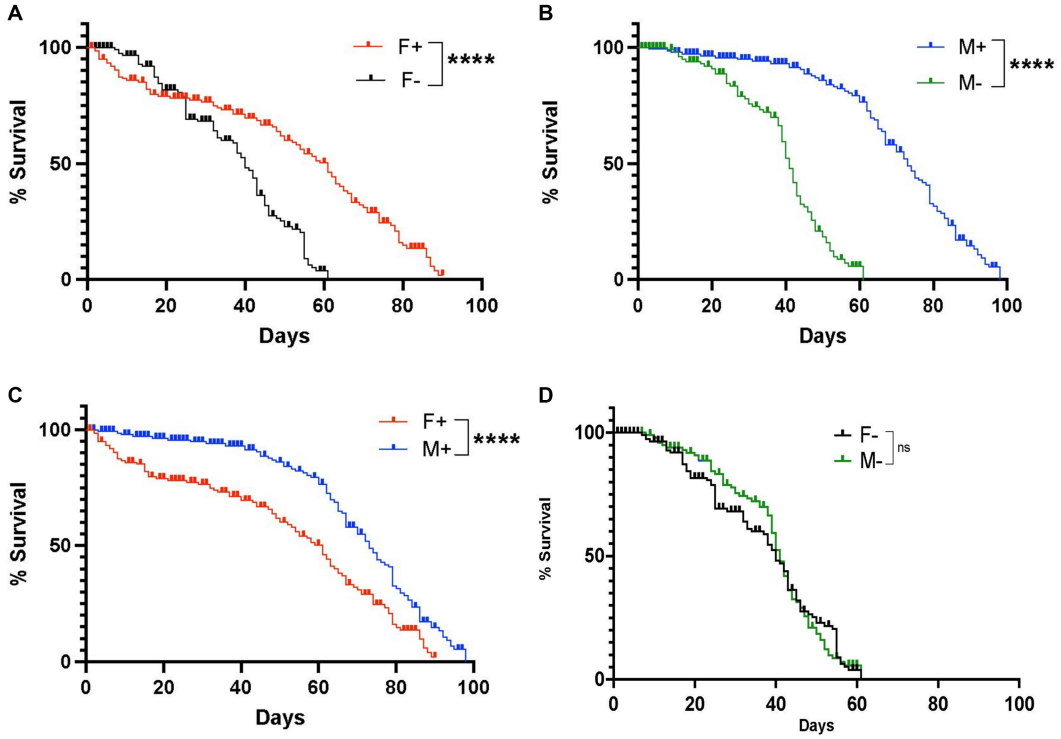

FIGURE 1
Lifespan of *Drosophila melanogaster* wild type adult flies containing or lacking *Wolbachia* endosymbionts. **(A)** Percent survival of *D. melanogaster* Canton-S female adult flies carrying (F+) or lacking (F–) *Wolbachia* endosymbionts (****$p < 0.0001$). **(B)** Percent survival of *D. melanogaster* Canton-S male adult flies carrying (M+) or lacking (M-) *Wolbachia* endosymbionts. **(C)** Percent survival of *D. melanogaster* Canton-S female and male adult flies carrying *Wolbachia* endosymbionts (F+ and M+, respectively) (****$p < 0.0001$). **(D)** Percent survival of *D. melanogaster* Canton-S female and male adult flies lacking *Wolbachia* endosymbionts (F– and M–, respectively); ns, non-significant difference ($n = 150$ flies of each sex).

methyltransferase and RNA-dependent RNA polymerase (Elshahawi et al., 2019; Song et al., 2021). We found that female flies carrying *Wolbachia* had significantly lower expression of Zika virus *NS5* compared to females without the endosymbionts (Figure 3A). In contrast, there were no significant differences in Zika virus *NS5* fold change between males with *Wolbachia* and those lacking the endosymbiotic bacteria (Figure 3B). These results demonstrate that the effect of *Wolbachia* endosymbionts on Zika virus replication in *D. melanogaster* Canton-S is sex-specific and the presence of the endosymbionts confers resistance to female, but not male, adult flies.

Presence of *Wolbachia* in *Drosophila melanogaster* Canton-S adult flies infected with Zika virus does not affect the expression of genes in the RNA interference pathway

We first tested whether the presence of *Wolbachia* in *D. melanogaster* adults infected with Zika virus modifies the transcriptional gene expression levels of *Dicer-2* and *Ago-2*. We found no significant changes in the transcript levels of *Dicer-2* and *Ago-2* between Zika virus infected female flies (Figure 4A) and male flies (Figure 4B) carrying or lacking *Wolbachia* endosymbionts. These results suggest that *Wolbachia* endosymbionts do not affect RNAi signaling activity in *D. melanogaster* adults in the context of Zika virus infection.

Presence of *Wolbachia* in *Drosophila melanogaster* Canton-S infected with Zika virus upregulates the expression of *Drosocin*

To test whether the presence of *Wolbachia* affects the NF-κB signaling activity in *D. melanogaster* adults following intrathoracic challenge with Zika virus, we used qPCR and gene-specific primers to estimate the expression of frequently-measured readout genes in the Toll and Imd pathways. We observed no statistical differences in the expression levels of *Drosomycin* and *Defensin* (Toll pathway) between female or male flies carrying or lacking *Wolbachia* endosymbionts (Figures 5A,B). Interestingly, we noticed significantly higher levels of *Drosocin* expression, an antimicrobial peptide encoding gene that acts as readout for the regulation of Imd pathway, in female flies carrying *Wolbachia* compared to those lacking the endosymbionts (Figure 5C). The difference in *Drosocin* expression was not observed between male flies carrying or lacking the endosymbiotic bacteria (Figure 5D). Similarly, no changes in *Diptericin* expression were noted in female and male flies regardless of the presence or absence of *Wolbachia* (Figures 5C,D). These results imply that *Wolbachia* endosymbionts can induce the expression of

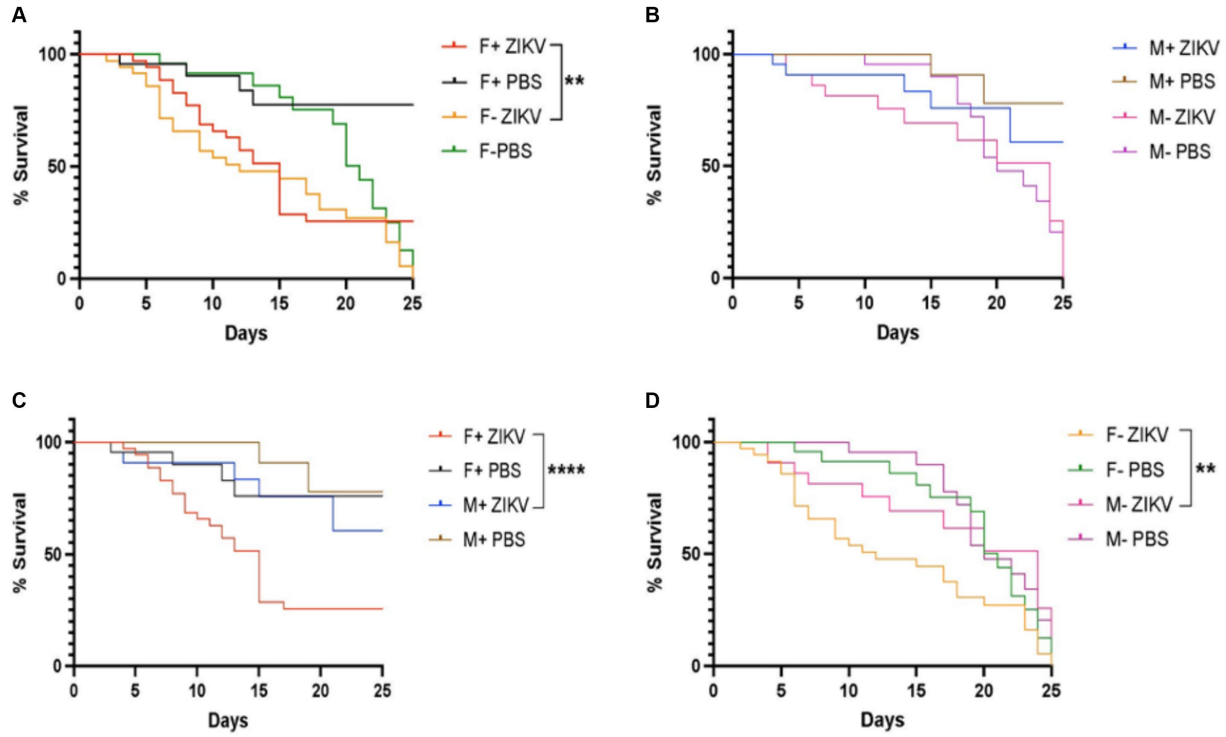

FIGURE 2
Wolbachia endosymbionts promote the survival of wild type *Drosophila melanogaster* against Zika virus infection. **(A)** Percent survival of *D. melanogaster* Canton-S female adult flies carrying or lacking *Wolbachia* endosymbionts following infection with Zika virus (ZIKV) (F+ ZIKV and F− ZIKV, respectively). Uninfected flies were injected with sterile PBS (F+ PBS and F− PBS) and acted as controls (**$p < 0.01$). **(B)** Percent survival of male flies carrying or lacking *Wolbachia* endosymbionts following infection with Zika virus (M+ ZIKV and M− ZIKV, respectively). Fly infections with PBS served as uninfected controls (M+ PBS and M− PBS). **(C)** Percent survival of *D. melanogaster* Canton-S female and male adult flies containing *Wolbachia* endosymbionts after infection with Zika virus (F+ ZIKV and M+ ZIKV, respectively). Uninfected control flies were injected with sterile PBS only (F+ PBS and M+ PBS) (****$p < 0.0001$). **(D)** Percent survival of *D. melanogaster* Canton-S female and male adult flies lacking *Wolbachia* endosymbionts following Zika virus infection (F− ZIKV and M− ZIKV, respectively). Uninfected flies were injected with sterile PBS (F− PBS and M− PBS) (**$p < 0.01$).

certain antimicrobial peptide-encoding genes in Zika virus infected *D. melanogaster* adults in a sex-specific manner.

Presence of *Wolbachia* in *Drosophila melanogaster* Canton-S adults infected with Zika virus alters Jak/Stat and Jnk signaling activity in sex-specific manner

To study the effect of *Wolbachia* on Jak/Stat and Jnk signaling pathway activity in *D. melanogaster* flies infected with Zika virus, we assessed through qPCR the expression level of four representative readout genes. For the JAK/STAT pathway, there were no significant differences in *TotA* and *TotM* gene expression levels between Zika virus infected female flies carrying *Wolbachia* and those lacking the endosymbionts (Figure 6A). A similar gene expression pattern was also observed for *TotA* in male flies (Figure 6B). However, we found that male wild type flies containing *Wolbachia* had significantly higher *TotM* expression compared to those without the endosymbionts (Figure 6B). For Jnk signaling, there was significant upregulation of *Puckered*, but not *Basket*, in Zika virus infected wild type female adult flies carrying *Wolbachia* compared to those without the bacteria (Figure 6C). Finally, there were no statistically significant differences in *Puckered* and *Basket* gene expression levels between Zika virus infected male flies irrespective of their *Wolbachia* status (Figure 6D). These findings denote that *Wolbachia* endosymbionts can alter Jak/Stat and Jnk signaling activity in male and female *D. melanogaster* adults, respectively, during Zika virus infection.

Discussion

Here we explored the potential effect of *Wolbachia* on the regulation of innate immune signaling and function of the *D. melanogaster* model against infection with the nonnatural pathogen, Zika virus. Our results provide evidence that *Wolbachia* can modulate the fly immune response in a sex-specific manner. More precisely, we show that the presence of *Wolbachia* prolongs the lifespan of adult flies, increases the survival of *D. melanogaster* females in response to Zika virus infection, and confers significant resistance to female, but not male, adult flies. Also, we find upregulation of the antimicrobial peptide gene *Drosocin* in Zika virus infected flies carrying the endosymbionts, but no changes in RNAi and Toll pathway regulated genes. Finally, we demonstrate that male and female flies containing *Wolbachia* have altered Jak/Stat and Jnk signaling activity during Zika virus infection. This information is important because it reveals that certain bacterial endosymbionts can be an important component of the host antiviral innate immune response against Zika virus and maybe other flaviviruses.

First, we observed that *Wolbachia* extends the lifespan of *D. melanogaster* Canton-S adult flies, which is conserved in both males and females. This information suggests that *Wolbachia* endosymbionts confer a fitness advantage to this *D. melanogaster* line. Previous research indicates that in most cases *Wolbachia* can provide fitness benefits for the insect host; however, the effect of *Wolbachia* on lifespan is variable and appears to depend on the genetic background of the fly and the strain of the endosymbiont (reviewed in Maistrenko et al., 2016). For instance, both increased and decreased lifespan effects have been found before in *D. melanogaster* and flies carrying the *wMel* strain of *Wolbachia* have shorter lifespan compared to flies free of endosymbionts (Min and Benzer, 1997; Martinez et al., 2015). In contrast to these previous findings, our results show that *wMel*-containing Canton-S flies have longer lifespan, which reinforce the concept that *D. melanogaster* longevity relies on the fly and *Wolbachia* strain.

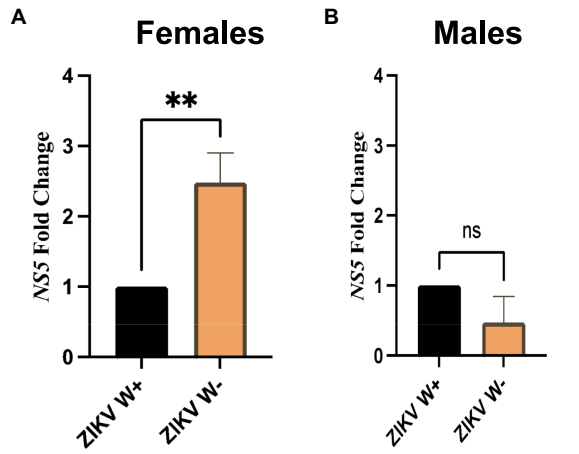

FIGURE 3
Zika virus replication in *Drosophila melanogaster* adults containing or lacking *Wolbachia* endosymbionts. **(A)** Expression of Zika virus (ZIKV) *NS5* in *D. melanogaster* Canton-S female adult flies carrying (W+) or lacking (W–) *Wolbachia* endosymbionts at 4 days following intrathoracic injection (**$p < 0.01$). **(B)** Expression of Zika virus (ZIKV) NS5 in *D. melanogaster* Canton-S male adult flies carrying (W+) or lacking (W–) *Wolbachia* endosymbionts at 4 days following virus infection (ns, non-significant difference; $n = 360$ flies of each sex). All data were normalized to the housekeeping gene *RpL32*, shown relative to flies injected with PBS.

The differences in *D. melanogaster* survival ability between female and male flies carrying or lacking *Wolbachia* following infection with Zika virus adds to our previous observations indicating sex-specific antiviral immune responses. In particular, we have recently shown that Zika virus infected *Dicer-2* female mutant flies have reduced food consumption rates compared to male mutants and Zika virus replicates at higher rates in adult *brat*^{chs} mutants to cause motor dysfunction in a sex-dependent manner (Tafesh-Edwards et al., 2022, 2023). Also, *D. melanogaster* prophenoloxidase 1 (PPO1) is essential for male survival following Zika virus infection, while mutation of PPO2 triggers higher RNAi, Toll, Imd, and Jak/Stat immune signaling in female flies but not in male individuals, thus implying sex-specific immune responses during Zika virus infection (Tafesh-Edwards and Eleftherianos, 2023). Our current findings emphasize the complexity of antiviral defense in *D. melanogaster* through the potential involvement of *Wolbachia* endosymbionts in regulating host survival phenotypes and immune signaling activity differently in the two sexes.

In terms of the involvement of *Wolbachia* in altering the immune signaling in *D. melanogaster* challenged with Zika virus, we find that the presence of the endosymbionts in female or male adult flies fails to modify the expression of *Dicer-2* and *Ago-2* genes upon Zika virus infection. In *D. melanogaster*, RNAi plays an instrumental role in antiviral response (Carthew and Sontheimer, 2009). We paid attention to the expression of *Dicer-2* and *Ago-2* genes, which are components of the exogenous siRNA pathway that leads to the degradation of viral dsRNA molecules (Kim et al., 2006; Peters and Meister, 2007). More precisely, Dicer-2 recognizes exogenous dsRNAs and processes them into small-interfering RNAs (siRNAs), while Ago-2 is the central

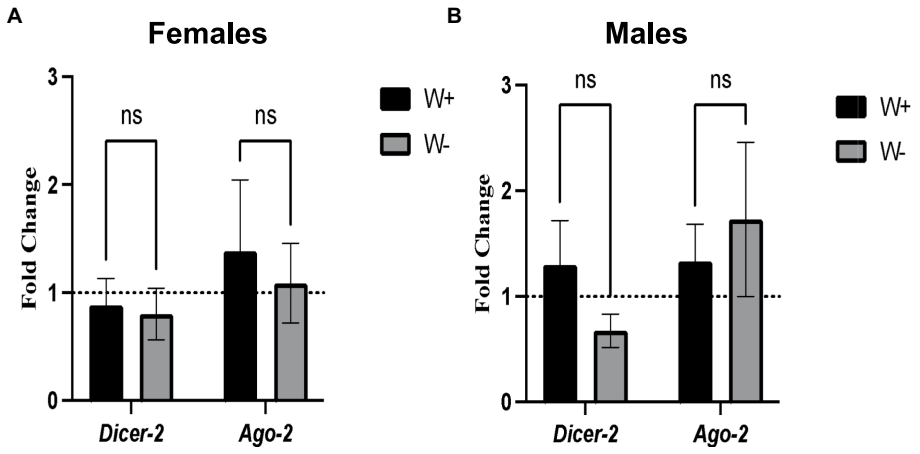

FIGURE 4
Expression of RNA interference pathway genes in Zika virus infected *Drosophila melanogaster* in the presence or absence of *Wolbachia* endosymbionts. **(A)** Expression of *Dicer-2* and *Ago-2* in *D. melanogaster* Canton-S female flies containing (W+) or lacking (W–) *Wolbachia* endosymbionts after Zika virus infection (ns, non-significant difference). **(B)** Expression of *Dicer-2* and *Ago-2* in *D. melanogaster* Canton-S male flies containing (W+) or lacking (W–) *Wolbachia* endosymbionts (ns, non-significant difference). Gene expression levels were normalized to the housekeeping gene *RpL32*. The horizontal dotted line indicates gene expression in uninfected controls treated with PBS ($n = 360$ flies of each sex).

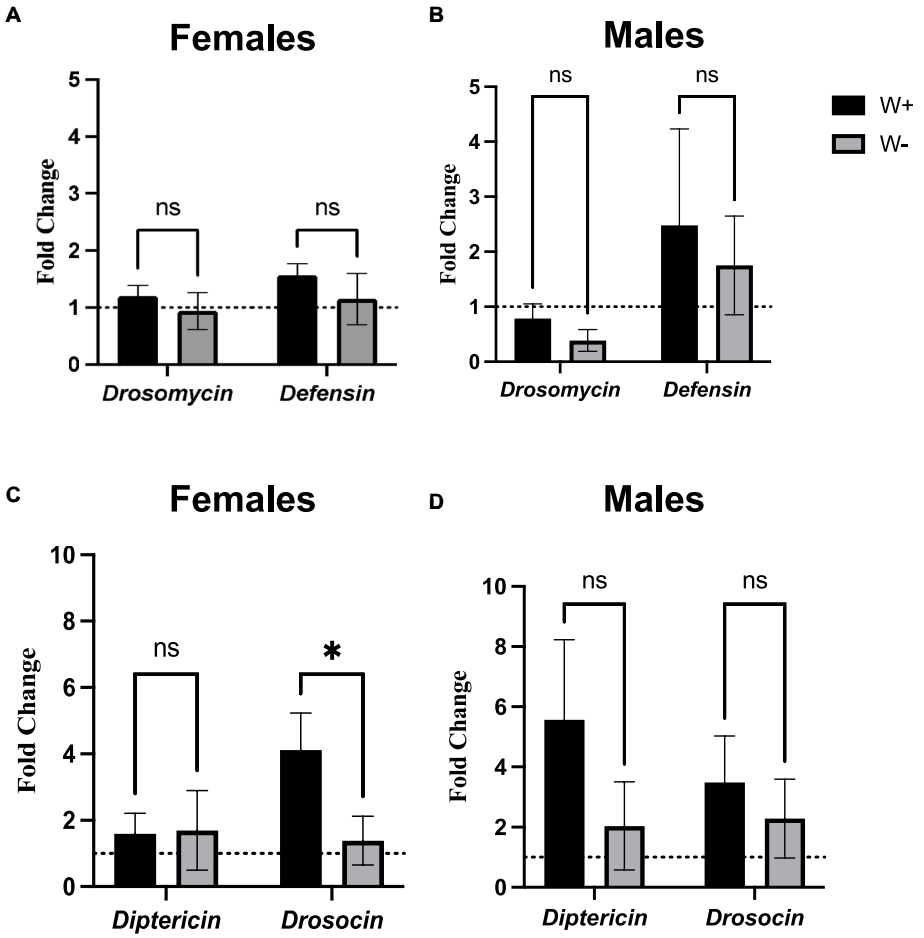

FIGURE 5
Toll and Immune deficiency pathway gene expression in Zika virus infected *Drosophila melanogaster* in the presence or absence of *Wolbachia* endosymbionts. Expression of *Drosomycin* and *Defensin* (Toll pathway) in *D. melanogaster* Canton-S **(A)** female and **(B)** male flies carrying (W+) or lacking (W–) *Wolbachia* endosymbionts following Zika virus infection (ns, non-significant differences). Expression of *Diptericin* and *Drosocin* (Imd pathway) in *D. melanogaster* Canton-S **(C)** female and **(D)** male flies carrying (W+) or lacking (W–) *Wolbachia* endosymbionts following Zika virus infection (*$p < 0.01$). Gene expression levels were normalized to the housekeeping gene *RpL32*. The horizontal dotted line indicates gene expression in uninfected controls treated with PBS ($n = 360$ flies of each sex).

catalytic component of the RNA-induced silencing complex (RISC) and essential for antiviral defense (Galiana-Arnoux et al., 2006; van Rij et al., 2006). Previous research has indicated that *Wolbachia*-mediated protection of *D. melanogaster* adults against *Drosophila* C virus (DCV) is not RNAi dependent because fly mortality was slower in *Wolbachia* containing RNAi loss-of-function mutants compared to the *Wolbachia*-free individuals (Hedges et al., 2012). Our findings further imply the lack of participation of *Wolbachia* in altering RNAi signaling activity in both female and male flies following Zika virus injection.

We also find that with the exception of *Drosocin* transcriptional expression in female flies, *Wolbachia* presence in Zika virus infected *D. melanogaster* adults does not affect the mRNA levels of certain antimicrobial peptide-encoding genes. These results denote that Imd signaling activity can be modified in *Wolbachia*-containing female flies during Zika virus infection at least to some extent. The Imd pathway has been previously found to participate in the immune response of *D. melanogaster* against Cricket Paralysis virus, which is a natural viral pathogen of the fruit fly (Costa et al., 2009). In the context of Zika virus infection, the Imd pathway target gene *Diptericin A* has been shown to be upregulated in whole flies and heads, supporting the involvement of the Imd arm of the Rel/NF-κB pathway (Liu et al., 2018). Also, we have recently showed that Zika virus infection fails to activate Imd-mediated immunity in male *D. melanogaster* adult flies (Tafesh-Edwards and Eleftherianos, 2023). Interestingly, the *Drosocin* gene encodes two separate antimicrobial peptides with different specificity against distinct pathogens (Hanson et al., 2022). In addition, *Drosocin* was one of the antimicrobial peptide genes which was substantially upregulated in response to Sigma virus infection in *D. melanogaster* adult flies (Tsai et al., 2008). Whether the upregulation of *Drosocin* in female flies is directly attributed to *Wolbachia* or is an indirect effect as well as the role of this antimicrobial peptide in *Wolbachia* mediated protection to Zika virus infection will be the subject of future investigations.

Here we find that expression of the Jnk regulated gene *Puckered* increases during Zika virus infection in *Wolbachia* containing female flies. Previously, it has been shown that expression of the Puckered phosphatase, an inhibitor of Jnk activity, suppresses the expression of antimicrobial peptide genes in *D. melanogaster* (Delaney et al., 2006). Therefore, we speculate that the presence of *Wolbachia* specifically in female flies infected with Zika virus could possibly lead to the differential

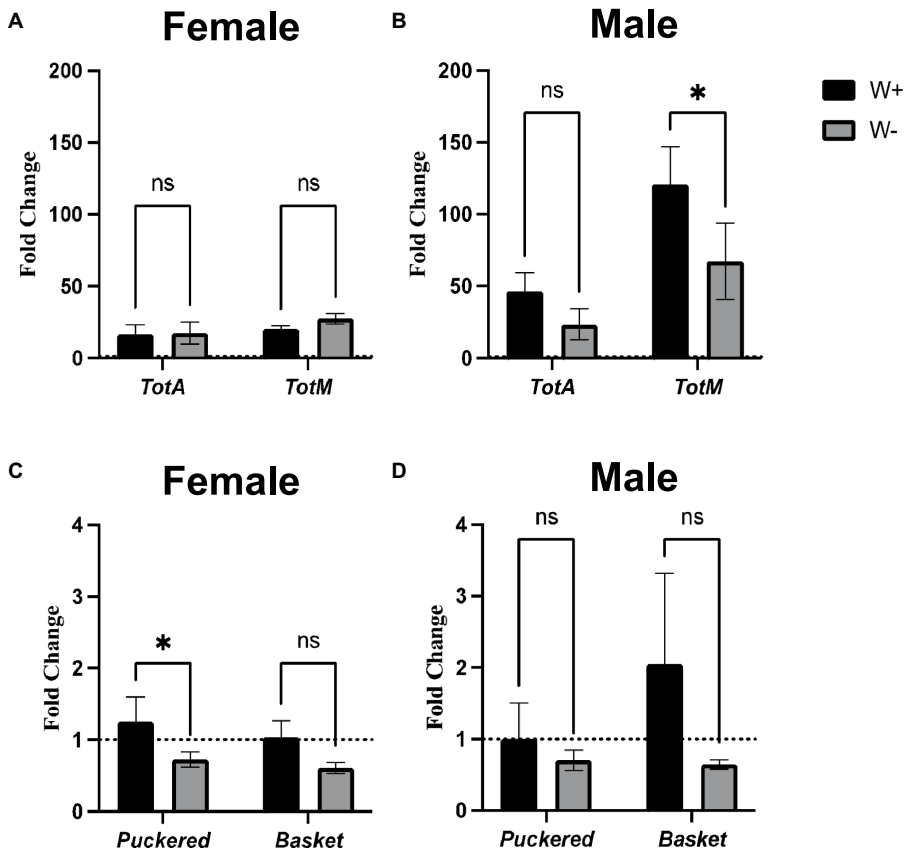

FIGURE 6
Jak/Stat and Jnk pathway activity in Zika virus infected *Drosophila melanogaster* in the presence or absence of *Wolbachia* endosymbionts. Expression of *TotaA* and *TotM* (Jak/Stat pathway) in *D. melanogaster* Canton-S **(A)** female and **(B)** male adult flies carrying (W+) or lacking (W–) *Wolbachia* endosymbionts following Zika virus infection (ns, non-significant differences). Expression of *Puckered* and *Basket* (Jnk pathway) in *D. melanogaster* Canton-S **(C)** female and **(D)** male flies carrying (W+) or lacking (W–) *Wolbachia* endosymbionts following Zika virus infection (*$p < 0.01$). Gene expression levels were normalized to the housekeeping gene *RpL32*. The horizontal dotted line indicates gene expression in uninfected controls treated with PBS ($n = 360$ flies of each sex).

activation of Jnk signaling through the expression of *Puckered*, which in turn could potentially affect the expression of certain antimicrobial peptides, like Drosocin. The interaction between Jnk and Imd signaling by *Wolbachia* endosymbionts could be regulated through the TGF-beta activated kinase 1 (TAK1), which has been previously shown to act as an essential factor in Jnk signaling for the expression of antimicrobial peptides (Silverman et al., 2003; Delaney et al., 2006). Finally, we find that *Wolbachia*-containing male flies challenged with Zika virus have increased expression of the Jak/Stat regulated stress-induced *TotM* gene (Ekengren and Hultmark, 2001; Brun et al., 2006), and that male flies containing *Wolbachia* die at a slower rate by Zika virus compared to those lacking the endosymbiont, although there is no statistically significant difference. It is possible that *Wolbachia* presence in *D. melanogaster* males provides a slight protective effect against this virus and this effect is controlled through the activation of the Jak/Stat pathway. These various possibilities remain to be confirmed in future studies.

In conclusion, our findings point to a sex-specific effect of *Wolbachia* on the *D. melanogaster* immune response against Zika virus infection. The phenotypic effect of the endosymbionts is primarily demonstrated by the expansion in the survival of female adult flies after intrathoracic injection of Zika virus. The extended survival in *D. melanogaster* females is accompanied by reduced viral titers and changes in innate immune signaling. The latter is mainly expressed through the increased expression of the antimicrobial peptide gene *Drosocin* which is regulated by the Imd pathway, and the increased expression of the gene *Puckered* which is regulated by the Jnk pathway. The exact mechanism of decreased Zika virus replication in female flies carrying *Wolbachia* is currently unknown and it will be explored more in future studies. Further efforts will focus on testing whether the observed effects are specific to the *D. melanogaster* line Canton-S and the *Wolbachia pipientis* strain *w*Mel, and also to other *Drosophila* species. Considering that recent research has indicated that antiviral immunity in the fly is age dependent (Sheffield et al., 2021), it is intriguing to investigate the influence of age on the *Wolbachia* protective effect against Zika virus infection in female flies. Because hemocytes, autophagy, and the prophenoloxidase system contribute to *D. melanogaster* antiviral immunity (Lamiable et al., 2016; Tafesh-Edwards and Eleftherianos, 2023), potential input of *Wolbachia* to these aspects of the immune response against Zika virus will also be examined. Analyzing the dose-dependent and tissue-specific interaction of the innate immune response to oral infection with Zika virus in adult flies or larvae containing various concentration of the endosymbiotic bacteria will provide more detailed information about the prevalence of the current observations. Such information will

contribute to a better understanding of the molecular and functional bases of endosymbiont-mediated resistance to Zika virus in mosquito vectors, which could reduce the transmission capacity of this viral pathogen and possibly other arboviruses.

Data availability statement

The datasets presented in this study can be found in the NCBI Gene database. The accession numbers can be found in Table 1. Further inquiries can be directed to the corresponding author.

Ethics statement

The manuscript presents research on animals that do not require ethical approval for their study.

Author contributions

GT-E: Writing – review & editing, Visualization, Validation, Supervision, Methodology, Investigation, Formal analysis, Data curation, Conceptualization. MK: Writing – original draft, Visualization, Validation, Methodology, Investigation, Formal analysis. KM: Writing – review & editing, Methodology, Investigation. DB: Writing – review & editing, Validation, Resources, Methodology. SC: Writing – review & editing, Validation, Supervision, Resources, Conceptualization. IE: Writing – review & editing, Writing – original draft, Supervision, Project administration, Funding acquisition, Conceptualization.

Funding

The author(s) declare that financial support was received for the research, authorship, and/or publication of this article. This work was supported by Facilitating Funds from the Columbian College of Arts and Sciences at George Washington University (GWU) to IE; and Harlan funds from the GWU Department of Biological Sciences to GT-E and MK.

Acknowledgments

We thank members of the I.E. lab for maintaining and amplifying the laboratory fly lines and members of the Department of Biological Sciences at George Washington University for providing feedback to the project.

Conflict of interest

The authors declare that the research was conducted in the absence of any commercial or financial relationships that could be construed as a potential conflict of interest.

Publisher's note

References

Araújo, N. J. S., Macêdo, M. J. F., de Morais, L. P., da Cunha, F. A. B., de Matos, Y. M. L. S., de Almeida, R. S., et al. (2022). Control of arboviruses vectors using biological control by *Wolbachia pipientis*: a short review. *Arch. Microbiol.* 204:376. doi: 10.1007/s00203-022-02983-x

Bi, J., and Wang, Y. F. (2020). The effect of the endosymbiont *Wolbachia* on the behavior of insect hosts. *Insect Sci.* 27, 846–858. doi: 10.1111/1744-7917.12731

Brownlie, C. J., and Johnson, K. N. (2009). Symbiont-mediated protection in insect hosts. *Trends Microbiol.* 17, 348–354. doi: 10.1016/j.tim.2009.05.005

Brun, S., Vidal, S., Spellman, P., Takahashi, K., Tricoire, H., and Lemaitre, B. (2006). The MAPKKK Mekk1 regulates the expression of *Turandot* stress genes in response to septic injury in *Drosophila*. *Genes Cells* 11, 397–407. doi: 10.1111/j.1365-2443.2006.00953.x

Caragata, E. P., Rancès, E., Hedges, L. M., Gofton, A. W., Johnson, K. N., O'Neill, S. L., et al. (2013). Dietary cholesterol modulates pathogen blocking by *Wolbachia*. *PLoS Pathog.* 9:e1003459. doi: 10.1371/journal.ppat.1003459

Carthew, R. W., and Sontheimer, E. J. (2009). Origins and mechanisms of miRNAs and siRNAs. *Cell* 136, 642–655. doi: 10.1016/j.cell.2009.01.035

Chen, W., White, M. A., and Cobb, M. H. (2002). Stimulus-specific requirements for MAP3 kinases in activating the JNK pathway. *J. Biol. Chem.* 277, 49105–49110. doi: 10.1074/jbc.M204934200

Chow, J., and Kagan, J. C. (2018). The Fly way of antiviral resistance and disease tolerance. *Adv. Immunol.* 140, 59–93. doi: 10.1016/bs.ai.2018.08.002

Chowdhury, A., Modahl, C. M., Tan, S. T., Wei, W., Xiang, B., Missé, D., et al. (2020). JNK pathway restricts DENV2, ZIKV and CHIKV infection by activating complement and apoptosis in mosquito salivary glands. *PLoS Pathog.* 16:e1008754. doi: 10.1371/journal.ppat.1008754

Chrostek, E., Marialva, M. S., Yamada, R., O'Neill, S. L., and Teixeira, L. (2014). High anti-viral protection without immune upregulation after interspecies *Wolbachia* transfer. *PLoS One* 9:e99025. doi: 10.1371/journal.pone.0099025

Contamine, D., Petitjean, A. M., and Ashburner, M. (1989). Genetic resistance to viral infection: the molecular cloning of a *Drosophila* gene that restricts infection by the rhabdovirus sigma. *Genetics* 123, 525–533. doi: 10.1093/genetics/123.3.525

Costa, A., Jan, E., Sarnow, P., and Schneider, D. (2009). The Imd pathway is involved in antiviral immune responses in *Drosophila*. *PLoS One* 4:e7436. doi: 10.1371/journal.pone.0007436

Dale, C., and Moran, N. A. (2006). Molecular interactions between bacterial symbionts and their hosts. *Cell* 126, 453–465. doi: 10.1016/j.cell.2006.07.014

Delaney, J. R., Stöven, S., Uvell, H., Anderson, K. V., Engström, Y., and Mlodzik, M. (2006). Cooperative control of *Drosophila* immune responses by the JNK and NF-kappaB signaling pathways. *EMBO J.* 25, 3068–3077. doi: 10.1038/sj.emboj.7601182

Dostert, C., Jouanguy, E., Irving, P., Troxler, L., Galiana-Arnoux, D., Hetru, C., et al. (2005). The Jak-STAT signaling pathway is required but not sufficient for the antiviral response of drosophila. *Nat. Immunol.* 6, 946–953. doi: 10.1038/ni1237

Edenborough, K. M., Flores, H. A., Simmons, C. P., and Fraser, J. E. (2021). Using *Wolbachia* to eliminate dengue: will the virus fight Back? *J. Virol.* 95:e0220320. doi: 10.1128/JVI.02203-20

Ekengren, S., and Hultmark, D. (2001). A family of Turandot-related genes in the humoral stress response of *Drosophila*. *Biochem. Biophys. Res. Commun.* 284, 998–1003. doi: 10.1006/bbrc.2001.5067

Eleftherianos, I., Atri, J., Accetta, J., and Castillo, J. C. (2013). Endosymbiotic bacteria in insects: guardians of the immune system? *Front. Physiol.* 4:46. doi: 10.3389/fphys.2013.00046

Elshahawi, H., Syed Hassan, S., and Balasubramaniam, V. (2019). Importance of Zika virus NS5 protein for viral replication. *Pathogens* 8:169. doi: 10.3390/pathogens8040169

Ferreira, Á. G., Naylor, H., Esteves, S. S., Pais, I. S., Martins, N. E., and Teixeira, L. (2014). The toll-dorsal pathway is required for resistance to viral oral infection in *Drosophila*. *PLoS Pathog.* 10:e1004507. doi: 10.1371/journal.ppat.1004507

Galiana-Arnoux, D., Dostert, C., Schneemann, A., Hoffmann, J. A., and Imler, J. L. (2006). Essential function *in vivo* for Dicer-2 in host defense against RNA viruses in drosophila. *Nat. Immunol.* 7, 590–597. doi: 10.1038/ni1335

Gubler, D. J., Vasilakis, N., and Musso, D. (2017). History and emergence of Zika virus. *J. Infect. Dis.* 216, S860–S867. doi: 10.1093/infdis/jix451

Hanson, M. A., Kondo, S., and Lemaitre, B. (2022). *Drosophila* immunity: the *Drosocin* gene encodes two host defense peptides with pathogen-specific roles. *Proc. Biol. Sci.* 289:20220773. doi: 10.1098/rspb.2022.0773

Harsh, S., Fu, Y., Kenney, E., Han, Z., and Eleftherianos, I. (2020). Zika virus non-structural protein NS4A restricts eye growth in *Drosophila* through regulation of JAK/STAT signaling. *Dis. Model. Mech.* 13:dmm040816. doi: 10.1242/dmm.040816

Harsh, S., Ozakman, Y., Kitchen, S. M., Paquin-Proulx, D., Nixon, D. F., and Eleftherianos, I. (2018). Dicer-2 regulates resistance and maintains homeostasis against Zika virus infection in *Drosophila*. *J. Immunol.* 201, 3058–3072. doi: 10.4049/jimmunol.1800597

Hedges, L. M., Brownlie, J. C., O'Neill, S. L., and Johnson, K. N. (2008). *Wolbachia* and virus protection in insects. *Science* 322:702. doi: 10.1126/science.1162418

Hedges, L. M., Yamada, R., O'Neill, S. L., and Johnson, K. N. (2012). The small interfering RNA pathway is not essential for *Wolbachia*-mediated antiviral protection in *Drosophila melanogaster*. *Appl. Environ. Microbiol.* 78, 6773–6776. doi: 10.1128/AEM.01650-12

Huang, Z., Wang, W., Xu, P., Gong, S., Hu, Y., Liu, Y., et al. (2023). *Drosophila ectoderm-expressed 4* modulates JAK/STAT pathway and protects flies against *Drosophila* C virus infection. *Front. Immunol.* 14:1135625. doi: 10.3389/fimmu.2023.1135625

Iturbe-Ormaetxe, I., and O'Neill, S. L. (2007). *Wolbachia*-host interactions: connecting phenotype to genotype. *Curr. Opin. Microbiol.* 10, 221–224. doi: 10.1016/j.mib.2007.05.002

Kaur, R., Shropshire, J. D., Cross, K. L., Leigh, B., Mansueto, A. J., Stewart, V., et al. (2021). Living in the endosymbiotic world of *Wolbachia*: a centennial review. *Cell Host Microbe* 29, 879–893. doi: 10.1016/j.chom.2021.03.006

Kim, K., Lee, Y. S., Harris, D., Nakahara, K., and Carthew, R. W. (2006). The RNAi pathway iniated by Dicer-2 in *Drosophila*. *Cold Spring Harb. Symp. Quant. Biol.* 71, 39–44. doi: 10.1101/sqb.2006.71.008

Lamiable, O., Arnold, J., de Faria, I. J. D. S., Olmo, R. P., Bergami, F., Meignin, C., et al. (2016). Analysis of the contribution of Hemocytes and autophagy to *Drosophila* antiviral immunity. *J. Virol.* 90, 5415–5426. doi: 10.1128/JVI.00238-16

Landmann, F. (2019). The *Wolbachia* endosymbionts. *Microbiol. Spectr.* 7. doi: 10.1128/microbiolspec.BAI-0018-2019

Liu, Y., Gordesky-Gold, B., Leney-Greene, M., Weinbren, N. L., Tudor, M., and Cherry, S. (2018). Inflammation-induced, STING-dependent autophagy restricts Zika virus infection in the *Drosophila* brain. *Cell Host Microbe* 24, 57–68.e3. doi: 10.1016/j.chom.2018.05.022

Livak, K. J., and Schmittgen, T. D. (2001). Analysis of relative gene expression data using realtime quantitative PCR, and the 2–11CT method. *Methods* 25, 402–408. doi: 10.1006/meth.2001.1262

Longdon, B., Obbard, D. J., and Jiggins, F. M. (2010). Sigma viruses from three species of *Drosophila* form a major new clade in the rhabdovirus phylogeny. *Proc. Biol. Sci.* 277, 35–44. doi: 10.1098/rspb.2009.1472

Lye, S. H., and Chtarbanova, S. (2018). *Drosophila* as a model to study brain innate immunity in health and disease. *Int. J. Mol. Sci.* 19:3922. doi: 10.3390/ijms19123922

Maistrenko, O. M., Serga, S. V., Vaiserman, A. M., and Kozeretska, I. A. (2016). Longevity-modulating effects of symbiosis: insights from *Drosophila-Wolbachia* interaction. *Biogerontology* 17, 785–803. doi: 10.1007/s10522-016-9653-9

Martinez, J., Cogni, R., Cao, C., Smith, S., Illingworth, C. J., and Jiggins, F. M. (2016). Addicted? Reduced host resistance in populations with defensive symbionts. *Proc. Biol. Sci.* 283:20160778. doi: 10.1098/rspb.2016.0778

Martinez, J., Longdon, B., Bauer, S., Chan, Y. S., Miller, W. J., Bourtzis, K., et al. (2014). Symbionts commonly provide broad spectrum resistance to viruses in insects: a comparative analysis of *Wolbachia* strains. *PLoS Pathog.* 10:e1004369. doi: 10.1371/journal.ppat.1004369

Martinez, J., Ok, S., Smith, S., Snoeck, K., Day, J. P., and Jiggins, F. M. (2015). Should symbionts be Nice or selfish? Antiviral effects of Wolbachia are costly but reproductive parasitism is not. *PLoS Pathog.* 11:e1005021. doi: 10.1371/journal.ppat.1005021

Martinez, J., Tolosana, I., Ok, S., Smith, S., Snoeck, K., Day, J. P., et al. (2017). Symbiont strain is the main determinant of variation in *Wolbachia*-mediated protection against viruses across *Drosophila* species. *Mol. Ecol.* 26, 4072–4084. doi: 10.1111/mec.14164

Min, K. T., and Benzer, S. (1997). *Wolbachia*, normally a symbiont of *Drosophila*, can be virulent, causing degeneration and early death. *Proc. Natl. Acad. Sci. USA* 94, 10792–10796. doi: 10.1073/pnas.94.20.10792

Myllymäki, H., and Rämet, M. (2014). JAK/STAT pathway in *Drosophila* immunity. *Scand. J. Immunol.* 79, 377–385. doi: 10.1111/sji.12170

Newton, I. L. G., and Rice, D. W. (2020). The Jekyll and Hyde symbiont: could *Wolbachia* be a nutritional mutualist? *J. Bacteriol.* 202, e00589–e00519. doi: 10.1128/JB.00589-19

Peters, L., and Meister, G. (2007). Argonaute proteins: mediators of RNA silencing. *Mol. Cell* 26, 611–623. doi: 10.1016/j.molcel.2007.05.001

Pietri, J. E., DeBruhl, H., and Sullivan, W. (2016). The rich somatic life of *Wolbachia*. *MicrobiologyOpen* 5, 923–936. doi: 10.1002/mbo3.390

Pimentel, A. C., Cesar, C. S., Martins, M., and Cogni, R. (2021). The antiviral effects of the symbiont Bacteria *Wolbachia* in insects. *Front. Immunol.* 11:626329. doi: 10.3389/fimmu.2020.626329

Plourde, A. R., and Bloch, E. M. (2016). A literature review of Zika virus. *Emerg. Infect. Dis.* 22, 1185–1192. doi: 10.3201/eid2207.151990

Porter, J., and Sullivan, W. (2023). The cellular lives of *Wolbachia*. *Nat. Rev. Microbiol.* 21, 750–766. doi: 10.1038/s41579-023-00918-x

Rancès, E., Johnson, T. K., Popovici, J., Iturbe-Ormaetxe, I., Zakir, T., Warr, C. G., et al. (2013). The toll and Imd pathways are not required for *Wolbachia*-mediated dengue virus interference. *J. Virol.* 87, 11945–11949. doi: 10.1128/JVI.01522-13

Rancès, E., Ye, Y. H., Woolfit, M., McGraw, E. A., and O'Neill, S. L. (2012). The relative importance of innate immune priming in *Wolbachia*-mediated dengue interference. *PLoS Pathog.* 8:e1002548. doi: 10.1371/journal.ppat.1002548

Schmittgen, T. D., and Livak, K. J. (2008). Analyzing real-time PCR data by the comparative CT method. *Nat. Protoc.* 3, 1101–1108. doi: 10.1038/nprot.2008.73

Sheffield, L., Sciambra, N., Evans, A., Hagedorn, E., Goltz, C., Delferd, M., et al. (2021). Age-dependent impairment of disease tolerance is associated with a robust transcriptional response following RNA virus infection in *Drosophila* 11:jkab116. doi: 10.1093/g3journal/jkab116

Silverman, N., Zhou, R., Erlich, R. L., Hunter, M., Bernstein, E., Schneider, D., et al. (2003). Immune activation of NF-kappaB and JNK requires *Drosophila* TAK1. *J. Biol. Chem.* 278, 48928–48934. doi: 10.1074/jbc.M304802200

Simhadri, R. K., Fast, E. M., Guo, R., Schultz, M. J., Vaisman, N., Ortiz, L., et al. (2017). The gut commensal microbiome of *Drosophila melanogaster* is modified by the endosymbiont *Wolbachia* 2, e00287–e00217. doi: 10.1128/mSphere.00287-17

Sluss, H. K., Han, Z., Barrett, T., Goberdhan, D. C., Wilson, C., Davis, R. J., et al. (1996). A JNK signal transduction pathway that mediates morphogenesis and an immune response in *Drosophila*. *Genes Dev.* 10, 2745–2758. doi: 10.1101/gad.10.21.2745

Song, W., Zhang, H., Zhang, Y., Chen, Y., Lin, Y., Han, Y., et al. (2021). Identification and characterization of Zika virus NS5 methyltransferase inhibitors. *Front. Cell. Infect. Microbiol.* 11:665379. doi: 10.3389/fcimb.2021.665379

Tafesh-Edwards, G., and Eleftherianos, I. (2020a). *Drosophila* immunity against natural and nonnatural viral pathogens. *Virology* 540, 165–171. doi: 10.1016/j.virol.2019.12.001

Tafesh-Edwards, G., and Eleftherianos, I. (2020b). JNK signaling in *Drosophila* immunity and homeostasis. *Immunol. Lett.* 226, 7–11. doi: 10.1016/j.imlet.2020.06.017

Tafesh-Edwards, G., and Eleftherianos, I. (2023). The *Drosophila melanogaster* prophenoloxidase system participates in immunity against Zika virus infection. *Eur. J. Immunol.* 53:e2350632. doi: 10.1002/eji.202350632

Tafesh-Edwards, G., Kalukin, A., Bunnell, D., Starbanova, S., and Eleftherianos, I. (2023). Temperature and sex shape Zika virus pathogenicity in the adult *brat* ^{cheesehead} brain: a *Drosophila* model for virus-associated neurological diseases. *iScience* 26:106424. doi: 10.1016/j.isci.2023.106424

Tafesh-Edwards, G., Kalukin, A., and Eleftherianos, I. (2022). Zika virus induces sex-dependent metabolic changes in *Drosophila melanogaster* to promote viral replication. *Front. Immunol.* 13:903860. doi: 10.3389/fimmu.2022.903860

Teixeira, L., Ferreira, A., and Ashburner, M. (2008). The bacterial symbiont *Wolbachia* induces resistance to RNA viral infection in *Drosophila melanogaster*. *PLoS Biol.* 6:e2. doi: 10.1371/journal.pbio.1000002

Tsai, C. W., McGraw, E. A., Ammar, E.-D., Dietzgen, R. G., and Hogenhout, S. A. (2008). *Drosophila melanogaster* mounts a unique immune response to the Rhabdovirus sigma virus. *Appl. Environ. Microbiol.* 74, 3251–3256. doi: 10.1128/AEM.02248-07

Vale, P. F., and Jardine, M. D. (2015). Sex-specific behavioural symptoms of viral gut infection and *Wolbachia* in *Drosophila melanogaster*. *J. Insect Physiol.* 82, 28–32. doi: 10.1016/j.jinsphys.2015.08.005

van Rij, R. P., Saleh, M. C., Berry, B., Foo, C., Houk, A., Antoniewski, C., et al. (2006). The RNA silencing endonuclease Argonaute 2 mediates specific antiviral immunity in *Drosophila melanogaster*. *Genes Dev.* 20, 2985–2995. doi: 10.1101/gad.1482006

Wong, Z. S., Brownlie, J. C., and Johnson, K. N. (2016). Impact of ERK activation on fly survival and *Wolbachia*-mediated protection during virus infection. *J. Gen. Virol.* 97, 1446–1452. doi: 10.1099/jgv.0.000456

Ye, Y. H., Seleznev, A., Flores, H. A., Woolfit, M., and McGraw, E. A. (2017). Gut microbiota in *Drosophila melanogaster* interacts with *Wolbachia* but does not contribute to *Wolbachia*-mediated antiviral protection. *J. Invertebr. Pathol.* 143, 18–25. doi: 10.1016/j.jip.2016.11.011

Yen, P. S., and Failloux, A. B. (2020). A review: *Wolbachia*-based population replacement for mosquito control shares common points with genetically modified control approaches. *Pathogens* 9:404. doi: 10.3390/pathogens9050404

frontiers | Frontiers in Microbiology

TYPE Original Research
PUBLISHED 18 July 2024
DOI 10.3389/fmicb.2024.1405287

OPEN ACCESS

EDITED BY
Yuval Gottlieb,
Hebrew University of Jerusalem, Israel

REVIEWED BY
Vipin Rana,
University of Maryland, United States
Ranju Manoj,
Cornell University, United States
Daisuke Kageyama,
National Agriculture and Food Research Organization (NARO), Japan

*CORRESPONDENCE
Kenneth Pfarr
✉ Kenneth.Pfarr@ukbonn.de
Lara Vanessa Behrmann
✉ Lara_Vanessa.Behrmann@ukbonn.de

†These authors have contributed equally to this work and share first authorship

RECEIVED 22 March 2024
ACCEPTED 02 July 2024
PUBLISHED 18 July 2024

CITATION
Behrmann LV, Meier K, Vollmer J, Chiedu CC, Schiefer A, Hoerauf A and Pfarr K (2024) *In vitro* extracellular replication of *Wolbachia* endobacteria. *Front. Microbiol.* 15:1405287. doi: 10.3389/fmicb.2024.1405287

In vitro extracellular replication of *Wolbachia* endobacteria

Lara Vanessa Behrmann[1*†], Kirstin Meier[1†], Jennifer Vollmer[1†], Chukwuebuka Chibuzo Chiedu[1], Andrea Schiefer[1], Achim Hoerauf[1,2] and Kenneth Pfarr[1,2*]

[1]Institute for Medical Microbiology, Immunology and Parasitology, University Hospital Bonn, Bonn, Germany, [2]German Center for Infection Research (DZIF), Partner Site Bonn-Cologne, Bonn, Germany

Obligate intracellular endobacteria of the genus *Wolbachia* are widespread in arthropods and several filarial nematodes. Control programs for vector-borne diseases (dengue, Zika, malaria) and anti-filarial therapy with antibiotics are based on this important endosymbiont. Investigating *Wolbachia*, however, is impeded by the need for host cells. In this study, the requirements for *Wolbachia w*AlbB growth in a host cell-free *in vitro* culture system were characterized via qPCRs. A cell lysate fraction from *Aedes albopictus* C6/36 insect cells containing cell membranes and medium with fetal bovine serum were identified as requisite for cell-free replication of *Wolbachia*. Supplementation with the membrane fraction of insect cell lysate increased extracellular *Wolbachia* replication by 4.2-fold. Replication rates in the insect cell-free culture were lower compared to *Wolbachia* grown inside insect cells. However, the endobacteria were able to replicate for up to 12 days and to infect uninfected C6/36 cells. Cell-free *Wolbachia* treated with the lipid II biosynthesis inhibitor fosfomycin had an enlarged phenotype, seen previously for intracellular *Wolbachia* in C6/36 cells, indicating that the bacteria were unable to divide. In conclusion, we have developed a cell-free culture system in which *Wolbachia* replicate for up to 12 days, providing an *in vitro* tool to elucidate the biology of these endobacteria, e.g., cell division by using compounds that may not enter the C6/36 cells. A better understanding of *Wolbachia* biology, and in particular host-symbiont interactions, is key to the use of *Wolbachia* in vector control programs and to future drug development against filarial diseases.

KEYWORDS

***Wolbachia*, cell-free, endosymbionts, intracellular bacteria, *in vitro* culture, filariasis, vector control**

1 Introduction

Wolbachia are intracellular Gram-negative alpha-proteobacteria found in arthropods and in some nematodes, including filarial nematode species pathogenic to humans (Taylor and Hoerauf, 2001; Fenn et al., 2006; Zug and Hammerstein, 2012). They reside in host-derived vesicles within cells of somatic tissues as well as the host germline through which they are transmitted vertically from the mother to the offspring (Casiraghi et al., 2007; Serbus and Sullivan, 2007). A common feature of endosymbiotic bacteria is the reduction of genome size due to the evolutionary adaptation to their host (Stepkowski and Legocki, 2001). This is also the case for *Wolbachia*, which possess a limited metabolic capacity. They lack almost all biosynthetic pathways to produce amino acids *de novo* and have retained almost only incomplete pathways for the synthesis of vitamins and cofactors, all of which are most probably

provided by their host (Wu et al., 2004; Foster et al., 2005; Slatko et al., 2010).

Wolbachia endosymbionts of arthropods are largely facultative and often exhibit a parasitic association with their hosts (Werren et al., 2008). The stability of *Wolbachia* transmission is ensured by reproductive manipulations such as male-killing, feminization, parthenogenesis, and cytoplasmic incompatibility between infected and uninfected organisms (Fenn and Blaxter, 2006). Of note, benefits of an infection with *Wolbachia*, e.g., in terms of protection against different pathogens, have been reported (Hedges et al., 2008; Teixeira et al., 2008; Kambris et al., 2009; Moreira et al., 2009). Here, especially anti-viral effects have gained great interest as *Wolbachia* could be used to control vector-borne human diseases such as dengue fever (Blagrove et al., 2012; Velez et al., 2023).

Wolbachia of filarial nematodes are, in contrast to *Wolbachia* of arthropods, intrinsically tied to their host. Here, they are mutualistic endosymbionts that depend on compounds produced by the host, but in turn are believed to provide metabolites that cannot be synthesized by the nematodes *de novo*, e.g., heme, purines, pyrimidines, FAD, and riboflavin, essential for worm survival (Wu et al., 2004; Foster et al., 2005; Slatko et al., 2010). It was demonstrated that *Wolbachia* depletion by the antibiotic doxycycline leads to block in development, sterility, and death of adult filarial worms (Hoerauf et al., 2001; Taylor et al., 2012). Thus, filarial *Wolbachia* are an effective target for anti-filarial therapy.

The cultivation of *Wolbachia* as obligate intracellular bacteria is challenging. To date, filarial *Wolbachia* cannot be cultured *in vitro* (Slatko et al., 2014) and only a few culture systems exist, in which insect cell lines are stably infected with *Wolbachia* strains from arthropods (Fenollar et al., 2003a; McMeniman et al., 2008; Conceição et al., 2021). In these culture systems, *Wolbachia* are protected from the environment by at least three lipid membrane barriers: the insect cell membrane, vesicle membrane, and the *Wolbachia* cell membranes. Therefore, molecular biology techniques, e.g., genetic transformation, cannot be applied. Additionally, many molecules cannot pass the insect cell membrane, which hampers the elucidation of *Wolbachia* biology and its symbiosis with the host cell.

However, since *Wolbachia* are transmitted from somatic tissue to the germline (Frydman et al., 2006; Landmann et al., 2012), and also horizontally between host species (Dyson et al., 2002; White et al., 2017), even with plants as temporary hosts (Li et al., 2017), they require an extracellular stage (Nevalainen et al., 2023). This stage has been observed in the hemolymph of insects, foregut of ants, and pseudocoelomic cavity of filarial nematodes (Fischer et al., 2011; Andersen et al., 2012; Frost et al., 2014). Rasgon et al. (2006) showed that *Wolbachia* purified from insect cells could be maintained in cell-free culture medium for at least 1 week without loss of viability or infectivity. More recently, the metabolic activity of extracellular *Wolbachia* was measured via phenotypic microarrays over 4 days (Krafsur et al., 2020). However, *Wolbachia* in these cultures did not replicate outside the insect cell (Rasgon et al., 2006; Krafsur et al., 2020).

For a few intracellular bacteria, e.g., *Coxiella burnetii*, *Chlamydia trachomatis*, *Ehrlichia chaffeensis,* and *Anaplasma phagocytophilum*, cell-free culture systems were developed that support metabolic activity (Omsland et al., 2008, 2012; Eedunuri et al., 2018; Zhang et al., 2021). After further modifications, cell-free growth of *Coxiella burnetii* was made possible, accelerating genetic transformation (Omsland et al., 2009, 2011). An adapted medium allows for the non-antibiotic-based selection of genetic transformants (Sandoz et al., 2016).

In this study, we provide first evidence of *Wolbachia* replication in a host cell-free *in vitro* culture. Growth of *Wolbachia w*AlbB was observed when the medium was supplemented with total lysate from *Aedes albopictus* C6/36 insect cells. Furthermore, we could show that the necessary components for the replication of the endobacteria in cell-free medium are contained in the membrane fraction of the insect cell lysate and in fetal bovine serum (FBS).

2 Materials and methods

2.1 C6/36 insect cell culture

The *Aedes albopictus* C6/36 insect cell line, uninfected or infected with the *Wolbachia pipientis* supergroup B strain of *Aedes albopictus* (*w*AlbB), were cultured as previously described (Turner et al., 2006; Henrichfreise et al., 2009). Infected and uninfected C6/36 cells were grown at 26°C in 75 cm^2 culture flasks (Greiner, Frickenhausen, Germany) with 15 mL standard medium consisting of Leibovitz's L15 medium (Thermo Fisher Scientific, Waltham, Massachusetts, United States) supplemented with 5% fetal bovine serum (FBS; PAA Laboratories, Cölbe, Germany or PAN-Biotech, Aidenbach, Germany), 1% MEM non-essential amino acids (PAA Laboratories or Thermo Fisher Scientific), 2% tryptose phosphate broth (Sigma-Aldrich, Steinheim, Germany) and 1% penicillin/streptomycin (PAA Laboratories or Thermo Fisher Scientific). The standard 5% FBS in the culture media was changed to 20% to increase the percentage of infected cells (Clare et al., 2015) for later experiments as indicated.

2.2 Isolation of *Wolbachia* from insect cells

Wolbachia were purified from infected C6/36 cells either as described by Rasgon et al. (2006) or by an abbreviated protocol. The C6/36 cells were grown to ~90% confluence. Cells were harvested with a cell lifter (Corning, New York, United States) in 10 mL standard medium and lysed by vortexing with 100 sterile 3 mm borosilicate glass beads (Sigma-Aldrich) for 5 min. Cell debris was removed by centrifugation at 2,500 g for 10 min at 4°C (Heraeus Multifuge 4 KR, Heraeus, Hanau, Germany) and the supernatant was filtered through a 5 µm syringe filter (Sartorius, Göttingen, Germany). Our abbreviated protocol ended here, so that the insect cell lysate remained in the suspension. For purification following the procedure of Rasgon et al. (2006), *Wolbachia* were pelleted from the filtered supernatant by centrifugation at 18,400 g for 5 min at 4°C (Eppendorf Centrifuge 5,424 R, Eppendorf, Hamburg, Germany) on a 250 mM sucrose cushion (Sigma-Aldrich) and suspended in 10 mL standard medium. In contrast to Rasgon et al. (2006), the subsequent filtration was not performed with a 2.7 µm filter, but with a 1.2 µm syringe filter (Sartorius). The genomic DNA (gDNA) was isolated and the number of *Wolbachia* was determined by quantitative real-time PCR (qPCR) of the single-copy *Wolbachia* 16S rRNA gene as previously described (Makepeace et al., 2006).

2.3 Cell-free *Wolbachia* culture

To investigate the effect of insect cell lysate (see below) on isolated *Wolbachia,* the bacteria were purified from C6/36 either using the

procedure published by Rasgon et al. (2006) or by the abbreviated procedure in which the insect cell lysate was retained. Isolated *Wolbachia* were diluted 1:5 in standard medium and incubated in 25 cm^2 plug-sealed cell culture flasks (Greiner) at 26°C for 15 days. The number of *Wolbachia* was determined by 16S rRNA gene qPCR every one to three days. In the following assays, 200 µL cell-free *Wolbachia* extracted by the abbreviated protocol were incubated in F-bottom 96-well plates (Greiner) at 26°C for 12 days, and *Wolbachia* numbers were quantified by qPCR on day 0 and subsequently every three days.

For insect cell lysate titration assays, isolated *Wolbachia* (0.5–1.5 × 10^3 16S rRNA gene copies/µL) were added to total insect cell lysate equivalent to final concentrations of 0.95 × 10^6 cells/mL, 1.9 × 10^6 cells/mL, or 3.8 × 10^6 cells/mL uninfected C6/36 cells as counted prior to lysis. Dilutions were prepared in standard medium. For *Wolbachia* cell number titration assays, different amounts of *Wolbachia* ranging from 10^2 to 10^5 16S rRNA gene copies/µL were diluted in total cell lysate prepared from 0.95 × 10^6 uninfected C6/36 cells and standard medium.

2.4 Preparation of insect cell lysate

2.4.1 Total insect cell lysate

Insect cell lysate was generated from uninfected C6/36 cells. Briefly, cells were harvested in 10 mL standard medium and the amount of uninfected C6/36 cells was calculated using a Neubauer counting chamber (Laboroptik, Bad Homburg, Germany). Then, C6/36 cells were lysed by vortexing with 100 sterile 3 mm borosilicate glass beads for 5 min. Cell debris was removed by centrifugation at 2,500 g for 10 min at 4°C and the supernatant was filtered through a 5 µm syringe filter.

2.4.2 Fractionation of insect cell lysate

Total insect cell lysate was fractionated by centrifugation at 20,000 g for 30 min at 4°C (Eppendorf Centrifuge 5,424 R) or at 100,000 g for 1 h at 4°C (Sorvall Discovery M120 SE, Sorvall, Waltham, USA), respectively. The supernatants containing microsomes and plasma membranes (Fraction 1) or the soluble cytoplasmic content (Fraction 3), respectively, were retained. Since ultracentrifugation could not be performed under sterile conditions, the supernatant obtained after centrifugation at 100,000 g for 1 h was sterile filtered through a 0.2 µm syringe filter (Sartorius), and the pellet was discarded. The pellet obtained after centrifugation at 20,000 g for 30 min containing nuclear debris and large organelles (Fraction 2) was dissolved in the same volume of standard medium as the starting volume of total lysate. Fractions were used for the preparation of cell-free *Wolbachia* cultures with a concentration of 0.5–1 × 10^3 16S rRNA gene copies/µL. The final concentration of fraction added to the culture was equivalent to 0.95 × 10^6 C6/36 cells/mL as counted prior to lysis. For testing combinations of fractions, the final concentration of each fraction was 0.95 × 10^6 cells/mL, and standard medium with 20% FBS was used. *Wolbachia* cultures with fractions were incubated at 26°C for 12 days. When supplementation with freshly prepared Fraction 1 on day 9 was tested, standard medium with 20% FBS was used, and growth was monitored until day 15.

2.4.3 Insect cell lysate with and without FBS

Wolbachia were purified as described above. Two different insect cell lysates were prepared in cell culture medium with and without FBS. Prior to the preparation of insect cell lysate without FBS, the C6/36 cells were washed once in cell culture medium lacking FBS. Both lysates were centrifuged at 20,000 g for 30 min at 4°C and the supernatants were retained (Fraction 1). *Wolbachia* cultures containing Fraction 1 with and without FBS were incubated at 26°C for 12 days. A control containing *Wolbachia* incubated only in standard medium with FBS was included. The initial *Wolbachia* concentration was 0.1–1 × 10^4 16S rRNA gene copies/µL and the final concentration of Fraction 1 was equivalent to 0.95 × 10^6 cells/mL.

2.5 Supplementation of cell-free culture with cholesterol

Cell-free *Wolbachia* cultures were prepared as described above with 0.5–1 × 10^3 16S rRNA gene copies/µL isolated *Wolbachia* and Fraction 1 from insect cell lysate equivalent to 0.95 × 10^6 cells/mL diluted in standard medium with 20% FBS, cultured in 96-well plates at 26°C and supplemented with 0.1 or 1 mg/mL water-soluble cholesterol (Sigma-Aldrich) for 12 days.

2.6 Infection of C6/36 insect cells with *Wolbachia* from cell-free culture

Cell-free *Wolbachia* cultures were prepared as described above with 0.5 × 10^3 16S rRNA gene copies/µL isolated *Wolbachia* and Fraction 1 from insect cell lysate equivalent to 0.95 × 10^6 cells/mL diluted in standard medium and cultured in 96-well plates at 26°C for 12 days. After 9 days, uninfected C6/36 cells were seeded in an F-bottom 24-well plate (Greiner) with 10^5 cells/well in triplicate. On day 12, the medium was removed from the uninfected C6/36 cells and 750 µL of the cell-free *Wolbachia* culture were added, corresponding to a multiplicity of infection (MOI) of 14. As a negative control, *Wolbachia* were heated at 95°C for 10 min, before adding them to the uninfected C6/36 cells. The cells, covered with cell-free *Wolbachia* culture, were centrifuged at 2,000 g for 1 h at 15°C and subsequently incubated at 26°C overnight. On the next day, cells were transferred into an F-bottom 6-well plate (Greiner) containing 1.5 mL standard medium with 10% FBS and incubated at 26°C. After 6 days, the C6/36 cells were harvested in fresh standard medium and transferred into an 8-well culture slide (BD Falcon, Corning, United States). Additionally, samples were taken for qPCR. C6/36 cells were grown on culture slides for 1 day. *Wolbachia* infection was subsequently examined by immunofluorescence microscopy using rabbit anti-*w*PAL primary antiserum (1:1,000 in PBST; Taylor Laboratory, Liverpool School of Tropical Medicine, Liverpool, UK) and a goat anti-rabbit Alexa 488-conjugated secondary antibody (1:200 in PBST; Thermo Fisher Scientific) and counterstained with 0.25 µg/mL DAPI (Sigma-Aldrich) as described previously (Turner et al., 2009; Vollmer et al., 2013). Cells were then analyzed with a Zeiss Axio Observer.Z1 fluorescence microscope (Carl Zeiss AG, Oberkochen, Germany) at the respective wavelengths.

2.7 Quantitative real-time PCR

gDNA was extracted from 200 µL using the QIAamp DNA Mini Kit (Qiagen, Hilden, Germany) following the manufacturer's instructions for DNA purification from blood or body fluids with an adjusted elution volume of 50 µL in a QIAcube robotic workstation (Qiagen). *Wolbachia* cell numbers were calculated by quantification of 16S rRNA gene copies by qPCR as previously described (Makepeace

et al., 2006) using the HotStar Taq Polymerase Kit (Qiagen). A qPCR reaction contained 1x HotStar Taq polymerase buffer, 3 mM $MgCl_2$, 200 µM dNTPs, 0.2 µL SYBR Green (1,000-fold diluted in DMSO; Fermentas, St. Leon-Rot, Germany), 0.5 µM 16S rRNA primers (forward: 5'-TTGCTATTAGATGAGCCTATATTAG-3′, reverse: 5'-GTGTGGCTGATCATC CTCT-3′; Microsynth, Balgach, Switzerland), 0.5 U HotStar Taq polymerase and 2 µL of extracted gDNA (1:20 diluted in AE buffer for cell culture samples, undiluted for cell-free samples). qPCR conditions included a heat activation step at 95°C for 15 min followed by 45 cycles of 95°C for 10 s, 55°C for 15 s, and 72°C for 20 s. Actin qPCRs were applied to control for C6/36 replication (Henrichfreise et al., 2009). For actin qPCRs, a reaction mixture contained 1x HotStar Taq polymerase buffer, 1 mM $MgCl_2$, 200 µM dNTPs, 0.2 µL SYBR Green (1,000-fold diluted in DMSO), 0.3 µM actin primers (forward: 5'-ACGAACTGGGACGATATGGA-3′, reverse: 5'-GCCTCTGTCAGGAGAACTGG-3′; Microsynth, Balgach, Switzerland), 0.5 U HotStar Taq polymerase and 2 µL of extracted gDNA (1:20 diluted in AE buffer for cell culture samples, undiluted for cell-free samples). qPCR conditions included a heat activation step at 95°C for 15 min followed by 45 cycles of 95°C for 10 s, 57°C for 15 s, and 72°C for 20 s. Melt curve analysis showed a specific peak for all positive samples. Data were analyzed using Rotor-Gene 6,000 software version 1.7 (Corbett Life Sciences, Sydney, Australia). The fold change in 16S rRNA gene and actin copies is calculated by dividing the value of each time point by the mean copy number at D0 and indicates replication of *Wolbachia* and C6/36 cells, respectively.

2.8 Fluorescence microscopy of antibiotic-treated cell-free *Wolbachia*

Cell-free *Wolbachia* cultures were prepared as described above with 0.5×10^3 16S rRNA gene copies/µL isolated *Wolbachia* and Fraction 1 from insect cell lysate equivalent to 0.95×10^6 cells/mL diluted in standard medium with 20% FBS, cultured in 96-well plates at 26°C for 12 days and treated with 512 µg/mL fosfomycin (Infectofos, InfectoPharm, Heppenheim, Germany) daily or every three days with ampicillin (Sigma-Aldrich), bacitracin (AppliChem, Darmstadt, Germany), or vancomycin (Sigma-Aldrich). 50 µL of cell-free *Wolbachia* were dried on a microscopy slide and stained as described for the infection experiment. Cell diameter of fosfomycin-treated cells was measured based on the *w*Pal staining using ImageJ (Version 2.0.0-rc-43/1.50e, https://imagej.nih.gov/ij/).

2.9 Statistical analysis

For statistical analysis, GraphPad Prism version 10.1.2 for Windows (GraphPad Software, Boston, Massachusetts United States, www.graphpad.com) was used.

3 Results

3.1 *Wolbachia* replicate under cell-free conditions

As a first step toward establishing an insect cell-free culture of replicating *Wolbachia*, it was investigated whether lysate from disrupted host cells is sufficient for wolbachial growth. For this, two different cell-free *Wolbachia* suspensions were prepared. The first suspension contained *Wolbachia* purified according to the procedure published by Rasgon et al. (2006). The second suspension contained *Wolbachia* purified according to an abbreviated protocol in which the high-speed centrifugation on a sucrose cushion and the subsequent filtration step through a 1.2 µm filter were omitted, which retained more of the insect cell lysate. A 1:5 dilution of each suspension in standard medium was incubated in 25 cm^2 cell culture flasks at 26°C for up to 15 days. Samples were removed every one to three days (exact timing is shown in figures) and the number of *Wolbachia* was determined by qPCR. Gene copy numbers were normalized to the counts on day 0 of the culture. In the cell-free *Wolbachia* culture with retained insect cell lysate, 16S rRNA gene copies increased 3.2-fold by day 5 and 13-fold by day 13 (Figure 1). In contrast, the number of cell-free *Wolbachia*, purified as described by Rasgon et al. (2006) and thus without insect cell lysate, decreased by 88% from day 0 to day 3 and remained unchanged until day 9. An apparent increase was observed on day 11; however, considering the absence of subsequent replication and this time point being a single replicate, this data point was considered an outlier. *Actin* copy numbers were monitored to exclude the possibility that intact C6/36 cells remained in the culture; no increase in *actin* copy number was measured (Supplementary Figure S1). In the following, *Wolbachia* were purified using the abbreviated protocol.

We wanted to further characterize the conditions for cell-free growth of *Wolbachia* to enable consistent assays. In addition, faster growth of cell-free *Wolbachia* would be desirable to allow easy application, e.g., for antibiotic assays. Since the starting amount of C6/36 cells was not measured, our next step was to first determine the optimal amount of insect cell lysate.

3.2 *Wolbachia* replication is inversely dependent on the amount of lysate from uninfected C6/36 cells

Purified *Wolbachia* ($0.5–1.5 \times 10^3$ 16S rRNA gene copies/µL) were incubated with different dilutions of total cell lysate prepared from uninfected C6/36 cells. *Wolbachia* replication was detected in all dilutions of cell lysate, with the highest overall copy number of the 16S rRNA gene on day 9 (Figure 2). In lysate equivalent to 3.8×10^6 cells/mL, *Wolbachia* numbers increased up to 1.9-fold compared to day 0. In more diluted insect cell lysates, the *Wolbachia* replication rate was even higher, achieving an up to 2.9-fold increase with lysate from 1.9×10^6 cells/mL and up to 5.1-fold with lysate from 0.95×10^6 cells/mL. *Wolbachia* growth was achieved from day 0 to day 9 when using the two higher-concentrated lysates, whereas lower *Wolbachia* concentrations were measured on day 12. For the lowest lysate concentration, growth was also observed to day 12. Based on these results, cell lysate prepared from uninfected C6/36 cells equivalent to 0.95×10^6 cells/mL was used for further experiments.

3.3 Replication in cell-free medium is *Wolbachia* density-dependent

Next, the optimal initial density of *Wolbachia* for growth in cell-free culture was titrated. *Wolbachia* were purified from infected C6/36 cells and total cell lysate from uninfected C6/36 cells was prepared.

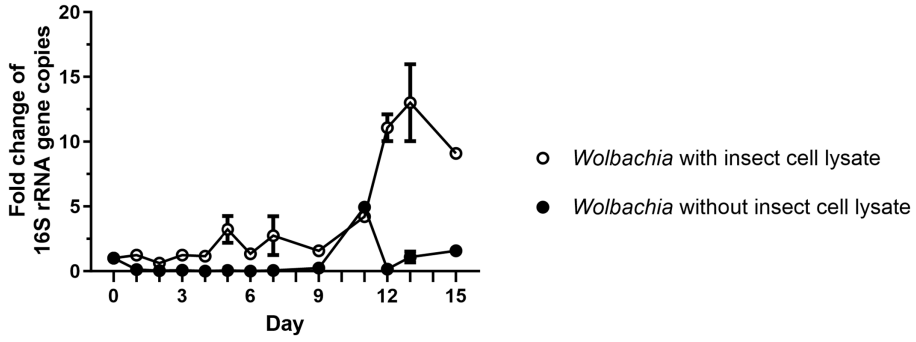

FIGURE 1
Isolated *Wolbachia* replicate in medium when the C6/36 cell membranes are retained. *Wolbachia* were purified from C6/36 cells via ultracentrifugation (Rasgon et al., 2006), or were purified by an abbreviated protocol that retained more of the insect cell lysate. Cell-free cultures were incubated at 26°C for 15 days and samples were taken every one to three days. *Wolbachia* were quantified by qPCR of the 16S rRNA gene. Copy numbers were normalized to day 0. Data were pooled from two independent experiments. For days 2, 4, 6 (experiment 1) and days 9, 11, 15 (experiment 2), the data from only one experiment is shown. For the other days, the mean ± SEM of 2–5 wells is shown.

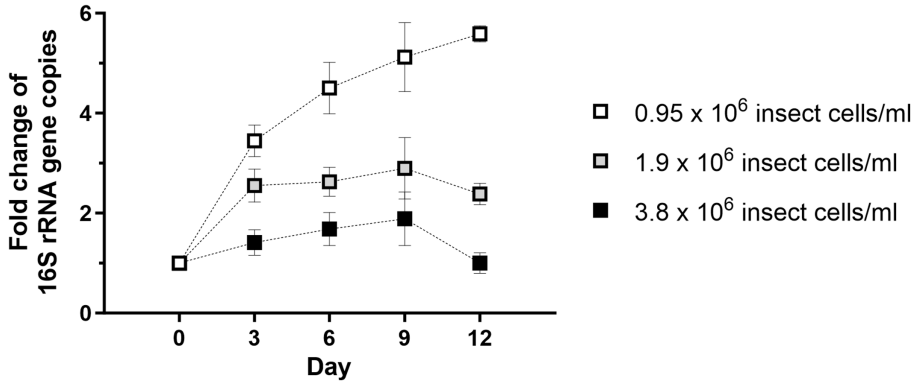

FIGURE 2
Wolbachia replication in cell-free culture is dose-dependent on the amount of C6/36 cell lysate. Total cell lysate from uninfected C6/36 cells was prepared from the depicted cell numbers determined in a Neubauer counting chamber prior to cell lysis. Purified *Wolbachia* ($0.5–1.5 \times 10^3$ 16S rRNA gene copies/µL) were incubated at 26°C for 12 days with the three indicated dilutions of insect cell lysate. Growth was monitored by 16S rRNA gene qPCR every three days and data were normalized to day 0. Data were pooled from two independent experiments. For every time point, the mean ± SEM of six wells is shown.

Decreasing concentrations of *Wolbachia* from 10^5 to 10^2 16S rRNA gene copies/µL were suspended in standard medium containing total insect cell lysate. In cell-free culture containing high *Wolbachia* counts of 10^5 or 10^4 16S rRNA gene copies/µL, the counts slightly increased 1.6- and 1.9-fold, respectively, until day 9 (Figure 3). In contrast, cultures containing 10^3 or 10^2 16S rRNA gene copies/µL had higher replication rates between days 0 and 9, increasing 3.6- and 4.7-fold, respectively. At all concentrations, *Wolbachia* numbers decreased to day 12. Therefore, unless otherwise stated, initial *Wolbachia* concentrations between 10^2 and 10^3 16S rRNA gene copies/µL were used for further experiments.

3.4 Insect cell membranes are essential for *Wolbachia* replication

Wolbachia replication might be dependent on soluble signaling molecules or growth factors provided by the C6/36 cells. As a first step to verify this possibility, insect cell lysate was separated by centrifugation to achieve a rough fractionation of C6/36 cell components (Lodish et al., 2000). For this, insect cell lysate was centrifuged at 20,000 g for 30 min or ultracentrifuged at 100,000 g for 60 min. The supernatant after 20,000 g centrifugation containing cytosol, microsomes, and plasma membranes of the C6/36 cells was retained (Fraction 1), and the corresponding pellet containing nuclear debris and large cell organelles was resuspended in standard medium (Fraction 2). The supernatant after ultracentrifugation containing soluble cytoplasmic contents was also retained (Fraction 3). All three fractions equivalent to 0.95×10^6 cells/mL were incubated separately with 10^3 16S rRNA gene copies/µL of purified *Wolbachia*. As controls, *Wolbachia* were grown in total insect cell lysate and in standard medium without lysate.

Wolbachia incubated with Fraction 1 had equivalent replication as *Wolbachia* incubated with total insect cell lysate, reaching 7-fold mean replication on day 9 compared to day 0. However, the group with Fraction 1 showed growth until day 12 (Figure 4). *Wolbachia*

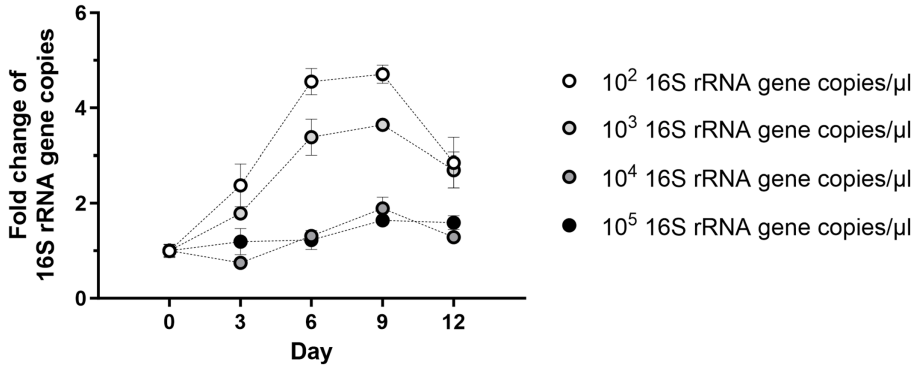

FIGURE 3
Starting density of *Wolbachia* influences cell-free replication. Different starting concentrations of *Wolbachia* were incubated with total insect cell lysate (equivalent to 0.95 × 10^6 uninfected C6/36 cells) at 26°C for 12 days. Growth was monitored by 16S rRNA gene qPCR every three days and data were normalized to day 0. The graph is representative of two independent experiments. For every time point, the mean ± SEM of three wells is shown.

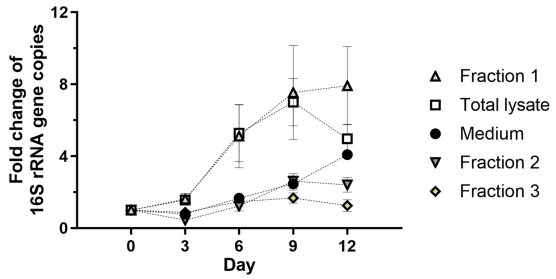

FIGURE 4
The cell membrane-containing fraction from C6/36 cells is required for *Wolbachia* replication in a cell-free culture. Total cell lysate was prepared from 0.95 × 10^6 uninfected C6/36 cells. A portion of cell lysate was fractionated by centrifugation at 20,000 g for 30 min or 100,000 g for 60 min. *Wolbachia* were incubated in the supernatant retained after 20,000 g centrifugation (Fraction 1, microsomes and membranes), the corresponding pellet resuspended in cell culture medium (Fraction 2, nuclear debris and organelles), or the supernatant retained after 100,000 g (Fraction 3, soluble cytoplasmic molecules) at 26°C for 12 days. Growth was compared to reactions containing total insect cell lysate or medium alone. The initial concentration of *Wolbachia* was 10^3 16S rRNA gene copies/µL. Growth was monitored by 16S rRNA gene qPCR every three days and data were normalized to day 0. Data were pooled from two independent experiments. For every time point, the mean ± SEM of six wells is shown, except for the medium group for which the mean ± SEM of three wells is shown.

incubated in medium alone or supplemented with Fraction 2 or Fraction 3 had similar growth curves until day 9 when they had replicated 2- to 3-fold. The medium group continued to replicate until day 12, never reaching more than 50% growth compared to the culture with Fraction 1, while the other two had a slight decrease. To investigate whether Fraction 2 or 3 contain compounds with an inhibitory effect on extracellular wolbachial growth, combinations of all fractions were tested. Replication rates were lower for Fraction 1 in combination with Fraction 2 or Fraction 3 than for Fraction 1 alone, indicating inhibitory effects (Supplementary Figure S2). Therefore, for all further experiments, cell-free *Wolbachia* cultures were supplemented with Fraction 1 (= membrane fraction).

To further extend cell-free growth, freshly prepared Fraction 1 was applied to the culture on day 9 and replication was monitored via qPCR until day 15. Growth rates were slightly higher in the supplemented group on day 12 (5-fold) than in the standard cell-free culture (4-fold), but growth was not prolonged since both groups showed a decrease to day 15 (Figure 5A). A second supplementation with fresh Fraction 1 on day 12 also did not extend cell-free *Wolbachia* replication (data not shown). Insufficient amounts of cholesterol were also considered to be a potential limiting factor of cell-free *Wolbachia* growth. Thus, freshly prepared water-soluble cholesterol was added to the cell-free culture with Fraction 1, but no increase in replication was observed (Figure 5B).

3.5 FBS is essential for *Wolbachia* replication

The growth rate of C6/36 insect cells in cell culture medium is slower in FBS-free medium (Kuno, 1983). The exact components of FBS are not known but many hormones, growth factors, and nutrients are provided with the serum. Thus, it was investigated whether FBS also supports or is necessary for *Wolbachia* replication in the cell-free system. *Wolbachia* grown in standard medium supplemented with Fraction 1 replicated as seen before, reaching a 4.2-fold increase on day 12 (Figure 6). In contrast, *Wolbachia* incubated in medium barely replicated, with a 1.3-fold increase on day 12. No increase of cell-free *Wolbachia* was detected when grown in FBS-free medium supplemented with Fraction 1 derived from uninfected C6/36 cells also harvested in FBS-free medium. These results show that both FBS and Fraction 1 are necessary for replication of cell-free *Wolbachia*; one without the other is not sufficient.

3.6 *Wolbachia* from cell-free culture can infect C6/36 cells

Rasgon et al. (2006) and Nevalainen et al. (2023) demonstrated that purified *Wolbachia* can infect uninfected insect cells. Therefore, we wanted to determine if *Wolbachia* that replicated in our cell-free culture system had maintained the infective phenotype. The infectivity of *Wolbachia* was examined by infecting uninfected C6/36 cells with *Wolbachia* grown in cell-free culture for 12 days (Figure 7A). For cell-free cultured *Wolbachia* incubated with Fraction 1, the number of *Wolbachia* increased 2.7-fold to day 12 (Figure 7A). *Wolbachia* from day

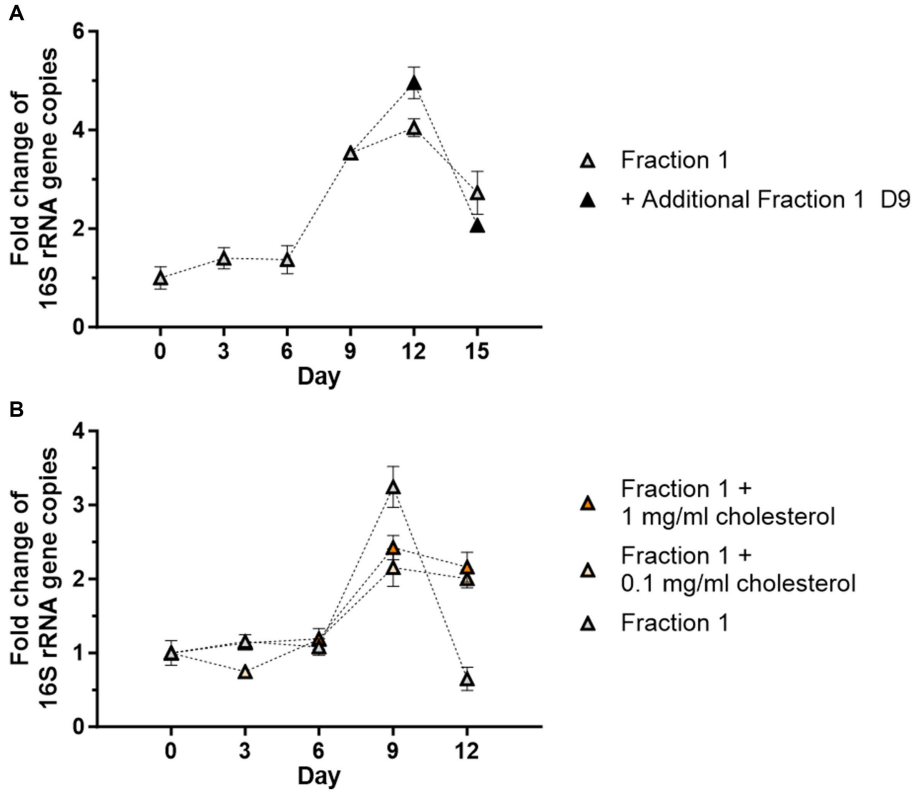

FIGURE 5
Addition of fresh Fraction 1 or cholesterol do not support cell-free replication. **(A)** Cell-free *Wolbachia* (2×10^2 16S rRNA gene copies/µL) were incubated with Fraction 1 from uninfected C6/36 cells (equivalent to 0.95×10^6 cells/mL) at 26°C for 15 days. On day 9, fresh Fraction 1 was added to half of the remaining wells. Growth was monitored by 16S rRNA gene qPCR every three days and data were normalized to day 0. The graph is representative of two independent experiments. For every time point, the mean ± SEM of three wells is shown. **(B)** Cell-free *Wolbachia* (0.5×10^3 16S rRNA gene copies/µL) were incubated with Fraction 1 from uninfected C6/36 cells (equivalent to 0.95×10^6 cells/mL) with or without water-soluble cholesterol (0.1 or 1 mg/mL) at 26°C for 12 days. Growth was monitored by 16S rRNA gene qPCR every three days and data were normalized to day 0. For every time point, the mean ± SEM of six wells is shown.

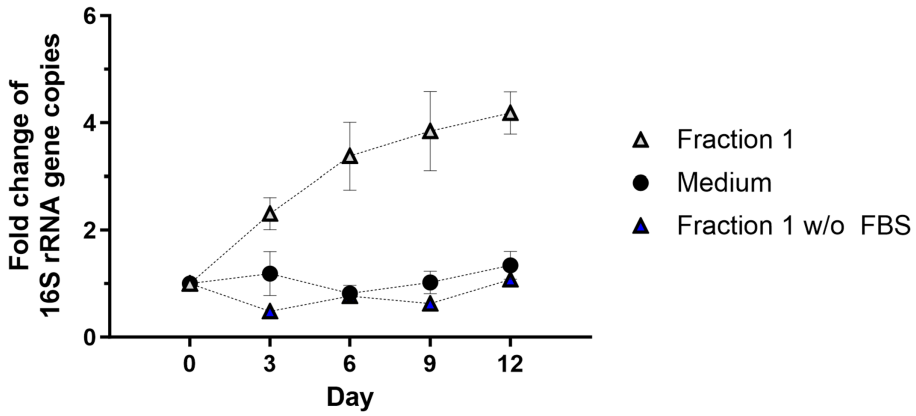

FIGURE 6
FBS is required for *Wolbachia* replication in a cell-free culture. Cell-free *Wolbachia* ($0.1–1 \times 10^4$ 16S rRNA gene copies/µL) were incubated with Fraction 1 from uninfected C6/36 cells (equivalent to 0.95×10^6 cells/mL) harvested in cell culture medium either with or without FBS and incubated at 26°C for 12 days. Growth was monitored by 16S rRNA gene qPCR every three days and data were normalized to day 0. Data were pooled from two independent experiments. For every time point, the mean ± SEM of six wells is shown.

12 of this cell-free culture were used to infect C6/36 cells. Six days post-infection, ~140 16S rRNA gene copies/µL were measured in the cell culture (Figure 7B). In contrast, only eight 16S rRNA gene copies/µL were detected in C6/36 cells infected with heat-killed *Wolbachia* from the same cell-free culture. Immunofluorescence microscopy using a *Wolbachia*-specific antiserum against *w*Pal confirmed the presence of

10.3389/fmicb.2024.1405287

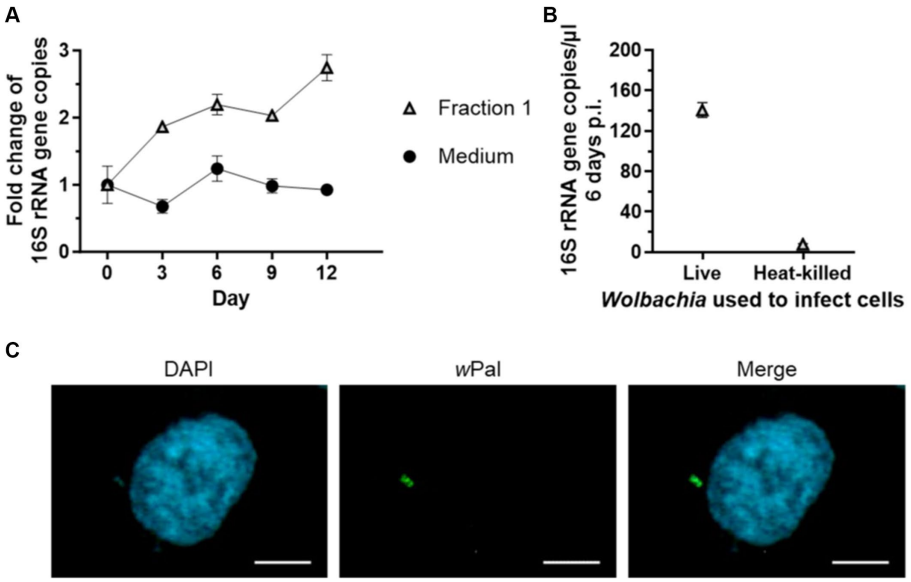

FIGURE 7
Cell-free cultured *Wolbachia* infect uninfected C6/36 cells. **(A)** Cell-free *Wolbachia* (0.5×10^3 16S rRNA gene copies/µL) were incubated with Fraction 1 from uninfected C6/36 cells (equivalent to 0.95×10^6 cells/mL) at 26°C for 12 days. Growth was monitored by 16S rRNA gene qPCR every three days. For every time point, the mean ± SEM of three wells is shown. **(B)** On day 12, 750 µL of this cell-free *Wolbachia* culture were added to uninfected C6/36 cells grown in a 24-well plate. As a negative control, *Wolbachia* were heat-killed at 95°C for 10 min prior to addition to the uninfected C6/36 cells. After centrifugation at 2,000 g for 1 h at 15°C, the plate was incubated overnight at 26°C. On the next day, the medium was removed and fresh cell culture medium was added. On day 6 post-infection, three samples were taken for 16S rRNA gene qPCR of C6/36 cells infected with *Wolbachia* and with heat-killed *Wolbachia* (mean ± SEM). Data are representative of two experiments. **(C)** Six days post-infection, C6/36 cells were grown on culture slides for 1 day and subsequently examined with a Zeiss Axio Observer.Z1 fluorescence microscope using immunofluorescence microscopy with *w*PAL anti-serum and an Alexa 488-conjugated secondary antibody (green, *Wolbachia*) and counterstained with DAPI (blue). Scale bar: 5 µm.

Wolbachia in the C6/36 cell culture 7 days post-infection when infected with live *Wolbachia* (Figure 7C).

3.7 *Wolbachia* replication rate is lower in cell-free culture

By supplementing standard medium with Fraction 1, *Wolbachia* were able to replicate for at least 9 days. To determine the stability and growth efficiency of *Wolbachia* in the cell-free culture system, growth rates of *Wolbachia* cultured with and without Fraction 1 were compared to *Wolbachia* cultured within the C6/36 cell line. For each culture system, the fold increase of 16S rRNA gene copies on day 9 was compared. Growth rates significantly differed between the groups (Figure 8). *Wolbachia* residing in C6/36 cells had a median growth rate of 14.8 (range 4.8–25.5; mean: 13.6). Cell-free *Wolbachia* cultured in standard medium had a median growth rate of 1.0 (range 0.6–6.8; mean: 1.7). Cell-free *Wolbachia* cultured in standard medium supplemented with Fraction 1 had a median growth rate of 4.2 (range 2–14.8; mean: 6.4).

3.8 Cell-free cultured *Wolbachia* are sensitive to fosfomycin treatment

It has been shown that *Wolbachia* are sensitive to fosfomycin (Henrichfreise et al., 2009), a specific inhibitor of MurA that catalyzes the first dedicated step of lipid II biosynthesis. Treatment of

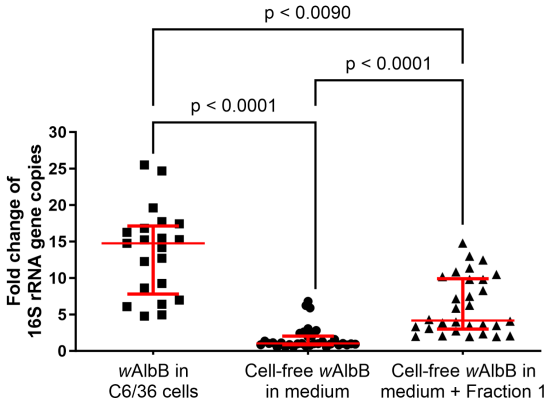

FIGURE 8
Variation in growth between *Wolbachia* cultured in cell-free medium ± Fraction 1 from C6/36 cell lysate compared to standard C6/36 cell culture. The replication of *Wolbachia* in cell-free culture with and without Fraction 1 from insect cell lysate or in C6/36 cells was compared on day 9, combining data from at least 20 independent experiments performed in duplicates (growth in C6/36 cells) or triplicates (cell-free growth), respectively. Cell-free *Wolbachia* with initial concentrations of 10^2–10^3 16S rRNA gene copies/µL were incubated with Fraction 1 from uninfected C6/36 cells (equivalent to 0.95×10^6 cells/mL). *Wolbachia* in C6/36 cells had initial concentrations of 10^3–10^4 16S rRNA gene copies/µL. Each dot represents one experiment. The median with interquartile range is shown (red lines). Statistical differences were determined using a Kruskal-Wallis test followed by a post-hoc Dunn's multiple comparisons test using GraphPad Prism 10.

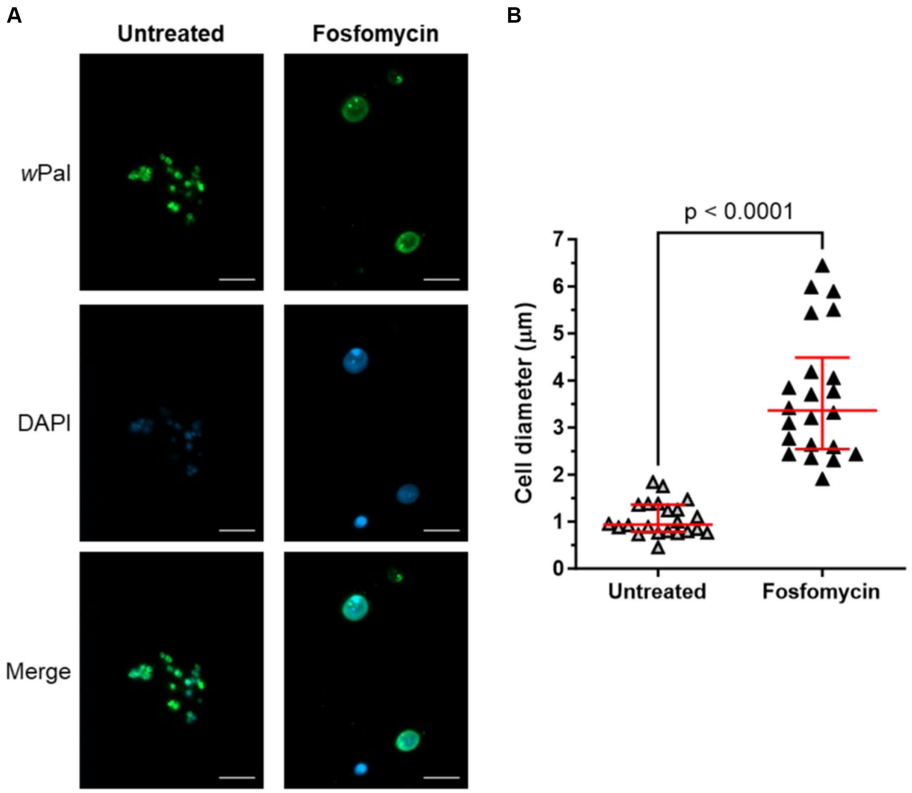

FIGURE 9
Cell-free cultured *Wolbachia* are sensitive to fosfomycin treatment. Cell-free *Wolbachia* (0.5×10^3 16S rRNA gene copies/µL) were incubated with Fraction 1 from uninfected C6/36 cells (equivalent to 0.95×10^6 cells/mL) at 26°C for 12 days, with or without daily 512 µg/mL fosfomycin treatment. **(A)** Cells were fixed and visualized by immunofluorescence microscopy using *w*PAL anti-serum and an Alexa 488-conjugated secondary antibody (green, *Wolbachia*) and counterstained with DAPI (blue). Scale bar: 5 µm. **(B)** Cell diameter (median with IQR, red lines) was measured with ImageJ based on the *w*Pal staining from three independent assays ($n = 22$). Statistical differences were determined using a Mann–Whitney test using GraphPad Prism 10.

Wolbachia-infected C6/36 cells with fosfomycin resulted in fewer and enlarged *Wolbachia* cells, demonstrating that the cell wall precursor lipid II is necessary for cell division in *Wolbachia* (Vollmer et al., 2013). To confirm that cell-free cultivated *Wolbachia* are suitable for antibiotic studies, e.g., to understand the reduced cell division machinery encoded in the genome, the phenotype of fosfomycin-treated endobacteria was analyzed via immunofluorescence microscopy using anti-*w*PAL. Untreated cell-free *Wolbachia* had a median (IQR) cell diameter of 0.94 µm (0.78–1.36 µm), whereas fosfomycin-treated *Wolbachia* were significantly larger with 3.36 µm (2.54–4.49 µm) (Figure 9). We only observed these enlarged cells when we also detected wolbachial replication via qPCR of the 16S rRNA gene. In contrast, the other cell wall biosynthesis-inhibiting antibiotics tested, i.e., ampicillin, bacitracin, and vancomycin did not affect the phenotype of cell-free *Wolbachia* (Supplementary Figure S3).

4 Discussion

In vitro culture systems of *Wolbachia* necessary for the elucidation of their biology are few and only *Wolbachia* strains naturally occurring in arthropods have been successfully cultured in insect cell lines (Fenollar et al., 2003a; McMeniman et al., 2008), while all attempts to culture *Wolbachia* of filarial nematodes have failed (McNulty et al., 2010; Slatko et al., 2014; Marriott et al., 2023). Molecular biological techniques are mostly impossible to apply to *Wolbachia* cultured in insect cell lines, e.g., genetic transformation or treatment of *Wolbachia* with large antibiotics such as aminoglycosides, polymyxins, lipo-and glycopeptide antibiotics that might not pass the insect cell membranes. Therefore, the extracellular cultivation of *Wolbachia* would provide an excellent tool for understanding the biology and symbiosis of *Wolbachia*. However, *Wolbachia* purified from insect cells have only been maintained without replication in cell-free cultures (Rasgon et al., 2006; Krafsur et al., 2020). Further attempts regarding *ex vivo* growth failed, but some components were advantageous regarding survival of *Wolbachia*, e.g., compatible solutes, actin, and mammalian blood (Uribe-Alvarez et al., 2018).

For other intracellular species such as *Coxiella burnetii* a complex medium has been designed in which cell-free growth occurred (Omsland et al., 2009). However, contrary to *Wolbachia*, *Coxiella burnetii* exhibit a less symbiotic interaction with their host cell and can even persist in an extracellular environment (Heinzen et al., 1999). Furthermore, attempts to generate a complex medium for cell-free growth of *Chlamydia*, which have a lifestyle that is more similar to that of *Wolbachia*, were unsuccessful (Omsland et al., 2012). This points out the complexity of cell-free growth of obligate intracellular bacteria that are tightly associated with their host. Compared to *Coxiella burnetii*, *Wolbachia* and *Chlamydia* possess a

substantially reduced genome, which might make cell-free growth even more difficult.

In the present study, we could demonstrate that *Wolbachia* were not only viable when maintained in a cell-free culture, but underwent replication when insect cell lysate from uninfected C6/36 cells was added to the medium. In some experiments, a slight increase in *Wolbachia* numbers was observed in standard cell culture medium without insect cell lysate, but it never reached the levels observed when supplementing the cell-free medium, and in most cases no growth was detected. It is possible that the *Wolbachia* suspension generated from infected C6/36 cells contained sufficient components that allowed for a weak replication rate.

Viability and infectivity of *Wolbachia* from a 12-day-old cell-free *Wolbachia* culture were confirmed by infecting uninfected C6/36 cells, with *Wolbachia* DNA and intracellular *Wolbachia* detectable six and seven days post-infection. With a maximum of 1–2 *Wolbachia* per C6/36 cell, the insect cells were considerably less infected than the Aa23 and JW18 cells of Rasgon et al. (2006) and Nevalainen et al. (2023), respectively. While this could be supported by different uptake efficiencies of the *Wolbachia* subspecies and insect cells, it is most likely explained by the different MOIs used for infection. We used an MOI of 14, whereas Rasgon et al. (2006) used an MOI of 2,600 and Nevalainen et al. (2023) used an MOI of 20:1 host cell equivalents (i.e., the *Wolbachia* contents from 20 infected cells per seeded uninfected cell). Our MOI was low because of the low *Wolbachia* numbers required for cell-free replication. We also used a comparatively high number of C6/36 cells to have confluent growth and thereby increase the likelihood of *Wolbachia* coming into contact with a C6/36 cell. When *Wolbachia* were killed by heating prior to infection of uninfected C6/36 cells, only minimal amounts of DNA were detected in the cells 6 days post-infection, confirming the results from Nevalainen et al. (2023) that *Wolbachia* are not only passively taken up but also facilitate their uptake. No *Wolbachia* could be detected by immunofluorescence microscopy (data not shown). Thus, detected DNA most probably represents residual DNA from dead *Wolbachia*.

Wolbachia growth in the insect cell-free culture was dependent on the initial *Wolbachia* concentrations, with higher concentrations resulting in lower levels of replication. A first explanation might be an insufficient supply of nutrients, e.g., pyruvate and intermediates of the tricarboxylic acid cycle derived from amino acids (Foster et al., 2005). However, in the insect cell-free *Wolbachia* culture, essential and nonessential amino acids are provided in excess by the cell culture medium as well as pyruvate and sugars. *Wolbachia* replicate slowly in the culture and competition for nutrients is unlikely. Instead, *Wolbachia* densities might be regulated by a yet unknown, intrinsic, or host cell-derived mechanism. It is striking that cell-free *w*AlbB showed the highest replication rates at an initial concentration of $0.1–1 \times 10^3$ 16S rRNA gene copies/µL. In contrast, in cell-free cultures containing higher densities of *Wolbachia* with 10^4 or 10^5 16S rRNA gene copies/µL, *Wolbachia* numbers only slightly increased. This indicates that *Wolbachia* might sense densities and regulate cell division by internal communication patterns. The two-component regulatory system (TCS) is the predominant form of signaling used in a majority of prokaryotes, including bacteria (Beier and Gross, 2006). It is composed of a sensor histidine kinase and a paired response regulator (Mitrophanov and Groisman, 2008; Jung et al., 2012). Stimuli such as nutrients, osmolarity, oxygen, salinity, and quorum sensing cues are recognized by sensor histidine kinases (Mascher et al., 2006). This activates cognate response regulators which, e.g., coordinate induction of sporulation, regulation of bacterial differentiation, or formation of biofilms (Stock et al., 2000). TCS genes are highly conserved in various *Wolbachia* strains, but very little is known about their function to date (Cheng et al., 2006; Brilli et al., 2010). A bioinformatics study showed that wolbachial TCS genes are consistently found clustered with metabolic genes within several *Wolbachia* strains, including *w*AlbB and *w*Bm (Christensen and Serbus, 2015). Considering these findings, it might be hypothesized that *Wolbachia* are able to sense, e.g., nutrients or quorum sensing molecules and consequently regulate cell division and density. This could explain why cell-free *Wolbachia* growth stops after 9–12 days of incubation and could further explain the observation that *Wolbachia* cell numbers inside C6/36 cells do not reach a density that would negatively affect the survival of their host cell. Nevertheless, how *Wolbachia* growth is regulated remains to be elucidated.

It was also observed that increasing the amount of uninfected C6/36 cells used to prepare total insect cell lysate had a detrimental effect on *Wolbachia* growth rather than increasing replication. *Wolbachia* replication inside their host cells is a complex and tightly regulated process (McGraw et al., 2002; Ruang-areerate et al., 2004). The C6/36 cell culture was originally generated from *A. albopictus* larvae and therefore consists of cells of different cell cycle stages and of different cell types (Singh, 1967; Igarashi, 1978). Hence, it should be considered that *Wolbachia* growth-inhibiting factors present in a subset of C6/36 cells might accumulate when larger numbers of cells are used for lysate preparation. Fraction 1 (containing microsomes and plasma membranes) induced *Wolbachia* growth. However, almost no replication occurred when Fraction 2 (nuclear debris and large organelles) or Fraction 3 (soluble cytoplasmic content) of the C6/36 cells were used to supplement the medium. Since a combination of Fraction 1 with either Fraction 2 or Fraction 3 decreased growth, we hypothesize an inhibiting effect of these fractions. Supplementation with fresh Fraction 1 on day 9 enhanced growth to day 12 but could not extend growth. A second supplementation with fresh Fraction 1 on day 12 also failed to prolong growth. The factor limiting cell-free growth to 12 days remains unclear. As the fresh Fraction 1 was only added to existing cultures and the medium was not completely exchanged, there might be degradation products present that prevented further growth of the cell-free *Wolbachia*.

Notably, it has been shown that survival of endobacteria of the species *Ehrlichia chaffeensis* and *Anaplasma phagocytophilum*, which are closely related to *Wolbachia* spp., is dependent on the incorporation of cholesterol derived from their host cell (Lin and Rikihisa, 2003). Like *Wolbachia*, *Ehrlichia chaffeensis* and *Anaplasma phagocytophilum* do not synthesize lipid A and it was proposed that cholesterol might be necessary to promote membrane stability as a substitute for lipopolysaccharides (Lin and Rikihisa, 2003; Wu et al., 2004). There are indications that *Wolbachia*-infected insect cells might indeed incorporate cholesterol (Caragata et al., 2013; Geoghegan et al., 2017). Further, *Wolbachia* reside in cholesterol-rich Golgi-related vesicles derived from the host which form a vacuole surrounding each bacterium (Cho et al., 2011). Insects assimilate cholesterol from their environment which is incorporated into the plasma membrane and internal membranes such as those from the Golgi apparatus (Rolls et al., 1997). Thus, cholesterol might be a limiting factor for cell-free *w*AlbB replication, and supplementation with the membrane fraction

of an insect cell lysate might not be sufficient to sustain growth for more than 12 days. However, the supplementation of water-soluble cholesterol did not lead to increased cell numbers under the conditions tested, indicating that this compound cannot be the only potential limiting growth factor. Apart from cholesterol, eukaryotic sphingomyelin was found in membranes of *Chlamydia trachomatis* (Carabeo et al., 2003), and it was shown that *Chlamydia* need these host lipids for expansion and replication (Feldkamp et al., 2017). Insects do not have sphingomyelin but instead contain ceramide phosphorylethanolamine (Luukkonen et al., 1973). Therefore, the sphingolipids sphingomyelin or ceramide phosphorylethanolamine, respectively, might be taken up by *Wolbachia* residing in different hosts and be essential for replication.

Nevertheless, components of Fraction 1 such as cholesterol cannot be the only necessary factor for *Wolbachia* growth outside their host cell since *Wolbachia* were not able to grow in cell-free medium supplemented with Fraction 1 derived from C6/36 cells harvested in medium without FBS. The composition of FBS is unknown but it is very likely that the serum, similar to the eukaryotic host cells in cell culture, provides proteins, carbohydrates, lipids, vitamins, and other factors essential for *Wolbachia* viability and replication. Similarly, extracellular growth of *Coxiella burnetii* was initially found to be FBS-dependent as well (Omsland et al., 2009), although a defined medium without FBS was developed later (Sandoz et al., 2016).

A prerequisite for bacterial cell division is the proper assembly of the divisome and disturbance of this process results in an aberrant phenotype characterized by swelling or filamentation of bacteria (Goehring et al., 2005; Park et al., 2005). For *Wolbachia* cultured in C6/36 cells, enlarged cells were observed subsequent to the blockade of lipid II biosynthesis by fosfomycin, demonstrating that the cell wall precursor lipid II is essential for the cell division of *Wolbachia* (Vollmer et al., 2013). A similar phenotype was induced by fosfomycin in intracellular *Protochlamydia* and *Waddlia chondrophila* (Pilhofer et al., 2013; Scherler et al., 2020). In the cell-free *Wolbachia* culture, the same aberrant phenotype was observed, indicating that the bacteria are indeed replicating in the cell-free system and that replication can be inhibited by fosfomycin. This was underlined by the fact that we only detected enlarged *Wolbachia* when we measured an increase of 16S rRNA gene copies via qPCR. The fosfomycin-treated cell-free *Wolbachia* were significantly enlarged with 3.36 µm (2.54–4.49 µm) [median (IQR)]. The determined cell diameter of 0.94 µm (0.78–1.36 µm) of the untreated cell-free *Wolbachia* fits well with the 0.8–1.5 µm determined by Hertig, showing that the cell-free *Wolbachia* display their normal morphology (Hertig, 1936).

We hypothesized a phenotype similar to the fosfomycin-induced for other cell wall biosynthesis-inhibiting antibiotics and thus tested ampicillin, bacitracin, and vancomycin. Belonging to the class of beta-lactam antibiotics, ampicillin binds to penicillin-binding proteins (Suginaka et al., 1972; Tipper, 1979). Since bacitracin and vancomycin are large antibiotics that might not be taken up by the C6/36 cells, we were interested in a possible effect on cell-free *Wolbachia*. Bacitracin binds to the pyrophosphate moiety of undecaprenyl pyrophosphate (C55-PP) and vancomycin binds to the D-Ala-D-Ala of lipid II (Perkins, 1969; Storm and Strominger, 1973). For all three, no effect on the phenotype of cell-free *Wolbachia* was observed although their intracellular targets are present (Henrichfreise et al., 2009; Vollmer et al., 2013; Atwal et al., 2021). Possibly, bacitracin and vancomycin are not reaching their targets due to the outer membrane of *Wolbachia* (Nikaido, 1989). Beta-lactams have previously been found to not affect intracellular *Wolbachia* *w*AlbB in cell culture, the reason is unclear (Fenollar et al., 2003b; Fallon, 2018). In contrast, for *Chlamydia*, an aberrant phenotype is induced by beta-lactams (Matsumoto and Manire, 1970; Kramer and Gordon, 1971), and for *Waddlia chondrophila*, an aberrant phenotype is induced by both beta-lactams and vancomycin (Scherler et al., 2020). Further investigation is necessary to determine why these cell wall biosynthesis-inhibiting antibiotics do not have a similar effect for *Wolbachia*.

Although close attention was paid to using consistent conditions, the cell-free cultures often did not grow. We also observed a decrease in cell-free growth rates over time, which could be due to a new FBS batch (Liu et al., 2023). In the calculation of the median growth rate, only the assays in which the *Wolbachia* replicated were included. The variance of growth rates between independent experiments in cell-free culture containing Fraction 1 was similar to those of *Wolbachia* cultured inside C6/36 cells. In both culture systems, we observed growth variability occurring over time that might originate from variances of medium or cell culture passage. However, the median growth rate of *Wolbachia* in cell-free medium is ~3.5 times lower compared to *Wolbachia* cultured in C6/36 cells. This indicates that in addition to the need for Fraction 1 for cell-free *Wolbachia* cultivation, further constituents are needed.

Previous studies indicate that replication of *Wolbachia* is dependent on the stage of the host life cycle, tissue-specific control mechanism, and host cell replication (Min and Benzer, 1997; McGraw et al., 2002; Ruang-areerate et al., 2004; Landmann et al., 2012). These findings provide insight into the complexity of *Wolbachia* replication, which will in turn influence the cell-free cultivation of the bacteria. In the cell-free culture, the differences in cell types and cell cycle stages of the C6/36 cells used to generate the lysate, and thus Fraction 1, could therefore have a major effect on replication. Further elucidation of this culture system will be necessary to achieve greater and sustained *Wolbachia* growth outside their host cells and to gain insight into the multiple mechanisms that influence and regulate replication in the symbiosis.

Nevertheless, the establishment of this culture system represents a further step in the effort to cultivate *Wolbachia* extracellularly and might also provide important cues for the extracellular cultivation of other endobacteria that could not be cultivated *in vitro* yet. Moreover, a powerful tool for the exploration of *Wolbachia* biology and *Wolbachia*-host interactions is provided by *Wolbachia* cultivated in an insect cell-free *in vitro* system.

Data availability statement

The raw data supporting the conclusions of this article will be made available by the authors, without undue reservation.

Author contributions

LB: Data curation, Formal analysis, Funding acquisition, Visualization, Writing – original draft, Writing – review & editing, Investigation, Methodology. KM: Data curation, Formal analysis, Visualization, Writing – original draft, Writing – review & editing,

Investigation, Methodology. JV: Data curation, Formal analysis, Visualization, Writing – original draft, Writing – review & editing, Funding acquisition, Investigation, Methodology. CC: Data curation, Formal analysis, Writing – review & editing, Investigation. AS: Conceptualization, Writing – review & editing. AH: Conceptualization, Funding acquisition, Writing – review & editing, Supervision. KP: Conceptualization, Funding acquisition, Project administration, Writing – review & editing, Methodology, Supervision.

Funding

The authors received support for this project from German Research Foundation (Deutsche Forschungsgemeinschaft, DFG) grants to KP and AH [FOR 854, PF673/3-1, PF673/3-2, TRR261 (project ID 398967434)]. AH and KP are members of the German Center for Infection Research (DZIF). AH is a member and KP is an associate member of the Excellence Cluster Immunosensation (DFG, EXC 1023). LB received a PhD scholarship from the Studienstiftung des deutschen Volkes. JV received a PhD scholarship from the Jürgen Manchot Stiftung. This work was supported by the Open Access Publication Fund of the University of Bonn.

Acknowledgments

We thank Prof. M. Taylor, University of Liverpool, UK for providing us with *w*PAL anti-serum (Turner et al., 2009). Furthermore, we thank H. Neufeld for excellent technical assistance with the cell culture and J. Nadal for advice on statistical analysis.

Conflict of interest

The authors declare that the research was conducted in the absence of any commercial or financial relationships that could be construed as a potential conflict of interest.

The author(s) declared that they were an editorial board member of Frontiers, at the time of submission. This had no impact on the peer review process and the final decision.

Publisher's note

Supplementary material

The Supplementary material for this article can be found online at: https://www.frontiersin.org/articles/10.3389/fmicb.2024.1405287/full#supplementary-material

References

Andersen, S. B., Boye, M., Nash, D. R., and Boomsma, J. J. (2012). Dynamic *Wolbachia* prevalence in *Acromyrmex* leaf-cutting ants: potential for a nutritional symbiosis. *J. Evol. Biol.* 25, 1340–1350. doi: 10.1111/j.1420-9101.2012.02521.x

Atwal, S., Chuenklin, S., Bonder, E. M., Flores, J., Gillespie, J. J., Driscoll, T. P., et al. (2021). Discovery of a diverse set of Bacteria that build their cell walls without the canonical peptidoglycan polymerase aPBP. *MBio* 12:e0134221. doi: 10.1128/mBio.01342-21

Beier, D., and Gross, R. (2006). Regulation of bacterial virulence by two-component systems. *Curr. Opin. Microbiol.* 9, 143–152. doi: 10.1016/j.mib.2006.01.005

Blagrove, M. S., Arias-Goeta, C., Failloux, A. B., and Sinkins, S. P. (2012). *Wolbachia* strain wMel induces cytoplasmic incompatibility and blocks dengue transmission in *Aedes albopictus*. *Proc. Natl. Acad. Sci. USA* 109, 255–260. doi: 10.1073/pnas.1112021108

Brilli, M., Fondi, M., Fani, R., Mengoni, A., Ferri, L., Bazzicalupo, M., et al. (2010). The diversity and evolution of cell cycle regulation in alpha-proteobacteria: a comparative genomic analysis. *BMC Syst. Biol.* 4:52. doi: 10.1186/1752-0509-4-52

Carabeo, R. A., Mead, D. J., and Hackstadt, T. (2003). Golgi-dependent transport of cholesterol to the *Chlamydia trachomatis* inclusion. *Proc. Natl. Acad. Sci. USA* 100, 6771–6776. doi: 10.1073/pnas.1131289100

Caragata, E. P., Rancès, E., Hedges, L. M., Gofton, A. W., Johnson, K. N., O'Neill, S. L., et al. (2013). Dietary cholesterol modulates pathogen blocking by *Wolbachia*. *PLoS Path.* 9:e1003459. doi: 10.1371/journal.ppat.1003459

Casiraghi, M., Ferri, E., and Bandi, C. (2007). "*Wolbachia*: evolutionary significance in nematodes" in *Wolbachia*: A Bug's life in another bug. eds. A. Hoerauf and R. U. Rao. *5th* ed (Basel: Karger), 15–30.

Cheng, Z., Kumagai, Y., Lin, M., Zhang, C., and Rikihisa, Y. (2006). Intra-leukocyte expression of two-component systems in *Ehrlichia chaffeensis* and *Anaplasma phagocytophilum* and effects of the histidine kinase inhibitor closantel. *Cell. Microbiol.* 8, 1241–1252. doi: 10.1111/j.1462-5822.2006.00704.x

Cho, K.-O., Kim, G.-W., and Lee, O.-K. (2011). *Wolbachia* bacteria reside in host Golgi-related vesicles whose position is regulated by polarity proteins. *PLoS One* 6:e22703. doi: 10.1371/journal.pone.0022703

Christensen, S., and Serbus, L. R. (2015). Comparative analysis of *Wolbachia* genomes reveals streamlining and divergence of minimalist two-component systems. *G3 Genes Genomes Genet.* 5, 983–996. doi: 10.1534/g3.115.017137

Clare, R. H., Cook, D. A. N., Johnston, K. L., Ford, L., Ward, S. A., and Taylor, M. J. (2015). Development and validation of a high-throughput anti-*Wolbachia* whole-cell screen: a route to Macrofilaricidal drugs against onchocerciasis and lymphatic Filariasis. *J. Biomol. Screen.* 20, 64–69. doi: 10.1177/1087057114551518

Conceição, C. C., da Silva, J. N., Arcanjo, A., Nogueira, C. L., de Abreu, L. A., de Oliveira, P. L., et al. (2021). *Aedes fluviatilis* cell lines as new tools to study metabolic and immune interactions in mosquito-*Wolbachia* symbiosis. *Sci. Rep.* 11:19202. doi: 10.1038/s41598-021-98738-7

Dyson, E. A., Kamath, M. K., and Hurst, G. D. (2002). *Wolbachia* infection associated with all-female broods in *Hypolimnas bolina* (Lepidoptera: Nymphalidae): evidence for horizontal transmission of a butterfly male killer. *Heredity* 88, 166–171. doi: 10.1038/sj.hdy.6800021

Eedunuri, V. K., Zhang, Y., Cheng, C., Chen, L., Liu, H., Omsland, A., et al. (2018). Protein and DNA synthesis demonstrated in cell-free *Ehrlichia chaffeensis* organisms in axenic medium. *Sci. Rep.* 8:9293. doi: 10.1038/s41598-018-27574-z

Fallon, A. M. (2018). Strain-specific response to ampicillin in *Wolbachia*-infected mosquito cell lines. *Vitro Cell. Dev. Biol. Anim.* 54, 580–588. doi: 10.1007/s11626-018-0279-x

Feldkamp, M. L., Ward, D. M., Pysher, T. J., and Chambers, C. T. (2017). *Chlamydia trachomatis* is responsible for lipid Vacuolation in the amniotic epithelium of fetal Gastroschisis. *Birth Defects Res.* 109, 1003–1010. doi: 10.1002/bdr2.1062

Fenn, K., and Blaxter, M. (2006). *Wolbachia* genomes: revealing the biology of parasitism and mutualism. *Trends Parasitol.* 22, 60–65. doi: 10.1016/j.pt.2005.12.012

Fenn, K., Conlon, C., Jones, M., Quail, M. A., Holroyd, N. E., Parkhill, J., et al. (2006). Phylogenetic relationships of the *Wolbachia* of nematodes and arthropods. *PLoS Path.* 2:e94. doi: 10.1371/journal.ppat.0020094

Fenollar, F., La Scola, B., Inokuma, H., Dumler, J. S., Taylor, M. J., and Raoult, D. (2003a). Culture and phenotypic characterization of a *Wolbachia pipientis* isolate. *J. Clin. Microbiol.* 41, 5434–5441. doi: 10.1128/jcm.41.12.5434-5441.2003

Fenollar, F., Maurin, M., and Raoult, D. (2003b). *Wolbachia pipientis* growth kinetics and susceptibilities to 13 antibiotics determined by immunofluorescence staining and real-time PCR. *Antimicrob. Agents Chemother.* 47, 1665–1671. doi: 10.1128/aac.47.5.1665-1671.2003

Fischer, K., Beatty, W. L., Jiang, D., Weil, G. J., and Fischer, P. U. (2011). Tissue and stage-specific distribution of *Wolbachia* in *Brugia malayi*. *PLoS Negl. Trop. Dis.* 5:e1174. doi: 10.1371/journal.pntd.0001174

Foster, J., Ganatra, M., Kamal, I., Ware, J., Makarova, K., Ivanova, N., et al. (2005). The *Wolbachia* genome of *Brugia malayi*: endosymbiont evolution within a human pathogenic nematode. *PLoS Biol.* 3:e121. doi: 10.1371/journal.pbio.0030121

Frost, C. L., Pollock, S. W., Smith, J. E., and Hughes, W. O. (2014). *Wolbachia* in the flesh: symbiont intensities in germ-line and somatic tissues challenge the conventional view of *Wolbachia* transmission routes. *PLoS One* 9:e95122. doi: 10.1371/journal.pone.0095122

Frydman, H. M., Li, J. M., Robson, D. N., and Wieschaus, E. (2006). Somatic stem cell niche tropism in *Wolbachia*. *Nature* 441, 509–512. doi: 10.1038/nature04756

Geoghegan, V., Stainton, K., Rainey, S. M., Ant, T. H., Dowle, A. A., Larson, T., et al. (2017). Perturbed cholesterol and vesicular trafficking associated with dengue blocking in *Wolbachia*-infected *Aedes aegypti* cells. *Nat. Commun.* 8:526. doi: 10.1038/s41467-017-00610-8

Goehring, N. W., Gueiros-Filho, F., and Beckwith, J. (2005). Premature targeting of a cell division protein to midcell allows dissection of divisome assembly in *Escherichia coli*. *Genes Dev.* 19, 127–137. doi: 10.1101/gad.1253805

Hedges, L. M., Brownlie, J. C., O'Neill, S. L., and Johnson, K. N. (2008). *Wolbachia* and virus protection in insects. *Science* 322:702. doi: 10.1126/science.1162418

Heinzen, R. A., Hackstadt, T., and Samuel, J. E. (1999). Developmental biology of *Coxiella burnetii*. *Trends Microbiol.* 7, 149–154. doi: 10.1016/S0966-842X(99)01475-4

Henrichfreise, B., Schiefer, A., Schneider, T., Nzukou, E., Poellinger, C., Hoffmann, T. J., et al. (2009). Functional conservation of the lipid II biosynthesis pathway in the cell wall-less bacteria *Chlamydia* and *Wolbachia*: why is lipid II needed? *Mol. Microbiol.* 73, 913–923. doi: 10.1111/j.1365-2958.2009.06815.x

Hertig, M. (1936). The Rickettsia, *Wolbachia pipientis* (gen. Et sp.n.) and associated inclusions of the mosquito *Culex pipiens*. *Parasitology* 28, 453–486. doi: 10.1017/S0031182000022666

Hoerauf, A., Mand, S., Adjei, O., Fleischer, B., and Büttner, D. W. (2001). Depletion of *Wolbachia* endobacteria in *Onchocerca volvulus* by doxycycline and microfilaridermia after ivermectin treatment. *Lancet* 357, 1415–1416. doi: 10.1016/S0140-6736(00)04581-5

Igarashi, A. (1978). Isolation of a Singh's *Aedes albopictus* cell clone sensitive to dengue and chikungunya viruses. *J. Gen. Virol.* 40, 531–544. doi: 10.1099/0022-1317-40-3-531

Jung, K., Fried, L., Behr, S., and Heermann, R. (2012). Histidine kinases and response regulators in networks. *Curr. Opin. Microbiol.* 15, 118–124. doi: 10.1016/j.mib.2011.11.009

Kambris, Z., Cook, P. E., Phuc, H. K., and Sinkins, S. P. (2009). Immune activation by life-shortening *Wolbachia* and reduced filarial competence in mosquitoes. *Science* 326, 134–136. doi: 10.1126/science.1177531

Krafsur, A. M., Ghosh, A., and Brelsfoard, C. L. (2020). Phenotypic response of *Wolbachia pipientis* in a cell-free medium. *Microorganisms* 8:60. doi: 10.3390/microorganisms8071060

Kramer, M. J., and Gordon, F. B. (1971). Ultrastructural analysis of the effects of penicillin and chlortetracycline on the development of a genital tract *Chlamydia*. *Infect. Immun.* 3, 333–341. doi: 10.1128/iai.3.2.333-341.1971

Kuno, G. (1983). Cultivation of mosquito cell lines in serum-free media and their effects on dengue virus replication. *In Vitro* 19, 707–713. doi: 10.1007/BF02628962

Landmann, F., Bain, O., Martin, C., Uni, S., Taylor, M. J., and Sullivan, W. (2012). Both asymmetric mitotic segregation and cell-to-cell invation are required for stable germline transmission of *Wolbachia* in filarial nematodes. *Biol. Open* 1, 536–547. doi: 10.1242/bio.2012737

Li, S.-J., Ahmed, M. Z., Lv, N., Shi, P.-Q., Wang, X.-M., Huang, J.-L., et al. (2017). Plantmediated horizontal transmission of *Wolbachia* between whiteflies. *ISME J.* 11, 1019–1028. doi: 10.1038/ismej.2016.164

Lin, M., and Rikihisa, Y. (2003). *Ehrlichia chaffeensis* and *Anaplasma phagocytophilum* lack genes for lipid a biosynthesis and incorporate cholesterol for their survival. *Infect. Immun.* 71, 5324–5331. doi: 10.1128/iai.71.9.5324-5331.2003

Liu, S., Yang, W., Li, Y., and Sun, C. (2023). Fetal bovine serum, an important factor affecting the reproducibility of cell experiments. *Sci. Rep.* 13:1942. doi: 10.1038/s41598-023-29060-7

Lodish, H., Berk, A., Zipursky, S. L., Matsudaira, P., Baltimore, D., and Darnell, J. (2000). "5.2 purification of cells and their parts" in Molecular cell biology (4th edition). ed. W. H. Freeman (New York: Palgrave Macmillan).

Luukkonen, A., Brummer-Korvenkontio, M., and Renkonen, O. (1973). Lipids of cultured mosquito cells (*Aedes albopictus*). Comparison with cultured mammalian fibroblasts (BHK 21 cells). *Biochim. Biophys. Acta* 326, 256–261. doi: 10.1016/0005-2760(73)90251-8

Makepeace, B. L., Rodgers, L., and Trees, A. J. (2006). Rate of elimination of *Wolbachia pipientis* by doxycycline in vitro increases following drug withdrawal. *Antimicrob. Agents Chemother.* 50, 922–927. doi: 10.1128/aac.50.3.922-927.2006

Marriott, A. E., Dagley, J. L., Hegde, S., Steven, A., Fricks, C., DiCosty, U., et al. (2023). Dirofilariasis mouse models for heartworm preclinical research. *Front. Microbiol.* 14:1208301. doi: 10.3389/fmicb.2023.1208301

Mascher, T., Helmann, J. D., and Unden, G. (2006). Stimulus perception in bacterial signal-transducing histidine kinases. *Microbiol. Mol. Biol. Rev.* 70, 910–938. doi: 10.1128/mmbr.00020-06

Matsumoto, A., and Manire, G. P. (1970). Electron microscopic observations on the effects of penicillin on the morphology of *Chlamydia psittaci*. *J. Bacteriol.* 101, 278–285. doi: 10.1128/jb.101.1.278-285.1970

McGraw, E. A., Merritt, D. J., Droller, J. N., and O'Neill, S. L. (2002). *Wolbachia* density and virulence attenuation after transfer into a novel host. *Proc. Natl. Acad. Sci. USA* 99, 2918–2923. doi: 10.1073/pnas.052466499

McMeniman, C. J., Lane, A. M., Fong, A. W., Voronin, D. A., Iturbe-Ormaetxe, I., Yamada, R., et al. (2008). Host adaptation of a *Wolbachia* strain after long-term serial passage in mosquito cell lines. *Appl. Environ. Microbiol.* 74, 6963–6969. doi: 10.1128/AEM.01038-08

McNulty, S. N., Foster, J. M., Mitreva, M., Dunning Hotopp, J. C., Martin, J., Fischer, K., et al. (2010). Endosymbiont DNA in endobacteria-free filarial nematodes indicates ancient horizontal genetic transfer. *PLoS One* 5:e11029. doi: 10.1371/journal.pone.0011029

Min, K. T., and Benzer, S. (1997). *Wolbachia*, normally a symbiont of Drosophila, can be virulent, causing degeneration and early death. *Proc. Natl. Acad. Sci. USA* 94, 10792–10796. doi: 10.1073/pnas.94.20.10792

Mitrophanov, A. Y., and Groisman, E. A. (2008). Signal integration in bacterial two-component regulatory systems. *Genes Dev.* 22, 2601–2611. doi: 10.1101/gad.1700308

Moreira, L. A., Iturbe-Ormaetxe, I., Jeffery, J. A., Lu, G., Pyke, A. T., Hedges, L. M., et al. (2009). A *Wolbachia* symbiont in *Aedes aegypti* limits infection with dengue, chikungunya, and plasmodium. *Cell* 139, 1268–1278. doi: 10.1016/j.cell.2009.11.042

Nevalainen, L. B., Layton, E. M., and Newton, I. L. G. (2023). *Wolbachia* promotes its own uptake by host cells. *Infect. Immun.* 91:e0055722. doi: 10.1128/iai.00557-22

Nikaido, H. (1989). Outer membrane barrier as a mechanism of antimicrobial resistance. *Antimicrob. Agents Chemother.* 33, 1831–1836. doi: 10.1128/aac.33.11.1831

Omsland, A., Beare, P. A., Hill, J., Cockrell, D. C., Howe, D., Hansen, B., et al. (2011). Isolation from animal tissue and genetic transformation of *Coxiella burnetii* are facilitated by an improved axenic growth medium. *Appl. Environ. Microbiol.* 77, 3720–3725. doi: 10.1128/aem.02826-10

Omsland, A., Cockrell, D. C., Fischer, E. R., and Heinzen, R. A. (2008). Sustained axenic metabolic activity by the obligate intracellular bacterium *Coxiella burnetii*. *J. Bacteriol.* 190, 3203–3212. doi: 10.1128/jb.01911-07

Omsland, A., Cockrell, D. C., Howe, D., Fischer, E. R., Virtaneva, K., Sturdevant, D. E., et al. (2009). Host cell-free growth of the Q fever bacterium *Coxiella burnetii*. *Proc. Natl. Acad. Sci. USA* 106, 4430–4434. doi: 10.1073/pnas.0812074106

Omsland, A., Sager, J., Nair, V., Sturdevant, D. E., and Hackstadt, T. (2012). Developmental stage-specific metabolic and transcriptional activity of *Chlamydia trachomatis* in an axenic medium. *Proc. Natl. Acad. Sci. USA* 109, 19781–19785. doi: 10.1073/pnas.1212831109

Park, I.-S., Kim, J.-H., and Kim, B.-G. (2005). The effects of ftsZ mutation on the production of recombinant protein in *Bacillus subtilis*. *Appl. Microbiol. Biotechnol.* 69, 57–64. doi: 10.1007/s00253-005-1953-y

Perkins, H. R. (1969). Specificity of combination between mucopeptide precursors and vancomycin or ristocetin. *Biochem. J.* 111, 195–205. doi: 10.1042/bj1110195

Pilhofer, M., Aistleitner, K., Biboy, J., Gray, J., Kuru, E., Hall, E., et al. (2013). Discovery of chlamydial peptidoglycan reveals bacteria with murein sacculi but without FtsZ. *Nat. Commun.* 4:2856. doi: 10.1038/ncomms3856

Rasgon, J. L., Gamston, C. E., and Ren, X. (2006). Survival of *Wolbachia pipientis* in cell-free medium. *Appl. Environ. Microbiol.* 72, 6934–6937. doi: 10.1128/AEM.01673-06

Rolls, M. M., Marquardt, M. T., Kielian, M., and Machamer, C. E. (1997). Cholesterol-independent targeting of Golgi membrane proteins in insect cells. *Mol. Biol. Cell* 8, 2111–2118. doi: 10.1091/mbc.8.11.2111

Ruang-areerate, T., Kittayapong, P., McGraw, E. A., Baimai, V., and O'Neill, S. L. (2004). *Wolbachia* replication and host cell division in *Aedes albopictus*. *Curr. Microbiol.* 49, 10–12. doi: 10.1007/s00284-003-4245-8

Sandoz, K. M., Beare, P. A., Cockrell, D. C., and Heinzen, R. A. (2016). Complementation of arginine Auxotrophy for genetic transformation of *Coxiella burnetii* by use of a defined axenic medium. *Appl. Environ. Microbiol.* 82, 3042–3051. doi: 10.1128/aem.00261-16

Scherler, A., Jacquier, N., Kebbi-Beghdadi, C., and Greub, G. (2020). Diverse stress-inducing treatments cause distinct aberrant body morphologies in the *Chlamydia*-related bacterium, *Waddlia chondrophila*. *Microorganisms* 8:89. doi: 10.3390/microorganisms8010089

Serbus, L. R., and Sullivan, W. (2007). A cellular basis for *Wolbachia* recruitment to the host germline. *PLoS Path.* 3:e190. doi: 10.1371/journal.ppat.0030190

Singh, K. R. P. (1967). Cell cultures derived from larvae of *Aedes Albopictus* (SKUSE) and *Aedes aegypti*. *Curr. Sci.* 36, 506–507.

Slatko, B. E., Luck, A. N., Dobson, S. L., and Foster, J. M. (2014). *Wolbachia* endosymbionts and human disease control. *Mol. Biochem. Parasitol.* 195, 88–95. doi: 10.1016/j.molbiopara.2014.07.004

Slatko, B. E., Taylor, M. J., and Foster, J. M. (2010). The *Wolbachia* endosymbiont as an anti-filarial nematode target. *Symbiosis* 51, 55–65. doi: 10.1007/s13199-010-0067-1

Stepkowski, T., and Legocki, A. B. (2001). Reduction of bacterial genome size and expansion resulting from obligate intracellular lifestyle and adaptation to soil habitat. *Acta Biochim. Pol.* 48, 367–381. doi: 10.18388/abp.2001_3922

Stock, A. M., Robinson, V. L., and Goudreau, P. N. (2000). Two-component signal transduction. *Annu. Rev. Biochem.* 69, 183–215. doi: 10.1146/annurev.biochem.69.1.183

Storm, D. R., and Strominger, J. L. (1973). Complex formation between bacitracin peptides and isoprenyl pyrophosphates. The specificity of lipid-peptide interactions. *J. Biol. Chem.* 248, 3940–3945. doi: 10.1016/S0021-9258(19)43823-4

Suginaka, H., Blumberg, P. M., and Strominger, J. L. (1972). Multiple penicillin-binding components in *Bacillus subtilis*, *Bacillus cereus*, *Staphylococcus aureus*, and *Escherichia coli*. *J. Biol. Chem.* 247, 5279–5288. doi: 10.1016/S0021-9258(20)81102-8

Taylor, M. J., Ford, L., Hoerauf, A., Pfarr, K., Foster, J. M., Kumar, S., et al. (2012). "Drugs and targets to perturb the symbiosis of *Wolbachia* and filarial nematodes" in *Parasitic Helminths: Targets, Screens, Drugs and Vaccines*. ed. C. R. Caffrey Weinheim, Germany: Wiley-VCH. 251–265.

Taylor, M. J., and Hoerauf, A. (2001). A new approach to the treatment of filariasis. *Curr. Opin. Infect. Dis.* 14, 727–731. doi: 10.1097/00001432-200112000-00011

Teixeira, L., Ferreira, A., and Ashburner, M. (2008). The bacterial symbiont *Wolbachia* induces resistance to RNA viral infections in *Drosophila melanogaster*. *PLoS Biol.* 6:e2. doi: 10.1371/journal.pbio.1000002

Tipper, D. J. (1979). Mode of action of beta-lactam antibiotics. *Rev. Infect. Dis.* 1, 39–53. doi: 10.1093/clinids/1.1.39

Turner, J. D., Langley, R. S., Johnston, K. L., Egerton, G., Wanji, S., and Taylor, M. J. (2006). *Wolbachia* endosymbiotic bacteria of Brugia malayi mediate macrophage tolerance to TLR-and CD40-specific stimuli in a MyD88/TLR2-dependent manner. *J. Immun.* 177, 1240–1249. doi: 10.4049/jimmunol.177.2.1240

Turner, J. D., Langley, R. S., Johnston, K. L., Gentil, K., Ford, L., Wu, B., et al. (2009). *Wolbachia* lipoprotein stimulates innate and adaptive immunity through toll-like receptors 2 and 6 to induce disease manifestations of filariasis. *J. Biol. Chem.* 284, 22364–22378. doi: 10.1074/jbc.M901528200

Uribe-Alvarez, C., Chiquete-Félix, N., Morales-García, L., Bohórquez-Hernández, A., Delgado-Buenrostro, N. L., Vaca, L., et al. (2018). *Wolbachia pipientis* grows in *Saccharomyces cerevisiae* evoking early death of the host and deregulation of mitochondrial metabolism. *Microbiol. Open* 8:675. doi: 10.1002/mbo3.675

Velez, I. D., Tanamas, S. K., Arbelaez, M. P., Kutcher, S. C., Duque, S. L., Uribe, A., et al. (2023). Reduced dengue incidence following city-wide wMel *Wolbachia* mosquito releases throughout three Colombian cities: interrupted time series analysis and a prospective case-control study. *PLoS Negl. Trop. Dis.* 17:e0011713. doi: 10.1371/journal.pntd.0011713

Vollmer, J., Schiefer, A., Schneider, T., Jülicher, K., Johnston, K. L., Taylor, M. J., et al. (2013). Requirement of lipid II biosynthesis for cell division in cell wall-less *Wolbachia*, endobacteria of arthropods and filarial nematodes. *Int. J. Med. Microbiol.* 303, 140–149. doi: 10.1016/j.ijmm.2013.01.002

Werren, J. H., Baldo, L., and Clark, M. E. (2008). *Wolbachia*: master manipulators of invertebrate biology. *Nat. Rev. Microbiol.* 6, 741–751. doi: 10.1038/nrmicro1969

White, P. M., Pietri, J. E., Debec, A., Russell, S., Patel, B., and Sullivan, W. (2017). Mechanisms of horizontal cell-to-cell transfer of *Wolbachia* spp. in *Drosophila melanogaster*. *Appl. Environ. Microbiol.* 83:16. doi: 10.1128/aem.03425-16

Wu, M., Sun, L. V., Vamathevan, J., Riegler, M., Deboy, R., Brownlie, J. C., et al. (2004). Phylogenomics of the reproductive parasite *Wolbachia pipientis* wMel: a streamlined genome overrun by mobile genetic elements. *PLoS Biol.* 2:e69. doi: 10.1371/journal.pbio.0020069

Zhang, Y., Chen, L., Kondethimmanahalli, C., Liu, H., and Ganta, R. R. (2021). Protein and DNA biosynthesis demonstrated in host cell-free phagosomes containing *Anaplasma phagocytophilum* or *Ehrlichia chaffeensis* in axenic media. *Infect. Immun.* 89:20. doi: 10.1128/iai.00638-20

Zug, R., and Hammerstein, P. (2012). Still a host of hosts for *Wolbachia*: analysis of recent data suggests that 40% of terrestrial arthropod species are infected. *PLoS One* 7:e38544. doi: 10.1371/journal.pone.0038544

frontiers | Frontiers in Microbiology

TYPE Original Research
PUBLISHED 22 August 2024
DOI 10.3389/fmicb.2024.1416057

OPEN ACCESS

EDITED BY
Naser Safaie,
Tarbiat Modares University, Iran

REVIEWED BY
Astrid Collingro,
University of Vienna, Austria
Sergio López-Madrigal,
Indiana University Bloomington, United States

*CORRESPONDENCE
Didier Bouchon
didier.bouchon@univ-poitiers.fr

RECEIVED 11 April 2024
ACCEPTED 15 July 2024
PUBLISHED 22 August 2024

CITATION
Grève P, Moumen B and Bouchon D (2024) Three feminizing *Wolbachia* strains in a single host species: comparative genomics paves the way for identifying sex reversal factors. *Front. Microbiol.* 15:1416057. doi: 10.3389/fmicb.2024.1416057

Three feminizing *Wolbachia* strains in a single host species: comparative genomics paves the way for identifying sex reversal factors

Pierre Grève, Bouziane Moumen and Didier Bouchon*

Université de Poitiers, Ecologie et Biologie des Interactions, UMR CNRS 7267, Poitiers, France

Introduction: Endosymbiotic bacteria in the genus *Wolbachia* have evolved numerous strategies for manipulating host reproduction in order to promote their own transmission. This includes the feminization of males into functional females, a well-studied phenotype in the isopod *Armadillidium vulgare*. Despite an early description of this phenotype in isopods and the development of an evolutionary model of host sex determination in the presence of *Wolbachia*, the underlying genetic mechanisms remain elusive.

Methods: Here we present the first complete genomes of the three feminizing *Wolbachia* (*w*VulC, *w*VulP, and *w*VulM) known to date in *A. vulgare*. These genomes, belonging to *Wolbachia* B supergroup, contain a large number of mobile elements such as WO prophages with eukaryotic association modules. Taking advantage of these data and those of another *Wolbachia*-derived feminizing factor integrated into the host genome (*f* element), we used a comparative genomics approach to identify putative feminizing factors.

Results: This strategy has enabled us to identify three prophage-associated genes secreted by the Type IV Secretion System: one ankyrin repeat domain-containing protein, one helix-turn-helix transcriptional regulator and one hypothetical protein. In addition, a latrotoxin-related protein, associated with phage relic genes, was shared by all three genomes and the *f* element.

Conclusion: These putative feminization-inducing proteins shared canonical interaction features with eukaryotic proteins. These results pave the way for further research into the underlying functional interactions.

KEYWORDS

***Wolbachia*, feminization, *Armadillidium vulgare*, genomics, isopod crustacean, effectors, *f* element**

Introduction

The central role of host-symbiont interactions in the biology, ecology and evolution of the biotic world is now well recognized, which has led to the popularization of the holobiont concept (McFall-Ngai et al., 2013; Bordenstein and Theis, 2015). There are therefore no macroorganisms that do not host symbionts. Among these symbionts is *Wolbachia pipientis* (hereafter *Wolbachia*), a bacterium originally described in the mosquito *Culex pipiens* (Hertig and Wolbach, 1924). Since

then, many studies have shown that this maternally inherited intracellular symbiont, belonging to the order Rickettsiales of the Alphaproteobacteria, exhibited exceptional traits. It is the most widespread endosymbiont in the animal world, representing a very wide diversity of strains infecting ~50% of arthropods and several nematodes (Zug and Hammerstein, 2012; Kaur et al., 2021). This enormous genetic diversity is reflected in the classification of *Wolbachia* where at least 17 phylogenetic supergroups (named A-F, H-Q and S; Supergroups A and B being the most numerous) can be identified to date (Kaur et al., 2021). Furthermore, these bacteria, often referred to as reproductive parasites, have attracted attention for the diversity of phenotypes they induce in their terrestrial arthropod hosts. Indeed, one of the main characteristics of *Wolbachia* is its remarkable ability to interfere with the reproduction of its hosts, through four main phenotypes, to optimize its own transmission, which has earned it the title of master manipulator (Werren et al., 2008).

Cytoplasmic Incompatibility (CI) represents the most common *Wolbachia*-induced phenotype (Werren et al., 2008; Landmann, 2019), resulting in embryonic death in crosses between infected males and uninfected females. It has been observed in Insecta as well as in Acari and in Isopoda (Landmann, 2019). The molecular basis of CI has recently been demonstrated by the identification of two genes, *cifA* and *cifB*, from the Eukaryotic Association Module (EAM) of *Wolbachia*'s prophage WO (Shropshire and Bordenstein, 2019; Shropshire et al., 2020). The other three *Wolbachia*-induced phenotypes lead to sex ratio biases in the host. Male-killing (MK), first described in the ladybird *Adalia bipunctata*, results in males death favoring female survival (Hurst et al., 1999; Fukui et al., 2015). As for CI, a candidate MK gene (termed WO-mediated killing *wmk*) was identified in the EAM of WO prophage (Perlmutter et al., 2019). *Wolbachia*-induced parthenogenesis (PI) was first described in *Trichogramma* Hymenoptera (Stouthamer et al., 1990) in which infected females can produce daughters from unfertilized eggs (Ma and Schwander, 2017). Recently, two putative PI-inducing factors (PifA and PifB) has been identified, also localized in EAM (Fricke and Lindsey, 2024). *Wolbachia*-induced feminization, which consists in the feminization of genetic males, is a reproductive manipulation that has been widely described in isopods and also observed in two insect species (Hiroki et al., 2002; Negri et al., 2006; Bouchon et al., 2008). However, the mechanisms involved are different: in butterflies, the feminizing *Wolbachia* interact with the master regulator genes that control sex determination, whereas in crustaceans, they interact with the hormonal regulatory genes (Kageyama et al., 2017; Herran et al., 2021).

The first description of feminization in isopods was due to the pioneering work on the pill bug *Armadillidium vulgare* (Juchault et al., 1974). The identification of *Wolbachia* (*w*VulC strain) as the feminizing factor came later (Rousset et al., 1992; Bouchon et al., 1998). Two additional *Wolbachia* (*w*VulM and *w*VulP strains), have been identified in *A. vulgare* (Cordaux et al., 2004; Verne et al., 2007). In *A. vulgare*, genetically (ZZ) male embryos carrying *Wolbachia* inherited from the mother develop into functional females morphologically undistinguishable from genetic females (ZW). Several studies have suggested that feminization of genetic males results from inhibition of androgenic gland differentiation that produce the androgenic hormone [review in Bouchon et al. (2008) and Herran et al. (2020)]. As males inverted in females produce female-biased broods, all *Wolbachia*-infected females were ZZ individuals in natural populations (Juchault et al., 1993). This situation has given rise to strong genetic conflicts with major evolutionary consequences for interactions between *Wolbachia* and *A. vulgare* (Rigaud, 1997). In particular, it has been suggested that a feminizing factor called *f* element, derived from the *w*VulC *Wolbachia* strain, was at the origin of a new W-type chromosome (Juchault and Mocquard, 1993). This hypothesis has recently been verified, as the *f* element corresponds to the insertion of a large part of the *Wolbachia w*VulC chromosome into the *A. vulgare* genome (Leclercq et al., 2016). It has also been shown that *w*VulC and the *f* element never co-occur (Durand et al., 2023).

Until now, genomic data on *Wolbachia* endosymbionts from woodlice has been very fragmentary, with only two genome assemblies. One is *w*Con, known to induce CI in *Cylisticus convexus* (Moret et al., 2001; Badawi et al., 2018). The other one available in databases is an assembly of 10 contigs from the genome of *w*VulC. In this study, we performed a comparative genomic analysis of the three *Wolbachia* strains identified so far in *A. vulgare*. We obtained the complete genomes of *w*VulC, *w*VulM using both short and long read sequencing and *w*VulP strains using long read sequencing. Our data shed light on the evolution of *Wolbachia* strains in *A. vulgare* and highlighted putative candidate feminization genes.

Materials and methods

Host lineages and DNA extraction

Four *A. vulgare* lineages were used in this study: a *Wolbachia*-free lineage (called BF) collected in 1967 in Nice (France), a *w*VulC-infected lineage (called ZN) collected in 1991 in Celles-sur-Belle (France), a *w*VulM-infected lineage (called BI) collected in 1999 in Méry sur Cher (France) and a *w*VulP-infected lineage (called CP) collected in 2007 in Poitiers (France) (Cordaux et al., 2004; Verne et al., 2007). These lineages have since been stably maintained in the laboratory, at 20°C under natural photoperiod, with food *ad libitum* (dead lime leaves and carrots). Controlled rearing on a standard diet homogenizes the diversity of the gut microbiota and no other sex-parasitic bacteria have been identified (Dittmer et al., 2014; Dittmer and Bouchon, 2018).

The sex ratios observed in the lineages were recorded each year. The *Wolbachia*-free BF lineage is used as a control for genetic sex determination as attempts to cure individuals with antibiotics have been unsuccessful (Rigaud and Juchault, 1998). The proportion of males was determined in each brood over 5 years and visualized by boxplots using arcsine transformations. Comparison of the mean male ratio was performed in R version 4.3.2 (R Core Team, 2023) through a generalized linear mixed model with host lineage as fixed effect and clutch size and year as random effects. Assessment of the model was performed using the *performance* package (Lüdecke et al., 2021).

DNA extraction was carried out by homogenizing ovaries of 30 to 50 infected females with a Dounce tissue grinder B in a PBS solution supplemented with sucrose (0.25 M) and L-glutamine (5 mM) which allow the cells to be crushed but not the nuclei. Large fragments were removed by passing the solution through a 5 µm filter. The remaining nuclei were pelleted after centrifugation at 200 x g (4°C, 20 min.). The supernatant was then centrifuged at 4100 x g to pellet the bacteria (4°C, 20 min.). DNA purification was performed using the Qiagen DNeasy Blood and Tissue Kit as follows. The *Wolbachia*-enriched pellet was first resuspended in 180 µL ATL buffer plus 20 µL of proteinase K (10 mg/mL) and incubated for 1 h at 54°C. After treatment with RNase A (0.2 µg/µL, at 37°C for 15 min.), DNA was recovered following the manufacturer's instructions. DNA quantification was

performed using a Nanodrop 1000 spectrophotometer (Thermo Scientific) and the Qubit 2.0 fluorimeter (Invitrogen).

Genome sequencing, assembly, and annotation

Library preparation for nanopore sequencing was performed using the protocols for the SQK-LSK109 Ligation Sequencing Kit (Oxford Nanopore Technologies, UK). Libraries were sequenced on R9.4.1 flowcells on a MinION sequencer for 48 h. Base-calling was performed using the Guppy base-caller software v4.2.2 (Oxford Nanopore Technologies, UK) using high-accuracy mode, with a quality score cut-off of 9 and minimum read length filter set of 200. Adapters were trimmed with Porechop 0.2.4[1] on the basecalled reads.

Prior to Illumina sequencing, targeted genome enrichment was used for *w*VulC and *w*VulM strains as described in Geniez et al. (2012). Illumina libraries were prepared and samples were sequenced at HudsonAlpha Genome Sequencing Center (Hunstville AL35806, USA) on the Illumina HiSeq 2000 (Geniez, 2013).

These two sequencing strategies led to 2,001,609 and 2,581,285 Nanopore long reads and 72,894,720 and 64,625,816 Illumina reads for *w*VulC and *w*VulM, respectively. The *w*VulP genome was assembled from 1,795,327 Nanopore long reads.

Bacterial genome assembly was performed using the long reads assembler Flye v2.8.1 (Kolmogorov et al., 2019). The best assembly was chosen based on the expected size and circular status of the genome, after comparing meta and single mode assembly using several overlap parameters. The resulting assemblies were first polished with Nanopore reads using Nanopolish v0.14.0 (Loman et al., 2015). Additional Illumina polishing using Medaka v1.6.0 was performed on assemblies for *w*VulC and *w*VulM strains after assessing the quality of Illumina reads with FastQC v0.11.9 (Andrews, 2010) and removing adapters and quality filtering using Fastp v0.21.0 (Chen et al., 2018). Genome completeness was assessed by using the Benchmarking Universal Single-Copy Orthologs (BUSCO) pipeline v5.4.6 and the rickettsiales_odb10 database (Manni et al., 2021). The polished assemblies with the highest BUSCO score were selected for further analysis.

The genomes were functionally annotated using the NCBI Prokaryotic Genome Annotation Pipeline (PGAP) (Tatusova et al., 2016).

Comparative genomics and phylogenomics

The three *Wolbachia* genomes were presented starting with *dnaA* gene as for wMel (Wu et al., 2004) and most other *Wolbachia* genomes. Comparisons between the three genomes were performed and visualized using FastANI v1.3.3 (Jain et al., 2018) implemented in the NanoGalaxy platform (de Koning et al., 2020) and Mauve v2.4.0 progressive alignments (Darling et al., 2010) using Circos software v0.69–9 (Krzywinski et al., 2009).

Comparisons of *w*VulC genome with a previous draft genome (GCA_001027565.1) and the *w*VulC inserts identified into the pill bug nuclear genome (Leclercq et al., 2016) were performed using FastANI v1.3.3 (Jain et al., 2018) implemented in the NanoGalaxy platform (de Koning et al., 2020).

Orthofinder v2.5.5 (Emms and Kelly, 2019) implemented in the NanoGalaxy platform (de Koning et al., 2020) was used to identify orthologous sequences and infer the species tree from 29 *Wolbachia* genomes belonging to the six A-F supergroups. Four hundred and fourteen single-copy proteins were aligned with MAFFT v. 7.505 (Katoh et al., 2017). The concatenated alignment was used for phylogenetic reconstruction by maximum-likelihood with the iQtree 2.1.2 (Minh et al., 2020) implemented in the NanoGalaxy platform (de Koning et al., 2020). The best model (JTT + F + R6) was selected by ModelFinder (Kalyaanamoorthy et al., 2017), implemented in IQ-TREE, based on Bayesian Information Criterion. Branch support was assessed using ultrafast bootstrap with 1,000 replicates. The resulting consensus tree was drawn using iTol v6.8.2 (Letunic and Bork, 2021).

Analyses of *Wolbachia* prophage regions, mobile elements, T4SS, effectors, and biotin operon

Prophage regions (WO prophages) in the three *Wolbachia* assemblies were estimated using the PHASTEST web server (Wishart et al., 2023). WO phage genomic maps were drawn using the *gggenes* package v.0.5.1 in R (Wilkins, 2023). EAMs (Bordenstein and Bordenstein, 2016; Bordenstein and Bordenstein, 2022) were identified by annotating CDSs flanking or located within the PHASTEST-predicted prophage regions through BLASTp queries using the NCBI clustered protein database. Alignment of the large serine recombinase of the WO prophages was generated with MAFFT v. 7.505 (Katoh et al., 2017) and the phylogeny was inferred by maximum likelihood using the iQtree server v1.6.12 (Trifinopoulos et al., 2016). The best substitution model (JTT + F + G4) was selected by ModelFinder (Kalyaanamoorthy et al., 2017) and tree topology was tested by ultrafast bootstrap (Minh et al., 2013) of 1,000 iterations.

Insertion sequence (IS) elements were determined in the three genomes using the ISEScan v1.7.2.3 (Xie and Tang, 2017) implemented in the NanoGalaxy platform (de Koning et al., 2020). Candidate intron sequences were identified using RASTtk pipeline (Brettin et al., 2015) and BLASTp searches against the Database for Bacterial Group II Introns (Candales et al., 2012). The comparative location of mobile elements between the three genomes was represented using Circos software v0.69–9 (Krzywinski et al., 2009).

Prediction of intact secretion systems and secreted proteins was performed using EffectiveDB queries v5.2 (Eichinger et al., 2016).

Genes of the biotin operon were identified by BLASTn using the sequences previously identified in the *w*VulC draft genome. Comparison of the structure of the operons in the three *Wolbachia* genomes was visualized using *gggenes* R package (Wilkins, 2023).

Results

Sex ratio bias in *Wolbachia*-infected host lineages

The *Wolbachia* strains sequenced in this study have been isolated from females belonging to three different lineages of *A. vulgare,* which

1 https://github.com/rrwick/Porechop

exhibit sex ratio biases (Figure 1; Supplementary Table S1; Supplementary Figure S1). The male proportions (mean ± se) were 19.71 ± 0.03% for ZN lineage (infected with *w*VulC), 23.45 ± 0.03% for BI lineage (infected with *w*VulM), and 19.96 ± 0.03% for CP lineage (infected with *w*VulP) with no significant differences. The greater variance in male proportions in the infected lineages reflected variations in the *Wolbachia* transmission rate (Figure 1). In contrast, the uninfected BF control line showed a balanced sex ratio of close to 50% (49.9 ± 0.01%).

Comparative genomics of the three feminizing strains

The three *Wolbachia* genomic sequences were assembled into single molecules of 1,711,483 bp for the *w*VulC strain, 1,638,198 bp for the *w*VulM strain and 1,566,000 bp for the *w*VulP strain, with a G + C content ranging from 34.8 to 34.9% (Figure 2). The two *w*VulC and *w*VulM genomes were circularized and even though *w*VulP was not completely closed, it was a genome of the same quality assembled into a single scaffold. The general features of the genomes are presented in Table 1. Their sizes were comparable to those of other *Wolbachia* strains inducing reproductive phenotypes (Sun et al., 2001), with each genome containing between 1,282 and 1,484 protein-coding genes (Table 1). The *w*VulC, *w*VulM, and *w*VulP assemblies were assessed by BUSCO, showing a very small number of fragmented and missing genes (Table 1), resulting in high scores (99.8, 99.5 and 98.3% for *w*VulC, *w*VulM, and *w*VulP, respectively). The three genomes were very similar as shown by the high ANI value obtained from pairwise comparisons (> 98%, Supplementary Table S2). However, numerous genomic rearrangements have been identified, particularly in the *w*VulP genome (Figures 2, 3; Supplementary Figures S2A–C). Orthofinder analysis of the three genomes revealed 1,094 orthogroups in common out of 1,259 (Supplementary Table S3). *w*VulC and *w*VulM shared 126 orthogroups whereas each of these strains shared only 15 and 10 orthogroups with *w*VulP. Finally, one to 11 specific orthogoups corresponded to four, three and twenty-four specific genes of *w*VulC, *w*VulM, and *w*VulP, respectively (Supplementary Table S3). The *w*VulC specific genes were two hypothetical protein paralogs (wVulc_000316 and wVulc_000382; 100% amino acid identity) and two DUF4815 domain-containing protein paralogs (wVulc_000708 and wVulc_001210; 99.7% amino acid identity). In *w*VulM, the three specific genes were paralogs of recombinase (wVulm_000691, wVulm_001174 and wVulm_001253; 100% amino acid identity) corresponding to the third recombinase in the core module prophage WOVulM1_2, WOVulM3_4, and WOvulM5_6 (see below). As to the *w*VulP-specific genes, five were duplicated mobile elements (IS and group II introns), one was a duplicated phage tail protein, one was a duplicated SET domain-containing protein, one was a duplicated ANK gene and three were duplicated hypothetical proteins. Each duplicated gene was 100% identical with the exception of the phage tail paralogs which were 77% identical (Supplementary Table S3).

Furthermore, comparison of the complete, closed *w*VulC genome with a previous draft genome obtained by Sanger sequencing showed a high ANI value of 99.9%. The non-collinearity between these two sequences was due to artificial joining of the 10 contigs in the Sanger draft assembly (Supplementary Figure S3). Comparison of the *w*VulC genome was also carried out with the *f* element (derived from *w*VulC) which comprised nine scaffolds spanning 3.13 Mb (Leclercq et al., 2016). This showed a high average nucleotide identity of 99.6% (Supplementary Figure S4) but revealed numerous genomic rearrangements indicating multiple insertion and duplication events of the *f* element in the *A. vulgare* genome.

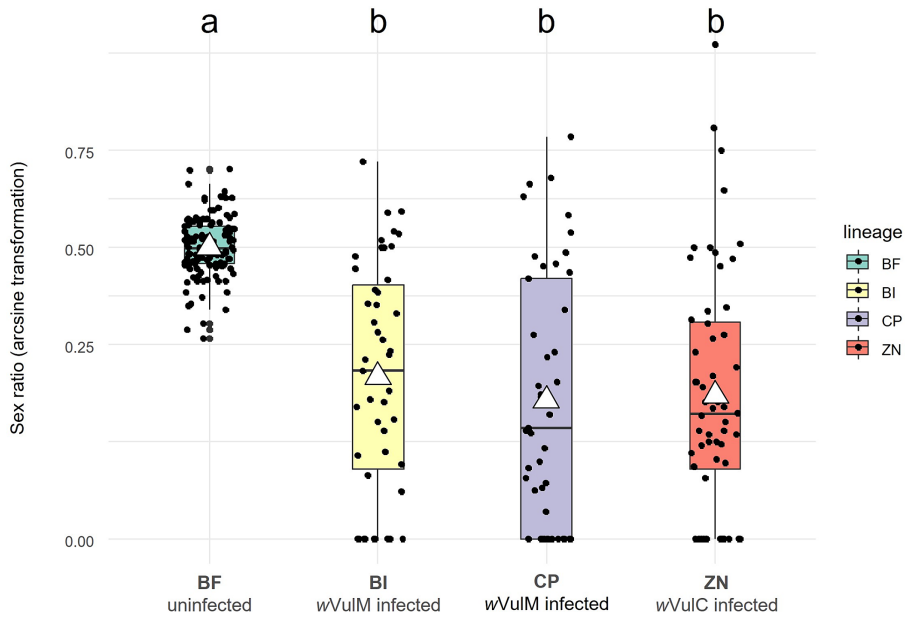

FIGURE 1
Boxplot showing sex ratios (proportion of males) of the four laboratory lineages of *A. vulgare* (BF, BI, CP, and ZN) over five years. BF lineage is uninfected whereas BI, CP, and ZN lineages are infected with *w*VulM, *w*VulP, and *w*VulC *Wolbachia* strains, respectively. Sex ratios have been arcsine transformed. White triangles correspond to mean values. Statistical analysis was performed using a Generalized Linear Mixed Model (conditional R-squared = 0.222).

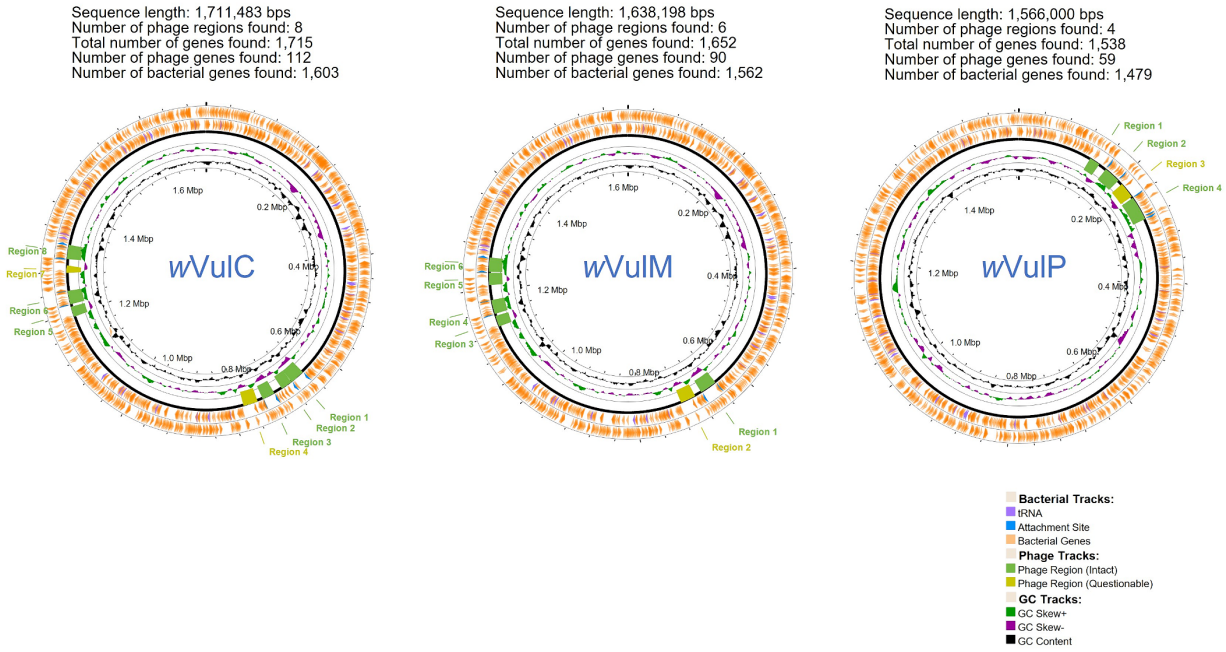

FIGURE 2
Graphical representation of the circular genome map of the three *Wolbachia* strains *w*VulC, *w*VulM, *w*VulP. PHASTEST description, from the outside to the center: (1) Predicted CDSs transcribed in the counterclockwise direction. (2) Predicted CDSs transcribed in the clockwise direction. (3) Predicted phage regions (intact and questionable). (4) GC skew. (5) GC content.

TABLE 1 Comparative statistics and BUSCO assessment of the three *Wolbachia* genomes *w*VulC, *w*VulM, and *w*VulP isolated from *A. vulgare*.

	Strain		
	*w*VulC	*w*VulM	*w*VulP
Length (bp)	1,711,483	1,638,198	1,566,000
%GC	34.91	34.84	34.85
Genes	1,708	1,649	1,535
CDS	1,666	1,607	1,494
Protein-coding genes	1,448	1,386	1,282
Pseudogenes	218	221	212
rRNA	3	3	3
tRNA	35	35	34
ncRNA	3	3	3
tmRNA	1	1	1
BUSCO assessment			
Complete and Single	362	361	356
Duplicated	1	1	2
Fragmented	0	1	4
Missing	1	1	2

Phylogenomic relationships

The phylogenomic position of the three *Wolbachia* from *A. vulgare* was determined by comparison with 26 publicly available and annotated *Wolbachia* genomes, including five from supergroup A, thirteen from supergroup B, three from supergroup C, three from supergroup D and one for supergroup E and F strains from various host species (Supplementary Table S4). A total of 415 single-copy gene ortholog clusters were used to reconstruct the phylogenomic tree (Figure 4; Supplementary Table S5). The three *Wolbachia* strains isolated from *A. vulgare* belonged to the supergroup B, forming a separated clade, with *w*VulC and *w*VulM being closely related (bootstrap support 100, Figure 4).

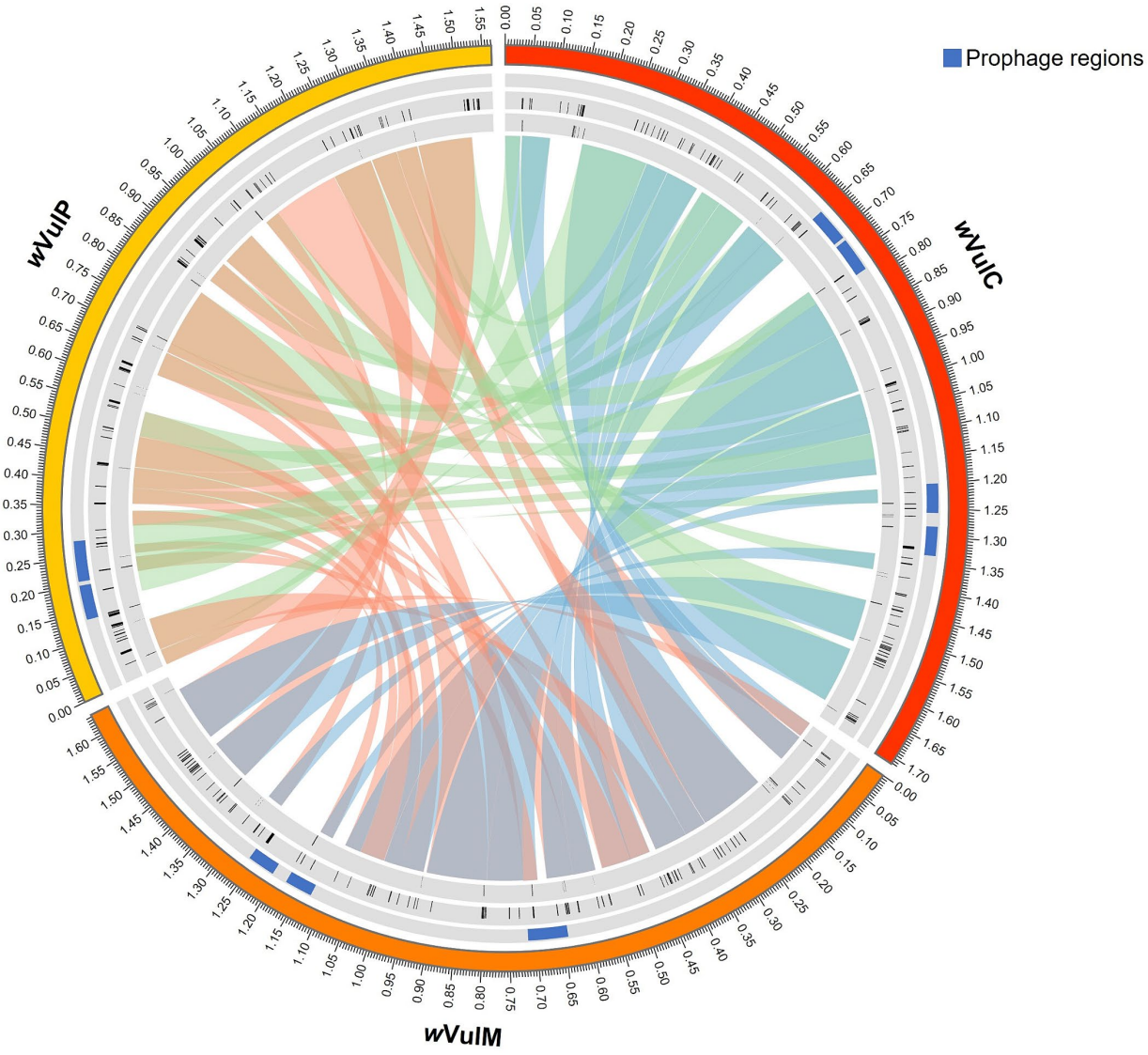

FIGURE 3
Circos representation of the progressive Mauve alignment and mobilome of the three *Wolbachia* strains (*w*VulC, *w*VulM, *w*VulP) of *A. vulgare*. First inner ring: WO prophage regions in blue. Second inner ring: complete IS elements in black. Third inner ring: group II introns in black.

Mobilome identification

ISEScan predicted 105, 103 and 77 complete IS elements from 10 different families in *w*VulC, *w*VulM and *w*VulP, respectively, representing around 8% of the genome size (Supplementary Table S6). The IS families most represented in the three genomes, when complete sequences were taken into account, were IS110, IS256, IS3, IS4, IS5 with the exception of *w*Vulp where IS3 had only one representative. Specific IS clusters were ISNCY_191 for *w*VulC, IS110_236, new_343 and IS4_64 for *w*VulP (Supplementary Table S6). Many IS element positions coincided with regions where synteny breaks occurred (Figure 3), suggesting that IS elements may have contributed to the genomic rearrangements among the three genomes.

RASTtk annotations and BLASTp searches against the Database for Bacterial Group II Introns showed 29, 25 and 29 group II intron-associated genes in *w*VulC, *w*VulM and *w*VulP, respectively (Supplementary Table S7). The sum of the lengths of these genes was 17,892 bp, 14,556 bp, and 13,332 bp respectively, representing 0.9–1% of the genome size. The distribution of these introns was not homogeneous and regions of several successive genes were observed (Figure 3). As with IS elements, these group II introns are often located in regions of synteny breaks (Figure 3).

Prophage regions were identified by PHASTEST and BLASTp searches using annotated CDS, both in predicted and flanking regions. The results were also manually curated using the recently published WO prophage annotations (Bordenstein and Bordenstein, 2022). This strategy enabled us to extend the regions initially predicted by PHASTEST (Figure 2), notably by including EAMs (Bordenstein and Bordenstein, 2016). Functional annotations of these regions were shown in Supplementary Table S8.

We identified four complete prophage regions in *w*VulC measuring 70,719 bp (WOVulC1_2), 57,601 bp (WOVulC3_4), 55,840 bp (WOVulC5_6), and 64,755 bp (WOVulC7_8). WOVulC1_2 and WOVulC3_4 formed a continuous region with two sets of all

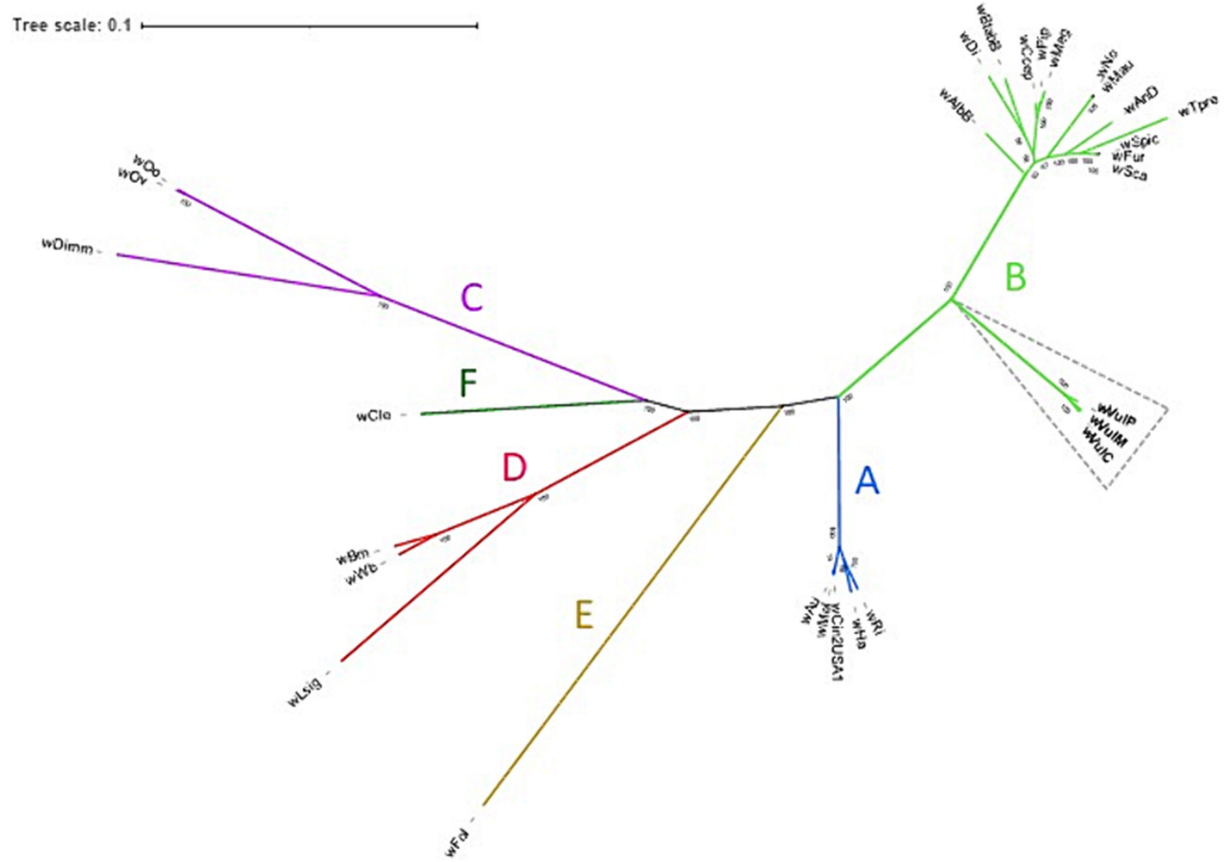

FIGURE 4
Unrooted maximum-likelihood consensus tree based on concatenated alignments of 415 single-copy orthologues in 29 *Wolbachia* genomes. Newly assembled genomes are shown in bold. Tree scale bar represents substitutions per site. Bootstrap support values (> 50%) from 1,000 replicates are shown at the edges.

core prophage modules separated by two EAMs (Figure 5A; Supplementary Table S8). Three complete prophage regions were identified in *w*VulM measuring 63,169 bp (WOVulM1_2), 55,822 bp (WOVulM3_4) and 63,644 bp (WOVulM5_6) (Figure 5B; Supplementary Table S8). In *w*VulP, only two prophage regions of 63,842 bp (WOVulP1_2) and 75,199 bp (WOVulP3_4) were found (Figure 5C; Supplementary Table S8). They formed a continuous prophage region separated by two EAMs. In addition, WOVulP3_4 is interrupted by an internal EAM. Overall, these prophages accounted for around 10% of each genome. The core genomic content of each prophage WO began with a large serine recombinase and ended with a patatin. With the exception of prophages WOVulC3_4 and WOVulP1_2, the majority of prophages contained two different serine recombinase genes, the second downstream of the first. In tandem to the latter, a third short recombinase was specifically present in all three prophage regions of *w*VulM (Figure 5B; Supplementary Table S8).

Four distinct WO variants (sr1WO-sr4WO) have been described based on the large serine recombinase phylogeny and core module synteny (Bordenstein and Bordenstein, 2022). Based on the phylogeny of the first serine recombinase genes marking the start of the core modules, classification of the WO prophages of the three *Wolbachia* strains showed that they all belonged to the sr3WO group (Figure 6). The general structure of these prophages corresponded to the module synteny described for sr3WO variants, which includes an internal core prophage WO region flanked by EAM genes (Bordenstein and Bordenstein, 2022). Although the synteny of genes within each core module was consistent with the sr3WO organization (i.e., connector/baseplate, head, replication & repair, tail), variations between prophages were observed, some due to the presence of mobile elements (transposases and group II introns). These variations were consistent with the phylogenetic position established with the serine recombinase gene, with the closest prophages sharing a better synteny. In particular, strong collinearity is observed between the closely related core prophage modules WOVulC1_2 and WOVulM1_2, WOVulC5_6 and WOVulM_3_4 and WOVulC7_8 and WOVulM5_6 (Figure 6). In contrast, WOVulP3_4 had a particular structure with 3 EAM-like regions, including one region localized within the core prophage module (Figure 5C).

Using PHASTEST, we also examined the wCon assembly of 237 contigs and identified one large serine recombinase (locus wCon_01757) in an incomplete prophage region due to the end of the contig. This sequence was added in the phylogenetic tree, showing a putative prophage belonging to sr1WO cluster (Figure 6). This could reflect different prophage features depending on the *Wolbachia* reproductive phenotype.

Genes encoding proteins containing an ankyrin repeat domain (ANK genes) were localized in each core prophage module with a

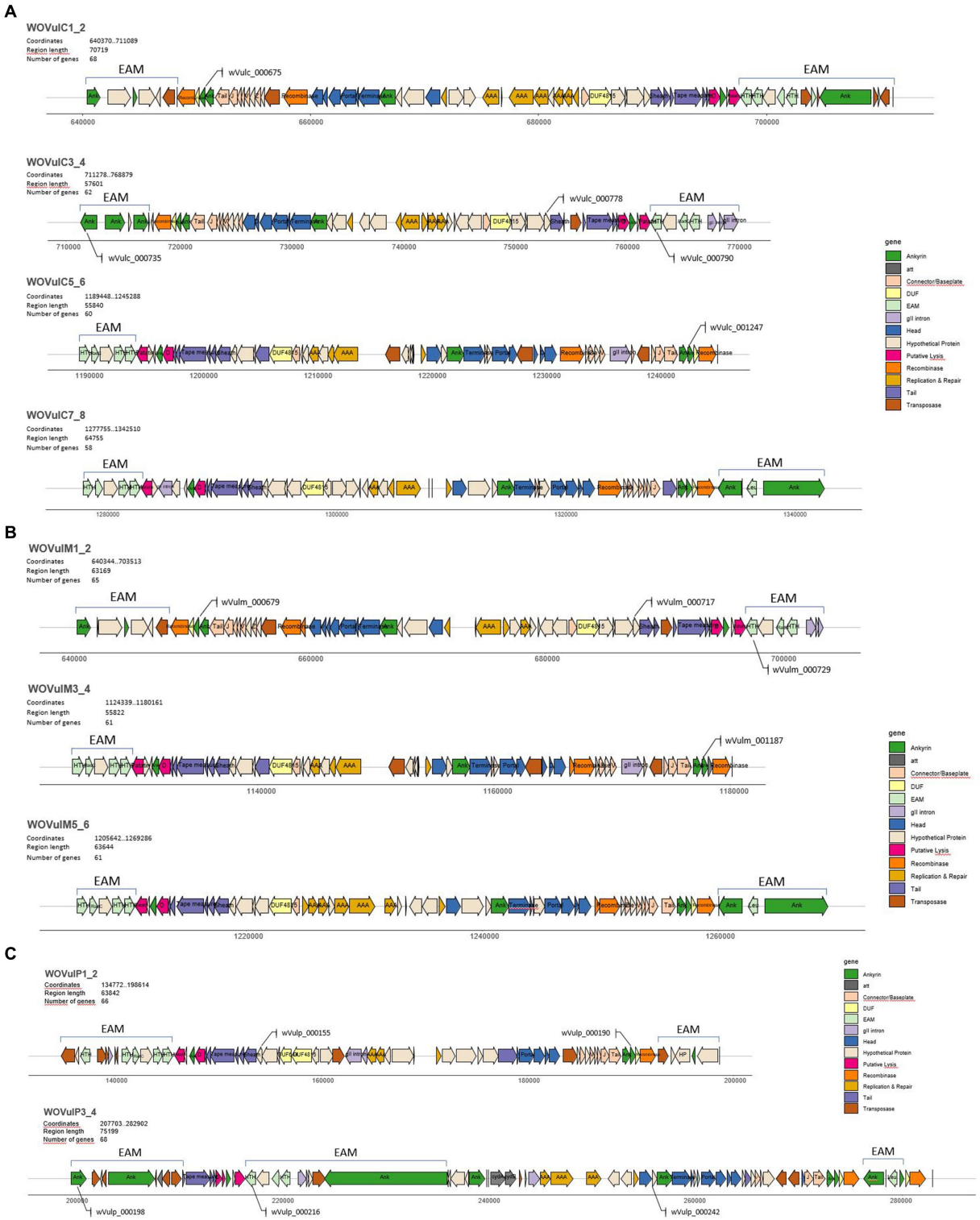

FIGURE 5
Annotation of prophage regions of *w*VulC, *w*VulM, *w*VulP by PHASTEST and manual curation. **(A)** *w*VulC harbors four intact prophage regions (70.7 kb, 57.6 kb, 55.8 kb and 64.8 kb). **(B)** *w*VulM harbors three intact prophage regions (63.2 kb, 55.8 kb, and 63.6 kb) and **(C)** *w*VulP harbors two intact prophage regions (63.8 kb and 75.2 kb). Lengths of the graphs are proportional to the size (bp) of the prophages. The legends indicate the color coding of the modules. EAM-like regions are highlighted. Locus tags of T4SS effectors are indicated.

highly conserved arrangement in the three *Wolbachia* genomes (Figures 5A–C). At the beginning of the module, two contiguous ANK genes were located just after a DUF2924 domain-containing protein downstream of the large serine recombinase, then toward the middle, one ANK located just after the phage terminase large subunit gene (except for WOVulP1_2) and at the end of the module, one ANK gene

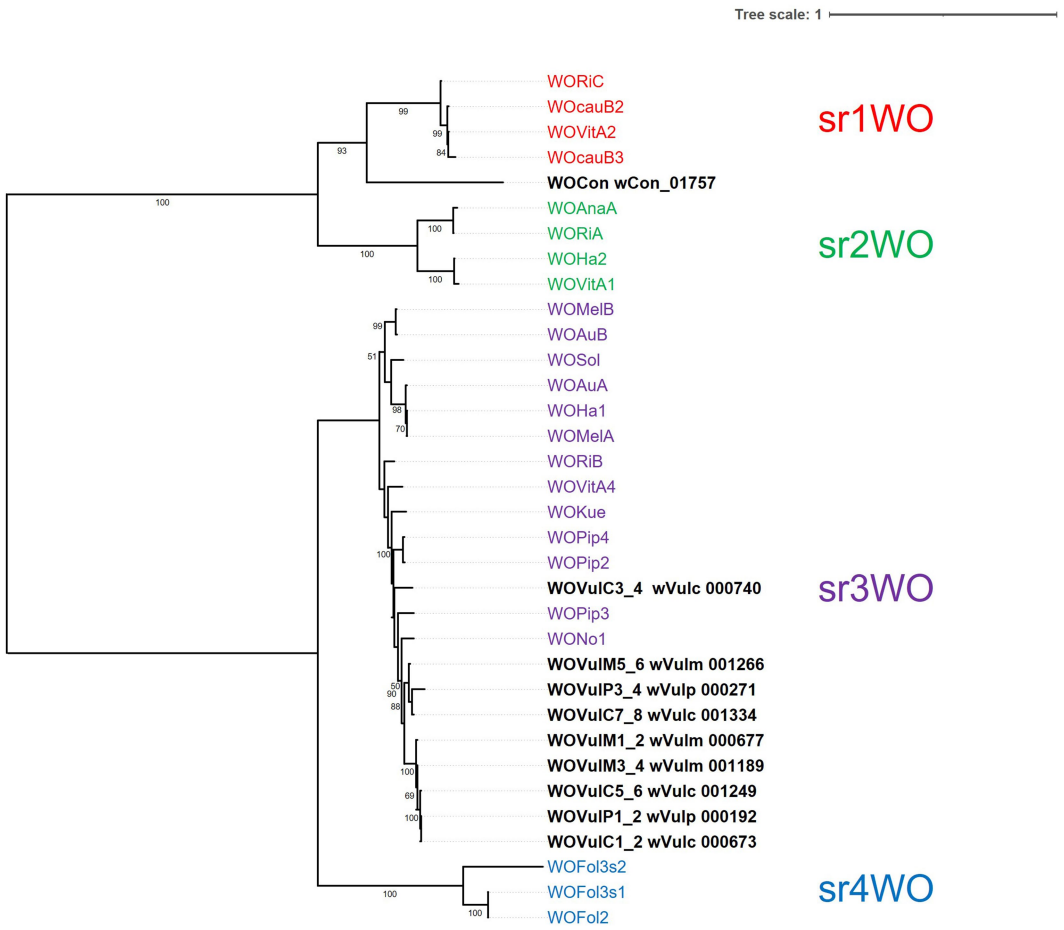

FIGURE 6
Maximum-likelihood phylogeny based on the large serine recombinase of *Wolbachia* prophage regions. The phylogeny was generated from 34 sequences (630 amino acid sites) using the JTT + F + G4 model. The tree was rooted at the mid-point. Tree scale bar represents substitutions per site.

located between a patatin-like phospholipase and a holin-like protein constituting a lytic cassette (Bordenstein and Bordenstein, 2022).

Regions similar to EAMs previously reported in other *Wolbachia* genomes were also observed in *w*VulC, *w*VulM and *w*VulP prophage regions (Figures 5A–C). These EAM-like regions contained genes encoding transcription regulators (helix-turn-helix HTH domain-containing protein) and ankyrin repeat proteins that might be involved in the host manipulation (Bordenstein and Bordenstein, 2022). *RadC* genes encoding JAB domain-containing proteins were also identified in EAMs from WOVulC1_2, WOVulC3_4, WOVulM1_2, and WOVulP1_2 prophages. Finally, mobile elements (Group II introns and transposases) were also frequent in EAMs. Here again, there was a strong collinearity between the EAMs of closely related prophages, with most EAMs being very similar in composition and structure, with the exception of those of WOVulP3_4.

T4SS and phage-related putative feminizing effectors

The two operons characteristic of the T4SS were identified in the three genomes (Supplementary Table S9). The *virB3-virB6* operon was constituted of *virB3*, *virB4* and four *virB6* genes. The *virB8-virD4* operon was constituted of *virB8*, *virB9*, *virB10*, *virB11* and *virD4* genes. All these genes were highly conserved between the three genomes (96 to 100% of amino acid identity) with the exception of the second duplicated virB6 (83% amino acid identity).

The prediction of secreted proteins showed a high number of potential T4SS effectors among the total number of effectors: 97 (92 unique genes) out of 1,530 for *w*VulC, 100 (96 unique genes) out of 1,474 for *w*VulM and 83 (82 unique genes) out of 1,353 for *w*VulP (Supplementary Table S9). Among these T4SS effectors, particular attention was paid to genes present in the prophage regions and common to all three genomes and the *f* element. This led to the identification of genes encoding an ankyrin-repeat protein, an HTH-domain protein and a hypothetical protein.

Ten ANK genes were shared by all the three *Wolbachia* strains, including one which is localized in the core prophage modules. It is represented by two homologs (wVulc_000675 and wVulc_001247) in WOVulC1_2 and WOVulC5_6, two homologs (wVulm_000679 and wVulm_001187) in WOVulM1_2 and WOVulM3_4, and one homolog (wVulp_000190) in WOVulP1_2 (Figures 5A–C). These five ANK genes were highly conserved, from 98.9 to 100% amino-acid identity (Supplementary Table S9). Moreover, seven homologs of this gene were also present in the *f* insert (Wxf_00764, Wxf_00854, Wxf_01743, Wxf_02351, Wxf_02903, Wxf_0307 and, Wxf_03107)

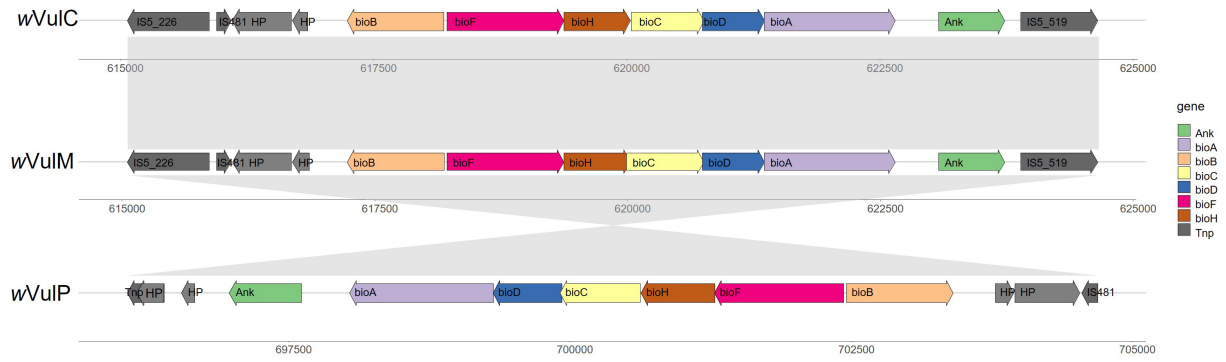

FIGURE 7
Comparison of the biotin operon of *w*VulC, *w*VulM, and *w*VulP and flanking regions showing collinearity.

with an amino acid identity ranging from 77.2 to 97.4% (Supplementary Table S9).

A gene encoding a transcriptional regulator (HTH domain protein) shared by all three strains and the *f* element, was also predicted as a T4SS effector (Supplementary Table S9). This gene was localized in the EAMs of the WOVulC3_4 (wVulc_000790), WOVulM1_2 (wVulm_000729) and WOVulP3_4 (wVulp_000216) prophages (Figures 5A–C). Interestingly, five homologs (Wxf_00824, Wxf_00827, Wxf_00907, Wxf_01690 and Wxf_02404) of this gene were annotated in the largest scaffold of the *f* element. Conservation of residues of these sequences was low (around 37% of amino acid identity) but the HTH domain is still present.

Finally, 18 hypothetical proteins common to all three genomes were also predicted as T4SS effectors. Among them, one with 100% amino acid identity, was located in the WOVulC3_4, WOVulM1_2, and WOVulP1_2 (wVulc_000778, wVulm_000717 and wVulp_000155 respectively) (Supplementary Table S8; Figures 5A–C). This hypothetical protein was also identified in the *f* element, with a degree of conservation of around 70% (Supplementary Table S8; Wxf_00810, Wxf_00893, Wxf_01704, and Wxf_02390).

Another T4SS effector shared by the three genomes, a latrotoxin-related protein (wVulc_001131, wVulm_001070, and wVulp_000491) might be involved in host-*Wolbachia* interactions. This gene present a latrotoxin C-terminal domain characteristic of the latrotoxins of the black widow spider (Grishin, 1998). It was not located in the prophages but in a region containing phage relic, just two CDS upstream a phage terminase large subunit encoding gene. Interestingly, one homolog (Wxf_02470; 90.4% amino acid identity) was also present in the *f* element (Supplementary Table S9).

Conservation of the biotin pathway

A highly conserved biotin operon was identified in the three *Wolbachia* genomes (Figure 7), suggesting a potential supply of this vitamin by the bacteria, although this role is probably not essential given the non-obligatory nature of the association. This operon contained the six canonical biotin genes [*bioB*, *bioF*, *bioH*, *bioC*, *bioD* and *bioA;* (Gerth and Bleidorn, 2016)] which are highly conserved (99 to 100% amino acid sequence identity). This operon was inverted in the *w*VulP genome. The structure of the nearby flanking regions was also conserved, bordered by IS elements and containing two identical hypothetical proteins and one ankyrin gene (97 to 99% amino acid sequence identity) (Figure 7). In *w*VulC and *w*VulM, this region was bordered by identical IS5 elements belonging to two different clusters (IS5_226 and IS5_519) (Supplementary Table S6).

Discussion

Although studies on *Wolbachia* have gained momentum since the late 1990s, the mechanisms involved in host-*Wolbachia* interactions are still poorly understood (Landmann, 2019). Indeed, the search for bacterial factors responsible for the different phenotypes induced by *Wolbachia* has long been the subject of intensive study (Rice et al., 2017; Carpinone et al., 2018). The sequencing of numerous *Wolbachia* genomes over the last twenty years has provided access to all the bacterium's genetic information and opened up the way to comparative genomic analyses (Kaur et al., 2021). The presence of prophages in most of these genomes was of particular interest, as these mobile elements could carry effectors of the feminizing phenotype of this endosymbiont, in particular genes involved in mutualistic relationships or in the manipulation of host reproduction (Bordenstein and Bordenstein, 2016). Although in most *Wolbachia* genomes the prophages appeared to be sedentary, it has been shown in the parasitoid wasp *Nasonia vitripennis* that they can still be active and propagate (Bordenstein et al., 2006). In this *Wolbachia* strain, it was also shown that the sedentarized copies had undergone numerous rearrangements (Bordenstein and Bordenstein, 2022). In the end, these prophage analyses identified the *cifA* and *cifB* genes as well as the *wmk* gene, involved in CI and MK, respectively (LePage et al., 2017; Perlmutter et al., 2019). While the genome of the *Wolbachia* strain of *Trichogramma* contained only degenerated prophage regions (Lindsey et al., 2016), two putative PI factors were identified in a degraded EAM (Fricke and Lindsey, 2024).

In this study, we performed a comparative genomic analysis of the three *Wolbachia* strains *w*VulC, *w*VulM, and *w*VulP infecting *A. vulgare*, focusing on the identification of putative feminizing factors.

Since their collection from the wild, the three *Wolbachia*-infected lineages of *A. vulgare* were stably maintained in the laboratory. The sex-ratio of the progenies as well as the presence of the corresponding *Wolbachia* strains in female genitors were regularly monitored by

diagnostic PCR. Although multiple strains may coexist in *A. vulgare* populations, no individual has been found to be multiinfected (Verne et al., 2007). Moreover, feminization led to cytoplasmic sex determination in natural populations where all infected *Wolbachia*-infected females were ZZ reversed males (Juchault et al., 1993; Rigaud et al., 1997). This implies variations in offspring sex ratios as a function of *Wolbachia* transmission rate, as it has been demonstrated in *A. vulgare* populations infected with either *w*VulC or *w*VulM (Cordaux et al., 2004). In the three laboratory lineages of *A. vulgare*, male biased ratio may be thus observed in some offspring of infected females. Far from being surprising, this confirms that these females were necessarily ZZ inverted males, which can produce male biased offspring when the *Wolbachia* transmission rate falls below 50%. In contrast, the balanced male ratio observed in the uninfected control line was the result of chromosomal sex determination with individuals of ZZ and WZ genotypes. All these observations confirmed the feminizing phenotype of the three *Wolbachia* strains of *A. vulgare*, leading to transmission rate-dependent cytoplasmic sex determination.

Consistent with previous single gene (16S rDNA, *ftsZ*, *wsp*, and *GroE*) phylogenies (Bouchon et al., 1998; Cordaux et al., 2001; Wiwatanaratanabutr et al., 2009), as well as multi-locus sequence typing data (Sicard et al., 2014), *w*VulC, *w*VulM and *w*VulP belonged to the supergroup B forming a separated clade in phylogenomic analyses (bootstrap support 100, Figure 3). This reflected a general pattern of *Wolbachia* from terrestrial isopods, which clustered in a monophyletic clade (referred as the *Oni* clade for Oniscidea; (Cordaux et al., 2001)) within supergroup B. This result also confirmed the genetic proximity of the *w*VulC and *w*VulM strains.

The *w*VulC, *w*VulM, and *w*VulP genomes were between 1.7 and 1.6 Mb in size and contained between 1,700 and 1,500 genes, corresponding to a coding density of 75 to 67% (Table 1). These characteristics correlated with genome size, *w*VulC being the largest and *w*VulP the smallest. They were also consistent with the features of the B supergroup of *Wolbachia* which are known to have a larger number of genes than the A supergroup (Vancaester and Blaxter, 2023). The genome length of the three strains was among the longest known for *Wolbachia* (Scholz et al., 2020). These sizes were highly correlated with the extent of the mobilome (including prophages, IS elements and group II introns), representing a total of 415,545 bp for *w*VulC, 338,395 bp for *w*VulM and 287,918 bp for *w*VulP, i.e., from 24 to 18% of the genome. The high density of mobile and repeated elements in the three genomes, in particular IS belonging to the IS110 and IS256 families, could explain the genomic rearrangements observed (Figure 3; Supplementary Figures S2A–C). The copy number of group II introns was also one of the highest reported in *Wolbachia* genomes (Leclercq et al., 2011). These features were, to varying degrees, common to *Wolbachia* reproductive parasites, as demonstrated by the first sequenced genomes (Wu et al., 2004; Klasson et al., 2008, 2009). Particular attention was paid to the *w*VulC strain, as a Sanger sequence assembly (GCA_001027565.1) and *w*VulC inserts identified into the pill bug nuclear genome are publicly available (Leclercq et al., 2016). Consistently, genomic comparisons have confirmed that locally collinear blocks are conserved, but that significant genomic rearrangements are probably due to the impact of the mobilome, in particular the IS and group II introns (Figure 3; Supplementary Figures S2A–C, S3, S4). This is particularly obvious in the comparison with the nine scaffolds of the *f* element where, despite a high average nucleic identity, collinearity remains low. This pattern was also evident when only the longest scaffold of 2,798,100 bp (LYUU01002088.1) is included in the comparison (Leclercq et al., 2016). It has long been known that *Wolbachia* can recombine with several implications on the evolution of these bacteria (Jiggins et al., 2001; Werren and Bartos, 2001). Based on single gene analyses, two recombination events have been shown in feminizing *Wolbachia* and more specifically in *w*VulP (Verne et al., 2007) and complete pathway for homologous recombination pathway was found in *w*VulC (Badawi et al., 2014). *Wolbachia*'s great ability for recombination could therefore explain the genomic plasticity observed.

A complete biotin operon has been identified in the three genomes, suggesting that these *Wolbachia* strains were capable of synthesizing B vitamins. It was also conserved in the *f* element inserted into the genome of *A. vulgare*. Although generally absent from most *Wolbachia* genomes, a complete biotin operon has been identified in around fifteen *Wolbachia* strains (Beliavskaia et al., 2023). However, it has been shown that only the *Wolbachia w*Cle from the bedbug *Cimex lectularius* supplies B vitamins to its host (Nikoh et al., 2014). This beneficial symbiosis was not demonstrated in the other strains harboring the biotin operon. For example, biotin supplementation remains unlikely in the *w*CfeF strain of *Ctenochephalides felis*, since the *bioB* gene is frameshifted (Beliavskaia et al., 2023). Similarly, the *w*Oo strain of *Onchocerca ochengi* has a completely disrupted biotin operon (Darby et al., 2012; Nikoh et al., 2014). It therefore seems that this operon undergoes evolutionary events leading to its degradation, presumably due to the absence of a selective advantage for the host. In the particular case of *A. vulgare*, although the biotin operon is complete in the three *Wolbachia* genomes and also in the *f* element, and may supply B vitamins as well, the absence of an obligate association with the host may indicate that this contribution is not essential. Finally, the presence of IS and transposases in the flanking regions of the operon is consistent with an acquisition by lateral gene transfer, supported by the lack of congruence between the phylogenies of the biotin genes and the *Wolbachia* (Nikoh et al., 2014; Driscoll et al., 2020; Beliavskaia et al., 2023). Accordingly, phylogenetic analyses support the hypothesis of at least three independent acquisition of the biotin operon by Rickettsiales (Driscoll et al., 2020; Lefoulon et al., 2020).

Multiple copies of the WO prophages were identified in the genomes of all three feminizing strains. However, copy number differs from genome to genome, *w*VulC having 4 copies representing a total of 248,915 bp (including the EAM-like regions), followed by *w*VulM with three copies representing 182,635 bp and *w*VulP with only 2 copies representing 139,041 bp. This copy number contributes to the size of the genomes, with *w*VulC being the largest and *w*VulP the smallest, representing between 9 and 10% of the total. Multiple phage infections have been observed in many *Wolbachia* strains from different arthropod host species (Gavotte et al., 2006). In particular, PCR amplification of the minor capsid gene *orf7* showed the presence of 4 to 6 copies of the WO phage in the terrestrial isopods *A. vulgare*, *Porcellionides pruinosus*, and *Porcellio dilatatus* (Braquart-Varnier et al., 2005). In agreement with our genomic data, the four copies of the *orf7* amplified in *A. vulgare*, corresponded to the capsid assembly proteins (wVulc_000689, wVulc_000754, wVulc_001230, and wVulc_0001319), annotated, respectively, in the core regions of prophages WOVulC1_2, WOVulC3_4, WOVulC5_6, and WOVulC7_8 of the *w*VulC genome.

The prophage loci were not restricted to the core modules of the prophage regions, and WO-like Islands (Bordenstein and

Bordenstein, 2022) corresponding to "relic" prophages have been annotated in all three genomes. Due to the presence of numerous hypothetical proteins, it was difficult to define the precise boundaries of these regions. However, a general pattern seemed to emerge for the three genomes with two main WO-like islands. The first island comprised two portal proteins associated with two ankyrin repeat proteins in *w*VulC (from wVulc_000522 to wVulm_000527) and in *w*VulM (from wVulm_000522 to wVulm_000527) and only one portal protein and one ANK gene in *w*VulP (from wVulp_000412 to wVulp_000415). The second WO-like island had a structure comprising a terminase large subunit, an ANK gene, a hypothetical protein, a DNA modification methylase, a Holliday junction resolvase and a RhuM domain containing protein. This module was colinear in all three genomes, ranging from wVulc_000813 to wVulc_000818 in *w*VulC, from wVulm_000751 to wVulm_000756 in *w*VulM, and, with reverse synteny, from wVulp_000974 to wVulp_000969 in *w*VulP. These results were in line with those observed in various *Wolbachia* strains where RhuM virulence genes are located close to prophage genes encoding Holliday junction resolvase and DNA methylase proteins (Kent and Bordenstein, 2010; Fallon, 2020). Finally, single prophage genes encoding proteins of head, baseplate and tail, flanked either by hypothetical proteins or mobile elements (group II intron and IS) were annotated in the three genomes. These regions are too short to constitute genomic islands, but they testify to WO prophage degradation processes in *Wolbachia* genomes (Bordenstein and Bordenstein, 2022). Apart from this common pattern, a small cluster of prophage WO-like genes was identified in *w*VulP. This region (wVulp_000778 to wVulp_000780), flanked by two hypothetical proteins, contained genes encoding one head-tail connector protein, one DUF3168 domain-containing protein and one phage tail tube protein.

The T4SS is an efficient way for *Wolbachia* to transfer DNA and/or proteins to eukaryotic cells (Lindsey, 2020). Indeed, putative T4SS substrates have been already described in *Wolbachia* (Sheehan et al., 2016; Rice et al., 2017; Carpinone et al., 2018). This secretion system, consisting of *virB* and *virD* genes clustered at two loci, was conserved in *Wolbachia* reproductive parasites (Pichon et al., 2009). In line with this work, the presence of these two operons were confirmed in the three genomes. The ubiquitous presence of these operons in *Wolbachia* strains strongly suggested that they were functional, and led to an extensive search for potential substrates (Rice et al., 2017; Carpinone et al., 2018). Off all the hundred proteins identified as putatively secreted by the T4SS, three were located in the prophage regions of all three strains and had homologs in the *f* element: one ankyrin repeat domain-containing protein, one HTH domain-containing protein and one hypothetical protein. ANK motifs in bacterial proteins were thought to mimic eukaryotic protein–protein interactions, enabling bacteria to interact with host factors (Jernigan and Bordenstein, 2014). T4SS-secreted ANK proteins that interact with host cells has already been identified in bacteria such as *Legionella pneumophila*, *Anaplasma phagocytophilum* or *Ehrlichia chaffeenis* (Rikihisa and Lin, 2010; Yu et al., 2018). They were therefore ideal candidates as symbiotic factors in reproductive parasitism. In addition, protein–protein interactions were demonstrated between an MK inducer, Oscar, a *Wolbachia* protein containing ankyrin repeats, and the Masc protein involved in both masculinization and dosage compensation in the moth *Ostrinia furnacalis* (Katsuma et al., 2022). The induced reduction in Masc accumulation led to the inhibition of masculinization and the failure of dosage compensation, resulting in the death of male offspring (Katsuma et al., 2022). Another MK factor (SpAID), a protein with ANK repeats and a OTU (ovarian tumor) deubiquitinase domain, has been identified in *Spiroplasma poulsonii* (Harumoto and Lemaitre, 2018). The authors proposed a model in which the OTU domain induced nuclear localization, allowing SpAID to interact through its ANK domain with the Male Specific Lethal complex, thereby disrupting dosage compensation that led to male-killing phenotype. Interestingly, this is the only ANK protein identified in the *Spiroplasma* genome. In *w*Mel genome, a MK gene candidate (*wmk*) encoding two HTH, XRE family DNA-binding domains has been identified in the EAM of the prophage WOMelB, next to the *cifA* and *cifB* genes that are involved in CI (Perlmutter et al., 2019). Homologs of *wmk* were also found in prophage EAMs from different MK strains. This protein likely interacts with DNA through its two HTH domains and could act as a transcriptional regulator potentially also targeting dosage compensation mechanisms. Based on this work, the ANK gene and the HTH-domain gene identified in this study were therefore be strong putative candidates for feminization. These genes were present, as expected, both in the feminizing *Wolbachia* genomes and in the *f* element, the latter also inducing a feminizing phenotype in the host into whose genome it has been inserted (Leclercq et al., 2016). In the three feminizing strains, the ANK gene was part of the WO prophage core modules whereas the HTH domain-containing gene was localized in an EAM, like the *Wolbachia* CI and MK factors (LePage et al., 2017; Shropshire et al., 2020). Nevertheless, putative factors inducing PI in parasitoid wasps have been identified in *Wolbachia* prophage relics (Fricke and Lindsey, 2024). This is why we also paid attention to a latrotoxin-related protein localized near isolated phage genes, evoking phage relics and present in all feminizing strains and the *f* element. After processing of the latrotoxin C-terminal domain, the toxin encoded by this gene may be able to form ion-permeable membrane pores leading to host cell lysis, as does the latrotoxin of widow spiders venom in the cells of their prey (Zhang et al., 2012). Spider latrotoxins appear to have been acquired by lateral transfer from a bacterial endosymbiont (Bordenstein and Bordenstein, 2016). Such toxins could also be involved in the feminizing phenotype. Indeed, previous data have shown that *Wolbachia* do not directly target the androgenic hormone neither its receptors, but more likely the nerve centres that control the activity of the receptors (Juchault and Legrand, 1985; Herran et al., 2021). The toxin could therefore target these nerve centers and disrupt androgen receptor function.

Overall, our study highlighted three strong candidates for feminization of *A. vulgare* males. Further experiments need to be performed to confirm that these candidates disrupt the androgenic hormone pathway. Indeed, these genes need to be expressed during embryonic development, at the stage where the androgenic hormone expression that induces male differentiation is inhibited in infected animals. Besides, the *Wolbachia* load increases just at this stage, defining the window of action enabling the bacteria to counteract the

masculinizing effect of the androgen hormone and induce the development of male embryos into females (Herran et al., 2020). Monitoring the expression of these candidate genes during the development of the offspring of *Wolbachia*-infected females could provide further support for our hypotheses. To decipher the mechanisms of feminization, it will be necessary to identify host targets with which these candidates can interact.

Data availability statement

The *Wolbachia* genomes of *A. vulgare* recovered in this study were deposited in GenBank (https://www.ncbi.nlm.nih.gov/genbank) under BioProjects PRJNA1093130, PRJNA1093132, and PRJNA1093134 and the genomes are available under the accession numbers CP156068, CP156069, and CP156070.

Ethics statement

Ethical approval was not required for the study involving animals in accordance with the local legislation and institutional requirements because animals are invertebrates and are not subject to any ethical declaration.

Author contributions

PG: Conceptualization, Investigation, Methodology, Formal analysis, Writing – original draft, Writing – review & editing. BM: Data curation, Methodology, Formal analysis, Writing – review & editing. DB: Conceptualization, Funding acquisition, Investigation, Methodology, Formal analysis, Writing – original draft, Writing – review & editing.

Funding

The author(s) declare that financial support was received for the research, authorship, and/or publication of this article. This work was funded by the 2015–2020 State-Region Planning Contracts (CPER), European Regional Development Fund (FEDER) (BiodivUP project, coordinator DB), and intramural funds from the Centre National de la Recherche Scientifique (CNRS) and the University of Poitiers.

Acknowledgments

We would like to thank Yann Dussert from the EBI laboratory for his invaluable help in using the Circos software and Alexandra Lafitte from the EBI laboratory for animal rearing.

Conflict of interest

The authors declare that the research was conducted in the absence of any commercial or financial relationships that could be construed as a potential conflict of interest.

Publisher's note

Supplementary material

The Supplementary material for this article can be found online at: https://www.frontiersin.org/articles/10.3389/fmicb.2024.1416057/full#supplementary-material

SUPPLEMENTARY TABLE S1
Sex ratio of progenies in four different laboratory lineages of *A. vulgare* over 5 years. BI, CP, and ZN were lineages naturally infected with *w*VulM, *w*VulP, and *w*VULC *Wolbachia* strains, respectively. BF was an uninfected lineage.

SUPPLEMENTARY TABLE S2
Pairwise comparison of average nucleotide identity (ANI) values between *w*VulC, *w*VulM, and *w*VulP genomes (*w*VulC as reference).

SUPPLEMENTARY TABLE S3
OrthoFinder analysis to identify orthologous groups of genes from the three *Wolbachia* genomes.

SUPPLEMENTARY TABLE S4
Wolbachia genomes used in the phylogenomic analysis.

SUPPLEMENTARY TABLE S5
Orthogroup analysis from 29 *Wolbachia* complete genomes.

SUPPLEMENTARY TABLE S6
Annotations of IS elements predicted by ISEScan analysis.

SUPPLEMENTARY TABLE S7
Annotations of group II intron-associated genes.

SUPPLEMENTARY TABLE S8
Annotations of the phage regions.

SUPPLEMENTARY TABLE S9
EffectiveDB predictions of Type IV Secretion Systems (T4SS) and potential effectors.

SUPPLEMENTARY FIGURE S1
Plot of mean male ratio of progeny from the four laboratory lines of *A. vulgare* (BF, BI, CP, and ZN) per year over five-years. BF lineage is uninfected whereas BI, CP, and ZN lineages are infected with *w*VulM, *w*VulP, and *w*VulC *Wolbachia* strains, respectively. White circles correspond to mean values and whiskers represent standard error.

SUPPLEMENTARY FIGURE S2
Alignment of the three *Wolbachia* genomes: **(A)** Collinearity between *w*VulC and *w*VulM. **(B)** Collinearity between *w*VulC and *w*VulP. **(C)** Collinearity between *w*VulM and *w*VulP. Pairwise comparisons were performed by BLASTn using FastANI 1.3 software. Each red line segment indicates a reciprocal match between two sequences. The colored bar indicates the percentage of identity. Homologous regions are indicated by segments of the same color.

SUPPLEMENTARY FIGURE S3
Alignment of the complete *w*VulC genome obtained by ONT sequencing technology (this study) with the previous draft genome (GCA_001027565.1; unpublished) obtained by Sanger technology. Collinearity detected by BLASTn using FastANI 1.3 software. Each red line segment denotes a reciprocal match between two sequences. Homologous regions are indicated by segments of the same color. The colored bar indicates the percentage of identity.

SUPPLEMENTARY FIGURE S4
Alignment of the complete *w*VulC genome with the concatenated eight scaffolds of the *Wolbachia* inserts (*f* element; Leclercq et al., 2016) in the nuclear genome of *A. vulgare*. Collinearity detected by BLASTn using FastANI 1.3 software. Each red line segment denotes a reciprocal match between two sequences. Homologous regions are indicated by segments of the same color. The colored bar indicates the percentage of identity.

References

Andrews, S. (2010). FastQC: A quality control tool for high throughput sequence data. Available online at: http://www.bioinformatics.babraham.ac.uk/projects/fastqc (Accessed January 23, 2023).

Badawi, M., Giraud, I., Vavre, F., Grève, P., and Cordaux, R. (2014). Signs of neutralization in a redundant gene involved in homologous recombination in *Wolbachia* endosymbionts. *Genome Biol. Evol.* 6, 2654–2664. doi: 10.1093/gbe/evu207

Badawi, M., Moumen, B., Giraud, I., Grève, P., and Cordaux, R. (2018). Investigating the molecular genetic basis of cytoplasmic sex determination caused by *Wolbachia* endosymbionts in terrestrial isopods. *Genes (Basel)* 9:290. doi: 10.3390/genes9060290

Beliavskaia, A., Tan, K.-K., Sinha, A., Husin, N. A., Lim, F. S., Loong, S. K., et al. (2023). Metagenomics of culture isolates and insect tissue illuminate the evolution of *Wolbachia*, rickettsia and bartonella symbionts in Ctenocephalides spp. fleas. *Microb Genom* 9:mgen001045. doi: 10.1099/mgen.0.001045

Bordenstein, S. R., and Bordenstein, S. R. (2016). Eukaryotic association module in phage WO genomes from *Wolbachia*. *Nat. Commun.* 7:13155. doi: 10.1038/ncomms13155

Bordenstein, S. R., and Bordenstein, S. R. (2022). Widespread phages of endosymbionts: phage WO genomics and the proposed taxonomic classification of Symbioviridae. *PLoS Genet.* 18:e1010227. doi: 10.1371/journal.pgen.1010227

Bordenstein, S. R., Marshall, M. L., Fry, A. J., Kim, U., and Wernegreen, J. J. (2006). The tripartite associations between bacteriophage, *Wolbachia*, and arthropods. *PLoS Pathog.* 2:e43. doi: 10.1371/journal.ppat.0020043

Bordenstein, S. R., and Theis, K. R. (2015). Host biology in light of the microbiome: ten principles of Holobionts and Hologenomes. *PLoS Biol.* 13:e1002226. doi: 10.1371/journal.pbio.1002226

Bouchon, D., Cordaux, R., and Grève, P. (2008). "Feminizing *Wolbachia* and the evolution of sex determination in isopods" in Insect Symbiosis. Contemporary Topics in Entomology, vol. *3* (Boca Raton, FL: CRC Press), 273–294.

Bouchon, D., Rigaud, T., and Juchault, P. (1998). Evidence for widespread *Wolbachia* infection in isopod crustaceans: molecular identification and host feminization. *Proc. Royal Soc. London Series B Biol. Sci.* 265, 1081–1090. doi: 10.1098/rspb.1998.0402

Braquart-Varnier, C., Grève, P., Félix, C., and Martin, G. (2005). Bacteriophage WO in *Wolbachia* infecting terrestrial isopods. *Biochem. Biophys. Res. Commun.* 337, 580–585. doi: 10.1016/j.bbrc.2005.09.091

Brettin, T., Davis, J. J., Disz, T., Edwards, R. A., Gerdes, S., Olsen, G. J., et al. (2015). RASTtk: a modular and extensible implementation of the RAST algorithm for building custom annotation pipelines and annotating batches of genomes. *Sci. Rep.* 5:8365. doi: 10.1038/srep08365

Candales, M. A., Duong, A., Hood, K. S., Li, T., Neufeld, R. A. E., Sun, R., et al. (2012). Database for bacterial group II introns. *Nucleic Acids Res.* 40, D187–D190. doi: 10.1093/nar/gkr1043

Carpinone, E. M., Li, Z., Mills, M. K., Foltz, C., Brannon, E. R., Carlow, C. K. S., et al. (2018). Identification of putative effectors of the type IV secretion system from the *Wolbachia* endosymbiont of *Brugia malayi*. *PLoS One* 13:e0204736. doi: 10.1371/journal.pone.0204736

Chen, S., Zhou, Y., Chen, Y., and Gu, J. (2018). Fastp: an ultra-fast all-in-one FASTQ preprocessor. *Bioinformatics* 34, i884–i890. doi: 10.1093/bioinformatics/bty560

Cordaux, R., Michel-Salzat, A., and Bouchon, D. (2001). *Wolbachia* infection in crustaceans: novel hosts and potential routes for horizontal transmission. *J. Evol. Biol.* 14, 237–243. doi: 10.1046/j.1420-9101.2001.00279.x

Cordaux, R., Michel-Salzat, A., Frelon-Raimond, M., Rigaud, T., and Bouchon, D. (2004). Evidence for a new feminizing *Wolbachia* strain in the isopod *Armadillidium vulgare*: evolutionary implications. *Heredity* 93, 78–84. doi: 10.1038/sj.hdy.6800482

Darby, A. C., Armstrong, S. D., Bah, G. S., Kaur, G., Hughes, M. A., Kay, S. M., et al. (2012). Analysis of gene expression from the *Wolbachia* genome of a filarial nematode supports both metabolic and defensive roles within the symbiosis. *Genome Res.* 22, 2467–2477. doi: 10.1101/gr.138420.112

Darling, A. E., Mau, B., and Perna, N. T. (2010). Progressive mauve: multiple genome alignment with gene gain, loss and rearrangement. *Plos One* 5:e11147. doi: 10.1371/journal.pone.0011147

de Koning, W., Miladi, M., Hiltemann, S., Heikema, A., Hays, J. P., Flemming, S., et al. (2020). Nano galaxy: nanopore long-read sequencing data analysis in galaxy. *GigaScience* 9:giaa105. doi: 10.1093/gigascience/giaa105

Dittmer, J., Beltran-Bech, S., Lesobre, J., Raimond, M., Johnson, M., and Bouchon, D. (2014). Host tissues as microhabitats for *Wolbachia* and quantitative insights into the bacterial community in terrestrial isopods. *Mol. Ecol.* 23, 2619–2635. doi: 10.1111/mec.12760

Dittmer, J., and Bouchon, D. (2018). Feminizing *Wolbachia* influence microbiota composition in the terrestrial isopod *Armadillidium vulgare*. *Sci. Rep.* 8:6998. doi: 10.1038/s41598-018-25450-4

Driscoll, T. P., Verhoeve, V. I., Brockway, C., Shrewsberry, D. L., Plumer, M., Sevdalis, S. E., et al. (2020). Evolution of *Wolbachia* mutualism and reproductive parasitism: insight from two novel strains that co-infect cat fleas. *PeerJ* 8:e10646. doi: 10.7717/peerj.10646

Durand, S., Lheraud, B., Giraud, I., Bech, N., Grandjean, F., Rigaud, T., et al. (2023). Heterogeneous distribution of sex ratio distorters in natural populations of the isopod *Armadillidium vulgare*. *Biol. Lett.* 19:20220457. doi: 10.1098/rsbl.2022.0457

Eichinger, V., Nussbaumer, T., Platzer, A., Jehl, M.-A., Arnold, R., and Rattei, T. (2016). EffectiveDB—updates and novel features for a better annotation of bacterial secreted proteins and type III, IV, VI secretion systems. *Nucleic Acids Res.* 44, D669–D674. doi: 10.1093/nar/gkv1269

Emms, D. M., and Kelly, S. (2019). OrthoFinder: phylogenetic orthology inference for comparative genomics. *Genome Biol.* 20:238. doi: 10.1186/s13059-019-1832-y

Fallon, A. M. (2020). Computational evidence for antitoxins associated with RelE/ParE, RatA, fic, and AbiEii-family toxins in *Wolbachia* genomes. *Mol. Gen. Genomics.* 295, 891–909. doi: 10.1007/s00438-020-01662-0

Fricke, L. C., and Lindsey, A. R. I. (2024). Identification of parthenogenesis-inducing effector proteins in *Wolbachia*. *Genome Biol. Evol.*:evae036. doi: 10.1093/gbe/evae036

Fukui, T., Kawamoto, M., Shoji, K., Kiuchi, T., Sugano, S., Shimada, T., et al. (2015). The endosymbiotic bacterium *Wolbachia* selectively kills male hosts by targeting the masculinizing gene. *PLoS Pathog.* 11:e1005048. doi: 10.1371/journal.ppat.1005048

Gavotte, L., Henri, H., Stouthamer, R., Charif, D., Charlat, S., Bouletreau, M., et al. (2006). A survey of the bacteriophage WO in the endosymbiotic bacteria *Wolbachia*. *Mol. Biol. Evol.* 24, 427–435. doi: 10.1093/molbev/msl171

Geniez, S. (2013). Investigation of *Wolbachia* symbiosis in isopods and filarial nematodes by genomic and interactome studies. Poitiers: Université de Poitiers.

Geniez, S., Foster, J. M., Kumar, S., Moumen, B., LeProust, E., Hardy, O., et al. (2012). Targeted genome enrichment for efficient purification of endosymbiont DNA from host DNA. *Symbiosis* 58, 201–207. doi: 10.1007/s13199-012-0215-x

Gerth, M., and Bleidorn, C. (2016). Comparative genomics provides a timeframe for *Wolbachia* evolution and exposes a recent biotin synthesis operon transfer. *Nat. Microbiol.* 2, 1–7. doi: 10.1038/nmicrobiol.2016.241

Grishin, E. V. (1998). Black widow spider toxins: the present and the future. *Toxicon* 36, 1693–1701. doi: 10.1016/S0041-0101(98)00162-7

Harumoto, T., and Lemaitre, B. (2018). Male-killing toxin in a drosophila bacterial symbiont. *Nature* 557, 252–255. doi: 10.1038/s41586-018-0086-2

Herran, B., Geniez, S., Delaunay, C., Raimond, M., Lesobre, J., Bertaux, J., et al. (2020). The shutting down of the insulin pathway: a developmental window for *Wolbachia* load and feminization. *Sci. Rep.* 10:67428. doi: 10.1038/s41598-020-67428-1

Herran, B., Houdelet, C., Raimond, M., Delaunay, C., Cerveau, N., Debenest, C., et al. (2021). Feminising *Wolbachia* disrupt *Armadillidium vulgare* insulin-like signalling pathway. *Cell. Microbiol.* 23:e13381. doi: 10.1111/cmi.13381

Hertig, M., and Wolbach, S. B. (1924). Studies on rickettsia-like micro-organisms in insects. *J. Med. Res.* 44:7.

Hiroki, M., Kato, Y., Kamito, T., and Miura, K. (2002). Feminization of genetic males by a symbiotic bacterium in a butterfly, Eurema hecabe (lepidoptera: Pieridae). *Naturwissenschaften* 89, 167–170. doi: 10.1007/s00114-002-0303-5

Hurst, G. D. D., Jiggins, F. M., von der Schulenburg, J. H. G., Bertrand, D., West, S. A., Goriacheva, I. I., et al. (1999). Male-killing *Wolbachia* in two species of insect. *Proc. Biol. Sci.* 266:735. doi: 10.1098/rspb.1999.0698

Jain, C., Rodriguez-R, L. M., Phillippy, A. M., Konstantinidis, K. T., and Aluru, S. (2018). High throughput ANI analysis of 90K prokaryotic genomes reveals clear species boundaries. *Nat. Commun.* 9:5114. doi: 10.1038/s41467-018-07641-9

Jernigan, K. K., and Bordenstein, S. R. (2014). Ankyrin domains across the tree of life. *PeerJ* 2:e264. doi: 10.7717/peerj.264

Jiggins, F. M., Schulenburg, J. H. G. V. D., Hurst, G. D. D., and Majerus, M. E. N. (2001). Recombination confounds interpretations of *Wolbachia* evolution. *Proc. R. Soc. Lond. B* 268, 1423–1427. doi: 10.1098/rspb.2001.1656

Juchault, P., and Legrand, J. J. (1985). Contribution to the study of refractory state mechanism in the androgenic hormone in *Armadillidium vulgare* Latr (Crustaceae, isopoda, Oniscoida) sheltering a feminizing bacteria. *Gen. Comp. Endocrinol.* 60, 463–467. doi: 10.1016/0016-6480(85)90082-6

Juchault, P., Legrand, J.-J., and Martin, G. (1974). Action interspecifique du facteur epigenetique feminisant responsable de la thelygenie et de l'intersexualite du crustace *Armadillidium vulgare* (isopode oniscoide). *Ann. Embryol. Morphogenese* 7, 265–276.

Juchault, P., and Mocquard, J. P. (1993). Transfer of a parasitic sex factor to the nuclear genome of the host: a hypothesis on the evolution of sex-determining mechanisms in the terrestrial isopod *Armadillidium vulgare* Latr. *J. Evol. Biol.* 6, 511–528. doi: 10.1046/j.1420-9101.1993.6040511.x

Juchault, P., Rigaud, T., and Mocquard, J.-P. (1993). Evolution of sex determination and sex ratio variability in wild populations of *Armadillidium vulgare* (Latr.) (crustacea, isopoda): a case study in conflict resolution. *Acta Oecol. Int. J. Ecol.* 14, 547–562.

Kageyama, D., Ohno, M., Sasaki, T., Yoshido, A., Konagaya, T., Jouraku, A., et al. (2017). Feminizing *Wolbachia* endosymbiont disrupts maternal sex chromosome inheritance in a butterfly species. *Evol. Lett.* 1, 232–244. doi: 10.1002/evl3.28

Kalyaanamoorthy, S., Minh, B. Q., Wong, T. K. F., von Haeseler, A., and Jermiin, L. S. (2017). ModelFinder: fast model selection for accurate phylogenetic estimates. *Nat. Methods* 14, 587–589. doi: 10.1038/nmeth.4285

Katoh, K., Rozewicki, J., and Yamada, K. D. (2017). MAFFT online service: multiple sequence alignment, interactive sequence choice and visualization. *Brief. Bioinform.* 20, 1160–1166. doi: 10.1093/bib/bbx108

Katsuma, S., Hirota, K., Matsuda-Imai, N., Fukui, T., Muro, T., Nishino, K., et al. (2022). A *Wolbachia* factor for male killing in lepidopteran insects. *Nat. Commun.* 13:6764. doi: 10.1038/s41467-022-34488-y

Kaur, R., Shropshire, J. D., Cross, K. L., Leigh, B., Mansueto, A. J., Stewart, V., et al. (2021). Living in the endosymbiotic world of *Wolbachia*: a centennial review. *Cell Host Microbe* 29, 879–893. doi: 10.1016/j.chom.2021.03.006

Kent, B. N., and Bordenstein, S. R. (2010). Phage WO of *Wolbachia*: lambda of the endosymbiont world. *Trends Microbiol.* 18, 173–181. doi: 10.1016/j.tim.2009.12.011

Klasson, L., Walker, T., Sebaihia, M., Sanders, M. J., Quail, M. A., Lord, A., et al. (2008). Genome evolution of *Wolbachia* strain wPip from the *Culex pipiens* group. *Mol. Biol. Evol.* 25, 1877–1887. doi: 10.1093/molbev/msn133

Klasson, L., Westberg, J., Sapountzis, P., Näslund, K., Lutnaes, Y., Darby, A. C., et al. (2009). The mosaic genome structure of the *Wolbachia* wRi strain infecting *Drosophila simulans*. *Proc. Natl. Acad. Sci. USA* 106, 5725–5730. doi: 10.1073/pnas.0810753106

Kolmogorov, M., Yuan, J., Lin, Y., and Pevzner, P. A. (2019). Assembly of long, error-prone reads using repeat graphs. *Nat. Biotechnol.* 37, 540–546. doi: 10.1038/s41587-019-0072-8

Krzywinski, M. I., Schein, J. E., Birol, I., Connors, J., Gascoyne, R., Horsman, D., et al. (2009). Circos: an information aesthetic for comparative genomics. *Genome Res.* doi: 10.1101/gr.092759.109

Landmann, F. (2019). The *Wolbachia* endosymbionts. *Microbiol Spectr* 7:2019. doi: 10.1128/microbiolspec.BAI-0018-2019

Leclercq, S., Giraud, I., and Cordaux, R. (2011). Remarkable abundance and evolution of Mobile group II introns in *Wolbachia* bacterial endosymbionts. *Mol. Biol. Evol.* 28, 685–697. doi: 10.1093/molbev/msq238

Leclercq, S., Thézé, J., Chebbi, M. A., Giraud, I., Moumen, B., Ernenwein, L., et al. (2016). Birth of a W sex chromosome by horizontal transfer of *Wolbachia* bacterial symbiont genome. *Proc. Natl. Acad. Sci.* 113, 15036–15041. doi: 10.1073/pnas.1608979113

Lefoulon, E., Clark, T., Borveto, F., Perriat-Sanguinet, M., Moulia, C., Slatko, B. E., et al. (2020). Pseudoscorpion *Wolbachia* symbionts: diversity and evidence for a new supergroup S. *BMC Microbiol.* 20:188. doi: 10.1186/s12866-020-01863-y

LePage, D. P., Metcalf, J. A., Bordenstein, S. R., On, J., Perlmutter, J. I., Shropshire, J. D., et al. (2017). Prophage WO genes recapitulate and enhance *Wolbachia*-induced cytoplasmic incompatibility. *Nature* 543, 243–247. doi: 10.1038/nature21391

Letunic, I., and Bork, P. (2021). Interactive tree of life (iTOL) v5: an online tool for phylogenetic tree display and annotation. *Nucleic Acids Res.* 49, W293–W296. doi: 10.1093/nar/gkab301

Lindsey, A. R. I. (2020). Sensing, Signaling, and secretion: a review and analysis of Systems for Regulating Host Interaction in *Wolbachia*. *Genes (Basel)* 11:813. doi: 10.3390/genes11070813

Lindsey, A. R. I., Werren, J. H., Richards, S., and Stouthamer, R. (2016). Comparative genomics of a parthenogenesis-inducing *Wolbachia* symbiont. *G3 (Bethesda)* 6, 2113–2123. doi: 10.1534/g3.116.028449

Loman, N. J., Quick, J., and Simpson, J. T. (2015). A complete bacterial genome assembled de novo using only nanopore sequencing data. *Nat. Methods* 12, 733–735. doi: 10.1038/nmeth.3444

Lüdecke, D., Ben-Shachar, M., Patil, I., Waggoner, P., and Makowski, D. (2021). Performance: an R package for assessment, comparison and testing of statistical models. *JOSS* 6:3139. doi: 10.21105/joss.03139

Ma, W.-J., and Schwander, T. (2017). Patterns and mechanisms in instances of endosymbiont-induced parthenogenesis. *J. Evol. Biol.* 30, 868–888. doi: 10.1111/jeb.13069

Manni, M., Berkeley, M. R., Seppey, M., Simão, F. A., and Zdobnov, E. M. (2021). BUSCO update: novel and streamlined workflows along with broader and deeper phylogenetic coverage for scoring of eukaryotic, prokaryotic, and viral genomes. *Mol. Biol. Evol.* 38, 4647–4654. doi: 10.1093/molbev/msab199

McFall-Ngai, M., Hadfield, M. G., Bosch, T. C. G., Carey, H. V., Domazet-Lošo, T., Douglas, A. E., et al. (2013). Animals in a bacterial world, a new imperative for the life sciences. *Proc. Natl. Acad. Sci.* 110, 3229–3236. doi: 10.1073/pnas.1218525110

Minh, B. Q., Nguyen, M. A. T., and von Haeseler, A. (2013). Ultrafast approximation for phylogenetic bootstrap. *Mol. Biol. Evol.* 30, 1188–1195. doi: 10.1093/molbev/mst024

Minh, B. Q., Schmidt, H. A., Chernomor, O., Schrempf, D., Woodhams, M. D., von Haeseler, A., et al. (2020). IQ-TREE 2: new models and efficient methods for phylogenetic inference in the genomic era. *Mol. Biol. Evol.* 37, 1530–1534. doi: 10.1093/molbev/msaa015

Moret, Y., Juchault, P., and Rigaud, T. (2001). *Wolbachia* endosymbiont responsible for cytoplasmic incompatibility in a terrestrial crustacean: effects in natural and foreign hosts. *Heredity (Edinb)* 86, 325–332. doi: 10.1046/j.1365-2540.2001.00831.x

Negri, I., Pellecchia, M., Mazzoglio, P. J., Patetta, A., and Alma, A. (2006). Feminizing *Wolbachia* in Zyginidia pullula (Insecta, Hemiptera), a leafhopper with an XX/X0 sex-determination system. *Proc. R. Soc. B Biol. Sci.* 273, 2409–2416. doi: 10.1098/rspb.2006.3592

Nikoh, N., Hosokawa, T., Moriyama, M., Oshima, K., Hattori, M., and Fukatsu, T. (2014). Evolutionary origin of insect-*Wolbachia* nutritional mutualism. *Proc. Natl. Acad. Sci. USA* 111, 10257–10262. doi: 10.1073/pnas.1409284111

Perlmutter, J. I., Bordenstein, S. R., Unckless, R. L., LePage, D. P., Metcalf, J. A., Hill, T., et al. (2019). The phage gene wmk is a candidate for male killing by a bacterial endosymbiont. *PLoS Pathog.* 15:e1007936. doi: 10.1371/journal.ppat.1007936

Pichon, S., Bouchon, D., Cordaux, R., Chen, L., Garrett, R. A., and Greve, P. (2009). Conservation of the type IV secretion system throughout *Wolbachia* evolution. *Biochem. Biophys. Res. Commun.* 385, 557–562. doi: 10.1016/j.bbrc.2009.05.118

R Core Team (2023). R: A language and environment for statistical Computing_. Vienna, Austria: R Foundation for Statistical Computing.

Rice, D. W., Sheehan, K. B., and Newton, I. L. G. (2017). Large-scale identification of *Wolbachia pipientis* effectors. *Genome Biol. Evol.* 9, 1925–1937. doi: 10.1093/gbe/evx139

Rigaud, T. (1997). "Inherited microorganisms and sex determination of arthropod hosts" in Influential passengers: Inherited microorganisms and arthropod reproduction (Oxford: Oxford University Press), 81–101.

Rigaud, T., and Juchault, P. (1998). Sterile intersexuality in an isopod induced by the interaction between a bacterium (*Wolbachia*) and the environment. *Can. J. Zool.* 76, 493–499. doi: 10.1139/z97-216

Rigaud, T., Juchault, P., and Mocquard, J. (1997). The evolution of sex determination in isopod crustaceans. *Bio Essays* 19, 409–416. doi: 10.1002/bies.950190508

Rikihisa, Y., and Lin, M. (2010). *Anaplasma phagocytophilum* and *Ehrlichia chaffeensis* type IV secretion and Ank proteins. *Curr. Opin. Microbiol. Host* 13, 59–66. doi: 10.1016/j.mib.2009.12.008

Rousset, F., Bouchon, D., Pintureau, B., Juchault, P., and Solignac, M. (1992). *Wolbachia* endosymbionts responsible for various alterations of sexuality in arthropods. *Proc. Royal Soc. London Series B Biol. Sci.* 250, 91–98. doi: 10.1098/rspb.1992.0135

Scholz, M., Albanese, D., Tuohy, K., Donati, C., Segata, N., and Rota-Stabelli, O. (2020). Large scale genome reconstructions illuminate *Wolbachia* evolution. *Nat. Commun.* 11:5235. doi: 10.1038/s41467-020-19016-0

Sheehan, K. B., Martin, M., Lesser, C. F., Isberg, R. R., and Newton, I. L. G. (2016). Identification and characterization of a candidate *Wolbachia pipientis* type IV effector that interacts with the actin cytoskeleton. *MBio* 7, e00622–e00616. doi: 10.1128/mBio.00622-16

Shropshire, J. D., and Bordenstein, S. R. (2019). Two-by-one model of cytoplasmic incompatibility: synthetic recapitulation by transgenic expression of cifA and cifB in drosophila. *PLoS Genet.* 15:e1008221. doi: 10.1371/journal.pgen.1008221

Shropshire, J. D., Rosenberg, R., and Bordenstein, S. R. (2020). The impacts of cytoplasmic incompatibility factor (cifA and cifB) genetic variation on phenotypes. *Genetics* 217:iyaa007. doi: 10.1093/genetics/iyaa007

Sicard, M., Bouchon, D., Ceyrac, L., Raimond, R., Thierry, M., Le Clec'h, W., et al. (2014). Bidirectional cytoplasmic incompatibility caused by *Wolbachia* in the terrestrial isopod *Porcellio dilatatus*. *J. Invertebr. Pathol.* 121, 28–36. doi: 10.1016/j.jip.2014.06.007

Stouthamer, R., Luck, R. F., and Hamilton, W. D. (1990). Antibiotics cause parthenogenetic Trichogramma (Hymenoptera/Trichogrammatidae) to revert to sex. *Proc. Natl. Acad. Sci. USA* 87, 2424–2427. doi: 10.1073/pnas.87.7.2424

Sun, L. V., Foster, J. M., Tzertzinis, G., Ono, M., Bandi, C., Slatko, B. E., et al. (2001). Determination of *Wolbachia* genome size by pulsed-field gel electrophoresis. *J. Bacteriol.* 183, 2219–2225. doi: 10.1128/JB.183.7.2219-2225.2001

Tatusova, T., DiCuccio, M., Badretdin, A., Chetvernin, V., Nawrocki, E. P., Zaslavsky, L., et al. (2016). NCBI prokaryotic genome annotation pipeline. *Nucleic Acids Res.* 44, 6614–6624. doi: 10.1093/nar/gkw569

Trifinopoulos, J., Nguyen, L.-T., von Haeseler, A., and Minh, B. Q. (2016). W-IQ-TREE: a fast online phylogenetic tool for maximum likelihood analysis. *Nucleic Acids Res.* 44, W232–W235. doi: 10.1093/nar/gkw256

Vancaester, E., and Blaxter, M. (2023). Phylogenomic analysis of *Wolbachia* genomes from the Darwin tree of life biodiversity genomics project. *PLoS Biol.* 21:e3001972. doi: 10.1371/journal.pbio.3001972

Verne, S., Johnson, M., Bouchon, D., and Grandjean, F. (2007). Evidence for recombination between feminizing *Wolbachia* in the isopod genus Armadillidium. *Gene* 397, 58–66. doi: 10.1016/j.gene.2007.04.006

Werren, J. H., Baldo, L., and Clark, M. E. (2008). *Wolbachia*: master manipulators of invertebrate biology. *Nat. Rev. Microbiol.* 6, 741–751. doi: 10.1038/nrmicro1969

Werren, J. H., and Bartos, J. D. (2001). Recombination in *Wolbachia*. *Curr. Biol.* 11, 431–435. doi: 10.1016/S0960-9822(01)00101-4

Wilkins, D. (2023). Gggenes: draw gene arrow maps in "ggplot2". R package version 0.1. Available online at: https://wilkox.org/gggenes/ (Accessed January 23, 2023).

Wishart, D. S., Han, S., Saha, S., Oler, E., Peters, H., Grant, J. R., et al. (2023). PHASTEST: faster than PHASTER, better than PHAST. *Nucleic Acids Res.* 51, W443–W450. doi: 10.1093/nar/gkad382

Wiwatanaratanabutr, I., Kittayapong, P., Caubet, Y., and Bouchon, D. (2009). Molecular phylogeny of *Wolbachia* strains in arthropod hosts based on groE-homologous gene sequences. *Zool. Sci.* 26, 171–177. doi: 10.2108/zsj.26.171

Wu, M., Sun, L. V., Vamathevan, J., Riegler, M., Deboy, R., Brownlie, J. C., et al. (2004). Phylogenomics of the reproductive parasite *Wolbachia pipientis* wMel: a streamlined genome overrun by Mobile genetic elements. *PLoS Biol.* 2:e69. doi: 10.1371/journal.pbio.0020069

Xie, Z., and Tang, H. (2017). ISEScan: automated identification of insertion sequence elements in prokaryotic genomes. *Bioinformatics* 33, 3340–3347. doi: 10.1093/bioinformatics/btx433

Yu, X., Noll, R. R., Romero Dueñas, B. P., Allgood, S. C., Barker, K., Caplan, J. L., et al. (2018). Legionella effector AnkX interacts with host nuclear protein PLEKHN1. *BMC Microbiol.* 18:5. doi: 10.1186/s12866-017-1147-7

Zhang, D., de Souza, R. F., Anantharaman, V., Iyer, L. M., and Aravind, L. (2012). Polymorphic toxin systems: comprehensive characterization of trafficking modes, processing, mechanisms of action, immunity and ecology using comparative genomics. *Biol. Direct* 7:18. doi: 10.1186/1745-6150-7-18

Zug, R., and Hammerstein, P. (2012). Still a host of hosts for *Wolbachia*: analysis of recent data suggests that 40% of terrestrial arthropod species are infected. *PLoS One* 7:e38544. doi: 10.1371/journal.pone.0038544

Frontiers in Microbiology

Explores the habitable world and the potential of microbial life

The largest and most cited microbiology journal which advances our understanding of the role microbes play in addressing global challenges such as healthcare, food security, and climate change.

Discover the latest Research Topics

See more →

Frontiers

Avenue du Tribunal-Fédéral 34
1005 Lausanne, Switzerland
frontiersin.org

Contact us

+41 (0)21 510 17 00
frontiersin.org/about/contact